NASA

Earth Resources
A Continuing
Bibliography
with Indexes

NASA SP-7041(37)
April 1983

National Aeronautics and
Space Administration

25

25th Anniversary
1958-1983

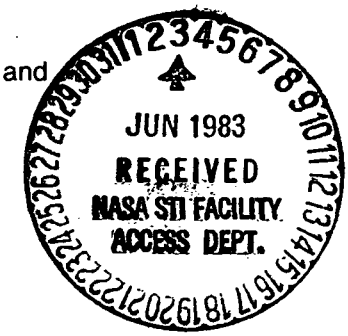

(NASA-SP-7041(37)) EARTH RESOURCES: A CONTINUING BIBLIOGRAPHY WITH INDEXES (ISSUE 37) (National Aeronautics and Space Administration) 140 p HC A07 CSCL 05B

N83-26123

Unclas
00/43 11834

Earth Resources

Earth Resources

Earth Resources

ACCESSION NUMBER RANGES

Accession numbers cited in this Supplement fall within the following ranges.

STAR (N-10000 Series)	N83-10001 - N83-16274
IAA (A-10000 Series)	A83-10001 - A83-19623

This bibliography was prepared by the NASA Scientific and Technical Information Facility operated for the National Aeronautics and Space Administration by PRC Government Information Systems.

NASA SP-7041(37)

EARTH RESOURCES

A CONTINUING BIBLIOGRAPHY WITH INDEXES

Issue 37

A selection of annotated references to unclassified reports and journal articles that were introduced into the NASA scientific and technical information system and announced between January 1 and March 31, 1983 in

- *Scientific and Technical Aerospace Reports (STAR)*
- *International Aerospace Abstracts (IAA).*

NASA Scientific and Technical Information Branch 1983
National Aeronautics and Space Administration
Washington, DC

This supplement is available as NTISUB/038/093 from the National Technical Information Service (NTIS), Springfield, Virginia 22161 at the price of $12.50 domestic; $25.00 foreign for standing orders. Please note: Standing orders are subscriptions which do not terminate at the end of a year, as do regular subscriptions, but continue indefinitely unless specifically terminated by the subscriber.

INTRODUCTION

The technical literature described in this continuing bibliography may be helpful to researchers in numerous disciplines such as agriculture and forestry, geography and cartography, geology and mining, oceanography and fishing, environmental control, and many others. Until recently it was impossible for anyone to examine more than a minute fraction of the Earth's surface continuously. Now vast areas can be observed synoptically, and changes noted in both the Earth's lands and waters, by sensing instrumention on orbiting spacecraft or on aircraft.

This literature survey lists 512 reports, articles, and other documents announced between January 1 and March 31, 1983 in *Scientific and Technical Aerospace Reports (STAR)*, and *International Aerospace Abstracts (IAA)*.

The coverage includes documents related to the identification and evaluation by means of sensors in spacecraft and aircraft of vegetation, minerals, and other natural resources, and the techniques and potentialities of surveying and keeping up-to-date inventories of such riches. It encompasses studies of such natural phenomena as earthquakes, volcanoes, ocean currents, and magnetic fields; and such cultural phenomena as cities, transportation networks, and irrigation systems. Descriptions of the components and use of remote sensing and geophysical instrumentation, their subsystems, observational procedures, signature and analyses and interpretive techniques for gathering data are also included. All reports generated under NASA's Earth Resources Survey Program for the time period covered in this bibliography will also be included. The bibliography does not contain citations to documents dealing mainly with satellites or satellite equipment used in navigation or communication systems, nor with instrumentation not used aboard aerospace vehicles.

The selected items are grouped in nine categories. These are listed in the Table of Contents with notes regarding the scope of each category. These categories were especially chosen for this publication, and differ from those found in *STAR* and *IAA*.

Each entry consists of a standard bibliographic citation accompanied by an abstract. The citations and abstracts are reproduced exactly as they appeared originally in *STAR*, or *IAA*, including the original accession numbers from the respective announcement journals.

Under each of the nine categories, the entries are presented in one of two groups that appear in the following order:

IAA entries identified by accession number series A83-10,000 in ascending accession number order;

STAR entries identified by accession number series N83-10,000 in ascending accession number order.

After the abstract section, there are six indexes:

subject, personal author, corporate source, contract number, report/accession number, and accession number.

AVAILABILITY OF CITED PUBLICATIONS

IAA ENTRIES (A83-10000 Series)

All publications abstracted in this Section are available from the Technical Information Service, American Institute of Aeronautics and Astronautics, Inc. (AIAA), as follows: Paper copies of accessions are available at $8.00 per document. Microfiche[1] of documents announced in *IAA* are available at the rate of $4.00 per microfiche on demand, and at the rate of $1.35 per microfiche for standing orders for all *IAA* microfiche.

Minimum air-mail postage to foreign countries is $2.50 and all foreign orders are shipped on payment of pro-forma invoices.

All inquiries and requests should be addressed to AIAA Technical Information Service. Please refer to the accession number when requesting publications.

STAR ENTRIES (N83-10000 Series)

One or more sources from which a document announced in *STAR* is available to the public is ordinarily given on the last line of the citation. The most commonly indicated sources and their acronyms or abbreviations are listed below. If the publication is available from a source other than those listed, the publisher and his address will be displayed on the availability line or in combination with the corporate source line.

Avail: NTIS. Sold by the National Technical Information Service. Prices for hard copy (HC) and microfiche (MF) are indicated by a price code preceded by the letters HC or MF in the *STAR* citation. Current values for the price codes are given in the tables on page vii.

Documents on microfiche are designated by a pound sign (#) following the accession number. The pound sign is used without regard to the source or quality of the microfiche.

Initially distributed microfiche under the NTIS SRIM (Selected Research in Microfiche) is available at greatly reduced unit prices. For this service and for information concerning subscription to NASA printed reports, consult the NTIS Subscription Section, Springfield, Va. 22161.

NOTE ON ORDERING DOCUMENTS: When ordering NASA publications (those followed by the * symbol), use the N accession number. NASA patent applications (only the specifications are offered) should be ordered by the US-Patent-Appl-SN number. Non-NASA publications (no asterisk) should be ordered by the AD, PB, or other *report* number shown on the last line of the citation, not by the N accession number. It is also advisable to cite the title and other bibliographic identification.

Avail: SOD (or GPO). Sold by the Superintendent of Documents, U.S. Government Printing Office, in hard copy. The current price and order number are given following the availability line. (NTIS will fill microfiche requests, as indicated above, for those documents identified by a # symbol.)

Avail: NASA Public Document Rooms. Documents so indicated may be examined at or purchased from the National Aeronautics and Space Administration, Public Document Room (Room 126), 600 Independence Ave., S.W., Washington, D.C. 20546, or public document rooms located at each of the NASA research centers, the NASA Space Technology Laboratories, and the NASA Pasadena Office at the Jet Propulsion Laboratory.

(1) A microfiche is a transparent sheet of film, 105 by 148 mm in size containing as many as 60 to 98 pages of information reduced to micro images (not to exceed 26.1 reduction).

Avail: DOE Depository Libraries. Organizations in U.S. cities and abroad that maintain collections of Department of Energy reports, usually in microfiche form, are listed in *Energy Research Abstracts.* Services available from the DOE and its depositories are described in a booklet, *DOE Technical Information Center - Its Functions and Services* (TID-4660), which may be obtained without charge from the DOE Technical Information Center.

Avail: Univ. Microfilms. Documents so indicated are dissertations selected from *Dissertation Abstracts* and are sold by University Microfilms as xerographic copy (HC) and microfilm. All requests should cite the author and the Order Number as they appear in the citation.

Avail: USGS. Originals of many reports from the U.S. Geological Survey, which may contain color illustrations, or otherwise may not have the quality of illustrations preserved in the microfiche or facsimile reproduction, may be examined by the public at the libraries of the USGS field offices whose addresses are listed in this introduction. The libraries may be queried concerning the availability of specific documents and the possible utilization of local copying services, such as color reproduction.

Avail: HMSO. Publications of Her Majesty's Stationery Office are sold in the U.S. by Pendragon House, Inc. (PHI), Redwood City, California. The U.S. price (including a service and mailing charge) is given, or a conversion table may be obtained from PHI.

Avail: BLL (formerly NLL): British Library Lending Division, Boston Spa, Wetherby, Yorkshire, England. Photocopies available from this organization at the price shown. (If none is given, inquiry should be addressed to the BLL.)

Avail: Fachinformationszentrum, Karlsruhe. Sold by the Fachinformationszentrum Energie, Physik, Mathematik GMBH, Eggenstein Leopoldshafen, Federal Republic of Germany, at the price shown in deutschmarks (DM).

Avail: Issuing Activity, or Corporate Author, or no indication of availability. Inquiries as to the availability of these documents should be addressed to the organization shown in the citation as the corporate author of the document.

Avail: U.S. Patent and Trademark Office. Sold by Commissioner of Patents and Trademarks, U.S. Patent and Trademark Office, at the standard price of 50 cents each, postage free.

Other availabilities: If the publication is available from a source other than the above, the publisher and his address will be displayed entirely on the availability line or in combination with the corporate author line.

ADDRESSES OF ORGANIZATIONS

American Institute of Aeronautics and Astronautics
Technical Information Service
555 West 57th Street, 12th Floor
New York, New York 10019

British Library Lending Division,
Boston Spa, Wetherby, Yorkshire,
England

Commissioner of Patents and Trademarks
U.S. Patent and Trademark Office
Washington, D.C. 20231

Department of Energy
Technical Information Center
P.O. Box 62
Oak Ridge, Tennessee 37830

ESA-Information Retrieval Service
ESRIN
Via Galileo Galilei
00044 Frascati (Rome) Italy

Fachinformationszentrum Energie, Physik, Mathematik GMBH
7514 Eggenstein Leopoldshafen
Federal Republic of Germany

Her Majesty's Stationery Office
P.O. Box 569, S.E. 1
London, England

NASA Scientific and Technical Information Facility
P.O. Box 8757
B.W.I. Airport, Maryland 21240

National Aeronautics and Space Administration
Scientific and Technical Information Branch (NIT-41)
Washington, D.C. 20546

National Technical Information Service
5285 Port Royal Road
Springfield, Virginia 22161

Pendragon House, Inc.
899 Broadway Avenue
Redwood City, California 94063

Superintendent of Documents
U.S. Government Printing Office
Washington, D.C. 20402

University Microfilms
A Xerox Company
300 North Zeeb Road
Ann Arbor, Michigan 48106

University Microfilms, Ltd.
Tylers Green
London, England

U.S. Geological Survey Library
National Center – MS 950
12201 Sunrise Valley Drive
Reston, Virginia 22092

U.S. Geological Survey Library
2255 North Gemini Drive
Flagstaff, Arizona 86001

U.S. Geological Survey
345 Middlefield Road
Menlo Park, California 94025

U.S. Geological Survey Library
Box 25046
Denver Federal Center, MS 914
Denver, Colorado 80225

NTIS PRICE SCHEDULES

Schedule A

STANDARD PAPER COPY PRICE SCHEDULE

(Effective January 1, 1983)

Price Code	Page Range	North American Price	Foreign Price
A01	Microfiche	$ 4.50	$ 9.00
A02	001-025	7.00	14.00
A03	026-050	8.50	17.00
A04	051-075	10.00	20.00
A05	076-100	11.50	23.00
A06	101-125	13.00	26.00
A07	126-150	14.50	29.00
A08	151-175	16.00	32.00
A09	176-200	17.50	35.00
A10	201-225	19.00	38.00
A11	226-250	20.50	41.00
A12	251-275	22.00	44.00
A13	276-300	23.50	47.00
A14	301-325	25.00	50.00
A15	326-350	26.50	53.00
A16	351-375	28.00	56.00
A17	376-400	29.50	59.00
A18	401-425	31.00	62.00
A19	426-450	32.50	65.00
A20	451-475	34.00	68.00
A21	476-500	35.50	71.00
A22	501-525	37.00	74.00
A23	526-550	38.50	77.00
A24	551-575	40.00	80.00
A25	576-600	41.50	83.00
A99	601-up	-- 1	-- 2

1/ Add $1.50 for each additional 25 page increment or portion thereof for 601 pages up.

2/ Add $3.00 for each additional 25 page increment or portion thereof for 601 pages and more.

Schedule E

EXCEPTION PRICE SCHEDULE

Paper Copy & Microfiche

Price Code	North American Price	Foreign Price
E01	$ 6.50	$ 13.50
E02	7.50	15.50
E03	9.50	19.50
E04	11.50	23.50
E05	13.50	27.50
E06	15.50	31.50
E07	17.50	35.50
E08	19.50	39.50
E09	21.50	43.50
E10	23.50	47.50
E11	25.50	51.50
E12	28.50	57.50
E13	31.50	63.50
E14	34.50	69.50
E15	37.50	75.50
E16	40.50	81.50
E17	43.50	88.50
E18	46.50	93.50
E19	51.50	102.50
E20	61.50	123.50
E-99 - Write for quote		
N01	35.00	45.00

TABLE OF CONTENTS

Page

Category 01 Agriculture and Forestry 1
Includes crop forecasts, crop signature analysis, soil identification, disease detection, harvest estimates, range resources, timber inventory, forest fire detection, and wildlife migration patterns.

Category 02 Environmental Changes and Cultural Resources 18
Includes land use analysis, urban and metropolitan studies, environmental impact, air and water pollution, geographic information systems, and geographic analysis.

Category 03 Geodesy and Cartography 23
Includes mapping and topography.

Category 04 Geology and Mineral Resources 30
Includes mineral deposits, petroleum deposits, spectral properties of rocks, geological exploration, and lithology.

Category 05 Oceanography and Marine Resources 38
Includes sea-surface temperature, ocean bottom surveying imagery, drift rates, sea ice and icebergs, sea state, fish location

Category 06 Hydrology and Water Management 49
Includes snow cover and water runoff in rivers and glaciers, saline intrusion, drainage analysis, geomorphology of river basins, land uses, and estuarine studies.

Category 07 Data Processing and Distribution Systems 54
Includes film processing, computer technology, satellite and aircraft hardware, and imagery.

Category 08 Instrumentation and Sensors 67
Includes data acquisition and camera systems and remote sensors.

Category 09 General 72
Includes economic analysis.

Subject Index A-1
Personal Author Index B-1
Corporate Source Index C-1
Contract Number Index D-1
Report / Accession Number Index E-1
Accession Number Index F-1

TYPICAL CITATION AND ABSTRACT FROM *STAR*

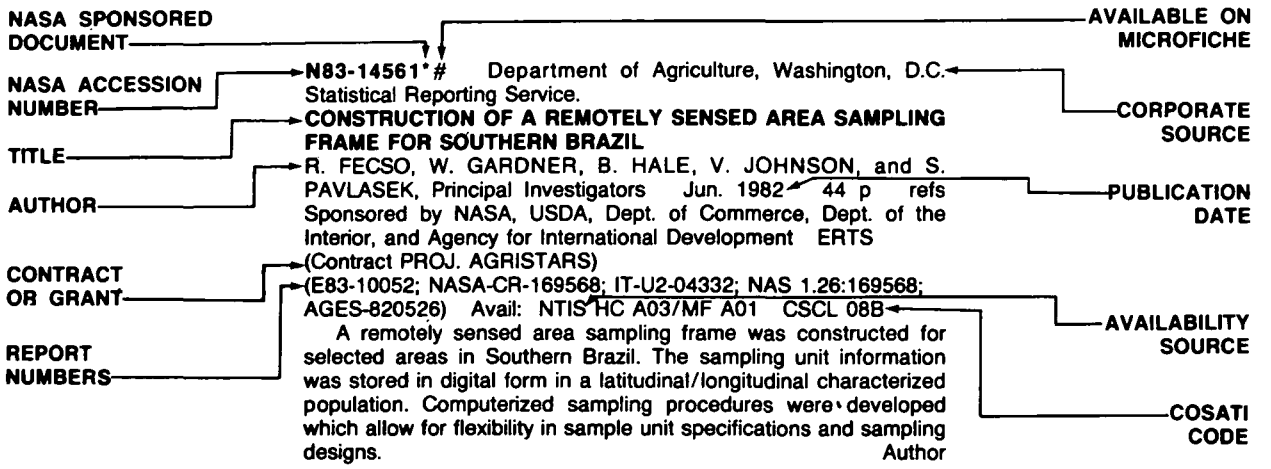

TYPICAL CITATION AND ABSTRACT FROM *IAA*

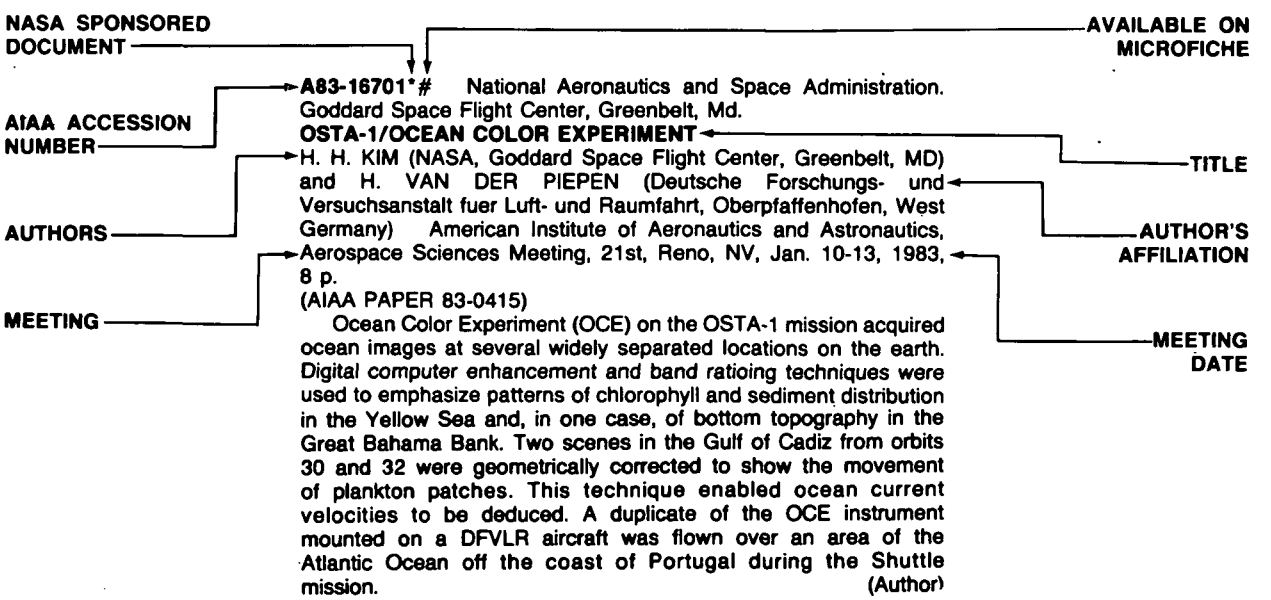

EARTH RESOURCES

A Continuing Bibliography (Issue 37)

APRIL 1983

01

AGRICULTURE AND FORESTRY

Includes crop forecasts, crop signature analysis, soil identification, disease detection, harvest estimates, range resources, timber inventry, forest fire detection, and wildlife migration patterns.

A83-10061* Geological Survey, Reston, Va.
SEASAT L-BAND RADAR RESPONSE TO FOREST VEGETATION IN EASTERN VIRGINIA
M. D. KROHN, N. M. MILTON, D. SEGAL, J. CROWLEY (U.S. Geological Survey, Reston, VA), and A. ENGLAND (NASA, Johnson Space Center, Houston, TX) In: International Geoscience and Remote Sensing Symposium, Washington, DC, June 8-10, 1981, Digest. Volume 1. New York, Institute of Electrical and Electronics Engineers, 1981, p. 617, 618.

A83-10095* National Aeronautics and Space Administration. Lyndon B. Johnson Space Center, Houston, Tex.
AGRISTARS - PLANS AND FIRST-YEAR ACHIEVEMENTS
F. G. HALL (NASA, Johnson Space Center, Houston, TX), R. C. HOGG (NASA, Washington, DC), and C. E. CAUDILL (U.S. Department of Agriculture, Washington, DC) In: International Geoscience and Remote Sensing Symposium, Washington, DC, June 8-10, 1981, Digest. Volume 2. New York, Institute of Electrical and Electronics Engineers, 1981, p. 1133-1153.

The results of the agriculture and resources inventory surveys through aerospace remote sensing (AgRISTARS) program managed by the USDA for exploring the use of satellite data for domestic and global commodity information needs are discussed. The program was intended to gather early warning of changes affecting production and quality of commodities and renewable resources, for predicting commodity production, land use classification and quantification, for inventories and assessments of renewable resources, land productivity measurements, assessment of conservation practices, and for pollution detection and impact evaluation. Up to 20 crop/region combinations in 7 countries were covered by the experiments, which comprised NOAA 6 and Landsat data analyses. Attempts to reduce variances through improved machine classification techniques are reported, together with soil moisture profiling, and the use of airborne sensors for providing comparative data. M.S.K.

A83-10096* Purdue Univ., Lafayette, Ind.
APPLICATION OF COMPUTER AXIAL TOMOGRAPHY /CAT/ TO MEASURING CROP CANOPY GEOMETRY
V. C. VANDERBILT and R. W. KILGORE (Purdue University, West Lafayette, IN) In: International Geoscience and Remote Sensing Symposium, Washington, DC, June 8-10, 1981, Digest. Volume 2. New York, Institute of Electrical and Electronics Engineers, 1981, p. 1162-1167. refs
(Contract NAS9-15466)
(Previously announced in STAR as N82-23600)

A83-10097
LANDSAT MONITORING OF DESERT LOCUST BREEDING GROUNDS IN AFRICA, THE NEAR EAST AND SOUTHWEST ASIA
J. U. HIELKEMA (United Nations, Food and Agriculture Organization, Rome, Italy) In: International Geoscience and Remote Sensing Symposium, Washington, DC, June 8-10, 1981, Digest. Volume 2. New York, Institute of Electrical and Electronics Engineers, 1981, p. 1168-1170.

A83-10106
REMOTE SENSING OF DIELECTRIC MEDIA WITH PERIODIC ROUGH SURFACES
S. L. CHUANG and J. A. KONG (MIT, Cambridge, MA) In: International Geoscience and Remote Sensing Symposium, Washington, DC, June 8-10, 1981, Digest. Volume 2. New York, Institute of Electrical and Electronics Engineers, 1981, p. 1274-1279. Research supported by the Charles C. Draper Laboratory, Inc refs
(Contract F19628-80-C-0052; NSF ENG-78-23145)

A method is developed to study the scattering of electromagnetic waves from periodic rough surfaces of dielectric media in order to improve the theory of the microwave remote sensing of plowed vegetation fields with row structures. The results of the theoretical investigation are also compared with experimental data obtained at optical frequencies, and they are found to be in excellent agreement. It is concluded that these results explain the serious discrepancies that existed in previous examinations of theory and experiment where only a perfect conductor model was used. N.B.

A83-10107* Kansas Univ. Center for Research, Inc., Lawrence.
A BACKSCATTER MODEL FOR A RANDOMLY PERTURBED PERIODIC SURFACE
F. T. ULABY, F. KOUYATE, and A. K. FUNG (University of Kansas Center for Research, Inc., Lawrence, KS) In: International Geoscience and Remote Sensing Symposium, Washington, DC, June 8-10, 1981, Digest. Volume 2. New York, Institute of Electrical and Electronics Engineers, 1981, p. 1280-1293. refs
(Contract NAG5-30)

A backscatter model for a randomly perturbed periodic surface has been developed to explain backscatter measurements from a bare soil surface with row structure. It is assumed that the row-direction effect can be included by integrating the scattering coefficient due to the random roughness component over the underlying periodic component of the soil surface. It is found that the row-direction effect is strongly dependent upon the rate of change of this scattering coefficient with the local angle, and that the maximum difference between looking parallel and perpendicular to the row direction occurs around an incidence angle whose tangent is equal to the slope of the periodic surface at the inflection point. (Author)

A83-10108* National Aeronautics and Space Administration. Lyndon B. Johnson Space Center, Houston, Tex.
A PARAMETRIC STUDY OF TILLAGE EFFECTS ON RADAR BACKSCATTER
R. G. FENNER, G. F. PELS (NASA, Johnson Space Center, Experiment Systems Div., Houston, TX), and S. C. REID (Lockheed Engineering and Management Services Co., Inc., Houston, TX) In: International Geoscience and Remote Sensing Symposium, Washington, DC, June 8-10, 1981, Digest. Volume 2. New York, Institute of Electrical and Electronics Engineers, 1981, p. 1294-1308. refs

An experiment was conducted to study the effects of tillage and row spacing on radar backscatter without the variables of moisture and vegetation. To accomplish this objective, a test site was selected in an area characterized by minimal rainfall and sparse vegetation, and simulation rows were plowed on two adjacent 762 x 152.4 m plots, across the 762-m dimension on one plot and along the 762-m dimension on the other plot. It is found that row direction is a significant contributor to radar linearly polarized backscatter from cropland and must be considered when making radar measurements over bare or sparsely vegetated fields. Although the effect decreases with increasing frequency, it is still large (5 dB) at 13.3 13.3 GHz. It is also found that row effects may not exist in cross-polarized radar returns, in which case further measurements with an improved scatterometer system (30-35 dB cross-polarization isolation) are needed. V.L.

A83-10109
PERFORMANCE ASSESSMENT OF FUTURE EUROPEAN REMOTE SENSING SYSTEMS
J. BODECHTEL (Zentralstelle fuer Geo- Photogrammetrie und Fernerkundung, Munich, West Germany) In: International Geoscience and Remote Sensing Symposium, Washington, DC, June 8-10, 1981, Digest. Volume 2. New York, Institute of Electrical and Electronics Engineers, 1981, p. 1309-1314B. refs

A study has been carried out to investigate the possibility of detecting agricultural crops in Europe using spaceborne remote sensing means. For this purpose, a U.S. crop information model based on Landsat data was modified in accordance with European demands and used in the study. Data taken into consideration included real data from Landsat, Skylab, and other remote sensing missions as well as data obtained from simulations of future satellite platforms carried out on the basis of ground measurements. The main purpose of the investigation was to differentiate between wheat and other crops or vegetation types. Results are presented in the form of rms errors for the detectability of wheat for the existing and future remote sensing systems. V.L.

A83-10117* South Dakota State Univ., Brookings.
COMBINING LAND USE DATA ACQUIRED FROM LANDSAT WITH SOIL MAP DATA
F. C. WESTIN and T. M. BRANDNER (South Dakota State University, Brookings, SD) In: International Geoscience and Remote Sensing Symposium, Washington, DC, June 8-10, 1981, Digest. Volume 2. New York, Institute of Electrical and Electronics Engineers, 1981, p. 1413-1424. Research supported by South Dakota State University; U.S. Department of Agriculture refs
(Contract USDA-53-3148-200; NAS1-5345)

A method currently used to derive agrophysical units (APUs), i.e., geographical areas having definable/comparable agronomic and physical parameters which reflect a range in agricultural use and management, is discussed with reference to results obtained for South Dakota and an area in China. The method consists of combining agricultural land use data acquired from Landsat with soil map data. The resulting map units are soil associations characterized by cropland use intensity, and they can be used to identify major cropland areas and to develop a rating reflecting the relative potential of the soils in the delineated area for crop production, as well as to update small-scale soil maps. V.L.

A83-10118* National Aeronautics and Space Administration. Earth Resources Labs., Bay St. Louis, Miss.
SOIL SPECTRAL CHARACTERIZATION
E. R. STONER (NASA, National Space Technology Laboratories, Earth Resources Laboratory, Bay St. Louis, MS) and M. F. BAUMGARDNER (Purdue University, West Lafayette, IN) In: International Geoscience and Remote Sensing Symposium, Washington, DC, June 8-10, 1981, Digest. Volume 2. New York, Institute of Electrical and Electronics Engineers, 1981, p. 1426-1436. refs

The spectral characterization of soils is discussed with particular reference to the bidirectional reflectance factor as a quantitative measure of soil spectral properties, the role of soil color, soil parameters affecting soil reflectance, and field characteristics of soil reflectance. Comparisons between laboratory-measured soil spectra and Landsat MSS data have shown good agreement, especially in discriminating relative drainage conditions and organic matter levels in unvegetated soils. The capacity to measure both visible and infrared soil reflectance provides information on other soil characteristics and makes it possible to predict soil response to different management conditions. Field and laboratory soil spectral characterization helps define the extent to which intrinsic spectral information is available from soils as a consequence of their composition and field characteristics. V.L.

A83-10119
ANALYZING AND MAPPING REGIONAL LAND USE TRENDS BY COMBINING LANDSAT AND TOPOGRAPHIC DATA
H. P. FOOTE, S. C. BLAIR, G. W. WUKELIC, V. L. COBURN (Pacific Northwest Laboratory, Richland, WA), and L. S. LEONHART (Rockwell Hanford Operations, Richland, WA) In: International Geoscience and Remote Sensing Symposium, Washington, DC, June 8-10, 1981, Digest. Volume 2. New York, Institute of Electrical and Electronics Engineers, 1981, p. 1437-1442.

Digital Landsat data and U-2 aerial photography for the Columbia Plateau region of eastern Washington and Oregon have been analyzed in order to estimate the amount of growth in irrigated cropland between 1975 and 1979. The classified scenes were registered with a stereographic map projection using USGS digital terrain data files and merged into one file. Irrigated cropland, water, and other land cover classes within this file were edited to conform with U-2 aerial photographs and Landsat color composite prints from 1975 and 1979. Land use data derived from 1975 Landsat imagery were registered to the same map projection and, a map displaying irrigated cropland in 1979 and growth of irrigated cropland between 1975 and 1979 was produced using the discrete table lookup method. The total irrigated cropland for 1979 was found to be 4281 square miles, which represents a 20% increase over 1975 with an accuracy of 90%. The amount and location of the new irrigated cropland provides essential input into ongoing ground water studies for this region. (Author)

A83-10717
SATELLITE ORBITAL DYNAMICS AND OBSERVATION STRATEGIES IN SUPPORT OF AGRICULTURAL APPLICATIONS
J. C. PRICE (U.S. Department of Agriculture, Hydrology Laboratory, Beltsville, MD) Photogrammetric Engineering and Remote Sensing, vol. 48, Oct. 1982, p. 1603-1611. refs

The operational satellites (GOES, NOAA) and the proto-operational satellite (Landsat) acquire data suitable for agricultural applications representing a wide range of coverage frequencies and spatial resolution. The geosynchronous (GOES) satellites provide highly repetitive low spatial resolution data appropriate for monitoring atmospheric variability, the Landsats provide infrequent (80 m)-squared spatial resolution data appropriate for detailed study of vegetation and surface characteristics, and the NOAA series (especially the instrument Advanced Very High Resolution Radiometer - AVHRR) represent an intermediate observing regime. A discussion of satellite orbital characteristics in the context of agricultural applications suggests advantages to placing both the AVHRR and a high resolution imager (e.g., Multispectral Scanner of Landsat) on an early

afternoon satellite having the capability for in-flight orbit maintenance. (Author)

A83-12315*# Arizona Univ., Tucson.
ATMOSPHERIC EFFECTS ON RADIATION REFLECTED FROM SOIL AND VEGETATION AS MEASURED BY ORBITAL SENSORS USING VARIOUS SCANNING DIRECTIONS
P. N. SLATER (Arizona, University, Tucson, AZ) and R. D. JACKSON (U.S. Department of Agriculture, Water Conservation Laboratory, Phoenix, AZ) Applied Optics, vol. 21, Nov. 1, 1982, p. 3923-3931. Research supported by the U.S. Geological Survey; U.S. Department of Agriculture refs
(Contract USDA-12-14-5001-38; NAG5-196)

Ground-measured spectral reflectance data for Avondale loam and drought-stressed and unstressed wheat were converted into digital counts for spectral bands 5 and 7 of the Landsat Multispectral Scanner System (MSS). For dry loam, the differences between ratios of MSS bands 7-5 as determined from space and from ground level measurements were 2.3 percent for clear and 5.6 percent for turbid atmospheric conditions. By contrast, for wet loam the differences were 10.4 and 29.5 percent. It is found that atmospheric conditions may cause a delay of from 3 to 7 days in the discrimination between drought-stressed and unstressed wheat. For oblique angle observations the atmospheric modification of ground-measured reflectances increased with angle at a greater rate in the 0/180 deg azimuth than in the 90/270 deg azimuth. Implications of this result are discussed for oblique angle Systeme Probatoire d'Observation de la Terre (SPOT), Mapsat, future multispectral linear array system imagery, and wide-angle imagery collected from scanners in high-altitude aircraft. (Author)

A83-12603*# Colorado State Univ., Fort Collins.
REFLECTANCE OF A VEGETATION CANOPY USING THE ADDING METHOD
K. COOPER, J. A. SMITH (Colorado State University, Fort Collins, CO), and D. PITTS (NASA, Johnson Space Center, Earth Resources Branch, Houston, TX) Applied Optics, vol. 21, Nov. 15, 1982, p. 4112-4118. refs
(Contract NGT-06-002-800; DAAG29-79-C-0199)

A modified vegetation reflectance model based on the Adding method is presented as a means to measure the interaction of shortwave radiation within a vegetation canopy. The canopy is conceptualized with reflecting and transmitting leaf facets, with the leaf orientations described by a leaf slope distribution, thereby yielding scattering matrices for canopy layers. The model predictions, when compared with ground-truth measurements, show good agreement except at visible wavelengths, where overestimations are observed. Conditions under which the model satisfies the reciprocity theorem are defined. Extension of the model by including azimuth is indicated. M.S.K.

A83-12604*# National Aeronautics and Space Administration. Goddard Space Flight Center, Greenbelt, Md.
RADIATIVE TRANSFER MODEL FOR HETEROGENEOUS 3-D SCENES
D. S. KIMES and J. A. KIRCHNER (NASA, Goddard Space Flight Center, Earth Resources Branch, Greenbelt, MD) Applied Optics, vol. 21, Nov. 15, 1982, p. 4119-4129. refs

A general mathematical framework for simulating processes in heterogeneous 3-D scenes is presented. Specifically, a model was designed and coded for application to radiative transfers in vegetative scenes. The model is unique in that it predicts (1) the directional spectral reflectance factors as a function of the sensor's azimuth and zenith angles and the sensor's position above the canopy, (2) the spectral absorption as a function of location within the scene, and (3) the directional spectral radiance as a function of the sensor's location within the scene. The model was shown to follow known physical principles of radiative transfer. Initial verification of the model as applied to a soybean row crop showed that the simulated directional reflectance data corresponded relatively well in gross trends to the measured data. However, the model can be greatly improved by incorporating more sophisticated and realistic anisotropic scattering algorithms (Author)

A83-14121
ACTION PLAN FOR REMOTE SENSING APPLICATIONS FOR RICE PRODUCTION
A. DEEPAK, (ED.) (Institute for Atmospheric Optics and Remote Sensing, Hampton, VA) Hampton, VA, Spectrum Press, 1982. 34 p.
(IFAORS-207)

The use of remote sensing in research on water, crops, soil, plant pests and diseases, and modeling is discussed, and sensor and data management is addressed. Water-related parameters that need to be inventoried and monitored are given, as are sampling intervals for land cropping and water-related projection parameters. Water management needs are listed. Steps to establish crop environmental and crop production plans are described, and data needs are given for delineating areas of soils in which nutrient deficiency and toxicity problems occur. Recommendations for soil management in the next ten years are stated. Objectives and approaches for applying remote sensing toward developing models of the effects of environmental stress and cultural practices on crop growth are discussed. Rice diseases and pests which need remote sensing are listed, and the required measurements are stated. The types of observations that can be made from meteorological satellites, aircraft, and ground-based platforms are shown. C.D.

A83-14229#
SATELLITE REMOTE SENSING FOR DOMESTIC CROP REPORTING IN THE UNITED STATES AND CANADA - A LOOK TO THE FUTURE
R. A. RYERSON, R. J. BROWN (Canada Centre for Remote Sensing, Ottawa, Canada), and R. S. SIGMAN (U.S. Department of Agriculture, Economics and Statistics Service, Washington, DC) In: Canadian Symposium on Remote Sensing, 7th, Winnipeg, Canada, September 8-11, 1981, Proceedings. Ottawa, Canadian Aeronautics and Space Institute, 1982, p. 30-41. refs

A83-14231#
A PROCEDURE TO OVERLAY THEMATIC MAP AND DOMINION LAND SURVEY SYSTEM DATA TO GEOMETRICALLY-CORRECTED LANDSAT IMAGES AND ITS APPLICATION TO AGRICULTURAL LAND USE STUDIES IN WESTERN CANADA
R. STEFFENSON (Geostudio Consultants, Ltd., Ottawa, Canada), J. A. SHIELDS, A. R. MACK (Department of Agriculture, Land Resource Research Institute, Ottawa, Canada), and L. C. GOODFELLOW (Canada Centre for Remote Sensing, Ottawa, Canada) In: Canadian Symposium on Remote Sensing, 7th, Winnipeg, Canada, September 8-11, 1981, Proceedings. Ottawa, Canadian Aeronautics and Space Institute, 1982, p. 51-62. Research supported by the Department of Supply and Services and Department of Agriculture of Canada. refs

A83-14233#
APPLICATION OF LANDSAT IMAGERY TO FLOOD CONTROL AND MANAGEMENT OF AGRICULTURAL LAND - A CASE STUDY OF NORTHERN INDIA
K. S. MISRA (Manitoba, University, Winnipeg, Canada) In: Canadian Symposium on Remote Sensing, 7th, Winnipeg, Canada, September 8-11, 1981, Proceedings. Ottawa, Canadian Aeronautics and Space Institute, 1982, p. 67-73.

A83-14235#
VISUAL ANALYSIS OF 1:250,000 LANDSAT DATA FOR FORAGE ASSESSMENT DURING THE 1980 DROUGHT IN WESTERN MANITOBA
R. A. RYERSON (Canada Centre for Remote Sensing, Ottawa, Canada) and R. ARNASON (Cargill Grain Co., Winnipeg, Canada) In: Canadian Symposium on Remote Sensing, 7th, Winnipeg, Canada, September 8-11, 1981, Proceedings. Ottawa, Canadian Aeronautics and Space Institute, 1982, p. 83-87.

A83-14236#
VEGETATION CHANGE DETECTION IN AN AGRICULTURAL AREA - A SIMPLE APPROACH FOR USE WITH GEO-DATA BASE
R. YAZDANI, E. E. DERENYI (New Brunswick, University, Fredericton, Canada), and R. A. RYERSON (Canada Centre for Remote Sensing, Ottawa, Canada) In: Canadian Symposium on Remote Sensing, 7th, Winnipeg, Canada, September 8-11, 1981, Proceedings. Ottawa, Canadian Aeronautics and Space Institute, 1982, p. 88-92. Research supported by the Natural Sciences and Engineering Research Council. refs

A simple method was developed for monitoring changes in vegetation cover conditions and for classifying crop cover types into three classes: potatoes, grain and hay. Vegetation indices (VI) are computed for two key dates during the growing season according to the formula: VI = /(MSS7 - MSS5)/(MSS7 + MSS5)/ K, where the MSS numbers designate Landsat MSS bands and K is a scale factor. Differences between VI values for the two dates provide a Multi-Temporal Vegetation Index (MTVI), which is a good indicator of changes in the vegetation vigour. All computations can be performed in a general purpose computer. The method was successfully tested, using June and August, 1979 Landsat-2 MSS data, acquired over Grand Falls, NB. (Author)

A83-14240#
POTENTIALS OF LANDSAT-D AND SPOT-1 FOR CROP IDENTIFICATION IN THE MARITIMES
E. DERENYI and R. YAZDANI (New Brunswick, University, Fredericton, Canada) In: Canadian Symposium on Remote Sensing, 7th, Winnipeg, Canada, September 8-11, 1981, Proceedings. Ottawa, Canadian Aeronautics and Space Institute, 1982, p. 120-125.

An experiment was recently completed at U.N.B. to ascertain what improvements will the next generation of earth observation satellite sensors provide for the identification of agricultural crops and the delineation of farm fields in the Maritimes. Airborne MSS digital data, covering Grand Falls, NB and vicinity, was resampled to simulate Landsat-D TM and SPOT-1 HRV data for this purpose. Landsat-2 MSS data was also available. Each digital data set was geometrically corrected and registered to the U.T.M. grid. Supervised classification was then carried out on the CIAS for potato and grain and fields. The results indicated that Landsat-D and SPOT sensors will be able to identify crops grown in small, narrow, irregularly shaped fields, can differentiate between different variety of potatoes and can detect irregularities in the development of crops within fields, better than the current Landsat sensors. The Landsat-D simulated data gave marginally better classification accuracy compared to the SPOT data. (Author)

A83-14241#
LAND USE/LAND COVER MAPPING FROM ENHANCED LANDSAT IMAGERY OF THE EASTERN PROVINCES OF THE PEOPLE'S REPUBLIC OF CHINA
S. HATHOUT (Winnipeg, University, Winnipeg, Canada) and V. SMIL (Manitoba, University, Winnipeg, Canada) In: Canadian Symposium on Remote Sensing, 7th, Winnipeg, Canada, September 8-11, 1981, Proceedings. Ottawa, Canadian Aeronautics and Space Institute, 1982, p. 126-134. refs

The three eastern provinces, Jiangsu, Anhue and Zhejiang, are among the world's most intensively farmed areas, where field multicropping is augmented by animal production, cultivation of water plants and tree crops, and fish breeding. The objective of this study is to compile a Land use/Land cover map of east China with particular emphasis on the agricultural land from enhanced Landsat linagery by using the diazo and density slicing techniques. Because of the lack of ground truth, the authors depend on various other sources of published and unpublished information on these provinces. Area measurement results from constructed Landsat mosaic of the major land use; irrigated cropland and total farmland are very close to the published figures. This study has revealed the usefulness of Landsat imagery for detecting and plotting recently reclaimed land, irrigated cropland with two patterns of multicropping, non-irrigated land, hilly cropland, valley cropland, swamp cropland, and mixed range cropland. (Author)

A83-14244#
WATERFOWL HABITAT INVENTORY OF ALBERTA, SASKATCHEWAN AND MANITOBA BY REMOTE SENSING
T. BARNARD, R. J. MACFARLANE, T. NERAASEN (Ducks Unlimited /Canada/, Winnipeg, Canada), R. P. MROCZYNSKI (Purdue University, West Lafayette, IN), J. JACOBSEN, and R. SCHMIDT (Interdisciplinary Systems, Ltd., Winnipeg, Canada) In: Canadian Symposium on Remote Sensing, 7th, Winnipeg, Canada, September 8-11, 1981, Proceedings. Ottawa, Canadian Aeronautics and Space Institute, 1982, p. 150-158. refs

A waterfowl habitat inventory is described which reflects an attempt to map and describe wetlands across prairie, parkland and forest-edge regions of Manitoba, Saskatchewan, and Alberta using Landsat data. It is noted that wetlands that held water at the time of the Landsat overpass were consistently and accurately classified and were rarely confused with upland classes. However, wetlands that had gone dry because of drainage or evaporation could not be distinguished and therefore were not classified. The problem of dry wetlands was most pronounced in late scenes, mainly those imaged in August. C.R.

A83-14245#
OPTICAL CHARACTERISTICS OF ALBERTA RANGELAND AS RELATED TO REMOTE SENSING
F. J. AHERN, R. J. BROWN, K. P. B. THOMSON (Canada Centre for Remote Sensing, Ottawa, Canada), C. M. PEARCE (Calgary, University, Calgary, Alberta, Canada), G. FEDOSEJEVS (Intera Environmental Consultants, Ltd., Ottawa, Canada), and K. STAENZ (Zurich, Universitaet, Zurich, Switzerland) In: Canadian Symposium on Remote Sensing, 7th, Winnipeg, Canada, September 8-11, 1981, Proceedings. Ottawa, Canadian Aeronautics and Space Institute, 1982, p. 159-173. Research supported by Alberta Environment. refs

Attention is given to interband correlations, to the role of grass, forbs, shrubs, litter, carryover, and soil in determining the spectral reflectance of two rangeland types, and to the optical manifestation of soil moisture and plant moisture. Simulated thematic mapper imagery is also investigated. It is noted that the investigation has led to a greater understanding of the optical behavior of individual rangeland vegetation components throughout the growing season and has aided in interpreting Landsat images for a qualitative assessment of range conditions. It is found that a qualitative assessment of range conditions is difficult in the rough fescue prairie with green-red-infrared composite color imagery but shows promise with imagery that includes the mid-infrared region to be provided with the thematic mapper. C.R.

A83-14246#
THE USE OF R.B.V., COLOUR ADDITIVE VIEWER AND M.S.S. PRODUCTS IN THE BRITISH COLUMBIA FOREST INVENTORY DEPLETION MONITORING PROGRAM
R. V. QUENET, F. HEGYI, and J. NEMETH (Ministry of Forests, Victoria, British Columbia, Canada) In: Canadian Symposium on Remote Sensing, 7th, Winnipeg, Canada, September 8-11, 1981, Proceedings. Ottawa, Canadian Aeronautics and Space Institute, 1982, p. 174-177.

Since 1981, the British Columbia Ministry of Forests has engaged in complete annual updates of the provincial forest inventory to determine the extent and location of all logged areas and areas significantly disturbed by fire, insects, disease, windthrow, or other causes since the last inventory. The present paper considers the potential contributions of data sources other than conventional medium- and small-scale photography to the annual forest depletion updates. Operational procedures and results obtained are discussed for pilot studies conducted with satellite-borne return beam vidicon (RBV) imagery, temporally classified MSS imagery, and color additive viewer (CAV) imagery. It is concluded that both RBV and MSS data are well suited to the identification and delineation of forest depletion boundaries,

while CAV products are a useful and effective means for the quality control of depletion monitoring programs. A.L.W.

A83-14248#
ASSESSMENT OF SPRUCE BUDWORM DEFOLIATION USING DIGITAL AIRBORNE MSS DATA
D. G. LECKIE and F. A. GOUGEON (Canadian Forestry Service, Petawawa National Forestry Institute, Chalk River, Ontario, Canada) In: Canadian Symposium on Remote Sensing, 7th, Winnipeg, Canada, September 8-11, 1981, Proceedings. Ottawa, Canadian Aeronautics and Space Institute, 1982, p. 190-196. refs

A83-14249#
DIGITAL COLOUR ENHANCEMENT OF LANDSAT DATA FOR MAPPING VEGETATION OF BARRENGROUND CARIBOU WINTER RANGE IN NORTHERN MANITOBA
R. J. DIXON (Manitoba Remote Sensing Center, Winnipeg, Canada) and L. HORN (Department of Natural Resources, Wildlife Branch, Thompson, Manitoba, Canada) In: Canadian Symposium on Remote Sensing, 7th, Winnipeg, Canada, September 8-11, 1981, Proceedings. Ottawa, Canadian Aeronautics and Space Institute, 1982, p. 197-205. refs

A83-14252#
INTEGRATION OF LANDSAT IMAGERY INTO A PROGRAM FOR AERIAL SURVEYING OF DEER POPULATIONS IN ALBERTA
M. BOYD (Alberta Recreations and Parks, Research and Systems Branch, Edmonton, Canada), W. HALL, A. COOK (Alberta Fish and Wildlife, Edmonton, Canada), and G. LANGFORD (G. Langford Associates, Ltd., Edmonton, Alberta, Canada) In: Canadian Symposium on Remote Sensing, 7th, Winnipeg, Canada, September 8-11, 1981, Proceedings. Ottawa, Canadian Aeronautics and Space Institute, 1982, p. 222-227. refs

A83-14253#
LANDSAT-BASED FOREST MAPPING IN ONTARIO NORTH OF LATITUDE 52 DEG NORTH
S. PALA and A. JANO (Ontario Centre for Remote Sensing, Toronto, Canada) In: Canadian Symposium on Remote Sensing, 7th, Winnipeg, Canada, September 8-11, 1981, Proceedings. Ottawa, Canadian Aeronautics and Space Institute, 1982, p. 228-232. refs

The Ontario Centre for Remote Sensing (OCRS) has initiated an operational forest cover mapping program in Ontario north of latitude 52 deg N, based on the digital analysis of Landsat data and an innovative computerized map production technique. At present, only a reconnaissance inventory is required for this 400,000-sq km region. The OCRS program provides statistics on and maps of several major forest types and non-productive classes. The classification accuracy is highest for homogeneous areas, such as the dense, uniform forest cover types which represent most of the timber volume in this region. Although the Landsat-based method has inherent limitations, it can provide a reliable, low-cost inventory to serve as the basis for future detailed resource surveys. (Author)

A83-14254#
MULTITEMPORAL ANALYSIS OF LANDSAT DATA FOR FOREST CUTOVER MAPPING - A TRIAL OF TWO PROCEDURES
A. V. BANNER (Intertech Remote Sensing, Ltd., Ottawa, Canada) and T. LYNHAM (Canadian Forestry Service, Great Lakes Forest Research Centre, Saulte Sainte Marie, Ontario, Canada) In: Canadian Symposium on Remote Sensing, 7th, Winnipeg, Canada, September 8-11, 1981, Proceedings. Ottawa, Canadian Aeronautics and Space Institute, 1982, p. 233-240. refs

A trial was conducted to evaluate two procedures to map forest cutovers using Landsat data; a multitemporal band 5 overlay and a multitemporal vegetation index difference. The satellite data had been geometrically corrected using the Digital Image Correction System (DICS). Both techniques were applied using the Canada Centre for Remote Sensing Image Analysis System (CIAS). Results of this study indicate that the 'multitemporal band 5 overlay' technique shows great potential as a cutover monitoring technique. The procedure is effective for cutovers with a grass or regeneration cover as well as for those with bare soil. According to this trial, the 'multitemporal vegetation index difference' is impractical for delineation of cutover boundaries. The vegetation index indicates the presence of grass or other vegetation within cutovers. Clear-cuts with an ingrowth of vegetation appear uncut using this procedure. The two methods are discussed using Landsat data, photography taken concurrently with the second Landsat pass, and ground reference data. (Author)

A83-14255#
AERIAL SURVEY OF CROP LOSSES DUE TO GRASSHOPPERS /ORTHOPTERA - ACRIDIDAE/ IN SASKATCHEWAN
O. OLFERT (Department of Agriculture, Research Station, Saskatoon, Saskatchewan, Canada) In: Canadian Symposium on Remote Sensing, 7th, Winnipeg, Canada, September 8-11, 1981, Proceedings. Ottawa, Canadian Aeronautics and Space Institute, 1982, p. 241-246. refs

A83-14257#
THE APPLICATION OF REMOTE SENSING IN SOUTHERN ALBERTA'S MOUNTAIN PINE BEETLE MANAGEMENT
E. WINQUEST and J. V. BRINK (Department of Energy, Mines and Resources, Alberta Forest Service, Edmonton, Canada) In: Canadian Symposium on Remote Sensing, 7th, Winnipeg, Canada, September 8-11, 1981, Proceedings. Ottawa, Canadian Aeronautics and Space Institute, 1982, p. 265-268. refs

A83-14259#
PREDICTING FOREST LAND ATTRIBUTES FROM AERIAL PHOTO INTERPRETATION VARIABLES
F. C. MARTIN, JR. (Montana, University, Missoula, MT) and F. L. GERLACH (U.S. Department of Agriculture, Forest Service, Missoula, MT) In: Canadian Symposium on Remote Sensing, 7th, Winnipeg, Canada, September 8-11, 1981, Proceedings. Ottawa, Canadian Aeronautics and Space Institute, 1982, p. 278-285. Research supported by the U.S. Department of Agriculture. refs

High-altitude panchromatic photography has been applied to the prediction of forest and land attributes in two areas of Montana. The technique utilizes photointerpretation variables consisting of five landform characteristics, five vegetation characteristics, and one combination variable: a land and overstory modifier. Each unit was then classified according to eleven photointerpretation variables. Prediction equations were formulated using multiple linear regression and dummy variables. Discriminant analysis predicted habitat and forest types. The mapping system utilized the digital terrain information system and the RID-POLY technique developed by Russell et al., 1975. S.C.S.

A83-14261#
LANDSAT FOR DELINEATION AND MAPPING OF SALINE SOILS IN DRYLAND AREAS IN SOUTHERN ALBERTA
M. D. THOMPSON (Intera Environmental Consultants, Ltd., Calgary, Alberta, Canada), N. A. PROUT (Intera Environmental Consultants, Ltd., Ottawa, Canada), and T. G. SOMMERFELDT (Department of Agriculture, Lethbridge, Alberta, Canada) In: Canadian Symposium on Remote Sensing, 7th, Winnipeg, Canada, September 8-11, 1981, Proceedings. Ottawa, Canadian Aeronautics and Space Institute, 1982, p. 294-303. Department of Supply and Services refs
(Contract DSS-0S2-80-00026)

A83-14264#
PREDICTING PERMAFROST CONDITIONS WITH INFRARED SENSING TECHNIQUES
H. SCHREIER (British Columbia, University, Vancouver, Canada) and C. SELBY (Department of Agriculture, Land Resource Research Institute, Vancouver, Canada) In: Canadian Symposium on Remote Sensing, 7th, Winnipeg, Canada, September 8-11, 1981, Proceedings. Ottawa, Canadian Aeronautics and Space Institute, 1982, p. 323-330. Department of Supply and Services refs
(Contract DSS-O6SU-323-8050)

In order to investigate how the conditions and depth of the active layer can be predicted with IR remote sensing technology, the relationships between terrain, vegetation, permafrost, and surface temperature regimes were investigated using thermal IR imagery and color IR air photos in a 50 x 50 km test area in the Richardson Mountains of the Yukon Territory. Three out of five identified plant communities were found to indicate permafrost conditions which were significantly different from one another in terms of depth of active layer, moisture content in the active layer, and temperature at 20 cm depth. The vegetation distribution thus reflected the spatial pattern of the active layer. While the thermal data was found to be less reliable than the color IR data, when processed it was found to be of considerable use where nonindicator plants were present. C.D.

A83-14269#
OFFICE AUTOMATION IN RESOURCE-MANAGEMENT - THE FUTURE IS NOW
J. P. HESSION (Canada Centre for Remote Sensing, Ottawa, Canada) In: Canadian Symposium on Remote Sensing, 7th, Winnipeg, Canada, September 8-11, 1981, Proceedings. Ottawa, Canadian Aeronautics and Space Institute, 1982, p. 364-368. refs

During the summer of 1981, the Canada Center for Remote Sensing participated in a commercial Telidon project in southwestern Manitoba. In this project (called 'GRASSROOTS') CCRS provided thematic images showing agricultural land use derived from Landsat data for distribution in a network that included terminals installed in ag rep offices, crop insurance offices, grain elevator offices and in the homes of private farmers. Remote sensing information on estimated acreages of rapeseed and fallow fields were transmitted along with current weather maps and commodity prices. Early user experiences indicate that low cost Canadian videotex technology may be a feasible tool for disseminating text and graphic information to improve decision-making and productivity in the primary and resource industry sectors. (Author)

A83-14301
A SYSTEM FOR THE COMPLEX PROCESSING OF AERIAL AND SPACE DATA FOR AGRICULTURE [O SISTEME KOMPLEKSNOI OBRABOTKI AEROKOSMICHESKOI INFORMATSII DLIA SEL'SKOGO KHOZIAISTVA]
G. I. BELCHANSKII, G. G. ANDREEV, N. V. SAZONOV, and V. I. TORSHIN (Vsesoiuznyi Nauchno-Issledovatel'skii i Proektno-Tekhnologicheskii Institut Kibernetiki, Moscow, USSR) Issledovanie Zemli iz Kosmosa, Sept.-Oct. 1982, p. 5-11. In Russian.

The hardware and software requirements for a typical aerial- and space-data reduction system for agricultural applications are briefly discussed. Some practical results obtained during the use of such a system for processing images generated by the Fragment satellite-borne multispectral scanning system are reviewed. V.L.

A83-14306
REMOTE MEASUREMENT OF BIOMASS [DISTANTSIONNOE IZMERENIE FITOMASSY]
B. V. VINOGRADOV (Akademiia Nauk SSSR, Institut Okeanologii, Leningrad; Akademiia Nauk SSSR, Institut Evoliutsionnoi Morfologii i Ekologii Zhivotnykh, Moscow, USSR) Issledovanie Zemli iz Kosmosa, Sept.-Oct. 1982, p. 36-45. In Russian. refs

Generalized functions are presented for determining grass and shrub biomass on the basis of the luminance factor and optical density of photographic negatives in the red (0.6-0.7 micron) and near infrared (0.7-1.3 micron) spectral regions. The exponential nature of the remote indicators of biomass is discussed. A two-parameter method is developed for measuring the biomass on the basis of its optical characteristics with an accuracy to within 10%. V.L.

A83-14307
DETERMINATION OF FOREST FIRE SPREAD RATES FROM INFRARED PHOTOGRAPHS [IDENTIFIKATSIIA SKOROSTEI RASPROSTRANENIIA LESNYKH POZHAROV PO IKH INFRAKRASNYM SNIMKAM]
E. N. VALENDIK, G. A. DORRER, N. A. KALININA, A. I. SUKHININ, and B. A. KHREBTOV (Akademiia Nauk SSSR, Institut Lesa i Drevesiny; Sibirskii Tekhnologicheskii Institut, Krasnoyarsk, USSR) Issledovanie Zemli iz Kosmosa, Sept.-Oct. 1982, p. 46-53. In Russian. refs

Methods for estimating the spread rates of forest fires from a series of remote infrared images taken at given intervals of time are examined. Algorithms are presented which have been proven useful in interpreting infrared photographs of forest fires and which might be also useful in designing airborne instrumentation for similar applications. V.L.

A83-14310
DETERMINATION OF HUMUS IN SOIL ON THE BASIS OF SPECTRAL MEASUREMENTS [VOZMOZHNOSTI OPREDELENIIA GUMUSA V POCHVAKH PO DANNYM SPEKTRAL'NYKH IZMERENII]
P. P. FEDCHENKO (Vsesoiuznyi Nauchno-Issledovatel'skii Institut Sel'skokhoziaistvennoi Meteorologii, Obninsk, USSR) Issledovanie Zemli iz Kosmosa, Sept.-Oct. 1982, p. 72-79. In Russian. refs

A study has been carried out with a view to establishing a quantitative relationship between the color coordinates and the humus content of soils. With reference to comprehensive experimental data, it is demonstrated that remote monitoring of soil humus from aircraft is possible in principle. A regional map showing humus contents which has been derived from airborne spectral measurements is presented. V.L.

A83-14665* South Dakota State Univ., Brookings.
AERIAL THERMAL INFRARED CENSUS OF CANADA GEESE IN SOUTH DAKOTA
R. G. BEST, D. HAUSE, M. WEHDE (South Dakota State University, Brookings, SD), and R. FOWLER (South Dakota Department of Game, Fish and Parks, Pierre, SD) Photogrammetric Engineering and Remote Sensing, vol. 48, Dec. 1982, p. 1869-1877. Research supported by the South Dakota Department of Game, Fish and Parks refs
(Contract NGL-42-003-007)

A83-14666
A MULTISPECTRAL APPROACH TO REMOTE DETECTION OF DEER
M. M. TRIVEDI (Louisiana State University, Baton Rouge, LA), C. L. WYATT (Utah State University of Agriculture and Applied Science, Logan, UT), and D. R. ANDERSON (U.S. Fish and Wildlife Service Cooperative Wildlife Research Unit, Logan, UT) Photogrammetric Engineering and Remote Sensing, vol. 48, Dec. 1982, p. 1879-1889. Research supported by the U.S. Fish and Wildlife Service. refs

A83-14856
EFFECTS OF VEGETATION COVER ON THE RADAR SENSITIVITY TO SOIL MOISTURE
F. T. ULABY, A. ASLAM, and M. C. DOBSON (Kansas, University, Lawrence, KS) IEEE Transactions on Geoscience and Remote Sensing, vol. GE-20, Oct. 1982, p. 476-481. refs

Measurements of the backscattering coefficient, made for bare and vegetation-covered fields, are used in conjunction with a simple backscattering model to evaluate the effects of vegetation cover on the estimation accuracy of soil moisture when derived from radar observations. The results indicate that for soil moisture values

below 50% of field capacity, the backscatter contribution of the vegetation cover limits the radar's ability to predict soil moisture with an acceptable degree of accuracy. However, for moisture values in the range between 50 and 150% of field capacity, the measured backscattering coefficient is dominated by the soil contribution and the effects of vegetation cover become secondary in importance. It is estimated that in this upper soil moisture range, which is the primary range of interest in hydrology and agriculture, a radar soil moisture prediction algorithm would predict soil moisture with an error of less than 15% of field capacity in 90% of the cases. (Author)

A83-14859
A BACKSCATTER MODEL FOR A RANDOMLY PERTURBED PERIODIC SURFACE
F. T. ULABY, F. KOUYATE, A. K. FUNG (University of Kansas Center for Research, Inc., Remote Sensing Laboratory, Lawrence, KS), and A. J. SIEBER (Deutsche Forschungs- und Versuchsanstalt fuer Luft- und Raumfahrt, Institut fuer Hochfrequenztechnik, Oberpfaffenhofen, West Germany) IEEE Transactions on Geoscience and Remote Sensing, vol. GE-20, Oct. 1982, p. 518-528. refs

A backscatter model for a randomly perturbed periodic surface has been developed to explain backscatter measurements from a bare soil surface with row structure. It is assumed that the row-direction effect can be included by integrating the scattering coefficient due to the random roughness component over the underlying periodic component of the soil surface. It is found that the row-direction effect is strongly dependent upon the rate-of-change of the scattering coefficient with the local angle and that for sinusoidal surfaces, the maximum difference between looking parallel and perpendicular to the row direction occurs around an incidence angle whose tangent is usually smaller than the slope of the periodic surface at the inflection point. (Author)

A83-15889
REMOTE DETERMINATION OF HUMUS CONTENT IN SOILS [DISTANTSIONNOE OPREDELENIE SODERZHANIIA GUMUSA V POCHVAKH]
K. IA. KONDRATEV and P. P. FEDCHENKO Akademiia Nauk SSSR, Doklady, vol. 266, no. 6, 1982, p. 1477-1479. In Russian.

A procedure for constructing a calibration curve for the determination of humus content in soils on the basis of aerial measurements is described. This procedure was used in compiling a 1:1,500,00 scale soil-humus maps of the Ukraine and Moldavia. A portion of this map for the Kiev region is presented here. It is concluded that there exists a relationship between the humus content in soil and soil color coordinates. Aerial measurements of spectral brightness coefficients can be used to make a quantitative determination of humus content in soils. B.J.

A83-16907
REFLECTANCE MEASUREMENT OF ARTIFICIALLY INDUCED ULTRAVIOLET RADIATION STRESS ON COTTON LEAVES
H. W. GAUSMAN (U.S. Department of Agriculture, Agricultural Research Service, Lubbock, TX) and D. E. ESCOBAR (U.S. Department of Agriculture, Agricultural Research Service, Weslaco, TX) Remote Sensing of Environment, vol. 12, Dec. 1982, p. 485-490. refs

A83-16908
POLARIZED VISIBLE LIGHT AS AN AID TO VEGETATION CLASSIFICATION
P. J. CURRAN (Sheffield, University, Sheffield, England) Remote Sensing of Environment, vol. 12, Dec. 1982, p. 491-499. Natural Environment Research Council refs
(Contract NERC-GR/3/4076)

Radiation which is reflected from the earth's surface can be described in terms of radiance and its polarization. However, in connection with remote sensing applications, only radiation measurements were generally performed. It has been found that the degree to which light is linearly polarized is negatively correlated with surface roughness and, to a lesser extent, radiance. Polarized visible light has been used by researchers as a measure of surface roughness, to distinguish between dry, rough soils and smooth wet soils. NASA has now recognized the importance of polarization data, and included polarization filters on the Multispectral Resource Sampler (MRS), which is a satellite-borne pushbroom scanner that may be launched in the mid-1980s. The present investigation is concerned with the utility of aerial measurements of percent reflected visible light (percent RVL) and percent polarized visible light (percent PVL) for the discrimination of land cover types in an area of seminatural vegetation. G.R.

A83-16909
REFLECTANCE DIFFERENCES BETWEEN UNTREATED AND MEPIQUAT CHLORIDE-TREATED, FIELD-GROWN COTTON THROUGH A GROWING SEASON
A. J. RICHARDSON and H. W. GAUSMAN (U.S. Department of Agriculture, Agricultural Research Service, Weslaco, TX) Remote Sensing of Environment, vol. 12, Dec. 1982, p. 501-507. refs

A83-16910* National Aeronautics and Space Administration. Lyndon B. Johnson Space Center, Houston, Tex.
THE USE OF LARGE-AREA SPECTRAL DATA IN WHEAT YIELD ESTIMATION
T. L. BARNETT and D. R. THOMPSON (NASA, Johnson Space Center, Houston, TX) Remote Sensing of Environment, vol. 12, Dec. 1982, p. 509-518. refs

Large-area relations between satellite spectral data and end-of-season crop yield were investigated. Green Index Number (GIN) values from Landsat MSS data of sample segments throughout the U.S. Great Plains winter wheat belt in 1978 were correlated to county USDA-SRS reported yields. A linear relation between GIN and yield appeared to exist up to GIN values of 40 or 50, covering cases of severe to moderate stress. In a test on 1978 Texas winter wheat at the county level, GIN values for sample segments in the counties were used in conjunction with an agronomic-meteorological yield model. The combined fit explained significantly more of the observed yield variation at the county level than the agromet model alone. (Author)

N83-12482*# Agricultural Research Service, Pullman, Wash.
INFLUENCE OF ENVIRONMENTAL FACTORS DURING SEED DEVELOPMENT AND AFTER FULL-RIPENESS ON PRE-HARVEST SPROUTING IN WHEAT
A. J. CIHA, H. MURRAY (Washington State Univ., Pullman), M. G. HAGEMANN (Washington State Univ., Pullman), and W. A. GOLDSTEIN, Principal Investigators Jun. 1982 43 p refs Sponsored by NASA, USDA, Dept. of Commerce, Dept. of the Interior, and Agency for International Development ERTS (Contract PROJ. AGRISTARS)
(E83-10002; NASA-CR-169493; EW-U2-04319; JSC-18254; NAS 1.26:169493) Avail: NTIS HC A03/MF A01 CSCL 02C

Results on environmental and genotypic factors influencing preharvest sprouting of wheat are summarized. Other possible areas where additional research is needed is suggested. A.R.H.

N83-12483*# Missouri Univ., Columbia.
SECOND GENERATION CROP YIELD MODELS REVIEW
T. HODGES, Principal Investigator Mar. 1982 37 p refs Prepared in cooperation with Dept. of Agriculture, Columbia, Mo. Sponsored by NASA, USDA, Dept. of Commerce, Dept. of the Interior, and Agency for International Development ERTS (Contract PROJ. AGRISTARS)
(E83-10003; NASA-CR-169492; YM-12-04306; JSC-18245)
Avail: NTIS HC A03/MF A01 CSCL 02C

Second generation yield models, including crop growth simulation models and plant process models, may be suitable for large area crop yield forecasting in the yield model development project. Subjective and objective criteria for model selection are defined and models which might be selected are reviewed. Models may be selected to provide submodels as input to other models; for further development and testing; or for immediate testing as forecasting tools. A plant process model may range in complexity from several dozen submodels simulating (1) energy,

carbohydrates, and minerals; (2) change in biomass of various organs; and (3) initiation and development of plant organs, to a few submodels simulating key physiological processes. The most complex models cannot be used directly in large area forecasting but may provide submodels which can be simplified for inclusion into simpler plant process models. Both published and unpublished models which may be used for development or testing are reviewed. Several other models, currently under development, may become available at a later date. Author

N83-12484*# Purdue Univ., Lafayette, Ind. Lab. for Applications of Remote Sensing.
PERFORMANCE COMPARISON FOR BARNES MODEL 12-1000, EXOTECH MODEL 100, AND IDEAS INC. BIOMETER MARK 2
B. ROBINSON, Principal Investigator 22 Apr. 1981 32 p Sponsored by NASA, USDA, Dept. of Commerce, Dept. of the Interior, and Agency for International Development ERTS
(Contract NAS9-15466; PROJ. AGRISTARS)
(E83-10004; NASA-CR-167646; SR-P1-04090; NAS 1.26:167646)
Avail: NTIS HC A03/MF A01 CSCL 02C

Results of tests show that all channels of all instruments, except channel 3 of the Biometer Mark 2, were stable in response to input signals were linear, and were adequately stable in response to temperature changes. The Biometer Mark 2 is labelled with an inappropriate description of the units measured and the dynamic range is a inappropriate for field measurements causing unnecessarily high fractional errors. This instrument is, therefore, quantization limited. The dynamic range and noise performance of the Model 12-1000 are appropriate for remote sensing field research. The field of view and performance of the Model 100A and the Model 12-1000 are satisfactory. The Biometer Mark 2 has not, as yet, been satisfactorily equipped with an acceptable field of view determining device. Neither the widely used aperture plate nor the 24 deg cone are acceptable. A.R.H.

N83-12485*# Kansas Univ. Center for Research, Inc., Lawrence. Remote Sensing Lab.
A THREE-PART GEOMETRIC MODEL TO PREDICT THE RADAR BACKSCATTER FROM WHEAT, CORN, AND SORGHUM
F. T. ULABY, Principal Investigator, G. W. EGER, III, and E. T. KANEMASU Apr. 1982 211 p refs Sponsored by NASA, USDA, Dept. of Commerce, Dept. of the Interior, and Agency for International Development ERTS
(Contract NAS9-15421; PROJ. AGRISTARS)
(E83-10005; NASA-CR-167713; SR-K2-04313; RSL-TR-360-18)
Avail: NTIS HC A10/MF A01 CSCL 02C

A model to predict the radar backscattering coefficient from crops must include the geometry of the canopy. Radar and ground-truth data taken on wheat in 1979 indicate that the model must include contributions from the leaves, from the wheat head, and from the soil moisture. For sorghum and corn, radar and ground-truth data obtained in 1979 and 1980 support the necessity of a soil moisture term and a leaf water term. The Leaf Area Index (LAI) is an appropriate input for the leaf contribution to the radar response for wheat and sorghum, however the LAI generates less accurate values for the backscattering coefficient for corn. Also, the data for corn and sorghum illustrate the importance of the water contained in the stalks in estimating the radar response. Author

N83-12486*# National Aeronautics and Space Administration. Lyndon B. Johnson Space Center, Houston, Tex.
AGRISTARS. SEMIANNUAL PROGRAM REVIEW PRESENTATION TO LEVEL 1, INTERAGENCY COORDINATION COMMITTEE
15 Apr. 1982 104 p Sponsored by NASA, USDA, Dept. of Commerce, Dept. of the Interior, and Agency for International Development ERTS
(Contract PROJ. AGRISTARS)
(E83-10006; NASA-TM-84878; ITJ2-04267; JSC-17830; NAS 1.15:84878) Avail: NTIS HC A06/MF A01 CSCL 02C

Results are presented for (1) spring small grains; (2) summer crops/corn and soybeans; and (3) crop signature characterization. The development of an early season approach, profile and segment based change estimation, and future satellite and sensor system requirements are discussed. Documentation for the inventory technology development project is included. A.R.H.

N83-12487*# Lockheed Engineering and Management Services Co., Inc., Houston, Tex.
EVALUATION OF SMALL AREA CROP ESTIMATION TECHNIQUES USING LANDSAT- AND GROUND-DERIVED DATA Final Report, 1980 - 1981
M. L. AMIS, M. V. MARTIN, W. G. MCGUIRE, and S. S. SHEN, Principal Investigators Aug. 1982 146 p refs Sponsored by NASA, USDA, Dept. of Commerce, Dept. of the Interior, and Agency for International Development ERTS
(Contract NAS9-15800)
(E83-10008; NASA-CR-167752; DC-L2-04264; JSC-17829; NAS 1.26:167752; LEMSCO-17597) Avail: NTIS HC A07/MF A01 CSCL 02C

Studies completed in fiscal year 1981 in support of the clustering/classification and preprocessing activities of the Domestic Crops and Land Cover project. The theme throughout the study was the improvement of subanalysis district (usually county level) crop hectarage estimates, as reflected in the following three objectives: (1) to evaluate the current U.S. Department of Agriculture Statistical Reporting Service regression approach to crop area estimation as applied to the problem of obtaining subanalysis district estimates; (2) to develop and test alternative approaches to subanalysis district estimation; and (3) to develop and test preprocessing techniques for use in improving subanalysis district estimates. Author

N83-12488*# Agricultural Research Service, Phoenix, Ariz. Water Conservation Lab.
DISCRIMINATION OF GROWTH AND WATER STRESS IN WHEAT BY VARIOUS VEGETATION INDICES THROUGH A CLEAR A TURBID ATMOSPHERE
R. D. JACKSON, P. M. SLATER, and P. J. PINTER, Principal Investigators May 1982 44 p refs Sponsored by NASA, USDA, Dept. of Commerce, Dept. of the Interior, and Agency for International Development ERTS
(Contract PROJ. AGRISTARS)
(E83-10009; NASA-CR-169491; EW-U2-04298; JSC-18241; NAS 1.26:169491) Avail: NTIS HC A03/MF A01 CSCL 02C

Reflectance data were obtained over a drought-stressed and a well-watered wheat plot with a hand-held radiometer having bands similar to the MSS bands of the LANDSAT satellites. Data for 48 clear days were interpolated to yield reflectance values for each day of the growing season, from planting until harvest. With an atmospheric path radiance model and LANDSAT-2 calibration data, the reflectance were used to simulate LANDSAT digital counts (not quantized) for the four LANDSAT bands for each day of the growing season, through a clear (approximately 100 km meteorological range) and a turbid (approximately 10 km meteorological range) atmosphere. Several ratios and linear combinations of bands were calculated using the simulated data, then assessed for their relative ability to discriminate vegetative growth and plant stress through the two atmospheres. The results show that water stress was not detected by any of the indices until after growth was retarded, and the sensitivity of the various indices to vegetation depended on plant growth stage and atmospheric path radiance. Author

N83-12489*# Department of Agriculture, Houston, Tex.
OPTICAL PARAMETERS OF LEAVES OF SEVEN WEED SPECIES
H. W. GAUSMAN, R. M. MENGES, A. J. RICHARDSON, H. WALTER, R. R. RODRIGUEZ, and S. TAMEZ, Principal Investigators Jun. 1982 9 p refs Sponsored by NASA, USDA, Dept. of Commerce, Dept. of the Interior, and Agency for International Development ERTS
(Contract PROJ. AGRISTARS)
(E83-10010; NASA-CR-169490; EW-U2-04328; JSC-18259; NAS 1.26:169490) Avail: NTIS HC A02/MF A01 CSCL 02C

The absorption coefficient (k), infinite reflectance (R), and scattering coefficient (s) were tabulated for five wavelengths and analyzed for statistical differences for seven weed species. The wavelengths were: 0.55-micrometer, 0.65-micrometers, 0.85-micrometer, 1.65-micrometers, and 2.20-micrometer. The R of common lambsquarters (Chenopodium album L.), Johnsongrass (Sorghum halepense (L.) Pers.), and annual sowthistle (Sonchus oleraceus L.) leaves at the 0.85-micrometer wavelength were significantly ($p=0.05$) higher than for sunflower (Heliantus annus L.), ragweed parthenium (Parthenium hysterophorus L.), or London rocket (Sisymbrium irio L.). Annual sowthistle had the largest k value, and Plamer amaranth (Amaranthus palmer S. Wats.) had the smallest k value at the 0.65 approximately chlorophyll absorption wavelength. In general, john-songress, ragweed parthenium, or London rocket had the largest s values among the five wavelengths, wereas annual sowthistle and plamar amaranth were usually lowest. Author

N83-12491*# Arkansas Univ., Fayetteville. Dept. of Electrical Engineering.
MEASUREMENT OF SOIL MOISTURE USING REMOTE SENSING MULTISENSOR RADIATION TECHNIQUES Final Report
W. P. WAITE, Principal Investigator May 1982 12 p Sponsored by NASA, USDA, Dept. of Commerce, Dept. of the Interior, and Agency for International Development ERTS
(Contract NAS9-14251; PROJ. AGRISTARS)
(E83-10012; NASA-CR-167648; SM-A2-04322; NAS 1.26:167648)
Avail: NTIS HC A02/MF A01 CSCL 02C

Theoretical modeling as well as laboratory and field measurement were coupled with analysis of aircraft data obtained from controlled sites in an effort to enhance understanding of the microwave response due to soil moisture so as to specify sensor parameters and develop inversion algorithms. Models to predict the complex dielectric constant were produced which led to the interpretation of the results in terms of a matrix potential rather than simply moisture content. Similar advances were made in the development of coherent and incoherent radiative transfer models and rough surface scattering models. A.R.H.

N83-12492*# Department of Agriculture, Sydney, Mont.
WINTER WHEAT STAND DENSITY DETERMINATION AND YIELD ESTIMATES FROM HANDHELD AND AIRBORNE SCANNERS
J. K. AASE, J. P. MILLARD, and F. H. SIDDOWAY, Principal Investigators Jun. 1982 20 p refs Sponsored by NASA, USDA, Dept. of Commerce, Dept. of the Interior, and Agency for International development Original contains imagery. Original photography may be purchased from the EROS Data Center, Sioux Falls, S.D. 57198 ERTS
(Contract PROJ. AGRISTARS)
(E83-10013; NASA-CR-169489; EW-U2-04327; JSC-18258)
Avail: NTIS HC A02/MF A01 CSCL 02C

Radiance measurments from handheld (Exotech 100-A) and air-borne (Daedalus DEI 1260) radiometers were related to wheat (Triticum aestivum L.) stand densities (simulated winter wheat winterkill) and to grain yield for a field located 11 km northwest of Sidney, Montana, on a Williams loam soil (fine-loamy, mixed Typic Argiborolls) where a semidwarf hard red spring wheat cultivar was needed to stand. Radiances were measured with the handheld radiometer on clear mornings throughout the growing season. Aircraft overflight measurements were made at the end of tillering and during the early stem extension period, and the mid-heading period. The IR/red ratio and normalized difference vegetation index were used in the analysis. The aircraft measurements corroborated the ground measurements inasmuch as wheat stand densities were detected and could be evaluated at an early enough growth stage to make management decision. The aircraft measurements also corroborated handheld measurements when related to yield prediction. The IR/red ratio, although there was some growth stage dependency, related well to yield when measured from just past tillering until about the watery-ripe stage. Author

N83-12493*# Lockheed Engineering and Management Services Co., Inc., Houston, Tex.
DEVELOPMENT OF A CORN AND SOYBEAN LABELING PROCEDURE FOR USE WITH PROFILE PARAMETER CLASSIFICATION
E. R. MAGNESS, Principal Investigator Jun. 1982 184 p refs Sponsored by NASA, USDA, Dept. of Commerce, Dept. of the Interior, and Agency for International Development ERTS
(Contract NAS9-15800; PROJ. AGRISTARS)
(E83-10014; NASA-CR-167720; SR-L2-00750; JSC-18257; NAS 1.26:167720; LEMSCO-17765) Avail: NTIS HC A09/MF A01 CSCL 02C

Some essential processes for the development of a green-number-based logic for identifying (labeling) crops in LANDSAT imagery are documented. The supporting data and subsequent conclusions that resulted from development of a specific labeling logic for corn and soybean crops in the United States are recorded. Author

N83-12494*# Texas A&M Univ., College Station. Dept. of Mathematics.
DEVELOPMENT OF ADVANCED ACREAGE ESTIMATION METHODS Final Report, 1 Nov. 1980 - 30 Jun. 1982
L. F. GUSEMAN, JR., Principal Investigator Jun. 1982 275 p refs Sponsored by NASA, USDA, Dept. of Commerce, Dept. of Interior, and Agency for International Development ERTS
(Contract NAS9-14689; PROJ. AGRISTARS)
(E83-10015; NASA-CR-167701; SR-T2-04371; NAS 1.26:167701)
Avail: NTIS HC A12/MF A01 CSCL 05B

The development of an accurate and efficient algorithm for analyzing the structure of MSS data, the application of the Akaiki information criterion to mixture models, and a research plan to delineate some of the technical issues and associated tasks in the area of rice scene radiation characterization are discussed. The AMOEBA clustering algorithm is refined and documented.

N83-12495*# Texas A&M Univ., College Station.
SYSTEM SUPPORT DOCUMENTATION: IDIMS FUNCTION AMOEBA Final Report
J. BRYANT *In its* Develop. of Advan. Acreage Estimation Methods 189 p Jun. 1982 ERTS
Avail: NTIS HC A12/MF A01 CSCL 05B

A listing is provided for AMOEBA, a clustering program based on a spatial-spectral model for image data. The program is fast and automatic (in the sense that no parameters are required), and classifies each picture element into classes which are determined internally. As an IDIMS function, no limit on the size of the image is imposed. Author

N83-12496*# Texas A&M Univ., College Station. Remote Sensing Center.
RICE SCENE RADIATION RESEARCH PLAN Final Report
J. HEILMAN *In its* Develop. of Advan. Acreage Estimation Methods 12 p Jun. 1982 ERTS
Avail: NTIS HC A12/MF A01 CSCL 05B

Data requirements, tasks to be accomplished, and the technical approaches to be used in identifying the characteristics of rice for crop inventories are listed as well as methods for estimating crop development and assessing its conditions. A.R.H.

N83-12497*# Houston Univ., Tex. Dept. of Mathematics.
THE POSSIBLE MODIFICATIONS OF THE HISSE MODEL FOR PURE LANDSAT AGRICULTURAL DATA
C. PETERS *In* Texas A and M Univ. Develop. of Advan. Acreage Estimation Methods 14 p Jun. 1982 refs ERTS
(Contract NAS9-14689)
Avail: NTIS HC A12/MF A01 CSCL 05B

An idea, due to A. Feiveson, is presented for relaxing the assumption of class conditional independence of LANDSAT spectral measurements within the same patch (field). Theoretical arguments are given which show that any significant refinement of the model beyond Feiveson's proposal will not allow the reduction, essential to HISSE, of the pure data to patch summary statistics. A slight alteration of the new model is shown to be a reasonable approximation to the model which describes pure data elements from the same patch as jointly Quassian with a covariance function which exhibits exponential decay with respect to spatial separation. Author

N83-12499*# Kansas Univ. Center for Research, Inc., Lawrence. Remote Sensing Lab.
DATA DOCUMENTATION FOR THE 1981 SUMMER VEGETATION EXPERIMENT Interim Report
F. T. ULABY, Principal Investigator, B. BRISCO, and C. ALLEN May 1982 117 p Sponsored by NASA, USDA, Dept. of Commerce, Dept. of the Interior, and Agency for International Development ERTS
(Contract NAS9-15421; PROJ. AGRISTARS)
(E83-10016; NASA-CR-167718; SR-K2-04336; NAS 1.26:167718)
Avail: NTIS HC A06/MF A01 CSCL 02C

The mobile agricultural radar sensor was used to collect data from 31 fields in the floodplain of the Kansas River east of Lawrence, Kansas during the summer of 1981. Corn, soybeans, and wheat crops were observed from May 1 to November 11. Radar backscattering measurements were acquired at 10.2 GHz for VV and VH polarizations at 50 deg incidence angles for all fields and at 30 deg, 40 deg, 50 deg, 60 deg, and 70 deg for nine of the 31 fields. Target parameters describing the vegatation and soil characteristics, such as plant moisture, plant height, soil moisture, etc., were also measured. The methodology, radar backscatter data and associated ground-truth data obtained during this experiment are documented. Author

N83-12500*# Environmental Research Inst. of Michigan, Ann Arbor. Infrared and Optics Div.
DEVELOPMENT, IMPLEMENTATION AND EVALUATION OF SATELLITE-AIDED AGRICULTURAL MONITORING SYSTEMS Semiannual Report
R. CICONE, E. P. CRIST, M. METZLER, and D. NUESCH Jun. 1982 58 p refs Sponsored by NASA, USDA, Dept. of Commerce, Dept. of the Interior, and Agency for International Development Original contains imagery. Original photography may be purchased from the EROS Data Center, Sioux Falls, S.D. 57198 ERTS
(Contract NAS9-16538; PROJ. AGRISTARS)
(E83-10017; NASA-CR-167702; IT-E2-04311; ERIM-160300-18-P)
Avail: NTIS HC A04/MF A01 CSCL 02C

Research activities in support of AgRISTARS Inventory Technology Development Project in the use of aerospace remote sensing for agricultural inventory described include: (1) corn and soybean crop spectral temporal signature characterization; (2) efficient area estimation techniques development; and (3) advanced satellite and sensor system definition. Studies include a statistical evaluation of the impact of cultural and environmental factors on crop spectral profiles, the development and evaluation of an automatic crop area estimation procedure, and the joint use of SEASAT-SAR and LANDSAT MSS for crop inventory. A.R.H.

N83-12501*# Environmental Research Inst. of Michigan, Ann Arbor. Infrared and Optics Div.
ANALYSIS OF THE PROFILE CHARACTERISTICS OF CORN AND SOYBEANS USING FIELD REFLECTANCE DATA Technical Report, 1 Jan. - 31 May 1982
E. P. CRIST Jun. 1982 52 p refs Sponsored by NASA, USDA, Dept. of Commerce, Dept. of the Interior, and Agency for International Development ERTS
(Contract NAS9-16538; PROJ. AGRISTARS)
(E83-10018; NASA-CR-167729; IT-E2-04310; NAS 1.26:167729; ERIM-160300-19-T) Avail: NTIS HC A04/MF A01 CSCL 02C

The typical patterns of spectral development (profiles) for corn and soybeans are presented, based on field-collected reflectance data transformed to correspond to LANDSAT-MSS Tasseled Cap coordinates. Reasonable variations in field conditions and cultural practices are shown to significantly influence profile features. The separability of the two crops is determined to be primarily related to the maximum value of the reflectance equivalent of Greenness, and to the plateau effect seen in corn Greenness profiles. The impact of changes in conditions on separability is described. In addition, association is made between profile features and stages of development for corn and soybeans. Corn is shown to peak at a stage well before tasseling or maximum LAI, while the characteristics of the soybean profile are shown to be unrelated to any particular stage of development. Author

N83-12502*# Lockheed Engineering and Management Services Co., Inc., Houston, Tex. Experiment Support Dept.
AGRISTARS DOCUMENTS TRACKING LIST REPORT
J. L. HAWKINS Jun. 1982 90 p Sponsored by NASA, USDA, Dept. of Commerce, Dept. of the Interior, and Agency for International Development ERTS
(Contract NAS9-15800; PROJ. AGRISTARS)
(E83-10019; NASA-CR-167728; AP-L2-04116; NAS 1.26:167728)
Avail: NTIS HC A05/MF A01 CSCL 05B

A quarterly listing of those documents and related publications that have been issued and placed in the AgRISTARS tracking system is presented. The Tracking List Report provides a catalog, by project, of technical publications arranged by type of document and gives the reference AgRISTARS document numbers, title and date of publication, the issuing organization, and the National Technical Information Service reference number. Author

N83-12503*# Kansas Univ. Center for Research, Inc., Lawrence. Remote Sensing Lab.
ASSESSMENT OF RADAR RESOLUTION REQUIREMENTS FOR SOIL MOISTURE ESTIMATION FROM SIMULATED SATELLITE IMAGERY
F. T. ULABY, Principal Investigator, M. C. DOBSON, and S. MOEZZI Aug. 1982 109 p refs Sponsored by NASA, USDA, Dept. of Commerce, Dept. of the Interior, and Agency for International Development Original contains imagery. Original photography may be purchased from the EROS Data Center, Sioux Falls, S.D. 57198 ERTS
(Contract NAS9-16419; PROJ. AGRISTARS)
(E83-10020; NASA-CR-167748; SM-K2-04356; NAS 1.26:167748; RSL-TR-551-2) Avail: NTIS HC A06/MF A01 CSCL 08M

Radar simulations were performed at five-day intervals over a twenty-day period and used to estimate soil moisture from a generalized algorithm requiring only received power and the mean elevation of a test site near Lawrence, Kansas. The results demonstrate that the soil moisture of about 90% of the 20-m by 20-m pixel elements can be predicted with an accuracy of + or - 20% of field capacity within relatively flat agricultural portions of the test site. Radar resolutions of 93 m by 100 m with 23 looks or coarser gave the best results, largely because of the effects of signal fading. For the distribution of land cover categories, soils, and elevation in the test site, very coarse radar resolutions of 1 km by 1 km and 2.6 km by 3.1 km gave the best results for wet moisture conditions while a finer resolution of 93 m by 100 m was found to yield superior results for dry to moist soil conditions. A.R.H.

N83-12504*# Purdue Univ., Lafayette, Ind. Lab. for Applications of Remote Sensing.
EXTENSION OF LABORATORY-MEASURED SOIL SPECTRA TO FIELD CONDITIONS
E. R. STONER, M. F. BAUMGARDNER, R. A. WEISMILLER, L. L. BIEHL, and B. F. ROBINSON Jun. 1982 7 p refs Repr. from Soil Sci. Soc. Am. J., v. 44, 1980 p 572-574 Sponsored by NASA, USDA, Dept. of Commerce, Dept. of the Interior, and Agency for International Development ERTS
(Contract NAS9-15466; PROJ. AGRISTARS)
(E83-10021; NASA-CR-167722; SR-P2-04326; LARS-052680)
Avail: NTIS HC A02/MF A01 CSCL 08M

Spectral responses of two glaciated soils, Chalmers silty clay loam and Fincastle silt loam, formed under prairie grass and forest vegetation, respectively, were measured in the laboratory under controlled moisture equilibria using an Exotech Model 20C spectroradiometer to obtain spectral data in the laboratory under artificial illumination. The same spectroradiometer was used outdoors under solar illumination to obtain spectral response from dry and moistened field plots with and without corn residue cover, representing the two different soils. Results indicate that laboratory-measured spectra of moist soil are directly proportional to the spectral response of that same field-measured moist bare soil over the 0.52 micrometer to 1.75 micrometer wavelength range. The magnitudes of difference in spectral response between identically treated Chalmers and Fincastle soils are greatest in the 0.6 micrometers to 0.8 micrometer transition region between the visible and near infrared, regardless of field condition or laboratory preparation studied. Author

N83-12505*# Texas A&M Univ., College Station. Inst. of Statistics.
MISSING OBSERVATIONS IN MULTIYEAR ROTATION SAMPLING DESIGNS
E. E. GBUR and R. L. SIELKEN, JR., Principal Investigators Jun. 1982 125 p Sponsored by NASA, USDA, Dept. of Commerce, Dept. of the Interior, and Agency for International Development ERTS
(Contract NAS9-14689; PROJ. AGRISTARS)
(E83-10022; NASA-CR-167700; IT-T2-04323) Avail: NTIS HC A06/MF A01 CSCL 02C

Because Multiyear estimation of at-harvest stratum crop proportions is more efficient than single year estimation, the behavior of multiyear estimators in the presence of missing acquisitions was studied. Only the (worst) case when a segment proportion cannot be estimated for the entire year is considered. The effect of these missing segments on the variance of the at-harvest stratum crop proportion estimator is considered when missing segments are not replaced, and when missing segments are replaced by segments not sampled in previous years. The principle recommendations are to replace missing segments according to some specified strategy, and to use a sequential procedure for selecting a sampling design; i.e., choose an optimal two year design and then, based on the observed two year design after segment losses have been taken into account, choose the best possible three year design having the observed two year parent design. Author

N83-12506*# Purdue Univ., Lafayette, Ind. Lab. for Applications of Remote Sensing.
REMOTE SENSING OF AGRICULTURAL CROPS AND SOILS Final Annual Technical Summary Report
M. E. BAUER, Principal Investigator May 1982 208 p Sponsored by NASA, USDA, Dept. of Commerce, Dept. of the Interior, and Agency for International Development Original contains imagery. Original photography may be purchased from the EROS Data Center, Sioux Falls, S.D. 57198 ERTS
(Contract NAS9-15466; PROJ. AGRISTARS)
(E83-10023; NASA-CR-167721; SR-P2-04266; NAS 1.26:167721; LARS-113081) Avail: NTIS HC A10/MF A01 CSCL 02C

Research results and accomplishments of sixteen tasks in the following areas are described: (1) corn and soybean scene radiation research; (2) soil moisture research; (3) sampling and aggregation research; (4) pattern recognition and image registration research; and (5) computer and data base services. Author

N83-13517 Iowa State Univ. of Science and Technology, Ames.
REMOTE SENSING OF LAND RESOURCES: APPLICATION OF LANDSAT SATELLITE IMAGERY Ph.D. Thesis
J. GOLCHIN 1982 197 p
Avail: Univ. Microfilms Order No. DA8221189

LANDSAT satellite images were used to study the major factors which affect water consumption by irrigation in west-central Iowa. These factors are soil moisture, area under irrigation, and crop types. Once the monitoring system of these factors is established, the amount of water withdrawn for upplementary irrigation can be estimated. The use of the microdensitometer and measurement of image reflectivity was emphasized in the soil moisture portion. The results indicated that there is a linear relation between the measured reflectivity from the LANDSAT image and the generalized surface oil moisture. Applying a simple manual interpretation method of black and white and false color composite prints and transparencies, both irrigated lands and crop types were identified. The main instrument used in this part was the Zoom Transfer Scope. The results for both experiments were promising and supported the methods of interpretation. Examination of the methods introduced in this study showed that the manual interpretation of LANDSAT imagery is a low-cost and easy approach to monitor the irrigated areas and the crop types. Dissert. Abstr.

N83-13519*# Instituto de Pesquisas Espaciais, Sao Jose dos Campos (Brazil).
USE OF LANDSAT IMAGES TO STUDY CERRADO VEGETATION [UTILIZACAO DE IMAGENS ORBITAIS DO SATELITE LANDSAT PARA ESTUDO DA VEGETACAO DE CERRADO]
N. D. J. PARADA, Principal Investigator and P. H. FILHO Aug. 1982 6 p refs In PORTUGUESE; ENGLISH summary Presented at the Congr. Nacional sobre Essencias Nativas, Campos do Jordao, 12-18 Sep. 1982 Sponsored by NASA ERTS
(E83-10025; NASA-CR-169498; NAS 1.26:169498; INPE-2526-PRE/195) Avail: NTIS HC A02/MF A01

Channel 5 and 7 LANDSAT imagery at the scale of 1:250,000 made during passes in the dry and rainy seasons were used to select the optimal season for cerrado characterization in Mato Grosso do Sul State. The study area is located around the cities of Campo Grande and Tres Lagoas, a region being used for reforestation and rangeland activities. Imagery acquired during the dry season permitted a good discrimination between 'cerrado' (woodsy pasture) vegetation and reforestation. In relation to the altered areas, only the recently modified area presented good discrimination of cerrado vegetation. Imagery of the rainy season did not provide a reasonable separation between cerrado and reforestation areas but the altered area could be easily discriminated. A.R.H.

N83-13529*# National Aeronautics and Space Administration. Lyndon B. Johnson Space Center, Houston, Tex.
DEVELOPMENT OF THEMATIC MAPPER VEGETATIVE INDICES FOR ASSESSING BIOMASS IN CORN, SOYBEANS AND WHEAT
B. R. GARDNER, D. R. THOMPSON, K. E. HENDERSON, and B. L. BLAD, Principal Investigators Aug. 1982 88 p refs Sponsored by NASA, USDA, Dept. of Commerce, Dept. of the Interior, and Agency for International Development ERTS
(Contract PROJ. AGRISTARS)
(E83-10035; NASA-TM-85170; SR-J2-04337; JSC-18264; NAS 1.15:85170) Avail: NTIS HC A05/MF A01 CSCL 02C

Spectral transformations that utilize thematic mapper (TM) bands were found to be highly related to various agronomic parameters such as leaf area index, percent ground cover, total fresh biomass, and plant moisture for corn, soybeans, and wheat. It was found that different spectral transformations are necessary in order to obtain the maximum predictability for each agronomic variable. The TM bands in the water absorption region (1.55 micrometers to 1.75 micrometer and 2.08 micrometer 2.35

micrometer) appear to provide information concerning the water condition of the canopy. Author

N83-13535*# National Oceanic and Atmospheric Administration, Columbia, Mo.
EVALUATION OF THE WILLIAMS-TYPE SPRING WHEAT MODEL IN NORTH DAKOTA AND MINNESOTA
S. LEDUC, Principal Investigator Jan. 1982 45 p refs Sponsored by NASA, USDA, Dept. of Commerce, Dept. of the Interior, and Agency for International Development ERTS
(Contract PROJ. AGRISTARS)
(E83-10041; NASA-CR-169549; YM-U2-04286; JSC-18233; NAS 1.26:169549; YM-1-4-4(80-01.1)) Avail: NTIS HC A03/MF A01 CSCL 02C

The Williams type model, developed similarly to previous models of C.V.D. Williams, uses monthly temperature and precipitation data as well as soil and topological variables to predict the yield of the spring wheat crop. The models are statistically developed using the regression technique. Eight model characteristics are examined in the evaluation of the model. Evaluation is at the crop reporting district level, the state level and for the entire region. A ten year bootstrap test was the basis of the statistical evaluation. The accuracy and current indication of modeled yield reliability could show improvement. There is great variability in the bias measured over the districts, but there is a slight overall positive bias. The model estimates for the east central crop reporting district in Minnesota are not accurate. The estimate of yield for 1974 were inaccurate for all of the models. Author

N83-13536*# Agricultural Research Service, Weslaco, Tex.
ESTIMATING TOTAL STANDING HERBACEOUS BIOMASS PRODUCTION WITH LANDSAT MSS DIGITAL DATA Progress Report
A. J. RICHARDSON, J. H. EVERITT, and C. L. WIEGAND, Principal Investigators Jun. 1982 26 p refs Sponsored by NASA, USDA, Dept. of Commerce, Dept. of the Interior, and Agency for International Development ERTS
(Contract PROJ. AGRISTARS)
(E83-10045; NASA-CR-169606; EW-U2-04320; JSC-18255; NAS 1.26:169606) Avail: NTIS HC A03/MF A01 CSCL 02C

Rangeland biomass data were correlated with spectral vegetation indices, derived from LANDSAT MSS data. LANDSAT data from five range and three other land use sites in Willacy and Cameron Counties were collected on October 17 and December 10, 1975, and on July 31 and September 23, 1976. The overall linear correlation of total standing herbaceous biomass with the LANDSAT derived perpendicular vegetation index was highly significant ($r = 0.90^{**}$) for these four dates. The standard error of estimate was 722 kg/ha. Biomass data were recorded for two of these range sites for 8 months (March through October) during the 1976 growing season. Standing green biomass accounted for most of the increase in herbage, starting in June and ending about September and October. These results indicate that satellite data may be useful for the estimation of total standing herbaceous biomass production that could aid range managers in assessing range condition and animal carrying capacities of large and inaccessible range holdings. Author

N83-14554*# National Aeronautics and Space Administration. Lyndon B. Johnson Space Center, Houston, Tex.
MONITORING GLOBAL VEGETATION
R. B. MACDONALD, A. G. HOUSTON, R. P. HEYDORN, D. B. BOTKIN, J. E. ESTES, and A. H. STRAHLR Jun. 1981 22 p refs Presented at the 7th Intern. Symp. on Machine Process. of Remotely Sensed Data, West Lafayette, Ind., 23-26 Jun. 1981 Sponsored by NASA, USDA, Dept. of Commerce, Dept. of the Interior, and Agency for International Development Prepared in cooperation with California Univ., Santa Barbara Original contains imagery. Original photography may be purchased from the EROS Data Center, Sioux Falls, S.D. 57198 ERTS
(Contract PROJ. AGRISTARS)
(E83-10044; NASA-TM-85166; SR-J2-04300; JSC-18242; NAS 1.15:85166) Avail: NTIS HC A02/MF A01 CSCL 02C

An attempt is made to identify the need for, and the current capability of, a technology which could aid in monitoring the Earth's vegetation resource on a global scale. Vegetation is one of our most critical natural resources, and accurate timely information on its current status and temporal dynamics is essential to understand many basic and applied environmental interrelationships which exist on the small but complex planet Earth. Author

N83-14557*# Texas A&M Univ., College Station. Remote Sensing Center.
INVESTIGATION OF REMOTE SENSING TECHNIQUES OF MEASURING SOIL MOISTURE Interim Report, 1 Mar. 1980 - 31 Jan. 1981
R. W. NEWTON, Principal Investigator, A. J. BLANCHARD, J. L. NIEBER, R. LASCANO, L. TSANG, and C. H. M. VANBAVEL Jan. 1981 51 p refs Sponsored by NASA, USDA, Dept. of Commerce, Dept. of the Interior, and Agency for International Development ERTS
(Contract NAG5-31; PROJ. AGRISTARS)
(E83-10048; NASA-CR-169564; SM-T2-04363; NAS 1.26:169564; RSC-4242-1) Avail: NTIS HC A04/MF A01 CSCL 02C

Major activities described include development and evaluation of theoretical models that describe both active and passive microwave sensing of soil moisture, the evaluation of these models for their applicability, the execution of a controlled field experiment during which passive microwave measurements were acquired to validate these models, and evaluation of previously acquired aircraft microwave measurements. The development of a root zone soil water and soil temperature profile model and the calibration and evaluation of gamma ray attenuation probes for measuring soil moisture profiles are considered. The analysis of spatial variability of soil information as related to remote sensing is discussed as well as the implementation of an instrumented field site for acquisition of soil moisture and meteorologic information for use in validating the soil water profile and soil temperature profile models. A.R.H.

N83-14558*# Agricultural Research Service, Weslaco, Tex. Remote Sensing Research Unit.
USE OF NEAR-INFRARED VIDEO RECORDING SYSTEM FOR THE DETECTION OF FREEZE DAMAGED CITRUS LEAVES
D. E. ESCOBAR, R. L. BOWEN, H. W. GAUSMAN, and G. COOPER, Principal Investigators Sep. 1982 12 p refs Sponsored by NASA, USDA, Dept. of Commerce, Dept. of the Interior, and Agency for International Development Original contains imagery. Original photography may be purchased from the EROS Data Center, Sioux Falls, S.D. 57198 ERTS
(Contract PROJ. AGRISTARS)
(E83-10049; NASA-CR-169565; EW-U2-04351; JSC-18563; NAS 1.26:169565) Avail: NTIS HC A02/MF A01 CSCL 02C

A video recording system with a visible light blocking filter to give sensitivity in the 0.78 m to 1.1 m waveband detected freeze-damaged citrus leaves rapidly. With this technique, the time to analyze images can be decreased from about one day for conventional photography to less than one hour for video recording. Author

N83-14559*# Department of Agriculture, Phoenix, Ariz. Water Conservation Lab.
DIURNAL PATTERNS OF WHEAT SPECTRAL REFLECTANCES AND THEIR IMPORTANCE IN THE ASSESSMENT OF CANOPY PARAMETERS FROM REMOTELY SENSED OBSERVATIONS
P. J. PINTER, JR., R. D. JACKSON, S. B. IDSO, and R. J. REGINATO, Principal Investigators Sep. 1982 49 p refs ERTS
(Contract PROJ. AGRISTARS)
(E83-10050; NASA-CR-169566; EW-U2-04349; JSC-18561; NAS 1.26:169566) Avail: NTIS HC A03/MF A01 CSCL 02C

Spectral reflectances of Produra wheat were measured at 13 different times of the day at Phoenix, Arizona, during April 1979 using a nadir-oriented hand-held 4-band radiometer which had bandpass characteristics similar to those on LANDSAT satellites. Different Sun altitude and azimuth angles caused significant diurnal changes in radiant return in both visible and near-IR regions of the spectrum and in several vegetation indices derived from them. The magnitude of these changes were related to different canopy architecture, percent cover and green leaf area conditions. Spectral measurements taken at each time period were well correlated with green leaf area index but the nature of the relationship changed significantly with time of day. Thus, a significant bias in the estimation of the green leaf area index from remotely sensed spectral data could occur if sun angles are not properly accounted for. Author

N83-14561*# Department of Agriculture, Washington, D.C. Statistical Reporting Service.
CONSTRUCTION OF A REMOTELY SENSED AREA SAMPLING FRAME FOR SOUTHERN BRAZIL
R. FECSO, W. GARDNER, B. HALE, V. JOHNSON, and S. PAVLASEK, Principal Investigators Jun. 1982 44 p refs Sponsored by NASA, USDA, Dept. of Commerce, Dept. of the Interior, and Agency for International Development ERTS
(Contract PROJ. AGRISTARS)
(E83-10052; NASA-CR-169568; IT-U2-04332; NAS 1.26:169568; AGES-820526) Avail: NTIS HC A03/MF A01 CSCL 08B

A remotely sensed area sampling frame was constructed for selected areas in Southern Brazil. The sampling unit information was stored in digital form in a latitudinal/longitudinal characterized population. Computerized sampling procedures were developed which allow for flexibility in sample unit specifications and sampling designs. Author

N83-14562*# Agricultural Research Service, Phoenix, Ariz. Water Conservation Lab.
ADJUSTING THE TASSELED CAP BRIGHTNESS AND GREENNESS FACTORS FOR ATMOSPHERIC PATH RADIANCE AND ABSORPTION ON A PIXEL BY PIXEL BASIS
R. D. JACKSON, P. N. SLATER, and P. J. PINTER, Principal Investigators Jul. 1982 24 p refs Sponsored by NASA, USDA, Dept. of Commerce, Dept. of the Interior, and Agency for International Development ERTS
(Contract DI-12-14-5001-38; PROJ. AGRISTARS)
(E83-10053; NASA-CR-169569; EW-U2-04334; JSC-18260; NAS 1.26:169569) Avail: NTIS HC A02/MF A01 CSCL 20F

A radiative transfer model was used to convert ground measured reflectances into the radiance at the top of the atmosphere, for several levels of atmospheric path radiance. The radiance in MSS7 (0.8 to 1.1 m) was multiplied by the transmission fraction for atmospheres having different levels of precipitable water. The radiance values were converted to simulated LANDSAT digital counts for four path radiance levels and four levels of precipitable water. These values were used to calculate the Kauth-Thomas brightness, greenness, yellowness, and nonsuch factors. Brightness was affected by surface conditions and path radiance. Greenness was affected by surface conditions, path radiance, and precipitable water. Yellowness was affected by path radiance and nonsuch by precipitable water, and both factors changed only slightly with surface conditions. Yellowness and nonsuch were used to adjust brightness and greenness to produce factors that were affected only by surface conditions such as soils and vegetation, and not by path radiance and precipitable water. Author

N83-14563*# National Oceanic and Atmospheric Administration, Columbia, Mo.
CROP WEATHER MODELS OF CORN AND SOYBEANS FOR AGROPHYSICAL UNITS (APU'S) IN IOWA USING MONTHLY METEOROLOGICAL PREDICTORS
S. LEDUC, Principal Investigator Sep. 1982 79 p refs Sponsored by NASA, USDA, Dept. of Commerce, Dept. of the Interior, and Agency for International Development ERTS
(Contract PROJ. AGRISTARS)
(E83-10054; NASA-CR-169612; YM-I2-04348; JSC-18272; NAS 1.26:169612) Avail: NTIS HC A05/MF A01 CSCL 02C

Models based on multiple regression were developed to estimate corn and soybean yield from weather data for agrophysical units (APU) in Iowa. The predictor variables are derived from monthly average temperature and monthly total precipitation data at meteorological stations in the cooperative network. The models are similar in form to the previous models developed for crop reporting districts (CRD). The trends and derived variables were the same and the approach to select the significant predictors was similar to that used in developing the CRD models. The APU's were selected to be more homogeneous with respect crop to production than the CRDs. The APU models are quite similar to the CRD models, similar explained variation and number of predictor variables. The APU models are to be independently evaluated and compared to the previously evaluated CRD models. That comparison should indicate the preferred model area for this application, i.e., APU or CRD. Author

N83-14564*# Agricultural Research Service, Weslaco, Tex. Soil and Water Conservation Research Service.
COMPARISON OF LANDSAT-2 AND FIELD SPECTROMETER REFLECTANCE SIGNATURES OF SOUTH TEXAS RANGELAND PLANT COMMUNITIES
A. J. RICHARDSON, D. E. ESCOBAR, H. W. GAUSMAN, and J. H. EVERITT, Principal Investigators Jul. 1982 23 p refs Sponsored by NASA, USDA, Dept. of Commerce, Dept. of the Interior, and Agency for International Development ERTS
(Contract NASA ORDER S-53876-AG; PROJ. AGRISTARS)
(E83-10055; NASA-CR-169570; EW-U2-04335; JSC-18261; NAS 1.26:169570) Avail: NTIS HC A02/MF A01 CSCL 02C

The accuracy was assessed for an atmospheric correction method that depends on clear water bodies to infer solar and atmospheric parameters for radiative transfer equations by measuring the reflectance signature of four prominent south Texas rangeland plants with the LANDSAT satellite multispectral scanner (MSS) and a ground based spectroradiometer. The rangeland plant reflectances produced by the two sensors were correlated with no significant deviation of the slope from unity or of the intercept from zero. These results indicated that the atmospheric correction produced LANDSAT MSS estimates of rangeland plant reflectances that are as accurate as the ground based spectroradiometer. A.R.H.

N83-14565*# National Oceanic and Atmospheric Administration, Columbia, Mo. Environmental Data and Information Service.
COMPARISON OF THE CEAS AND WILLIAMS-TYPE BARLEY YIELD MODELS FOR NORTH DAKOTA AND MINNESOTA
S. LEDUC, Principal Investigator Mar. 1982 57 p refs Sponsored by NASA, USDA, Dept. of Commerce, Dept. of the Interior, and Agency for International Development ERTS
(Contract PROJ. AGRISTARS)
(E83-10056; NASA-CR-169571; YM-U2-04290; JSC-18237; NAS 1.26:169571; YMD-1-4-2(82-1.2)) Avail: NTIS HC A04/MF A01 CSCL 02C

The CEAS and Williams type models were compared based on specified selection criteria which includes a ten year bootstrap test (1970-1979). Based on this, the models were quite comparable; however, the CEAS model was slightly better overall. The Williams type model seemed better for the 1974 estimates. Because that

year spring wheat yield was particularly low, the Williams type model should not be excluded from further consideration. Author

N83-14567*# Agricultural Research Service, Weslaco, Tex.
COMPARISONS AMONG A NEW SOIL INDEX AND OTHER TWO- AND FOUR-DIMENSIONAL VEGETATION INDICES
C. L. WIEGAND and A. J. RICHARDSON, Principal Investigators Sep. 1982 22 p refs Sponsored by NASA, USDA, Dept. of Commerce, Dept. of the Interior, and Agency for International Development ERTS
(Contract NASA ORDER S-70251-AG; NASA ORDER S-53876-AG; PROJ. AGRISTARS)
(E83-10058; NASA-CR-169592; EW-U2-04350; JSC-18562; NAS 1.26:169592) Avail: NTIS HC A02/MF A01 CSCL 02C

The 2-D difference vegetation index (DVI) and perpendicular vegetation index (PVI), and the 4-D green vegetation index (GVI) are compared in LANDSAT MSS data from grain sorghum (Sorghum bicolor, L. Moench) fields for the years 1973 to 1977. PVI and DVI were more closely related to LAI than was GVI. A new 2-D soil line index (SLI), the vector distance from the soil line origin to the point of intersection of PVI with the soil line, is defined and compared with the 4-D soil brightness index, SBI. SLI (based on MSS and MSS7) and SL16 (based on MSS 5 and MSS 6) were smaller in magnitude than SBI but contained similar information about the soil background. These findings indicate that vegetation and soil indices calculated from the single visible and reflective infrared band sensor systems, such as the AVHRR of the TIROS-N polar orbiting series of satellites, will be meaningful for synoptic monitoring of renewable vegetation. Author

N83-14568*# National Oceanic and Atmospheric Administration, Columbia, Mo.
CROP WEATHER MODELS OF BARLEY AND SPRING WHEAT YIELD FOR AGROPHYSICAL UNITS IN NORTH DAKOTA
S. LEDUC, Principal Investigator Jun. 1982 36 p refs Sponsored by NASA, USDA, Dept. of Commerce, Dept. of the Interior, and Agency for International Development ERTS
(Contract PROJ. AGRISTARS)
(E83-10059; NASA-CR-169572; YM-12-04321; JSC-18256; NAS 1.26:169572) Avail: NTIS HC A03/MF A01 CSCL 02C

Models based on multiple regression were developed to estimate barley yield and spring wheat yield from weather data for Agrophysical units(APU) in North Dakota. The predictor variables are derived from monthly average temperature and monthly total precipitation data at meteorological stations in the cooperative network. The models are similar in form to the previous models developed for Crop Reporting Districts (CRD). The trends and derived variables were the same and the approach to select the significant predictors was similar to that used in developing the CRD models. The APU models show sight improvements in some of the statistics of the models, e.g., explained variation. These models are to be independently evaluated and compared to the previously evaluated CRD models. The comparison will indicate the preferred model area for this application, i.e., APU or CRD. Author

N83-14569*# National Aeronautics and Space Administration. Lyndon B. Johnson Space Center, Houston, Tex.
EVALUATION OF THE WILLIAMS-TYPE MODEL FOR BARLEY YIELDS IN NORTH DAKOTA AND MINNESOTA
T. L. BARNETT, Principal Investigator Dec. 1981 50 p Sponsored by NASA, USDA, Dept. of Commerce, Dept. of the Interior, and Agency for International Development ERTS
(Contract PROJ. AGRISTARS)
(E83-10060; NASA-TM-85169; YM-U2-04287; JSC-18234; NAS 1.15:85169; YMD-1-4-1(81-12.2)) Avail: NTIS HC A03/MF A01 CSCL 02C

The Williams-type yield model is based on multiple regression analysis of historial time series data at CRD level pooled to regional level (groups of similar CRDs). Basic variables considered in the analysis include USDA yield, monthly mean temperature, monthly precipitation, soil texture and topographic information, and variables derived from these. Technologic trend is represented by piecewise linear and/or quadratic functions of year. Indicators of yield reliability obtained from a ten-year bootstrap test (1970-1979) demonstrate that biases are small and performance based on root mean square appears to be acceptable for the intended AgRISTARS large area applications. The model is objective, adequate, timely, simple, and not costly. It consideres scientific knowledge on a broad scale but not in detail, and does not provide a good current measure of modeled yield reliability. Author

N83-14574*# Instituto de Pesquisas Espaciais, Sao Jose dos Campos (Brazil).
AN AUTOMATIC AGRICULTURAL ZONE CLASSIFICATION PROCEDURE FOR CROP INVENTORY SATELLITE IMAGES [UM PROCEDIMENTO AUTOMATICO PARA CLASSIFICACAO DE AREAS AGRICOLAS EM IMAGENS DE SATELITE, PARA USO EM PREVISAO DE SAFRAS]
N. D. J. PARADA, Principal Investigator, G. C. NETO, F. R. D. VELASCO, and M. O. B. DEOLIVEIRA Jul. 1982 11 p refs In PORTUGUESE; ENGLISH summary Presented at the 34th Reuniao da SBPC, Campinas, Sao Paulo, Brazil, 6-14 Jul. 1982 Sponsored by NASA ERTS
(E83-10065; NASA-CR-169576; NAS 1.26:169576; INPE-2482-PRE/166) Avail: NTIS HC A02/MF A01 CSCL 02C

A classification procedure for assessing crop areal proportion in multispectral scanner image is discussed. The procedure is into four parts: labeling; classification; proportion estimation; and evaluation. The procedure also has the following characteristics: multitemporal classification; the need for a minimum field information; and verification capability between automatic classification and analyst labeling. The processing steps and the main algorithms involved are discussed. An outlook on the future of this technology is also presented. M.G.

N83-14576*# Instituto de Pesquisas Espaciais, Sao Jose dos Campos (Brazil).
AN APPLICATION OF CLUSTER ANALYSIS FOR DETERMINING HOMOGENEOUS SUBREGIONS: THE AGROCLIMATOLOGICAL POINT OF VIEW
N. D. J. PARADA, Principal Investigator and C. A. CAPPELLETTI Jul. 1982 11 p refs Presented at the 16th Intern. Symp. on Remote Sensing of Environ., Buenos Aires, 2-9 Jun. 1982 Sponsored by NASA ERTS
(E83-10067; NASA-CR-169578; NAS 1.26:169578; INPE-2490-PRE/173) Avail: NTIS HC A02/MF A01 CSCL 02C

A stratification oriented to crop area and yield estimation problems was performed using an algorithm of clustering. The variables used were a set of agroclimatological characteristics measured in each one of the 232 municipalities of the State of Rio Grande do Sul, Brazil. A nonhierarchical cluster analysis was used and the pseudo F-statistics criterion was implemented for determining the 'cut point' in the number of strata. Author

N83-14577*# Instituto de Pesquisas Espaciais, Sao Jose dos Campos (Brazil).
VEGETATION SURVEY IN AMAZONIA USING LANDSAT DATA
N. D. J. PARADA, Principal Investigator, Y. E. SHIMABUKURO, J. R. DOSSANTOS, and L. C. S. DEAQUINO (Comissao Estadual de Planejamento Agricola, Manaus, Brazil) May 1982 8 p refs Presented at the 16th Intern. Symp. on Remote Sensing of Environ., Buenos Aires, 2-9 Jun. 1982 Sponsored by NASA Original contains imagery. Original photography may be purchased from the EROS Data Center, Sioux Falls, S.D. 57198 ERTS
(E83-10068; NASA-CR-169579; NAS 1.26:169579; INPE-2409-PRE/118) Avail: NTIS HC A02/MF A01 CSCL 08F

Automatic Image-100 analysis of LANDSAT data was performed using the MAXVER classification algorithm. In the pilot area, four vegetation units were mapped automatically in addition to the areas occupied for agricultural activities. The Image-100 classified results together with a soil map and information from RADAR images, permitted the establishment of the final legend with six classes: semi-deciduous tropical forest; low land evergreen tropical forest;

secondary vegetation; tropical forest of humid areas, predominant pastureland and flood plains. Two water types were identified based on their sediments indicating different geological and geomorphological aspects. A.R.H.

N83-14579*# Instituto de Pesquisas Espaciais, Sao Jose dos Campos (Brazil).
REMOTE SENSING TECHNIQUES FOR CONSERVATION AND MANAGEMENT OF NATURAL VEGETATION ECOSYSTEMS [SENSORIAMENTO REMOTO NA CONSERVACAO E MANEJO DE ECOSSISTEMAS NATURAIS VEGETAIS]
N. D. J. PARADA, Principal Investigator, J. J. VERDESIO, and J. R. DOSSANTOS Nov. 1981 26 p refs In PORTUGUESE; ENGLISH summary Presented at the 3rd Simposio Nacio nal de Ecologia, Belo Horizonte, Brazil, 27-31 Jul. 1981 Sponsored by NASA ERTS
(E83-10070; NASA-CR-169581; NAS 1.26:169581; INPE-2264-PRE/045) Avail: NTIS HC A03/MF A01 CSCL 02F

The importance of using remote sensing techniques, in the visible and near-infrared ranges, for mapping, inventory, conservation and management of natural ecosystems is discussed. Some examples realized in Brazil or other countries are given to evaluate the products from orbital platform (MSS and RBV imagery of LANDSAT) and aerial level (photography) for ecosystems study. The maximum quantitative and qualitative information which can be obtained from each sensor, at different level, are discussed. Based on the developed experiments it is concluded that the remote sensing technique is a useful tool in mapping vegetation units, estimating biomass, forecasting and evaluation of fire damage, disease detection, deforestation mapping and change detection in land-use. In addition, remote sensing techniques can be used in controling implantation and planning natural/artificial regeneration. Author

N83-14585*# Instituto de Pesquisas Espaciais, Sao Jose dos Campos (Brazil).
EVALUATION OF REFORESTATION USING REMOTE SENSING TECHNIQUES
N. D. J. PARADA, Principal Investigator, P. H. FILHO, Y. E. SHIMABUKURO, and J. R. DOSSANTOS May 1982 9 p refs Presented at the 16th Intern. Symp. on Remote Sensing of Environ., Buenos Aires, 2-9 Jun. 1982 Sponsored by NASA ERTS
(E83-10076; NASA-CR-169587; NAS 1.26:169587; INPE-2413-PRE/121) Avail: NTIS HC A02/MF A01 CSCL 02F

The utilization of remotely sensed orbital data for forestry inventory. The study area (approximately 491,100 ha) encompasses the municipalities of Ribeirao Preto, Altinopolis, Cravinhos, Serra Azul, Luis Antonio, Sao Simao, Sant Rita do Passa Quatro and Santa Rosa do Viterbo (Sao Paulo State). Materials used were LANDSAT data from channels 5 and 7 (scale 1:250,000) and CCT's. Visual interpretation of the imagery showed that for 1977 a total of 37,766.00 ha and for 1979 38,003.75 ha were reforested with Pinus and Eucalyptus within the area under study. The results obtained show that LANDSAT data can be used efficiently in forestry inventory studies. Author

N83-14586*# Instituto de Pesquisas Espaciais, Sao Jose dos Campos (Brazil).
ESTIMATION OF THE SUGAR CANE CULTIVATED AREA FROM LANDSAT IMAGES USING THE TWO PHASE SAMPLING METHOD
N. D. J. PARADA, Principal Investigator, C. A. CAPPELLETTI, F. J. MENDONCA, D. C. L. LEE, and Y. E. SHIMABUKURO Jul. 1982 6 p refs Presented at the 16th Intern. Symp. on Remote Sensing of Environ., Buenos Aires, 2-9 Jun. 1982 Sponsored by NASA ERTS
(E83-10077; NASA-CR-169588; NAS 1.26:169588; INPE-2489-PRE/172) Avail: NTIS HC A02/MF A01 CSCL 02C

A two phase sampling method and the optimal sampling segment dimensions for the estimation of sugar cane cultivated area were developed. This technique employs visual interpretations of LANDSAT images and panchromatic aerial photographs considered as the ground truth. The estimates, as a mean value of 100 simulated samples, represent 99.3% of the true value with a CV of approximately 1%; the relative efficiency of the two phase design was 157% when compared with a one phase aerial photographs sample. Author

N83-14619# Katholieke Universiteit te Leuven (Belgium). Lab. voor Bodemgenese en Bodemgeografie.
MULTITEMPORAL SOIL AND VEGETATION OBSERVATIONS BY METEOSAT OVER CENTRAL AFRICA
J. MAES, R. GOMBEER, and J. DHOORE *In* ESA Satellite Remote Sensing for Developing Countries p 87-94 Jun. 1982 refs
Avail: NTIS HC A11/MF A01

The extent to which METEOSAT could contribute to the study of dynamic land surface features in central Africa was verified. The rain forest-humid savanna limit can be distinguished through intercomparison of multitemporal data. In the savanna area, response patterns in the visible and in the thermal infrared channel agree with soil distribution patterns. The expansion or retraction of lakes and marshes and the progress of the drying out of vegetation with the advance of the dry season was also followed. Author (ESA)

N83-14624# Copenhagen Univ. (Denmark). Inst. of Geography.
MULTITEMPORAL ANALYSIS OF LANDSAT DATA FOR INVESTIGATIONS OF AGRICULTURAL LAND USE: PROBLEMS AND POTENTIALS
K. RASMUSSEN *In* ESA Satellite Remote Sensing for Developing Countries p 145-151 Jun. 1982 refs Sponsored by Danish Natural Science Research Council
Avail: NTIS HC A11/MF A01

The great demands on computer time, the decreased spatial *resolution due to inaccuracies in digital overlay of two or more* LANDSAT scenes, and the difficulties in using standard classification algorithms on multitemporal data sets are considered. Ways of minimizing these problems are mentioned, and examples drawn from a Danish crop identification study are shown. Two examples of use of multitemporal analysis in current projects in developing countries are presented. In Zambia the intensity of land use in a shifting cultivation system is being studied, and by means of multitemporal analysis the intensification process can be detected. In Kenya within and between year variations of amount and location of grazing resources are studied as a means of understanding migration patterns of pastoral nomads.
Author (ESA)

N83-14625# Center for Remote Sensing, Colombo (Sri Lanka). Survey Dept.
MULTISTAGE LAND USE MAPPING AND CHANGE MONITORING IN SRI LANKA
U. GEISER, M. SOMMER, H. HAEFNER (Eidgenoessische Tech. Hochschule, Zurich), and K. I. ITTEN (Eidgenoessische Tech. Hochschule, Zurich) *In* ESA Satellite Remote Sensing for Developing Countries p 153-160 Jun. 1982 refs
Avail: NTIS HC A11/MF A01

A 1:100,000 scale land use/land cover map series of Sri Lanka was produced. Analog interpretation of computer enhanced and bulk LANDSAT imagery, and aerial photography, based on extensive ground truth, were used in a medium technological level multistage approach. Rice yield forecasting images and forest cover change maps are presented. Author (ESA)

N83-14626# Joint Research Centre of the European Communities, Ispra (Italy).
USE OF REMOTE SENSING TECHNIQUES FOR RICE PRODUCTION FORECASTING IN WEST AFRICA (MALI AND GUINEA: NIGER-BANI PROJECT)
A. BERG and J. M. GREGOIRE *In* ESA Satellite Remote Sensing for Developing Countries p 161-168 Jun. 1982 refs
Avail: NTIS HC A11/MF A01

The west African rice system under controlled submersion conditions is described, and data on visual and digital interpretation

of LANDSAT images of the Mali test site are presented to show the potential and limitations of that imagery for the assessment of the harvestable areas one month before harvest. The same assessment is feasible from the interpretation of IR photographs with a six rice-class classification. Interpretation of RBV imagery acquired during the 1980 campaign allows forecasting to be extended to 3 months before harvest as a result of the recognition of the flooded areas. This indicates that the maximum extension of flooding constitutes the main limiting factor of rice production. Author (ESA)

N83-14653# Army Engineer Topographic Labs., Fort Belvoir, Va.

EFFECTS OF GROUND COVER AND LEAF AREA ON THE SPECTRAL REFLECTANCE OF VEGETATION-SOIL TARGET

M. B. SATTERWHITE and P. HENLEY 23 Sep. 1982 12 p refs

(AD-A119714; ETL-R039) Avail: NTIS HC A02/MF A01 CSCL 20F

The relations between spectral reflectance, percent ground cover, and leaf area index (LAI) for vegetation-soil targets were evaluated for green vegetation against either a light-toned sand and a dark-toned organic loam soil. The percent ground cover and LAI were calculated for the ground area in the radiometer's field of view. The special reflectances of the different targets were measured in the 400 to 1100 nm region. For the vegetation-organic loam targets, the present cover and LAI varied directly with the target reflectance in the green (520-600 nm) and the infrared (700-1100 nm) regions, but varied inversely with reflectance in the red region (650-700 nm). For the vegetation-sand targets, the percent cover and LAI varied inversely with reflectance in the visible region and directly in the IR region. Results show that the major change in reflectance of vegetation-soils was related more to the change in percent cover. For less than 100 percent cover, the LAI varied directly with percent ground cover. A change in LAI produced less change in target reflectance than did a change in percent cover. Once the canopy is closed, i.e., 100 percent cover, variation in LAI had little effect. Author (GRA)

N83-14655# Army Engineer Topographic Labs., Fort Belvoir, Va.

SPECIAL REFLECTANCE OF SOME PLANT INDICATORS OF SALINE AND NONSALINE SOILS

M. B. SATTERWHITE and J. W. EASTES 23 Sep. 1982 12 p refs

(AD-A119727; ETL-R038) Avail: NTIS HC A02/MF A01 CSCL 20F

The task of finding a water supply in an arid region and determining something of its potability can be aided by using various remote sensing techniques for gathering geological, botanical, and terrain data. The objective of this study was to determine if salt-tolerant and salt-intolerant plant species could be distinguished by some unique spectral bandpass in the 0.4 to 1.1 micrometers spectral region. A number of study sites in Nevada having either salt-tolerant or intolerant plant species were selected. Spectral measurements were made on six salt-tolerant and two salt-intolerant species during June-July when the plants were in full vegetative stage and not under any apparent water deficit stress. The reflectance spectra of the halophyte and nonhalophyte species showed that they could not be differentiated using selected bandpasses because the spectral characteristics (intensity and wavelength range) were too similar for both groups. Comparison of individual spectra showed some salt-tolerant and intolerant species could be distinguished by their reflectance spectra. Even so, different species occupying similar landform conditions had similar spectral reflectance signatures. The canopy geometry and background were important factors affecting these spectral signatures. Author (GRA)

N83-15740*# National Aeronautics and Space Administration. Earth Resources Labs., Bay St. Louis, Miss.

AUTOMATED SEGMENT MATCHING ALGORITHM-THEORY, TEST, AND EVALUATION

M. T. KALCIC, Principal Investigator Jun. 1982 46 p refs Sponsored by NASA, USDA, Dept. of Commerce, Dept. of the Interior, and Agency for International Development Original contains color imagery. Original photography may be purchased from the EROS Data Center, Sioux Falls, S.D. 57198 ERTS

(Contract PROJ. AGRISTARS)

(E83-10096; NASA-TM-85192; DC-Y2-04325; NSTL/ERL-209; NAS 1.15:85192) Avail: NTIS HC A03/MF A01 CSCL 02C

Results to automate the U.S. Department of Agriculture's process of segment shifting and obtain results within one-half pixel accuracy are presented. Given an initial registration, the digitized segment is shifted until a more precise fit to the LANDSAT data is found. The algorithm automates the shifting process and performs certain tests for matching and accepting the computed shift numbers. Results indicate the algorithm can obtain results within one-half pixel accuracy. A.R.H.

N83-15741*# National Aeronautics and Space Administration. Ames Research Center, Moffett Field, Calif.

GATES TO GREGG HIGH VOLTAGE TRANSMISSION LINE STUDY

V. BERGIS, K. MAW, W. NEWLAND, D. SINNOTT, G. THORNBURY, P. EASTERWOOD, and J. BONDERUD Dec. 1982 152 p refs Prepared in cooperation with Technicolor Government Services, Inc., Moffett Field, Calif. and Pacific Gas and Electric Co., San Francisco Original contains color imagery. Original photography may be purchased from the EROS Data Center, Sioux Falls, S.D. 57198 ERTS

(Contract NAS2-11101)

(E83-10097; NASA-TM-84314; A-9182; NAS 1.15:84314) Avail: NTIS HC A08/MF A01 CSCL 08B

The usefulness of LANDSAT data in the planning of transmission line routes was assessed. LANDSAT digital data and image processing techniques, specifically a multi-date supervised classification aproach, were used to develop a land cover map for an agricultural area near Fresno, California. Twenty-six land cover classes were identified, of which twenty classes were agricultural crops. High classification accuracies (greater than 80%) were attained for several classes, including cotton, grain, and vineyards. The primary products generated were 1:24,000, 1:100,000 and 1:250,000 scale maps of the classification and acreage summaries for all land cover classes within four alternate transmission line routes. Author

N83-15743*# Lockheed Engineering and Management Services Co., Inc., Houston, Tex.

COMPUTER PROGRAM DOCUMENTATION FOR THE PASTURE/RANGE CONDITION ASSESSMENT PROCESSOR

K. S. MCINTYRE and T. G. MILLER, Principal Investigators Jul. 1982 46 p Sponsored by NASA, USDA, Dept. of Commerce, Dept. of the Interior, and Agency for International Development ERTS

(Contract NAS9-15800; PROJ. AGRISTARS)

(E83-10100; NASA-CR-167746; EW-L2-04340; JSC-18265; NAS 1.26:167746; LEMSCO-18627) Avail: NTIS HC A03/MF A01 CSCL 02C

The processor which drives for the RANGE software allows the user to analyze LANDSAT data containing pasture and rangeland. Analysis includes mapping, generating statistics, calculating vegetative indexes, and plotting vegetative indexes. Routines for using the processor are given. A flow diagram is included. A.R.H.

N83-15747*# Pennsylvania State Univ., University Park. Office for Remote Sensing of Earth Resources.
DEVELOPMENT OF A DATA MANAGEMENT FRONT END FOR USE WITH A LANDSAT BASED INFORMATION SYSTEM Final Report, Feb. 1981 - Jan. 1982
B. J. TURNER, Principal Investigator Jan. 1982 34 p refs Original contains imagery. Original photography may be purchased from the EROS Data Center, Sioux Falls, S.D. 57198 ERTS
(Contract NAS5-26468)
(E83-10104; NASA-CR-170461; NAS 1.26:170461) Avail: NTIS HC A03/MF A01 CSCL 05B

A user friendly front end was constructed to facilitate access to the LANDSAT mosaic data base supplied by JPL and to process both LANDSAT and ancillary data. Archieval and retrieval techniques were developed to efficiently handle this data base and make it compatible with requirements of the Pennsylvania Bureau of Forestry. Procedures are ready for: (1) forming the forest/nonforest mask in ORSER compressed map format using GSFC-supplied classification procedures; (2) registering data from a new scene (defoliated) to the mask (which may involve mosaicking if the area encompasses two LANDSAT scenes; (3) producing a masked new data set using the MASK program; (4) analyzing this data set to produce a map showing degrees of defoliation, output on the Versatec plotter; and (5) producing color composite maps by a diazo-type process. A.R.H.

N83-15749*# Utah Univ., Salt Lake City. Center for Remote Sensing and Cartography.
DETECTION OF ASPEN-CONIFER FOREST MIXES FROM LANDSAT DIGITAL DATA
R. A. JAYNES and J. A. MEROLA 1982 30 p refs Sponsored by Dept. of Agriculture ERTS
(Contract NAGW-95)
(E83-10106; NASA-CR-169680; NAS 1.26:169680; CRSC-82-4)
Avail: NTIS HC A03/MF A01 CSCL 08F

Aspen, conifer and mixed aspen/conifer forests were mapped for a 15-quadrangle study area in the Utah-Idaho Bear River Range using LANDSAT multispectral scanner data. Digital classification and statistical analysis of LANDSAT data allowed the identification of six groups of signatures which reflect different types of aspen/conifer forest mixing. Photo interpretations of the print symbols suggest that such classes are indicative of mid to late seral aspen forests. Digital print map overlays and acreage calculations were prepared for the study area quadrangles. Further field verification is needed to acquire additional information about the nature of the forests. Single date LANDSAT analysis should be a cost effective means to index aspen forests which are at least in the mid seral phase of conifer invasion. Since aspen canopies tend to obscure understory conifers for early seral forests, a second date analysis, using data taken when aspens are leafless, could provide information about early seral aspen forests.
Author

N83-15750*# National Aeronautics and Space Administration. Goddard Space Flight Center, Greenbelt, Md.
SPECTRAL CHARACTERIZATION OF THE LANDSAT-D MULTISPECTRAL SCANNER SUBSYSTEMS
B. L. MARKHAM, Principal Investigator and J. L. BARKER Jun. 1982 65 p refs Submitted for publication ERTS
(E83-10107; NASA-TM-83955; NAS 1.15:83955) Avail: NTIS HC A04/MF A01 CSCL 20F

Relative spectral response data for the multispectral scanner subsystems (MSS) to be flown on LANDSAT-D and LANDSAT-D backup, the protoflight and flight models, respectively, are presented and compared to similar data for the Landsat 1,2, and 3 subsystems. Channel-bychannel (six channels per band) outputs for soil and soybean targets were simulated and compared within each band and between scanners. The two LANDSAT-D scanners proved to be nearly identical in mean spectral response, but they exhibited some differences from the previous MSS's. Principal differences between the spectral responses of the D-scanners and previous scanners were: (1) a mean upper-band edge in the green band of 606 nm compared to previous means of 593 to 598 nm; (2) an average upper-band edge of 697 nm in the red band compared to previous averages of 701 to 710 nm; and (3) an average bandpass for the first near-IR band of 702-814 nm compared to a range of 693-793 to 697-802 nm for previous scanners. These differences caused the simulated D-scanner outputs to be 3 to 10 percent lower in the red band and 3 to 11 percent higher in the first near-IR band than previous scanners for the soybeans target. Otherwise, outputs from soil and soybean targets were only slightly affected. The D-scanners were generally more uniform from channel to channel within bands than previous scanners. Author

N83-15751*# Texas A&M Univ., College Station. Remote Sensing Center.
MICROWAVE REMOTE SENSING OF SOIL MOISTURE, VOLUME 1 Final Report
M. J. MCFARLAND, Principal Investigator, S. W. THEIS, W. D. ROSENTHAL, and C. L. JONES Feb. 1982 144 p refs Original contains imagery. Original photography may be purchased from the EROS Data Center, Sioux Falls, S.D. 57198 ERTS
(Contract NSG-5134)
(E83-10108; NASA-CR-166822; NAS 1.26:166822;
RSC-3458-129-VOL-1) Avail: NTIS HC A07/MF A01 CSCL 08M

Multifrequency sensor data from NASA's C-130 aircraft were used to determine which of the all weather microwave sensors demonstrated the highest correlation to surface soil moisture over optimal bare soil conditions, and to develop and test techniques which use visible/infrared sensors to compensate for the vegetation effect in this sensor's response to soil moisture. The L-band passive microwave radiometer was found to be the most suitable single sensor system to estimate soil moisture over bare fields. The perpendicular vegetation index (PVI) as determined from the visible/infrared sensors was useful as a measure of the vegetation effect on the L-band radiometer response to soil moisture. A linear equation was developed to estimate percent field capacity as a function of L-band emissivity and the vegetation index. The prediction algorithm improves the estimation of moisture significantly over predictions from L-band emissivity alone.
A.R.H.

N83-15753*# Aster Consulting Associates, Binghamton, N.Y.
A REVIEW OF CROP CANOPY REFLECTANCE MODELS
N. S. GOEL, Principal Investigator 1 Aug. 1982 55 p refs ERTS
(Contract NAS9-16505)
(E83-10110; NASA-CR-167716; NAS 1.26:167716) Avail: NTIS HC A04/MF A01 CSCL 02C

Various models for calculating crop canopy reflectance, in the visible and infrared wavelengths, from the optical and geometrical properties of a canopy and its constituents are reviewed. The radiative transfer equation is discussed as well as both analytical and numerical crop reflectance models which are manifestations of the solution of this equation. Recommendations are made for further work in modeling of canopy reflectance. Author

N83-15756*# Texas A&M Univ., College Station. Remote Sensing Center.
RANGELAND BIOMASS ESTIMATION DEMONSTRATION Final Report
R. W. NEWTON, Principal Investigator, W. E. BOYD, and B. V. CLARK Feb. 1982 58 p refs Original contains imagery. Original photography may be purchased from the EROS Data Center, Sioux Falls, S.D. 57198 ERTS
(Contract NAS9-16369)
(E83-10113; NASA-CR-167634; NAS 1.26:167634;
RSC-4496-132) Avail: NTIS HC A04/MF A01 CSCL 02C

Because of their sensitivity to chlorophyll density, green leaf density, and leaf water density, two hand-held radiometers which have sensor bands coinciding with thematic mapper bands 3, 4, and 5 were used to calibrate green biomass to LANDSAT spectral ratios as a step towards using portable radiometers to speed up ground data acquisition. Two field reflectance panels monitored

incoming radiation concurrently with sampling. Software routines were developed and used to extract data from uncorrected tapes of MSS data provided in NASA LANDSAT universal format. A LANDSAT biomass calibration curve estimated the range biomass over a four scene area and displayed this information spatially as a product in a format of use to ranchers. The regional biomass contour map is discussed. A.R.H.

N83-15758*# Kansas Univ. Center for Research, Inc., Lawrence. Space Technology Center.
CROP-PHENOLOGY AND LANDSAT-BASED IRRIGATED LANDS INVENTORY IN THE HIGH PLAINS Interim Report, 1 Dec. 1980 - 31 Jan. 1981
E. A. MARTINKO, Principal Investigator, J. PORACSKY, E. R. KIPP, and H. KRIEGER 31 Jan. 1981 80 p ERTS
(Contract NAG2-57)
(E83-10115; NASA-CR-169698; NAS 1.26:169698; IR-2) Avail: NTIS HC A05/MF A01 CSCL 02C

Crop calendars for 1979 and 1980 were investigated in support of an effort to develop techniques for mapping the High Plains aquifer region. Optimal LANDSAT image dates for 1980 were preliminarily identified based on ESS weekly crop weather reports and 1979 ESS agricultural statistics were entered into the computer. A questionnaire was compiled and sent to ASCS county agents with the approval of the Extension Directors in each state involved. Data from returning questionnaires were tabulated and development started on a set of computer programs to allow the preparation of computer assisted graphic displays of much of the collected data. A.R.H.

N83-15760*# National Aeronautics and Space Administration. Lyndon B. Johnson Space Center, Houston, Tex.
CROP PROPORTION ESTIMATION PROBLEMS IN AGRISTARS
R. P. HEYDORN *In* Texas A and M Univ. Proc. of the NASA Workshop on Surface Fitting p 7-26 1982 ERTS
Avail: NTIS HC A10/MF A01 CSCL 02C

Some mathematical/statistical problems within the AgRISTARS program amendable to investigations involving the use of surface fitting techniques are overviewed. The Bayes and maximum likelihood rules, bias determination, regression estimators, parameter estimation, and classifier design are addressed. M.G.

N83-15790*# Cornell Univ., Ithaca, N. Y. School of Civil and Environmental Engineering.
REMOTE SENSING PROGRAM Semiannual Status Report, 1 Jun. - 30 Nov. 1982
W. R. PHILIPSON, Principal Investigator, T. LIANG, and W. D. PHILPOT Jan. 1983 261 p refs Original contains imagery. Original photography may be purchased from the EROS Data Center, Sioux Falls, S.D. 57198 ERTS
(Contract NGL-33-010-171)
(E83-10120; NASA-CR-169723; NAS 1.26:169723) Avail: NTIS HC A12/MF A01 CSCL 05B

Field spectroradiometric and airborne multispectral scanner data were related to vineyard yield and other agronomic variables in an attempt to determine the optimum wavelengths for yield prediction modeling. Reflections between vine canopy reflectance and several management practices were also considered. Spectral analysis of test vines found that, although some correlations with vine yield were significant, they were inadequate for producing a yield prediction model. The findings also indicate that the vines examined through the field spectroradiometers were not truly representative. Geologic linears identified from aerial photographys, LANDSAT images, and maps were compared to gas well locations in three New York' counties. Correlations were found between the dominant trends in regional liners and gas field boundaries and trends. Other projects being conducted under the grant include determining vegetable acreage in mucklands, site selection for windmills, spectral effects of sulfur dioxide, and screening tomato seedlings for salt tolerance. A.R.H.

N83-15793*# Lockheed Engineering and Management Services Co., Inc., Houston, Tex.
FORTRAN IMPLEMENTATION OF FRIEDMAN'S TEST FOR SEVERAL RELATED SAMPLES
S. A. DAVIDSON Feb. 1982 25 p refs Sponsored by NASA, USDA, Dept. of Commerce, Dept. of the Interior, and Agency for International Development ERTS
(Contract NAS9-15800; PROJ. AGRISTARS)
(E83-10123; NASA-CR-169726; SM-L2-04234; JSC-17816; NAS 1.26:169726; LEMSCO-17502) Avail: NTIS HC A02/MF A01 CSCL 02C

The FRIEDMAN program is a FORTRAN-coded implementation of Friedman's nonparametric test for several related samples with one observation per treatment/-block combination, or as it is sometimes called, the two-way analysis of variance by ranks. The FRIEDMAN program is described and a test data set and its results are presented to aid potential users of this program. Author

02

ENVIRONMENTAL CHANGES AND CULTURAL RESOURCES

Includes land use analysis, urban and metroplitan studies, environmental impact, air and water pollution, geographic information systems, and geographic analysis.

A83-10083
ONGOING MICROWAVE REMOTE SENSING-ACTIVITIES FOR LAND APPLICATIONS IN GERMANY
P. HARTL (Berlin, Technische Universitaet, Berlin, West Germany) and A. SIEBER (Deutsche Forschungs- und Versuchsanstalt fuer Luft- und Raumfahrt, Institut fuer Hochfrequenztechnik, Wessling, West Germany) In: International Geoscience and Remote Sensing Symposium, Washington, DC, June 8-10, 1981, Digest. Volume 2. New York, Institute of Electrical and Electronics Engineers, 1981, p. 913-919. refs

A program is discussed that entails the design, development, and testing of microwave remote sensing systems and techniques intended to overcome the weather-related visibility limitations of optical sensors. The program includes the design and development of an experimental X-band SLAR and a dual-frequency L-band scatterometer, the development of radar-signature analysis techniques, design studies for spaceborne microwave sensors, and an experiment to verify design assumptions pertaining to SAR image information. The development of SAR data processing equipment is briefly noted. F.G.M.

A83-11626
EVIDENCE FOR A CENTRAL EURASIAN SOURCE AREA OF ARCTIC HAZE IN ALASKA
G. E. SHAW (Alaska, University, Fairbanks, AK) Nature, vol. 299, Oct. 28, 1982, p. 815-818. refs
(Contract N00014-C-0435; NSF DPP-79-19816)

Three strong episodes of arctic haze that occurred in interior Alaska during late winter 1982 are investigated by means of laser and X-ray spectrometry, by tracing back air trajectories from central Alaska at the 500-mbar level, and by examining satellite photographs of the possible source area. It is found that the air masses involved in the haze episodes came from arctic regions west of Alaska and were charged with suspended submicrometer heavy-metal particles apparently derived from anthropogenic sources of pollution. The back air trajectories are traced to the central Eurasian sector of the Arctic, in particular, the area of the Taimyr Peninsula in Siberia. A Landsat image of the area around the large polymetallic ore mining and smelting complex at Norilsk in the Taimyr district is presented that shows two large plumes emanating from smelters processing sulfide-rich Ni-Cu ores. F.G.M.

A83-11866
PHOTOINTERPRETATION, REMOTE SENSING, AND PHOTOGRAMMETRIC ELEMENTS APPLIED TO ROAD-PLANNING STUDIES [PHOTO-INTERPRETATION, TELEDETECTION ET ELEMENTS PHOTOGRAMMETRIQUES APPLIQUES AUX ETUDES ROUTIERES]
C. CAZABAT and J. DENEGRE (Institut Geographique National, Saint-Mande, Val-de-Marne, France) Laboratoires des Ponts et Chausees, Bulletin de Liaison, vol. 110, Nov.-Dec. 1980, p. 73-79. In French.

Photointerpretation and photogrammetry have numerous applications in road-planning studies in developing countries. This paper examines the products of these two methods for the treatment of aerial photographs (and of remotely sensed data in general), including products associated with photographic techniques (types of emulsion and processing), photoidentification (geomorphology and hydrology), and photogrammetric plotting (relief and planimetry). Attention is also given to the automation of geographical techniques, in the area of computer-aided design as well as in the area of image processing. B.J.

A83-12671* National Aeronautics and Space Administration. Goddard Space Flight Center, Greenbelt, Md.
LANDSAT OBSERVATIONS OF MOUNT ST. HELENS
C. G. BOHN (NASA, Goddard Space Flight Center, Missions Utilization Office, Greenbelt, MD) and B. G. BLY (Computer Sciences Corp., Silver Spring, MD) In: Electro-optical instrumentation for resources evaluation; Proceedings of the Meeting, Washington, DC, April 21, 22, 1981. Bellingham, WA, SPIE - The International Society for Optical Engineering, 1981, p. 32-40.

The eruption of Mount St. Helens on May 18, 1980, and subsequent destruction of approximately 593 square kilometers (229 square miles) of vegetation, clearly provided a unique opportunity for earth-oriented satellite remote sensing systems. Landsat, a relatively high resolution Multispectral Scanner (MSS) system, imaged Mount St. Helens both before and after its major eruption. Digital data have been used to create a damage assessment map and a change detection image. Several classes of timber damage and land cover modification have been developed. Acreages for each class have been tabulated. (Author)

A83-12672
MOUNT ST. HELENS QUICK RESPONSE DAMAGE ASSESSMENT USING HIGH-ALTITUDE INFRARED PHOTOGRAPHY
R. E. HINKLE, J. C. PRILL (Lockheed Engineering and Management Services Co., Inc., Houston, TX), and J. R. PRUITT (U.S. Forest Service, Portland, OR) In: Electro-optical instrumentation for resources evaluation; Proceedings of the Meeting, Washington, DC, April 21, 22, 1981. Bellingham, WA, SPIE - The International Society for Optical Engineering, 1981, p. 41-48. U.S. Department of Agriculture
(Contract USDA-53-3187-0-29)

A rapid assessment was needed to devise land management plans for timber sale operations, rehabilitation efforts, and fire protection activities. High-altitude color-infrared photography was collected in May and June by the Ames Research Center. The photographs, together with information from a helicopter trip into the area, formed the basis for the construction of 58 map-registered overlays within a three-week period. These overlays gave detailed depictions of the damage to timber resources, the transportation network, and the watershed. Using the 14 timber loss overlays, the Department of Agriculture (Forest Service) digitized cells depicting ownership, degree of damage, and the preeruption cover classes. These digitized data furnished such information as the total area affected within and outside the national forest, the total timber acreage destroyed or damaged, the sizes of the timber destroyed, and the acreage of barren land before and after the eruption. The hydrology and transportation overlays provided information for an alert system to locate areas needing comprehensive studies. C.R.

A83-14095
THE RELATIONSHIPS BETWEEN REFLECTANCE IN THE LANDSAT WAVEBANDS AND THE COMPOSITION OF AN AUSTRALIAN SEMI-ARID SHRUB RANGELAND
R. D. GRAETZ and M. R. GENTLE (Commonwealth Scientific and Industrial Research Organization, Div. of Land Resources Management, Deniliquin, New South Wales, Australia) Photogrammetric Engineering and Remote Sensing, vol. 48, Nov. 1982, p. 1721-1730. refs

A83-14228#
RENEWABLE RESOURCES MONITORING NEEDS IN MANITOBA
J. CIHLAR (Canada Center for Remote Sensing, Ottawa, Canada), W. G. BEST (Manitoba Remote Sensing Centre, Winnipeg, Canada), and G. REMPEL (MacLaren Engineers, Planners and Scientists, Inc., Winnipeg, Canada) In: Canadian Symposium on Remote Sensing, 7th, Winnipeg, Canada, September 8-11, 1981, Proceedings. Ottawa, Canadian Aeronautics and Space Institute, 1982, p. 20-29.

A83-14230#
OPERATIONAL LAND COVER TYPE MAPPING IN ONTARIO BY LANDSAT BASED DIGITAL ANALYSIS AND MAP PRODUCTION
S. PALA, T. J. ELLIS, and D. B. WHITE (Ontario Centre for Remote Sensing, Toronto, Canada) In: Canadian Symposium on Remote Sensing, 7th, Winnipeg, Canada, September 8-11, 1981, Proceedings. Ottawa, Canadian Aeronautics and Space Institute, 1982, p. 42-50. refs

A83-14232#
A POSITION-BASED RESOURCE MAPPING STUDY OF THE KANANASKIS VALLEY USING LANDSAT
G. D. LODWICK and S. H. PAINE (Calgary, University, Calgary, Alberta, Canada) In: Canadian Symposium on Remote Sensing, 7th, Winnipeg, Canada, September 8-11, 1981, Proceedings. Ottawa, Canadian Aeronautics and Space Institute, 1982, p. 63-66. refs

For effective management of natural resources, environmental monitoring is necessary on a temporal basis. To enable quantitative evaluation of changes, details are also required concerning the spatial distribution of ground-cover types. All this information can be stored efficiently using a position-based land information system. In non-urban areas, Landsat data can be used to provide a basic framework for such a land information system. The coverage, the repetitive nature of the imagery and the resolution are all suitable for resources monitoring. This paper describes the application of a general position-based resource mapping system using Landsat, recently developed in Australia, to environmental monitoring in the Kananaskis Valley, Alberta. A common grid, used to resample the rectified pixel data, provides the basis for the land information system to which conventional survey and mapping data can be appended. (Author)

A83-14238#
ENVIRONMENTAL MONITORING OF THE ATHABASCA OIL SANDS REGION
S. ARONOFF (California, University, Berkeley, CA), G. A. ROSS, and W. A. ROSS (Calgary, University, Calgary, Alberta, Canada) In: Canadian Symposium on Remote Sensing, 7th, Winnipeg, Canada, September 8-11, 1981, Proceedings. Ottawa, Canadian Aeronautics and Space Institute, 1982, p. 100-109. Research supported by the Canada Centre for Remote Sensing, Alberta Oil Sands Environmental Research Program, and TES Research and Consulting, Ltd. refs

This study was designed to examine the application of remote sensing to environmental monitoring of the 30,000 square km region under the jurisdiction of the Alberta Oil Sands Environmental Research Program (AOSERP) and to demonstrate appropriate ways to integrate field-acquired and remotely-sensed data. False color infrared aerial photography acquired during the period of maximum foliage development was found to be most valuable for vegetation

mapping and the detection of environmental disturbance. Thermal infrared night-time imagery, used with true color aerial photography, was found to be most valuable in the detection of thermal anomalies related to water features and in the analysis of oil sands plant sites. Landsat color composite transparencies were found to be valuable in providing an overview of the major ecological communities in the area, and of the progress of land-clearing operations. Digital analysis of two summer images was done using the computer-based image analysis system at the Canada Centre for Remote Sensing in Ottawa. Change detection analysis of open water, cleared land, and vegetation appeared to be the most valuable application of Landsat digital data to environmental monitoring of the region (Author)

A83-14242#
VEGETATION AND HUMAN IMPACT MAPPING FOR THE MANAGEMENT OF THE SUNSHINE AREA, CANADIAN ROCKY MOUNTAINS
M. PRICE (F. G. Bercha and Associates, Ltd., Calgary, Alberta, Canada) In: Canadian Symposium on Remote Sensing, 7th, Winnipeg, Canada, September 8-11, 1981, Proceedings. Ottawa, Canadian Aeronautics and Space Institute, 1982, p. 137-141. Research supported by Parks Canada, Sunshine Village, Ltd., and University of Calgary. refs

A83-14250#
ECOLOGICAL LAND CLASSIFICATION IN THE YUKON
E. T. OSWALD (Canadian Forestry Service, Pacific Forest Research Centre, Victoria, British Columbia, Canada) In: Canadian Symposium on Remote Sensing, 7th, Winnipeg, Canada, September 8-11, 1981, Proceedings. Ottawa, Canadian Aeronautics and Space Institute, 1982, p. 206-210. refs

A multistage inventory procedure using several remote sensing techniques has been used to assess the renewable resources of the Yukon territory. Satellite imagery provides a broad overview of the terrain and identifies large-scale vegetational differences. It is also useful for identifying such dynamic events as forest fires. Conventional photography is useful for more detailed work, such as identifying surficial materials and specific types of vegetation or soil. Photographs taken by hand-held 35-mm cameras are useful for field checking in connection with other remotely sensed data. S.C.S.

A83-14263#
REMOTE SENSING AND WASTE MANAGEMENT
J. E. HAYNES (Gartner Lee Associates, Ltd., Markham, Ontario, Canada), G. M. WOOD (Ontario Ministry of the Environment, Waste Management Branch, Toronto, Canada), G. LAWRENCE (Intertech Remote Sensing, Ltd., Ottawa, Canada), and H. H. BOURQUE (M. M. Dillon, Ltd., Edmonton, Alberta, Canada) In: Canadian Symposium on Remote Sensing, 7th, Winnipeg, Canada, September 8-11, 1981, Proceedings. Ottawa, Canadian Aeronautics and Space Institute, 1982, p. 316-322.

Four remote sensing techniques - archival black and white, color, and color infrared photography plus thermograph - are examined to ascertain which is most suitable for waste management. Six landfill sites in southern Ontario are used in evaluating techniques for locating landfilled areas, monitoring operational practices, and monitoring surface discharges of leachate. The suitability of color and color infrared photography and thermography for monitoring active leachate discharge from landfill sites is discussed. Color and color infrared film exposed at either 1:8000 or 1:6000 scale throughout 1980 is analyzed, noting that predawn thermography was flown in March, April, and November 1980. It is found that the 1980 photography and thermography identified current site conditions and located some surface leachate discharges. Site conditions and restrictions inherent in each remote sensing technique, however, prevented complete detection of leachate discharge. What is more, all the data required some understanding of landfills and site physical setting to be fully interpreted. C.R.

A83-14277#
THE USE OF SATELLITE INFORMATION IN WEATHER FORECASTING AT THE PACIFIC WEATHER CENTRE
L. R. LEGAL (Department of the Environment, Atmospheric Environment Service, Vancouver, Canada) In: Canadian Symposium on Remote Sensing, 7th, Winnipeg, Canada, September 8-11, 1981, Proceedings. Ottawa, Canadian Aeronautics and Space Institute, 1982, p. 429-435. refs

Projected impacts of the development of a satellite meteorological ground station in Vancouver to compensate for the termination of an ocean-based meteorological station, Papa, are assessed. Currently, GOES satellite data, containing imagery, derived vertical temperature and moisture profiles, and winds aloft data are received in San Francisco and relayed to Vancouver, while polar orbitting satellite data are received in Edmonton for relay. Of primary meteorological interest in Canada are migratory high and low pressure systems on a scale of 1000-5000 km. It is noted that predictions of frost onset, low clouds, fog, thunderstorms, and icing hazards using satellite data have been historically verified. The new station will accept visual and IR images, have color enhancement, animation, and overlay capabilities for use with the GOES data. M.S.K.

A83-14292#
RESULTS OF STEREOSCOPIC IMAGE SIMULATIONS FOR THE SPOT HRV CARRIED OUT AT THE GUN LAKE SITE IN BRITISH COLUMBIA [RESULTATS DE SIMULATIONS D'IMAGES STEREOSCOPIQUES HRV SPOT SUR LE SITE DE GUN LAKE, C.B.]
R. SIMARD (Department of Energy, Mines, and Resources, Ottawa, Canada) In: Canadian Symposium on Remote Sensing, 7th, Winnipeg, Canada, September 8-11, 1981, Proceedings. Ottawa, Canadian Aeronautics and Space Institute, 1982, p. 541-551. In French. refs

Results are presented of simulations of stereoscopic visible high resolution images taken by the French SPOT satellite over an 18 square kilometer area in the Canadian Rockies. The simulated images were produced with the help of MSS data from the Daedalus sensor and of a numerical model of the terrain. The methodology is discussed for both vertical and lateral views of the terrain and for the automated reconstitution of the numerical model. The results are presented in the form of stereoscopic pairs which can be viewed three-dimensionally by means of a pocket stereoscope. C.D.

A83-14305
INVESTIGATING THE POSSIBILITY OF PRODUCING A LAND-USE MAP FOR CUBA ON THE BASIS OF SPACE IMAGERY [ISSLEDOVANIE VOZMOZHNOSTI SOSTAVLENIIA KARTY ISPOL'ZOVANIIA ZEMEL' TERRITORII KUBY PO KOSMICHESKIM SNIMKAM]
L. FERNANDES (Moskovskii Gosudarstvennyi Universitet, Moscow, USSR) Issledovanie Zemli iz Kosmosa, Sept.-Oct. 1982, p. 29-35. In Russian.

An attempt is made to use space imagery in conjunction with standard photogrammetric devices and interpretation tools for producing a land-use map for one of the eastern regions of Cuba. It is shown that the use of the space techniques makes it possible to obtain simultaneously, in the shortest time possible, a series of small land-use maps without having to await the production of larger-scale maps. V.L.

A83-14504
A STUDY OF ATMOSPHERIC DIFFUSION FROM THE LANDSAT IMAGERY
Y. VISWANADHAM and J. A. TORSANI (Instituto de Pesquisas Espaciais, Sao Jose dos Campos, Sao Paulo, Brazil) Journal of Geophysical Research, vol. 87, Nov. 20, 1982, p. 9621-9635. Financiadora de Estudos e Projetos refs
(Contract FINEP-B/54-81-042-00-00)

Landsat multispectral scanner (MSS) data of smoke plumes that originated in eastern Cabo Frio (22 deg, 59 min S; 42 deg, 02 min W), in Brazil, and crossed over into the Atlantic are analyzed

and presented to illustrate the way in which high-resolution Landsat imagery can aid in evaluating specific air pollution events. Conventional interpretation techniques are applied to analyze the images in such a way as to arrive at certain plume characteristics. Analysis of the visible smoke plumes reveals that the plume was 130 km long and attained a maximum width of 937 m, 10 km away from the chimney emitting the effluent. The results show that diffusion is governed mainly by water and air temperature differences. With colder water, low-level air is extremely stable and the vertical diffusion is minimal; water warmer than the air, however, induces vigorous diffusion. C.R.

A83-14632
AN OPTIMUM STATISTICAL TECHNIQUE FOR OZONE PROFILE RETRIEVAL FROM BACKSCATTERED UV RADIANCES
W. H. SCHNEIDER, P. K. BHARTIA, K. F. KLENK (Systems and Applied Sciences Corp., Riverdale, MD), and C. L. MATEER (Department of the Environment, Atmospheric Environment Service, Downsview, Ontario, Canada) In: Conference on Atmospheric Radiation, 4th, Toronto, Canada, June 16-18, 1981, Preprints. Boston, MA, American Meteorological Society, 1981, p. 33-37.

A83-16713#
AUTOMATED MEASUREMENTS OF ATMOSPHERIC VISIBILITY
W. VIEZEE and W. E. EVANS (SRI International, Menlo Park, CA) American Institute of Aeronautics and Astronautics, Aerospace Sciences Meeting, 21st, Reno, NV, Jan. 10-13, 1983, 7 p. Research supported by the Electric Power Research Institute.
(AIAA PAPER 83-0436)

The concept of using a solid-state, linear-array imaging device coupled with computerized scene analysis and display to measure daytime atmospheric visibility is described. Computer software is implemented for routine conversion of observed target and sky radiances into measurements of horizon contrast, visual range, target color impairment, and target modulation depth, i.e., target texture and clarity. An assembled, working instrument has been applied to field measurements. Several examples of field measurements are presented. The instrument is fully automated, and is available for visibility research; its applicability to routine visibility monitoring and as an operational tool for aircraft operations is explored. (Author)

A83-16714#
ARCTIC HAZE AND THE ARCTIC GAS AND AEROSOL SAMPLING PROGRAM /AGASP/
R. C. SCHNELL (Cooperative Institute for Research in Environmental Sciences, Boulder, CO) American Institute of Aeronautics and Astronautics, Aerospace Sciences Meeting, 21st, Reno, NV, Jan. 10-13, 1983, 7 p. NOAA-Navy-Army-supported research. refs
(AIAA PAPER 83-0439)

The spring atmosphere in the Arctic has been observed to have anthropogenic pollution levels (Arctic haze) equivalent to those in cities such as Denver and Los Angeles. These high carbon content aerosols (efficient energy absorbers) have a probable Eurasian source. Model studies suggest that aerosol-induced heating has the potential of reducing the Arctic ice cap. A multi-agency group is undertaking an airborne study of the phenomenon using the long range NOAA WP-3D research aircraft. This research will characterize the physical and chemical aspects of the haze constituents and determine their distribution and trajectories. In situ radiative effects will also be measured. Together, these measurements will allow for closing the loop on theory and modeling of the effects of Arctic haze. Aerosol data will be used to determine the applicability of using the proposed NOAA-Air Force-NASA Wind Satellite (WINDSAT) for the measurement of tropospheric wind in the Arctic. (Author)

A83-17248
RADAR SIGNATURES OF TERRAIN - USEFUL MONITORS OF RENEWABLE RESOURCES
F. T. ULABY (University of Kansas Center for Research, Inc., Lawrence, KS) IEEE, Proceedings, vol. 70, Dec. 1982, p. 1410-1428. refs

A general overview of the backscattering behavior of terrain surfaces is presented, and the potential use of radar in the monitoring of renewable resources is examined. Imaging radar fundamentals are discussed with regard to real-aperture radar, synthetic-aperture radar, and the Seasat SAR. The backscattering behavior of natural targets is considered with attention given to penetration depth, angular response, and frequency response. Three applications of remote sensing are examined: the mapping of soil moisture content, the identification of crop types and the monitoring of crop vigor, and the monitoring of snowpack dynamics. Possible future trends in the development of space SARs are considered. B.J.

N83-10645*# General Electric Co., Philadelphia, Pa. Space Systems Div.
TECHNOLOGY NEEDS ASSESSMENT OF AN ATMOSPHERIC OBSERVATION SYSTEM FOR TROPOSPHERIC RESEARCH MISSIONS, PART 1 Final Report, Jul. 1980 - Mar. 1981
D. R. ALVARADO, M. H. BORTNER, R. N. GRENDA, G. G. FRIPPEL, H. HALSEY, S. L. NESTE, H. KRITIKOS (Pennsylvania Univ., Philadelphia), L. S. KEAFER (NASA, Langley Research Center), and L. J. DERYDER Washington NASA Sep. 1982 249 p refs
(Contract NAS1-16312)
(NASA-CR-3556; NAS 1.26:3556) Avail: NTIS HC A11/MF A01 CSCL 13B

The technology advancements needed to implement the atmospheric observation satellite systems for air quality research were identified. Tropospheric measurements are considered. The measurements and sensors are based on a model of knowledge objectives in atmospheric science. A set of potential missions and attendant spacecraft and sensors is postulated. The results show that the predominant technology needs will be in passive and active sensors for accurate and frequent global measurements of trace gas concentration profiles. Author

N83-10646*# General Electric Co., Philadelphia, Pa. Space Systems Div.
TECHNOLOGY NEEDS ASSESSMENT OF AN ATMOSPHERIC OBSERVATION SYSTEM FOR MULTIDISCIPLINARY AIR QUALITY/METEOROLOGY MISSIONS, PART 2 Final Report, Mar. 1981 - Feb. 1982
U. R. ALVARADO, M. H. BORTNER, R. N. GRENDA, W. F. BREHM, G. G. FRIPPEL, F. ALYEA, H. KRAIMAN, P. FOLDER, and L. KROWITZ (Krowitz (Lowell) Associates) Washington NASA Sep. 1982 252 p refs
(Contract NAS1-16312)
(NASA-CR-3557; NAS 1.26:3557) Avail: NTIS HC A12/MF A01 CSCL 13B

The technology advancements that will be necessary to implement the atmospheric observation systems are considered. Upper and lower atmospheric air quality and meteorological parameters necessary to support the air quality investigations were included. The technology needs were found predominantly in areas related to sensors and measurements of air quality and meteorological measurements. Author

N83-11639# Geological Survey, Washington, D. C.
GEOGRAPHIC RESEARCH IN THE US GEOLOGICAL SURVEY: BIBLIOGRAPHY, 1966 - 1980
M. E. GRAZIANI 1982 63 p
(USGS-CIRC-865) Avail: NTIS HC A04/MF A01

Geographic research, particularly research utilizing remotely sensed data is reported in approximately 390 references. Testing the use of satellite and high altitude remotely sensed data in a geographic context is covered. N.W.

N83-12507*# National Aeronautics and Space Administration. Ames Research Center, Moffett Field, Calif.
LANDSAT LAND COVER ANALYSIS COMPLETED FOR CIRSS/SAN BERNARDINO COUNTY PROJECT Final Report
W. LIKENS, K. MAW (Technicolor Graphic Services, Inc., Mountain View, Calif.), and D. SINNOTT, Principal Investigators Oct. 1982 29 p refs ERTS
(E83-10024; NASA-TM-84244; A-8920; NAS 1.15:84244) Avail: NTIS HC A03/MF A01 CSCL 08B

The LANDSAT analysis carried out as part of Ames Research Center's San Bernardino County Project, one of four projects sponsored by NASA as part of the California Integrated Remote Sensing System (CIRSS) effort for generating and utilizing digital geographic data bases; is described. Topics explored include use of data-base modeling with spectral cluster data to improve LANDSAT data classification, and quantitative evaluation of several change techniques. Both 1976 and 1979 LANDSAT data were used in the project. Author

N83-12599# World Meteorological Organization, Geneva (Switzerland).
ON THE DEVELOPMENT OF MULTIMEDIA MONITORING OF ENVIRONMENTAL POLLUTION
1980 551 p refs Symp. held in Riga, USSR, 12-15 Dec. 1978 Original contains color illustrations
(WMO-563; SER-15; ISBN-92-63-10563-4) Avail: NTIS MF A01; print copy available at WMO, Geneva

Theoretical and practical approaches to integrated monitoring, including migration of pollutants between different geophysical media, and effects of pollutants on flora and fauna are discussed. Sessions were devoted to the scientific basis and aims of monitoring systems, levels of pollution, the spread and cycles of pollutants, and assessment and forecasting of the impact of pollutants on ecosystems and climate.

N83-12620# Hydrometeorological Centre of the USSR (Moscow). Inst. of Applied Geophysics.
AIRCRAFT AND REMOTE MEASUREMENTS OF ATMOSPHERIC TRANSPORT OF POLLUTANTS WITHIN THE GLOBAL INTEGRATED MONITORING SYSTEM
V. A. IONOV, I. M. NAZAROV, and S. D. FRIDMAN *In* WMO On the Develop. of Multimedia Monitoring of Environ. Pollution p 211-217 1980 refs
Avail: NTIS MF A01; print copy available at WMO, Geneva

The value of aircraft sampling for obtaining data on circulation and transport of air pollutants for determinations of concentrations is pointed out. Active remote sensing techniques using lasers, and passive methods using the Sun or the studied gas itself as electromagnetic radiation sources are mentioned. The concentration field of mercury vapor was investigated over the USSR and adjacent seas, and concentrations of sulfates from industrial sources and the eruption of the Tolbachik volcano in 1975 were studied partly through aircraft sampling. Maximum sulfate concentrations observed at altitudes near the 850 to 925 mb surfaces show the necessity for data exchange using the 925 mb level. Author (ESA)

N83-12648# Hydrometeorological Centre of the USSR (Moscow). Voeikov Main Geophysical Observatory.
MONITORING OF METEOROLOGICAL ELEMENTS IN A COMPOSITE PROGRAM FOR ENVIRONMENTAL POLLUTION STUDIES
N. A. PETROV *In* WMO On the Develop. of Multimedia Monitoring of Environ. Pollution p 497-506 1980 refs
Avail: NTIS MF A01; print copy available at WMO, Geneva

The need for meteorological observations for the assessment and prediction of pollution dispersion and for measuring the impact of pollution on weather and climate is examined. Methods using spatial comparison can be used for studying mesoscale phenomena, such as the influence of a large city on weather and climate. Methods of temporal comparison, when atmospheric response before and after the event are appropriate for analyses of severe short-term events, such as volcanic eruptions are given. Remaining problems to be solved as part of environmental monitoring efforts include: (1) optimal unification and task distribution in the information acquisition between individual observing subsystems (ground based, satellites, aircraft, etc.); (2) development of new measuring techniques, especially for radiation characteristics, and their metrological maintenance; (3) establishment of subsystems for data collection, processing and retrieval; and (4) development of scientific guidance for the observing systems and techniques. Author (ESA)

N83-12650# Hydrometeorological Centre of the USSR (Moscow). Inst. of Experimental Meteorology.
INSTRUMENTS AND METHODS FOR MONITORING BACKGROUND SOIL POLLUTION
E. BABKINA, G. BELOV, T. BOBOVNIKOVA, E. VIRCHENKO, Y. GAZIEV, S. MALAKHOV, E. MAKHONKO, L. NAZAROV, and A. SHILINA *In* WMO On the Develop. of Multimedia Monitoring of Environ. Pollution p 507-570 1980 refs
Avail: NTIS MF A01; print copy available at WMO, Geneva

Airborne instruments used for aerosol sampling in the troposphere include an airlock aerosol sampler Vega-I and a three-stage impactor IFAZ with outlet filter. Measurements are made at flight heights between 0.5 and 10 km. Volumetric sampler output at the indicated speed of the aircraft of 350 km/hr amounts to 160 and 230 cu m/hr at heights of 0.5 and 10 km for Vega-I and for IFAZ impactor 470 and 720 cum/hr respectively. A multistage impactor which can obtain nine dispersed phases of aerosols is used for surface aerosol sampling. Pesticides are sampled on slides impregnated with ethylene glycol. Soil sampling is carried out using the method of soil geochemical profiles, i.e., a narrow soil section stretched in one direction that crosses different elements of relief and biogeocenoses. Gas chromatography, atomic absorption spectroscopy and neutron activation are used for trace element determination. Author (ESA)

N83-13703# Instituto de Pesquisas Espaciais, Sao Jose dos Campos (Brazil). Div. de Aplicacoes Meteorologicas.
AN INTRODUCTION TO PROJECT FREEZE [PROJETO GEADA: APRESENTACAO]
F. C. ALMEIDA Jun. 1982 30 p refs In PORTUGUESE; ENGLISH summary
(INPE-2435-NTE/186) Avail: NTIS HC A03/MF A01

The use of infrared imagery from meteorological satellites to record and locate freezing temperatures in subtropical Brazil is described. Techniques employed during the testing phase of the project are examined. The use of environmental satellites for freeze monitoring and the application of these methods to monitor the severe frosts of the winter of 1981 are discussed.
Transl. by J.D.

N83-14571*# California Inst. of Tech., Pasadena.
DEVELOPMENT OF MATHEMATICAL TECHNIQUES FOR THE ASSIMILATION OF REMOTE SENSING DATA INTO ATMOSPHERIC MODELS Final Technical Report
J. H. SEINFELD, Principal Investigator 1982 106 p refs ERTS
(Contract NAG1-71)
(E83-10062; NASA-CR-169574; NAS 1.26:169574) Avail: NTIS HC A06/MF A01 CSCL 13B

The problem of the assimilation of remote sensing data into mathematical models of atmospheric pollutant species was investigated. The data assimilation problem is posed in terms of the matching of spatially integrated species burden measurements to the predicted three-dimensional concentration fields from atmospheric diffusion models. General conditions were derived for the reconstructability of atmospheric concentration distributions from data typical of remote sensing applications, and a computational algorithm (filter) for the processing of remote sensing data was developed. M.G.

N83-14581*# Instituto de Pesquisas Espaciais, Sao Jose dos Campos (Brazil).
METHOD OF INTERPRETATION OF REMOTELY SENSED DATA AND APPLICATIONS TO LAND USE [METODOGIA DE INTERPRETACAO DE DADOS DE SENSORIAMENTO REMOTO E APLICACOES NO USO DA TERRA]
N. D. J. PARADA, Principal Investigator, A. P. DOSSANTOS, C. FORESTI, E. M. L. DEMORAESNOVO, M. NIERO, and M. A. LOMBARDO Nov. 1981 65 p refs In PORTUGUESE; ENGLISH summary Sponsored by NASA ERTS
(E83-10072; NASA-CR-169583; NAS 1.26:169583; INPE-2261-MD/016) Avail: NTIS HC A04/MF A01 CSCL 08B

Instructional material describing a methodology of remote sensing data interpretation and examples of applicatons to land use survey are presented. The image interpretation elements are discussed for different types of sensor systems: aerial photographs, radar, and MSS/LANDSAT. Visual and automatic LANDSAT image interpretation is emphasized. Author

N83-14615# Environmental Analysis and Remote Sensing, Delft (Netherlands).
THE GROUP AGROMET MONITORING PROJECT (GAMP)
A. ROSEMA *In* ESA Satellite Remote Sensing for Developing Countries p 61-67 Jun. 1982
Avail: NTIS HC A11/MF A01

The GAMP project, which uses METEOSAT data to monitor rainfall, evaporation, soil moisture, and germination in arid and semiarid regions is described. An area of the Sahelian zone of Mali was monitored in 20 X 30 km blocks using 5 climatic stations and 16 rain gages. The test period was 17 days at the beginning of the growing season. At the start of the period substantial rainfall caused germination, but the young plants were killed by a later drought. Author (ESA)

N83-14622# Florence Univ. (Italy). Ist. Elettronica.
AGROECOLOGICAL CLASSIFICATION BY REMOTE SENSING TECHNIQUES
V. CAPPELLINI, C. CONESE, G. P. MARACCHI, F. MIGLIETTA, and P. PAMPALONI *In* ESA Satellite Remote Sensing for Developing Countries p 111-129 Jun. 1982 refs Prepared in cooperation with CNR, Florence
Avail: NTIS HC A11/MF A01

Temporal multispectral clustering (TMC) and radiation and land morphology automatic mapping (RM) techniques are introduced. Land use classification and inventory maps are presented. The TMC consists of a nonhierarchical cluster algorithm and a multivariate data ordination code. It separates optical scanner data according to their temporal variations. For RM, global radiation values can be obtained by an empirical relationship which depends on the solar coordinates and on the slope and exposure of an identified landscape unity. The slope of each landscape unity can be defined as the ratio between the lowest distance between two points of known elevation, and the relative height increase; its exposure is the geographical direction of this line. The RM algorithm automatically calculates these values, using a digitized contour lines data bank. Author (ESA)

N83-14623# Lund Univ. (Sweden). Lab. of Remote Sensing.
APPROACHES TO DESERTIFICATION MONITORING IN THE SUDAN
U. HELLDEN, L. OLSSON, and M. STERN *In* ESA Satellite Remote Sensing for Developing Countries p 131-144 Jun. 1982 refs
Avail: NTIS HC A11/MF A01

A project for the development, testing and application of environmental monitoring methods for regional studies of desertification and its control, using LANDSAT data, was formulated. Data processing using a geographical data base, population density monitoring, and land use appropriateness versus theoretically optimal land use were studied. Results indicate that LANDSAT can contribute significantly to the development of models which explain desertification status and rate as functions of physical, biological, agricultural, and socioeconomic variables. Author (ESA)

N83-15752*# Utah Univ., Salt Lake City. Center for Remote Sensing and Cartography.
IDENTIFYING ENVIRONMENTAL FEATURES FOR LAND MANAGEMENT DECISIONS Semiannual Report
8 May 1981 32 p refs ERTS
(Contract NSG-7226)
(E83-10109; NASA-CR-169681; NAS 1.26:169681) Avail: NTIS HC A03/MF A01 CSCL 08B

The benefits of changes in management organization and facilities for the Center for Remote Sensing and Cartography in Utah are reported as well as interactions with and outreach to state and local agencies. Completed projects are described which studied (1) Unita Basin wetland/land use; (2) Davis County foothill development; (3) Farmington Bay shoreline fluctuation; (4) irrigation detection; and (5) satellite investigation of snow cover/mule deer relationships. Techniques developed for composite computer mapping, contrast enhancement, U-2 CIR/LANDSAT digital interface; factor analysis, and multivariate statistical analysis are described. A.R.H.

N83-15757*# Kansas Univ., Lawrence. Space Technology Center.
THE APPLICATION OF REMOTE SENSING TO RESOURCE MANAGEMENT AND ENVIRONMENTAL QUALITY PROGRAMS IN KANSAS Annual Report, 1 Apr. 1981 - 31 Mar. 1982
B. G. BARR and E. A. MARTINKO, Principal Investigators Jul. 1982 234 p Original contains imagery. Original photography may be purchased from the EROS Data Center, Sioux Falls, S.D. 57198 ERTS
(Contract NGL-17-004-024)
(E83-10114; NASA-CR-169697; NAS 1.26:169697) Avail: NTIS HC A11/MF A01 CSCL 05A

Capabilities to process data for state agencies in Kansas were upgraded through the vehicle of a low cost data processing system. Short term projects in which agencies identified areas of immediate needs, and longer terms projects, continued from previous years, are described including studies of Arkansas River irrigation; evaluation of rangeland in the Cimarron National Grassland; a model of the Walnut Creek watershed groundwater; selection of a pronghorn antelope release site; the establishment of a geographical data base for tax reassement in Finney County; a land use/land cover inventory and hazards assessment; and applied R & D in agricultural remote sensing. The topics discussed at a short course in remote sensing and publications are listed. A.R.H.

03

GEODESY AND CARTOGRAPHY

Includes mapping and topography.

A83-10078* Jet Propulsion Lab., California Inst. of Tech., Pasadena.
DRUMLIN FIELDS AND GLACIATED MOUNTAINS - A CONTRAST IN GEOMORPHIC PERCEPTION FROM SEASAT RADAR IMAGES
J. P. FORD (California Institute of Technology, Jet Propulsion Laboratory, Pasadena, CA) In: International Geoscience and Remote Sensing Symposium, Washington, DC, June 8-10, 1981, Digest. Volume 2. New York, Institute of Electrical and Electronics Engineers, 1981, p. 864-869. refs
(Contract NAS7-100)

Digitally correlated Seasat synthetic-aperture radar (SAR) images of the Alaska Range, Alaska, and the drumlin-drift belt in Ireland are analyzed for the perception and identification of geomorphic features. The two terrains display strongly contrasted

types of glacial topography whose identification in each case is related to the geometry of the Seasat imaging radar. Identification of terrain shape and form is important within the caveats imposed by the intrinsic distortions on the radar images. Image texture serves coarsely to distinguish topography. Image tones are scene-dependent and do not uniquely identify specific targets. Extensive alignments of linear and curvilinear features provide some of the more important image information from which to make geologic interpretations in each case. (Author)

A83-10981
LOW THRESHOLD INGAASP/INP LASERS WITH MICROCLEAVED MIRRORS SUITABLE FOR MONOLITHIC INTEGRATION
U. KOREN, A. HASSON, K. L. YU, T. R. CHEN, S. MARGALIT, and A. YARIV (California Institute of Technology, Pasadena, CA) Applied Physics Letters, vol. 41, Nov. 1, 1982, p. 791-793. Navy-USAF-supported research. refs

Low threshold InGaAsP/InP injection lasers on semiinsulating InP substrates have been developed with mirrors fabricated by the microcleavage technique. Miniature suspended bridges containing the laser channels have been formed and then microcleavage has been accomplished by the use of ultrasonic vibrations. Lasers with current thresholds as low as 18 mA with 140 micron cavity length and with 35-45 percent differential quantum efficiency have been obtained. (Author)

A83-12877
DEFENSE MAPPING AGENCY /DMA/ OVERVIEW OF MAPPING, CHARTING, AND GEODESY /MC&G/ APPLICATIONS OF DIGITAL IMAGE PATTERN RECOGNITION
W. C. MAHONEY (U.S. Defense Mapping Agency, Aerospace Center, St. Louis, MO) In: Techniques and applications of image understanding; Proceedings of the Meeting, Washington, DC, April 21-23, 1981. Bellingham, WA, SPIE - The International Society for Optical Engineering, 1981, p. 11-23.

DMA applications of digital image pattern recognition are discussed with reference to geometric modeling; data base stereo reconstruction; the application of stereo reconstruction functions; the complexity of mapping, charting, and geodesy pattern recognition processes; and the design of hierarchical rule-structures. The complexity of pattern recognition interaction with the digital processes is indicated, especially as it affects geometric modeling in the generation of digital terrain elevation data and digital feature analysis data. The current standards of manhour performance associated with these data bases are presented, and the need for an improved capability to extract data at all required levels of detail density is discussed. It is concluded that digital image processing and exploitation has already demonstrated application to a wide range of individual mapping, charting, and geodesy problems. B.J.

A83-14237#
MONITORING REVISION REQUIREMENTS FOR CANADIAN MAPS
E. FLEMING (Department of Energy, Mines and Resources, Topographical Survey Div., Ottawa, Canada) In: Canadian Symposium on Remote Sensing, 7th, Winnipeg, Canada, September 8-11, 1981, Proceedings. Ottawa, Canadian Aeronautics and Space Institute, 1982, p. 93-99.

The two principal topographic map series for Canada are the 1:250,000 for which there is complete coverage of the country and the 1:50,000 which is 66% complete. The total maps in these two series which are entered into revision cycles now numbers 9491 and is increasing at the rate of 400 maps per year. Innovative techniques using Landsat imagery are being developed which will facilitate map revision in many parts of the country. Revision of 1:250,000 maps using Landsat as the primary information source is proving operationally feasible. Change detection studies at 1:50,000 are making it possible to plan aerial photography over the areas showing most change and to re-validate those maps on which no change is detected. The geographical areas of the country where these techniques are applicable are being defined. (Author)

A83-14303
LINEAMENTS AND RING STRUCTURES ON THE TERRITORY OF POLAND [LINEAMENTY I KOL'TSEVYE OBRAZOVANIIA TERRITORII POL'SKOI NARODNOI RESPUBLIKI]
IU. BAZHINSKII, B. DANEL-DANELSKAIA, M. GRANICHNYI, and M. VILCHINSKII (Polska Akademia Nauk, Instytut Geologii, Warsaw, Poland) Issledovanie Zemli iz Kosmosa, Sept.-Oct. 1982, p. 20-22. In Russian.

A tectonic map of Poland is presented which shows lineaments and ring structures derived from space imagery. It is suggested that the origin of the lineaments is associated with the tectonic shifts of the folded basement, in particular those that occurred during the recent epoch. V.L.

A83-14857
A SIMPLE RELATION BETWEEN ACTIVE AND PASSIVE MICROWAVE REMOTE SENSING MEASUREMENTS OF EARTH TERRAIN
L. TSANG, A. J. BLANCHARD, R. W. NEWTON (Texas A & M University, College Station, TX), and J. A. KONG (MIT, Cambridge, MA) IEEE Transactions on Geoscience and Remote Sensing, vol. GE-20, Oct. 1982, p. 482-485. refs
(Contract NSF ECS-80-14579)

A simple approximate relation between backscattering coefficient and emissivity measurements is derived. The relation is applicable to active and passive microwave remote sensing of earth terrain where volume scattering plays a dominant role. From the relation, one can obtain a rough estimate of the backscattering coefficient from the emissivity and vice versa. Such estimation is useful in checking experimental measurements and also helps to ascertain the validity of theoretical models. It also safeguards against obtaining arbitrarily high values for both backscattering coefficients and emissivities. (Author)

A83-16239* Geological Survey, Flagstaff, Ariz.
THE GEOLOGY OF EUROPA
B. K. LUCCHITTA and L. A. SODERBLOM (U.S. Geological Survey, Flagstaff, AZ) In: Satellites of Jupiter. Tucson, AZ, University of Arizona Press, 1982, p. 521-555, 940, 941. refs
(Contract PROJECT VOYAGER; NASA ORDER W-13709; NASA ORDER W-08395)

The map units and lineations of Europa are detailed, and the geologic processes, and history, and thick and thin ice models of the satellite are discussed. It is concluded that Europa lacks evidence of a horizontally stratified crust; the geology appears characterized by disruption of the crust and intrusions into an icy shell. The surface consists of plains and mottled terrain, the former being older. Numerous straight and curved lineations, streaks, stripes, and bands cross EuropA's surface on a global and surface scale. Most lineations appear related to fractures in the crust. Five fresh craters in the 10 to 30 km diameter range are visible. The dark spots, stripes, and bands that appear to have replaced sections of the crust suggest that material was transported to the surface from the subjacent silicate lithosphere. The apparent low density of craters superposed on Europa's surface suggests that the surface is about 100 million years old. C.D.

A83-17679
CONCERNING A METHOD FOR THE DETERMINATION OF INITIAL GEODETIC DATA [OB ODNOM METODE USTANOVLENIIA ISKHODNYKH GEODEZICHESKIKH DANNYKH]
F. KH. LAN (Moskovskii Institut Inzhenerov Geodezii, Aerofotos'emki i Kartografii, Moscow, USSR) Geodeziia i Aerofotos'emka, no. 5, 1982, p. 75-78. In Russian. refs

A method for the determination of initial geodetic data is proposed which is based on the use of planetary heights of the quasi-geoid. It is shown that, within the limits of the territory of Vietnam, the rms deviation of the real geoid from the Krasovskii ellipsoid oriented by this method does not exceed 6 m. It is noted

that the proposed method is suitable for constructing an astronomical-geodetic network over the entire territory which is studied, and is effective in approximating the quasi-geoid to the reference ellipsoid. B.J.

N83-10693# California Univ., Livermore. Lawrence Livermore Lab.
AERIAL GEOLOGIC LOG FROM LIVERMORE, CALIFORNIA TO THE NEVADA TEST SITE, NYE COUNTY, NEVADA
J. L. WAGONER Jan. 1982 121 p refs
(Contract W-7405-ENG-48)
(DE82-018392; UCRL-53217) Avail: NTIS HC A06/MF A01

Some geologic and cultural points of interest along Lawrence Livermore National Laboratory's F-27 flight between Livermore, California, and the Nevada Test Site, Navada are outlined. A geologic history is given for each of the four geologic provinces. Approximately 60 air photos are included which will help the traveler identify specific geologic features. Geologic cross sections of the area from Livermore Valley to Gold Mountain describe the geologic structure across the geologic provinces. A LANDSAT mosaic of the flight path is also included. DOE

N83-11563 Bayerische Akademie der Wissenschaften, Munich (West Germany).
REPORT ON THE SPECIAL PROGRAM 78 SATELLITE GEODESY OF THE TECHNICAL UNIVERSITY OF MUNICH Progress Report, 1980 [DIE ARBEITEN DES SONDERFORSCHUNGSBEREICHES 78 SATELLITENGEODAESIE DER TECHNISCHE UNIVERSITAET NUEMCHEN IM JAHRE 1980]
M. SCHNEIDER Bayerischen Akademie der Wissenschaften. 1981 216 p refs In GERMAN
(ASTRON-GEODAET-ARB-41; ISBN-3-7696-9784-7; ISSN-0340-7691) Avail: Issuing Activity

Various topics include: (1) direction finding; (2) range finding; (3) Doppler measurements; (4) construction of a receiver for radio interferometry; (5) mobile laser range finding system; (6) figure-and field parameter determination/geopotential; (7) dynamics of the Earth-Moon system; and (8) kinematics of geodetic point fields. Author (ESA)

N83-11564 Bayerische Akademie der Wissenschaften, Munich (West Germany).
THEORETICAL AND EXPERIMENTAL INVESTIGATIONS ON THE ACCURACY OF CLOSE-RANGE PHOTOGRAMMETRY Ph.D. Thesis - Stuttgart Univ. [THEORETISCHE UND EXPERIMENTELLE UNTERSUCHUNGEN ZUR GENAUIGKEIT DER NAHBEREICHSPHOTOGRAMMETRIE]
W. U. BOETTINGER Bayerischen Akademie der Wissenschaften 1981 148 p refs In GERMAN
(SER-C-266; ISBN-3-7696-9318-3; ISSN-0065-5325) Avail: Issuing Activity

Theoretical and experimental investigations were performed in order to obtain indications, concerning the accuracy in the entire domain of close-range photogrammetry. For all important steps, a theoretical simulation was done and experimentally verified, using well chosen cases. A measuring chamber with high internal stability and equipped with geodetical instruments was constructed. An average point accuracy of + or - 0.05 mm was obtained. The investigation of a conventional calibration and orientation system with regard to its applicability in close-range photogrammetry led to modifications in the system. The orientation accuracy corresponds approximately to that of aerial photography. Adding a third picture for orientation, according to the bundle method, improves the result by 15%. A 50% accuracy improvement occurs in the registration direction for convergence angle of about 30 deg arc and a basis height ratio of 1:1. All theoretical and experimental investigations show that this is the best situation for close-range photogrammetry. Author (ESA)

N83-11571# Naval Surface Weapons Center, Dahlgren, Va.
EVALUATION OF GEODETIC PRODUCTS PRODUCED BY THE NSWC REDUCTION OF SEASAT RADAR ALTIMETER DATA Final Report
S. L. SMITH, III and T. I. HICKS Jun. 1981 36 p refs
(AD-A117837; NSWC/TR-81-260) Avail: NTIS HC A03/MF A01 CSCL 08E

An estimation is made of the possible errors associated with the processing by NSWC of raw SEASAT altimetry data to produce ocean geodetic data, e.g., geoid heights and vertical deflections. Also the noise level of the SEASAT radar altimetry is estimated. Then the SEASAT geodetic data are examined for self-consistency on repeat-track sequences and compared with other independent geodetic data obtained from ocean gravity surveys by ships. Anomalies in the comparisons are examined to determine probable causes. Author (GRA)

N83-12107# Texas Univ., Austin. Applied Research Lab.
OPERATION AND MAINTENANCE OF GEODETIC SATELLITE OBSERVATORY, MCMURDO, ANTARCTICA Semiannual Report, 1 Oct. 1980 - 31 Mar. 1981
D. L. HONEA and A. J. TUCKER 13 Nov. 1981 16 p 2 Vol.
(Contract NSF DPP-68-00508)
(PB82-187923; ARL-TR-81-49) Avail: NTIS HC A02/MF A01 CSCL 22D

Data acquisition and tracking procedures for navigation and beacon satellites maintenance and repair of electronic equipment, and physical upkeep of the station are summarized. The data gathered were used in geodetic studies, ionospheric investigations, and for navigational purposes. In addition, a program utilizing the refraction term error from the Doppler tracking data as a diagnostic to investigate certain characteristics of the ionsphere was brought into full operation. GRA

N83-13521*# Survey of India, Dehra Dun. Geodetic and Research Branch.
ANALYSIS OF MAGSAT DATA OF THE INDIAN REGION Progress Report, 2 Feb. - 31 May 1982
G. C. AGARWAL and M. G. ARUR 30 Jun. 1982 4 p Sponsored by NASA ERTS
(E83-10027; NASA-CR-169500; NAS 1.26:169500; REPT-4)
Avail: NTIS HC A02/MF A01 CSCL 02C

Data tapes were decoded and 24 tracks over the Indian region were reduced to common elevation. Profiles of raw scalar and vector field data and the residuals along few passes were prepared. An anomaly data set was created from the Investigator-B tape. Data was sampled on an 0.5 deg by 0.5 deg grid. A.R.H.

N83-13524*# Indian Inst. of Geomagnetism, Bombay.
MAGSAT PROJECT Quarterly Report
8 May 1981 1 p Sponsored by NASA ERTS
(E83-10030; NASA-CR-169503) Avail: NTIS HC A02/MF A01 CSCL 05B

Programs for the conversion of MAGSAT tapes (both CHRONICLE and CHRONINT formats) from IBM binary to DEC 10 binary were developed in ASSEMBLY language) and programs for selection of only a particular part of CHRONICLE tape (e.g., passes over the Indian subcontinent) were also prepared. Data on a few selected quiet and disturbed days were studied by substracting the main field, and the anomalies over the Indian region were partly identified on few of the passes. A national Workshop on MAGSAT was arranged. The potentialities and usefulness of MAGSAT data particularly in the study of crustal lithology was discussed. Author

N83-13525*# Purdue Univ., Lafayette, Ind. Dept. of Geosciences.
GRAVITY AND MAGNETIC ANOMALY DATA ANALYSIS Quarterly Progress Report, Apr. - Jun. 1982
L. W. BRAILE, W. J. HINZE, and R. R. B. VONFRESE, Principal Investigators 30 Jun. 1982 1 p Sponsored by NASA ERTS
(E83-10031; NASA-CR-169504) Avail: NTIS HC A02/MF A01 CSCL 05B

Progress on the analysis MAGSAT data is reported. The MAGSAT data from 40 deg S to 70 deg N latitude and 30 deg W to 60 E longitude was reduced to radial polarization. In addition, gravity anomaly data from this area were processed and a variety of filtered maps were prepared for combined interpretation of the gravity and magnetic data in conjunction with structural and tectonic maps of the area. The VERSATEC listings and cross-reference maps of variable and array names for the spherical Earth analysis programs NVERTSM, SMFLD, NVERTG, and GFLD were also prepared. M.G.

N83-13526*# Indian Inst. of Geomagnetism, Bombay.
MAGSAT FOR GEOMAGNETIC STUDIES OVER INDIAN REGION Progress Report, 1 Apr. - 31 Jul. 1982
R. G. RASTOGI, Principal Investigator 1 Aug. 1982 13 p Sponsored by NASA ERTS
(E83-10032; NASA-CR-169505; NAS 1.26:169505; PR-3) Avail: NTIS HC A02/MF A01 CSCL 09B

Software was prepared for removal of the external field due to the ring current and the associated induced part. Fast Fourier transformation was used to analyse the field of lithosphere with and without external current (+ induced internal current) component. A vertical component in the equatorial electrojet current system was identified from MAGSAT records. A.R.H.

N83-13527*# North Carolina State Univ., Raleigh. Dept. of Marine, Earth and Atmospheric Sciences.
MAGSAT AND AEROMAGNETIC DATA OF THE CONTINENTAL US Progress Report
I. J. WON, Principal Investigator 18 Jun. 1982 1 p ERTS
(Contract NAS5-26157)
(E83-10033; NASA-CR-169506) Avail: NTIS HC A02/MF A01 CSCL 05B

The MAGSAT data were used to produce a scalar anomaly map of the U.S. In order to remove the east-west striping anomalies, which are believed to be caused by the low-order polynomials used to reduce the orbital bias errors, a 2-D spectral filtering using the Fourier transform method was applied. The resultant low-pass filtered map, with the east-west stripings removed, resembles much closer the surface aeromagnetic map based on the U.S. MAGNET data. The spectral filtering was also applied to the MAGSAT vector data. Department of Defense gravity data was processed to produce a filtered U.S. gravity map whose spectral contents are comparable to those of the MAGSAT magnetic map. M.G.

N83-13532*# Texas Univ., El Paso. Dept. of Geological Sciences.
CRUSTAL AND UPPER MANTLE STRUCTURE DATA ANALYSIS Quarterly Report, 1 Apr. - 30 Jun. 1982
G. R. KELLER and E. G. LIDIAK, Principal Investigators 30 Jun. 1982 1 p ERTS
(Contract NAS5-26326)
(E83-10038; NASA-CR-169510) Avail: NTIS HC A02/MF A01 CSCL 08G

Approximately 50 seismograms obtained from the National Geophysical and Solar-Terrestrial Data Center were digitized and analysis of surface wave dispersion was begun. M.G.

N83-13537*# Ohio State Univ., Columbus. Dept. of Geodetic Science and Surveying.
BASIC RESEARCH FOR THE GEODYNAMICS PROGRAM Semiannual Status Report, 1 Apr. - 30 Sep. 1982
I. I. MUELLER Oct. 1982 97 p refs Presented at the 18th Gen. Assembly of the Intern. Astron. Union, Patras, Greece, 17-26 Aug. 1982 Submitted for publication
(Contract NAS5-25888; NSG-5265; OSURF PROJ. 711055; OSURF PROJ. 712407)
(NASA-CR-169470; NAS 1.26:169470; SASR-9; SASR-6) Avail: NTIS HC A05/MFA01 CSCL 05B

Work performed and data obtained in geodynamic research is reported. The purpose was to obtain utilization of: (1) laser and very long baseline interferometry (VLBI); (2) range difference observation in geodynamics; (3) development of models for ice sheet and crustal deformations. The effects of adopting new precession, nutation and equinox corrections on the terrestrial reference frame are investigated.

N83-13538*# Ohio State Univ., Columbus. Dept. of Geodetic Science and Surveying.
EFFECTS OF ADOPTING NEW PRECESSION, NUTATION AND EQUINOX CORRECTIONS ON THE TERRESTRIAL REFERENCE FRAME
S. Y. ZHU and I. I. MUELLER *In its* Basic Res. for the Geodyn. Program p 2-18 Oct. 1982 refs
Avail: NTIS HC A05/MF A01

The effects of adopting new definitive precession and equinox corrections on the terrestrial reference frame was investigated. It is noted that: (1) the effect on polar motion is a diurnal periodic term with an amplitude increasing linearly in time whole on UT1 it is a linear term; (2) general principles are given to determine the effects of small rotations of the frame of a conventional inertial reference system (CIS) on the frame of the conventional terrestrial reference system (CTS); (3) seven CTS options are presented, one of which is necessary to accommodate such rotation. Accommodating possible future changes in the astronomical nutation is discussed. The effects of differences which may exist between the various CTS's and CIS's on Earth rotation parameters (ERP) and how these differences can be determined are examined. It is shown that the CTS differences can be determined from observations made at the same site, while the CIS differences by comparing the ERP's determined by the different techniques during the same time period. E.A.K.

N83-13539*# Ohio State Univ., Columbus.
UTILIZATION OF RANGE-DIFFERENCE OBSERVATIONS IN GEODYNAMICS
In its Basic Res. for the Geodyn. Program p 19-45 Oct. 1982
(Contract NAS5-25888)
Avail: NTIS HC A05/MF A01

The utilization of simultaneous laser range differences (SRD) for the determination of Earth orientation and baseline variations is summarized. Results from the Aug. 1980 Lageos data collected during the short MERIT campaign, and simulations for a possible station arrangement for the main campaign are reported. E.A.K.

N83-13540*# Ohio State Univ., Columbus. Dept. of Geodetic Science and Surveying.
GEOMETRIC ADJUSTMENT OF SIMULTANEOUS DOPPLER-DERIVED RANGE DIFFERENCES
C. ZHANG and I. I. MUELLER *In its* Basic Res. for the Geodyn. Program p 46-94 Oct. 1982 refs
Avail: NTIS HC A05/MF A01

A mathematical model for the use of simultaneous Doppler derived correlated ranges in the geometric mode is presented. The model was tested with data taken during the EDOC-2 campaign with different integration intervals. The results of this adjustment are compared with the EDOC-2 adopted solution and those from an uncorrelated model used earlier to provide more economical calculations. It is shown that the correlated mode is superior to the uncorrelated one when the optimum integration interval of 23 seconds is used. E.A.K.

N83-13550# Army Engineer Topographic Labs., Fort Belvoir, Va.
AN ANALYSIS OF A RELAXATION SCHEME TO IMPROVE TERRAIN ELEVATION DATA
M. A. CROMBIE and J. A. SHINE Jul. 1982 27 p refs
(Contract DA PROJ. 4A7-62707-A-855)
(AD-A119257; ETL-0298) Avail: NTIS HC A03/MF A01 CSCL 08B

Elevation matrices derived from correlation of digital stereo images often contain errors resulting from a breakdown of the correlation process. One such matrix was corrected using a relaxation algorithm where each point was given a reliability based on comparison with its nearest and next-nearest neighbors. These reliabilities were then used to determine if and how much a point was to be corrected; the process was iterated. The algorithm removed small error areas, but large erroneous regions were not corrected, even when terrain slope classification information was considered. Author

N83-14566*# Business and Technological Systems, Inc., Seabrook, Md.
MAGSAT ANOMALY FIELD INVERSION AND INTERPRETATION FOR THE US Final Report
M. A. MAYHEW, Principal Investigator 1 Dec. 1982 67 p refs Sponsored by NASA ERTS
(E83-10057; NASA-CR-169591; NAS 1.26:169591; BTS33-82-79/RB) Avail: NTIS HC A04/MF A01 CSCL 08N

Long wavelength anomalies in the total magnetic field measured by MAGSAT over the United States and adjacent areas are inverted to an equivalent layer crustal magnetization distribution. The model is based on an equal area dipole grid at the Earth's surface. Model resolution, defined as the closest dipole spacing giving a solution having physical significance, is about 220 km for MAGSAT data in the elevation range 300-500 km. The magnetization contours correlate well with large scale tectonic provinces. A higher resolution (200 km) model based on relatively noise free synthetic 'pseudodata' is also presented. Magnetic anomaly component data measured by MAGSAT is compared with synthetic anomaly component fields arising from an equivalent source dipole array at the Earth's surface generated from total field anomaly data alone. An excellent inverse correlation between apparent magnetization and heat flow in the western U.S. is demonstrated. A regional heat flow map which is presented and compared with published maps, predicts high heat flow in Nebraska and the Dakotas, suggesting the presence of a 'blind' geothermal area of regional extent. A.R.H.

N83-14589*# Tokyo Univ. (Japan). Geophysics Research Lab.
JAPANESE MAGSAT TEAM Progress Report, 1 Apr. - 31 Jul. 1982
N. FUKUSHIMA, Principal Investigator 5 Aug. 1982 12 p Sponsored by NASA ERTS
(E83-10080; NASA-CR-169590; NAS 1.26:169590; PR-6) Avail: NTIS HC A02/MF A01 CSCL 08G

CHRONINT and investigator B tapes as well as CHRONFIN data are being analyzed using a graphical display to illustrate X,Y,Z components as well as their residuals from the MGST (4/81) model. In addition to surveys of the vicinity of Japan, an aerial magnetic survey was conducted around Syowa Station in the Antarctic. Relative data collected by polar orbiting satellites are also being studied. Techniques used to separate external and internal fields from the vector data along the orbital paths; analysis of the frequency of the toroidal current in the equatorial ionosphere; investigation of the sudden storm commencement observed by MAGSAT; determination of the structure of field aligned currents associated with substorms; and calculation of the total electric current passing through the plane encircled by the MAGSAT orbit are discussed. A.R.H.

N83-14591*# Miami Univ., Fla. School of Marine and Atmospheric Science.
INVESTIGATIONS OF MEDIUM WAVELENGTH MAGNETIC ANOMALIES IN THE EASTERN PACIFIC USING MAGSAT DATA Interim Report, 1 Apr. - 30 Jun. 1982
C. G. A. HARRISON, Principal Investigator Jul. 1982 13 p Sponsored by NASA ERTS
(E83-10083; NASA-CR-169595; NAS 1.26:169595) Avail: NTIS HC A02/MF A01 CSCL 08G

A series of plots illustrating the inversion of MAGSAT scalar anomaly data and the production of scalar anomaly maps at constant altitude are presented and discussed. M.G.

N83-14592*# Office de la Recherche Scientifique et Technique Outre-Mer, Paris (France).
GRAVIMETRIC MAPS OF THE CENTRAL AFRICAN REPUBLIC
J. ALBOUY and R. GODIVIER, Principal Investigators 1982 14 p Sponsored by NASA ERTS
(E83-10084; NASA-CR-169596; NAS 1.26:169596) Avail: NTIS HC A02/MF A01 CSCL 08B

Gravimetric maps of the Central African Republic are described including a map of Bouguer anomalies at 1/1,000,000 in two sections (eastern sheet, western sheet) and a map, in color, of Bouguer anomalies at 1/2,000,000. Instrumentation, data acquisition, calibration, and data correction procedures are discussed. M.G.

N83-14594*# Wisconsin Univ., Madison.
INVESTIGATION OF ANTARCTIC CRUST AND UPPER MANTLE USING MAGSAT AND OTHER GEOPHYSICAL DATA Quarterly Status and Technical Progress Report
C. R. BENTLEY, Principal Investigator 1982 15 p refs ERTS
(Contract NAS5-15977)
(E83-10086; NASA-CR-169597; NAS 1.26:169597; QSTPR-10)
Avail: NTIS HC A02/MF A01 CSCL 08G

Antarctica is the perfect proving ground for testing data reduction procedures which are alternatives to the standard procedure employing polynomial fitting. Unreduced data (observed values minus corefield model theo each pass) were averaged in 3 degree bins. The resulting map was then high pass filtered using a finite Fourier transform filter so that spectral peaks between 4200 km and 5280 km were diminished by 1/3, peaks corresponding to wavelengths greater than or equal to 5280 km were diminished by 1/2, and the d.c. component was set equal to zero. The surface subtracted in this way differs from the polynomials used in the standard method in that it is static over the 5 north data window. The map produced is presented and the effects of the static model are compared to those of the dynamic mode. A.R.H.

N83-14596*# Lamont-Doherty Geological Observatory, Palisades, N. Y.
THE INTERMEDIATE WAVELENGTH MAGNETIC ANOMALY FIELD OF THE NORTH PACIFIC AND POSSIBLE SOURCE DISTRIBUTIONS Final Report
J. L. LABRECQUE, S. C. CANDE, and R. D. JARRARD, Principal Investigators (Arco Oil and Gas Co., Dallas, Tex.) 1983 78 p refs Original contains color illustrations ERTS
(Contract NAS5-25891)
(E83-10088; NASA-CR-169598; NAS 1.26:169598) Avail: NTIS HC A05/MF A01 CSCL 08N

A technique that eliminates external field sources and the effects of strike aliasing was used to extract from marine survey data the intermediate wavelength magnetic anomaly field for (B) in the North Pacific. A strong correlation exists between this field and the MAGSAT field although a directional sensitivity in the MAGSAT field can be detected. The intermediate wavelength field is correlated to tectonic features. Island arcs appear as positive anomalies of induced origin likely due to variations in crustal thickness. Seamount chains and oceanic plateaus also are manifested by strong anomalies. The primary contribution to many of these anomalies appears to be due to a remanent magnetization.

The source parameters for the remainder of these features are presently unidentified ambiguous. Results indicate that the sea surface field is a valuable source of information for secular variation analysis and the resolution of intermediate wavelength source parameters. Author

N83-14597*# MacQuarie Univ., North Ryde (Australia). Centre for Geophysical Exploration Research.
THE MAGSAT PROJECT IN AUSTRALIA Status Report
Sep. 1982 8 p Sponsored by NASA ERTS
(E83-10089; NASA-CR-169599; NAS 1.26:169599) Avail: NTIS HC A02/MF A01 CSCL 05B

The first version of the MAGSAT selection and reduction software was completed as well as a major enhancement to support geomagnetic vector data selection and reduction. All MAGSAT data over an area between 90 E and 180 E and between 0 and 50 S were reduced. This area includes the Australasian region and surrounding oceans. Nearly 200 profiles across Australia satisfied the criteria for data. The reduced geomagnetic field inferred to be caused by sources within the lithosphere was interpreted. During reduction, magnetic effects caused by all other causes were eliminated. Some possible correlation with major tectonic structures and known continental scale heat flow anomalies were noted. A.R.H.

N83-14599*# Energy, Mines and Resources Canada, Ottawa (Ontario). Earth Physics Branch.
THE REDUCTION, VERIFICATION AND INTERPRETATION OF MAGSAT MAGNETIC DATA OVER CANADA Progress Report
R. L. COLES, G. V. HAINES, G. J. VANBEEK, J. K. WALKER, and L. R. NEWITT, Principal Investigators Jul. 1982 2 p Sponsored by NASA ERTS
(E83-10091; NASA-CR-169601; NAS 1.26:169601; PR-6) Avail: NTIS HC A02/MF A01 CSCL 08N

Research into an approach for altitude adjustments for MAGSAT or similar data acquired over a range of altitudes is progressing. The technique shows promise not only in the production of refined anomaly maps but also in the derivation of regional charts of the magnetic elements from satellite and ground data. Correlations between MAGSAT anomalies and other geophysical and geological data are being explored further and quantitative modelling of some features has begun. The form of some anomalies may change as the maps are refined by the technique being developed. Emphasis is being given to the Canadian regions, although analogous features elsewhere are being considered. Author

N83-14600*# Applied Physics Lab., Johns Hopkins Univ., Laurel, Md. Space Physics and Instrumentation Group.
INVESTIGATION OF MAGSAT AND TRIAD MAGNETOMETER DATA TO PROVIDE CORRECTIVE INFORMATION ON HIGH-LATTITUDE EXTERNAL FIELDS Final Report
T. A. POTEMRA, Principal Investigator, M. SUGIURA, and L. J. ZANETTIC Jul. 1982 19 p refs Sponsored by NASA Original contains color imagery. Original photography may be purchased from the EROS Data Center, Sioux Falls, S.D. 57198 ERTS
(E83-10093; NASA-CR-169603; NAS 1.26:169603) Avail: NTIS HC A02/MF A01 CSCL 08N

Disturbances in the MAGSAT magnetometer data set due to high latitude phenomena were evaluated. Much of the categorization of disturbances due to Birkeland currents, ionospheric Hall currents, fine structure and wave phenomena was done with the MAGSAT data catalog. A color graphics technique was developed for the display of disturbances from multiple orbits, from which one can infer a 'global-image' of the current systems of the auroral zone. The MAGSAT 4/81 magnetic field model appears to represent the Earth's main field at high latitudes very well for the epoch 1980. MAGSAT's low altitude allows analysis of disturbances in the magnetometer data due to ionospheric electrojet currents. These current distributions were modeled properly for single events as a precursor to the inference of the Birkeland current system. MAGSAT's orbit was approximately shared with that of the Navy/APL TRIAD satellite. This allowed space-time studies of the magnetic disturbance signatures to be performed, the result being an approximately 75% agreement in, as well as high frequency of, signatures due to Birkeland currents. Thus the field-aligned currents are a steady-state participant in the Earth's magnetospheric current system. M.G.

N83-14601*# Business and Technological Systems, Inc., Seabrook, Md.
EQUIVALENT SOURCE MODELING OF THE MAIN FIELD USING MAGSAT DATA Final Report
M. A. MAYHEW and R. H. ESTES, Principal Investigators May 1982 38 p refs ERTS
(Contract NAS5-26047)
(E83-10094; NASA-CR-169604; NAS 1.26:169604; BTS33-82-60/BR) Avail: NTIS HC A03/MF A01 CSCL 08N

An iterative least squares estimation algorithm with the capability for including a priori statistical information was implemented to recover multiple magnetic dipole models of the Earth's main magnetic field. The dipoles are fixed to a specified radius at or below the core-mantle boundary and centered on equal area blocks. The algorithm can solve for dipole magnitudes only (fixed orientations), or allow full freedom of orientation and solve for vector components. External field parameters and observatory anomaly biases can also be estimated simultaneously. Time dependence is modeled using first time derivatives for dipole vector components. Single-epoch and time dependent dipole models are derived using MAGSAT and observatory annul means data. Equivalent spherical harmonic representation are computed in closed form from the dipole models and compared with truncated spherical harmonic models estimated in the standard way from the same data sets. In particular, a 21 deg spatial resolution model based on 93 dipoles was computed based on observatory annual means data and a selected MAGSAT data set and was compared with candidate IGRF 1975 models and their 1980 secular variation. M.G.

N83-14602*# Analytic Sciences Corp., Reading, Mass.
INVESTIGATING TECTONIC AND BATHYMETRIC FEATURES OF THE INDIAN OCEAN USING MAGSAT MAGNETIC ANOMALY DATA Quarterly Progress Report, 1 Apr. - 30 Jun. 1982
R. V. SAILOR and A. R. LAZAREWICZ, Principal Investigators 19 Jul. 1982 28 p refs Original contains color imagery. Original photography may be purchased from the EROS Data Center, Sioux Falls, S.D. 57198 ERTS
(Contract NAS5-26424)
(E83-10095; NASA-CR-169605; NAS 1.26:169605; PR-1325-6)
Avail: NTIS HC A03/MF A01 CSCL 08E

An equivalent source anomaly map and a map of the relative magnetization for the investigation region were produced. Gravimetry, bathymetry, and MAGSAT anomaly maps were contoured in pseudocolor displays. Finally, an autoregressive spectrum estimation technique was verified with synthetic data and shown to be capable of resolving exponential power spectra using small samples of data. Interpretations were made regarding the relationship between MAGSAT data spectra and crustal anomaly spectra. M.G.

N83-14605*# Joint Inst. for Lab. Astrophysics, Boulder, Colo.
PRELIMINARY STUDY OF GPS ORBIT DETERMINATION ACCURACY ACHIEVABLE FROM WORLDWIDE TRACKING DATA
D. R. LARDEN and P. L. BENDER (NBS, Boulder, Colo.) 1982 6 p refs
(NASA-CR-169693; NAS 1.26:169693) Avail: NTIS HC A02/MF A01 CSCL 08B

The improvement in the orbit accuracy if high accuracy tracking data from a substantially larger number of ground stations is available was investigated. Observations from 20 ground stations indicate that 20 cm or better accuracy can be achieved for the horizontal coordinates of the GPS satellites. With this accuracy, the contribution to the error budget for determining 1000 km baselines by GPS geodetic receivers would be only about 1 cm. E.A.K.

N83-14606*# Joint Inst. for Lab. Astrophysics, Boulder, Colo.
TOPEX ORBIT DETERMINATION USING GPS SIGNALS PLUS A SIDETONE RANGING SYSTEM
P. L. BENDER and D. R. LARDEN 1982 6 p refs Sponsored in part by NASA
(NASA-CR-169694; NAS 1.26:169694) Avail: NTIS HC A02/MF A01

The GPS orbit determination was studied to see how well the radial coordinate for altimeter satellites such as TOPEX could be found by on board measurements of GPS signals, including the reconstructed carrier phase. The inclusion on altimeter satellites of an additional high accuracy tracking system is recommended. It is suggested that a sidetone ranging system is used in conjunction with TRANET 2 beacons. E.A.K.

N83-14656# Naval Surface Weapons Center, Dahlgren, Va.
AN UPPER BOUND ON ERRORS IN THE MEAN-OF-DATE/INSTANTANEOUS EARTH-FIXED VECTOR TRANSFORMATION INDUCED BY INTERPOLATED NUTATION ANGLES Final Report
A. D. PARKS Jun. 1982 19 p
(AD-A119444; NSWC/TR-82-75) Avail: NTIS HC A02/MF A01 CSCL 12A

An analytic expression for the upper bound on the error induced into a vector modulus by the use of interpolated nutation angles in the coordinate transformation between the mean-of-date reference system and the instantaneous Earth-fixed reference system is derived through first order. This expression is applied to the six-point Lagrange interpolator, using interpolation intervals between 0.25 and 1.00 days, and a quantification of associated upper error bounds for Earth satellite position vector moduli is made. Author (GRA)

N83-14808# Cologne Univ. (West Germany).
DETERMINATION OF THE RADIATION BUDGET AT THE EARTH'S SURFACE FROM SATELLITE DATA
W. MOESER *In its* Satellite Meas. of the Earth Radiation Budget p 156-170 Jul. 1982 refs
Avail: NTIS HC A08/MF A01

The determination of the global Earth surface radiation budget and of the surface albedo is presented. The problem of determining the solar part of the radiation balance equation, especially the global radiation, was solved in various studies because of its interdisciplinary relevance not only for meteorology, but also for agriculture and solar energy purposes. The results show that the errors can be kept on the order of about 10% to 15% for hourly values, but high accuracy is obtained for longer time intervals. The problem of a proper comparison method between the two different measuring geometries (surface measurement - satellite measurement) remains. Surface albedos are to be derived from satellite images except for mountainous and inhomogeneous landscapes because of the various effects of shadowing which can hardly be simulated by radiative transfer theory.
Author (ESA)

N83-15742*# Colorado Univ., Boulder. Dept. of Astro-Geophysics.
DATA USE INVESTIGATION FOR THE MAGNETIC FIELD SATELLITE (MAGSAT) MISSION: GEOMAGNETIC FIELD FORECASTING AND FLUID DYNAMICS OF THE CORE Final Project Report, 27 Dec. 1979 - 26 Nov. 1982
E. R. BENTON, Principal Investigator 8 Oct. 1982 28 p ERTS
(Contract NAS5-25957)
(E83-10098; NASA-CR-169675; NAS 1.26:169675) Avail: NTIS HC A03/MF A01 CSCL 08G

MAGSAT data were used to construct a variety of spherical harmonic models of the main geomagnetic field emanating from Earth's liquid core at poch 1980. These models were used to: (1) accurately determine the radius of Earth's core by a magnetic method, (2) calculate estimates, of the long-term ange of variation of geomagnetic Gauss coefficients; (3) establish a preferred truncation level for current spherical harmonic models of the main geomagnetic field from the core; (4) evaluate a method for taking account of electrical conduction in the mantle when the magnetic field is downward continued to the core-mantle boundary; and (5) establish that upwelling and downwelling of fluid motion at the top of the core is probably detectable, observationally. A fluid dynamics forecast model was not produced because of insufficient data. A.R.H.

N83-15744*# Energy, Mines and Resources Canada, Ottawa (Ontario). Earth Physics Branch.
THE REDUCTION, VERIFICATION AND INTERPRETATION OF MAGSAT MAGNETIC DATA OVER CANADA Progress Report
R. L. COLES, Principal Investigator, G. V. HAINES, G. J. VANBEEK, J. K. WALKER, and L. R. NEWITT Nov. 1982 3 p Sponsored by NASA ERTS
(E83-10101; NASA-CR-169677; NAS 1.26:169677; PR-7) Avail: NTIS HC A02/MF A01 CSCL 05B

Consideration is being given to representing the magnetic field *in the area 40 deg N to 83 deg N by means of functions in* spherical coordinates. A solution to Laplace's equation for the magnetic potential over a restricted area was found, and programming and testing are currently being carried out. Magnetic anomaly modelling is proceeding. The program SPHERE, which was adapted to function correctly on the Cyber computer, is now operational, for deriving gravity and magnetic models in a spherical coordinate system. A.R.H.

N83-15748*# Phoenix Corp., McLean, Va.
GRAVSAT ERROR ANALYSIS BY MEANS OF GLOBAL SPECTRAL ANALYSES OF THE MARINE GEOID FROM SEASAT ALTIMETER DATA Final Report
29 Apr. 1982 38 p refs ERTS
(Contract NAS5-26579)
(E83-10105; NASA-CR-166819; NAS 1.26:166819) Avail: NTIS HC A03/MF A01 CSCL 08E

The geographical variability of short wavelength geoid power spectra (geoid roughness), was mapped for the world's oceans between latitudes 72 deg N and 72 deg S. A spectral analysis of SEASAT altimeter data, reduced to sea surface heights, was performed at 2 minute intervals for 15 consecutive days of the 3-day repeat orbit. The geoid roughness represented by these spectra for wavelengths shorter than about 220 km is separated from the total sea height variance and is displayed in the form of a global contour map. The global average geoid roughness is 32 cm RMS, varying from a high in excess of 2 m RMS near deep ocean trenches to a low of 2 cm RMS in the southeast Pacific near the East Pacific Rise. This average value agrees well with previous estimates based on gravimetry and GEOS-3 altimetry. In general, the smoothest areas in the marine geoid overlie relatively young seafloor adjacent mid-ocean spreading centers, where even short-wavelength topographic variations tend to be isostatically compensated. Author

N83-15755*# Business and Technological Systems, Inc., Seabrook, Md.
GEOMAGNETIC MODELING BY OPTIMAL RECURSIVE FILTERING Final Report
B. P. GIBBS and R. H. ESTES May 1981 119 p refs ERTS
(Contract NAS5-26250)
(E83-10112; NASA-CR-169696; NAS 1.26:169696;
BTS-FR-81-147) Avail: NTIS HC A06/MF A01 CSCL 08G

The results of a preliminary study to determine the feasibility of using Kalman filter techniques for geomagnetic field modeling are given. Specifically, five separate field models were computed using observatory annual means, satellite, survey and airborne data for the years 1950 to 1976. Each of the individual field models used approximately five years of data. These five models were combined using a recursive information filter (a Kalman filter written in terms of information matrices rather than covariance matrices.) The resulting estimate of the geomagnetic field and its secular variation was propogated four years past the data to the time of the MAGSAT data. The accuracy with which this field model matched the MAGSAT data was evaluated by comparisons with

predictions from other pre-MAGSAT field models. The field estimate obtained by recursive estimation was found to be superior to all other models. Author

N83-15763*# Utah Univ., Salt Lake City. Dept. of Mathematics.
SURFACES: REPRESENTATION AND APPROXIMATION
R. E. BARNHILL *In* Texas A and M Univ. Proc. of the NASA Workshop on Surface Fitting p 121-134 1982 refs ERTS
(Contract NSF MCS 81-01854)
Avail: NTIS HC A10/MF A01 CSCL 05B

Schemes for the representation and approximation of surfaces, based on Coon's and triangular patches and blending are discussed. The necessary criteria/characteristics for resulting spaces are outlined. M.G.

04

GEOLOGY AND MINERAL RESOURCES

Includes mineral deposits, petroleum deposits, spectral properties of rocks, geological exploration, and lithology.

A83-10057* Jet Propulsion Lab., California Inst. of Tech., Pasadena.
ROCK TYPE DISCRIMINATION TECHNIQUES USING LANDSAT AND SEASAT IMAGE DATA
R. BLOM, M. ABRAMS, and C. CONRAD (California Institute of Technology, Jet Propulsion Laboratory, Pasadena, CA) In: International Geoscience and Remote Sensing Symposium, Washington, DC, June 8-10, 1981, Digest. Volume 1. New York, Institute of Electrical and Electronics Engineers, 1981, p. 597-602. refs
(Contract NAS7-100)

Results of a sedimentary rock type discrimination project using Seasat radar and Landsat multispectral image data of the San Rafael Swell, in eastern Utah, are presented, which has the goal of determining the potential contribution of radar image data to Landsat image data for rock type discrimination, particularly when the images are coregistered. The procedure employs several images processing techniques using the Landsat and Seasat data independently, and then both data sets are coregistered. The images are evaluated according to the ease with which contacts can be located and rock units (not just stratigraphically adjacent ones) separated. Results show that of the Landsat images evaluated, the image using a supervised classification scheme is the best for sedimentary rock type discrimination. Of less value, in decreasing order, are color ratio composites, principal components, and the standard color composite. In addition, for rock type discrimination, the black and white Seasat image is less useful than any of the Landsat color images by itself. However, it is found that the incorporation of the surface textural measures made from the Seasat image provides a considerable and worthwhile improvement in rock type discrimination. N.B.

A83-10058* Maryland Univ., College Park.
THE ROLE OF GEOLOGICAL SURFACES IN DETERMINING VISIBLE-NEAR INFRA RED SPECTRAL SIGNATURES
S. E. SOMMER and W. F. BUCKINGHAM (Maryland, University, College Park, MD) In: International Geoscience and Remote Sensing Symposium, Washington, DC, June 8-10, 1981, Digest. Volume 1. New York, Institute of Electrical and Electronics Engineers, 1981, p. 603-607. NASA-supported research. refs

The goal of the study described here is to determine new criteria for improved target discrimination in areas of hydrothermal mineralization. It is noted that the portion of materials, that is, geological surfaces detected by sensing devices, must be accurately determined before elemental and mineralogical characterization. The depth from which visible-near infrared radiation is reflected from target surfaces depends on composition and fabric. Reflectance spectra are obtained from binary mixtures of hematite, goethite, kaolinite and montmorillonite with a reflecting sphere spectrometer over a wavelength range of 400-2500 nm. The reflection (or absorption) intensity is plotted vs. the sample thickness (determined by scanning electron microscopy) to determine the sample thickness at which absorption saturates. The optical depth is seen to vary as a function of mineralogy and wavelength. In general, the maximum depth from which reflection features are discerned is from 12 to 47 microns measured in the visible-near infrared spectral region. C.R.

A83-10059
DERIVATION OF COMPOSITIONAL INFORMATION FROM MULTISPECTRAL IMAGES
D. L. EVANS and J. B. ADAMS (Washington, University, Seattle, WA) In: International Geoscience and Remote Sensing Symposium, Washington, DC, June 8-10, 1981, Digest. Volume 1. New York, Institute of Electrical and Electronics Engineers, 1981, p. 608-613. refs

A technique is presented for searching multispectral images in which compositional information is retained throughout the computer processing. The images are examined for materials with known spectral signatures that are related to known composition. The technique involves determining what the spectral response of a material of interest would be at different wavelengths based on laboratory measurements, and searching a stack of spatially registered images for picture elements with the desired spectral signature. Laboratory spectral reflectance curves are compared to Viking Lander and Orbiter images of Mars and Landsat images of Hawaii, and it is concluded that it is possible to derive compositional information from multispectral images. Since the technique need not be limited to visible and near-infrared images, it represents an important tool for geological exploration. C.D.

A83-10060
USE OF REFLECTANCE SPECTRA OF NATIVE PLANT SPECIES FOR INTERPRETING AIRBORNE MULTISPECTRAL SCANNER DATA IN THE EAST TINTIC MOUNTAINS, UTAH
N. M. MILTON (U.S. Geological Survey, Reston, VA) In: International Geoscience and Remote Sensing Symposium, Washington, DC, June 8-10, 1981, Digest. Volume 1. New York, Institute of Electrical and Electronics Engineers, 1981, p. 614-616. refs

A83-10079* Jet Propulsion Lab., California Inst. of Tech., Pasadena.
IMAGING RADAR OBSERVATIONS OF VOLCANIC FEATURES IN MEDICINE LAKE HIGHLAND, CALIFORNIA
T. G. FARR, C. ELACHI, M. DAILY, and R. BLOM (California Institute of Technology, Jet Propulsion Laboratory, Pasadena, CA) In: International Geoscience and Remote Sensing Symposium, Washington, DC, June 8-10, 1981, Digest. Volume 2. New York, Institute of Electrical and Electronics Engineers, 1981, p. 872-877. refs

Synthetic aperture L-band radar images of Medicine Lake Highland, California, as obtained from the JPL-NASA aircraft and Seasat orbital systems, are presented. Image interpretation is based on two types of information: slope and topographic effects for geomorphic information, and reflectivity or backscatter in flat terrain which is related to surface roughness and to the surface dielectric constant. Cinder cones and lava tubes are visible (geomorphic features), and three types of lava surfaces are: aa, pahoehoe, and block. In addition, to infer lava flow relative ages, overlapping flow fronts and roughness attenuation observations may be used. It is hoped that this research will improve the understanding of the radar signature of volcanic areas, and will be helpful in interpreting data obtained from spaceborne sensors over the earth and, in particular, Venus. R.K.R.

A83-10080* Arkansas Univ., Fayetteville.
GEOLOGICAL TERRAIN MODELS
V. H. KAUPP, H. C. MACDONALD, and W. P. WAITE (Arkansas, University, Fayetteville, AR) In: International Geoscience and Remote Sensing Symposium, Washington, DC, June 8-10, 1981, Digest. Volume 2. New York, Institute of Electrical and Electronics Engineers, 1981, p. 879-885. refs
(Contract NAG9-3)

The initial phase of a program to determine the best interpretation strategy and sensor configuration for a radar remote sensing system for geologic applications is discussed. In this phase, terrain modeling and radar image simulation were used to perform parametric sensitivity studies. A relatively simple computer-generated terrain model is presented, and the data base, backscatter file, and transfer function for digital image simulation are described. Sets of images are presented that simulate the results obtained with an X-band radar from an altitude of 800 km and at three different terrain-illumination angles. The simulations include power maps, slant-range images, ground-range images, and ground-range images with statistical noise incorporated. It is concluded that digital image simulation and computer modeling provide cost-effective methods for evaluating terrain variations and sensor parameter changes, for predicting results, and for defining optimum sensor parameters. F.G.M.

A83-10099* Jet Propulsion Lab., California Inst. of Tech., Pasadena.
SOME EXAMPLES OF THE UTILITY OF HCMM DATA IN GEOLOGIC REMOTE SENSING
A. B. KAHLE, J. P. SCHIELDGE, M. J. ABRAMS, and R. E. ALLEY (California Institute of Technology, Jet Propulsion Laboratory, Pasadena, CA) In: International Geoscience and Remote Sensing Symposium, Washington, DC, June 8-10, 1981, Digest. Volume 2. New York, Institute of Electrical and Electronics Engineers, 1981, p. 1183-1188.
(Contract NAS7-100)

Examples of HCMM (Heat Capacity Mapping Mission) data in geologic remote sensing are presented, and the data set is composed of HCMM and aircraft digital scanner data and ground truth data from four western U.S. test sites. Data are used in the thermal model to test thermal data effectiveness, and changes in temperature with depth and time for dry soils are described by the model. It is found that the HCMM thermal inertia image is useful in the separability of bedrock and alluvium in Death Valley, and aa and pahoehoe flows in the Pisgah basalt flow. In a color composite of HCMM day temperature, night temperature, and day visible images of the Pisgah Crater test site, it is possible to distinguish alluvium, playa, aa and pahoehoe basalt flow, rhyolite intrusives, and other elements. Ground checking of units at a few points will extend capabilities to large areas and assist in creating telegeologic maps. R.K.R.

A83-11959
COSMOGEOLOGICAL STRUCTURES OF THE HISSAR ALAI AND THEIR ROLE IN THE DISTRIBUTION OF ENDOGENOUS MINERALIZATION [KOSMOGEOLOGICHESKIE STRUKTURY GISSARO-ALAIA I IKH ROL' V RAZMESHCHENII ENDOGENNOGO ORUDENENIIA]
R. B. BARATOV, K. I. LITVINENKO, and V. N. CHIZHIK (Akademiia Nauk Tadzhikskoi SSR, Institut Geologii; Upravlenie Geologii Tadzhikskoi SSR, Dyushambe, Tadzhik SSR) Akademiia Nauk SSSR, Doklady, vol. 266, no. 4, 1982, p. 928-930. In Russian.

A83-11988
ENVIRONMENTAL MONITORING OF THE ATHABASCA OIL SANDS USING LANDSAT DATA
S. ARONOFF, G. A. ROSS, and W. A. ROSS (Calgary, University, Calgary, Alberta, Canada) Photogrammetria, vol. 38, Oct. 1982, p. 77-86. Research supported by the Alberta Oil Sands Environmental Research Program. refs

The Athabasca Oil Sands have undergone rapid and extensive strip mine development. This activity is expected to resume as the cost of petroleum continues to rise. Sixteen spring, summer, and fall Landsat color composite transparencies at the 1/1 million scale were evaluated for use in environmental monitoring. Roads, cleared areas, and water features were best imaged on the May 1, 1976 color composite. Summer Product 8 imagery (July and August) was most useful for vegetation analysis and also had the best year to year signature consistency. For this reason, summer Product 8 imagery was considered most suitable for environmental monitoring of the oil sands region. Two summer images were overlayed and registered, then changes were classified using a supervised classification algorithm. Change detection analyses of open water, cleared land, and vegetation appeared to be the most valuable applications of Landsat digital data to environmental monitoring of the region. (Author)

A83-12036* Alaska Univ., Fairbanks.
RADAR AND INFRARED REMOTE SENSING OF GEOTHERMAL FEATURES AT PILGRIM SPRINGS, ALASKA
K. G. DEAN, R. B. FORBES, D. L. TURNER, F. D. EATON (Alaska, University, Fairbanks, AK), and K. D. SULLIVAN (NASA, Johnson Space Center, Houston, TX) Remote Sensing of Environment, vol. 12, Nov. 1982, p. 391-405. refs
(Contract NAG9-8)

High-altitude radar and thermal imagery collected by the NASA research aircraft WB57F were used to examine the structural setting and distribution of radiant temperatures of geothermal anomalies in the Pilgrim Springs, Alaska area. Like-polarized radar imagery with perpendicular look directions provides the best structural data for lineament analysis, although more than half the mapped lineaments are easily detectable on conventional aerial photography. Radiometer data and imagery from a thermal scanner were used to evaluate radiant surface temperatures, which ranged from 3 to 17 C. The evening imagery, which utilized density-slicing techniques, detected thermal anomalies associated with geothermal heat sources. The study indicates that high-altitude predawn thermal imagery may be able to locate relatively large areas of hot ground in site-specific studies in the vegetated Alaskan terrain. This imagery will probably not detect gentle lateral gradients.
S.C.S.

A83-12641
CONTRIBUTION OF LANDSAT IMAGERY TO THE STUDY OF VOLCANIC STRUCTURES
M. C. W. BAKER (Open University, Milton Keynes, Bucks., England) (Symposium on Volcanoes of the Earth and Planets, University of Lancaster, Lancaster, England, Mar. 17, 1981.) Geophysical Surveys, vol. 5, Oct. 1982, p. 281-293. Research supported by the Natural Environment Research Council. refs

The principal uses of Landsat imagery in volcanological studies are for regional reconnaisance, for the interpretation of large volcanic structures and to facilitate the comparison of structures in different parts of the world. Standard black and white single band prints and standard false color composites are the cheapest and most readily available forms of Landsat imagery. However, standard Landsat images have a poorer resolution and lower information content than enhanced images. The most generally useful enhancement techniques for volcanic studies have proved to be destriping, contrast stretching and edge enhancement. Enhancement techniques are illustrated with examples of young volcanic structures from the Central Andes. The next few years should see significant advances in satellite remote sensing technology with higher resolution imagery (down to 10-30 m) and imagery in a wider range of spectral bands becoming available.
(Author)

A83-13348* Jet Propulsion Lab., California Inst. of Tech., Pasadena.
SHUTTLE IMAGING RADAR EXPERIMENT
C. ELACHI, W. E. BROWN, J. B. CIMINO, T. DIXON, D. L. EVANS, J. P. FORD, R. S. SAUNDERS (California Institute of Technology, Jet Propulsion Laboratory, Pasadena, CA), C. BREED, H. MASURSKY (U.S. Geological Survey, Flagstaff, AZ), A. ENGLAND (NASA, Johnson Space Center, Houston, TX) et al. Science, vol. 218, Dec. 3, 1982, p. 996-1003. NASA-supported research. refs

The Shuttle imaging radar (SIR-A) acquired images of a variety of the earth's geologic areas covering about 10 million square kilometers. Structural and geomorphic features such as faults, folds, outcrops, and dunes are clearly visible in both tropical and arid regions. The combination of SIR-A and Seasat images provides additional information about the surface physical properties: topography and roughness. Ocean features were also observed, including large internal waves in the Andaman Sea. (Author)

A83-13349* Geological Survey, Flagstaff, Ariz.
SUBSURFACE VALLEYS AND GEOARCHEOLOGY OF THE EASTERN SAHARA REVEALED BY SHUTTLE RADAR
J. F. MCCAULEY, G. G. SCHABER, C. S. BREED, M. J. GROLIER (U.S. Geological Survey, Flagstaff, AZ), C. V. HAYNES (Arizona, University, Tucson, AZ), B. ISSAWI (Egyptian Geological Survey and Mining Authority, Cairo, Egypt), C. ELACHI, and R. BLOM (California Institute of Technology, Jet Propulsion Laboratory, Pasadena, CA) Science, vol. 218, Dec. 3, 1982, p. 1004-1020. Research supported by the U.S. Geological Survey and NASA. refs

Previously unknown buried valleys, geologic structures, and possible Stone Age occupation sites have been revealed through the Shuttle Imaging Radar (SIR-A) penetration of the extremely dry Selima Sand Sheet, dunes and drift sand of the eastern Sahara. Radar penetration of dry sand and soils varies with the wavelength of the incident signals, which is 24 cm for the SIR-A system, as well as incidence angle and electrical properties of the material which are largely determined by moisture content. The calculated depth of radar penetration of dry sand and granules has been established to be 5 m on the basis of laboratory measurements of Selima Sand Sheet sample electrical properties. September 1982 field studies in Egypt have verified SIR-A signal penetration depths of at least 1 m in the Selima Sand Sheet and drift sand, and 2 m or more in sand dunes. O.C.

A83-13350* Jet Propulsion Lab., California Inst. of Tech., Pasadena.
MINERAL IDENTIFICATION FROM ORBIT - INITIAL RESULTS FROM THE SHUTTLE MULTISPECTRAL INFRARED RADIOMETER
A. F. H. GOETZ (California Institute of Technology, Jet Propulsion Laboratory, Pasadena, CA), L. C. ROWAN, and M. J. KINGSTON (U.S. Geological Survey, Reston, VA) Science, vol. 218, Dec. 3, 1982, p. 1020-1024. Research supported by the U.S. Geological Survey and NASA. refs

The Shuttle multispectral IR radiometer (SMIRR) was designed to obtain surface reflectance data in ten spectral bands in order to evaluate the usefulness of a future imaging system for remote mineral identification. Attention was given to the 2.0-2.4 micron region, which has a wealth of spectral absorption features and appeared to have potential for the identification of CO3- and OH-bearing minerals such as the kaolinite and montmorillonite clays. SMIRR radiances were normalized by using a spectrum for dune sand collected in the Kharga Depression in Egypt. Direct identifications have been made of kaolinite-containing and carbonate material, indicating an exceptional potential for future orbital platform narrowband spectral imaging systems for mineralogical mapping. O.C.

A83-14256#
LANDSAT FOR RESOURCE EVALUATION AND MANAGEMENT IN THE ALBERTA FOOTHILLS
D. B. V. R. CLAASEN and G. A. ROSS (Calgary, University, Calgary, Alberta, Canada) In: Canadian Symposium on Remote Sensing, 7th, Winnipeg, Canada, September 8-11, 1981, Proceedings. Ottawa, Canadian Aeronautics and Space Institute, 1982, p. 247-263. Research supported by Gulf Canada Resources, Inc. refs

The operational role of Landsat imagery in the integrated resource survey process in Alberta has been evaluated noting that oil and gas exploration is a major land use project in the Alberta foothills. Premapping is discussed with reference to imagery selection and enhancement. Reconnaissance field work is described and analysis-mapping procedures are outlined in terms of: (1) the visual analysis of standard color composite images; (2) ecodistrict stratification on enhanced imagery; (3) terrain condition indicators; (4) the Landsat biophysical unit; and (5) biophysical unit mapping. S.C.S.

A83-14266#
MEASUREMENTS OF THE CHARACTERISTIC REFLECTANCE SPECTRA OF SURFICIAL DEPOSITS
V. SINGHROY (Ontario Centre for Remote Sensing, Toronto, Canada) and M. DUGGIN (New York, State University, Syracuse, NY) In: Canadian Symposium on Remote Sensing, 7th, Winnipeg, Canada, September 8-11, 1981, Proceedings. Ottawa, Canadian Aeronautics and Space Institute, 1982, p. 341-348. refs

Sensor output may be modelled to determine optimum sensor characteristics and data acquisition conditions. A major input to simulation models is the spectral reflectance of the target under investigation. The discriminability of various ground targets depends largely upon the spectral reflectance characteristics of those targets. In order to determine the feasibility of discriminating between surficial deposits, radiometric measurements were made under cloud-free conditions of the reflectance of major types of surficial deposits in the area of Syracuse, New York. The difference observed in reflectance spectra are reported and the implications of these differences for the discrimination of surficial deposits are discussed. (Author)

A83-14268#
SURFICIAL GEOLOGY MAPPING FROM LANDSAT-KAMINAK LAKE, N.W.T.
A. N. RENCZ (Canada Centre for Remote Sensing, Ottawa, Canada) and W. W. SHILTS (Geological Survey of Canada, Ottawa, Canada) In: Canadian Symposium on Remote Sensing, 7th, Winnipeg, Canada, September 8-11, 1981, Proceedings. Ottawa, Canadian Aeronautics and Space Institute, 1982, p. 358-363. refs

The present investigation has the objective to evaluate possibilities regarding a utilization of digital Landsat data for classification applications concerning surficial geology. The study region selected is located in the Canadian Arctic in a zone of continuous permafrost. The vegetation is tundra, developing only where soil moisture conditions permit it. Precambrian crystalline bedrock is exposed over more than 80% of the area. The results obtained in the investigation show that present Landsat data with a resolution of 80x60M can be used to classify surficial geology at a scale of 1:125,000 with a high level of accuracy. G.R.

A83-14302
A METHOD FOR THE QUANTITATIVE EVALUATION OF THE RESULTS OF SPACE IMAGERY INTERPRETATION IN PROSPECTING APPLICATIONS [METODIKA KOLICHESTVENNOI OBRABOTKI REZUL'TATOV DESHIFRIROVANIIA KOSMICHESKIKH SNIMKOV DLIA RESHENIIA GEOLOGOPOISKOVYKH ZADACH]
O. G. SHEREMET, V. M. MORALEV, IU. S. PERFILEV, and A. S. REITLINGER (Akademiia Nauk SSSR, Institut Litosfery; Proizvodstvennoe Geologicheskoe Ob'edinenie Aerogeologiia, Moscow, USSR) Issledovanie Zemli iz Kosmosa, Sept.-Oct. 1982, p. 12-19. In Russian.

A procedure has been developed for the quantitative evaluation of the results of space imagery interpretation with a view to identifying regions where the occurrence of ore deposits would be most likely. The proposed procedure involves determining geometric parameters of lineament sets, correlating these with ore manifestations selecting the optimum averaging area, searching for meaningful features, and predicting and verifying numerical solutions. The procedure is illustrated by an example. V.L.

A83-14315
AN EXAMPLE OF A STATISTICAL ANALYSIS OF THE RESULTS OF SPACE IMAGERY INTERPRETATION FOR THE EASTERN PART OF THE FERGANA VALLEY [PRIMER STATISTICHESKOGO ANALIZA REZUL'TATOV DESHIFRIROVANIIA KOSMICHESKIKH SNIMKOV TERRITORII VOSTOCHNOI CHASTI FERGANSKOI VPADINY]
A. D. BAKLANOV (Gosudarstvennyi Nauchno-Issledovatel'skii i Proizvodstvennyi Tsentr Priroda, USSR) Issledovanie Zemli iz Kosmosa, Sept.-Oct. 1982, p. 110, 111. In Russian.

A83-14667
EVALUATING THE EFFECTIVENESS OF LANDSAT DATA AS A TOOL FOR LOCATING BURIED PRE-GLACIAL VALLEYS IN EASTERN SOUTH DAKOTA
D. K. ZIGICH and K. E. KOLM (South Dakota School of Mines and Technology, Rapid City, SD) Photogrammetric Engineering and Remote Sensing, vol. 48, Dec. 1982, p. 1891-1901. Research supported by the U.S. Geological Survey. refs

A83-14852* Jet Propulsion Lab., California Inst. of Tech., Pasadena.
RESOLUTION VERSUS SPECKLE RELATIVE TO GEOLOGIC INTERPRETABILITY OF SPACEBORNE RADAR IMAGES - A SURVEY OF USER PREFERENCE
J. P. FORD (California Institute of Technology, Jet Propulsion Laboratory, Pasadena, CA) IEEE Transactions on Geoscience and Remote Sensing, vol. GE-20, Oct. 1982, p. 434-444. NASA-supported research. refs

A survey conducted to evaluate user preference for resolution versus speckle relative to the geologic interpretability of spaceborne radar images is discussed. Thirteen different resolution/looks combinations are simulated from Seasat synthetic-aperture radar data of each of three test sites. The SAR images were distributed with questionnaires for analysis to 85 earth scientists. The relative discriminability of geologic targets at each test site for each simulation of resolution and speckle on the images is determined on the basis of a survey of the evaluations. A large majority of the analysts respond that for most targets a two-look image at the highest simulated resolution is best. For a constant data rate, a higher resolution is more important for target discrimination than a higher number of looks. It is noted that sand dunes require more looks than other geologic targets. At all resolutions, multiple-look images are preferred over the corresponding single-look image. In general, the number of multiple looks that is optimal for discriminating geologic targets is inversely related to the simulated resolution. C.R.

A83-17841#
GEOMORPHOLOGICAL MAPPING USING LANDSAT IMAGERY - A CASE STUDY IN ARGENTINA
C. A. CANOBA (Rosario, Universidad Nacional, Rosario, Argentina) ITC Journal, no. 3, 1982, p. 324-329. refs

A description is presented of the application of Landsat imagery to geomorphological mapping at small scale in areas of low relief amplitude. The determination of the geomorphologic units and aspects of feature detection are considered for a sector of the Pampean Plain in the southern part of Santa Fe province. Aerial photographs and topographical maps at various scales were used in connection with the study of this sector. A mapping scale of 1:1,000,000 was chosen. The geological characteristics of the Pampean Plain are discussed along with the approaches employed in connection with the visual interpretation of Landsat MSS imagery. It is pointed out that false color composites enhanced some features and, combined with black and white images, improved the interpretation. Questions of geomorphologic interpretation and mapping are also investigated. G.R.

A83-17842#
SOME COMPARATIVE ASPECTS OF SLAR AND AIRPHOTO IMAGES FOR GEOMORPHOLOGIC AND GEOLOGIC INTERPRETATION
B. N. KOOPMANS (International Institute for Aerial Survey and Earth Sciences, Enschede, Netherlands) ITC Journal, no. 3, 1982, p. 330-337. refs

N83-10485# Bureau of Mines, Anchorage, Alaska. Field Operations Center.
CRITICAL AND STRATEGIC MINERALS IN ALASKA: COBALT, THE PLATINUM-GROUP METALS AND CHROMITE
J. C. BARKER, J. C. STILL, T. C. MOWATT, and J. J. MULLIGAN Feb. 1982 20 p refs
(PB82-193085; BM-IC-8869) Avail: NTIS HC A02/MF A01 CSCL 08I

The Bureau of Mines' Alaska Field Operations Center and the Bureau's research centers at Albany, Oreg., and Reno, Nev., are cooperating in a long-range program to investigate occurrences and delineate reserves of cobalt, the platinum-group metals, and chromite in Alaska. GRA

N83-12509# Instituto de Pesquisas Espaciais, Sao Jose dos Campos (Brazil).
REMOTE SENSING IN GEOLOGY: CURRENT TRENDS AND FUTURE PROSPECTS WITH SATELLITE DATA [SENSORES REMOTOS NA GEOLOGIA: TENDENCIA ATUAL E PERSPECTIVAS FUTURAS COM DADOS DE SATELITES]
W. R. PARADELLA and I. VITORELLO Aug. 1982 24 p refs In PORTUGUESE; ENGLISH summary Submitted for publication (INPE-2514-PRE/193) Avail: NTIS HC A02/MF A01

Orbital remote sensing products, especially LANDSAT imagery are discussed. The user's tendency was toward visual interpretation of aerial photography, radar mosaic, and LANDSAT image for geological applicatons. However, effective use of the information contained in these products depends on their manipulation based on the understanding of the nature and seasonal behavior of the interactions of electromagnetic energy and matter. Spectral regions that can offer the best remote sensing potential for lithological discrimination are also discussed. S.L.

N83-12512# Los Alamos Scientific Lab., N. Mex.
STATISTICAL TECHNIQUES APPLIED TO AERIAL RADIOMETRIC SURVEYS (STARRS): DISCRIMINANT-ANALYSIS METHODS APPLIED TO AERIAL RADIOMETRIC DATA AND THEIR APPLICATION TO URANIUM FAVORABILITY IN SOUTH TEXAS. NATION URANIUM RESOURCE EVALUATION
F. L. PIRKLE, N. K. STABLEIN, C. D. KOCH, M. E. JOHNSON, C. K. NEWMAN, T. R. BEMENT, and D. A. PATTERSON Jul. 1982 114 p refs Prepared in cooperation with Bendix Field Engineering Corp., Grand Junction
(Contract DE-AC13-76GJ-01664; W-7405-ENG-36)
(DE82-020961; GJBX-156-82) Avail: NTIS HC A06/MF A01

In an effort to establish radiometric signatures of geologic units, ten discriminant analysis techniques were applied to aerial radiometric data collected along the Texas Gulf Coast. Results show that partial discriminant analysis with the linear discriminant function applied to the raw data is useful for establishing radiometric signatures and for classifying new observations. Signatures for favorable and unfavorable units along the Texas Gulf Coast were established and new observations were then classified as being from units favorable or unfavorable for hosting uranium deposits based on the established training sets. DOE

N83-12513# High Life Helicopters, Inc., Puyallup, Wash.
AIRBORNE GAMMA-RAY SPECTROMETER AND MAGNETOMETER SURVEY. VOLUME 1. DETAIL AREAS, CHRISTMAS MOUNTAINS, SOLITARIO, GREEN VALLEY/0-2 RANCH, TEXAS Final Report
1982 98 p Prepared in cooperation with QEB, Inc.
(Contract DE-AC13-76GJ-01664)
(DE82-021614; GJBX-195-82-VOL-1) Avail: NTIS HC A05/MF A01

An airborne survey was made by a gamma-ray spectrometer with a large crystal volume, and with a high sensitivity proton precession magnetometer. Radiometric data were corrected for live time, aircraft and equipment background, cosmic background, atmospheric radon, Compton scatter, and altitude dependence. The corrected data were statistically evaluated, gridded, and contoured to produce maps of the radiometric variables, uranium, potassium, and thorium; their ratios; and the residual magnetic field. These maps were analyzed to produce a multivariant analysis contour map based on the radiometric response of the individual geological units. A geochemical anaysis was performed using the radiometric and magnetic contour maps, the multivariant analysis map, and factor analysis techniques to produce a geochemical analysis map for the area. Systems used in the survey, calibration of the systems, data collection procedures, data processing procedures, the data presentation, interpretation rationale, and interpretation methodology are described. DOE

N83-12584# Nevada Univ., Reno. Div. of Earth Sciences.
LOW- TO MODERATE-TEMPERATURE GEOTHERMAL RESOURCE ASSESSMENT FOR NEVADA: AREA SPECIFIC STUDIES, PUMPERNICKEL VALLEY, CARLIN AND MOANA Final Report, 1 Jun. 1981 - 31 Jul. 1982
D. T. TREXLER, T. FLYNN, B. A. KOENIG, E. J. BELL, and G. CHUSN, JR. 1982 197 p refs
(Contract DE-AC08-81NV-10220)
(DE82-018598; DOE/NV-10220/1) Avail: NTIS HC A09/MF A01

Geological, geophysical and geochemical surveys were used in conjunction with temperature gradient hole drilling to assess the geothermal resources in Pumpernickel Valley and Carlin, Nevada. A statewide assessment of geothermal resources that was completed in 1979 was used. The exploration techniques are based on previous federally-funded assessment programs that were completed in ix other areas in Nevada and include: literaure search and compilation of existing data, geologic reconnaissance, chemical sampling of thermal and non-thermal fluids, interpretation of satellite imagery, interpretation of low-sun angle aerial photographs, two-meter depth temperature probe survey, gravity survey, seismic survey, soil-mercury survey, and temperature gradient drilling. DOE

N83-12713# Autometric Corp., Inc., Falls Church, Va.
DETERMINATION OF THE CONTRIBUTION OF SIDE-LOOKING AIRBORNE RADAR TO STRUCTURAL GEOLOGIC MAPPING
R. F. PASCUCCI, A. F. SMITH, and J. E. PEARSON Dec. 1981 125 p refs Sponsored by Geological Survey
(PB82-185042) Avail: NTIS HC A06/MF A01

To assist the U.S. Geological Survey in carrying out the Congressional mandate to investigate the use of side looking airborne radar (SLAR), Autometric, Inc. has conducted a research program to determine the unique, incremental contribution of SLAR imagery to structural geologic mapping. Imagery from two SLAR systems and from three other remote sensing systems was interpreted, and the resulting information was quantified and intercompared using a computer assisted geographic information system. The study area includes three U.S. Geological Survey quadrangles. Author (GRA)

N83-13523*# Instituto de Pesquisas Espaciais, Sao Jose dos Campos (Brazil).
GEOLOGICAL-STRUCTURAL INTERPRETATION USING PRODUCTS OF REMOTE SENSING IN THE REGION OF CARRANCAS, MINAS GERAIS, BRAZIL [INTERPRETACAO GEOLOGICA-ESTRUTURAL UTILIZANDO PRODUTOS DE SENSORIAMENTO REMOTO NA REGIAO DE CARRANCAS. MINAS GERAIS, BRASIL]
N. D. J. PARADA, Principal Investigator, A. R. DOSSANTOS, C. E. DOSANJOS, M. P. BARBOSA, and P. VENEZIANI Sep. 1982 24 p refs In PORTUGUESE; ENGLISH summary Sponsored by NASA ERTS
(E83-10029; NASA-CR-169502; NAS 1.26:169502; INPE-2528-RPE/416) Avail: NTIS HC A02/MF A01 CSCL 08G

The efficiency of some criteria developed for the utilization of small scale and low resolution remote sensing products to map geological and structural features was demonstrated. Those criteria were adapted from the Logical Method of Photointerpretation which consists of textural qualitative analysis of landforms and drainage net patterns. LANDSAT images of channel 5 and 7, 4 LANDSAT-RBV scenes, and 1 radar mosiac were utilized. The region of study is characterized by supracrustal metassediments (quartzites and micaschist) folded according to a 'zig-zag' pattern and gnaissic basement. Lithological-structural definition was considered outstanding when compared to data acquired during field work, bibliographic data and geologic maps acquired in larger scales. Author

N83-13528*# Massachusetts Univ., Amherst. Dept. of Geology.
THE MINERALOGY OF GLOBAL MAGNETIC ANOMALIES Progress Report, Feb. - Aug. 1982
S. E. HAGGERTY, Principal Investigator 13 Aug. 1982 47 p refs ERTS
(Contract NAS5-26414)
(E83-10034; NASA-CR-169507; NAS 1.26:169507) Avail: NTIS HC A03/MF A01 CSCL 08G

The Curie Balance was brought to operational stage and is producing data of a preliminary nature. Substantial problems experienced in the assembly and initial operation of the instrument were, for the most part, rectified, but certain problems still exist. Relationships between the geology and the gravity and MAGSAT anomalies of West Africa are reexamined in the context of a partial reconstruction of Gondwanaland. A.R.H.

N83-14556*# Brown Univ., Providence, R. I. Dept. of Geological Sciences.
AN INVESTIGATION INTO THE UTILIZATION OF HCMM THERMAL DATA FOR THE DESCRIMINATION OF VOLCANIC AND EOLIAN GEOLOGICAL UNITS Quarterly Progress Report, 28 Feb. 1981 - 30 Aug. 1982
J. W. HEAD, III, Principal Investigator 30 Aug. 1982 3 p HCMM
(Contract NAS5-26728)
(E83-10047; NASA-CR-169563; NAS 1.26:169563) Avail: NTIS HC A02/MF A01 CSCL 08G

Analysis of HCMM data shows that the resolution provided by the thermal data is inadequate to permit the identification of individual lava flows within the volcanic test sites. Thermal data of southern California reveals that dune complexes at Kelso and Algodomes are found to be too small to permit adequate investigation of their structure. As part of the study of the San Francisco volcanic field, marked variations in the thermal properties of the region between Flagstaff and the Utah State border were observed. Several well-defined units within the Grand Canyon and the Colorado Plateau were recognized and appear to be very suitable for analysis with HCMM, SEASAT and LANDSAT images. Although individual volcanic constructs within the Cascade Range are too small to permit detailed characterization with the thermal data, the regional volcano/tectonic setting offers a good opportunity for comparing the possible thermal distinction between this area and sedimentary fold belts such as those found in the eastern United States. Strong intra-regional variations in vegetation cover were also tentatively identified for the Oregon test site. A.R.H.

N83-14570*# Arkansas Univ., Fayetteville. Remote Sensing Lab.
ANALYSIS OF GEOLOGIC TERRAIN MODELS FOR DETERMINATION OF OPTIMUM SAR SENSOR CONFIGURATION AND OPTIMUM INFORMATION EXTRACTION FOR EXPLORATION OF GLOBAL NON-RENEWABLE RESOURCES. PILOT STUDY: ARKANSAS REMOTE SENSING LABORATORY, PART 1, PART 2, AND PART 3
V. H. KAUPP, H. C. MACDONALD, W. P. WAITE, J. A. STILES, F. S. FROST, K. S. SHANMUGAM, S. A. SMITH, V. NARAYANAN, and J. C. HOLTZMAN, Principal Investigators 1982 133 p refs Prepared in cooperation with Kansas Univ. Center for Research, Inc., Lawrence Original contains imagery. Original photography may be purchased from the EROS Data Center, Sioux Falls, S.D. 57198 ERTS
(Contract NAG9-3)
(E83-10061; NASA-CR-169573; ARSL-TR-81-2) Avail: NTIS HC A07/MF A01 CSCL 08G

Computer-generated radar simulations and mathematical geologic terrain models were used to establish the optimum radar sensor operating parameters for geologic research. An initial set of mathematical geologic terrain models was created for three basic landforms and families of simulated radar images were prepared from these models for numerous interacting sensor, platform, and terrain variables. The tradeoffs between the various sensor parameters and the quantity and quality of the extractable geologic data were investigated as well as the development of automated techniques of digital SAR image analysis. Initial work on a texture analysis of SEASAT SAR imagery is reported. Computer-generated radar simulations are shown for combinations of two geologic models and three SAR angles of incidence. A.R.H.

N83-14575*# Instituto de Pesquisas Espaciais, Sao Jose dos Campos (Brazil).
AUTOMATIC INTERPRETATION OF MSS-LANDSAT DATA APPLIED TO COAL REFUSE SITE STUDIES IN SOUTHERN SANTA CATARINA STATE, BRAZIL
N. D. J. PARADA, Principal Investigator, H. J. H. KUX, and D. D. M. VALERIANO May 1982 12 p refs Presented at the 16th Intern. Symp. on Remote Sensing of Environ., Buenos Aires, 2-9 Jun. 1982 Sponsored by NASA Original contains imagery. Original photography may be purchased from the EROS Data Center, Sioux Falls, S.D. 57198 ERTS
(E83-10066; NASA-CR-169577; NAS 1.26:169577; INPE-2410-PRE/119) Avail: NTIS HC A02/MF A01 CSCL 05B

The coal mining district in southeastern Santa Catarina State is considered one of the most polluted areas of Brazil. The author has identified significant preliminary results on the application of MSS-LANDSAT digital data to monitor the coal refuse areas and its environmental consequences in this region. Author

N83-14578*# Instituto de Pesquisas Espaciais, Sao Jose dos Campos (Brazil).
SPECTRAL DISCRIMINATION OF LITHOLOGIC FACIES IN THE GRANITE OF THE PEDRA BRANCA GOIAS USING LANDSAT 1 DIGITAL IMAGERY [DISCRIMINACAO ESPECTRAL DAS AREAS DE GREISENIZA CAO NO GRANITO DA SERRA DA PEDRA BRANCA - GO, A TRAVES DE IMAGENS DIGITAIS DO SATELITE LANDSAT-1]
N. D. J. PARADA and R. ALMEIDO, JR. May 1982 14 p refs In PORTUGUESE; ENGLISH summary Presented at the 32nd Brazilian Geol. Congr., Salvador, Bahia, Brazil, 12-18 Sep. 1982 Sponsored by NASA Original contains imagery. Original photography may be purchased from the EROS Data Center, Sioux Falls, S.D. 57198 ERTS
(E83-10069; NASA-CR-169580; NAS 1.26:169580; INPE-2418-PRE/126) Avail: NTIS HC A02/MF A01 CSCL 08B

The applicability of LANDSAT MSS imagery for discriminating geobotanical associations observed in zones of cassiterite-rich metasomatic alterations in the granitic body of Serra da Pedra Branca was investigated. Computer compatible tapes of dry and rainy season imagery were analyzed. Image enlargement, corrections, linear contrast stretch, and ratioing of noncorrelated spectral bands were performed using the Image 100 with a grey scale of 256 levels between zero and 255. Only bands 5 and 7 were considered. Band ratioing of noncorrelated channels (5 and 7) of rainy season imagery permits distinction of areas with different vegetation coverage percentage, which corresponds to geobotanial associations in the area studied. The linear contrast stretch of channel 5, especially of the dry season image is very unsatisfactory in this area. A.R.H.

N83-14580*# Instituto de Pesquisas Espaciais, Sao Jose dos Campos (Brazil).
MULTITEMPORAL AND GEOBOTANICAL APPROACH IN THE REMOTE DETECTION OF GREISENIZATION AREAS IN THE SERRA DA PEDRA BRANCA GRANITE, GOIAS STATE, BRAZIL
N. D. J. PARADA, Principal Investigator and R. A. FILHO Jun. 1982 10 p refs Presented at the 16th Intern. Symp. on Remote Sensing of Environ., Buenos Aires, 2-9 Jun. 1982 Sponsored by NASA Original contains imagery. Original photography may be purchased from the EROS Data Center, Sioux Falls, S.D. 57198 ERTS
(E83-10071; NASA-CR-169582; NAS 1.26:169582; INPE-2446-PRE/145) Avail: NTIS HC A02/MF A01 CSCL 08F

A multiseasonal analysis of LANDSAT multispectral images in CCT format permitted the mapping of lithologic facies in the Pedra Branca Granite, using geobotanical associations, which occur in the form of variations in the density of the cerrado vegetation, as well as the predominance of certain distinct vegetation species. Dry season images did not show very good results in lithological differentiation due to anomalous illumination conditions related to

the low solar elevation and the homogeneity in the vegetation cover, specially the grass that becomes dry during this season. Rainy season images, on the other hand, allowed the separation of the lithological types, a fact that can be attributed to a greater differentiation among the geobotanical associations. The muscovite-granite facies with greisenization zones within the Serra da Pedra Branca were mapped. This methodology can be successfully applied to similar known granite bodies elsewhere in the Tin Province of Goias. Author

N83-14582*# Instituto de Pesquisas Espaciais, Sao Jose dos Campos (Brazil).
LANDSAT AND RADAR MAPPING OF INTRUSIVE ROCKS IN SE-BRAZIL
N. D. J. PARADA, Principal Investigator, A. R. DOSSANTOS, C. E. DOSANJOS, J. C. MOREIRA, M. P. BARBOSA, and P. VENEZIANI May 1982 12 p refs Presented at the 16th Intern. Symp. on Remote Sensing of Environ., Buenos Aires, 2-9 Jun. 1982 Sponsored by NASA ERTS
(E83-10073; NASA-CR-169584; NAS 1.26:169584; INPE-2417-PRE/125) Avail: NTIS HC A02/MF A01 CSCL 08B

The feasibility of intrusive rock mapping was investigated and criteria for regional geological mapping established at the scale of 1:500,00 in polycyclic and polymetamorphic areas using the logic method of photointerpretation of LANDSAT imagery and radar from the RADAMBRASIL project. The spectral behavior of intrusive rocks, was evaluated using the interactive multispectral image analysis system (Image-100). The region of Campos (city) in northern Rio de Janeiro State was selected as the study area and digital imagery processing and pattern recognition techniques were applied. Various maps at the 2:250,000 scale were obtained to evaluate the results of automatic data processing. Author

N83-14587*# Instituto de Pesquisas Espaciais, Sao Jose dos Campos (Brazil).
THE COMPUTER TREATMENT OF REMOTELY SENSED DATA: AN INTRODUCTION TO TECHNIQUES WHICH HAVE GEOLOGIC APPLICATIONS [O TRATAMENTO POR COPUTADOR DE DADOS DE SENSORES REMOTOS: UMA INTRODUCAO DE TECNICAS QUE VISAM APLICACOES GEOLOGICAS]
N. D. J. PARADA, Principal Investigator, W. R. PARADELLA, and I. VITORELLO May 1982 16 p refs In PORTUGUESE; ENGLISH summary Presented at the 32nd Brazilian Geol. Congr., Salvador, Bahia, 12-18 Sep. 1982 Sponsored by NASA Original contains imagery. Original photography may be purchased from the EROS Data Center, Sioux Falls, S.D. 57198 ERTS
(E83-10078; NASA-CR-169589; NAS 1.26:169589; INPE-2419-PRE/127) Avail: NTIS HC A02/MF A01 CSCL 08G

Several aspects of computer-assisted analysis techniques for image enhancement and thematic classification by which LANDSAT MSS imagery may be treated quantitatively are explained. On geological applications, computer processing of digital data allows, possibly, the fullest use of LANDSAT data, by displaying enhanced and corrected data for visual analysis and by evaluating and assigning each spectral pixel information to a given class. Author

N83-14590*# Iowa Univ., Iowa City. Dept. of Geology.
USE OF MAGSAT ANOMALY DATA FOR CRUSTAL STRUCTURE AND MINERAL RESOURCES IN THE US MIDCONTINENT Quarterly Report, period ending 30 Sep. 1982
R. S. CARMICHAEL, Principal Investigator 30 Sep. 1982 5 p ERTS
(Contract NAS 5-26425)
(E83-10082; NASA-CR-169594; NAS 1.26:169594; QR-7) Avail: NTIS HC A02/MF A01 CSCL 08G

Progress in the correlation of MAGSAT anomaly maps with geological and geophysical data sets is reported. An excerpt from Bouguer gravity map of the U.S. was filtered to retain wavelengths of 250 km, thus being physically somewhat analogous to MAGSAT data at 400 km height. Residual anomalies were extracted to compare with the satellite magnetics. M.G.

N83-14593*# Technicolor Graphic Services, Inc., Sioux Falls, S. Dak.
AN INVESTIGATION OF MAGSAT AND COMPLEMENTARY DATA EMPHASIZING PRECAMBRIAN SHIELDS AND ADJACENT AREAS OF WEST AFRICA AND SOUTH AMERICA Quarterly Report, 1 Apr. - 30 Sep. 1982
D. A. HASTINGS, Principal Investigator 30 Sep. 1982 4 p Sponsored by NASA ERTS
(Contract DI-14-08-0001-20129)
(E83-10085; NASA-CR-169607; NAS 1.26:169607) Avail: NTIS HC A02/MF A01 CSCL 08G

A mineral deposits overlay was prepared to the van der Grinten projection geological world map and coloring of the map was initiated. The Mercator projection version was proofread and some preliminary modeling of MAGSAT anomalies for South America were undertaken. A.R.H.

N83-14598*# California Univ., Santa Barbara. Geography Remote Sensing Unit.
NEOTECTONICS OF THE SAN ANDREAS FAULT SYSTEM: BASIN AND RANGE PROVINCE JUNCTURE Semiannual Progress Report, May - Oct. 1981
J. E. ESTES and J. C. CROWELL, Principal Investigators Oct. 1981 7 p ERTS
(Contract NAG5-177)
(E83-10090; NASA-CR-169600; NAS 1.26:169600) Avail: NTIS HC A02/MF A01 CSCL 08G

A thorough evaluation of all LANDSAT coverage of the study area (considering atmospheric clarity, seasonal aspects, specific swath location, and digital quality) resulted in the selection of two consequetive (continuously recorded) scenes for detailed analyses. The acquisition of HCMM and SEASAT imagery as well as high altitude U-2 uniform coverage is being considered. A bibliography of previous geological studies and methodological examples is estimated to be 70% complete. A.R.H.

N83-14620# Ecole Nationale Superieure des Mines, Sophia-Antipolis (France).
COMBINED USE OF DAILY THERMAL CYCLE OF METEOSAT IMAGERY AND MULTISPECTRAL LANDSAT DATA: APPLICATION TO THE BANDIAGARA PLATEAU, MALI
C. BARDINET, J. M. MONGET, and Y. PATOUREAUX (SODETEG, Leplessis-Robinson) *In* ESA Satellite Remote Sensing for Developing Countries p 95-101 Jun. 1982 refs
Avail: NTIS HC A11/MF A01

Combined use of LANDSAT and METEOSAT digital data for the mapping of various lithologies in the Sahel zones is summarized. The thermal inertia maps of Meteosat are particularly good for geology, but ground resolution is too low to permit better than large scale mapping. The LANDSAT data is particularly suited to detailed small scale studies, but does not contain enough multispectral information for proper lithologic discrimination during the dry season of the Sahel zone. Author (ESA)

N83-14627# Institute of Geological Sciences, Nottingham (England).
SATELLITE REMOTE SENSING IN MINERAL EXPLORATION IN DEVELOPING COUNTRIES
E. A. STEPHENS *In* ESA Satellite Remote Sensing for Developing Countries p 169-170 Jun. 1982
Avail: NTIS HC A11/MF A01

Appropriate levels of image processing and infrastructure for satellite remote sensing in mineral exploration by small developing nations are discussed. It is suggested that EARSeL has an important role to play in undertaking research to evaluate data from the next generation of satellites on behalf of and in cooperation with developing countries. The provision of access to sophisticated image processing equipment and to experienced personnel as an alternative to the smaller developing countries

investing their limited resources in remote sensing field is also important. Author (ESA)

N83-14628# Electromagnetic Systems Labs., Inc., Sunnyvale, Calif. Imagery Data Systems.
REMOTE SENSING APPLICATIONS TO THE DEVELOPMENT OF AN INTEGRATED DATA BASE FOR OIL AND GAS EXPLORATION
R. J. HALL *In* ESA Satellite Remote Sensing for Developing Countries p 171-174 Jun. 1982 refs
Avail: NTIS HC A11/MF A01

Techniques employed in oil and gas exploration and the utility of satellite data to the exploration process are discussed. The application of satellite information to geologic analysis, planimetric mapping and other data collection efforts associated with the search for oil and gas are considered. Geographic information and image processing features that were utilized in three projects are outlined and the potential of data sources such as LANDSAT-D is assessed. Experience shows that satellite imagery is of greatest benefit when it is integrated into a comprehensive data base with conventional data. Author (ESA)

N83-14629# Institute of Geological Sciences, Nottingham (England).
REMOTE SENSING OF THE GRANITES OF SOUTHEAST ASIA
D. I. J. MALLICK *In* ESA Satellite Remote Sensing for Developing Countries p 175-179 Jun. 1982 refs
Avail: NTIS HC A11/MF A01

Remote sensing using LANDSAT imagery and air photography in support of field investigations is shown to be useful in subdividing the granite bodies of the SE Asia tin belt. In many cases, however, the distinctions in chemistry and physical properties between the various phases of granite are so small that no remote sensing discrimination between them is possible. In NW Malaysia cloud cover and vegetation hamper imagery. Subdivisions of the granite bodies on the basis of morphological and vegetation variations correlate with lithological variations in the underlying granite. Most subdivisions of the more rugged, high relief and high altitude areas of granite are based on slight variations in morphology alone; the main variation in the vegetation is with altitude. Author (ESA)

N83-14634# Geological Survey of Norway, Trondheim.
DIGITAL METHODS FOR LINEAMENT ANALYSIS
B. RINDSTAD and B. FOLLESTAD *In* ESA Satellite Remote Sensing for Developing Countries p 211-214 Jun. 1982 refs
Avail: NTIS HC A11/MF A01

Lineaments taken from LANDSAT images from an area covering most of Finnmark, Norway, were studied. Data programs for digitalization, statistics, plotting and gridding, run on a HP 3000 computer (2 MB core, 750 MB disk) are described. Lineaments are digitalized by the DIGLIN program. This program, written in BASIC, is operated on a graphic terminal and converted with a digitalization table. A cross-hair is placed over the point to be digitalized and for which the coordinates are required. The data as x and y coordinates as well as an identification are then transferred from band cassette to a file on the HP 3000. The program LINER converts the data to a readable file for the program LINAMENT, which calculates a directional frequency and a directional length histogram, from specified group number, lineament length and subarea. The KONTUR program provides contour maps. For Finnmarksvidda, the lineament directions were gridded and presented as contour maps, facilitating manual and digital correlation with other geodata. Author (ESA)

N83-14797# Los Alamos Scientific Lab., N. Mex.
TECTONICS OF WEST CENTRAL MEXICO AND ADJACENT ARIZONA: A REMOTE SENSING AND FIELD STUDY IN ARID AND SEMI-ARID AREAS
W. S. BALDRIDGE, Y. BARTOV, and A. KRON 1981 8 p refs Presented at the Intern. Symp. on Remote Sensing on Environ., Cairo, Nov. 1981
(Contract W-7405-ENG-36)
(DE82-002393; LA-UR-81-2920; CONF-811133-1) Avail: NTIS HC A02/MF A01

Large scale fault zones in west central New Mexico and eastern Arizona were mapped using conventional fieldwork aided by Landsat and Seasat images and high altitude air photos. These faults, which are of post early Miocene age, trend NE-SW and N-S and extend over 200 km. The fault zones bound very large horst and graben blocks which, although located on the physiographic Colorado Plateau, are characteristic of Basin and Range deformation. Their intersection was the locus of extensive Cenozoic volcanism. The procedure developed in this project permitted investigation of an area of about 1.8 x 10 to the 5th power of arid and semiarid land whose structures previously were poorly defined. GRA

N83-15795*# Instituto de Pesquisas Espaciais, Sao Jose dos Campos (Brazil).
ANALYSIS OF THE CHARACTERISTICS APPEARING IN LANDSAT MULTISPECTRAL IMAGES IN THE GEOLOGICAL STRUCTURAL MAPPING OF THE MIDWESTERN PORTION OF THE RIO GRANDE DO SUL SHIELD M.S. Thesis - 25 Mar. 1982 [ANALISE DAS CARACTERISTICAS APRESENTADAS EM IMAGENS MULTIESPECTRAIS DO SATELITE LANDSAT NO MAPEAMENTO GEOLOGICO-ESTRUTURAL DA PORCAO CENTRO - OESTE DO ESCUDO SUL-RIOGRANDENSE]
N. D. J. PARADA, Principal Investigator and T. OHARA Sep. 1982 362 p refs In PORTUGUESE; ENGLISH summary Sponsored by NASA Original contains color imagery. Original photography may be purchased from the EROS Data Center, Sioux Falls, S.D. 57198 ERTS
(E83-10126; NASA-CR-169728; NAS 1.26:169728; INPE-2524-TDL/100) Avail: NTIS HC A16/MF A01 CSCL 08G

The central-western part of Rio Grande do Sul Shield was geologically mapped to test the use of MSS-LANDSAT data in the study of mineralized regions. Visual interpretation of the images a the scale of 1:500,000 consisted, in the identification and analysis of the different tonal and textural patterns in each spectral band. After the structural geologic mapping of the area, using visual interpretation techniques, the statistical data obtained were evaluated, specially data concerning size and direction of fractures. The IMAGE-100 system was used to enlarge and enhance certain imagery. The LANDSAT MSS data offer several advantages over conventional white and black aerial photographs for geological studies. Its multispectral characteristic (band 6 and false color composition of bands 4, 5 and 7 were best suitable for the study). Coverage of a large imaging area of about 35,000 sq km, giving a synoptical view, is very useful for perceiving the regional geological setting. A.R.H.

05

OCEANOGRAPHY AND MARINE RESOURCES

Includes sea-surface temperature, ocean bottom surveying imagery, drift rates, sea ice and icebergs, sea state, fish location.

A83-10068
DETECTION OF COASTAL ZONE ENVIRONMENTAL CONDITIONS USING SYNTHETIC APERTURE RADAR
R. A. SHUCHMAN, E. S. KASISCHKE (Michigan, Environmental Research Institute, Ann Arbor, MI), and G. A. MEADOWS (Michigan, University, Ann Arbor, MI) In: International Geoscience and Remote Sensing Symposium, Washington, DC, June 8-10, 1981, Digest. Volume 2. New York, Institute of Electrical and Electronics Engineers, 1981, p. 756-767. refs
(Contract N00014-76-C-1048; NOAA-MO-A01-78-00-4339)

Two SAR systems for monitoring oceanic and coastal zone environments are described. One system is airborne, uses both X- and L-band polarizations, while the second is on board the Seasat spacecraft and uses only L-band polarization. The SARs have been employed for detecting gravity waves, surface currents, fronts, surf zone conditions, coastal vegetation, and for performing bathymetry. The use of fast Fourier transforms for gravity wave analysis is mentioned, as are a semi-causal model and a one-step spectral estimation computer scheme. Comparisons with sea-truth data have shown the gravity wave data to be accurate in terms of direction of propagation and wavelength measurement. The SAR data are noted to lack recognizable information on wave height, and further studies to characterize the modulation transfer function more precisely are indicated. M.S.K.

A83-10071
A COMPARISON DATA SET FOR THE EVALUATION OF REMOTE SENSING SYSTEMS ABILITY FOR OCEAN WAVE DATA COLLECTION
D. E. LICHY and A. A. PUNCHAK (U.S. Army, Coastal Engineering Research Center, Fort Belvoir, VA) In: International Geoscience and Remote Sensing Symposium, Washington, DC, June 8-10, 1981, Digest. Volume 2. New York, Institute of Electrical and Electronics Engineers, 1981, p. 787-792.

A83-10088
THE APPLICATION OF MICROWAVE REMOTE SENSING FOR SNOW AND ICE RESEARCH
W. J. CAMPBELL (U.S. Geological Survey, Reston, VA) and P. GUDMANSEN (Danmarks Tekniske Hojskole, Copenhagen, Denmark) In: International Geoscience and Remote Sensing Symposium, Washington, DC, June 8-10, 1981, Digest. Volume 2. New York, Institute of Electrical and Electronics Engineers, 1981, p. 951-957.

The use of active and passive microwave remote sensing techniques in arctic and antarctic snow and ice research is reviewed. In particular, the research program proposed by NASA's Ice and Climate Experiment (ICEX) Science and Applications Working Group is discussed. Aerial and satellite microwave observations of polar sea ice are recounted, as are satellite radar altimeter measurements of Greenland. The proposed ICEX instrument ensemble is briefly described; it consists of a large-antenna multifrequency microwave radiometer, a wide-swath-imagery radar, a scatterometer, a radar ice-elevation altimeter system, and a laser ice-elevation altimeter system. It is noted that the ICEX instruments are to be deployed on satellites flying high-inclination orbits and that near-simultaneous observations of multiple ice and snow parameters by complementary sensors are needed for many of the cryospheric processes to be studied. F.G.M.

A83-10091* National Aeronautics and Space Administration. Goddard Space Flight Center, Greenbelt, Md.
MICROWAVE RADIANCE OF EARLY FALL SEA ICE AT 1.55 CM
F. D. CARSEY (NASA, Goddard Space Flight Center, Laboratory for Atmospheric Sciences, Greenbelt, MD) and K. F. HUEMMRICH (Computer Sciences Corp., Silver Spring, MD) In: International Geoscience and Remote Sensing Symposium, Washington, DC, June 8-10, 1981, Digest. Volume 2. New York, Institute of Electrical and Electronics Engineers, 1981, p. 989-994. refs

Satellite microwave radiance images at 1.55 cm are examined to determine the amount of ice which survives the arctic summer and to determine the regional variation of this multiyear ice emissivity. In the central arctic concentrations are measured in the range 0.75-0.95 and emissivities in the range 0.77 and 0.83 with high values of both near the Canadian Archipelago.
(Author)

A83-10092* National Aeronautics and Space Administration. Goddard Space Flight Center, Greenbelt, Md.
SATELLITE LASER ALTIMETER FOR MEASUREMENT OF ICE SHEET TOPOGRAPHY
J. L. BUFTON, J. E. ROBINSON, M. D. FEMIANO, and F. S. FLATOW (NASA, Goddard Space Flight Center, Greenbelt, MD) In: International Geoscience and Remote Sensing Symposium, Washington, DC, June 8-10, 1981, Digest. Volume 2. New York, Institute of Electrical and Electronics Engineers, 1981, p. 1003-1011. refs

Results of a preliminary conceptual design study are presented for a laser altimeter that is capable of high-resolution mapping of the polar ice sheets and is proposed for inclusion in the National Oceanic Satellite System spacecraft or other polar-orbiting satellites. The instrument consists of a pulsed-laser transmitter operating at a wavelength of 532 nm and a duration of 5 nsec, a receiver telescope, a photomultiplier-tube detector, data processing and control electronics, and an attitude sensing and measurement system; a laser footprint diameter of 70 m is planned. The altimeter components are described, and the accuracy of both the altimetry measurement and the attitude measurement is evaluated. A range precision of about 10 cm is estimated, along with an attitude measurement accuracy of approximately 10 arcsec. F.G.M.

A83-10093* National Aeronautics and Space Administration. Goddard Space Flight Center, Greenbelt, Md.
ICE-SHEET DYNAMICS BY SATELLITE LASER ALTIMETRY
H. J. ZWALLY, R. A. BINDSCHADLER (NASA, Goddard Space Flight Center, Oceans and Ice Branch, Greenbelt, MD), and R. H. THOMAS (OAO Corp., Beltsville, MD) In: International Geoscience and Remote Sensing Symposium, Washington, DC, June 8-10, 1981, Digest. Volume 2. New York, Institute of Electrical and Electronics Engineers, 1981, p. 1012-1022. refs

Glaciological applications of a satellite laser altimeter system with a range precision of approximately 10 cm and a footprint diameter of 70 m are discussed. Available data on ice-sheet dynamics are reviewed, and the measurement errors associated with the laser altimeter are examined. It is shown that information collected with the system could make it possible to detect changes in average elevation (i.e., in average ice thickness) of less than 15 cm for areas of hundreds of sq km to a few thousand sq km. Other possible applications of the system are briefly considered, including the mapping of the positions of ice-sheet margins, the mapping of the junction between a grounded ice sheet and a floating ice shelf, and the estimation of iceberg calving rates.
F.G.M.

A83-10094
FEASIBILITY OF MAPPING OCEAN SURFACE CURRENTS USING DELTA K-MICROWAVE RADARS MOUNTED ON GEOSTATIONARY SATELLITE PLATFORMS
R. E. MCINTOSH (Massachusetts, University, Amherst, MA) In: International Geoscience and Remote Sensing Symposium, Washington, DC, June 8-10, 1981, Digest. Volume 2. New York, Institute of Electrical and Electronics Engineers, 1981, p. 1083-1088.

The feasibility of developing a dual-frequency (delta k) microwave radar system that operates from two geostationary satellites is considered. The system would be used to obtain synoptic surface-current maps for large ocean areas. The measurement technique that would be employed is described, along with a possible scheme for illuminating the ocean surface area to be mapped by the radar system. Calculations of the total system S/N ratio are presented for various average power levels. It is shown that the overall system S/N ratios approach 10 dB for average power levels of 1 W when there is no atmospheric absorption and that, when atmospheric conditions are less favorable, reasonable S/N levels close to 10 dB can be obtained by increasing the average power. F.G.M.

A83-10104* National Aeronautics and Space Administration. Langley Research Center, Hampton, Va.
MICROWAVE REMOTE SENSING MEASUREMENTS OF OIL POLLUTION ON THE OCEAN
W. F. CROSWELL, H.-J. C. BLUME, and J. W. JOHNSON (NASA, Langley Research Center, Hampton, VA) In: International Geoscience and Remote Sensing Symposium, Washington, DC, June 8-10, 1981, Digest. Volume 2. New York, Institute of Electrical and Electronics Engineers, 1981, p. 1246-1251.

Microwave and optical remote sensors were flown over fresh and weathered crude oil released from a surface research vessel and also over a slick formed on the sea by frozen oleyl alcohol cubes released from a helicopter. For the crude oil experiments, microwave radiometric measurements at 1.43, 2.65, 22, and 31 GHz are reported, along with the variable incidence angle scattering measurements at 13.9 GHz. For these experiments, unusual depressions in the L-band brightness temperature were observed, possibly related to dispersants applied to the crude oil. Similar depressions, but with much larger values, were observed over the oleyl alcohol monomolecular slicks. Images obtained at 31 and 22 GHz were used to infer oil volume, yielding values which bound the known amounts spilled. Ku band measurements obtained in repeated passes over crude oil slicks are also discussed. V.L.

A83-10113
ON THE CIRCULATION OF THE WESTERN GULF OF MEXICO - A SATELLITE VIEW
P. CLEMENTE-COLON and R. LEGECKIS (NOAA, National Earth Satellite Service, Washington, DC) In: International Geoscience and Remote Sensing Symposium, Washington, DC, June 8-10, 1981, Digest. Volume 2. New York, Institute of Electrical and Electronics Engineers, 1981, p. 1391-1394. refs

The mechanisms of the predominant anticyclonic circulation of the western Gulf of Mexico are investigated on the basis of satellite IR observations of the relative sea surface temperature (SST). It is shown that the distribution of SST could serve as an indication of dynamical processes in the western and northwestern Gulf of Mexico, at least for the fall, winter, and spring seasons. Analysis of the data supports the hypothesis that the detached Loop Current rings are a source of anticyclonicity for the circulation regime of the western Gulf. V.L.

A83-10115
THE 100 DAYS OF SEASAT-A
S. W. MCCANDLESS, JR. (User Systems Engineering, Annandale, VA) In: International Geoscience and Remote Sensing Symposium, Washington, DC, June 8-10, 1981, Digest. Volume 2. New York, Institute of Electrical and Electronics Engineers, 1981, p. 1401-1406.

The accomplishments of Seasat-A are reviewed. The radar altimeter monitored average wave height to within 0.5 to 1 meter along a 2 to 12 m swath, and measured changes in the ocean geoid to a precision of 10 cm. The radar scatterometer measured wind speeds from 3 to 28 m/sec within 2 m/sec and direction within 20 deg over two 500 km swaths. The five-frequency microwave radiometer measured surface temperature by measuring the microwave brightness of the surface to within 1 C, measured foam brightness which can be converted into a measurement of high wind speed, mapped ice coverage, and provided atmospheric correction data to the active radars by measuring liquid and gaseous water content in the upper atmosphere. The Synthetic Aperture Radar provided detailed images of open ocean, coastal, inland geology and culture, and ice-covered regions. Relevant oceanographic satellite applications include offshore oil and gas, environmental forecasting, marine transportation, deep ocean mining, and marine fisheries. C.D.

A83-10826
INVESTIGATIONS OF THE ARCTIC, THE ANTARCTIC AND THE WORLD OCEAN; CONFERENCE-SEMINAR, MOSCOW, USSR, FEBRUARY 9-13, 1981, REPORTS [ISSLEDOVANIA ARKTIKI, ANTARKTIKI I MIROVOGO OKEANA; SOVESHCHANIE-SEMINAR, MOSCOW, USSR, FEBRUARY 9-13, 1981, DOKLADY]
E. I. TOLSTIKOV, (ED.) and N. A. KORNILOV Leningrad, Gidrometeoizdat, 1982. 192 p. In Russian.

The volume includes review papers as well as papers discussing individual aspects of meteorological, oceanographic, and hydrochemical investigations of the Arctic, the Antarctic, and the world ocean. Ice-cover studies are described, and attention is given to practical applications relating to ocean transport, shelf operations, marine engineering, fishing, and environmental monitoring. Questions relating to instrumentation and observation methods are discussed. B.J.

A83-10828
USING NEW METHODS IN MONITORING THE THERMAL REGIME OF THE ARCTIC [ISPOL'ZOVANIE NOVYKH METODOV V MONITORINGE TERMICHESKOGO REZHIMA ARKTIKI]
I. B. ESERKEPOVA, K. M. LUGINA, N. A. SPERANSKAIA (Gosudarstvennyi Gidrologicheskii Institut, Leningrad, USSR), R. L. KAGAN (Glavnaia Geofizicheskaia Observatoriia, Leningrad, USSR), I. P. SMIRNOVA, and V. V. SUBBOTIN (Gosudarstvennyi Komitet SSSR po Gidrometeorologii i Kontroliu Prirodnoi Sredy, Arkticheskii i Antarkticheskii Nauchno-Issledovatel'skii Institut, Leningrad, USSR) In: Investigations of the Arctic, the Antarctic and the world ocean; Conference-Seminar, Moscow, USSR, February 9-13, 1981, Reports. Leningrad, Gidrometeoizdat, 1982, p. 56-64. In Russian. refs

Data describing the characteristics of the spatial statistical structure of the average surface temperature of air during a month (January) and a year at high latitudes in the Northern Hemisphere are presented. Attention is given to the spatial averaging of meteorological fields and to a priori evaluations of the accuracy of various averaging methods depending on the number and arrangement of the stations. The theoretical averaging errors with the existing network of stations in the Arctic zone are estimated. C.R.

A83-10832
TIDAL PHENOMENA IN ARCTIC OCEAN ICE /ACCORDING TO SPACE DATA/ [PRILIVNYE IAVLENIIA VO L'DAKH SEVERNOGO LEDOVITOGO OKEANA /PO KOSMICHESKIM DANNYM/]
V. V. BOGORODSKII (Gosudarstvennyi Komitet SSSR po Gidrometeorologii i Kontroliu Prirodnoi Sredy, Arkticheskii i Antarkticheskii Nauchno-Issledovatel'skii Institut, Leningrad, USSR) and M. G. NAZIROV (Gosudarstvennyi Nauchno-Issledovatel'skii Tsentr Izucheniia Prirodnykh Resursov, Moscow, USSR) In: Investigations of the Arctic, the Antarctic and the world ocean; Conference-Seminar, Moscow, USSR, February 9-13, 1981, Reports. Leningrad, Gidrometeoizdat, 1982, p. 105-117. In Russian. refs

An analysis of satellite photographs is used to study the tidal factor conditioning the large-scale features of the spatial structure of the Arctic Ocean ice cover. Certain stable regional features of the transformation of tide waves in ice during their quasi-circumpolar course are identified. A relationship is established between the stationary formation of ice clearings (polyn'yas) and the orographic blockage of tide waves. B.J.

A83-10833
SOME FEATURES OF THE SPATIAL STRUCTURE OF THE ARCTIC OCEAN ICE COVER IN CONNECTION WITH TURBULENT FRICTION AND GEOSTROPHIC CAPTURE OF TIDE WAVES [NEKOTORYE CHERTY PROSTRANSTVENNOI STRUKTURY LEDIANOGO POKROVA ARKTICHESKIKH MOREI V SVIAZI S TURBULENTNYM TRENIEM I GEOSTROFICHESKIM ZAKHVATOM PRILIVNOI VOLNY]
M. G. NAZIROV and V. G. TROFIMOVA (Gosudarstvennyi Nauchno-Issledovatel'skii Tsentr Izucheniia Prirodnykh Resursov, Moscow, USSR) In: Investigations of the Arctic, the Antarctic and the world ocean; Conference-Seminar, Moscow, USSR, February 9-13, 1981, Reports. Leningrad, Gidrometeoizdat, 1982, p. 118-121. In Russian. refs

A83-10836
THE UTILIZATION OF INFRARED /IR/ AERIAL AND SPACE OBSERVATIONS OF ARCTIC SEAS IN NAVIGATION AND DURING THE SOLUTION OF OTHER NATIONAL-ECONOMIC PROBLEMS [ISPOL'ZOVANIE INFRAKRASNYKH /IK/ AEROKOSMICHESKIKH NABLIUDENII ARKTICHESKIKH MOREI V NAVIGATSII I PRI RESHENII DRUGIKH NARODNOKHOZIAISTVENNYKH ZADACH]
A. I. PARAMONOV and V. A. CHEBOTAREVA (Gosudarstvennyi Komitet SSSR po Gidrometeorologii i Kontroliu Prirodnoi Sredy, Arkticheskii i Antarkticheskii Nauchno-Issledovatel'skii Institut, Leningrad, USSR) In: Investigations of the Arctic, the Antarctic and the world ocean; Conference-Seminar, Moscow, USSR, February 9-13, 1981, Reports. Leningrad, Gidrometeoizdat, 1982, p. 159-169. In Russian. refs

Dimensionless parameters for remote IR measurements of the thickness of sea ice are proposed. The influence of tide and topographic waves on the structure of sea ice cover is discussed. The variability of the surface temperature field of two Arctic seas during the summer-autumn period over a number of years is examined. The heat balance components of these seas for September are calculated. B.J.

A83-11352
ESTIMATING WIND SPEED FROM HF SKYWAVE RADAR SEA BACKSCATTER
J. W. MARESCA, JR. and J. R. BARNUM (SRI International Remote Sensing Laboratory, Menlo Park, CA) IEEE Transactions on Antennas and Propagation, vol. AP-30, Sept. 1982, p. 846-852. refs
(Contract NOAA-03-7-022-35111)

Linear expressions are derived for different radar frequencies which relate ocean surface wind speed to a theoretical estimate of the -10 dB width of the HF sea echo Doppler spectrum. This spectrum width changes in a complex way with the continuum of second-order echoes which surround the stronger, first-order echo. The second-order echo amplitude is directly related to changes in the directional ocean wave spectrum, resulting in a high dependence of the wind speed estimates derived on the total energy and direction distribution of the wave field. Doppler spectra recorded under known ocean wind and wave conditions illustrate the difficulty of applying the present theoretical expressions to the estimation of wind speed. It is concluded that the -10 dB width is not an adequate wind speed estimator. O.C.

A83-12032
APPLICABILITY OF SATELLITE-DERIVED SEA-SURFACE TEMPERATURES IN THE FIJI REGION
R. L. MCKENZIE and R. M. NISBET (University of the South Pacific, Suva, Fiji) Remote Sensing of Environment, vol. 12, Nov. 1982, p. 349-361. Research supported by the University of South Pacific. refs

NOAA-5 satellite-derived sea-surface temperature data in the Fiji region for a one-year period starting September 1977 are examined. Time series analysis revealed that the satellite data has spatial and temporal resolutions characterized by a coherence time of about 4 days and a coherence length of 850 km. A systematic difference Delta I between ship and satellite readings was found to correlate significantly with the surface temperature itself, with latitude, and with vapor pressure. Several possible models to explain the behavior of Delta T are introduced. It is concluded that while surface emissivity variations, incomplete cloud decontamination, and cooling across the air-sea interface may all be contributory factors, the bulk of the discrepancy between ship and satellite readings arises from insufficient corrections being made for atmospheric attenuation. This highlights the difficulty of applying data for which globally averaged corrections have been made to a particular latitude band. (Author)

A83-12316* Illinois Univ., Urbana.
REMOTE SENSING OF SEA STATE USING LASER ALTIMETERS
B. M. TSAI and C. S. GARDNER (Illinois, University, Urbana, IL) Applied Optics, vol. 21, Nov. 1, 1982, p. 3932-3940. Research supported by the University of Illinois refs
(Contract NSG-5049)
(Previously announced in STAR as N82-14789)

A83-13057
THE ROLE OF CROSS-EQUATORIAL TROPICAL CYCLONE PAIRS IN THE SOUTHERN OSCILLATION
R. A. KEEN (Cooperative Institute for Research in Environmental Sciences, Boulder, CO) Monthly Weather Review, vol. 110, Oct. 1982, p. 1405-1415. NOAA-supported research. refs

The locations and frequencies of cross-equatorial tropical cyclone pairs over the Pacific Ocean are compared between years of contrasting equatorial Pacific sea surface temperature (SST) and atmospheric circulation anomalies, i.e., high versus low southern oscillation (SO) indices, during the period 1971-79. Weak southeast trade winds associated with low SO indices allow warm (29 C) surface water in the equatorial (0-5 S) zone to extend eastward across the dateline, encouraging formation of cyclone pairs near the dateline. The cyclone pairs, in turn, provide the linkage between warm water and equatorial convection (as indicated by Canton Island rainfall) during southern summer. In general, the occurrences of cyclone pairs vary in longitude with the eastward excursions of warm equatorial water; furthermore, cyclone pairs appear to provide a positive feedback by advancing the eastward warm water extent. The possibility is raised that the occurrence (or absence) of a single synoptic event may influence the outcome of an entire southern oscillation anomaly. (Author)

A83-13059*# National Aeronautics and Space Administration. Goddard Space Flight Center, Greenbelt, Md.
SATELLITE ESTIMATES OF OCEAN-AIR HEAT FLUXES DURING COLD AIR OUTBREAKS
S.-H. CHOU and D. ATLAS (NASA, Goddard Space Flight Center, Laboratory for Atmospheric Sciences, Greenbelt, MD) Monthly Weather Review, vol. 110, Oct. 1982, p. 1434-1450. refs

A method for estimating the heat and moisture fluxes of coastal waters using the cloud free path, the sea surface temperature, and the saturation water vapor mixing ratio is presented. Generalized nomograms for the surface sensible and latent heat fluxes are developed using the Stage and Businger (1981) mixed-layer model. The fluxes are found to be slightly dependent on wind speed. The results are found to be applicable to any path within the cloud-free region, with heat fluxes obtainable by multiplication of the mean heating by the mean wind speed in the boundary layer. Higher stability causes lowered heating. It is shown that the latent heat flux is linear. Applications of the method to lake-effect snowstorms and for verification of boundary-layer models are indicated. M.S.K.

A83-13270
EFFECTS OF MESOSCALE ATMOSPHERIC CONVECTION CELLS ON THE WATERS OF THE EAST CHINA SEA
C. L. TRUMP (U.S. Navy, Naval Research Laboratory, Washington, DC), S. J. NESHYBA, and W. V. BURT (Oregon State University, Corvallis, OR) Boundary-Layer Meteorology, vol. 24, Sept. 1982, p. 15-34. refs
(Contract N00014-76-C-0067; NSF BA-28004; NR PROJECT 083-102)

A83-14093
USE OF AERIAL PHOTOGRAPHY WITH LORAN C POSITIONING TO MAP OFFSHORE SURFACE CURRENTS
D. O. COOK, G. R. DAVIS, R. A. FRANKLIN (Raytheon Ocean Systems Co., East Providence, RI), and T. L. FLYNN (Aero-Marine Surveys, Inc., New London, CT) Photogrammetric Engineering and Remote Sensing, vol. 48, Nov. 1982, p. 1695-1700. U.S. Bureau of Land Management refs
(Contract BLM-AA550-CT6-53)

A technique has been developed for mapping surface currents in the offshore zone which involves aerial photographic tracking of small dye-emitting, radio-equipped tracers by using the Loran C system for positioning. From 60 to 100 aircraft-deployed tracers can be tracked for several days in a 25,000 sq km area, with tracer positions determined to an accuracy of plus or minus 114 m. Associated data processing includes digitizing the photographic tracer information and using a computer to make photogrammetric corrections and display results in various graphical and tabular formats. The proposed technique can be used for basic research on mixing across frontal zones and other physical processes with a surface expression in shelf waters. V.L.

A83-14239#
ON DETECTION OF OIL POLLUTION IN ICE ENVIRONMENT
S. PARASHAR, B. DAWE, J. SNELLEN, G. STAPLETON, and R. WORSFOLD (Remote Applications, Inc., St. John's, Newfoundland, Canada) In: Canadian Symposium on Remote Sensing, 7th, Winnipeg, Canada, September 8-11, 1981, Proceedings. Ottawa, Canadian Aeronautics and Space Institute, 1982, p. 110-119. Research supported by the Department of the Environment. refs

Two studies concerned with the detection of oil in the ice environment are summarized. In one, digital Landsat MSS data was used to detect oil spilled from the damaged 'Kurdistan' tanker. The separation among water, ice, and oil-ice mixture was found best on Band 4 and worst on Band 7. In another, four sensors (an impulse radar, an ultrasonic device, a microwave radiometer and gamma ray spectrometer) were experimentally tested in a laboratory for detecting oil under ice. All sensors were unsuccessful in this experiment in detecting oil under saline ice. Only the ultrasonic device was able to detect oil under the fresh-water ice. The potential role and utility of these and other remote sensors in detecting oil pollution in ice environment are discussed through a review of techniques being used for oil surveillance in the temperate oceans and for ice surveillance. (Author)

A83-14258#
APPLICATION OF REMOTE SENSING TECHNIQUES IN OCEANOGRAPHIC STUDIES OF THE BRITISH COLUMBIA SALMON FISHERY
G. A. BORSTAD, R. M. BROWN, D. TRUAX (Seakem Oceanography, Ltd., Sidney, British Columbia, Canada), T. R. MULLIGAN (Department of Fisheries and Oceans, Pacific Biological Station, Nanaimo, British Columbia, Canada), and J. F. F. GOWER (Department of Fisheries and Oceans, Institute of Ocean Sciences, Sidney, British Columbia, Canada) In: Canadian Symposium on Remote Sensing, 7th, Winnipeg, Canada, September 8-11, 1981, Proceedings. Ottawa, Canadian Aeronautics and Space Institute, 1982, p. 269-277. refs

A83-14278#
APPLICATIONS OF ROBERT'S GRADIENT OPERATOR FOR THE DIGITAL ENHANCEMENT OF ICEBERGS FROM SAR IMAGERY
M. E. KIRBY (Intertech Remote Sensing, Ltd., Ottawa, Canada) In: Canadian Symposium on Remote Sensing, 7th, Winnipeg, Canada, September 8-11, 1981, Proceedings. Ottawa, Canadian Aeronautics and Space Institute, 1982, p. 436-442.

The Roberts gradient operator was employed to develop a shape detector program for discerning icebergs from pack ice when digital X-band satellite imagery is analyzed. The Roberts operator is defined as the sum of absolute values of the differences between diagonally opposite neighboring pixels, thereby reducing the amount of texture in a picture while retaining or enhancing the edges. The operator was applied to an SAR subscene containing three icebergs in two polarizations, cross and parallel. The gradient operator was then combined with median filtering to further reduce the image texture and decrease detected gradients. The median filter involved a 3 x 3 pixel matrix, with the pixels ranked by intensity levels in order to choose the median value for the filter. It is demonstrated that larger, homogeneous zones are generated which more closely resemble icebergs than by use of only the Roberts operator. M.S.K.

A83-14284#
AN ALGORITHM TO INTERFACE NIMBUS-7 SMMR DATA WITH THE AES ICE MODELLING GRID FOR THE BEAUFORT SEA
S. E. WATERMAN, R. YATES, and L. SEELEY-HEUSE (McDonald, Dettwiler and Associates, Ltd., Richmond, British Columbia, Canada) In: Canadian Symposium on Remote Sensing, 7th, Winnipeg, Canada, September 8-11, 1981, Proceedings. Ottawa, Canadian Aeronautics and Space Institute, 1982, p. 485-496. Department of the Environment refs
(Contract DE-43SS-KM601-0-2050)

A resampling algorithm for transferring preprocessed scanning multichannel microwave radiometer (SMMR) data from the Nimbus-7 spacecraft to the Atmospheric Environment Service (AES) ice modelling grid is discussed. The SMMR uses 10 channels with vertical and horizontal polarization at five frequencies from 6.6-37 GHz. Data gathered from the SMMR can be used to measure sea ice concentration, multi-year ice fraction, and the ice surface temperature. The algorithm was developed to transfer the sea ice data to the AES grid to aid in modeling sea ice dynamics in the Beaufort Sea. The algorithm is applied in the output grid coordinate space, allowing resampling of multiple-orbit data sets. Irregularly spaced data are then resampled with an image function which is a group of local functions equal in value and first derivatives at their boundaries. Application to different raster display schemes is also possible with the algorithms. M.S.K.

A83-14316
CONCERNING THE DETERMINATION OF THE TEMPERATURE OF THE OCEAN SURFACE FROM MULTICHANNEL SATELLITE MEASUREMENTS OF RADIATION IN INFRARED ATMOSPHERIC WINDOWS [K VOPROSU OB OPREDELENII TEMPERATURY POVERKHNOSTI OKEANA PO MNOGOKANAL'NYM SPUTNIKOVYM IZMERENIIAM IZLUCHENIIA V 'OKNAKH PROZRACHNOSTI' IK-DIAPAZONA SPEKTRA]
A. I. CHAVRO (Akademiia Nauk SSSR, Institut Kosmicheskikh Issledovanii, Moscow, USSR) Issledovanie Zemli iz Kosmosa, Sept.-Oct. 1982, p. 112-115. In Russian. refs

A83-14502*# National Aeronautics and Space Administration. Goddard Space Flight Center, Greenbelt, Md.
ON THE USE OF LASER PROFILOMETRY FOR OCEAN WAVE STUDIES
C. R. MCCLAIN (NASA, Goddard Space Flight Center, Laboratory for Atmospheric Sciences, Greenbelt, MD), D. T. CHEN (U.S. Navy, Naval Research Laboratory, Washington, DC), and W. D. HART (Science Systems and Applications, Inc., Lanham, MD) Journal of Geophysical Research, vol. 87, Nov. 20, 1982, p. 9505-9515. refs
(Contract NAVY PROJECT RR-032-08-41; NASA TASK 146-40-15-25; NAVAIR TASK WF59553000)

Airborne laser profilometer measurements of wave skewness and spectra are presented. The measurements were made during high wind and sea state conditions in the North Atlantic. The sea states ranged from 4.5 to 8.7 m and varied from swell to wind wave dominated situations. Skewness values for the five cases ranged from 0.08 to 0.28 and compare favorably with other existing measurements. Also, the Phillips and Wallops spectral models show excellent agreement with profilometer spectra of developing seas. For one case where the seas were fully developed, the Pierson-Moskowitz spectrum provides the best representation. (Author)

A83-14851* Applied Physics Lab., Johns Hopkins Univ., Laurel, Md.
A TUTORIAL ASSESSMENT OF ATMOSPHERIC HEIGHT UNCERTAINTIES FOR HIGH-PRECISION SATELLITE ALTIMETER MISSIONS TO MONITOR OCEAN CURRENTS
J. GOLDHIRSH and J. R. ROWLAND (Johns Hopkins University, Applied Physics Laboratory, Laurel, MD) IEEE Transactions on Geoscience and Remote Sensing, vol. GE-20, Oct. 1982, p. 418-434. NASA-supported research refs
(Contract N0024-81-C-5301)

Information from a number of sources is synthesized, and an error budget is deduced giving the projected overall height uncertainty correction for a suggested next-generation high-precision radar altimeter. Uncertainties deriving from the wet and dry troposphere, clouds, and the ionosphere are reviewed. It is assumed that the next generation of precision altimeters will be dual-frequency (13.5 and 6 GHz) and will be designed to correct for the ionospheric error. The altimeter-carrying satellite will have a nadir pointing near coincident-beam dual-frequency microwave radiometer for mitigating the wet tropospheric uncertainty. Whereas there are a number of caveats, the combined uncertainty in the height correction due to the atmosphere for the suggested system should be nominally 3 cm rms compared with at least 6 cm associated with the Seasat-A mission. Improvements in height resolution of the kind discussed here are considered vital for future satellite missions designed to monitor ocean currents. C.R.

A83-14861* Rutgers Univ., New Brunswick, N. J.
OBSERVATIONS OF OCEANIC SURFACE-WIND FIELDS FROM THE NIMBUS-7 MICROWAVE RADIOMETER
J. R. MILLER, J. E. GEYSER (Rutgers University, New Brunswick, NJ), A. T. C. CHANG, and T. T. WILHEIT, JR. (NASA, Goddard Space Flight Center, Greenbelt, MD) IEEE Transactions on Geoscience and Remote Sensing, vol. GE-20, Oct. 1982, p. 549-554. refs
(Contract NAS5-26123)

Brightness temperatures from the five-frequency dual-polarized scanning multichannel microwave radiometer (SMMR) on Nimbus 7 have been used to obtain surface wind fields over the ocean. The satellite-derived wind field for 1200Z, Feb. 19, 1979, in the eastern North Pacific has been compared with an operationally generated surface-wind analysis field. Previous point comparisons at selected locations have indicated that satellite winds are accurate to 3 m/sec. The results, although of a preliminary nature, indicate that SMMR-derived winds may be used to determine large-scale wind fields over the ocean, particularly in areas of strong wind gradients such as found in cyclonic systems. (Author)

A83-15058
THE PERMANENTLY SPARSE AREAS OF ICE COVER IN THE OPEN REGIONS OF THE OKHTSK SEA [POSTOIANNYE RAZREZHENIIA LEDIANOGO POKROVA V OTKRYTYKH RAIONAKH OKHOTSKOGO MORIA]
V. A. KOVSHOV and IU. N. SINIURIN (Glavnyi Radiometeorologicheskii Tsentr, USSR) Meteorologiia i Gidrologiia, Nov. 1982, p. 76-81. In Russian.

NOAA and Meteor satellite data from 1977-1980 identified areas in the Okhotsk Sea where the ice cover is permanently sparse. The data show that these areas are governed by a system of permanent currents and Coriolis forces acting on the drifting ice. The areas coincide with cyclonic gyres and regions where currents diverge. S.C.S.

A83-16581*# Jet Propulsion Lab., California Inst. of Tech., Pasadena.
FLIGHT PATH DESIGN ISSUES FOR THE TOPEX MISSION
J. C. FRAUTNICK and E. CUTTING (California Institute of Technology, Jet Propulsion Laboratory, Pasadena, CA) American Institute of Aeronautics and Astronautics, Aerospace Sciences Meeting, 21st, Reno, NV, Jan. 10-13, 1983, 10 p. NASA-supported research. refs
(AIAA PAPER 83-0197)

The proposed Ocean Topography Experiment (TOPEX) is an earth satellite mission currently under consideration by NASA. The primary purpose of the experiment is to determine the general circulation of the oceans and its variability. High precision, space based altimeter measurements will be combined with surface measurements and ocean models to accomplish the mission objectives. The paper will discuss mission requirements on orbit design, orbit selection space, derived requirements on navigation and satellite design issues which impact orbit selection. Unique aspects of the TOPEX orbit design are highlighted, such as high precision repeating orbits, 'frozen orbit' values of eccentricity and periapses, precise maneuver and orbit determination requirements and insuring crossing arcs over a calibration-site. (Author)

A83-16701*# National Aeronautics and Space Administration. Goddard Space Flight Center, Greenbelt, Md.
OSTA-1/OCEAN COLOR EXPERIMENT
H. H. KIM (NASA, Goddard Space Flight Center, Greenbelt, MD) and H. VAN DER PIEPEN (Deutsche Forschungs- und Versuchsanstalt fuer Luft- und Raumfahrt, Oberpfaffenhofen, West Germany) American Institute of Aeronautics and Astronautics, Aerospace Sciences Meeting, 21st, Reno, NV, Jan. 10-13, 1983, 8 p.
(AIAA PAPER 83-0415)

Ocean Color Experiment (OCE) on the OSTA-1 mission acquired ocean images at several widely separated locations on the earth. Digital computer enhancement and band ratioing techniques were used to emphasize patterns of chlorophyll and sediment distribution

in the Yellow Sea and, in one case, of bottom topography in the Great Bahama Bank. Two scenes in the Gulf of Cadiz from orbits 30 and 32 were geometrically corrected to show the movement of plankton patches. This technique enabled ocean current velocities to be deduced. A duplicate of the OCE instrument mounted on a DFVLR aircraft was flown over an area of the Atlantic Ocean off the coast of Portugal during the Shuttle mission. (Author)

A83-17709
SKY-WAVE RADAR SEA-STATE SENSING - EFFECTS OF IONOSPHERIC MOVEMENT AND PROPAGATION GEOMETRY
P. A. BRADLEY, E. N. BRAMLEY (Science and Engineering Research Council, Rutherford Appleton Laboratory, Slough, Bucks., England), W. A. SANDHAM, E. D. R. SHEARMAN, and S. THEODORIDIS (Birmingham, University, Birmingham, England) International Journal of Remote Sensing, vol. 3, Oct.-Dec. 1982, p. 373-382. refs

In the sky-wave radar technique, the parameters of sea waves beyond the horizon are deduced from the Doppler spectra of ionospherically propagated sea echoes. Ionospheric movements and multipath can contaminate the sea echo spectrum from a given location. Measurements of the multipath and Doppler spread for a 700 km ionospheric path during MARSEN are reported. For one hop by way of the F2 layer, a typical r.m.s. Doppler shift over 10 min was 0.005 Hz and Doppler spread, to -10 dB, was 0.08 Hz. Multihop and side-scatter modes of propagation and their Doppler structure were identified. The possible use of side scatter at the sea surface is analyzed. (Author)

A83-17710* National Aeronautics and Space Administration. Langley Research Center, Hampton, Va.
MEASUREMENTS OF OCEAN SURFACE SPECTRUM FROM AN AIRCRAFT USING THE TWO-FREQUENCY MICROWAVE RESONANCE TECHNIQUE
J. W. JOHNSON (NASA, Langley Research Center, Hampton, VA), D. E. WEISSMAN (Hofstra University, Hempstead, NY), and W. L. JONES (General Electric Co., Valley Forge Space Center, Philadelphia, PA) International Journal of Remote Sensing, vol. 3, Oct.-Dec. 1982, p. 383-407. refs

The present investigation is concerned with the results of a two-frequency (Delta k) microwave radar experiment conducted from an aircraft and aimed primarily at the development of remote sensing techniques to measure ocean surface wave spectral characteristics. The experiment was conducted as part of the Maritime Remote Sensing (MARSEN) project in the North Sea during the autumn of 1979. The objective was to demonstrate the feasibility of and study the performance of the Delta k technique from a higher altitude platform, at shallower incidence angles, and at higher Doppler velocities than earlier stationary platform experiments allowed. A quantitative engineering evaluation of the results of two comprehensive flights is provided, and the qualitative significance of the results is discussed from a geophysical point of view in terms of the existing theory. G.R.

A83-17712
SPECTRAL SIGNAL TO CLUTTER AND THERMAL NOISE PROPERTIES OF OCEAN WAVE IMAGING SYNTHETIC APERTURE RADARS
W. ALPERS (Hamburg, Universitaet; Max-Planck-Institut fuer Meteorologie, Hamburg, West Germany) and K. HASSELMANN (Max-Planck-Institut fuer Meteorologie, Hamburg, West Germany) International Journal of Remote Sensing, vol. 3, Oct.-Dec. 1982, p. 423-446. refs

It is noted that in such cases as low-amplitude swell and the short wave-length end of a wind wave spectrum, the wave image spectrum may simply be lost in the background noise spectrum. This spectrum comprises the clutter spectrum, deriving from the random nature of the backscattering surface elements, and the normal thermal noise spectrum, originating in the SAR system itself. The spectral signal-to-background resolution limit is investigated, with particular emphasis placed on the short wavelength detection limit for wind seas. It is shown that for a given power, the maximum detection cut-off wavenumber is attained if the SAR resolution is selected in such a way that the clutter and noise spectra are equal at the cut-off wavenumber. To first order, incoherent multilook averaging is found to have no influence on the signal-to-background detection cut-off wavenumber, provided that the reduced Nyquist cut-off wavenumber resulting from the reduced multilook spatial resolution remains greater than the signal-to-background cut-off wavenumber. C.R.

A83-17714* Hamburg Univ. (West Germany).
THE EFFECT OF MONOMOLECULAR SURFACE FILMS ON THE MICROWAVE BRIGHTNESS TEMPERATURE OF THE SEA SURFACE
W. ALPERS (Hamburg, Universitaet; Max-Planck-Institut fuer Meteorologie, Hamburg, West Germany), H.-J. C. BLUME (NASA, Langley Research Center, Hampton, VA), W. D. GARRETT (U.S. Navy, Naval Research Laboratory, Washington, DC), and H. HUEHNERFUSS (Hamburg, Universitaet, Hamburg, West Germany) International Journal of Remote Sensing, vol. 3, Oct.-Dec. 1982, p. 457-474. Research supported by the Deutsche Forschungsgemeinschaft and U.S. Navy. refs

It is pointed out that monomolecular surface films of biological origin are often encountered on the ocean surface, especially in coastal regions. The thicknesses of the monomolecular films are of the order of 3 x 10 to the -9th m. Huehnerfuss et al. (1978, 1981) have shown that monomolecular surface films damp surface waves quite strongly in the centimeter to decimeter wavelength regime. Other effects caused by films are related to the reduction of the gas exchange at the air-sea interface and the decrease of the wind stress. The present investigation is concerned with experiments which reveal an unexpectedly large response of the microwave brightness temperature to a monomolecular oleyl alcohol slick at 1.43 GHz. Brightness temperature is a function of the complex dielectric constant of thy upper layer of the ocean. During six overflights over an ocean area covered with an artificial monomolecular alcohol film, a large decrease of the brightness temperature at the L-band was measured, while at the S-band almost no decrease was observed. G.R.

A83-17840#
SUPER HIGH ALTITUDE PHOTOGRAPHY FOR COASTAL GEOMORPHOLOGY
H. G. GIERLOFF-EMDEN (Muenchen, Universitaet, Munich, West Germany) ITC Journal, no. 3, 1982, p. 313-316.

The data acquisition techniques currently preferred for coastal studies include conventional aerial photography (usually from an altitude of approximately 3 km) and satellite remote sensing (from an altitude of approximately 900 km for Landsat). The employment of an intermediate range involves the use of super high altitude photography from an altitude of approximately 20 km. A description is provided of the results of detailed analyses of super high altitude photography to determine its applicability for coastal studies. It is pointed out that high altitude and super high altitude photography (SHAPh) has been used since the early 1960s to fill the gaps in small and medium scale mapping programs. Attention is given to applications of SHAPh to mapping, spatial resolution for coastal studies, and the interpretation of coastal features from SHAPh. G.R.

A83-18580* Miami Univ., Coral Gables, Fla.
PHYTOPLANKTON PIGMENT CONCENTRATIONS IN THE MIDDLE ATLANTIC BIGHT - COMPARISON OF SHIP DETERMINATIONS AND CZCS ESTIMATES
H. R. GORDON, J. W. BROWN (Miami, University, Coral Gables, FL), D. K. CLARK (NOAA, National Earth Satellite Service, Washington, DC), O. B. BROWN, R. H. EVANS (Miami, University, Miami, FL), and W. W. BROENKOW (Moss Landing Marine Laboratories; San Jose State University, Moss Landing, CA) Applied Optics, vol. 22, Jan. 1, 1983, p. 20-36. refs
(Contract N00014-80-C-0042; NAS5-22963; NSF OCE-80-16991 ; NOAA-NA-79SA00741; NOAA-04-8M01-129)

The processing algorithms used for relating the apparent color of the ocean observed with the Coastal-Zone Color Scanner on

Nimbus-7 to the concentration of phytoplankton pigments (principally the pigment responsible for photosynthesis, chlorophyll-a) are developed and discussed in detail. These algorithms are applied to the shelf and slope waters of the Middle Atlantic Bight and also to Sargasso Sea waters. In all, four images are examined, and the resulting pigment concentrations are compared to continuous measurements made along ship tracks. The results suggest that over the 0.08-1.5 mg/cu m range, the error in the retrieved pigment concentration is of the order of 30-40% for a variety of atmospheric turbidities. In three direct comparisons between ship-measured and satellite-retrieved values of the water-leaving radiance, the atmospheric correction algorithm retrieved the water-leaving radiance with an average error of about 10%. This atmospheric correction algorithm does not require any surface measurements for its application. (Author)

A83-18581*# National Aeronautics and Space Administration. Wallops Flight Center, Wallops Island, Va.
EXPERIMENTAL FEASIBILITY OF THE AIRBORNE MEASUREMENT OF ABSOLUTE OIL FLUORESCENCE SPECTRAL CONVERSION EFFICIENCY
F. E. HOGE (NASA, Wallops Flight Center, Wallops Island, VA) and R. N. SWIFT (EG & G Washington Analytical Services Center, Inc., Pocomoke City, MD) Applied Optics, vol. 22, Jan. 1, 1983, p. 37-47. refs

Airborne lidar oil spill experiments carried out to determine the practicability of the AOFSCE (absolute oil fluorescence spectral conversion efficiency) computational model are described. The results reveal that the model is suitable over a considerable range of oil film thicknesses provided the fluorescence efficiency of the oil does not approach the minimum detection sensitivity limitations of the lidar system. Separate airborne lidar experiments to demonstrate measurement of the water column Raman conversion efficiency are also conducted to ascertain the ultimate feasibility of converting such relative oil fluorescence to absolute values. Whereas the AOFSCE model is seen as highly promising, further airborne water column Raman conversion efficiency experiments with improved temporal or depth-resolved waveform calibration and software deconvolution techniques are thought necessary for a final determination of suitability. C.R.

N83-10473*# Ocean Data Systems, Inc., Monterey, Calif.
SEASAT-A SASS WIND PROCESSING
R. A. LANGLAND, P. L. STEPHENS, and G. G. PIHOS Mar. 1980 9 p Prepared for JPL, Pasadena
(Contract JPL-955370)
(NASA-CR-169433; JPL-9950-738; NAS 1.26:169433) Avail: NTIS HC A02/MF A01 CSCL 08C

The techniques used for ingesting SEASAT-A SASS wind retrievals into the existing operational software are described. The intent is to assess the impact of SEASAT data in he marine wind fields produced by the global marine wind/sea level pressure analysis. This analysis is performed on a 21/2 deg latitude/longitude global grid which executes at three hourly time increments. Wind fields with and without SASS winds are being compared. The problems of data volume reduction and aliased wind retrieval ambiquity are treated. A.R.H.

N83-10483# Rhode Island Univ., Narragansett. Dept. of Ocean Engineering.
REMOTE SENSING, A TOOL FOR MANAGING THE MARINE ENVIRONMENT: EIGHT CASE STUDIES
G. BEHIE and P. CORNILLON 1982 44 p
(Contract SG-NA79AA-D-00096)
(PB82-220864; URI-MTR-77; NOAA-81072405) Avail: NTIS HC A03/MF A01 CSCL 13B

The applications of remote sensing described are not confined to satellite-derived imagery. The common link between all eight applications, which involved several remote-sensing techniques, is the usefulness of remote sensing in making needed management decisions. Similar projects in the future will definitely use satellites in some instances, while in others aircraft may remain the best tool. The purpose in presenting these case studies is to suggest the variety of ways in which remote sensing can be useful in studying the coastal and marine environment. It is hoped that the diversity of applications described, of data sources and platforms used (satellite/aircraft), as well as the high-quality photographs that resulted, may identify for the reader potential applications in his or her own area of interest. Author

N83-10647*# National Aeronautics and Space Administration. Langley Research Center, Hampton, Va.
ANALYSIS OF HIGH ALTITUDE REMOTELY SENSED DATA COLLECTED IN THE NANTUCKET SHOALS EXPERIMENT 4-15 MAY, 1981
C. W. OHLHORST Sep. 1982 37 p refs
(NASA-TM-84547; NAS 1.15:84547) Avail: NTIS HC A03/MF A01 CSCL 13B

High altitude ocean color scanner ratios of band 2 (456 to 476 nanometers) to band 4 (539 to 559 nanometers) and band 1 (418 to 438 nanometers) to band 3 (498 to 518 nanometers) had high correlation coefficient values (-0.928 and 0.891 respectively) with seven boat sampled chlorophyll a measurements. The range of chlorophyll a concentrations was small (1.7-2.58 mg/cu m.). Each ratio was used to calculate chlorophyll a values for the center pixel of each scan line on flight lines 5 and 6. The two ratios produced dissimilar chlorophyll a trends. Due to the high noise level in the scanner data, no reliable synoptic chlorophyll a map could be generated with either ratio algorithm. S.L.

N83-10707# National Oceanic and Atmospheric Administration, Rockville, Md. Engineering Development Office.
EFFECTS OF DETECTION ALGORITHM ON ACCURACY DEGRADATION FROM LOGARITHMIC AND DIFFERENCE PROCESSING FOR AIRBORNE LASER BATHYMETRY RETURNS
G. C. GUENTHER Feb. 1982 45 p refs
(PB82-215138; NOAA-82041501; NOAA-TR-OTES-6) Avail: NTIS HC A03/MF A01 CSCL 14B

The Hydrographic Airborne Laser Sounder (HALS) system currently under construction for the Naval Ocean Research and Development Activity (NORDA) incorporates logarithmic amplification for dynamic range compression and a first difference processing circuit to reduce the volume scattering signal prior to the arrival of the bottom return. These non-linear signal processing steps distort the input waveforms and lead to depth measurement biases whose magnitudes depend on signal strengths, pulse location algorithms, and algorithm parameters. The behavior of the estimated biases for varying circuit parameters is shown to be sensitive to the assumed pulse shape. An appropriate gamma function representation is selected and discussed. Biases as a function of signal strengths are reported for two separate pulse location algorithms: linear fractional thresholds and a 'constant fraction discriminator' circuit as used in HALS. If return signal strengths are recorded by the operational system software, these bias predictors can be applied to field data as estimated bias correctors. Author

N83-10739# Environmental Research Inst. of Michigan, Ann Arbor. Applications Div.
RADIANCE CALCULATIONS FOR OPTIMIZATION OF SENSORS DESIGNED FOR REMOTE BATHYMETRY, VOLUME 1 Final Technical Report
F. J. TANIS and F. POLCYN Jul. 1982 137 p refs
(Contract N00014-81-C-2350)
(AD-A117743; ERIM-155800-1-F1) Avail: NTIS HC A07/MF A01 CSCL 08J

An extensive set of radiance calculations have been generated for each of twelve representative bottom types using an existing water radiance and atmospheric radiative transfer model. Total radiance values were calculated under two separate (Elterman) atmospheric states for a sensor platform altitude of 50 km. Calculations were also made for a sensor placed just below the sea surface. The model parameters were iterated over representative water depths and water types. A preliminary visual band optimization analysis was made over the input parameters.

The suitability of Landsat-D Thematic mapper (TM) bands is also addressed. Author (GRA)

N83-10740# National Oceanic and Atmospheric Administration, Boulder, Colo. Office of Marine Pollution Assessment.
OCEAN POLLUTION RESEARCH, DEVELOPMENT AND MONITORING Annual Report, FY 1981
Jan. 1982 117 p refs
(PB82-219049; NOAA-82042703) Avail: NTIS HC A06/MF A01 CSCL 08J

The research summaries follow the categories of concern developed in the Federal plan for ocean pollution research, development and monitoring. These categories are: marine waste disposal, marine mining, marine energy, marine transportation, accidental discharge of oil and hazardous materials, coastal land use, and ocean pollution assessment and management of cumulative effects. GRA

N83-11568# Naval Ocean Research and Development Activity, Bay St. Louis, Miss. Numerical Modeling Div.
COLLINEAR-TRACK ALTIMETRY IN THE GULF OF MEXICO FROM SEASAT: MEASUREMENTS, MODELS AND SURFACE TRUTH Final Report
J. D. THOMPSON, G. H. BORN (JPL, California Inst. of Tech., Pasadena), and G. A. MAUL Jun. 1982 36 p refs
(AD-A118160; NORDA-TN-57) Avail: NTIS HC A03/MF A01 CSCL 18C

From 17 September to 10 October 1978 SEASAT made collinear passes over the Gulf of Mexico. Altimeter data for eight, three-day repeat passes over the eastern Gulf were examined using an arc-segment fitting technique to determine the mesoscale temporal variability of the sea surface. The pattern of sea height variability was then compared with sea height data generated by a numerical model of the Gulf (Hurlburt and Thompson, 1980) from the simulation of a complete cycle of Loop Current intrusion and shedding of an anticyclonic eddy. The model data was found to match that from the SEASAT altimeter when an anticyclonic eddy separated from the Loop Current and the Loop began to repenetrate into the eastern Gulf. Analysis of sparse ground truth data from ship-of-opportunity XBT's, satellite infrared imagery of the Loop Current boundary, and synthetic aperture radar (SAR) imagery, also from SEASAT, tend to confirm the circulation patterns deduced from the altimeter data and the numerical model. Author (GRA)

N83-11570# Naval Surface Weapons Center, Dahlgren, Va.
MEAN EARTH ELLIPSOID DETERMINED FROM SEASAT ALTIMETER OBSERVATIONS Final Report
G. B. WEST Sep. 1981 21 p refs
(AD-A117910; NSWC/TR-252) Avail: NTIS HC A02/MF A01 CSCL 03A

The radius and the origin of a mean-Earth ellipsoid have been determined from SEASAT satellite radar altimeter observations of the ocean surface and potential coefficients. Assuming that the altimetric geoid is the best available, adjustments are made to the geoid derived from potential coefficients so that the geoid height differences are minimized. A least-squares fitting procedure based on mean geoid heights in 5 degrees x 5 degrees areas was used in the determination of the ellipsoidal parameters. Solutions from two different sets of altimetric geoid heights and geoid heights derived from potential coefficients gave a mean-Earth ellipsoid with radius, a = 6378134.9 m and origin shifts less than 1 m in the x and y components and approximately -2.5 m in the z component. Author (GRA)

N83-11692# Underwater Systems, Inc., Rockville, Md.
ANALYSES OF OCEANIC SUBSURFACE FEATURES USING SPACE BASED RADAR IMAGERY Final Report
S. W. MCCANDLESS and C. P. MRAZEK Jul. 1982 204 p refs
(Contract N00014-82-C-0114)
(AD-A118411) Avail: NTIS HC A10/MF A01 CSCL 08J

Bathymetric features are visible on some SEASAT SAR and SIR-A images. This study surveyed as wide a data base as possible and collected available ground truth to determine the limits of this visibility. Such parameters as tidal levels, currents, wind, rain, radar incidence angle, radar aspect angle and radar processing were all considered. Some dependence of visibility on current was discovered, and conversely, independence of radar incidence angle. The results were severely limited by the lack of detailed ground truth of an appropriate nature. Author (GRA)

N83-12037# Office of Naval Research, Arlington, Va.
NAVAL RESEARCH REVIEWS, VOLUME 34, NO. 1
W. J. LESCURE, III, ed. 1982 63 p refs
(AD-A117981) Avail: NTIS MF A01; SOD HC $11.00 CSCL 17E

Contents: Remote Sensing Research, Visible and Infrared Satellite Remote Sensing - A Status Report, Outbreaks of Polar Continental Air: Windows on the Mesoscale Structure of the Upper Ocean, Surface Wave Modulation Patterns in Radar Images, and Three Dimensional Representation of Clouds from Satellite Images. GRA

N83-12511# Naval Ocean Research and Development Activity, Bay St. Louis, Miss. Ocean Science and Technology Lab.
COMPARISON OF MULTICHANNEL AND TWO-SATELLITE METHODS FOR REMOTE MEASUREMENT OF SEA SURFACE TEMPERATURE Final Technical Report
R. HOLYER and J. HAWKINS Jul. 1982 16 p refs
(AD-A118736; NORDA-TN-162) Avail: NTIS HC A02/MF A01 CSCL 17E

Atmospheric correction of IR satellite data for retrieval of sea surface temperatures (SST) by means of differential absorption can take on two forms. The most popular method utilizes changes in the spectral transmittance of the atmosphere between two or more IR channels (multichannel). The second form employs path length differences in the same spectral band using two satellites. The multichannel and two satellite approaches are applied to coincident imagery and in situ data and compared. GRA

N83-12707# World Meteorological Organization, Geneva (Switzerland).
REPORT OF THE MONEX REVIEW MEETING Global Atmospheric Research Programme
1981 146 p refs Conf. held at Denpasar, Bali, 2-6 Nov. 1981 Prepared on cooperation with ICSU, Rome
(GARP-SPEC-REPT-38) Avail: Issuing Activity

Completion of Monex data management was planned and further monsoon investigations were proposed. Summer Monex data collection is summarized. The status of level 2 b data and nonmerged, non-FGGE data processing is reported. Winter Monex data management is surveyed. Upper air dropwindsonde and ship data for oceanic areas in the summer Monex region are given. Statistics of synoptic data from quick look tapes, stripped FGGE tapes, level 2 b tapes and ship observations during 1 - 7 May 1979 are available. Author (ESA)

N83-12724# World Meteorological Organization, Geneva (Switzerland).
GLOBAL WEATHER EXPERIMENT. THE GARP ATLANTIC TROPICAL EXPERIMENT (GATE) MONOGRAPH
Apr. 1982 462 p refs Prepared in cooperation with International Council of Scientific Unions, Rome
(GARP-PUB-SER-25) Avail: NTIS MF A01; print copy available at WMO, Geneva

Papers on GATE objectives and techniques are presented. Large-scale mean state, synoptic-scale motions, boundary layer,

and radiation studies are summarized. Tropical waves are analyzed theoretically. The A/B and B scale motions in the intertropical convergent zones are investigated. Clouds, convection, and the physics of the upper tropical ocean are examined.

N83-12735# Hydrometeorological Centre of the USSR (Moscow).
MAIN ACHIEVEMENTS OF GARP ATLANTIC TROPICAL EXPERIMENT (GATE) AND ITS IMPACT ON FGGE
M. A. PETROSSIANTS *In* WMO Global Weather Expt. The GARP Atlantic Tropical Expt. (GATE) Monograph p 467-477 Apr. 1982 refs
Avail: NTIS MF A01; print copy available at WMO, Geneva

The GATE results, concerning large-scale mean state, easterly waves, large-scale numerical modelling, oceanography, the intertropical convergent zones, convection, boundary layers, and radiation, are summarized. Observational techniques developed during GATE are described and the use of GATE experience for the implentation and management of FGGE is discussed.
Author (ESA)

N83-12801# World Meteorological Organization, Geneva (Switzerland).
MANUAL ON THE GLOBAL OBSERVING SYSTEM. VOLUME 1 (ANNEX TO THE WMO TECHNICAL REGULATIONS): GLOBAL ASPECTS, 1981 EDITION
1981 111 p
(WMO-544-VOL-1-ANNEX; ISBN-92-63-12544-9) Avail: NTIS MF A01; print copy available at WMO, Geneva

Technical regulations (standard or recommended practices and procedures) for the guidance of global observing system members are given. Surface and space based systems are covered. Observational requirements, requirements for horizontal spacing, reporting frequency, and reduction of level 1 data are treated. The values of physical functions and constants, barometer conventions and calculation procedures are presented. Quality control procedures are outlined. Author (ESA)

N83-12802# World Meteorological Organization, Geneva (Switzerland).
WORLD INTEGRATED OCEANIC SERVICES SYSTEM: GENERAL PLAN AND OPERATIONAL PROGRAM FOR 1982-1985 [SYSTEME MONDIAL INTEGRE DE SERVICES OCEANIQUES: PLAN GENERAL ET PROGRAMME DE MISE EN OEUVRE POUR 1982-1985]
Jan. 1982 49 p In FRENCH Prepared in cooperation with UNESCO's Commission Oceanographique Intergouvernementale
(WMO-582; ISBN-92-63-20582-5) Avail: NTIS MF A01; print copy available at WMO, Geneva

General principles as to the observation and study of the ocean and atmosphere, emphasizing their interaction, are outlined. The World Integrated Oceanic Services System (WIOSS) meets these requirements. The WIOSS observation system as well as the data processing and analysis system are described. Measures taken relative to telecommunications and the dissemination of WIOSS information are reported. Other activities related to WIOSS (training, R and D, operations management) are also mentioned.
Author (ESA)

N83-12803# World Meteorological Organization, Geneva (Switzerland).
COMMISSION FOR MARINE TECHNOLOGY: ABRIDGED REPORT OF THE 8TH SESSION Final Report
1981 126 p Presented at Hamburg, 14-25 Sep. 1981
(WMO-584; ISBN-92-63-10584-7) Avail: Issuing Activity

Marine meteorology, maritime navigation, and ocean exploration and exploitation are considered, stressing application of meteorology and international cooperation. Prediction and early warning of hazardous weather conditions and associated floods are discussed, particularly in respect to observing activities over the ocean, marine data collection, marine climatology and sea ice. The economic impact of marine meteorological information, e.g. ship weather routing, is pointed out. The need for rational use of ocean resources and environmental protection is mentioned. Tasks of the Commission are to contribute substantially to the World Weather Watch and the World Climate Program and to provide ocean data for medium-range and long-range weather forecasting and research. Author (ESA)

N83-12808# World Meteorological Organization, Geneva (Switzerland).
THE GLOBAL WEATHER EXPERIMENT. FIRST GARP GLOBAL EXPERIMENT (FGGE) OPERATIONS REPORT SERIES: VOLUME 5, SUMMARY OF DATA COLLECTED 5 JULY - DECEMBER 1979 Global Atmospheric Research Program
Oct. 1981 104 p refs Prepared in cooperation with ICSU, Rome
(GARP-FOR-5) Avail: NTIS MF A01; print copy available at WMO, Geneva

Information on the volume of data collected during the FGGE is presented. The frequency and the geographical distribution of observations is presented in two different ways. In map form, utilizing the gray-shading technique, the daily average number of each type of observation is shown for the whole globe from 80 deg S to 80 deg N and for the polar regions. In order to provide in more detail the distribution of the observations, the tables present the daily average number of observations for each 5 deg latitude by 5 deg longitude area. The gray-shaded maps illustrate roughly the global distribution of observations. Before drawing the isolines, the daily average number of observations was computed over a unit area of 1000 km by 1000 km centered in the middle of each 5 deg latitude by 5 deg longitude area on the globe. One result of this technique is that ocean-based observations from areas near the coastlines have an impact on the data coverage over adjacent continents and vice versa. Author (ESA)

N83-12828*# Washington Univ., Seattle. Dept. of Geography.
COMPARISON OF ENVIRONMENTAL CONDITIONS IN THE BERING SEA AND DAVIS STRAIT AND THE EFFECTS ON MICROWAVE SIGNATURE RETURNS; MARCH AND APRIL, 1979 Final Report
S. L. MCNUTT and S. MARTIN 15 Jun. 1982 95 p refs
(Contract NAG5-161)
(NASA-CR-169473; NAS 1.26:169473) Avail: NTIS HC A05/MF A01 CSCL 08J

Aircraft data collected in the Bering Sea in March, 1979 using a 6.6 GH sub z (C Band) microwave radiometer and a 13.9 GH sub z (Ku Band) scatterometer, reinforce the difficulties in interpreting first year ice types found near the ice edge in a marginal ice zone. An ice interpretation scheme using data taken with a 13.3 GH sub z (Ku Band) scatterometer and a 19.4 GH sub z (K Band) radiometer in Davis Strait also shows ambiguity in the first year ice signal and indicates that ice interpretation becomes more difficult near the ice edge and under warmer conditions. This report also compares X Band SAR data taken in Davis Strait with similar imagery collected in the Bering Sea. Ice core samples from the Bering test area offer a basis for speculation on changes in ice morphology which affect the signature return at the ice edge, and help explain the difficulty of the sensors in discerning the two different ice types found on the photography and in the core samples. Author

N83-13534*# Research Triangle Inst., Research Triangle Park, N.C. Office of Geosciences Programs.
A COMPARISON OF HCMM SURFACE TEMPERATURES WITH IN SITU TEMPERATURE DATA Quarterly Progress Report
F. M. VUKOVICH, Principal Investigator Jun. 1982 5 p HCMM
(Contract NAS5-26863)
(E83-10040; NASA-CR-169512; NAS 1.26:169512) Avail: NTIS HC A02/MF A01 CSCL 05B

All HCMM required were processed. Calibrated and atmospherically corrected sea surface temperatures were developed for the Nantucket Shoals and Gulf of Mexico regions. These data were analyzed and the sea surface temperatures along the various transacts were compared with in situ data. The

comparisons indicate that there is, on the average, a root mean square difference between the in situ data and the HCMM sea surface temperatures of + or - 1.0 C. The linear correlation coefficient was 0.97. A.R.H.

N83-13544*# National Aeronautics and Space Administration. Goddard Space Flight Center, Greenbelt, Md.
AIRCRAFT AND SATELLITE MEASUREMENT OF OCEAN WAVE DIRECTIONAL SPECTRA USING SCANNING-BEAM MICROWAVE RADARS
F. C. JACKSON, W. T. WALTON, and P. L. BAKER (Computer Sciences Corp., Silver Spring, Md.) May 1982 81 p refs Presented at the Wave Dyn. and Radio Probing of the Ocean Surface Symp., Miami, Fla., 14-20 May 1981; sponsored by NAS-NRC Submitted for publication
(NASA-TM-84008; NAS 1.15:84008) Avail: NTIS HC A05/MF A01 CSCL 17I

A microwave radar technique for remotely measuring the vector wave number spectrum of the ocean surface is described. The technique, which employs short-pulse, noncoherent radars in a conical scan mode near vertical incidence, is shown to be suitable for both aircraft and satellite application, the technique was validated at 10 km aircraft altitude, where we have found excellent agreement between buoy and radar-inferred absolute wave height spectra. Author

N83-13572*# National Aeronautics and Space Administration. Goddard Space Flight Center, Greenbelt, Md.
THE BERING SEA ICE COVER DURING MARCH 1979: COMPARISON OF SURFACE AND SATELLITE DATA WITH THE NIMBUS-7 SMMR Annual Report
S. MARTIN, D. J. CAVALIERI, P. GLOERSEN, and S. L. MCNUTT Jan. 1982 55 p refs Prepared in cooperation with Washington Univ.
(Contract NAG5-161; MO-A01-78-00-4335; NA81RAC000-13)
(NASA-CR-169393; NAS 1.26:169393; PB82-230400; NOAA-82051011) Avail: NTIS HC A04/MF A01 CSCL 08L

During March 1979, field operations were carried out in the Marginal Ice Zone (MIZ) of the Bering Sea. The field measurements which included oceanographic, meteorological and sea ice observations were made nearly coincident with a number of Nimbus-7 and Tiros-N satellite observations. The results of a comparison between surface and aircraft observations, and images from the Tiros-N satellite, with ice concentrations derived from the microwave radiances of the Nimbus-7 Scanning Multichannel Microwave Radiometer (SMMR) are given. Following a brief discussion of the field operations, including a summary of the meteorological conditions during the experiment, the satellite data is described with emphasis on the Nimbus-7 SMMR and the physical basis of the algorithm used to retrieve ice concentrations. GRA

N83-13773*# City Univ. Inst. of Marine and Atmospheric Sciences, New York.
THE MEASUREMENT OF THE SYNOPTIC SCALE WIND OVER THE OCEAN Technical Report, 1981 - 1982
W. J. PIERSON Dec. 1982 81 p refs
(Contract NAS1-15669; NAGW-266)
Avail: NTIS HC A05/MF A01 CSCL 08C

Mesoscale and microscale features of the turbulent winds over the ocean are related to the synoptic scale winds in terms of published spectral forms for the microscale, a mesoscale valley and published values of U*, VAR u', VAR v' and z/L, as defined in the text and as obtained for moderate to gale force winds. The frequencies involved correspond to periods longer than 1 hour and extend to the microscale, which starts at a period near 2 minutes, or so, and continues to the Kolmogorov inertial range. Nondimensional spectra that span both the mesoscale and the microscale are derived as a function of u, f(= n z/u) and z/L, where z is 10 meters, L is the Monin Obukov stability length and u is evaluated at 10 meters. For the same u, different values of z/L produce a range of values of u which in turn result in variations of the eddy structure of the mesoscale and microscale spectra. Both conventional anemometer averages and remotely sensed winds contain a random component of the mesoscale wind in their values. These components are differnces and not errors when winds are compared, and quantitative values for these differences are given. Ways to improve the measurement of the synoptic scale wind by transient ships, data buoys and scatterometers on future spacecraft are described. These ways are loner averaging times for ships and data buoys, depending on the synoptic conditions, and pooling spacecraft to form super observations. Design considerations for future remote sensing systems are given. Author

N83-13776*# Environmental Research Inst. of Michigan, Ann Arbor. Radar and Optics Div.
FURTHER SEASAT SAR COASTAL OCEAN WAVE ANALYSIS Final Report, Mar. 1980 - Sep. 1981
E. S. KASISCHKE, R. A. SHUCHMAN, G. A. MEADOWS, P. L. JACKSON, and Y. TSENG Sep. 1981 207 p refs Sponsored in part by NASA
(Contract MO-A01-78-00-4339)
(NASA-CR-169682; NAS 1.26:169682; PB82-230350; ERIM-138600-6-F; NOAA-82052402) Avail: NTIS HC A09/MF A01 CSCL 08C

Analysis techniques used to exploit SEASAT synthetic aperture radar (SAR) data of gravity waves are discussed and the SEASAT SAR's ability to monitor large scale variations in gravity wave fields in both deep and shallow water is evaluated. The SAR analysis techniques investigated included motion compensation adjustments and the semicausal model for spectral analysis of SAR wave data. It was determined that spectra generated from fast Fourier transform analysis (FFT) of SAR wave data were not significantly altered when either range telerotation adjustments or azimuth focus shifts were used during processing of the SAR signal histories, indicating that SEASAT imagery of gravity waves is not significantly improved or degraded by motion compensation adjustments. Evaluation of the semicausal (SC) model using SEASAT SAR data from Rev. 974 indicates that the SC spectral estimates were not significantly better than the FFT results. GRA

N83-14553 Royal Aircraft Establishment, Farnborough (England).
THE ACCURACY OF SEASAT-1 ALTIMETER ALTITUDE MEASURMENTS UNDER VARIOUS SEA STATE CONDITIONS
G. C. WHITE May 1982 56 p refs
(RAE-TR-82059; RAE-SPACE-616; BR82059) Avail: Issuing Activity

The accuracy with which the SEASAT 1 altimeter height measurement can be used to derive the spacecraft CG to mean sea level distance is derived. The shape of a reflected pulse which incorporates a realistic description of a wavefield's wave height probability distribution in its derivation is used to calculate this accuracy. A quantitative description of such a reflected pulse is developed. This description is then used in a simulation procedure to calculate values of the rms errors in the tracking and wave bias, hence the rms height error. This figure of accuracy, i.e., rms height error is derived for various sea state conditions. S.L.

N83-14555*# Research Triangle Inst., Research Triangle Park, N.C.
A COMPARISON OF SURFACES TEMPERATURES FROM HCMM INFRARED DATA WITH FIELD MEASUREMENTS Final Report
F. M. VUKOVICH, Principal Investigator Oct. 1982 58 p refs HCMM
(Contract NAS 5-26442)
(E83-10046; NASA-CR-169530; NAS 1.26:169530) Avail: NTIS HC A04/MF A01 CSCL 08C

Heat Capacity Mapping Mission surface temperatures were compared to field data obtained in the Mississippi River, in the Atlantic Ocean in the vicinity of the Nantucket Shoals, and in the eastern Gulf of Mexico. The absolute and relative accuracies of the infrared data were determined. M.G.

N83-14583*# Instituto de Pesquisas Espaciais, Sao Jose dos Campos (Brazil).
INTERPRETATION OF REMOTELY SENSED DATA AND ITS APPLICATIONS IN OCEANOGRAPHY [INTERPRETACAO DE DADOS DE SENSORIAMENTO REMOTO E APLICACOES EM OCEANOGRAFIA]
N. D. J. PARADA, Principal Investigator, K. TANAKA, H. M. INOSTROZA, and J. J. VERDESIO Apr. 1982 65 p refs In PORTUGUESE; ENGLISH summary Sponsored by NASA ERTS
(E83-10074; NASA-CR-169585; NAS 1.26:169585; INPE-2368-MD/019) Avail: NTIS HC A04/MF A01 CSCL 08C

The methodology of interpretation of remote sensing data and its oceanographic applications are described. The elements of image interpretation for different types of sensors are discussed. The sensors utilized are the multispectral scanner of LANDSAT, and the thermal infrared of NOAA and geostationary satellites. Visual and automatic data interpretation in studies of pollution, the Brazil current system, and upwelling along the southeastern Brazilian coast are compared. J.D.

N83-14603*# Washington Univ., Seattle. Dept. of Atmospheric Sciences.
JOINT AIR SEA INTERACTION (JASIN) EXPERIMENT, NORTHWEST COAST OF SCOTLAND Final Report
J. A. BUSINGER 1981 2 p refs
(Contract JPL-955528)
(NASA-CR-169631; NAS 1.26:169631) Avail: NTIS HC A02/MF A01 CSCL 08C

The joint air sea interaction (JASIN) experiment took place off the Northwest coast of Scotland. Sea surface and boundary layer parameters were measured. The JASIN data was used as ground truth for various sensors on the SEASAT satellite. S.L.

N83-14604*# Jet Propulsion Lab., California Inst. of Tech., Pasadena.
EVALUATION OF THE POTENTIAL OF ONE TO THREE SEASAT-SMMR CHANNELS IN RETRIEVING SEA SURFACE TEMPERATURE
P. C. PANDEY (Space Applications Centre, Ahmedabad, India) and S. KNIFFEN 15 Nov. 1982 36 p refs Sponsored by NASA and NAS-NRC
(NASA-CR-169660; JPL-PUB-82-89; NAS 1.26:169660) Avail: NTIS HC A03/MF A01 CSCL 08C

The scanning multichannel microwave radiometer (SMMR) aboard the SEASAT satellite measured emitted radiation in both horizontal and vertical polarizations at microwave frequencies of 6.6, 10.69, 18.0, 21.0 and 37.0 GHz. Retrieval algorithms, for sea surface temperature (SST) determination, from subsets of one to three SMMR channels are obtained by a two step statistical technique. The technique first selects the best subsets of a given size defined by an R2 criterion (coefficient of determination), of a given size by the application of an efficient 'leaps and bounds' technique on a statistical data base. It then performs a regression analysis on the selected subsets. The statistical data base employed a large (600) set of seasonally and geographically diverse atmospheric and surface parameters for radiative transfer calculations. The results of the study of one to three channel subset retrieval algorithms indicate the possibility of using 6.6V, 6.6H and 18V channels for SST determination from SEASAT-SMMR data. B.W.

N83-14636# Instituto de Investigaciones Pesqueras, Barcelona (Spain). Dept. de Oceanografia.
SPACE TRUTH IN OCEANOGRAPHY
A. BALLESTER and M. GARCIA *In* ESA Satellite Remote Sensing for Developing Countries p 219-223 Jun. 1981 refs
Avail: NTIS HC A11/MF A01

Validation of remotely sensed sea surface temperatures by a ground truth configured from data collected in situ is discussed. Thermal synoptic cartography data from the Spanish continental shelf were compared with Tiros-N and NOAA-6 values. The danger of comparing nonsynoptic ground truth with synoptic satellite observations is revealed. Author (ESA)

N83-14832*# National Aeronautics and Space Administration. Goddard Space Flight Center, Greenbelt, Md.
PROSPECTS FOR THE FUTURE
D. ATLAS *In* NASA. Marshall Space Flight Center The Conception, Growth, Accomplishments and Future of Meteorol. Satellites p 84-96 Nov. 1982
Avail: NTIS HC A06/MF A01 CSCL 04B

Atmospheric and surface fields produced from the TIROS N high resolution infrared sounder/microwave sounding unit data are discussed. The data were analyzed by direct physical inversion of the multispectral radiative transfer equation. Sea ice mapping and sea surface temperature determination are addressed. M.G.

N83-14835*# National Aeronautics and Space Administration. Goddard Space Flight Center, Greenbelt, Md.
NIMBUS 6 RANDOM ACCESS MEASUREMENT SYSTEM APPLICATIONS EXPERIMENTS
C. E. COTE, ed., R. TAYLOR, ed., and E. GILBERT, ed. Oct. 1982 103 p
(NASA-SP-457; LC-82-14553) Avail: NTIS HC A06/MF A01 CSCL 04B

The advantages of a technique in which data collection platforms randomly transmit signal to a polar orbiting satellite, thus eliminating satellite interrogation are demonstrated in investigations of the atmosphere; oceanographic parameters; Arctic regions and ice conditions; navigation and position location; and data buoy development.

N83-14837*# Bureau of Meteorology, Melbourne (Australia). Dept. of Science.
AUSTRALIAN DRIFTING BUOY
H. N. BRANN and D. E. HANDCOCK *In* NASA. Goddard Space Flight Center Nimbus 6 Random Access Meas. System Appl. Expt. p 12-13 Oct. 1982
Avail: NTIS HC A06/MF A01 CSCL 04B

The effectiveness of free floating buoys to support atmospheric modeling over the South Indian and Southern Pacific Oceans was investigated in an experiment conducted to: (1) measure air pressure and sea surface temperature from free drifting buoys in the South Indian Ocean; (2) use the data in the assessment of atmospheric modeling accuracy; and (3) study the practical and logistical problems in the deployment of free-floating buoys from ships of opportunity and to obtain information on buoy trajectories as a basis for planning buoy release points for continuous coverage of the South Indian and Southern Pacific Oceans between 60 deg and 150 deg east longitude. The position data from RAMS were of significant value in analysis but were usable for real-time operations because the data were not immediately available. The analysis showed that buoy data received within 6 h of real time would make significant improvement to real-time analyses in the Southern Hemisphere. A.R.H.

N83-14841*# Environment Canada, Victoria (British Columbia).
MESOSCALE OCEAN VARIABILITY
J. GARRETT *In* NASA. Goddard Space Flight Center Nimbus 6 Random Access Meas. System Appl. Expt. p 23 Oct. 1982
Avail: NTIS HC A06/MF A01 CSCL 04B

The Nimbus 6 random access measuring system was used in a mesoscale ocean variability experiment conducted to determine the horizontal extent of oceanic variables influenced by individual storms. Ten drifting buoys were used to determine the horizontal variability of velocities and temperatures in the upper layer of the ocean, at scales of 100 to 500 km, in a region expected to be stormy during the period of the experiment. In addition, 30 prototype buoys of the type to be used during the first GARP global experiment were tested to determine buoy reliability. Measurements reported by the buoys were analyzed to review the sources of error or uncertainty in such pressure measurements. It is concluded that barometric pressure measurements can be made from small buoys with accuracies of about + or - 1 mb under typical conditions.

To achieve uncertainties less than 2.0 mb under extreme conditions, it is probably necessary to average the transducer signal over several wave periods. A.R.H.

N83-14842*# Coast Guard, Washington, D.C. Oceanographic Unit.
LAGRANGIAN DRIFT MEASUREMENTS OF SEA SURFACE CURRENTS AND ICEBERG TRACKING
E. A. DELANEY and K. M. PALFREY *In* NASA. Goddard Space Flight Center Nimbus 6 Random Access System Appl. Expt. Oct. 1982
Avail: NTIS HC A06/MF A01 CSCL 04B

Drogued buoys were tracked by the Nimbus 6 random access measuring system for approximately 10 days in the U.S. East Coast Continental Shelf waters between Delaware Bay and Cape Hatteras in February 1976. The resulting drift values were used to check a numerical model developed at the U.S. Coast Guard Oceanographic Unit for predicting surface currents on the Continental Shelf. Similar buoys were also tracked on the Grand Banks of Newfoundland for the U.S. Coast Guard's International Ice Patrol. Lagrangian drift velocities were measured in or near the Labrador Current. Prediction numerical models that were then in use or proposed for use by the Commander, International Ice Patrol, who has the operational responsibility for warning. Following field studies in the area of the Ice Patrol, the lagrangian drift velocities gleaned from the Nimbus 6 RAMS were used to test a numerical model of time-dependent Ekman wind generated currents. Air droppable RAMS buoys deployed from C-130 aircraft were also deployed onto icebergs that break off from Greenland glaciers and drift into the North Atlantic shipping lanes. A.R.H.

N83-14845*# Norwegian Meteorological Inst., Blindern.
THE RAMS COLLECTION OF METEROLOGICAL AND POSITION DATA IN THE NORWEGIAN SEA
J. NORDO and C. K. JENSEN *In* NASA. Goddard Space Flight Center Nimbus 6 Random Access Meas. System Appl. Expt. p 35-36 Oct. 1982
Avail: NTIS HC A06/MF A01 CSCL 04B

The Norwegian Meteorological Institute developed an experiment using the Nimbus 6 RAMS to obtain meteorological data from remote areas of the Norwegian Sea and to determine the flow of ice in the Arctic Ocean. The purpose of the ice drift investigations were as follows: (1) To obtain ice drift speeds in the Svalbard-Greenland area and compare them with meteorological and oceanographical conditions. The results will be used to develop forecast rules (short range for sea ice movements). (2) To use ice drift speeds to determine the outflow of sea ice from the Arctic Basin and from the eastern part of the Svalbard Archipelago to verify numerical models for ice circulation in the Arctic Basin. (3) To study the tidal influence upon the ice drift and obtain average speed of sea surface currents. This information was used to aid fishing, shipping, and oil drilling operations. B.W.

N83-14847*# Research Triangle Inst., Research Triangle Park, N.C.
WESTERN BOUNDARY EDDIES OF THE GULF STREAM
F. V. VUKOVICH *In* NASA. Goddard Space Flight Center Nimbus 6 Random Access Meas. System Appl. Expt. p 39-40 Oct. 1982
Avail: NTIS HC A06/MF A01 CSCL 04B

Oceanic exchange processes between the water on the Continental Shelf and the Gulf Stream of the Southeast coast of the United States are discussed. Eddies on the western boundary of the Gulf Stream were observed using infrared imagery. It was shown that barotropic waves that interact with the current shear of the Gulf Stream will become unstable and propagate downstream along the shelf. Real-time temperature, depth, and salinity data were collected. The experiments revealed that a class of Gulf Stream western boundary eddies developed immediately downstream (within 100 km) from an along shore topographical feature called the Charleston Bump. The data indicated cyclonic motion associated with the western boundary eddies from the surface to about 300 m. R.J.F.

N83-14848*# Texas A&M Univ., College Station. Dept. of Oceanography.
DRIFT BUOY COMPONENT, NORPAX ANOMALY DYNAMICS STUDY
A. D. KIRWAN, JR. *In* NASA. Goddard Space Flight Center Nimbus 6 Random Access Meas. System Appl. Expt. p 42-44 Oct. 1982
Avail: NTIS HC A06/MF A01 CSCL 04B

Drifting buoys were used to map large-scale circulation in the North Pacific Ocean for an anomaly dynamics study. Large-scale response of the general circulation of the North Pacific to autumn and winter storm activity was studied to predict the formation and evolution of large-scale thermal anomalies. The temperature/time series for all the drifters showed the diurnal heating cycles as well as the long-term seasonal march from early summer through fall. Preliminary data showed wavelike features along with a number of eddy mesoscale structures. R.J.F.

N83-15799# Scripps Institution of Oceanography, La Jolla, Calif. Shore Processes Lab.
INFRARED SATELLITE DATA FROM THE FIRST COASTAL OCEAN DYNAMICS EXPERIMENT, MARCH - JULY 1981
K. A. KELLY Jul. 1981 60 p refs
(Contract N00014-75-C-0300; N00014-80-C-0440)
(AD-A120068; SIO-REF-82-15) Avail: NTIS HC A04/MF A01 CSCL 08J

As part of the Coastal Ocean Dynamics Experiment infrared images from the weather satellite NOAA-6 were collected from late March to mid-July 1981. Images which met certain quality criteria were registered to a common grid and were screened to eliminate data which were cloud-contaminated. Infrared images yield approximate sea-surface temperature maps via the blackbody relationship. This report contains photographs of the digital images and a brief description of the processing techniques which were used. Author (GRA)

06

HYDROLOGY AND WATER MANAGEMENT

Includes snow cover and water runoff in rivers and glaciers, saline intrusion, drainage analysis, geomorphology of river basins, land uses, and estuarine studies.

A83-10064* Kansas Univ. Center for Research, Inc., Lawrence.
RADAR SPECTRAL OBSERVATIONS OF SNOW
W. H. STILES, F. T. ULABY, A. K. FUNG, and A. ASLAM (University of Kansas Center for Research, Inc., Lawrence, KS) In: International Geoscience and Remote Sensing Symposium, Washington, DC, June 8-10, 1981, Digest. Volume 1. New York, Institute of Electrical and Electronics Engineers, 1981, p. 654-668. refs
(Contract NSG-5335)

Radar remote sensing experiments have been conducted at test sites in Kansas, Colorado, and South Dakota over the last six years to examine backscatter coefficient response to snowcovered terrain. Truck-mounted 1-35 GHz scatterometers were employed in conjunction with detailed ground-truth measurements. From these experiments and associated modeling efforts, most of the fundamental questions concerning backscatter behavior in response to important snow parameters have been, at least qualitatively, answered. The optimum angular range seems to be between 20 and 50 deg and, for these angles, the results indicate that the radar backscatter generally: (1) increases with increasing water equivalent, (2) decreases with increasing liquid water, (3) increases with increasing crystal size, (4) is insensitive to surface roughness for dry snow conditions, and (5) can be

sensitive to soil state if the snowcover is dry. This paper gives a summary of these results, along with empirical and theoretical models for describing the backscatter from snow. (Author)

A83-10065
MICROWAVE EMISSION SIGNATURES OF SNOW IN FINLAND
M. TIURI (Helsinki University of Technology, Esbo, Finland) In: International Geoscience and Remote Sensing Symposium, Washington, DC, June 8-10, 1981, Digest. Volume 1. New York, Institute of Electrical and Electronics Engineers, 1981, p. 670-675. refs

A83-10072* Arkansas Univ., Fayetteville.
WETLAND MAPPING WITH IMAGING RADAR
W. P. WAITE, H. C. MACDONALD, V. H. KAUPP, and J. S. DEMARCKE (Arkansas, University, Fayetteville, AR) In: International Geoscience and Remote Sensing Symposium, Washington, DC, June 8-10, 1981, Digest. Volume 2. New York, Institute of Electrical and Electronics Engineers, 1981, p. 794-799. refs
(Contract JPL-954940; NAG5-20)

An analysis of Seasat radar imagery is presented to identify the radar signature of vegetation-covered water surfaces. Imagery taken on Aug. 21, 1978 displayed anomalously high returns over swamp lands near Lafayette, LA. Landsat scans of the area two days later revealed uniform vegetation cover in the area, and ground examination found the area to be filled with cypress trees in swamps. Similar results were obtained during an overflight above a region of southeast Arkansas. Mechanisms producing the high degree of reflectance are explored, and the possibility that the strong return is due to an interaction of the vegetation cover and the specular water surface underneath is mentioned. Further studies to identify the exact mechanisms producing the anomalous returns are recommended, as well as optimization of the viewing angle for general classes of vegetation density. M.S.K.

A83-10073
REMOTE SENSING OF WATER QUALITY FOR ESTUARINE ENVIRONMENTS
A. L. GERACI (California, University, Berkeley, CA; Catania, Universita, Catania, Italy), R. N. COLWELL, and S. KHORRAM (California, University, Berkeley, CA) In: International Geoscience and Remote Sensing Symposium, Washington, DC, June 8-10, 1981, Digest. Volume 2. New York, Institute of Electrical and Electronics Engineers, 1981, p. 800-810. refs

The capabilities of remote sensing techniques for monitoring water quality in estuarine environments is assessed, particularly for the case of oil pollution. The techniques include multispectral imagery, radar, and lidar. Landsat MSS data from band 7, 0.8-1.1 micron, can identify the land-water interface, while the 0.43-0.50 micron blue band and the 0.53-0.60 micron green band yield information on water quality. SAR operated in the X- and L-bands have detected sewage and industrial waste plumes. The Landsat MSS readings, when compared with ground truth sampling for suspended particulates, has quantitatively measured suspended solids up to 900 ppm. Sea surface smoothing as a result of oil slicks can be detected by SAR due to a reduction of the radar scattering at the slick. Finally, UV wavelengths from 0.5-0.55 micron have been used to detect oil on the sea surface because of oil's higher reflectance. M.S.K.

A83-10090
ACCURACY OF OPERATIONAL SNOW AND ICE CHARTS
G. KUKLA and D. ROBINSON (Lamont-Doherty Geological Observatory, Palisades, NY) In: International Geoscience and Remote Sensing Symposium, Washington, DC, June 8-10, 1981, Digest. Volume 2. New York, Institute of Electrical and Electronics Engineers, 1981, p. 974-987. refs
(Contract NSF ATM-77-28522; NSF ATM-80-01470)

Operational snow and ice cover charts produced by NOAA, the Navy, and the U.S. Air Force Global Weather Central (AFGWC) were compared with ground station reports and original satellite imagery. It is concluded that the information on the extent of snow covers is sufficiently accurate for use in the recent generation of general circulation models in all seasons except autumn. However, information on surface albedo, on the thickness of snow covers, and on the proportion of open water within the pack ice needs to be considerably upgraded. (Author)

A83-10101
REMOTE DETERMINATION OF SURFACE EVAPORATION USING THERMAL IR MEASUREMENTS
T. N. CARLSON (Pennsylvania State University, University Park, PA) In: International Geoscience and Remote Sensing Symposium, Washington, DC, June 8-10, 1981, Digest. Volume 2. New York, Institute of Electrical and Electronics Engineers, 1981, p. 1202-1210.

A83-10102* Environmental Research and Technology, Inc., Concord, Mass.
SNOW HYDROLOGY STUDIES USING DATA FROM THE HEAT CAPACITY MAPPING MISSION
J. C. BARNES and C. J. BOWLEY (Environmental Research and Technology, Inc., Concord, MA) In: International Geoscience and Remote Sensing Symposium, Washington, DC, June 8-10, 1981, Digest. Volume 2. New York, Institute of Electrical and Electronics Engineers, 1981, p. 1211-1217. refs
(Contract NAS5-24316)

This paper describes a study of the snow hydrology application of thermal infrared (IR) data from the Heat Capacity Mapping Mission (HCMM) satellite. The HCMM data in both imagery and digital tape formats are analyzed for two study areas: the Salt-Verde Watershed in central Arizona and the southern Sierra Nevada in California. The analysis procedures are described, including the development of a unique contour plotting program that makes it possible to overlay HCMM thermal contours directly onto the visible channel imagery. The results indicate that satellite thermal-IR data can provide the hydrologist with additional useful information on snow cover. (Author)

A83-10120
AIRBORNE MEASUREMENT OF SURFICIAL SOIL MOISTURE USING NATURAL TERRESTRIAL GAMMA RADIATION
T. R. CARROLL (NOAA, National Weather Service, Minneapolis, MN) In: International Geoscience and Remote Sensing Symposium, Washington, DC, June 8-10, 1981, Digest. Volume 2. New York, Institute of Electrical and Electronics Engineers, 1981, p. 1443-1448. refs

A83-12038
ICE DISTRIBUTION AND WINTER SURFACE CIRCULATION PATTERNS, KACHEMAK BAY, ALASKA
L. W. GATTO (U.S. Army, Cold Regions Research and Engineering Laboratory, Hanover, NH) Remote Sensing of Environment, vol. 12, Nov. 1982, p. 421-435. refs

The development of the hydropower potential of Bradley Lake, Alaska would considerably increase winter freshwater discharge into Kachemak Bay. This could result in increased ice formation and related problems. In order to investigate winter surface circulation in the bay and ice distribution patterns, Landsat MSS bands 5 and 7 and RBV imagery with 70 percent cloud cover or less taken between 1 November and 30 April each year from 1972 to 1980 were examined. The results show that surface water circulation is driven more by tidal forces than by wind stress. The circulation patterns indicate that if additional ice is formed from the increased winter discharge, a greater ice cover would accumulate along Homer Spit and be blown into the outer bay by the dominant northerly winter winds. S.C.S.

A83-14234#
TOWARD AN OPERATIONAL, SATELLITE-BASED, WETLAND MONITORING PROGRAM FOR THE FRASER RIVER ESTUARY, BRITISH COLUMBIA
G. F. TOMLINS (B.C. Research, Vancouver, Canada) and K. P. B. THOMSON (Canada Centre for Remote Sensing, Ottawa, Canada) In: Canadian Symposium on Remote Sensing, 7th, Winnipeg, Canada, September 8-11, 1981, Proceedings. Ottawa, Canadian Aeronautics and Space Institute, 1982, p. 74-82. Research supported by the Canada Centre for Remote Sensing and Department of the Environment. refs

A83-14251#
REMOTE SENSING APPLICATIONS FOR BRITISH COLUMBIA WETLANDS USING 35 MM AERIAL PHOTOGRAPHY
E. K. WATSON (International Range Remote Sensing, Ltd., Kamloops, British Columbia, Canada) and A. L. VAN RYSWYK (Department of Agriculture, Range Research Station, Kamloops, British Columbia, Canada) In: Canadian Symposium on Remote Sensing, 7th, Winnipeg, Canada, September 8-11, 1981, Proceedings. Ottawa, Canadian Aeronautics and Space Institute, 1982, p. 211-221. Research supported by the Department of Agriculture. refs

The cost of conventional aerial photography often precludes its use for monitoring, assessment and management of natural resources. A pilot project, using 35 mm vertical/stereo aerial photography as a data base, was conducted during the summer of 1980 on a wetland area. Color and color-infrared 35 mm photographs at 1:20,000, 1:10,000 and 1:4,000 were used to produce a detailed 1:2,500 scale map of a fen and bog complex near Kamloops, British Columbia. The wetland classification used follows the system currently being developed by the British Columbia Ministry of the Environment. The comparison of conventional 23 cm vs. 35 mm aerial photography obtained using a Meyer 35 mm Aerial camera sidemount is discussed with reference to cost, area covered, mapping techniques and air photo resolution. The methodology of obtaining operational 35 mm color and color-infrared using both inexpensive and expensive 35 mm camera systems is presented. (Author)

A83-14262#
BANK EROSION AND FLOOD PLAIN STUDIES OF THE ANNAPOLIS RIVER - AN APPLICATION OF REMOTE SENSING DATA
V. SINGHROY (Ontario Centre for Remote Sensing, Toronto, Canada) and J. F. WIGHTMAN (Nova Scotia Land Survey Institute, Lawrencetown, Canada) In: Canadian Symposium on Remote Sensing, 7th, Winnipeg, Canada, September 8-11, 1981, Proceedings. Ottawa, Canadian Aeronautics and Space Institute, 1982, p. 304-315.

An important effect of the tidal power generating station being planned in the lower reaches of the Annapolis River basin is the greater penetration of seawater into the basin on each tidal cycle. The average water elevation will be increased in order to achieve the head differentials needed to operate the turbine, and this increased elevation will affect the stability of the river banks. The contributions which various types of remotely sensed data can make to the preparation of preliminary maps of the basin are considered. These maps are seen as the basis for detailed field investigations of bank erosion, the identification of areas of accelerated erosion, the mapping of the flood plain, and the mapping of land use and land cover. C.R.

A83-14287#
WATER SURVEY OF CANADA'S EXPERIENCE WITH DATA ACQUISITION AND TELEMETRY SYSTEMS
I. MCLAURIN (Water Survey of Canada, Winnipeg, Canada) In: Canadian Symposium on Remote Sensing, 7th, Winnipeg, Canada, September 8-11, 1981, Proceedings. Ottawa, Canadian Aeronautics and Space Institute, 1982, p. 507-512. refs

The features of the data acquisition and telemetry systems which gauge, store, and report lake level and streamflow information in Manitoba and northwestern Ontario are briefly described and their method of operation is discussed. At four sites, satellite data collection platforms (DCPs) are installed which transmit information several times daily via satellite to data processing facilities where the data are archived. The equipment, power source, and operation of a typical DCP are described. At one site, an autoanswer telephone and modem connected to the telephone network replace the transmitter and antenna. The power requirements, data processing capabilities of this data acquisition and telemetry system (DATS) are different from those for DCPs and are briefly discussed. The costs of these programs, their operation by persons with little formal training in electronics or data communications, and their applications are discussed. C.D.

A83-14574#
TEMPORARY LAKES AND SALT PLAINS IN THE HIGH PLATEAUS OF THE ANDES /BOLIVIA/ - A CONTINUING SURVEY OF PERIODIC HYDROLOGIC PHENOMENA USING THE GEOSTATIONARY SATELLITE GOES-EST [LACS TEMPORAIRES & PLAINES DE SEL DES HAUTS PLATEAUX DES ANDES /BOLIVIE/ - SUIVI DE PHENOMENES HYDROLOGIQUES PERIODIQUES A L'AIDE DU SATELLITE GEOSTATIONNAIRE GOES-EST]
B. GUILLOT (Office de la Recherche Scientifique et Technique d'Outre-Mer, Lannion, France) La Meteorologie, Dec. 1981, p. 5-9. In French.

A summary of the observational techniques and parameters during GOES and SMS satellites remote sensing of hydrologic features of Lakes Titicaca and Poopo in the Andes, together with neighboring salt plains, is presented. It is noted that the alternation of wet and dry seasons has provided ample opportunities for observing strong variations in reflected radiances. The SMS 1, 2, and GOES spacecraft sensors have been used to monitor the area, successively, since 1974. The sensors have included an IR channel operating at 10.5-12.5 microns and a visual channel at 0.55-0.75 micron. IR resolution has been 8 x 4 km, and visual, 1:1,000,000. Multitemporal comparative studies have been effected using the archived photography, revealing surface characteristics such as dry, wet, and snow-covered, along with corresponding changes over time. M.S.K.

A83-14668* Texas A&M Univ., College Station.
EVALUATING DEPTH TO SHALLOW GROUNDWATER USING HEAT CAPACITY MAPPING MISSION /HCMM/ DATA
J. L. HEILMAN (Texas A & M University, College Station, TX) and D. G. MOORE (South Dakota State University, Brookings, SD) Photogrammetric Engineering and Remote Sensing, vol. 48, Dec. 1982, p. 1903-1906. refs
(Contract NAS5-24206)

A83-14854
SNOW-COVER PARAMETERS RETRIEVED FROM NIMBUS-7 SCANNING MULTICHANNEL MICROWAVE RADIOMETER /SMMR/ DATA
K. F. KUNZI, S. PATIL (Bern, Universitaet, Berne, Switzerland), and H. ROTT (Innsbruck, Universitaet, Innsbruck, Austria) IEEE Transactions on Geoscience and Remote Sensing, vol. GE-20, Oct. 1982, p. 452-467. Research supported by the Swiss National Science Foundation and Bundesministerium fuer Wissenschaft und Forschung. refs

The multifrequency, dual-polarized microwave imager on the Nimbus-7 satellite is designed to sense the ocean surface, the atmosphere, and land surfaces. Reference is made to the fact that snow cover over land has a very distinct effect on the microwave signature of the earth's surface. The goal of the study described here is to show that the three snow-cover parameters, namely extent, snow water equivalent, and onset of snow melt, can be determined using scanning multichannel microwave radiometer data. The analysis demonstrates that these parameters are retrievable with sufficient accuracy to be of great value in climatology, meteorology, and hydrology. Snow cover extent is determined for a dry snow cover having a depth greater than about 5 cm; the snow water equivalent, it is shown, can be determined on a regional basis with approximately 2 g/sq cm rms

accuracy. The onset of snow melt is clearly visible through the detection of melt and refreeze cycles before snow runoff. It is pointed out that the algorithms derived are simple enough to be incorporated in fully automated operational data analysis schemes. C.R.

A83-15816
INVESTIGATIONS OF THE APPARENT TEMPERATURE OF SNOW COVER IN THE SUBMILLIMETER WAVELENGTH REGION
L. I. FEDOSEEV, I. V. KUZNETSOV, N. K. POLOVA, and A. A. SHVETSOV (Akademiia Nauk SSSR, Institut Prikladnoi Fiziki, Gorki, USSR) International Journal of Infrared and Millimeter Waves, vol. 3, Nov. 1982, p. 917-927. refs

Equipment and methods used for measuring the apparent temperature of snow cover in high mountains is described. The spectrum of dry snowpack emission in the wavelength region 0.85-1.3 mm is obtained. The dependence of the apparent temperature of snow cover on the atmospheric optical depth is determined. It is shown that in the first approximation the snow cover emission is described by the Lambert law and the snow albedo is within 0.6-0.67. (Author)

A83-17713* National Aeronautics and Space Administration. Langley Research Center, Hampton, Va.
PASSIVE MICROWAVE DETECTION OF RIVER-PLUME FRONTS IN THE GERMAN BIGHT
H.-J. C. BLUME (NASA, Langley Research Center, Hampton, VA) International Journal of Remote Sensing, vol. 3, Oct.-Dec. 1982, p. 447-455. Research supported by the Max-Planck-Institut fuer Meteorologie and Deutsches Hydrographisches Institut. refs

The NASA P-3 aircraft with the L- and S-band radiometer system on board participated in the MARSEN experiments carried out between August 30 and September 23, 1979. Measurements of surface temperature and salinity were concentrated on freshwater outflows of the Rivers Weser and Elbe in the German Bight. Three missions were carried out, on September 19, 22, and 23. The values of salinity are plotted as a function of geographic position, and contour maps of the salinity distribution are generated from the value plots. It is noted that on September 22, during a noon flood-tide, two river-plume salinity fronts were detected when a body of water with higher salinity existed in front of the Weser delta near Bremerhaven generating with the river outflow of lower saline waters a front of delta-S equals 5 per thousand. Another pocket of lower saline waters was found in front of the Elbe delta at Cuxhaven, which in turn set up a strong front of delta-S equals 6 per thousand. The morning low tide of September 23 did not exhibit this extreme condition. C.R.

N83-10466*# National Aeronautics and Space Administration. Goddard Space Flight Center, Greenbelt, Md.
A CASE STUDY IN THE PRACTICAL USE OF LANDSAT DATA
S. COX *In its* The LANDSAT Tutorial Workbook p 309-326 1982 Original contains color imagery. Original photography may be purchased from the EROS Data Center, Sioux Falls, S.D. 57198. ERTS
Avail: NTIS MF A01; SOD HC $55.00 CSCL 05B

The use of computer aided classification of LANDSAT data in developing water quality plans for New Jersey watersheds is used to exemplify how a state natural resource management program benefits from satellite imagery. The transition of a research and development system into an operational remote sensing system to help decision makers is demonstrated. Nontechnial issues that can assist (or hinder) an agency in adopting a new technology are examined. The progress of LANDSAT use by state government from the earliest stage of curiosity through to incorporation in actual state planning methods is charted. Potential applications of LANDSAT data to real information needs and solutions to management problems are examined. The problems and mistakes that occurred in using LANDSAT data in the past are discussed as well as the ways by which these problems were overcome. A.R.H.

N83-10730# National Oceanic and Atmospheric Administration, Boulder, Colo. Office of Weather Research and Modification.
FACE-2 DATA REDUCTIONS (PRIOR TO DISCLOSURE OF THE TREATMENT DECISIONS). PART 5: SATELLITE-ESTIMATED RAINFALL FROM A GEOSTATIONARY PLATFORM IN FACE-2
J. G. MEITIN, JR., W. L. WOODLEY, and C. G. GRIFFITH Oct. 1981 147 p refs
(PB82-216581; NOAA-82042903; NOAA-TM-ERL-OWRM-11)
Avail: NTIS HC A07/MF A01 CSCL 04B

Precipitation on the 51 FACE-2 B days was estimated for the Florida area cumulus experiment (FACE) target area and an extended surrounding area through use of the digital GOES infrared imagery. The satellite rain estimation technique is described. Daily rain volumes and daily isohyetal maps are given. The approach to determine the extra-area effects of seeding with these rainfall data is outlined. M.G.

N83-10734# Nebraska Univ., Lincoln.
SATELLITE OBSERVATIONS OF VARIATIONS IN NORTHERN HEMISPHERE SEASONAL SNOW COVER
K. F. DEWEY and R. HEIM, JR. Washington NOAA Dec. 1981 87 p refs Sponsored by NOAA
(PB82-196668; NOAA-TR-NESS-87) Avail: NTIS HC A05/MF A01 CSCL 04B

The usefulness of satellite derived snow cover data, the digitized archive of snow cover data for the Northern Hemisphere, and the various climatological products that can be derived from this data base are discussed. Weekly Snow and Ice Charts of the Northern Hemisphere, which were prepared by the National Earth Satellite Service (NESS), were analyzed for the period November 1966 through December 1980. Each of these weekly charts was digitized and then stored and displayed in formats in which a star symbol stood for 50% or more of a grid box covered with snow on an O stood for no snow cover. For display purposes, all water bodies were left completely blank to allow the above two symbols to define the land areas. Although ice cover was also digitized and stored in the data archive, only snow cover is analyzed. Author (GRA)

N83-10745# National Oceanic and Atmospheric Administration, Rockville, Md. Ocean Technology and Engineering Services.
WEATHER CONSTRAINTS ON AIRBORNE LASER HYDROGRAPHY OPERATIONS
R. SCOTT Jan. 1982 20 p refs
(PB82-189754; NOAA-82021005; NOAA-TM-OTES-3) Avail: NTIS HC A02/MF A01 CSCL 08J

The operational limitations imposed on laser hydrography by weather conditions are discussed. An estimate is developed of the probability of favorable weather conditions for airborne laser hydrography operations at seven sites on the east coast of the United States. For comparison purposes, similar estimates are made for launch based sonar hydrograhy and for stereo photobathymetry. Author (GRA)

N83-11569# Army Engineer Topographic Labs., Fort Belvoir, Va. Geographic Sciences Lab.
TERRAIN ANALYSIS PROCEDURAL GUIDE FOR DRAINAGE AND WATER RESOURCES (ETL SERIES ON GUIDES FOR ARMY TERRAIN ANALYSTS)
J. A. MESSMORE Apr. 1982 245 p refs
(Contract DA PROJ. 4A7-62707-A-855)
(AD-A118318; ETL-0285; REPT-8) Avail: NTIS HC A11/MF A01 CSCL 08B

This document is one in a series of terrain analysis procedural guides being developed in support of the Topographic Support System (TSS). It was written specifically for the U.S. Army's Terrain Analysts and presents the methodology for extracting, reducing, and recording information for the drainage and water resources data field. This data field is divided into 3 subfields: (1) water-courses and water bodies, (2) drainage basins, and (3) ground water. Step-by-step procedures are provided for producing a factor overlay and supporting data tables for each of the drainage and water resources data fields. Author (GRA)

N83-12514# World Meteorological Organization, Geneva (Switzerland).
HYDROLOGICAL DATA TRANSMISSION
A. F. FLANDERS 1981 45 p refs
(WMO-559; OHR-14; ISBN-92-63-10559-6) Avail: NTIS MF A01; print copy available at WMO, Geneva

Methods of data transmission, existing facilities and requirements for hydrological purposes are reviewed. The use of satellites, meteor bursts, and the global telecommunication system (gts) to meet these requirements is considered. The GTS could cope with operational and research needs which involve the exchange of information in real time. Satellites offer a data relay facility, linking ships, island stations, ocean buoys, etc. Meteor bursts minimize blockage due to terrain and allow coverage of vast areas. Author (ESA)

N83-12516# World Meteorological Organization, Geneva (Switzerland).
LONG-RANGE WATER SUPPLY FORECASTING
M. DYHR-NIELSEN 1982 28 p refs
(WMO-587; OHR-20; ISBN-92-63-10587-1) Avail: NTIS MF A01; print copy available at WMO, Geneva SwFr 6

Current methods of forecasting water supply over periods ranging from two to four months are reviewed along with the feasibility of combining conceptual deterministic models and statistical data simulation for such forecasts. The term water supply is used with its meaning of runoff volumes over a defined period, such as weekly, monthly or seasonal flows. The techniques described apply not only to water supply projects, but also to irrigation and hydroelectric power projects. Some are equally well-suited to long range forecasts of floods or low flows and such applications are discussed. Three methods of long-range water supply forecasting are highlighted: regression methods, conceptual models and time series. The operational use of forecasting methods is illustrated. The three methods, including data and computational requirements and accuracy, are compared. Results show that the potential of conceptual models for long-range water supply forecasting is large and, if the accuracy of long range weather forecasts continues to improve, it will be conceptual models which will adapt most efficiently. Author (ESA)

N83-13520*# Brigham Young Univ., Provo, Utah. Dept. of Civil Engineering.
HCMM HYDROLOGICAL ANALYSIS IN UTAH Final Report
A. W. MILLER, Principal Investigator May 1982 178 p refs
Original contains imagery. Original imagery may be purchased from NASA Goddard Space Flight Center, (code 601), Greenbelt, Md. 20770. Domestic users send orders to 'Attn: National Space Science Data Center'; non-domestic users send orders to 'Attn: World Data Center A for Rockets and Satellites'. HCMM
(Contract NAS5-26473)
(E83-10026; NASA-CR-170492; NAS 1.26:169499) Avail: NTIS HC A09/MF A01 CSCL 08H

The feasibility of applying a linear model to HCMM data in hopes of obtaining an accurate linear correlation was investigated. The relationship among HCMM sensed data surface temperature and red reflectivity on Utah Lake and water quality factors including algae concentrations, algae type, and nutrient and turbidity concentrations was established and evaluated. Correlation (composite) images of day infrared and reflectance imagery were assessed to determine if remote sensing offers the capability of using masses of accurate and comprehensive data in calculating evaporation. The effects of algae on temperature and evaporation were studied and the possibility of using satellite thermal data to locate areas within Utah Lake where significant thermal sources exist and areas of near surface groundwater was examined.
A.R.H.

N83-14572*# Soil Conservation Service, Denver, Colo.
SNOWMELT RUNOFF MODELING IN SIMULATION AND FORECASTING MODES WITH THE MARTINEC-MANGO MODEL Final Report
B. SHAFER, E. B. JONES, and D. M. FRICK, Principal Investigators May 1982 419 p refs · Prepared in cooperation with Resource Consultants, Inc., Fort Collins, Colo. ERTS
(Contract NAS5-26062; NASA ORDER S-63971-B)
(E83-10063; NASA-CR-170452; NAS 1.26:170452) Avail: NTIS HC A18/MF A01 CSCL 08H

The Martinec-Rango snowmelt runoff model was applied to two watersheds in the Rio Grande basin, Colorado-the South Fork Rio Grande, a drainage encompassing 216 sq mi without reservoirs or diversions and the Rio Grande above Del Norte, a drainage encompassing 1,320 sq mi without major reservoirs. The model was successfully applied to both watersheds when run in a simulation mode for the period 1973-79. This period included both high and low runoff seasons. Central to the adaptation of the model to run in a forecast mode was the need to develop a technique to forecast the shape of the snow cover depletion curves between satellite data points. Four separate approaches were investigated-simple linear estimation, multiple regression, parabolic exponential, and type curve. Only the parabolic exponential and type curve methods were run on the South Fork and Rio Grande watersheds for the 1980 runoff season using satellite snow cover updates when available. Although reasonable forecasts were obtained in certain situations, neither method seemed ready for truly operational forecasts, possibly due to a large amount of estimated clinatic data for one or two primary base stations during the 1980 season. A.R.H.

N83-14621# Reading Univ. (England). Dept. of Meteorology.
THE DETERMINATION OF SOIL MOISTURE BALANCES IN TROPICAL AFRICA BY SATELLITE INFRARED REMOTE SENSING: THE ATMOSPHERIC PROBLEM
G. G. WILKINSON, N. R. WARD, G. DUGDALE, and J. R. MILFORD *In* ESA Satellite Remote Sensing for Developing Countries p 103-110 Jun. 1982 refs Sponsored by UK Overseas Development Administration
Avail: NTIS HC A11/MF A01

The technique of remote sensing of soil moisture content by thermal inertia mapping from space is examined. The problem of applying a radiometric correction to Meteosat infrared channel radiances to derive ground surface temperature is considered. A model was used to calculate clear column window channel infrared absorption. The variability of atmospheric state and of its radiative transmission from day to day was assessed using radiosonde profiles from Niamey, Niger. Results indicate that atmospheric variability requires that regular ground truth measurements be obtained for accurate use of the satellite data for soil moisture determination. Author (ESA)

N83-14630# Krueger (I.) A/S, Copenhagen (Denmark).
APPLICATION OF SATELLITE DATA TO HYDROGEOLOGICAL INVESTIGATION IN DAMAGARAM-MOUNIO, NIGER
J. P. ZAFIRYADIS *In* ESA Satellite Remote Sensing for Developing Countries p 181-189 Jun. 1982 refs
Avail: NTIS HC A11/MF A01

The use of satellite data in a project which will drill 300 boreholes and dig 100 wells in an area of the Sahel subject to drought is outlined. Satellite data were used to identify negative drilling zones (zones where the crystalline bedrock is overlaid by sandy formation). These negative zones can be distinguished on LANDSAT images by their reflectance. About 80% of the holes drilled outside these zones contain water. Author (ESA)

N83-15754*# Instituto de Pesquisas Espaciais, Sao Jose dos Campos (Brazil).
VERIFICATION OF LANDSAT IMAGERY FOR MORPHAMETRIC AND TOPOLOGICAL STUDIES OF DRAINAGE BASINS IN A SECTION OF THE WESTERN PLATEAU OF SAO PAULO STATE: TIETE-AGUAPEI WATERSHED M.S. Thesis [AVALIACAO DAS IMAGENS LANDSAT PARA ESTUDOS MORFOMETRI COS E TOPOLOGICOS DE BACIAS HIDROGRAFICAS, EM UMA AREA DO PLANALTO OCIDENTAL PAULISTA: INTERFLUVIO TIETE-AGUAPEI (FEIO)]
N. D. J. PARADA, Principal Investigator and J. C. G. CAMARGO Jun. 1982 255 p refs In PORTUGUESE; ENGLISH summary Sponsored by NASA Original contains imagery. Original photography may be purchased from the EROS Data Center, Sioux Falls, S.D. 57198 ERTS
(E83-10111; NASA-CR-169695; NAS 1.26:169695; INPE-2444-TDL/093) Avail: NTIS HC A12/MF A01 CSCL 08B

The potential of using LANDSAT MSS imagery for morphometric and topological studies of drainage basins was verified. Using Tiete and Aguapei watershed (Western Plateau) as the test site because of its homogeneous landscape. Morphometric variables collected for ten drainage basins include: circularity index; river density; drainage density; topographic texture; areal and index length; basin parameter; and main river length 1st order and 2nd order channel length. The topographical variables determined were: order; magnitude; bifuraction ratio; weighted bifuraction ratio; number of segments; number of linking; trajectory length; and topological diameter. Data were collected on topographical maps at the scale of 1:250,000 and 1:59,000 and on LANDSAT imagery at the scale of 1:250,000. The results which were summarized on tables for further analysis, show that LANDSAT imagery can supply the lack of topographic charts for drainage studies. Author

07

DATA PROCESSING AND DISTRIBUTION SYSTEMS

Includes film processing, computer technology, satellite and aircraft hardware, and imagery.

A83-10075* National Aeronautics and Space Administration. Goddard Space Flight Center, Greenbelt, Md.
STANDARDIZATION OF COMPUTER COMPATIBLE TAPE FORMATS FOR REMOTE SENSING DATA
V. L. THOMAS (NASA, Goddard Space Flight Center, Greenbelt, MD) and F. E. GUERTIN (Canada Centre for Remote Sensing, Ottawa, Canada) In: International Geoscience and Remote Sensing Symposium, Washington, DC, June 8-10, 1981, Digest. Volume 2. New York, Institute of Electrical and Electronics Engineers, 1981, p. 834-839. refs

Standards and guidelines being developed for future CCT formats for use in Landsat receiving stations are presented, in order to solve the data compatability problem, and to consider user community requirements. Data exchange at the local, regional, national, or international level is an important user requirement, and data integration from various sources should be possible. The tape super structure allows various formats to be implemented. A volume directory identifies the volume, and a file descriptor confirms it. The data is then filed, and it is determined whether the data files are appropriate to already defined file classes. If not, a new class is established. Applications of this format are in three areas: satellite imagery, geocoded polygon data, and airborne remote sensing data. R.K.R.

A83-10084* Jet Propulsion Lab., California Inst. of Tech., Pasadena.
SAR SQUINT ANALYSIS OF DIRECTIONAL EXTENDED TARGETS
M. I. DAILY and T. J. BICKNELL (California Institute of Technology, Jet Propulsion Laboratory, Pasadena, CA) In: International Geoscience and Remote Sensing Symposium, Washington, DC, June 8-10, 1981, Digest. Volume 2. New York, Institute of Electrical and Electronics Engineers, 1981, p. 925-930. refs
(Contract NAS7-100)

Results are presented for multisquint processing of L-band like-polarized (HH) SAR data. Images of agricultural fields were generated by Doppler filtering of SAR signal film, with an angular width and step size of 0.8 deg. The results indicate that field reflectivities may vary by more than 10 dB over a range of less than 1 deg. Implications of observing extremely narrow-beamwidth targets are discussed for platform-pointing and antenna-stability requirements. It is suggested that a multiazimuth Venus-orbiting imaging radar could provide a significant amount of information at a relatively low weight penalty. F.G.M.

A83-10121* Jet Propulsion Lab., California Inst. of Tech., Pasadena.
POTENTIALS FOR CHANGE DETECTION USING SEASAT SYNTHETIC APERTURE RADAR DATA
M. L. BRYAN (California Institute of Technology, Jet Propulsion Laboratory, Pasadena, CA) In: International Geoscience and Remote Sensing Symposium, Washington, DC, June 8-10, 1981, Digest. Volume 2. New York, Institute of Electrical and Electronics Engineers, 1981, p. 1451-1457. refs
(Contract NAS7-100)

Synthetic aperture radars (SAR) image from a non-nadir position. Thus the orientation of the target and sensor to one another is of paramount importance. This has posed problems for data interpretation and with the potentials of radar data for change detection studies. It is possible to use Seasat radar data for change detection even though the look directions are fixed for each location. Especially in areas with repeated coverage on descending or ascending orbits or where the terrain is flat and the targets nonoriented, coverage may be sufficient to provide data for change detection. Examples of Los Angeles and the Everglades of Florida help develop and support the argument. (Author)

A83-11410* Lockheed Engineering and Management Services Co., Inc., Houston, Tex.
PROBABILISTIC CLUSTER LABELING OF IMAGERY DATA
T. C. MINTER, R. K. LENNINGTON, and C. B. CHITTINENI (Lockheed Engineering and Management Services Co., Inc., Houston, TX) In: Conference on Pattern Recognition and Image Processing, Dallas, TX, August 3-5, 1981, Proceedings. New York, Institute of Electrical and Electronics Engineers, Inc., 1981, p. 5-10. refs
(Contract NAS9-15800)
(Previously announced in STAR as N82-22590)

A83-11450
PATTERN RECOGNITION AND DIGITAL IMAGE PROCESSING AS APPLIED TO REMOTE SENSING IN INDIA
B. L. DEEKSHATULU (National Remote Sensing Agency, Technical Div., Hyderabad, India) In: Conference on Pattern Recognition and Image Processing, Dallas, TX, August 3-5, 1981, Proceedings. New York, Institute of Electrical and Electronics Engineers, Inc., 1981, p. 410-417. refs

It is pointed out that with the setting up of the National Remote Sensing Agency in the mid seventies, remote sensing activities have gathered momentum and a sizable user community has sprung up. Research being done by the agency and by the Space Applications Center of India is surveyed. The work done thus far in India includes (1) the development of remote sensing sensor hardware; (2) data processing, image processing and image interpretation techniques and hardware; and (3) the application to different fields, such as forestry, water resources, soils, geology, and agriculture. India is seen to be on a par with any other

developed country in the utilization of remote sensing technology in the visible and IR regions of the spectrum. C.R.

A83-11458
SCENE CLASSIFICATION OF LANDSAT MULTISPECTRAL SCANNER DATA BY MEANS OF THE ADAPTIVE LEARNING NETWORK METHODOLOGY
P. HORVATH and F. J. COOK (Adaptronics, Inc., McLean, VA) In: Conference on Pattern Recognition and Image Processing, Dallas, TX, August 3-5, 1981, Proceedings. New York, Institute of Electrical and Electronics Engineers, Inc., 1981, p. 473-477. refs
(Contract DACW39-79-M-3958)

An approach to pattern recognition and modeling known as the Adaptive Learning Network (ALN) methodology was used to classify a Landsat scene into three terrain classes: water, forest, and non-forest. The ALN classifier algorithm was derived from a training data set of 545 pixels and was used to classify 52,000 pixels of the evaluation set. The positive classification results based on a comparison with the actual terrain conditions and the large evaluation set as compared to the training data set, together with the speed and simplicity of the algorithm demonstrate that the ALN methodology is ideally suited to classification of large Landsat scenes in very short periods of time. (Author)

A83-11461
AUTOMATIC MULTITEMPORAL SEGMENTATION FOR DIACHRONIC ANALYSIS OF REMOTELY SENSED IMAGES
R. JEANSOULIN (Ecole Nationale Superieure d'Electrotechnique, d'Electronique, d'Informatique, et d'Hydraulique; Toulouse III, Universite, Toulouse, France) and W. FREI (Southern California, University, Marina del Rey, CA) In: Conference on Pattern Recognition and Image Processing, Dallas, TX, August 3-5, 1981, Proceedings. New York, Institute of Electrical and Electronics Engineers, Inc., 1981, p. 487-490. Research supported by the Centre National d'Etudes Spatiales. refs

A three-stage operation that greatly facilitates diachronic analysis is proposed. A region in each image of the sequence of interest is grown to encompass all the elements belonging to the fields initially designated by the user. This allows fields to be analyzed on an entity/entity basis rather than on a pixel/pixel basis, thus reducing susceptibility to noise and misregistration errors. A relative geometric deformation model for each image is determined, based upon a set of control points located by an automatic registration. The regions initially grown in the different images of the sequence are then compared, taking the geometric deformation models into account. One major advantage of the approach is that the problems caused by misregistration of successive views are eliminated, and manual intervention is reduced to the designation of one pixel within the area of interest in any image of the sequence to be analyzed, and to the initialization of the registration algorithms for each other image. C.D.

A83-11462
A RELATIONAL IMAGE DATA BASE SYSTEM FOR REMOTE SENSING /LAND DBMS/
M. NAGATA In: Conference on Pattern Recognition and Image Processing, Dallas, TX, August 3-5, 1981, Proceedings. New York, Institute of Electrical and Electronics Engineers, Inc., 1981, p. 491-495. refs

This paper describes the design and experimental implementation of a relational image data base system (DBMS) for remote sensing, whose name is LAND DBMS. The LAND DBMS provides faculties for hierarchical command, user oriented job control language (JCL) and concurrency file control mechanism. The hierarchical command is designed for convenience of the conceptual scheme of the DBMS. The user oriented JCL supports the external scheme for processing the accessed image data. The concurrency file control mechanism is designed to maintain the consistency of the data-base. The LAND DBMS retrieves tuples in the relation which contains indirect information of the remote sensing imagery. The LAND DBMS also processes the accessed image. The image data of remote sensing is a type of computer compatible tape collected by multispectral scanner (MSS) and A-D converted. The LAND DBMS is implemented on a computer, FACOM M150-F, the multiprogramming operating system of which is FACOM OS IV/X8. (Author)

A83-12035* Alaska Univ., Fairbanks.
EVALUATION OF PHOTOGRAPHIC ENHANCEMENTS OF LANDSAT IMAGERY
K. G. DEAN (Alaska, University, Fairbanks, AK) and J. P. SPENCER (U.S. Bureau of Land Management, Anchorage, AK) Remote Sensing of Environment, vol. 12, Nov. 1982, p. 381-390. refs
(Contract NGL-02-001-092)

The photographic processing of color Landsat imagery was evaluated to determine the optimal enhancement techniques. Twenty-six images were examined to explore the effects of gamma values upon image interpretation in a subarctic environment. Gamma values were varied on the images of bands 4 through 7 prior to the creation of the color composites. This yielded color-composited images with various color balances. These images were evaluated in terms of visible geological features (drainage, lineaments, landforms, etc.) and landcover features (exposed rock and ground, coniferous forest, etc.). The results indicate that the most informative images are created by using gamma values of 2.0 for band 4, 1.0 for band 5, and 2.0 for band 6 or 7. Other photographic enhancements tend to enhance some features at the expense of others. S.C.S.

A83-12037
A COMPARISON OF UNSUPERVISED CLASSIFICATION PROCEDURES ON LANDSAT MSS DATA FOR AN AREA OF COMPLEX SURFACE CONDITIONS IN BASILICATA, SOUTHERN ITALY
C. JUSTICE (ESA, Frascati, Italy) and J. TOWNSHEND (Reading, University, Reading, Berks., England) Remote Sensing of Environment, vol. 12, Nov. 1982, p. 407-420. refs

In this study, two unsupervised classification procedures are applied to ratioed and unratioed Landsat MSS data on an area of spatially complex vegetation and terrain. An objective accuracy assessment is undertaken on each classification and a comparison is made of the classification accuracies. By one procedure the entire area is clustered and by the other, a representative sample of the area is clustered and the resulting statistics are extrapolated to the remaining area using a maximum likelihood classifier. Classification of the unratioed data produced higher percentage accuracies than for the ratioed data and the monocluster block approach gave higher accuracies than clustering the entire area. The accuracy was increased to 84% by applying a 3 x 3 contextual filter to the classified image. The monocluster block approach was additionally the most economical in terms of computing time. (Author)

A83-12602#
BACKGROUND REFLECTANCE EFFECTS IN LANDSAT DATA
R. W. DANA (U.S. Department of Agriculture, Forest Service, Fort Collins, CO) Applied Optics, vol. 21, Nov. 15, 1982, p. 4106-4111. refs

A regression analysis was performed on Landsat MSS data to investigate the dependence of object radiance on the radiance of adjacent areas. The object radiance is increased by a path radiance component attributed to forward scattering in the atmosphere after reflection of solar radiation from the object background. Inclusion of average radiance of a few concentric rings with object reflectance in the regression model for satellite-measured radiance improves the least-squares fit at all sites tested. Multiple regression analysis indicates that radiance of an object is significantly affected by reflectance of background objects up to 500 m away. (Author)

A83-12678* Ocean Data Systems, Inc., Monterey, Calif.
TECHNOLOGY AND FUTURE GROUND PROCESSING SYSTEMS
B. J. WOOD and K. W. RUGGLES (Ocean Data Systems, Inc., Monterey, CA) In: Electro-optical instrumentation for resources evaluation; Proceedings of the Meeting, Washington, DC, April 21, 22, 1981. Bellingham, WA, SPIE - The International Society for Optical Engineering, 1981, p. 104-115. refs
(Contract NAS5-26025)

Land-observing satellites with multiple thematic mappers will produce data at rates of 100 to 300 Mbps. When coupled with a high daily scene production rate, these rates will require new approaches to ground processing. Consideration is given here to future downlink rates and data volumes, and requirements peculiar to the future user community are discussed. The advanced technologies required to attain an operational system in the years 1985-1990 are considered, together with advances foreseen in communications, mass storage, bulk memories, and data processing. Using advanced devices, a centralized data processing system capable of handling the 100 Mbps data rate is described. New approaches, among them a parallel pipelined calibration front-end, real-time browse image production, a high bandwidth optical disk archive, regional image broadcast and massively parallel product production, are considered. A distributed system capable of handling the 300 Mbps data rate is then described. Designs for a hub system and a regional processing center are presented. C.R.

A83-12683
ANALYTICAL PLOTTER FOR DATA INPUT INTO GEO-BASED INFORMATION SYSTEMS
R. R. S. CHAMARD (Helava Associates, Inc., Southfield, MI) In: Electro-optical instrumentation for resources evaluation; Proceedings of the Meeting, Washington, DC, April 21, 22, 1981. Bellingham, WA, SPIE - The International Society for Optical Engineering, 1981, p. 147-153.

The analytical plotter is shown to be economical, accurate, and fast in gathering data in a digital format for 'action' plans. It is thought possible that, by using very small scale aerial photography, the analytical stereoplotter will be very competitive with conventional data gathering for macro systems. This may be in the offing because of the ready availability of small scale aerial photography. The U.S. Geological Survey is now obtaining cyclic aerial photography at a scale of approximately 1:80,000. Combined with the analytic stereoplotter, this could well make data acquisition for any geo-based systems more economical and accurate than is the case in macro geo-based information systems. It is pointed out that this would also reduce the need for a micro system by furnishing data at a middle ground accuracy. C.R.

A83-12685
IMAGE ENHANCEMENT THROUGH FILM RECORDER RESPONSE CONTOURING
J. E. BOYD (Technicolor Graphic Services, Inc., EROS Data Center, Sioux Falls, SD) In: Electro-optical instrumentation for resources evaluation; Proceedings of the Meeting, Washington, DC, April 21, 22, 1981. Bellingham, WA, SPIE - The International Society for Optical Engineering, 1981, p. 157-166. U.S. Geological Survey
(Contract USGS-14-08-001-16439)

Even though digitization involves several extra steps in the preproduction of the imagery, it permits manipulation or enhancement of the data for special uses. For example, image data enhancement techniques can be applied to partially restore contrast lost because of atmospheric luminance and scatter. What is more significant, the digital-to-analog transfer function of the film recorder can be modified to simulate certain characteristics of other film types. Manipulation of a film's apparent gamma, relative speed, and linear-response region is easily effected by mapping the input data to a new distribution in real time using a hardware-implemented lookup table. However, to accomplish the desired photographic results, full cooperation and communication between photographic, electronic, and computer technologists is essential. C.R.

A83-12882
RECONNAISSANCE APPLICATIONS OF IMAGE UNDERSTANDING
J. L. ROBERTS (Central Intelligence Agency, Imagery Exploitation Research Div., Washington, DC) In: Techniques and applications of image understanding; Proceedings of the Meeting, Washington, DC, April 21-23, 1981. Bellingham, WA, SPIE - The International Society for Optical Engineering, 1981, p. 80-84. refs

Numerous DARPA and privately pursued image understanding research efforts are related to various phases of reconnaissance image interpretation. These efforts can contribute directly to the various subtasks associated with each phase of the interpretation. Three major categories to which DARPA research in image understanding may be applied are considered: object detection, target monitoring, and in-depth analysis. B.J.

A83-12885
REGISTRATION OF A SYNTHETIC APERTURE RADAR /SAR/ RECONNAISSANCE IMAGE WITH A MAP REFERENCE DATA BASE
G. K. KIREMIDJIAN (ESL, Inc., Sunnyvale, CA) In: Techniques and applications of image understanding; Proceedings of the Meeting, Washington, DC, April 21-23, 1981. Bellingham, WA, SPIE - The International Society for Optical Engineering, 1981, p. 110-115. refs

The problem of registering a reconnaissance side-looking synthetic aperture radar (SAR) image to a three-dimensional reference map is examined by developing a technique which is based on computing an image-to-date base correspondence in terms of a SAR sensor model as a function of such parameters as altitude, range, scale, etc. If their exact values are known, registration is accomplished by utilizing the model to predict the two-dimensional image coordinates for any three-dimensional data base point. In general, the platform ephemeris (PE) data provides only coarse model parameter estimates. The objective, then, is to refine them so that the model can predict the image location of any data base point within a desired accuracy range. The results obtained in this paper demonstrate the feasibility of achieving location accuracy within 50 m. (Author)

A83-12889
RELAXATION MATCHING APPLIED TO AERIAL IMAGES
K. E. PRICE (Southern California, University, Los Angeles, CA) In: Techniques and applications of image understanding; Proceedings of the Meeting, Washington, DC, April 21-23, 1981. Bellingham, WA, SPIE - The International Society for Optical Engineering, 1981, p. 207-210.

A symbolic matching system has been developed which can be used for a variety of matching tasks in scene analysis. The system is designed to handle many of the problems encountered in the analysis of real scenes, including noisy feature values, missing elements, extra pieces of objects, many features, and many objects. The system is based on a relaxation matchi2g scheme; a variety of relaxation procedures have been used with varying results. This paper describes the overall matching system and discusses the performance of the various relaxation techniques. B.J.

A83-13845#
QUALITY ASSESSMENT OF REMOTE-SENSING DATA - THE SAR CASE
S. BRUZZI (ESA, European Space Research Institute, Frascati, Italy), J.-P. GUIGNARD (ESA, Payload Technology Dept., Noordwijk, Netherlands), and T. PIKE (Marconi Communication Systems, Ltd., Research Centre, Chelmsford, Essex, England) ESA Journal, vol. 6, no. 3, 1982, p. 271-281.

In the context of a continuing effort to develop tools for quality controlling digital image products from remote-sensing satellites, quality-control procedures and measurements are reported for images generated from Synthetic Aperture Radar (SAR) data. The particular case considered here is the data set collected during the Earthnet SAR-580 campaign in June-July 1981. The results demonstrate (a) the possibility of discriminating between different

SAR products and therefore the validity of the instruments employed for measurements; (b) the practical usability of the instruments and procedures in the light of operational quality control of SAR data. (Author)

A83-14243#
COMPARISON STUDY OF FUTURE SPOT AND LANDSAT-D SATELLITE PRODUCTS FROM A SIMULATION FLIGHT [ETUDE COMPARATIVE DES PRODUITS DES FUTURS SATELLITES SPOT ET LANDSAT-D A PARTIR D'UN SURVOL DE SIMULATION]
F. BONN, G. CLICHE, and C. TOUTANT (Sherbrooke, Universite, Sherbrooke, Quebec, Canada) In: Canadian Symposium on Remote Sensing, 7th, Winnipeg, Canada, September 8-11, 1981, Proceedings. Ottawa, Canadian Aeronautics and Space Institute, 1982, p. 142-149. In French. Research supported by the Ministere de l'Education du Quebec. refs

An airborne simulation of SPOT and Landsat D images was done in August 1980 in the Granby-Mont Yamaska region, Quebec, using a 1260 Daedalus sensor (11 channels) modified by the Canada Centre for Remote Sensing. Analysis of images obtained indicated that because of its spectral characteristics Landsat D is a useful tool for crop discrimination and that, because of its spatial resolution, SPOT should be used in urban and semi-urban regions and for road and building location (Author)

A83-14247#
APPLICATION OF LANDSAT IMAGERY TO NATURAL RESOURCES MANAGEMENT IN SIERRA LEONE, WEST AFRICA
S. M. RINGROSE, J. P. JOLLY (Geological, Hydrological, and Hydrogeological Consultants, Ottawa, Canada), P. LARGE (Deloitte Haskins and Sells Associates, Ottawa, Canada), and W. D. BRUCE (Canada Centre for Remote Sensing, Ottawa, Canada) In: Canadian Symposium on Remote Sensing, 7th, Winnipeg, Canada, September 8-11, 1981, Proceedings. Ottawa, Canadian Aeronautics and Space Institute, 1982, p. 178-189. Research supported by the Geological, Hydrological and Hydrogeological Consultants, Canada Centre for Remote Sensing, and International Development Research Centre. refs

Digital enhancement techniques were used to obtain basic natural resources information for Sierra Leone and adjacent parts of Guinea, West Africa. Preliminary results indicate that geological land use information (mineral extraction) and engineering terrain classification can be achieved through standard unsupervised classification techniques. Linear mapping for possible diamond exploration was accomplished using contrast stretch and biomass ratio data. Seasonal Landsat MSS imagery is required to obtain information on the hydrological dynamics of the coastal swamps (mangrove) and inland swamps (bollilands). General information enabling the identification of vegetation and land use patterns can be discerned from colour composite data. Contrast stretch and biomass data appear to best enhance the visual distinction of vegetative cover and the identification of potential mangrove swamp areas. (Author)

A83-14260#
CONSTRUCTION AND INTERPRETATION OF A THERMAL INERTIA IMAGE USING AIRBORNE DATA [CONSTRUCTION ET INTERPRETATION D'UNE IMAGE D'INERTIE THERMIQUE A PARTIR DE DONNEES AEROPORTEES]
F. BONN, M. BERNIER, and R. BROCHU (Sherbrooke, Universite, Sherbrooke, Quebec, Canada) In: Canadian Symposium on Remote Sensing, 7th, Winnipeg, Canada, September 8-11, 1981, Proceedings. Ottawa, Canadian Aeronautics and Space Institute, 1982, p. 286-293. In French. Natural Sciences and Engineering Research Council of Canada refs
(Contract NSERC-A-6043)

A high-resolution (4 m) thermal inertia image of the earth's surface was constructed using airborne data in the visible, near infrared and thermal infrared regions of the spectrum by combining digital images from a day flight and a night flight by means of the algorithm used for the HCMM (Heat Capacity Mapping Mission) satellite. Interpretation of the image showed a good relationship between thermal inertia and vegetation height, but no conclusive results could be obtained for soil humidity in the region studied, which was totally covered by vegetation and where the soil was near saturation. (Author)

A83-14265#
COLOUR LANDSAT IMAGES AND MOSAICS - BASIC TOOLS IN AREAL AND ECOLOGICAL DIFFERENTIATION IN CANADA
C. D. A. RUBEC, E. B. WIKEN, and N. R. MORRISON (Department of the Environment, Lands Directorate, Hull, Quebec, Canada) In: Canadian Symposium on Remote Sensing, 7th, Winnipeg, Canada, September 8-11, 1981, Proceedings. Ottawa, Canadian Aeronautics and Space Institute, 1982, p. 331-340. refs

Mosaics for the Canadian Arctic Islands are discussed in the light of current applications by Environment Canada to northern land use and ecological land surveys. The problems and merits associated with color satellite products are considered. The general development and applications of both color and panchromatic satellite mosaics are outlined. The use of color Landsat mosaics for ecodistrict mapping in the Lancaster sound region of the Arctic is discussed. A table in which panchromatic and color Landsat mosaics are listed by province and territory is included, as is a table indicating the mosaics most useful for studies on a 1:1,000,000 map sheet by sheet basis. C.R.

A83-14270#
A NATIONAL LANDSAT COLLECTION AND A PROPOSAL FOR A LIBRARY OF LANDSAT IMAGES
E. FLEMING (Department of Energy, Mines, and Resources, Topographical Survey Div., Ottawa, Canada) In: Canadian Symposium on Remote Sensing, 7th, Winnipeg, Canada, September 8-11, 1981, Proceedings. Ottawa, Canadian Aeronautics and Space Institute, 1982, p. 369-373.

There have been numerous proposals from interested user groups regarding an implementation of optimum procedures for preserving the Landsat image record of Canada and for making the image record of Canada available to a wider public. The present investigation is concerned with one proposal which is currently being implemented, and another which deserves serious consideration. The first proposal is related to the establishment of a national collection of images. A study group was set up to investigate a means of establishing a national collection of Landsat images in hard copy form, which could be used as a reference source for people desiring to know what could be seen on a good Landsat image of any particular area of the country in which they were interested. The second proposal is concerned with the establishment of a library of Landsat images. Images could be borrowed from this source for some predetermined time period, after which they would either be returned, bought, or reordered. G.R.

A83-14271#
AN EXPERIMENTAL LANDSAT QUICKLOOK SYSTEM FOR ALASKA
K. COX (MacDonald Dettwiler and Associates, Ltd., Richmond, British Columbia, Canada) In: Canadian Symposium on Remote Sensing, 7th, Winnipeg, Canada, September 8-11, 1981, Proceedings. Ottawa, Canadian Aeronautics and Space Institute, 1982, p. 374-383.

Many potential applications of Landsat imagery require that imagery be made available to users with minimal delay from acquisition. However, users frequently experience delays of 2 to 6 weeks from data acquisition to image delivery. The Quicklook Image Recording System (QLIRS) has been developed in response to the need for near-real-time image generation. This simple, inexpensive system is intended to be used by relatively low-budget groups for production of near-real-time, partially-corrected, full-resolution Landsat images. It is designed to supplement rather than replace existing Landsat image processing facilities. The QLIRS is mainly designed for the production of film images in monochrome and optionally in color. As another option, computer-compatible magnetic tapes of image and auxiliary data

can be produced for transfer to another computer system. (Author)

A83-14272#
DEFINITION AND POTENTIAL OF GEOCODED SATELLITE IMAGERY PRODUCTS
F. E. GUERTIN and E. SHAW (Canada Centre for Remote Sensing, Ottawa, Canada) In: Canadian Symposium on Remote Sensing, 7th, Winnipeg, Canada, September 8-11, 1981, Proceedings. Ottawa, Canadian Aeronautics and Space Institute, 1982, p. 384-394. refs

In the next ten years, there will be an increase in the number of imaging satellites following similar quasi-polar but different orbits. For the most suitable utilization of images from multiple complementary spaceborne (and airborne) missions and their integration with geocoded databases, it is important for remote sensing data processing and distribution agencies to develop and offer mission independent standard products in a fixed and common cartographic projection such as the Universal Transverse Mercator (UTM) projection. In Canada, the UTM projection is being used for most national and provincial databases. Imagery which is transformed to a cartographic projection and is independent of the sensor characteristics and orbital parameters of the platform is called 'geocoded'. G.R.

A83-14273#
REMOTE SENSING SOFTWARE FOR AIRBORNE IMAGE ANALYSIS
B. GUINDON, P. M. TEILLET, D. G. GOODENOUGH, J.-F. MEUNIER, and K. DICKINSON (Canada Centre for Remote Sensing, Ottawa, Canada) In: Canadian Symposium on Remote Sensing, 7th, Winnipeg, Canada, September 8-11, 1981, Proceedings. Ottawa, Canadian Aeronautics and Space Institute, 1982, p. 395-409. refs

The high resolution and large look angles of airborne synthetic aperture radar (SAR) and multispectral scanner (MSS) sensors introduce image processing problems not encountered with the present satellite (Landsat) data. During the last three years, studies have been conducted at the Canada Centre for Remote Sensing (CCRS) with the objective to develop suitable airborne image processing algorithms and to implement them on the CCRS Image Analysis System (CIAS). A description of the resulting software is provided. A synopsis of software is presented, taking into account Digital Elevation Model (DEM) processing, aspects of geometric correction, radiometric effects, loss of information in connection with shadow and layover phenomena, and spatial feature generation. G.R.

A83-14280#
CARTOGRAPHIC ASPECTS OF DUAL-FREQUENCY DUAL-POLARIZATION SAR IMAGERY
E. DERENYI and L. SZABO (New Brunswick, University, Fredericton, Canada) In: Canadian Symposium on Remote Sensing, 7th, Winnipeg, Canada, September 8-11, 1981, Proceedings. Ottawa, Canadian Aeronautics and Space Institute, 1982, p. 450-453. Research supported by the Department of Energy, Mines and Resources and Natural Sciences and Engineering Research Council of Canada.

Radar imagery was obtained using four-channel SAR equipment on board an aircraft to define the cartographic performance of the bands. The tests were performed over Ontario by flying three lines, each 60 km long, with the sensor in a shallow angle mode. An altitude of 6 km was maintained to obtain a 6 km wide ground swath. Data analysis was performed to examine the four sets of images to identify inconsistencies in scale, compare the accuracies available from each channel, and assay the accuracy for the registration of output from each channel to a base map. A two-stage transformation was employed to produce residual errors for comparisons. Significant differences in scale were found, together with scale inequalities in the aximuth and range direction, thereby making the operations of overlay of the different channels' data difficult. An X-band, like-polarization produced the best cartographic accuracy. Segmentation improved the accuracy of image-to-image or image-to-map registration. M.S.K.

A83-14281#
A REFINED DESTRIPING PROCEDURE FOR LANDSAT MSS DATA PRODUCTS
J. MURPHY (Canada Centre for Remote Sensing, Ottawa, Canada) In: Canadian Symposium on Remote Sensing, 7th, Winnipeg, Canada, September 8-11, 1981, Proceedings. Ottawa, Canadian Aeronautics and Space Institute, 1982, p. 454-470.

Two refinements to the destriping procedures included in the Canadian Centre for Remote Sensing software are described, together with quality control methods used for all Landsat imagery at the Centre. Existing processing consists of a choice of a reference detector in each band and a definition of correlations necessary to define an absolute scale, the calculation of the relative differences between all other detectors and the reference detector in each band, and the combination of the absolute calibration with the relative corrections between the six detectors of each band. Details of the refinements to the relative correction procedure are presented, including histogram preprocessing to exclude false data values. Histogram inspection is discussed, together with steps taken to test the refinements. It is shown that the corrected imagery contains very little striping. M.S.K.

A83-14285#
SOME EFFECTS ON THE GCP SUCCESS RATE
K. TSUCHIYA (National Space Development Agency of Japan, Earth Observation Systems Dept., Tokyo, Japan) and K. ARAI (National Space Development Agency of Japan, Earth Observation Center, Hatoyama, Saitama, Japan) In: Canadian Symposium on Remote Sensing, 7th, Winnipeg, Canada, September 8-11, 1981, Proceedings. Ottawa, Canadian Aeronautics and Space Institute, 1982, p. 497-502. refs

An examination of the causes of registration errors which cause geometric distortions during Landsat MSS data processing is carried out, and various ground control points (GCPs) are ranked for effectiveness. Experimental examination of precision registration processing has shown that a success rate is dependent on the seasonal and weather conditions independent of the type of satellite. A negative correlation has been demonstrated between the sequential similarity detecting algorithm and the registration errors in the direction normal to the satellite track. A negative correlation has also been found between the number of ground control points and the registration errors. It is shown that refinement in yaw estimation is necessary to compensate for image skew. Breakwaters were calculated to be the most effective GCPs. M.S.K.

A83-14286#
REFERENCE QUICKLOOK IMAGES FOR MONITOR OF LANDSAT IMAGE DATA ACQUISITION
H. SATO and T. IGARASHI (National Space Development Agency of Japan, Earth Observation Center, Hatoyama, Saitama, Japan) In: Canadian Symposium on Remote Sensing, 7th, Winnipeg, Canada, September 8-11, 1981, Proceedings. Ottawa, Canadian Aeronautics and Space Institute, 1982, p. 503-506.

The results of an attempt to define a reference quality for quick-look CRT displays nominally put on the screen during transmission of satellite imagery to ground receiving stations are discussed. The reference imagery is classified into normal and abnormal groups. The normal group comprises test patterns, ordinary Landsat MSS and RBV images, cloud-coverage images, gamma-curve-enhanced images, pseudo-color enhanced images, and images from a high gain mode. The abnormal group covers images interfered with by solar noise and radio transmitters, images disturbed with by on-board operational problems, images affected by unusual spacecraft attitudes, and pseudo-pulse mode images. Image deterioration occurs when, for instance, the solar noise reaches a predetermined level, and it is recommended that a predictive method for determining the sun-satellite coincidence be developed. Finally, a technique is described for storage and retrieval of archived false color images. M.S.K.

A83-14304
THE ACCURACY OF A COMPONENT ANALYSIS IN SPACE STUDIES OF NATURAL ENVIRONMENTS [TOCHNOST' KOMPONENTNOGO ANALIZA PRI KOSMICHESKIKH ISSLEDOVANIIAKH PRIRODNOI SREDY]
B. B. SERAPINAS (Moskovskii Gosudarstvennyi Universitet, Moscow, USSR) Issledovanie Zemli iz Kosmosa, Sept.-Oct. 1982, p. 23-28. In Russian.

Simple methods are presented for estimating the number of the principal components to be isolated and evaluating the accuracy of the correlation matrix eigenvalues and object coordinates within the principal component system when interpreting multispectral aerial and space imagery. The practical use of the proposed methods is illustrated by examples involving identification of agricultural fields from space imagery. V.L.

A83-14311
AUTOMATION OF THE SEARCH FOR AND RECOGNITION OF REFERENCE ZONES FOR PRECISE COORDINATE CONTROL OF SPACE IMAGERY [VOPROSY AVTOMATIZATSII PROTSESSA POISKA I RASPOZNAVANIIA OPORNYKH ZON PRI TOCHNOI KOORDINATNOI PRIVIAZKE KOSMICHESKOI VIDEOINFORMATSII]
G. A. AVANESOV and V. A. VAVAEV (Akademiia Nauk SSR, Institut Kosmicheskikh Issledovanii, Moscow, USSR) Issledovanie Zemli iz Kosmosa, Sept.-Oct. 1982, p. 80-86. In Russian.

An algorithm is developed for the automatic search for reference zones, their identification with the available standards, and determination of their coordinates. Experimental results confirming the efficiency of the proposed algorithm, which has been implemented in a computer program, are presented. V.L.

A83-14598* Jet Propulsion Lab., California Inst. of Tech., Pasadena.
RADAR IMAGES OF THE EARTH FROM SPACE
C. ELACHI (California Institute of Technology, Jet Propulsion Laboratory, Pasadena, CA) Scientific American, vol. 247, Dec. 1982, p. 54-61.

The operational principles and imagery available from microwave SAR radars for earth observations from aircraft, the Shuttle, and Seasat are explored. Using microwave frequencies is noted to offer imagery access in day or night, all-weather conditions. SAR radar functions by obtaining a series of reflected signals over a single path, with data processing combining the echoes into an image corresponding to what may be obtained with a large antenna. A stable, reference signal is added to the incoming signals in order to establish the phase and amplitude of echoes. Because the wavelengths of the images can be precisely controlled, Doppler shifts can be detected, thus allowing point by point scattering analysis in two-dimensions. The Shuttle SIR-A and the Seasat radar feature a ground resolution of 25 m. Applications of the satellite systems to terrain, ice mapping, and for a Venus radar mapper mission are described. M.S.K.

A83-14664
TO MIX OR MATCH - ON CHOOSING MATCHED SAMPLES IN COMPARATIVE AERIAL SURVEYS
L. D. MAXIM and L. HARRINGTON (Everest Consulting Associates, Princeton Junction, NJ) Photogrammetric Engineering and Remote Sensing, vol. 48, Dec. 1982, p. 1863-1867. refs

The problem of sampling design in repetitive aerial surveys is addressed. Specifically, the trade-offs in sampling design to maximize either the precision of an estimate of the change in a population (between two surveys) or of an estimate of the current level of a survey variable are examined. Optimal designs for change detection require that a matched set of quadrats be selected. But optimal designs for estimation of levels of the survey variable often involve taking unmatched quadrats. Practical designs attempt to strike a balance between these objectives. This design problem is described and illustrated. (Author)

A83-14853* Computer Sciences Corp., Silver Spring, Md.
ESTIMATION OF CONTEXT FOR STATISTICAL CLASSIFICATION OF MULTISPECTRAL IMAGE DATA
J. C. TILTON (Computer Sciences Corp., Silver Spring, MD), S. B. VARDEMAN (Iowa State University of Science and Technology, Ames, IA), and P. H. SWAIN (Purdue University, West Lafayette, IN) IEEE Transactions on Geoscience and Remote Sensing, vol. GE-20, Oct. 1982, p. 445-452. refs
(Contract NAS9-15466; NSF MCS-78-04366)

Recent investigations have demonstrated the effectiveness of a contextual classifier that combines spatial and spectral information employing a general statistical approach. This statistical classification algorithm exploits the tendency of certain ground cover classes to occur more frequently in some spatial contexts than in others. Indeed, a key input to this algorithm is a statistical characterization of the context: the context function. An unbiased estimator of the context function is discussed which, besides having the advantage of statistical unbiasedness, has the additional advantage over other estimation techniques of being amenable to an adaptive implementation in which the context-function estimate varies according to local contextual information. Results from applying the unbiased estimator to the contextual classification of three real Landsat data sets are presented and contrasted with results from noncontextual classifications and from contextual classifications utilizing other context-function estimation techniques. (Author)

A83-14944
THE DIGITAL IMAGE PROCESSING SYSTEM MOBI-DIVAH [DAS DIGITALE BILDVERARBEITUNGSSYSTEM MOBI-DIVAH]
E. DENNERT-MOELLER, M. EHLERS, D. KOLOUCH, and P. LOHMANN (Hannover, Universitaet, Hanover, West Germany) Bildmessung und Luftbildwesen, vol. 50, Nov. 1, 1982, p. 201-203. In German.

The digital image processing procedures considered in the present investigation make use of a digital interactive image processing facility (DIVAH) and a modular off-line image processing program package (MOBI). MOBI consists of five main programs, and most programs are written in Fortran. DIVAH contains a minicomputer with a computer memory of 32 K and 16-bit words. MOBI and DIVAH are both used for the processing of image data of the different sensors. Statistic procedures for the digital multispectral classification of Landsat imagery are used to produce a map of the sediment of tidal flats. A basis for further geometrical processing for the determination of water depths is obtained by making use of suitable processes involving the filtering of the interferometric sonar data. G.R.

A83-14945
PREPARATION OF A SEDIMENT MAP OF THE NORTH FRISIAN SHOAL AREAS ON THE BASIS OF LANDSAT IMAGERY [ERSTELLUNG EINER SEDIMENTKARTE DER NORDFRIESISCHEN WATTGEBIETE AUS LANDSAT-BILDDATEN]
E. DENNERT-MOELLER (Hanover, Universitaet, Hanover, West Germany) Bildmessung und Luftbildwesen, vol. 50, Nov. 1, 1982, p. 204-206. In German. refs

A83-14946
RECTIFICATION OF SEASAT RADAR ON LANDSAT MSS WITH THE AID OF DIGITAL IMAGE CORRELATION [ENTZERRUNG VON SEASAT-RADAR AUF LANDSAT-MSS MIT HILFE DIGITALER BILDKORRELATION]
M. EHLERS (Hanover, Universitaet, Hanover, West Germany) Bildmessung und Luftbildwesen, vol. 50, Nov. 1, 1982, p. 210-213. In German. refs

In connection with the rectification of remote sensing imagery with respect to a reference image, digital image correlation was found to provide a successful approach for the determination of control points for the rectification procedure. Ehlers (1982) has reported a sensor-independent concept for the rectification of remote-sensing imagery with the aid of digital correlation processes. The present investigation is concerned with an application of this

concept in the processing of imagery data provided by an active sensor, i.e. radar. The investigation makes use of a data provided by a synthetic aperture radar (SAR) of the Seasat satellite. Seasat was placed into orbit in 1978. A corresponding Landsat imagery section was selected as reference image for the rectification procedure. G.R.

A83-16831* National Aeronautics and Space Administration. Goddard Space Flight Center, Greenbelt, Md.
DUAL-WAVELENGTH CORRELATION MEASUREMENTS WITH AN AIRBORNE PULSED CARBON DIOXIDE LIDAR SYSTEM
J. L. BUFTON, T. ITABE (NASA, Goddard Space Flight Center, Greenbelt, MD), and D. A. GROLEMUND (NASA, Goddard Space Flight Center, Greenbelt; Bendix Field Engineering Corp., Columbia, MD) Optics Letters, vol. 7, Dec. 1982, p. 584-586. refs

Dual-wavelength correlation data are presented for ground-level and airborne measurements of topographic and ocean backscatter near the 9.5-micron wavelength. Data were acquired with a pulsed carbon dioxide, dual-laser, dual-wavelength lidar system. The best system performance gave a dual-wavelength uncorrelated noise component of 2.8% and 9% standard deviation for ground-based and airborne data, respectively. This sets one limit on lidar measurement accuracy with a single pulse pair. (Author)

A83-16904* New York State Univ., Albany.
AN EVALUATION OF SEASAT SAR IMAGERY FOR URBAN ANALYSIS
F. M. HENDERSON (New York, State University, Albany, NY) Remote Sensing of Environment, vol. 12, Dec. 1982, p. 439-461. refs
(Contract NAS5-26032)

Digitally processed Seasat SAR imagery of the Denver, Colorado, area is analyzed with regard to the types of urban data that can be detected and/or inferred from satellite-borne L-band systems. Black-and-white images of the scene were generated at three scales to determine the advantages and detail discernible at each level of display. The large-scale imagery was density-sliced to evaluate the feasibility of producing a semiautomated land-cover classification from the SAR data. Gray level classes were assigned colors to aid interpretation and subsequently compared with the black-and-white images to assess the contribution of each technique and benefits of combining the data from both procedures. (Author)

A83-16905* New South Wales Univ., Kensington (Australia).
A MEANS FOR UTILIZING ANCILLARY INFORMATION IN MULTISPECTRAL CLASSIFICATION
J. A. RICHARDS (New South Wales, University, Kensington, Australia), D. A. LANDGREBE, and P. H. SWAIN (Purdue University, West Lafayette, IN) Remote Sensing of Environment, vol. 12, Dec. 1982, p. 463-477. refs
(Contract NAS9-15466)

Attention is given to a method which makes it possible to incorporate information from ancillary data sources into the results of an existing classification of remotely sensed data. The method is based upon probabilistic label relaxation procedures which are used for imbedding spatial context data in image-labeling problems. The source of ancillary information is utilized in the form of a set of probabilities. These are introduced into a modified relaxation method called supervised relaxation labeling which, on application, develops a labeling for remotely sensed data that strikes a balance in consistency between spectral, spatial, and ancillary data sources of information. A description is given of results of a forestry classification in which accuracy is improved from 68% to 81% by incorporating topographic elevation in the outlined manner. G.R.

A83-17299
RESULTS OF PHOTOTRIANGULATION ON THE BASIS OF SPACE PHOTOGRAPHS [O REZUL'TATAKH FOTOTRIANGULIROVANIIA PO KOSMICHESKIM SNIMKAM]
A. A. BALASHOV, E. A. RESHETOV, and B. I. SAVELEV Geodeziia i Kartografiia, Nov. 1982, p. 27-30. In Russian. refs

The feasibility of using satellite photographs to construct three-dimensional photogrammetric networks with the ultimate aim of mapping remote areas was investigated, with emphasis on the application of analytic phototriangulation. Particular consideration was given to the precision with which the coordinates of points could be measured on space photographs. It is concluded that the use of space photographs for purposes of large-scale mapping requires the solution of a number of technical problems, including the need to increase the precision with which points are identified and coordinates are measured. B.J.

N83-10459*# National Aeronautics and Space Administration. Goddard Space Flight Center, Greenbelt, Md.
SOME FUNDAMENTAL CONCEPTS IN REMOTE SENSING
In its The LANDSAT Tutorial Workbook p 9-38 1982 refs Original contains color imagery. Original photography may be purchased from the EROS Data Center, Sioux Falls, S.D. 57198. ERTS
Avail: NTIS MF A01; SOD HC $55.00 CSCL 05B

The term remote sensing is defined as well as ideas such as class, pattern, feature, pattern recognition, feature extraction, and theme. The electromagnetic spectrum is examined especially those wavelength regions available to remote sensing. Relevant energy and wave propagation laws are discussed and the characteristics of emitted and reflected radiation and their detection are investigated. The identification of classes by their spectral signatures, the multispectral approach, and the principal types of sensors and platforms used in remote sensing are also considered. A.R.H.

N83-10460*# National Aeronautics and Space Administration. Goddard Space Flight Center, Greenbelt, Md.
FAMILIARIZATION WITH LANDSAT IMAGERY
In its The LANDSAT Tutorial Workbook p 39-80 1982 refs Original contains color imagery. Original photography may be purchased from the EROS Data Center, Sioux Falls, S.D. 57198. ERTS
Avail: NTIS MF A01; SOD HC $55.00 CSCL 05B

Learning objectives of the activities provided include: (1) reading the annotation of a LANDSAT image; (2) becoming acquainted with the characteristics of 1:1,000,000 scale transparencies and prints of MSS images; (3) noting the general information visible in LANDSAT photo products; (4) observing changes of appearance of any ground feature or class in the black and white images made from the four MSS bands and the characteristic color of each class in color composites; (5) determining the degree to which a LANDSAT image meets map accuracy standards and can be fitted to map projections; (6) assessing the effects of LANDSAT enlargements and scale changes and of the limitations of satellite resolution relative to aerial photos; (7) observing the influence of time of acquisition (season) on a scene; (8) getting a feel for image quality as dependent on processing and photoreproduction; (9) appreciating the characteristics of the RBV and thermal band imagery obtained from LANDSAT-3; and (10) becoming familiar with certain attributes of adjacent LANDSAT images which permit them to be joined in mosaics and to be viewed in stereo. A.R.H.

N83-10461*# National Aeronautics and Space Administration. Goddard Space Flight Center, Greenbelt, Md.
SOME SPECTRAL AND SPATIAL CHARACTERISTICS OF LANDSAT DATA
In its The LANDSAT Tutorial Workbook p 81-99 1982 refs Original contains color imagery. Original photography may be purchased from the EROS Data Center, Sioux Falls, S.D. 57198. ERTS
Avail: NTIS MF A01; SOD HC $55.00 CSCL 05B

Activities are provided for: (1) developing insight into the way in which the LANDSAT MSS produces multispectral data; (2) promoting understanding of what a 'pixel' means in a LANDSAT image and the implications of the term 'mixed pixel'; (3) explaining the concept of spectral signatures; (4) deriving a simple signature for a class or feature by analysis: of the four band images; (5) understanding the production of false color composites; (6) appreciating the use of color additive techniques; (7) preparing Diazo images; and (8) making quick visual identifications of major land cover types by their characteristic gray tones or colors in LANDSAT images. A.R.H.

N83-10462*# National Aeronautics and Space Administration. Goddard Space Flight Center, Greenbelt, Md.
PHOTOINTERPRETATION OF LANDSAT IMAGES
In its The LANDSAT Tutorial Workbook p 101-143 1982 refs Original contains color imagery. Original photography may be purchased from the EROS Data Center, Sioux Falls, S.D. 57198. ERTS
Avail: NTIS MF A01; SOD HC $55.00 CSCL 05B

Learning objectives include: (1) developing a facility for applying conventional techniques of photointerpretation to small scale (satellite) imager; (2) promoting the ability to locate, identify, and interpret small natural and man made surface features in a LANDSAT image; (3) using supporting imagery, such as aerial and space photography, to conduct specific applications analyses; (4) learning to apply change detection techniques to recognize and explain transient and temporal events in individual or seasonal imagery; (5) producing photointerpretation maps that define major surface units, themes, or classes; (6) classifying or analyzing a scene for specific discipline applications in geology, agriculture, forestry, hyrology, coastal wetlands, and environmental pollution; and (7) evaluating both advantages and shortcomings in relying on the photointerpretive approach (rather than computer based analytical approach) for extracting information from LANDSAT data. A.R.H.

N83-10463*# National Aeronautics and Space Administration. Goddard Space Flight Center, Greenbelt, Md.
COMPUTER PROCESSED LANDSAT DATA
In its The LANDSAT Tutorial Workbook p 145-232 1982 refs Original contains color imagery. Original photography may be purchased from the EROS Data Center, Sioux Falls, S.D. 57198. ERTS
Avail: NTIS MF A01; SOD HC $55.00 CSCL 05B

Background information and exercises are provided to: (1) establish or expand understanding of the concepts, methods, and terminology of computer processing of image producing data; (2) develop insight into the advantages of computer based image processing compared with the photointerpretation approach for processing, classifying, interpreting, and applying remote sensing data; (3) foster a broad perspective on the principal of the main techniques for image enhancement, pattern recognition, and thematic classification; (4) appreciate the pros and cons of batch and interactive modes of image analysis; (5) examine and evaluate some specific computer generated products for subscenes in Pennsylvania and New Jersey; and (6) interrelate these particular examples of output with more theoretical explanations of computer processing strategies and procedures. A.R.H.

N83-10464*# National Aeronautics and Space Administration. Goddard Space Flight Center, Greenbelt, Md.
NEAR SURFACE OBSERVATIONS
In its The LANDSAT Tutorial Workbook p 233-276 1982 refs Original contains imagery. Original photography may be purchased from the EROS Data Center, Sioux Falls, S.D. 57198. ERTS
Avail: NTIS MF A01; SOD HC $55.00 CSCL 05B

Learning objectives include: (1) developing an understanding of the implications of the term 'near surface observations'; (2) associating the appearance of large ground features as seen in satellite imagery with their appearance as seen from the ground; (3) grasping criteria and procedures for selecting training sites on the ground for use in supervised classification; (4) running through an example of training site selection; (5) becoming familiar with several methods of accuracy assessment; (6) becoming aware of the approach and value of making supporting measurements of the spectral and physical properties of materials on the ground and from aircraft; (7) taking note of the different types of instruments used in making specific ground measurements; and (8) appreciating the rationale underlying laboratory and field studies on or near the Earth's surface for the purpose of developing new sensor systems. A.R.H.

N83-10465*# National Aeronautics and Space Administration. Goddard Space Flight Center, Greenbelt, Md.
GEOGRAPHIC INFORMATION SYSTEMS
W. J. CAMPBELL *In its* The LANDSAT Tutorial Workbook p 277-308 1982 refs Original contains color imagery. Original photography may be purchased from the EROS Data Center, Sioux Falls, S.D. 57198. ERTS
Avail: NTIS MF A01; SOD HC $55.00 CSCL 05B

Information and activities are provided to: (1) enhance the ability to distinguish between a Geographic Information System (GIS) and a data management system; (2) develop understanding of spatial data handling by conventional methods versus the automated approach; (3) promote awareness of GIS design and capabilities; (4) foster understanding of the concepts and problems of data base development and management; (5) facilitate recognition of how a computerized GIS can model conditions in the present 'real world' to project conditions in the future; and (6) appreciate the utility of integrating LANDSAT and other remotely sensed data into the GIS. A.R.H.

N83-11391# Rensselaer Polytechnic Inst., Troy, N. Y. Electrical, Computer, and Systems Engineering.
IMAGE PROCESSING TECHNIQUES
L. A. GERHARDT *In* AGARD Image Process. Tech. 5 p May 1982
Avail: NTIS HC A11/MF A01

Image generation, image processing, image transmission, image enhancement, and interpretation are discussed. Author

N83-11400# Deutsche Forschungs- und Versuchsanstalt fuer Luft- und Raumfahrt, Oberpfaffenhofen (West Germany). Inst. Fuer Optoelektronik.
IMAGE PROCESSING OF REMOTELY SENSED PHENOMENA
K. A. ULBRICHT *In* AGARD Image Process. Tech. 18 p May 1982 refs Original document contains color illustrations
Avail: NTIS HC A11/MF A01

A review of application possibilities of digital image processing of remotely sensed phenomena of the Earth is given. Several application examples processed on DIBIAS and representing different disciplines are discussed, showing possibilities of image processing. Among them are geologic, oceanographic, and cartographic examples, as well as applications in the field of atmospheric physics, correlation of SEASAT SAR to a LANDSAT scene, and an evaluation of a commercial compression algorithm. Author

N83-12490*# Lockheed Engineering and Management Services Co., Inc., Houston, Tex.
OPERATION PLAN FOR THE DATA 100/LARS TERMINAL SYSTEM
A. J. BOWEN, JR. Jul. 1980 23 p Sponsored by NASA, USDA, Dept. of Commerce, Dept. of the Interior, and Agency for International Development ERTS
(Contract NAS9-15800; PROJ. AGRISTARS)
(E83-10011; NASA-CR-167754; JSC-16747; NAS 1.26:167754; LEMSCO-15128) Avail: NTIS HC A02/MF A01 CSCL 09B

The Data 100/LARS terminal system provides an interface for processing on the IBM 3031 computer system at Purdue University's Laboratory for Applications of Remote Sensing. The environment in which the system is operated and supported is discussed. The general support responsibilities, procedural mechanisms, and training established for the benefit of the system users are defined. A.R.H.

N83-12498*# Tulsa Univ., Okla. Div. of Mathematical Sciences.
THE AKAIKE INFORMATION CRITERION AND ITS APPLICATION TO MIXTURE PROPORTION ESTIMATION Final Report
R. A. REDNER, G. KITAGAWA, and W. A. COBERLY *In* Texas A and M Univ. Develop. of Advan. Acreage Estimation Methods 48 p Jun. 1982 refs ERTS
(Contract NAS9-14689)
Avail: NTIS HC A12/MF A01 CSCL 05B

The theory and applications of the Akaike information criterion (AIC) Mixture model simulations and the application of the AIC to a large portion of a LANDSAT segment are presented. A.R.H.

N83-12508# Ministere de l'Energie et des Ressources (Quebec).
CONFERENCE ON USING NEXT GENERATION EARTH OBSERVATION SATELLITES: SUMMARY HANDBOOK [COLLOQUE SUR L'UTILISATION DE LA PROCHAINE GENERATION DE SATELLITES D'OBSERVATION DE LA TERRE: MANUEL DE SYNTHESE]
H. AUDET, ed. and K. P. B. THOMSON, ed. (Centre Canadien de Teledetection) 1981 79 p refs In FRENCH and ENGLISH Conf. held in Montreal, 24-25 Mar. 1981
Avail: NTIS HC A05/MF A01

Presentations and discussions of the different techniques needed to process the data to be provided by the high resolution visible sensor on SPOT and the thematic mapper on LANDSAT D are highlighted. Experiments conducted to simulate data from these two instruments are described and results, conclusions, and recommendations from each effort are summarized.
Transl. by A.R.H.

N83-12866*# Lockheed Engineering and Management Services Co., Inc., Houston, Tex.
EARTH OBSERVATIONS DIVISION VERSION OF THE LABORATORY FOR APPLICATIONS OF REMOTE SENSING SYSTEM (EOD-LARSYS) USER GUIDE FOR THE IBM 370/148. VOLUME 1: SYSTEM OVERVIEW
P. J. AUCOIN and M. F. MCKAY, Principal Investigators May 1980 184 p Sponsored by NASA, USDA, Dept. of Commerce, Dept. of the Interior, and Agency for International Development ERTS
(Contract NAS9-15800; PROJ. AGRISTARS)
(E83-10007; NASA-CR-167755; JSC-13821-VOL-1-REV-A; LEMSCO-12653-VOL-1-REV-A; NAS 1.26:167755) Avail: NTIS HC A09/MF A01 CSCL 09B

A system overview is presented for those interested in the EOD-LARSYS as programmed on the Purdue University IBM 370/148 (recently replaced by the IBM 3031) computer. All processors in the system are described and all control cards are summarized. EOD-LARSYS is the JSC version of an integrated batch system for analysis of multispectral scanner imagery data. The system is operational from remote terminals at Johnson Space Center under the virtual machine/conversational monitor system environment. A.R.H.

N83-13518 Bayerische Akademie der Wissenschaften, Munich (West Germany).
PASS POINT DETERMINATION AND GEOMETRICAL PRECISION OF THE RELATIVE RECTIFICATION OF SCANNER DATA Ph.D. Thesis - Karlsruhe Univ., West Germany [PASSPUNKTBESTIMMUNG UND GEOMETRISCHE GENAUIGKEIT BEI DER RELATIVEN ENTZERRUNG VON ABTASTDATEN]
W. J. WIESEL 1981 74 p refs In GERMAN
(SER-C-268; ISBN-3-7696-93205; ISSN-0065-5325) Avail.: Issuing Activity

An iterative method for the relative geometrical rectification of image scanning data, based on pass points, was developed and tested on three data processing systems of an airborne multispectral scanner. The pass points were determined by means of correlation methods. A testing system using the original image data, for the coordinate measuring accuracy obtained by cross correlation, is proposed. The accuracy limits of 0.10 to 0.25 image elements calculated with this testing system, are nearly obtained with the rectification method. Average coordinate errors of 0.15 to 0.27 image elements are obtained on correlation points. These accuracies are sufficient to fit data of different times and/or different sensors into each other. Author (ESA)

N83-13522*# Florida Univ., Gainesville. Inst. of Food and Agricultural Sciences.
USE OF THERMAL INERTIA DETERMINED BY HCMM TO PREDICT NOCTURNAL COLD PRONE AREAS IN FLORIDA Progress Report, 16 Dec. 1981 - 15 Jun. 1982
L. H. ALLEN, JR., Principal Investigator, E. CHEN, J. D. MARTSOLF, and P. H. JONES 15 Jun. 1982 10 p Original contains imagery. Original imagery may be purchased from NASA Goddard Space Flight Center, (code 601), Greenbelt, Md. 20770. Domestic users send orders to 'Attn: National Space Science Data Center'; non-domestic users send orders to 'Attn: World Data Center A for Rockets and Stellites'. HCMM
(Contract NAS5-26453)
(E83-10028; NASA-CR-169501; NAS 1.26:169501) Avail: NTIS HC A02/MF A01 CSCL 08B

A different model is being adapted to handle Florida HCMM data and conditions in an effort to overcome difficulties encountered in extracting data from computer compatible tapes. A.R.H.

N83-13530*# Jet Propulsion Lab., California Inst. of Tech., Pasadena.
GEOLOGIC INTERPRETATION OF HCMM AND AIRCRAFT THERMAL DATA
25 Feb. 1982 5 p Sponsored by NASA HCMM
(E83-10036; NASA-CR-169508) Avail: NTIS HC A02/MF A01 CSCL 05B

Progress on the Heat Capacity Mapping Mission (HCMM) follow-on study is reported. Numerous image products for geologic interpretation of both HCMM and aircraft thermal data were produced. These include, among others, various combinations of the thermal data with LANDSAT and SEASAT data. The combined data sets were displayed using simple color composites, principal component color composites and black and white images, and hue, saturation intensity color composites. Algorithms for incorporating both atmospheric and elevation data simultaneously into the digital processing for creation of quantitatively correct thermal inertia images, are in the final development stage. A field trip to Death Valley was undertaken to field check the aircraft and HCMM data. M.G.

N83-13531*# Environmental Research Inst. of Michigan, Ann Arbor. Radar and Optics Div.
EVALUATION OF ERIM OPTICALLY PROCESSED SEASAT SAR DATA Informal Information Report, Aug. 1981 - Apr. 1982
R. SHUCHMAN, D. R. LYZENGA, Principal Investigators, A. KLOOSTER, JR., and J. MARKS Apr. 1982 45 p refs Original contains imagery. Original imagery may be purchased from the EROS Data Center, Sioux Falls, S.D. 57198 ERTS
(Contract NAS7-100; JPL-956105)
(E83-10037; NASA-CR-169509; NAS 1.26:169509;
ERIM-157800-1-F) Avail: NTIS HC A03/MF A01 CSCL 05B

The results of three studies on the radiometric and geometric properties of optically processed SEASAT SAR imagery are summarized. The accuracy with which the image scale can be predicted based upon a knowledge of the SAR platform and recording system parameters and the processor characteristics was evaluated. The considerations involved in making radiometric measurements from image films, the use of point targets for calibrating the effects of Doppler spectrum shifts on the radiometric calibration of the SAR image data over extended swath lengths was evaluated A.R.H.

N83-13533*# Purdue Univ., Lafayette, Ind. Lab. for Applications of Remote Sensing.
LANDSAT-4 IMAGE DATA QUALITY ANALYSIS Progress Report, 9 Aug. - 9 Nov. 1982
P. E. ANUTA, Principal Investigator Nov. 1982 22 p ERTS
(Contract NAS5-26859)
(E83-10039; NASA-CR-169511; NAS 1.26:169511;
LARS-CR-110982; PR-1) Avail: NTIS HC A02/MF A01 CSCL 05B

Work done on evaluating the geometric and radiometric quality of early LANDSAT-4 sensor data is described. Band to band and channel to channel registration evaluations were carried out using a line correlator. Visual blink comparisons were run on an image display to observe band to band registration over 512 x 512 pixel blocks. The results indicate a .5 pixel line misregistration between the 1.55 to 1.75, 2.08 to 2.35 micrometer bands and the first four bands. Also a four 30M line and column misregistration of the thermal IR band was observed. Radiometric evaluation included mean and variance analysis of individual detectors and principal components analysis. Results indicate that detector bias for all bands is very close or within tolerance. Bright spots were observed in the thermal IR band on an 18 line by 128 pixel grid. No explanation for this was pursued. The general overall quality of the TM was judged to be very high. Author

N83-13707# Instituto de Pesquisas Espaciais, Sao Jose dos Campos (Brazil).
IMAGE ANALYSIS UNIT (UAI-R) FOR METEOROLOGICAL APPLICATIONS [UNIDADE DE ANALISE DE IMAGENS PARA APLICACOES METEOROLOGICAL UAI-R]
Jun. 1982 10 p In PORTUGESE Original contains color illustrations
(INPE-2428-NTE/185) Avail: NTIS HC A02/MF A01

The remote version of the image analysis unit (UAI-R) is described. The UAI acquires and animates images obtained by the GOES satellite which are shown on a black and white or color television screen. The images are transmitted by telephone (1200 bits/sec) in real time from the master unit (UAI-M) which is coupled to the INPE GOES station. Estimated user fees are presented. Meteorological information from the prototype UAI-1 is used in synoptic weather forecasting, precipitation estimation, forecasting and observation of frosts, and observation of ocean currents. J.D.

N83-14573*# Instituto de Pesquisas Espaciais, Sao Jose dos Campos (Brazil).
CNPQ/INPE-LANDSAT SYSTEM REPORT OF ACTIVITIES Report, 1 May 1981 - 30 Sep. 1982
N. D. J. PARADA, Principal Investigator and M. N. BARBOSA Oct. 1982 41 p Presented at the LANDSAT Tech. Working Group Meeting, LANDSAT Ground Station Operations Working Group Meeting, and Data Distribution Working Group Meeting, Greenbelt, Md., 20-28 Oct. 1982 Sponsored by NASA Original contains color imagery. Original photography may be purchased from the EROS Data Center, Sioux Falls, S.D. 57198 ERTS
(E83-10064; NASA-CR-169575; NAS 1.26:169575;
INPE-2554-PRE-208) Avail: NTIS HC A03/MF A01 CSCL 14B

The status of the Brazilian LANDSAT facilities and the results achieved are presented. In addition, a LANDSAT product sales/distribution analysis is provided. Data recording and processing capabilities and planned products are addressed. M.G.

N83-14584*# Instituto de Pesquisas Espaciais, Sao Jose dos Campos (Brazil).
INPE LANDSAT-D THEMATIC MAPPER COMPUTER COMPATIBLE TAPE FORMAT SPECIFICATION
N. D. J. PARADA, Principal Investigator and R. C. M. DESOUZA 4 Oct. 1982 68 p Presented at LANDSAT Tech. Working Group Meeting, Greenbelt, Md., 20-22 Oct. 1982 Sponsored by NASA ERTS
(E83-10075; NASA-CR-169586; NAS 1.26:169586;
INPE-2553-PRE/207) Avail: NTIS HC A04/MF A01 CSCL 09B

The format of the computer compatible tapes (CCT) which contain Thematic Mapper (TM) imagery data acquired from the LANDSAT D and D Prime satellites by the INSTITUTO DE PERSQUISAS ESPACIALS (CNPq-INPE/BRAZIL) is defined. Author

N83-14595*# Purdue Univ., Lafayette, Ind.
CONTEXTUAL CLASSIFICATION OF MULTISPECTRAL IMAGE DATA: AN UNBIASED ESTIMATOR FOR THE CONTEXT DISTRIBUTION
J. C. TILTON, P. H. SWAIN, Principal Investigators, and S. B. VARDEMAN (Iowa State Univ. of Science and Technology) 1981 9 p refs Presented at the Machine Process. of Remotely Sensed Data Symp., 1981 Original contains imagery. Original photography may be purchased from the EROS Data Center, Sioux Falls, S.D. 57198 ERTS
(Contract NAS9-15466; NSF MCS-78-04366)
(E83-10087; NASA-CR-167633; NAS 1.26:167633;
LARS-TR-070381) Avail: NTIS HC A02/MF A01 CSCL 09B

A key input to a statistical classification algorithm, which exploits the tendency of certain ground cover classes to occur more frequently in some spatial context than in others, is a statistical characterization of the context: the context distribution. An unbiased estimator of the context distribution is discussed which, besides having the advantage of statistical unbiasedness, has the additional advantage over other estimation techniques of being amenable to an adaptive implementation in which the context distribution estimate varies according to local contextual information. Results from applying the unbiased estimator to the contextual classification of three real LANDSAT data sets are presented and contrasted with results from non-contextual classifications and from contextual classifications utilizing other context distribution estimation techniques. A.R.H.

N83-14617# Zentralstelle fuer Geo-Photogrammetrie und Fernerkundung, Munich (West Germany).
SOME ASPECTS OF THE PRESENTATION OF REMOTE SENSING DATA
R. HAYDN *In* ESA Satellite Remote Sensing for Developing Countries p 77-80 Jun. 1982 refs
Avail: NTIS HC A11/MF A01

Problems inherent in remote sensing data transfer procedures, and processing techniques which provide improved and

standardized images are discussed. Commonly available image products do not demonstrate the capabilities and applicability of multispectral satellite remote sensing techniques. They do not motivate potential users to consider remote sensing as anything other than a source of synoptic representations. Application optimized images can be obtained from intensity, hue, saturation systems and quasi-stereo effects. These data present subtle surface characteristics in a perceivable and understandable way. The processing techniques are suited for the definition of standardized enhancement schemes. Author (ESA)

N83-14618# Graz Univ. (Austria). Inst. for Image Processing and Computer Graphics.
THE APPLICABILITY OF SATELLITE REMOTE SENSING TO SMALL AND MEDIUM SCALE MAPPING
F. W. LEBERL *In* ESA Satellite Remote Sensing for Developing Countries p 81-85 Jun. 1982 refs
Avail: NTIS HC A11/MF A01

The usefulness of satellite remote sensing images to the generation and updating of general purpose maps at scales 1: 50,000 to 1:100,000 is considered. It is argued that the needs of conventional medium and small scale mapping will not be satisfied by space imagery, unless attitudes and value systems in mapping change, or space imagery at geometric resolution of 3 m or better is available. Author (ESA)

N83-14635# Canada Centre for Remote Sensing, Toronto (Ontario).
A PRACTICAL AUTOMATED MAPPING SYSTEM
S. PALA *In* ESA Satellite Remote Sensing for Developing Countries p 217-218 Jun. 1982
Avail: NTIS HC A11/MF A01

A system for the computerized production of maps directly from the digital analysis of LANDSAT data is described. The system is based on the Applicon Color Plotter, a computerized printer which plots lines, curves and polygons at any selected scale on ordinary paper measuring 86 cm by 56 cm. By using three ink jets, each applying a single basic color, the plotter prints map features in up to 256 different shades of color. The system uses a PDP 11/34 computer. It takes 2 hr to process the digital analysis results onto a tape in a format acceptable to the Applicon printer. Printing of the map can then be completed within 15 min.
Author (ESA)

N83-14637# Oslo Univ. (Norway). Dept. of Geography.
DIGITAL ANALYSIS OF LANDSAT SATELLITE IMAGERY IN TURKANA, NORTHERN KENYA
K. O. FREDHJEM *In* ESA Satellite Remote Sensing for Developing Countries p 225-226 Jun. 1982 refs
Avail: NTIS HC A11/MF A01

Digital LANDSAT scanner data was enhanced and compared with color infrared air photos. Results show that false color composite (FCC) images made from ratio or principal component bands add little new information to the information contained in the standard FCC. Best is the FCC: PC2=R, MSS5=G, and PC1=B. The FCC: MSS4/5=R, MSS6=G, and MSS5/6=P is also good. It is easier to obtain good results from the supervised than from the unsupervised classification technique.
Author (ESA)

N83-14830*# National Science Foundation, Washington, D.C. Div. of Atmospheric Sciences.
KEY SCIENTIFIC QUESTIONS AND THE ROLE OF SATELLITES
E. W. BIERLY *In* NASA. Marshall Space Flight Center The Conception, Growth, Accomplishments and Future of Meteorol. Satellites p 48-71 Nov. 1982
Avail: NTIS HC A06/MF A01 CSCL 04B

Some of the research opportunities that are available from geostationary satellite data, especially from MONEX during the Global Weather Experiment are described. In addition, the International Cloud Climatology Program is described and the use of satellite imagery in studying mesoscale convection complexes is discussed. Finally, information derived from satellite data on ocean winds is examined. M.G.

N83-15745*# Florida Univ., Gainesville. Inst. of Food and Agricultural Sciences.
USE OF THERMAL INERTIA DETERMINED BY HCMM TO PREDICT NOCTURNAL COLD PRONE AREAS IN FLORIDA Progress Report, 16 Jun. - 15 Nov. 1982
L. H. ALLEN, JR., Principal Investigator, E. CHEN, J. D. MARTSOLF, P. H. JONES, T. N. CARLSON, and G. DELVALLE 15 Nov. 1982 7 p refs ERTS
(Contract NAS5-26453)
(E83-10102; NASA-CR-169678; NAS 1.26:169678) Avail: NTIS HC A02/MF A01 CSCL 04B

Registered data sets were used to develop qualititative temperature and delta T maps of a band across north Florida and across south Florida for use with Carlson's boundary layer energy model balance model. Thermal inertia and moisture availability computations for north Florida are being used to investigate model sensitivity and to evaluate input parameters. Temperature differences of day-night HCMM overpasses clearly differentiate wetlands and uplands areas. A.R.H.

N83-15746*# Agricultural Research Service, Weslaco, Tex.
METHODS OF EDITING CLOUD AND ATMOSPHERIC LAYER AFFECTED PIXELS FROM SATELLITE DATA Final Report, 5 Dec. 1980 - 5 Jun. 1982
P. R. NIXON, Principal Investigator, C. L. WIEGAND, A. J. RICHARDSON, and M. P. JOHNSON Nov. 1982 48 p refs Sponsored by NASA Original contains color imagery. Original imagery may be purchased from NASA Goddard Space Flight Center, (code 601), Greenbelt, Md. 20770. Domestic users send orders to 'Attn: National Space Science Data Center'; non-domestic users send orders to 'Attn: World Data Center A for Rockets and Satellites'. HCMM
(E83-10103; NASA-CR-169679; NAS 1.26:169679) Avail: NTIS HC A03/MF A01 CSCL 05B

Practical methods of computer screening cloud-contaminated pixels from data of various satellite systems are proposed. Examples are given of the location of clouds and representative landscape features in HCMM spectral space of reflectance (VIS) vs emission (IR). Methods of screening out cloud affected HCMM are discussed. The character of subvisible absorbing-emitting atmospheric layers (subvisible cirrus or SCi) in HCMM data is considered and radiosonde soundings are examined in relation to the presence of SCi. The statistical characteristics of multispectral meteorological satellite data in clear and SCi affected areas are discussed. Examples in TIROS-N and NOAA-7 data from several states and Mexico are presented. The VIS-IR cluster screening method for removing clouds is applied to a 262, 144 pixel HCMM scene from south Texas and northeast Mexico. The SCi that remain after cluster screening are sited out by applying a statistically determined IR limit. A.R.H.

N83-15759*# Texas A&M Univ., College Station. Dept. of Mathematics.
PROCEEDINGS OF THE NASA WORKSHOP ON SURFACE FITTING
L. F. GUSEMAN, JR., Principal Investigator 1982 217 p refs Workshop held at College Station, Tex., 17-19 May 1982 ERTS
(Contract NAS9-16447)
(E83-10117; NASA-CR-167779; NAS 1.26:167779) Avail: NTIS HC A10/MF A01 CSCL 05B

Surface fitting techniques and their utilization are addressed. Surface representation, approximation, and interpolation are discussed. Along with statistical estimation problems associated with surface fitting.

N83-15761*# Texas A&M Univ., College Station. Dept. of Mathematics.
FITTING SURFACES TO SCATTERED DATA
L. L. SCHUMAKER *In its* Proc. of the NASA Workshop on Surface Fitting p 27-94 1982 refs ERTS
Avail: NTIS HC A10/MF A01 CSCL 05B

A variety of numerical methods for fitting a function to data given at a set of points scattered throughout a domain in the plane are surveyed. Four classes of methods are discussed: (1) global interpolation; (2) local interpolation; (3) global approximation; and (4) local approximation. Also, two-stage methods and contouring are discussed. The surfaces constructed include polynomials, spline functions, and rational functions, among others. M.G.

N83-15762*# Jet Propulsion Lab., California Inst. of Tech., Pasadena.
C-1 SURFACE INTERPOLATION FOR SCATTERED DATA ON A SPHERE
C. L. LAWSON *In* Texas A and M Univ. Proc. of the NASA Workshop on Surface Fitting p 95-119 1982 refs ERTS
Avail: NTIS HC A10/MF A01 CSCL 05B

An algorithm is described for constructing a smooth computable function, f, defined over the surface of a sphere and interpolating a set of n data values, u sub i, associated with n locations, P sub i, on the surface of the sphere. The interpolation function, f, will be continuous and have continuous first partial derivatives. The locations, p sub i, are not required to lie on any type of regular grid. M.G.

N83-15764*# Iowa State Univ. of Science and Technology, Ames. Engineering Research Inst.
SURFACE FITTING WITH BIHARMONIC AND HARMONIC MODELS
R. L. HARDY *In* Texas A and M Univ. Proc. of the NASA Workshop on Surface Fitting p 135-146 1982 refs ERTS
Avail: NTIS HC A10/MF A01 CSCL 05B

The physical and geometric interpretation of a surface fitting technique, multiquadric equations (MQ), is discussed. The relation of this method and its reciprocal form to biharmonic and harmonic techniques respectively, is pointed out. In both forms the solutions may be viewed as being numerical approximations of an integral equation in which an unknown density function is the physical source for disturbing potential (reciprocal-MQ) or elastic displacement (MQ). M.G.

N83-15765*# California Polytechnic State Univ., San Luis Obispo. Dept. of Computer Science.
BSPLASH: A THREE-STAGE SURFACE INTERPOLANT TO SCATTERED DATA
T. A. FOLEY *In* Texas A and M Univ. Proc. of the NASA Workshop on Surface Fitting p 147-178 1982 refs ERTS
Avail: NTIS HC A10/MF A01 CSCL 05B

Given N distinct points (X sub i, Y sub i) and N real numbers Z sub i, BSPLASH constructs a function G (x, y) that satisfies G (x sub i, y sub i) = Z sub i for i = 1,..., N. This C(2) interpolant consists of a bicubic spline approximation and Shepard's bivariate interpolant. M.G.

N83-15766*# Texas A&M Univ., College Station. Dept. of Mathematics.
PROCEEDINGS OF THE NASA WORKSHOP ON IMAGE ANALYSIS
L. F. GUSEMAN, JR., Principal Investigator 1982 149 p refs Workshop held in College Station, Tex., 28-30 Apr. 1982 Original contains imagery. Original photography may be purchased from the EROS Data Center, Sioux Falls, S.D. 57198 ERTS
(Contract NAS9-16447)
(E83-10118; NASA-CR-167778; NAS 1.26:167778) Avail: NTIS HC A07/MF A01 CSCL 05B

Three major topics of image analysis are addressed: segmentation, shape and texture analysis, and structural analysis.

N83-15767*# Virginia Polytechnic Inst. and State Univ., Blacksburg. Dept. of Computer Science.
IMAGE SEGMENTATION SURVEY
R. M. HARALICK *In* Texas A and M Univ. Proc. of the NASA Workshop on Image Anal. p 7-16 1982 refs ERTS
Avail: NTIS HC A07/MF A01 CSCL 05B

The methodologies and capabilities of image segmentation techniques are reviewed. Single linkage schemes, hybrid linkage schemes, centroid linkage schemes, histogram mode seeking, spatial clustering, and split and merge schemes are addressed. M.G.

N83-15768*# Maryland Univ., College Park. Computer Vision Lab.
COOPERATIVE PROCESSES IN IMAGE SEGMENTATION
L. S. DAVIS *In* Texas A and M Univ. Proc. of the NASA Workshop on Image Anal. p 17-50 1982 refs Original contains imagery. Original photography may be purchased from the EROS Data Center, Sioux Falls, S.D. 57198 ERTS
Avail: NTIS HC A07/MF A01 CSCL 05B

Research into the role of cooperative, or relaxation, processes in image segmentation is surveyed. Cooperative processes can be employed at several levels of the segmentation process as a preprocessing enhancement step, during supervised or unsupervised pixel classification and, finally, for the interpretation of image segments based on segment properties and relations. M.G.

N83-15769*# Maryland Univ., College Park. Computer Science Center.
SHAPE AND TEXTURE
A. ROSENFELD *In* Texas A and M Univ. Proc. of the NASA Workshop on Image Anal. p 57-84 1982 refs ERTS
Avail: NTIS HC A07/MF A01 CSCL 05B

Methods used to measure the geometrical properties of regions in a segmented image are discussed including the use of centroids, moments, and principle axes. In addition, statistical picture properties, particularly those which describe visual texture, are discussed. Gray level statistics, local property statistics, and autocorrelation and power spectrum are addressed. M.G.

N83-15770*# Florida Univ., Gainesville. Center for Information Research.
AUTOMATIC PHOTOINTERPRETATION VIA TEXTURE AND MORPHOLOGY ANALYSIS
J. T. TOU *In* Texas A and M Univ. Proc. of the NASA Workshop on Image Anal. p 87-88 1982 ERTS
Avail: NTIS HC A07/MF A01 CSCL 05B

Computer-based techniques for automatic photointerpretation based upon information derived from texture and morphology analysis of images are discussed. By automatic photointerpretation, is meant the determination of semantic descriptions of the content of the images by computer. To perform semantic analysis of morphology, a heirarchical structure of knowledge representation was developed. The simplest elements in a morphology are strokes, which are used to form alphabets. The alphabets are the elements for generating words, which are used to describe the function or property of an object or a region. The words are the elements for constructing sentences, which are used for semantic description of the content of the image. Photointerpretation based upon morphology is then augmented by textural information. Textural analysis is performed using a pixel-vector approach. M.G.

N83-15771*# Honeywell Systems and Research Center, Minneapolis, Minn.
FLIR TARGET SCREENING
R. AGGARWAL *In* Texas A and M Univ. Proc. of the NASA Workshop on Image Anal. p 89 1982 ERTS
Avail: NTIS HC A07/MF A01 CSCL 20F

Methods for the segmentation and recognition of individual targets sensed with forward looking infrared detectors are discussed. Particular attention is given to an adaptive multi-scenario target screener. M.G.

N83-15772*# Virginia Polytechnic Inst. and State Univ., Blacksburg. Dept. of Computer Science.
STRUCTURAL ANALYSIS TECHNIQES FOR REMOTE SENSING
L. G. SHAPIRO *In* Texas A and M Univ. Proc. of the NASA Workshop on Image Anal. p 91-132 1982 refs ERTS
Avail: NTIS HC A07/MF A01 CSCL 05B

The structural analysis of remotely sensed imagery is defined and basic techniques for implementing the process are described. Structural analysis uses knowledge of the properties of an entity, its parts and their relationships, and the relationships in which it participates at a higher level to locate and recognize objects in a visual scene. The representation of structural knowledge, the development of algorithms for using the knowledge to help analyze an image, and techniques for storage and retrieval of relational models are addressed. M.G.

N83-15773*# Illinois Univ., Urbana. Coordinated Science Lab.
DETERMINING 3-D MOTION AND STRUCTURE FROM IMAGE SEQUENCES
T. S. HUANG *In* Texas A and M Univ. Proc. of the NASA Workshop on Image Anal. p 134-149 1982 refs ERTS
Avail: NTIS HC A07/MF A01 CSCL 05B

A method of determining three-dimensional motion and structure from two image frames is presented. The method requires eight point correspondences between the two frames, from which motion and structure parameters are determined by solving a set of eight linear equations and a singular value decomposition of a 3x3 matrix. It is shown that the solution thus obtained is unique. M.G.

N83-15774*# Texas A&M Univ., College Station. Dept. of Mathematics.
PROCEEDINGS OF THE NASA WORKSHOP ON DENSITY ESTIMATION AND FUNCTION SMOOTHING
L. F. GUSEMAN, JR., Principal Investigator 1982 491 p refs Workshop held at College Station, Tex., 11-13 Mar. 1982 ERTS
(Contract NAS9-16447)
(E83-10119; NASA-CR-167780; NAS 1.26:167780) Avail: NTIS HC A21/MF A01 CSCL 05B

Statistical model identification techniques being developed to provide workable solutions to problems in density estimation and function smoothing are examined.

N83-15775*# McGill Univ., Montreal (Quebec). School of Computer Science.
TOPICS IN GLOBAL CONVERGENCE OF DENSITY ESTIMATES
L. DEVROYE *In* Texas A and M Univ. Proc. of the NASA Workshop on Density Estimation and Function Smoothing p 9-19 1982 refs Sponsored by Natural Sciences and Engineering Research Council ERTS
Avail: NTIS HC A21/MF A01 CSCL 05B

The problem of estimating a density f on R sup d from a sample Xz(1),...,X(n) of independent identically distributed random vectors is critically examined, and some recent results in the field are reviewed. The following statements are qualified: (1) For any sequence of density estimates f(n), any arbitrary slow rate of convergence to 0 is possible for E(integral/f(n)-fl); (2) In theoretical comparisons of density estimates, integral/f(n)-f/ should be used and not integral/f(n)-f/sup p, p 1; and (3) For most reasonable nonparametric density estimates, either there is convergence of integral/f(n)-f/ (and then the convergence is in the strongest possible sense for all f), or there is no convergence (even in the weakest possible sense for a single f). There is no intermediate situation. Author

N83-15776*# Brown Univ., Providence, R. I. Div. of Applied Mathematics.
CROSS-VALIDATION FOR DENSITIES AND REGRESSIONS
S. GEMAN *In* Texas A and M Univ. Proc. of the NASA Workshop on Density Estimation and Function Smoothing p 20-31 1982 refs ERTS
(Contract DAAG29-80-K-0006; AF-AFOSR-3514-78)
Avail: NTIS HC A21/MF A01 CSCL 05B

Virtually all nonparametric (infinite dimensional) problems require the choice of a smoothing parameter. It is natural to attempt to use the data to guide the choice of this parameter. The most widely applicable data driven technique is cross validation. The method of cross validation is introduced and results are presented which establish consistency for certain cross validated density estimators and consistency as well as asymptotic normality for rigid regression. A.R.H.

N83-15777*# Brown Univ., Providence, R. I. Div. of Applied Mathematics.
CHARACTERIZATION OF A MAXIMUM-LIKELIHOOD NONPARAMETRIC DENSITY ESTIMATOR OF KERNEL TYPE
S. GEMAN and D. E. MCCLURE *In* Texas A and M Univ. Proc. of the NASA Workshop on density Estimation and Function Smoothing p 38-47 1982 refs ERTS
(Contract DAAG-80-K-0006; AF-AFOSR-3514-78)
Avail: NTIS HC A21/MF A01 CSCL 05B

Kernel type density estimators calculated by the method of sieves. Proofs are presented for the characterization theorem: Let x(1), x(2),...x(n) be a random sample from a population with density f(0). Let sigma 0 and consider estimators f of f(0) defined by (1). A.R.H.

N83-15778*# Wisconsin Univ., Madison. Dept. of Statistics.
REMOTE SENSING OF TEMPERATURE PROFILES IN THE ATMOSPHERE
F. OSULLIVAN *In* Texas A and M Univ. Proc. of the NASA Workshop on Density Estimation and Function Smoothing p 48-59 1982 refs ERTS
(Contract DAAG29-80-K-0042)
Avail: NTIS HC A21/MF A01 CSCL 04B

Methods of regularized and generalized cross validation can be used to estimate the atmosphere's temperature, moisture, and wind structure from a finite number m noisy measurements by meteorological satellites on the intensity of upwelling radiation in selected channel frequencies. The inversion of the equation of radiative transfer is discussed for data obtained by TIROS N satellite. A.R.H.

N83-15791*# EROS Data Center, Sioux Falls, S. Dak.
LANDSAT 4 INVESTIGATIONS OF THEMATIC MAPPER AND MULTISPECTRAL SCANNER APPLICATIONS Quarterly Report
D. T. LAUER, Principal Investigator 30 Dec. 1982 3 p Sponsored by NASA ERTS
(E83-10121; NASA-CR-169724; NAS 1.26:169724) Avail: NTIS HC A02/MF A01 CSCL 05B

Initial data screening, data handling and program testing were completed on the four-band Detroit scene and the seven-band northeast Arkansas scene. Data were received in early December for one primary eastern test site (Washington, D.C.) and one secondary eastern test site (Allegheny National Forest). A comprehensive digital data base was built for a portion of the Black Hills test site and is composed of historic LANDSAT MSS data; elevation, slope, and aspect data; land cover data; geologic data; thematic mapper simulator data; and digitized high altitude aircraft data. The thematic mapper and multispectral scanner data of the Washington area were resampled at 25 and 50 meters respectively, with map projection to UTM grid. A.R.H.

N83-15792*# EROS Data Center, Sioux Falls, S. Dak.
LANDSAT 3 RETURN BEAM VIDICON RESPONSE ARTIFACTS: A REPORT ON RBV PHOTOGRAPHIC PRODUCT CHARACTERISTICS AND QUALITY CODING SYSTEM
B. P. CLARK Aug. 1981 14 p Prepared in cooperation with Computer Sciences-Technicolor Associates, Greenbelt, Md. Original contains imagery. Original photography may be purchased from the EROS Data Center, Sioux Falls, S.D. 57198 ERTS
(E83-10122; NASA-CR-169725; NAS 1.26:169725) Avail: NTIS HC A02/MF A01 CSCL 05B

Analysis of large volumes of LANDSAT 3 RBV digital data that were converted to photographic form led to the firm identification of several visible artifacts (objects or structures not normally present, but producted by an external agency or action) in the imagery. These artifacts were identified, categorized, and traced directly to specific sensor response characteristics. None of these artifacts is easily removed and all cases remain under active study of possible future enhancement. The seven generic categories of sensor response artifacts identified to date include: (1) shading and stairsteps; (2) corners out of focus; (3) missing reseaus; (4) reseau distortion and data distortion; (5) black vertical line; (6) grain effect; and (7) faceplate contamination. An additional category under study, but not yet determined to be caused by sensor response, is a geometric anomaly. Examples of affected imagery are presented to assist in distinguishing between image content and innate defects caused by the sensor system. A.R.H.

N83-15794*# Environmental Systems Research Inst., Redlands, Calif.
CIRSS VERTICAL DATA INTEGRATION, SAN BERNARDINO COUNTY STUDY PHASES 1-A, 1-B Annual Report
J. CHRISTENSON and R. MICHEL, Principal Investigators Aug. 1981 251 p Original contains imagery. Original photography may be purchased from the EROS Data Center, Sioux Falls, S.D. 57198 ERTS
(Contract NAS2-10741)
(E83-10124; NASA-CR-166355; NAS 1.26:166355) Avail: NTIS HC A12/MF A01 CSCL 05B

User needs, data types, data automation, and preliminary applications are described for an effort to assemble a single data base for San Bernardino County from data bases which exist at several administrative levels. Each of the data bases used was registered and converted to a grid-based data file at a resolution of 4 acres and used to create a multivariable data base for the entire study area. To this data base were added classified LANDSAT data from 1976 and 1979. The resulting data base thus integrated in a uniform format all of the separately automated data within the study area. Several possible interactions between existing geocoded data bases and LANDSAT data were tested. The use of LANDSAT to update existing data base is to be tested. A.R.H.

N83-15796*# Environmental Systems Research Inst., Redlands, Calif.
CIRSS VERTICAL DATA INTEGRATION, SAN BERNARDINO STUDY
W. HODSON, J. CHRISTENSON, and R. MICHEL, Principal Investigators Jun. 1982 317 p refs Original contains imagery. Original photography may be purchased from the EROS Data Center, Sioux Falls, S.D. 57198 ERTS
(Contract NAS2-10741)
(E83-10127; NASA-CR-166373; NAS 1.26:166373) Avail: NTIS HC A14/MF A01 CSCL 05B

The creation and use of a vertically integrated data base, including LANDSAT data, for local planning purposes in a portion of San Bernardino County, California are described. The project illustrates that a vertically integrated approach can benefit local users, can be used to identify and rectify discrepancies in various data sources, and that the LANDSAT component can be effectively used to identify change, perform initial capability/suitability modeling, update existing data, and refine existing data in a geographic information system. Local analyses were developed which produced data of value to planners in the San Bernardino County Planning Department and the San Bernardino National Forest staff. Author

08

INSTRUMENTATION AND SENSORS

Includes data acquisition and camera systems and remote sensors.

A83-10098
AN EVALUATION OF FOUR THERMAL MODELS USED IN THERMAL INERTIA ANALYSIS
J. K. DODD and E. H. CONROW (Aerospace Corp., Los Angeles, CA) In: International Geoscience and Remote Sensing Symposium, Washington, DC, June 8-10, 1981, Digest. Volume 2. New York, Institute of Electrical and Electronics Engineers, 1981, p. 1172-1181. refs

The conversion of remotely measured surface temperature into mappings of surface physical parameters requires the use of a well-constituted thermal model of the energy balance at the earth-atmosphere interface, in order to predict surface temperature across the area of interest. Four well-known models are examined: The Watson (1975) Fourier series model, the Pratt, Ellyett and Price (1979) Fourier series model, the Kahle (1977) thermal model, and the Carlson Boland and Dodd (1978) model. Although each of these begins with the surface energy budget equation, the physical and mathematical treatment of the component fluxes result in models radically different in their structure, accuracy, and applicability to particular remote sensing surveys. The design of each model is compared and the tradeoff between cost of execution and physical sophistication is discussed. All four models are used to simulate surface temperature for two test cases for which accurate surface truth data is available for comparison. Mean temperature errors are computed, and these errors are converted to errors in apparent thermal inertia. (Author)

A83-10715
AN AUTOMATED MAPPING SATELLITE SYSTEM /MAPSAT/
A. P. COLVOCORESSES (U.S. Geological Survey, Reston, VA) Photogrammetric Engineering and Remote Sensing, vol. 48, Oct. 1982, p. 1585-1591. refs

The fact that a remote sensing satellite orbits the earth with very high stability as long as no local perturbing forces are involved, and the existence of solid state linear array sensors having no moving parts and therefore exerting no perturbing forces on the satellite, are invoked in the proposal of a satellite imaging system designated 'Mapsat'. This system, which incorporates digital data from highly stabilized stereo linear arrays amenable to simplified processing that produces both planimetric imagery and elevation data, is expected to yield automated mapping in near real time. Image maps as large as 1:50,000 scale, with contours as close as a 20-m interval, may be produced from Mapsat data. O.C.

A83-10716
GEOMETRY OF A MAPPING SATELLITE
J. P. SNYDER (U.S. Geological Survey, Reston, VA) Photogrammetric Engineering and Remote Sensing, vol. 48, Oct. 1982, p. 1593-1602. refs

The proposed mapping satellite Mapsat is to consist of fixed fore, vertical, and aft linear detector arrays, any two of which may be used simultaneously to obtain digital images for one-dimensional stereo correlation. The satellite attitude may be varied according to Fourier series to enable a given detector on one array to follow closely the groundtrack sensed by the corresponding detector on another array throughout the orbit. These tracking errors are negligible for a satellite stable within anticipated ranges. The required computations have been programmed in FORTRAN IV. (Author)

A83-10718
SELECTION OF THE OPTIMUM SPECTRAL BANDS FOR THE SPOT SATELLITE
G. BEGNI (Centre National d'Etudes Spatiales, Toulouse, France) Photogrammetric Engineering and Remote Sensing, vol. 48, Oct. 1982, p. 1613-1620. refs

The choice of the locations and widths of the multispectral and panchromatic bands of the SPOT satellite have been optimized by taking into account both the spectral signature of ground objects and modifications introduced by the atmosphere. The spectral band B3 response has been separated from the water vapor absorption bands, and the width of the panchromatic band, which was initially 0.5-0.8 microns, has been reduced. Attention is given to the ways in which system characteristics influence the measurement of spectral signatures formed by the three optimized bands, as well as to the method of choosing the width of the panchromatic band, which involved a study of contrast over thermatically characterized objects. O.C.

A83-11239
KA-BAND PASSIVE/ACTIVE AIRBORNE RADAR
F. J. PORADISH (Texas Instruments, Inc., Dallas, TX) In: NAECON 1982; Proceedings of the National Aerospace and Electronics Conference, Dayton, OH, May 18-20, 1982. Volume 3. New York, Institute of Electrical and Electronics Engineers, Inc., 1982, p. 1262-1269. Research supported by Texas Instruments, Inc. refs

A multimode Ka-band radiometric imaging system is discussed. The basic operating principles of a conventional imaging radiometer are reviewed and two methods of image enhancement are presented for a typical battlefield scenario. The first enhancement method utilizes a low power bistatic illuminator in conjunction with a conventional radiometer. A passive image is subtracted from a coincident illuminated image to provide better contrast and improved detection of metallic targets. The second enhancement method incorporates an inverse filter algorithm to yield better than real beam resolution in high contrast images. A two dimensional spatial high pass filter is used to counteract the low pass filter effect of the antenna beam. A conceptual multi-mode imaging system is presented along with performance calculations for a typical airborne imaging scenario. A 36 GHz ground based radiometric test bed was developed to demonstrate the passive and illuminated modes. The system hardware and performance parameters are discussed and images from several scenarios are presented. (Author)

A83-11867
THE GDTA - REMOTE SENSING AT THE SERVICE OF USERS [LE GDTA - LA TELEDETECTION AU SERVICE DES UTILISATEURS]
G. GUEPET and B. ROND (Groupement pour le Developpement de la Teledetection Aerospatiale, Toulouse, France) Laboratoires des Ponts et Chausees, Bulletin de Liaison, vol. 110, Nov.-Dec. 1980, p. 80-82. In French.

The historical background behind the establishment of the GDTA (Groupement pour le Developpement de la Teledetection Aerospatiale) is briefly reviewed, and the objectives and activities of the GDTA are discussed. The relationship between the GDTA and Earthnet is considered, with attention given to the relationship between the GDTA and users, and prospects of the SPOT program. B.J.

A83-12605* Utah State Univ., Logan.
SPECTROSCOPIC IMAGING OF THE THERMOSPHERE FROM THE SPACE SHUTTLE
M. R. TORR, R. W. BASEDOW, and D. G. TORR (Utah State University of Agriculture and Applied Science, Logan, UT) Applied Optics, vol. 21, Nov. 15, 1982, p. 4130-4145. refs
(Contract NAS8-33992)

The design features, performance characteristics, and intended missions for the Imaging Spectrometric Observatory scheduled to fly on the first Spacelab Shuttle mission in 1983 are described. The instrument comprises an array of five imaging spectrometers covering the spectral range 300-1200 A. The spectrometers operate simultaneously, using CCDs as collector elements. Resolution on the first flight will be limited to 3 A, with coverage to containing the dynamic range from nocturnal signals to the bright earth. A minicomputer in the Spacelab will permit crewmember interaction with the measurements, while data will be telemetered in real-time to a ground station. Initial mission objectives include observations of dayglow, nightglow, and twilightglow over the full wavelength range capability. M.S.K.

A83-12669
ELECTRO-OPTICAL INSTRUMENTATION FOR RESOURCES EVALUATION; PROCEEDINGS OF THE MEETING, WASHINGTON, DC, APRIL 21, 22, 1981
F. J. DOYLE, (ED.) (U.S. Geological Survey, Reston, VA) Meeting sponsored by the SPIE - The International Society for Optical Engineering. Bellingham, WA, SPIE - The International Society for Optical Engineering (SPIE Proceedings. Volume 278), 1981. 175 p.
MEMBERS, $34.; NONMEMBERS, $40

Topics discussed include the monitoring of the eruption of Mount St. Helens, satellite systems for remote sensing, the ground processing of remote sensor data, and mensuration and interpretation equipment. Papers are presented on Landsat observations of Mount St. Helens, solid-state sensors for topographic mapping, a synthetic aperture radar coordinate processing system, and a computer-assisted photointerpretation system. Attention is also given to image enhancement through film recorder response contouring, future ground processing systems, planetary exploration sensor systems, and lidar measurements of Mount St. Helens effluents. C.R.

A83-12676* Jet Propulsion Lab., California Inst. of Tech., Pasadena.
EARTH RESOURCES OBSERVATION WITH THE SHUTTLE IMAGING RADAR
C. ELACHI (California Institute of Technology, Jet Propulsion Laboratory, Pasadena, CA) In: Electro-optical instrumentation for resources evaluation; Proceedings of the Meeting, Washington, DC, April 21, 22, 1981. Bellingham, WA, SPIE - The International Society for Optical Engineering, 1981, p. 73-78. refs
(Contract NAS7-100)

To fully understand the radar signature of different surface features and covers, observations must be made in a variety of sensor parameters (that is, frequency, polarization, and incidence angle). This makes it possible to choose those sensor parameters that will provide the greatest amount of information about the surface. The Shuttle Imaging Radar (SIR) will be able to obtain surface images at two frequencies (L-band and C-band), at multiple polarizations, and at all incidence angles from near vertical to near grazing. The SIR will operate in the synthetic aperture imaging mode and provide digital images of the surfaces with a resolution of approximately 20 m. As part of the SIR flights, a number of planned large-scale experiments will be carried out in the fields of geologic mapping, vegetation classification, land cover mapping, surface moisture measurements, and ocean surface observation.

A83-13347* National Aeronautics and Space Administration, Washington, D. C.
USE OF THE SPACE SHUTTLE FOR REMOTE SENSING RESEARCH - RECENT RESULTS AND FUTURE PROSPECTS
M. SETTLE and J. V. TARANIK (NASA, Office of Space Science and Applications, Washington, DC) Science, vol. 218, Dec. 3, 1982, p. 993-995.
(Contract NAGW-376)

The successful November 1981 test flight of the Space Shuttle Orbiter Columbia has demonstrated the Shuttle's utility and versatility for earth resources-related research. A series of remote sensing experiments is planned for the mid-1980s which will more fully exploit the Shuttle's earth observation capability. The OSTA-1 experiment package of the mission mentioned incorporated the Shuttle Imaging Radar, a synthetic aperture, side-looking device which artificially illuminated the earth's surface with horizontally

polarized microwave radiation transmitted at L-band frequency, the Shuttle Multispectral IR Radiometer, which measured the intensity of solar radiation reflected from the earth's surface, the Measurement of Air Pollution from Satellites experiment, which determined the concentration of CO in the earth's atmosphere, the proof-of-concept Feature Identification and Location Experiment, and the Night/Day Optical Survey of Lightning experiment. O.C.

A83-13726
TECHNICAL ISSUES IN FOCAL PLANE DEVELOPMENT; PROCEEDINGS OF THE MEETING, WASHINGTON, DC, APRIL 21, 22, 1981
E. KRIKORIAN, (ED.) (General Dynamics Corp., Pomona, CA) and W. C. CHAN (Aerospace Corp., El Segundo, CA) Meeting sponsored by the SPIE - The International Society for Optical Engineering Bellingham, WA, SPIE - The International Society for Optical Engineering (SPIE Proceedings. Volume 282), 1981. 136 p.
MEMBERS, $34.; NONMEMBERS, $40

Papers are presented in the areas of the specifications and requirements and performance limitations on focal plane imaging systems, and on the development of visible and infrared focal planes. Specific topics include the conceptual design of a pushbroom focal plane, a shutterless design for the correction of fixed pattern noise in infrared staring arrays, technical aspects of focal plane development for earth resource observations from space, signal processing in large focal plane arrays, and substrate interactions with passivant films on HgCdTe. A.L.W.

A83-13735* National Aeronautics and Space Administration. Goddard Space Flight Center, Greenbelt, Md.
TECHNICAL ISSUES IN FOCAL PLANE DEVELOPMENT FOR TERRESTRIAL RESOURCE OBSERVATIONS
L. L. THOMPSON (NASA, Goddard Space Flight Center, Greenbelt, MD) In: Technical issues in focal plane development; Proceedings of the Meeting, Washington, DC, April 21, 22, 1981. Bellingham, WA, SPIE - The International Society for Optical Engineering, 1981, p. 80-83.

Performance goals for solid-state detector arrays operating in the pushbroom scan mode for the high-resolution, high-accuracy remote sensing of earth resources from space are discussed and some of the focal plane and system trades involved are identified. Issues in the development of solid-state pushbroom arrays with radiometric calibration to 0.5% precision detector-to-detector over a dynamic range of 1000:1 are considered, with calibration, temporal stability and spectral response conditions noted. Factors influencing the geometric precision of satellite-borne pushbroom scan mode sensors are then examined, including satellite orbit track and attitude errors, and geometric and radiometric correlation between information in the various spectral bands. Approaches to the alignment of linear arrays of thousands of detectors are then discussed that take into account tradeoffs between fabrication and test complexity and ground processing requirements. Continuing science experiments are indicated as necessary to establish tolerances on performance goals. A.L.W.

A83-14040* Kansas Univ., Lawrence.
MICROWAVE REMOTE SENSING: ACTIVE AND PASSIVE. VOLUME 2 - RADAR REMOTE SENSING AND SURFACE SCATTERING AND EMISSION THEORY
F. T. ULABY, R. K. MOORE, and A. K. FUNG (Kansas, University, Lawrence, KS) Research supported by NASA, NSF, and U.S. Department of Defense. Reading, MA, Addison-Wesley Publishing Co., 1982, 624 p. refs
$49.50

The fundamental principles of radar backscattering measurements are presented, including measurement statistics, Doppler and pulse discrimination techniques, and associated ambiguity functions. The operation of real and synthetic aperture sidelooking airborne radar systems is described, along with the internal and external calibration techniques employed in scattering measurements. Attention is given to the physical mechanisms responsible for the scattering emission behavior of homogeneous and inhomogeneous media, through a discussion of surface roughness, dielectric properties and inhomogeneity, and penetration depth. Simple semiempirical models are presented. Theoretical models involving greater mathematical sophistication are also given for extended ocean and bare soil surfaces, and the more general case of a vegetation canopy over a rough surface. O.C.

A83-14275#
A FIELD PORTABLE REFLECTANCE SPECTROMETER
J. H. DAVIES, R. DICK, and C. CUMMING (Barringer Research, Ltd., Rexdale, Ontario, Canada) In: Canadian Symposium on Remote Sensing, 7th, Winnipeg, Canada, September 8-11, 1981, Proceedings. Ottawa, Canadian Aeronautics and Space Institute, 1982, p. 416-422. refs

To permit improved interpretation of aerial photographs and satellite imagery and to permit improved selection of band pass filters for future sensors of the earth's reflectance, a field portable reflectance spectrometer (REFSPEC) has been fabricated. Spectra from 420 to 2450 nm are recorded in 90 seconds. Spectral resolution varies from about 1.5 to 4 nm. Unique chopper design and signal processing gives directly the spectral reflectance of the target scene. Applications including geobotanical and geological studies and satellite ground truthing are described, as well as design and operational features of REFSPEC. (Author)

A83-14289#
THE CCRS SAR PROCESSING SYSTEM
D. N. DAVIS and G. J. PRINCZ (Canada Centre for Remote Sensing, Ottawa, Canada) In: Canadian Symposium on Remote Sensing, 7th, Winnipeg, Canada, September 8-11, 1981, Proceedings. Ottawa, Canadian Aeronautics and Space Institute, 1982, p. 520-526. refs

The SHARP (Synthetic Aperture Radar Processing) system is a recently acquired component of the Canada Centre for Remote Sensing synthetic aperture radar (SAR) sensor and processing facility. The SHARP system hardware consists of a minicomputer with four terminals and with one megabyte of memory, tape and disk units, array processor and high density tape recorder (HDTR). The software is organized in terms of modular functions and transcribes, generates images and controls output quality. Each of these functions is described. The SHARP system product consists of computer-compatible tapes of both the signal data transcribed from the HDTR tape and the generated SAR image. C.D.

A83-14290#
THE MICROWAVE PAYLOAD FOR THE ESA REMOTE SENSING SATELLITE /ERS-1/
G. DIETERLE (ESA, Toulouse, France) In: Canadian Symposium on Remote Sensing, 7th, Winnipeg, Canada, September 8-11, 1981, Proceedings. Ottawa, Canadian Aeronautics and Space Institute, 1982, p. 527-537. refs

The instruments for the planned first European Remote Sensing Satellite (ERS-1) are discussed, describing their main specifications, indicating their measurement principles, and describing their basic design. The active microwave instrumentation (AMI) is an all C-band sensor that can be operated in an SAR imaging mode over land, ice, and coastal areas, and in a wind scatterometer mode, a wave scatterometer mode, and an interleaved wind and wave scatterometer mode over the oceans. Each of these modes is discussed, giving such specifications as spatial resolution, swath, incidence angle, frequency, mean RF power, data rate, antenna size, power consumption, and polarization. The radar altimeter (RA) is also discussed, and its specifications are given. The microwave payload and the ERS-1 program schedule are presented, block diagrams of the AMI and the RA are shown, and a possible inflight configuration for ERS-1 is depicted. C.D.

A83-14293#
APPLICATION OF THE AIRBORNE MICROWAVE RAIN-SCATTERED/RADIOMETER SYSTEM TO THE REMOTE SENSING OF RAINS AND WIND VECTOR MEASUREMENTS OVER THE OCEAN
H. MASUKO, K. OKAMOTO, S. YOSHIKADO, T. OJIMA, M. FUJITA, N. FUGONO (Ministry of Posts and Telecommunications, Radio Research Laboratories, Koganei, Tokyo, Japan), and H. INOMATA (Ministry of Posts and Telecommunications, Radio Research Laboratories, Kashima, Ibaraki, Japan) In: Canadian Symposium on Remote Sensing, 7th, Winnipeg, Canada, September 8-11, 1981, Proceedings. Ottawa, Canadian Aeronautics and Space Institute, 1982, p. 567-578. refs

The airborne microwave scatterometers and radiometers both operated at X-band (wavelength, 3 cm) and Ka-band (wavelength, 8.7 mm) have been applied to the observations of precipitations and microwave scattering and emission characteristics of the ocean. The rain rates are calculated both from the attenuations derived from the Ka-band back-scattered power from the sea surface and from the X-band radar reflectivity factor, Z. The relations between the rainfall rates and the antenna temperatures measured by the dual-wavelength radiometer are estimated. Typical displays of analyzed data are also shown. The differential back-scattering cross section of the sea surface for the X-band and the brightness temperatures of that for the X-band and Ka-band obtained under the wind speed condition of 6 kt are shown as a function of the incident angle (0 to approximately 60 deg), the azimuth angle (0 to approximately 360 deg), and the polarization (H/V). The differential back-scattering cross section is confirmed to be a periodic function of azimuth angle, and the wind vector estimated from the model analysis based on the result is compared with the sea truth data obtained by the meteorological buoy. The brightness temperature map is obtained and the Tsushima Current (warm ocean current) is found on the map. (Author)

A83-14308
THE POSSIBILITY OF MEASURING THE MOISTURE CONTENT OF THE UPPER LAYERS OF THE ATMOSPHERE USING RADIOMETRIC TECHNIQUES [O VOZMOZHNOSTI OPREDELENIIA VLAGOSODERZHANIIA VERKHNIKH SLOEV ATMOSFERY RADIOMETRICHESKIM METODOM]
K. P. GAIKOVICH and SH. D. KITAI (Nauchno-Issledovatel'skii Radiofizicheskii Institut, Gorki, USSR) Issledovanie Zemli iz Kosmosa, Sept.-Oct. 1982, p. 54-58. In Russian. refs

A method is proposed for extracting the moisture-content profiles of the stratosphere and the mesosphere from satellite measurements of thermal radio emission in the narrow band of H2O absorption resonance at 22.23508 and 183.31009 GHz. It is shown that the corresponding inverse problem is reduced to an Abel-type integral equation. The effect of measurement uncertainty on the accuracy of the solution is examined. V.L.

A83-14313
COORDINATE TRANSFORMATION DURING THE GEOMETRIC CORRECTION OF THE SPACE SCANNER IMAGERY OF THE EARTH [PREOBRAZOVANIE KOORDINAT PRI GEOMETRICHESKOI KORREKTSII SKANERNYKH KOSMICHESKIKH SKIMKOV ZEMLI]
V. I. KHIZHNICHENKO Issledovanie Zemli iz Kosmosa, Sept.-Oct. 1982, p. 96-103. In Russian. refs

A previously proposed approximate model for the scanner survey process is further developed and generalized to obtain sufficiently compact explicit expressions for coordinate transformation in the course of the geometric correction of scanner imagery. Computations are carried out for the case of TV scanner systems used for the remote sensing of earth resources from space. It is shown that the proposed model produces an approximation error that does not exceed one resolution element while reducing the processing time by about 15 times, compared with standard numerical procedures. V.L.

A83-14314
OPERATIONAL PLANNING OF THE PROCESS OF EARTH SURVEY BY SATELLITES [OPERATIVNOE PLANIROVANIE PROTSESSA S'EMKI ZEMNOI POVERKHNOSTI S POMOSHCH'IU AVTOMATICHESKOGO ISZ]
V. V. MALYSHEV and D. V. MOISEEV Issledovanie Zemli iz Kosmosa, Sept.-Oct. 1982, p. 104-109. In Russian. refs

A method is proposed for programming the operation of satellite-borne survey instrumentation with allowance for meteorological conditions and constraints imposed by the design limitations of the spaceborne data processing systems. The task of compiling operational schedules is reduced to that of solving a linear programming problem. The proposed method is illustrated by an example. V.L.

A83-14943
INVESTIGATIONS OF INTERPRETABILITY OF IMAGES BY DIFFERENT SENSORS AND PLATFORMS FOR SMALL SCALE MAPPING [UNTERSUCHUNGEN UEBER DIE INTERPRETIERBARKEIT VON BILDERN UNTERSCHIEDLICHER SENSOREN UND PLATTFORMEN FUER DIE KLEINMASSSTAEBIGE KARTIERUNG]
G. KONECNY, W. SCHUHR, and J. WU (Hannover, Universitaet, Hanover, West Germany) Bildmessung und Luftbildwesen, vol. 50, Nov. 1, 1982, p. 187-200. In German. refs

Overlapping High Altitude Photography at scales varying from 1:35,000 to 1:125,000, satellite imagery (Skylab, Landsat) and radar imagery has been used to derive the mapping capability of topographic objects by monocular and, if applicable, stereoscopic observation. The interpretation of digital imagery has been simulated by digitizing the high alitude photographs on the Optronics Scanner using varying pixel sizes between 1 m and 100 m referred to the ground. Pixel sizes of about 3 m are required for monocular observation and 6 m for stereoscopic observation to detect objects to be shown on a 1:50,000 map. (Author)

A83-15458
SPECTRORADIOMETER MEASUREMENTS IN SUPPORT OF PHOTOVOLTAIC DEVICE TESTING
G. A. ZERLAUT and J. D. MAYBEE (DSET Laboratories, Inc., Phoenix, AZ) (U.S. Department of Energy, Commercial Photovoltaics Measurements Workshop, Vail, CO, July 27-29, 1981.) Solar Cells, vol. 7, Nov. 1982, p. 97-106.

The spectroradiometer is capable of complete solar spectral measurements approximately 7 min apart in both the global and the direct beam modes, all in the wavelength range 280-2500 nm. Global measurements can be made at any azimuth and altitude position; the field of view of the pyrheliometer comparison tube is 6 deg. Typical spectra show that the resolution is sufficient to identify Fraunhofer absorption bands in the surface of the sun. Data are presented that show the relationship between direct beam spectra and two specific microenvironments. The differences observed are analyzed in terms of the significance of microenvironment haze and pollution to the efficiency of concentrating photovoltaic devices. (Author)

A83-19585#
AIRBORNE ATMOSPHERIC TEMPERATURE STRUCTURE MEASUREMENTS OF A PACIFIC COAST MARINE INVERSION
L. J. OTTEN, III (USAF, Weapons Laboratory, Kirtland AFB, NM) and W. C. ROSE (Rose Engineering and Research, Inc., Incline Village, NV) American Institute of Aeronautics and Astronautics, Aerospace Sciences Meeting, 21st, Reno, NV, Jan. 10-13, 1983, 7 p. refs
(AIAA PAPER 83-0278)

A mobile airborne observation platform has been used to measure the temperature structure of a Pacific coast marine inversion. Data were collected using thin film and fine wire anemometry. Ground launched weather balloon data complemented the onboard meteorological observations. The technique provides the timely collection of vertical profile samples. The study indicated regions in the inversion where the wide-angle scattering of a propagating electromagnetic wave can be much

more severe than the best propagating bands. There also appears to be an optically quite region immediately above the inversion wherein the moisture level is considerably less than that found from the ocean surface to the top of the inversion. S.C.S.

N83-11565 Bayerische Akademie der Wissenschaften, Munich (West Germany).
INVESTIGATION OF THE GEOMETRICAL STABILITY OF A PHOTOGRAMMETRIC RECORDING SYSTEM Ph.D. Thesis - Bonn Univ. [UNTERSUCHUNG ZUR GEOMETRISCHEN STABILITAET EINES PHOTOGRAMMETRISCHEN AUFNAHMESYSTEMS]
K. H. ELLENBECK Bayerischen Akademie der Wissenschaften 1981 73 p refs In GERMAN
(SER-C-267; ISBN-3-7696-9319-1; ISSN-0065-5325) Avail: Issuing Activity

System parameters and their effect on the error of a photogrammetric recording system were investigated in order to evaluate the stability with respect to system errors and parameters. The possibilities of determination and separation of system errors is also explained. From the comparative investigations of different flights, the importance of a single system parameter for the photogrammetric result was deduced and requirements for the choice of system parameters in photogrammetric systems with high accuracy were deduced. The results show that the stability of the systems parameters and the possibility to register completely the system errors are closely dependent. Author (ESA)

N83-12396*# National Aeronautics and Space Administration. Goddard Space Flight Center, Greenbelt, Md.
AN EVALUATION OF THE NASA/GSFC BARNES FIELD SPECTRAL REFLECOMETER MODEL 14-758, USING SIGNAL/NOISE AS A MEASURE OF UTILITY
R. BELL and M. L. LABOVITZ Jul. 1982 42 p refs
(NASA-TM-83969; NAS 1.15:83969) Avail: NTIS HC A03/MF A01 CSCL 14B

A Barnes field spectral reflectometer which collected information in 373 channels covering the region from 0.4 to 2.5 micrometers was assessed for signal utility. A band was judged unsatisfactory if the probability was 0.1 or greater than its signal to noise ratio was less than eight to one. For each of the bands the probability of a noisy observation was estimated under a binomial assumption from a set of field crop spectra covering an entire growing season. A 95% confidence interval was calculated about each estimate and bands whose lower confidence limits were greater than 0.1 were judged unacceptable. As a result, 283 channels were deemed statistically satisfactory. Excluded channels correspond to portions of the electromagnetic spectrum (EMS) where high atmospheric absorption and filter wheel overlap occur. In addition, the analyses uncovered intervals of unsatisfactory detection capability within the blue, red and far infrared regions of vegetation spectra. From the results of the analysis it was recommended that 90 channels monitored by the instrument under consideration be eliminated from future studies. These channels are tabulated and discussed. B.W.

N83-13547*# National Aeronautics and Space Administration. Goddard Space Flight Center, Greenbelt, Md.
THE USE OF THEMATIC MAPPER SIMULATOR CALIBRATION DATA FOR ASSESSMENT OF DATA QUALITY
M. L. FORMAN Dec. 1980 23 p refs
(NASA-TM-82059; NAS 1.15:82059) Avail: NTIS HC A02/MF A01 CSCL 05B

In flight calibration data collected from the thematic mapper simulator (TMS) were used to assess the quality of Earth scan data. The following results are indicated: (1) based on limited samples, individual TMS channels have noise which varies from channel to channel, but remains constant within a channel; (2) short term variations of more than 5% in the average values of calibration source responses indicate problems; and (3) absolute radiometric calibration is unlikely to be meaningful in a temporal sense due to single point calibration methods used. E.A.K.

N83-13567# Messerschmitt-Boelkow-Blohm G.m.b.H., Ottobrunn (West Germany). Betriebsbereich.
A DIGITAL PHOTOGRAMMETRIC SYSTEM (DPS) FOR PRODUCING DIGITAL ELEVATION MODELS (DEM) AND ORTHOPLATES BY MEANS OF LINEAR ARRAY SCANNER IMAGERY
O. HOFMANN, P. NAVE, and H. EBNER (Tech. Univ., Munich) 1981 13 p refs
(MBB-UA-618/81) Avail: Issuing Activity

A digital procedure for the generation and processing of scanner images is presented. The terrain is scanned by an opto-electronic three-line scan camera from aircraft, missiles or spacecraft. Three linear sensor arrays are arranged in the focal plane of the camera objective perpendicularly to the flight course. Each sensor array produces an image strip of the covered terrain according to the pushbroom principle. Nodes of the DEM to be computed are selected in the middle image strip whose object planes are nearly vertical. The conjugate image points in the other two image strips are determined by area correlation methods. The coordinates of all these image points and a few control points are inserted into a least squares adjustment for computation of the orientation parameters of the camera along its entire flight course and the coordinates of the DEM. Raster plots of ortho and stereo orthophotos are produced after digital rectification of the image strips, utilizing the nodes of the DEM grid. Author (ESA)

N83-13750# Maryland Univ., College Park. Dept. of Meteorology.
SPATIAL AND TEMPORAL VARIATIONS OF LARGE-SCALE SUBSIDENCE AND CONVECTION REGIONS DERIVED FROM SATELLITE DATA
A. D. VERNEKAR *In* National Weather Service Proc. of the 6th Ann. Climate Diagn. Workshop p 261-267 Mar. 1982 refs
(Contract NA80AA-D-00035; NSF ATM-80-24881)
(PB82-219817) Avail: NTIS HC A16/MF A01 CSCL 04B

Geographical location and horizontal extent of large scale monthly mean subsidence regions and those of convection regions vary during a year and also vary from year to year. Anomalies in variations of subsidence regions over oceans can create anomalies in sea surface temperature and over land they can produce drought conditions. On the other hand, anomalies in variations of convection regions can create anomalies in rainfall patterns and in latent heat released. The variability of these systems from satellite data is determined. The data utilized is net outgoing infrared radiation (IR) at the top of the atmosphere. These data were derived from measurements made on scanning radiometer aboard the NOAA operational satellite. The global distribution of IR fields were available twice daily (9:00 a.m. and 9:00 p.m. local time) for 45 months. S.L.

N83-13767*# Washington Univ., Seattle. Dept. of Atmospheric Sciences.
VALIDATION AND APPLICATION OF THE SEASAT-SMMR GEOPHYSICAL ALGORITHMS Final Report
K. B. KATSAROS and L. A. MCMURDIE Feb. 1982 96 p refs Sponsored in part by NASA
(Contract NA78-SAC-04102)
(NASA-CR-169390; NAS 1.26:169390; PB82-237934; CONTRIB-616; NOAA-82051012) Avail: NTIS HC A05/MF A01 CSCL 04B

The work was concentrated on verification of the atmospheric water channels on SEASAT's Scanning Multichannel Microwave Radiometer (SMMR). Data from the Gulf of Alaska Experiment (GOASEX), tropical island stations, and particularly from the Joint Air Sea Interaction (JASIN) experiment have been used to compare with the SMMR algorithm predictions. SMMR's water vapor has been found to be at least as accurate as conventional radiosondes. Liquid water and rain rate have insufficient comparisons for statistical results, but can be said to show promise in a qualitative sense. The SEASAT SMMR maps of the atmospheric water components were found to be very useful in helping to locate fronts and cloudy and rainy areas in the JASIN experiment. Author (GRA)

N83-14588*# Instituto de Pesquisas Espaciais, Sao Jose dos Campos (Brazil).
COMPARISON OF DIVERSE METHODS FOR THE CORRECTION OF ATMOSPHERIC EFFECTS ON LANDSAT AND SKYLAB IMAGES [COMPARACAO DE DIVERSOS METODOS PARA A CORRECAO DE EFEITO ATMOSFERICO EM IMAGENS LANDSAT E SKYLAB]
N. D. J. PARADA, Principal Investigator, G. CAMARA, L. A. V. DIAS, N. D. D. MASCARENHAS, R. C. M. DESOUZA, and A. E. C. PEREIRA Jul. 1982 27 p refs In PORTUGUESE; ENGLISH summary Presented at the 33rd Reuniao Anual da SBPC, Salvador, Bahia, Jul. 1981 Sponsored by NASA ERTS (E83-10079; NASA-CR-165122; NAS 1.26:165122; INPE-2471-PRE/160) Avail: NTIS HC A03/MF A01 CSCL 05B

Earth's atmosphere reduces a sensors ability in currently discriminating targets. Using radiometric correction to reduce the atmospheric effects may improve considerably the performance of an automatic image interpreter. Several methods for radiometric correction from the open literature are compared leading to the development of an atmospheric correction system. A.R.H.

N83-14612*# National Aeronautics and Space Administration, Washington, D. C.
LAND REMOTE SENSING ACTIVITIES IN THE US
S. W. KELLER and K. J. ANDO *In* ESA Satellite Remote Sensing for Developing Countries p 37-45 Jun. 1982 refs
Avail: NTIS HC A11/MF A01

The LANDSAT D system, shuttle imaging radar instruments, the thermal infrared multispectral scanner system, the shuttle multispectral infrared radiometer, and the multispectral linear array program are described. These programs will develop advanced optical and microwave sensor technologies to support a broad spectrum of aircraft, shuttle and free flier missions for research in agriculture, geology, hydrology and geography. A broad based fundamental research effort coupled with the development of improved data acquisition and information extraction techniques is planned to improve fundamental understanding of the remote sensing process and fully exploit its capabilities. Author (ESA)

N83-14804# Cologne Univ. (West Germany).
THE CONICAL SCAN RADIOMETER
T. PROSCH and D. HENNINGS *In its* Satellite Meas. of the Earth Radiation Budget p 99-112 Jul. 1982 refs
Avail: NTIS HC A08/MF A01

A satellite-borne conical scan radiometer (CSR) is proposed, offering multiangular and multispectral measurements of Earth radiation fields, including the total radiances, which are not available from conventional radiometers. Advantages of the CSR for meteorological studies are discussed. In comparison to conventional cross track scanning instruments, the CSR is unique with respect to the selected picture element size which is kept constant by means of a specially shaped detector matrix at all scan angles. The conical scan mode offers the chance to improve angular sampling. Angular sampling gaps of previous satellite-borne radiometers can be interpolated and complemented by CSR data. Radiances are measured through 10 radiometric channels which are selected to study cloudiness, water vapor, ozone, surface albedo, ground and mean stratospheric temperature, and aerosols. Author (ESA)

N83-14805# Cologne Univ. (West Germany).
THE EARTH RADIATION BUDGET SATELLITE SYSTEM (ERBSS) OF THE UNITED STATES
E. RASCHKE *In its* Satellite Meas. of the Earth Radiation Budget p 113-119 Jul. 1982
Avail: NTIS HC A08/MF A01

A plan is presented which is accepted in the US to measure the radiation budget parameters simultaneously with wide field of view medium field of view and a scanning narrow field of view radiometer. The instrument parameters are summarized. Spectral and technical details are given. These instruments are planned to be flown in operational satellites of the NOAA series. A smaller low inclination satellite of the Atmospheric Explorer series can give valuable information sampled over tropical and subtropical regions of the Earth. The contributions of the different ERBSS members are grouped in four categories: modeling of instrumental performance; algorithms for data inversions; averaging of data in space and time; and consideration of the major aspects of most operational data evaluations and distributions to interested data users. Author (ESA)

N83-15344*# National Aeronautics and Space Administration. Goddard Space Flight Center, Greenbelt, Md.
DATA ANNOUNCEMENT BULLETIN: SPACE SHUTTLE OSTA 1 PAYLOAD DATA
Nov. 1982 2 p
(NASA-TM-84884; NSSDC/WDC-A-R/S-82-25; NAS 1.15:84884)
Avail: NTIS HC A02/MF A01 CSCL 12A

Data from the scientific payload, OSTA 1, is available. Images of the Earth's surface taken from the Shuttle Imaging Radar-A were processed, and can be obtained in the form of photographic prints, negatives, or positive transparencies. Magnetic tapes containing data for the ocean color experiment and the Shuttle multispectral infrared radiometer are also available. S.L.

N83-15797*# Hughes Aircraft Co., Los Angeles, Calif. Space and Communications Group.
MSS D MULTISPECTRAL SCANNER SYSTEM Final Report, Apr. 1978 - Nov. 1981
A. M. LAULETTA, R. L. JOHNSON, and K. L. BRINKMAN, Principal Investigators Apr. 1982 502 p refs ERTS
(Contract NAS5-25050)
(E83-10128; NASA-CR-170457; NAS 1.26:170457; HAC-E1966)
Avail: NTIS HC A22/MF A01 CSCL 05B

The development and acceptance testing of the 4-band Multispectral Scanners to be flown on LANDSAT D and LANDSAT D Earth resources satellites are summarized. Emphasis is placed on the acceptance test phase of the program. Test history and acceptance test algorithms are discussed. Trend data of all the key performance parameters are included and discussed separately for each of the two multispectral scanner instruments. Anomalies encountered and their resolutions are included. Author

09

GENERAL

Includes economic analysis.

A83-10429
EARTH OBSERVATION - EVOLUTION OF REQUIREMENTS AND SYSTEMS [OBSERVATION DE LA TERRE - EVOLUTION DES BESOINS ET DES SYSTEMES]
G. BRACHET (Centre National d'Etudes Spatiales, Paris, France) L'Aeronautique et l'Astronautique, no. 95, 1982, p. 21-25. In French.

The applications, operations, and types of space-based platforms for remote viewing of the earth are reviewed, together with projections of future developments. The spacecraft mainly produce imagery for ground-based analyses of scientific, meteorological, cartographical, or oceanographic data. Atmospheric phenomena, geological formations, temperature stratification, and sea-air interactions are monitored. The instrumentation comprises visual bands, SAR, and microwave passive sensing, with data transmission rates of 15 Mbits/sec for the Landsat 3 and a planned 50-100 Mbit/sec for the SPOT satellite. Signal receiving and data processing at ground stations are being continually upgraded in terms of data compression, image manipulation, and treatment in parallel and from storage. Future systems are projected to involve sequentially launched identical systems for keeping relatively continuous watch over a particular region, and also to experiment with spacecraft with newly developed instrumentation. Principal

features of the SPOT and Landsat-D spacecraft are detailed. M.S.K.

A83-11926
SPACELAB, SPACE PLATFORMS AND THE FUTURE; PROCEEDINGS OF THE FOURTH JOINT AAS/DGLR SYMPOSIUM AND TWENTIETH GODDARD MEMORIAL SYMPOSIUM, WASHINGTON, DC, MARCH 17-19, 1982
P. M. BAINUM, (ED.) (Howard University, Washington, DC) and D. E. KOELLE (Messerschmitt-Boelkow-Blohm GmbH, Ottobrunn, West Germany) Symposium sponsored by AAS, DGLR, AIAA, et al. San Diego, CA, Univelt, Inc. , 1982. 501 p. $43.25.

National and international program goals for the next generation of civil space missions are discussed. Attention was given to the instrumentation and hardware intended for the Spacelab flights, with specific details of material processing, remote sensing, life sciences, astrophysical, and solar physics experiments. Free-flying space platforms to be launched, serviced, and/or retrieved by the Shuttle are described, together with mission requirements attesting to the need for a permanently manned space station and also constraining its design. Earth-oriented space activities were surveyed, including microwave remote sensing apparatus for the Shuttle and autonomous satellites, data processing systems for earth resources satellites, and solid-state instrumentation concepts. NASA and ESA launch vehicles in the near term are projected, and the history of manned maneuvering units is traced. M.S.K.

A83-11932
ADVANCED OPERATIONAL EARTH RESOURCES SATELLITE SYSTEMS
S. W. MCCANDLESS (User Systems Engineering, Annandale, VA) and P. M. MAUGHAN (COMSAT General Corp., Washington, DC) In: Spacelab, space platforms and the future; Proceedings of the Fourth Joint AAS/DGLR Symposium and Twentieth Goddard Memorial Symposium, Washington, DC, March 17-19, 1982. San Diego, CA, Univelt, Inc., 1982, p. 293-308.
(AAS 82-128)

Spacecraft instrumentation and design, business objectives, and space technologies being developed and used by various nations in the near term are reviewed. The French are preparing the SPOT satellite for earth resouces mapping, while the ERS-1 spacecraft are being developed by both ESA and Japan, with capabilities similar to SEASAT and the GOES satellites. Communications satellites will implement the 30/20 GHz bands, multiple spot beam antennas, and large unmanned multiservice satellite systems. Predicted space missions in the period 1982-1991 are provided, including mention of satellite business communication services, direct broadcast television services, electronic mail, and international information services. At least four U.S. environmental monitoring satellites will be in orbit at any one time. Finally, the use of multisensor platforms is noted to potentially reduce the launch volume demands on the Shuttle and ballistic missile systems. M.S.K.

A83-11933
FUTURE LAND REMOTE SENSING DATA AND SERVICES - A COMMERCIAL PERSPECTIVE
T. M. ALEXANDER and P. M. MAUGHAN (COMSAT General Corp., Washington, DC) In: Spacelab, space platforms and the future; Proceedings of the Fourth Joint AAS/DGLR Symposium and Twentieth Goddard Memorial Symposium, Washington, DC, March 17-19, 1982. San Diego, CA, Univelt, Inc., 1982, p. 313-323.
(AAS 82-129)

The development of a market for satellite synoptic, repeat imagery of the earth is traced to the present, and necessities for full-scale commercial remote sensing operations are defined. The Landsat spacecraft produced multispectral imagery of the earth, based on technologies developed since World War II primarily for military applications. Rapid dissemination of the data was accomplished, but shortages in trained personnel, data processing, image generation, and interpretive and production hardware became evident. Additionally, government subsidies of the services created an artifically low cost, and foreign nations began to develop remote sensing satellites which offered the same services. It is suggested that the thematic mapper on the Landsat D should be evaluated for its actual use in commercial applications and replaced if it has none. Sensors which respond to commercial demands are recommended for development, together with commercially controlled remote sensing services. M.S.K.

A83-12673* National Aeronautics and Space Administration. Goddard Space Flight Center, Greenbelt, Md.
THE EARLY 1981 VIEW OF LANDSAT-D PROGRESS
V. V. SALOMONSON (NASA, Goddard Space Flight Center, Earth Survey Applications Div., Greenbelt, MD) In: Electro-optical instrumentation for resources evaluation; Proceedings of the Meeting, Washington, DC, April 21, 22, 1981. Bellingham, WA, SPIE - The International Society for Optical Engineering, 1981, p. 50-59. refs

The thematic mapper (TM) will provide a spatial resolution (30 m) higher than the radiometric observations provided from Landsats 1 through 3 (80 m); what is more, observations in new spectral bands (0.45 to 0.52, 1.55 to 1.75, and 2.08 to 2.35 microns) will be available. These characteristics will aid in identifying and assessing the acreage and condition of crops. Further advantages will be offered in mineral exploration and land resource assessment. In describing the flight segment, it is noted that the high-gain antenna (diameter, 6 ft) will be used to communicate with the Tracking and Data Relay Satellite System in the Ku-band (15 GHz). Direct transmission of TM data will be provided by the X-band antenna. The MSS data will be transmitted directly to foreign stations by the S-band antenna. A figure describing the Multimission Modular spacecraft is included. C.R.

A83-13715* National Aeronautics and Space Administration, Washington, D. C.
OSTA-1 - SHUTTLE'S FIRST SCIENTIFIC AND APPLICATIONS PAYLOAD
L. J. DEMAS (NASA, Office of Space Science, Washington, DC) and J. V. TARANIK (NASA, Office of Space and Terrestrial Applications, Washington, DC) In: NASA-ESA Spacelab systems and programs; Proceedings of the Seminar, Washington, DC, April 23, 24, 1981. Bellingham, WA, SPIE - The International Society for Optical Engineering, 1982, p. 118-123.

The Office of Space and Terrestrial Applications' OSTA-1 scientific and applications payload will be carried by the second Space Shuttle flight and be concerned primarily with the remote sensing of land resources, atmospheric phenomena and ocean conditions. Incorporated by the OSTA-1 payload are the Shuttle Multispectral IR Radiometer, the Feature Identification and Location Experiment, the Measurement of Air Pollution from Satellites experiment, the Ocean Color Experiment, the Night/Day Optical Survey of Lightning, and the Heflex Bioengineering Test. O.C.

A83-14226
CANADIAN SYMPOSIUM ON REMOTE SENSING, 7TH, WINNIPEG, CANADA, SEPTEMBER 8-11, 1981, PROCEEDINGS
W. G. BEST, (ED.) and S.-A. WESELAKE (Manitoba Remote Sensing Centre, Winnipeg, Canada) Symposium sponsored by CASI, Canada Centre for Remote Sensing, Department of Fisheries and Oceans of Canada, et al. Ottawa, Canadian Aeroanutics and Space Institute, 1982. 618 p. In English and French.

Overview presentations are provided, taking into account the development of airborne and satellite remote sensing applications, and the importance of remote sensing for Canada with respect to past achievements and future needs. Land use applications are considered, giving attention to renewable resource information needs in Manitoba, satellite remote sensing for domestic crop reporting in the U.S. and Canada, operational land cover type mapping in Ontario by Landsat-based digital analysis and map production, a position-based resource mapping study of the Kananskis valley using Landsat, and the application of Landsat imagery in flood control and management of agricultural land. Other topics discussed are related to ecological applications, earth science applications, and data management and acquisition. A description is provided of the Canadian synthetic aperture radar

satellite program, and the application of the airborne microwave rain-scatterometer/radiometer system to the remote sensing of rains and wind vector measurements over the ocean. G.R.

A83-14227#
THE IMPORTANCE OF REMOTE SENSING FOR CANADA - PAST ACHIEVEMENTS, FUTURE NEEDS
E. A. GODBY (Canada Centre for Remote Sensing, Ottawa, Canada) and J. THIE (Department of the Environment, Canada Lands Directorate, Hull, Quebec, Canada) In: Canadian Symposium on Remote Sensing, 7th, Winnipeg, Canada, September 8-11, 1981, Proceedings. Ottawa, Canadian Aeronautics and Space Institute, 1982, p. 8-19. refs

A survey of remote sensing activities and plans in Canada is presented. Attention is given to Landsat ground stations, computer-assisted data analysis, radar projects such as Canada's participation in the NASA Seasat project, and remote sensing programs in the individual Canadian provinces. Plans for the next decade are outlined. These include participation in projects involving Landsat D, the French SPOT satellite, the Japanese MOS-I satellite and Canada's own Radarsat satellite. S.C.S.

A83-17349
GLOBAL IMPLICATIONS OF SPACE ACTIVITIES; PROCEEDINGS OF THE CONFERENCE, ASPEN, CO, AUGUST 30-SEPTEMBER 4, 1981
J. GREY, (ED.) (American Institute of Aeronautics and Astronautics, Inc., New York, NY) and L. LEVY Conference sponsored by the American Institute of Aeronautics and Astronautics and Aspen Institute for Humanistic Studies. New York, American Institute of Aeronautics and Astronautics , 1982. 155 p.
MEMBERS, $18.50; NONMEMBERS, $24.50

The influence of present and future space activities on the world is discussed. The general topics addressed include space science, communications, and earth resources. Individual subjects considered include: the global implications of space; space science and humanistic concerns; motivations for the U.S. space program; international collaboration and military-civil interactions in space programs; space communications organizations and links; remote sensing programs and applications; institutional arrangements for remote sensing. C.D.

A83-17426#
EARTHNET PREPARES FOR LANDSAT-D
L. MARELLI (European Space Research Institute, Earthnet Programme Office, Frascati, Italy) ESA Bulletin, no. 32, Nov. 1982, p. 6-10.

Landsat-D incorporates a thematic mapper (TM) in addition to the more conventional multispectral scanner (MSS), thereby offering enhanced capabilities which are attractive in light of European requirements. Efforts are currently underway to upgrade the Earthnet Landsat stations at Fucino, Italy and Kiruna, Sweden, so that, when the Landsat-D payload becomes routinely available to Eathnet stations in mid-1983, European remote sensing data users will be able to employ this new tool for resource management. Four passes of Landsat-D MSS data have been acquired to date, and are undergoing evaluation. The first TM images are to be acquired before the end of 1983. Attention is given to the results of NASA's Landsat Image Data Quality Assessment program with respect to overall Landsat-D performance and especially that of its sensors. O.C.

A83-17775
SALYUT-7 FROM JUNE TO AUGUST ['SALIUT-7' S IUNIA PO AVGUST]
S. A. NIKITIN Priroda, Nov. 1982, p. 104, 105. In Russian.

Activities performed by the cosmonauts on Salyut-7 during June-August 1982 are briefly described. These activities included the unloading of Progress-13, biomedical studies, geophysical experiments, the remote sensing of earth resources, the testing of the Magma-F electric furnace for the Kristall space-manufacturing facility, astrophysical studies, and EVA. B.J.

N83-10458*# National Aeronautics and Space Administration. Goddard Space Flight Center, Greenbelt, Md.
THE LANDSAT TUTORIAL WORKBOOK: BASICS OF SATELLITE REMOTE SENSING
N. M. SHORT, Principal Investigator 1982 554 p refs Original contains color imagery. Original photography may be purchased from the EROS Data Center, Sioux Falls, S.D. 57198. ERTS
(E83-10001; NASA-RP-1078; NAS 1.61:1078; LC-81-600117)
Avail: NTIS MF A01; SOD HC $55.00 CSCL 05B

Most of the subject matter of a full training course in applying remote sensing is presented in a self-teaching mode in this how-to manual which combines a review of basics, a survey of systems, and a treatment of the principles and mechanics of image analysis by computers, with a laboratory approach for learning to utilize the data through practical experiences. All relevant image products are included.

N83-10467*# National Aeronautics and Space Administration. Goddard Space Flight Center, Greenbelt, Md.
OTHER REMOTE SENSING SYSTEMS: RETROSPECT AND OUTLOOK
In its The LANDSAT Tutorial Workbook p 327-387 1982 refs Original contains color imagery. Original photography may be purchased from the EROS Data Center, Sioux Falls, S.D. 57198. ERTS
Avail: NTIS MF A01; SOD HC $55.00 CSCL 05B

The history of remote sensing is reviewed and the scope and versatility of the several remote sensng systems already in orbit are discussed, especially those with sensors operating in other EM spectral modes. The multisensor approach is examined by interrelating LANDSAT observations with data from other satellite systems. The basic principles and practices underlying the use of thermal infrared and radar sensors are explored and the types of observations and interpretations emanating from the Nimbus, Heat Capacity Mapping Mission, and SEASAT programs are examined. Approved or proposed Earth resources oriented missions for the 1980's previewed include LANDSAT D, Stereosat, Gravsat, the French satellite SPOT-1, and multimission modular spacecraft launched from space shuttle. The pushbroom imager, the linear array pushbroom radiometer, the multispectral linear array, and the operational LANDSAT observing system, to be designed the LANDSAT-E series are also envisioned for this decade. A.R.H.

N83-10468*# National Aeronautics and Space Administration. Goddard Space Flight Center, Greenbelt, Md.
SOME CLOSING THOUGHTS: PRACTICAL PAYOFFS FROM SATELLITE SYSTEMS
In its The LANDSAT Tutorial Workbook p 389-407 1982 refs Original contains imagery. Original photography may be purchased from the EROS Data Center, Sioux Falls, S.D. 57198. ERTS
Avail: NTIS MF A01; SOD HC $55.00 CSCL 05B

The benefits-to-cost ratio of satellite remote sensing, both as a substitute for conventional methods of monitoring and assessing resources, and as a supplement to these methods is examined using a model which analyzes the cost of aerial photography versus satellite scanner for producing and interpreting an image of the Earth's surface sized to LANDSAT dimensions. Examples of cost savings are tabulated for ground surveys, aerial photos, and LANDSAT. Possible additional benefits from LANDSAT D are assessed. The way in which satellites fit into more comprehensive models for resources management is discussed. It is shown that remote sensing is but one essential component in a complex system that aggregates technical. Socioeconomics, political, cultural, and other factors in the human decision process.
A.R.H.

N83-10469*# National Aeronautics and Space Administration. Goddard Space Flight Center, Greenbelt, Md.
APPENDIX A: THE LANDSAT SYSTEM
S. C. FREDEN *In its* The LANDSAT Tutorial Workbook p 409-419 1982 refs ERTS
Avail: NTIS MF A01; SOD HC $55.00 CSCL 05B

The primary LANDSAT mission and the system requirements are summarized and pertinent parameters of the spacecraft, its orbit, and payload are tabulated. The history acquisition to entry into the archives for storage and product generation and dissemination is recounted. The LANDSAT D data handling plan is discussed showing requirements for both the MSS CCT and the thematic mapper CCT. A.R.H.

N83-10470*# National Aeronautics and Space Administration. Goddard Space Flight Center, Greenbelt, Md.
APPENDIX B: PRINCIPLES OF COMPUTER PROCESSING OF LANDSAT DATA
In its The LANDSAT Tutorial Workbook p 421-453 1982 refs Original contains color imagery. Original photography may be purchased from the EROS Data Center, Sioux Falls, S.D. 57198. ERTS
Avail: NTIS MF A01; SOD HC $55.00 CSCL 05B

Computer processing facilitates extraction of information from every pixel by executing a variety of functional operations, called processed algorithms, in general or specialized routines. The best results are obtained when data from more than one multispectral band are used together. Multivariate tatistical analysis, computer tape characteristics, processing modes, and a choice of systems (batch or interactive) are discussed. The major operations in computer processing elaborated include: preprocessing, enhancement, effects of rationing, and classification. Techniques for multisource data correlation are considered with emphasis on geobased systems. A.R.H.

N83-10471*# National Aeronautics and Space Administration. Goddard Space Flight Center, Greenbelt, Md.
APPENDIX C. LANDSAT: A WORLDWIDE PERSPECTIVE
In its The LANDSAT Tutorial Workbook p 455-475 1982 refs Original contains color imagery. Original photography may be purchased from the EROS Data Center, Sioux Falls, S.D. 57198. ERTS
Avail: NTIS MF A01; SOD HC $55.00 CSCL 05B

Images characteristics of geographic regions other than the northeastern part of the United States are presented for interpretation. Pre- and post-eruption imagery of Mt. St. Helens volcano serves to demonstrate the advantages of thermal infrared sensing, and the potential for developing a timely, decision oriented thematic map to be used in solving drought-related problems in Upper Volta is examined to show the applicability of satellite remote sensing in all geographic areas. A.R.H.

N83-11532# National Advisory Committee on Oceans and Atmosphere, Washington, D.C.
A REPORT TO THE PRESIDENT AND THE CONGRESS Annual Report
30 Jun. 1982 58 p refs
(AR-11) Avail: NTIS HC A04/MF A01

Atmospheric and marine issues of immediate and long-term consequence are reported. Remote sensing equipment, instrumented airplanes, and computers were examined. River and flood forecasting research is discussed. Funding for civil weather services is also discussed. Marine fisheries, minerals, and transportation are considered. Scientific diving standards and regulations, the Clean Water Act, ocean waste disposal, outer continental shelf revenue sharing, coastal barrier legislation, the Coast Guard, global oceanic processes, acid rain, and radioactive waste disposal are considered. Author

N83-12115# Indian Space Research Organization, Bangalore.
APPLICATIONS OF SPACE SCIENCE AND TECHNOLOGY
In its Natl. Paper of India for the 2d United Nations Conf. on Exploration and Peaceful Uses of Outer Space (UNISPACE 82) p 23-30 1982 refs
Avail: NTIS HC A04/MF A01 CSCL 22A

Space technology applications in the areas of communications, meteorology, geodesy, and remote sensing undertaken by Indian research organizations and international projects are discussed. The development of the INSAT system, the Satellite Instructional Television Experiment, the Satellite Telecommunications Experiments Project, and the APPLE satellite are specifically addressed. Indian participation in the MONEX experiment is also discussed. M.G.

N83-14560*# Agricultural Research Services, Beltsville, Md.
AGRICULTURAL RESEARCH SERVICE RESEARCH HIGHLIGHTS IN REMOTE SENSING FOR CALENDAR YEAR 1981 Annual Report
J. C. RITCHIE, comp. Jul. 1982 27 p Sponsored by NASA, USDA, Dept. of Commerce, Dept. of the Interior, and Agency for International Development ERTS
(Contract PROJ. AGRISTARS)
(E83-10051; NASA-CR-169567; EW-R2-04345; JSC-18268; NAS 1.26:169567) Avail: NTIS HC A03/MF A01 CSCL 02C

Selected examples of research accomplishments related to remote sensing are compiled. A brief statement is given to highlight the significant results of each research project. A list of 1981 publication and location contacts is given also. The projects cover emission and reflectance analysis, identification of crop and soil parameters, and the utilization of remote sensing data. M.G.

N83-14608# European Space Agency, Paris (France).
SATELLITE REMOTE SENSING FOR DEVELOPING COUNTRIES
N. LONGDON, ed. and G. LEVY, ed. Jun. 1982 245 p refs Proc. of EARSeL-ESA/ASSA Symp., Igls, Austria, 20-21 Apr. 1982
(ESA-SP-175; ISSN-0379-6566) Avail: NTIS HC A11/MF A01; ESA, Paris FF 125 (Member States and CV, AU, NO) + 20% others

Remote sensing technology transfer to developing nations was discussed. Data processing, particularly of LANDSAT data, was considered. Applications of remote sensing, and the role of ESA in meeting the remote sensing requirements of the Third World were examined. For individual titles, see N00-00001 through N00-00029.

N83-14609# Commission of the European Communities, Brussels (Belgium).
THE EUROPEAN COMMUNITY, DEVELOPMENT AND SATELLITE TECHNOLOGY
G. BOGGIO and C. WHITE *In* ESA Satellite Remote Sensing for Developing Countries p 11-18 Jun. 1982
Avail: NTIS HC A11/MF A01

European Community scientific and technical cooperation with developing nations, particularly in remote sensing technology, is discussed. Cooperation programs recognize the importance of improving the capabilities of the developing nations. In agriculture, the Community is studying the benefits of land use mapping for rice production in the Sahel. Mineral exploration and meteorological projects are also underway. Author (ESA)

N83-14610# European Space Agency, Toulouse (France). Earth Observation Programmes Dept.
THE EUROPEAN SPACE AGENCY'S EARTH OBSERVATION SATELLITE PROGRAMS IN THE 1980'S
D. LENNERTZ *In* ESA Satellite Remote Sensing for Developing Countries p 21-33 Jun. 1982
Avail: NTIS HC A11/MF A01

The METEOSAT, Sirio-2, Earthnet, Spacelab, and ERS-1 programs are described. METEOSAT will image the surface and cloud system in the visible and IR bands every 30 min. It will also

monitor water vapor absorption. Sirio 2 should have disseminated meteorological information to Africa and synchronized atomic clocks. Earthnet will disseminate LANDSAT, heat capacity mapping mission, Nimbus 7 and Seasat data. Spacelab experiments include photographic mapping and microwave remote sensing. The first ERS-1 mission is oriented towards ice and ocean monitoring.
Author (ESA)

N83-14611# Centre National de la Recherche Scientifique, Paris (France).
SPOT IN THE 1980'S
M. TAIZET *In* ESA Satellite Remote Sensing for Developing Countries p 35-36 Jun. 1982
Avail: NTIS HC A11/MF A01

The SPOT development program is outlined, and information transfer, storage, and management are discussed. The SPOT satellite is programmable and is designed for continuous remote sensing activities. The first satellite should operate from 1984 until 1986, when the launching of SPOT-2 is planned. Author (ESA)

N83-14614# Food and Agriculture Organization of the United Nations, Rome (Italy).
REMOTE SENSING IN DEVELOPING COUNTRIES. FAO'S INTERNATIONAL EXPERIENCE
J. A. HOWARD IN ESA Satellite Remote Sensing for Developming Countries p 55-59 Jun. 1982
Avail: NTIS HC A11/MF A01

The FAO remote sensing training scheme, assistance in establishing national remote sensing centers, experience of transfer of remote sensing technology to developing countries, and remote sensing of renewable resources are described. The FAO uses satellite imagery for land resources, water resources and soil surveys, forestry and wildlife monitoring, and fish location. Other projects include disaster forecasting, thematic mapping, agricultural statistics, and pasture and rangeland development.
Author (ESA)

N83-14616# Eidgenoessische Technische Hochschule, Zurich (Switzerland). Dept. of Geography.
REMOTE SENSING OF RENEWABLE NATURAL RESOURCES IN DEVELOPING COUNTRIES FOR NATIONAL PLANNING PURPOSES
H. HAEFNER and R. SCHOCH *In* ESA Satellite Remote Sensing for Developing Countries p 69-76 Jun. 1982 refs
Avail: NTIS HC A11/MF A01

The basic needs of a developing country regarding its renewable natural resources, exploitation of remote sensing technology as an aid to resource evaluation, planning and development, applications for which remote sensing techniques are of particular use, and the most appropriate approach to solving a defined application are considered. Case studies in the Yemen Arab Republic (inventory of land use acreage, monitoring seasonal and annual changes in renewable resources, forecasting agricultural yield) are reviewed. Experience suggests that systematic, accurate, synoptic, up to date information on renewable natural resources is indispensable for development planning. Only Earth resource satellites in combination with collatoral data can provide this information. Low to intermediate level technology is recommended. Author (ESA)

N83-14631# International Inst. for Aerial Survey and Earth Sciences, Delft (Netherlands).
SATELLITE REMOTE SENSING FOR DEVELOPING COUNTRIES: PROSPECTS AND CONSTRAINTS
C. VOUTE *In* ESA Satellite Remote Sensing for Developing Countries p 193-200 Jun. 1982 refs
Avail: NTIS HC A11/MF A01

Prospects and constraints of satellite remote sensing are discussed, focusing on the socioeconomic conditions and development objectives of the Third World and the necessity of preserving a sociocultural identity and pluriformity. It is concluded that endogenous adaptation of remote sensing techniques and methodologies should be promoted rather than a transfer of technology. This requires normative research in addition to application and technology oriented research. Author (ESA)

N83-14632# European Space Agency, Paris (France).
SATELLITE REMOTE SENSING: ESA'S EXPERIENCE WITH DEVELOPING COUNTRIES
V. A. HOOD *In its* Satellite Remote Sensing for Developing Countries p 201-204 Jun. 1982 refs
Avail: NTIS HC A11/MF A01

The data needs of developing nations, problems associated with remote sensing in Africa, Southeast Asia, and Latin America, and ESA satellite missions are discussed. METEOSAT, SPOT, the Spacelab metric camera, and ERS-1 all disseminate, or will disseminate, information to developing nations. Training programs are offered by ESA to these nations. A major criticism of cooperation projects is that the developing nations do not have enough time to assimilate and fully exploit a given program before it is replaced by a technologically more advanced one.
Author (ESA)

N83-14633# Bristol Univ. (England).
THE ROLE OF EARSEL AND EARSEL MEMBER LABORATORIES
E. C. BARRETT *In* ESA Satellite Remote Sensing for Developing Countries p 205-208 Jun. 1982
Avail: NTIS HC A11/MF A01

The role of EARSeL in method directory publication, data pooling, task force projects (especially in model testing and development), technical advice, education and training, and definition studies for future satellite products, sensors and systems is discussed. The establishment of an EARSeL Action Group to pursue such possibilities is urged. The advantages to the European Remote Sensing Community through greater exposure to and involvment in the pragmatic problem solving which situations in developing countries particularly demand are pointed out.
Author (ESA)

N83-15349*# National Aeronautics and Space Administration. Ames Research Center, Moffett Field, Calif.
TERRESTRIAL APPLICATIONS: AN INTELLIGENT EARTH-SENSING INFORMATION SYSTEM
In its Advan. Automation for Space Missions p 11-38 Nov. 1982 refs Document previously announced as A82-22149
Avail: NTIS HC A17/MF A01 CSCL 22B
For Abstract see A82-22149

N83-15739* General Electric Co., Fairfield, Conn.
LANDSAT-D: THE NEW ERA OF EARTH RESOURCES SURVEY
1982 12 p Sponsored by NASA Original contains color imagery. Original photography may be purchased from the EROS Data Center, Sioux Falls, S.D. 57198 ERTS
(E83-10125; NASA-CR-169727; NAS 1.26:169727) Avail: NTIS HC A02 CSCL 22B

The history of the development and utilization of LANDSAT satellites is summarized. Objectives of the LANDSAT D mission are listed and the capabilities of the 4-channel multispectral band scanner and the 7-channel radiometer (thematic mapper) to be carried on the satellite are described. Satellite components are illustrated and diagrams show the ground segment data management system, the data assessment system, and the operations control center. The flight segment of the mission and flight segment specifications are also described. Examples of digitally analyzed and ehanced imagery are included. A.R.H.

Typical Subject Index Listing

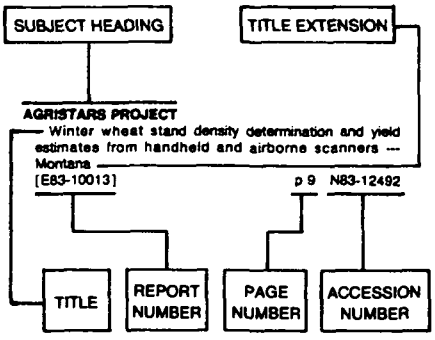

The subject heading is a key to the subject content of the document. The title is used to provide a description of the subject matter. When the title is insufficiently descriptive of the document content, the title extension is added, separated from the title by three hyphens. The (NASA or AIAA) accession number and the page number are included in each entry to assist the user in locating the abstract in the abstract section (of this supplement). If applicable, a report number is also included as an aid in identifying the document. Under any one subject heading, the accession numbers are arranged in sequence with the AIAA accession numbers appearing first.

A

ABSORPTIVITY
Optical parameters of leaves of seven weed species
[E83-10010] p 9 N83-12489
ACCURACY
Theoretical and experimental investigations on the accuracy of close-range photogrammetry
[SER-C-266] p 25 N83-11564
The applicability of satellite remote sensing to small and medium scale mapping p 64 N83-14618
ACID RAIN
A report to the President and the Congress
[AR-11] p 75 N83-11532
ADAPTIVE CONTROL
Scene classification of Landsat multispectral scanner data by means of the Adaptive Learning Network methodology p 55 A83-11458
AERIAL PHOTOGRAPHY
Analyzing and mapping regional land use trends by combining Landsat and topographic data p 2 A83-10119
The utilization of infrared /IR/ aerial and space observations of Arctic seas in navigation and during the solution of other national-economic problems p 40 A83-10836
A relational image data base system for remote sensing /LAND DBMS/ p 55 A83-11462
Mount St. Helens quick response damage assessment using high-altitude infrared photography p 19 A83-12672
Relaxation matching applied to aerial images p 56 A83-12889
Use of aerial photography with Loran C positioning to map offshore surface currents p 41 A83-14093
Monitoring revision requirements for Canadian maps p 24 A83-14237
Environmental monitoring of the Athabasca Oil Sands Region p 19 A83-14238
Vegetation and human impact mapping for the management of the sunshine area, Canadian Rocky Mountains p 20 A83-14242
Ecological land classification in the Yukon p 20 A83-14250
Remote sensing applications for British Columbia wetlands using 35 mm aerial photography p 51 A83-14251
Aerial survey of crop losses due to grasshoppers /Orthoptera - Acrididae/ in Saskatchewan p 5 A83-14255
Predicting forest land attributes from aerial photo interpretation variables p 5 A83-14259
Construction and interpretation of a thermal inertia image using airborne data p 57 A83-14260
Remote sensing and waste management p 20 A83-14263
Remote sensing software for airborne image analysis p 58 A83-14273
Cartographic aspects of dual-frequency dual-polarization SAR imagery p 58 A83-14280
A system for the complex processing of aerial and space data for agriculture p 6 A83-14301
Determination of forest fire spread rates from infrared photographs p 6 A83-14307
To mix or match - On choosing matched samples in comparative aerial surveys p 59 A83-14664
Aerial thermal infrared census of Canada geese in South Dakota p 6 A83-14665
Investigations of interpretability of images by different sensors and platforms for small scale mapping p 70 A83-14943
Remote determination of humus content in soils p 7 A83-15889
Super high altitude photography for coastal geomorphology --- from approximately 20 km altitude p 43 A83-17840
Some comparative aspects of SLAR and airphoto images for geomorphologic and geologic interpretation p 33 A83-17842
Aerial geologic log from Livermore, California to the Nevada Test Site, Nye County, Nevada
[DE82-018392] p 25 N83-10693
Investigation of the geometrical stability of a photogrammetric recording system --- systems stability
[SER-C-267] p 71 N83-11565
Determination of the contribution of side-looking airborne radar to structural geologic mapping
[PB82-185042] p 34 N83-12713
The Bering Sea ice cover during March 1979: Comparison of surface and satellite data with the Nimbus-7 SMMR
[NASA-CR-169393] p 47 N83-13572
Method of interpretation of remotely sensed data and applications to land use
[E83-10072] p 23 N83-14581
Tectonics of west central Mexico and adjacent Arizona: A remote sensing and field study in arid and semi-arid areas
[DE82-002393] p 37 N83-14797
AERIAL RECONNAISSANCE
Registration of a synthetic aperture radar /SAR/ reconnaissance image with a map reference data base p 56 A83-12885
Near surface observations p 61 N83-10464
Weather constraints on airborne laser hydrography operations
[PB82-189754] p 52 N83-10745
Statistical Techniques Applied to Aerial Radiometric Surveys (STARRS): Discriminant-analysis methods applied to aerial radiometric data and their application to uranium favorability in South Texas. Nation uranium resource evaluation
[DE82-020961] p 34 N83-12512
Airborne gamma-ray spectrometer and magnetometer survey. Volume 1. Detail areas, Christmas Mountains, Solitario, Green Valley/0-2 Ranch, Texas
[DE82-021614] p 34 N83-12513
AEROSOLS
Arctic haze and the Arctic gas and aerosol sampling program /AGASP/
[AIAA PAPER 83-0439] p 21 A83-16714
AEROSPACE SCIENCES
Global implications of space activities; Proceedings of the Conference, Aspen, CO, August 30-September 4, 1981 p 74 A83-17349
AEROSPACE TECHNOLOGY TRANSFER
Global implications of space activities; Proceedings of the Conference, Aspen, CO, August 30-September 4, 1981 p 74 A83-17349
AFRICA
An investigation of MAGSAT and complementary data emphasizing Precambrian shields and adjacent areas of West Africa and South America
[E83-10085] p 36 N83-14593
Multitemporal soil and vegetation observations by METEOSAT over Central Africa p 15 N83-14619
The determination of soil moisture balances in tropical Africa by satellite infrared remote sensing: The atmospheric problem p 53 N83-14621
AGRICULTURE
Action plan for remote sensing applications for rice production --- Book
[IFAORS-207] p 3 A83-14121
A procedure to overlay thematic map and dominion land survey system data to geometrically-corrected Landsat images and its application to agricultural land use studies in western Canada p 3 A83-14231
Potentials of Landsat-D and SPOT-1 for crop identification in the maritimes p 4 A83-14240
Landsat for delineation and mapping of saline soils in dryland areas in southern Alberta p 5 A83-14261
Office automation in resource-management - The future is now --- agricultural land use map dissemination p 6 A83-14269
A system for the complex processing of aerial and space data for agriculture p 6 A83-14301
The possible modifications of the Hisse model for pure LANDSAT agricultural data p 10 N83-12497
Development, implementation and evaluation of satellite-aided agricultural monitoring systems
[E83-10017] p 10 N83-12500
Multitemporal analysis of Landsat data for investigations of agricultural land use: Problems and potentials p 15 N83-14624
AGRISTARS PROJECT
AgRISTARS - Plans and first-year achievements --- Agriculture and Resources Inventory Surveys Through Aerospace Remote Sensing p 1 A83-10095
Influence of environmental factors during seed development and after full-ripeness on pre-harvest sprouting in wheat
[E83-10002] p 7 N83-12482
Second generation crop yield models review
[E83-10003] p 7 N83-12483
Performance comparison for Barnes model 12-1000, Exotech model 100, and Ideas Inc. Biometer Mark 2
[E83-10004] p 8 N83-12484
A three-part geometric model to predict the radar backscatter from wheat, corn, and sorghum
[E83-10005] p 8 N83-12485
AgRISTARS. Semiannual program review presentation to level 1, interagency Coordination Committee
[E83-10006] p 8 N83-12486
Evaluation of small area crop estimation techniques *using LANDSAT- and ground-derived data --- South* Dakota
[E83-10008] p 8 N83-12487
Discrimination of growth and water stress in wheat by various vegetation indices through a clear a turbid atmosphere
[E83-10009] p 8 N83-12488
Optical parameters of leaves of seven weed species
[E83-10010] p 9 N83-12489
Measurement of soil moisture using remote sensing multisensor radiation techniques
[E83-10012] p 9 N83-12491
Winter wheat stand density determination and yield estimates from handheld and airborne scanners --- Montana
[E83-10013] p 9 N83-12492
Development of a corn and soybean labeling procedure for use with profile parameter classification
[E83-10014] p 9 N83-12493

Development of advanced acreage estimation methods
[E83-10015] p 9 N83-12494
Data documentation for the 1981 summer vegetation experiment --- Kansas River floodplain
[E83-10016] p 10 N83-12499
Development, implementation and evaluation of satellite-aided agricultural monitoring systems
[E83-10017] p 10 N83-12500
Analysis of the profile characteristics of corn and soybeans using field reflectance data
[E83-10018] p 10 N83-12501
AgRISTARS documents tracking list report
[E83-10019] p 10 N83-12502
Assessment of radar resolution requirements for soil moisture estimation from simulated satellite imagery --- Kansas
[E83-10020] p 10 N83-12503
Extension of laboratory-measured soil spectra to field conditions
[E83-10021] p 11 N83-12504
Missing observations in multiyear rotation sampling designs
[E83-10022] p 11 N83-12505
Remote sensing of agricultural crops and soils
[E83-10023] p 11 N83-12506
Development of thematic mapper vegetative indices for assessing biomass in corn, soybeans and wheat
[E83-10035] p 11 N83-13529
Evaluation of the Williams-type spring wheat model in North Dakota and Minnesota
[E83-10041] p 12 N83-13535
Estimating total standing herbaceous biomass production with LANDSAT MSS digital data
[E83-10045] p 12 N83-13536
Monitoring global vegetation
[E83-10044] p 12 N83-14554
Investigation of remote sensing techniques of measuring soil moisture
[E83-10048] p 12 N83-14557
Diurnal patterns of wheat spectral reflectances and their importance in the assessment of canopy parameters from remotely sensed observations --- Phoenix, Arizona
[E83-10050] p 13 N83-14559
Construction of a remotely sensed area sampling frame for Southern Brazil
[E83-10052] p 13 N83-14561
Adjusting the tasseled cap brightness and greenness factors for atmospheric path radiance and absorption on a pixel by pixel basis
[E83-10053] p 13 N83-14562
Crop weather models of corn and soybeans for Agrophysical Units (APU's) in Iowa using monthly meteorological predictors
[E83-10054] p 13 N83-14563
Comparison of LANDSAT-2 and field spectrometer reflectance signatures of south Texas rangeland plant communities
[E83-10055] p 13 N83-14564
Comparison of the CEAS and Williams-type barley yield models for North Dakota and Minnesota
[E83-10056] p 13 N83-14565
Comparisons among a new soil index and other two- and four-dimensional vegetation indices
[E83-10058] p 14 N83-14567
Crop weather models of barley and spring wheat yield for agrophysical units in North Dakota
[E83-10059] p 14 N83-14568
Evaluation of the Williams-type model for barley yields in North Dakota and Minnesota
[E83-10060] p 14 N83-14569
Automated segment matching algorithm-theory, test, and evaluation
[E83-10096] p 16 N83-15740
Computer program documentation for the pasture/range condition assessment processor
[E83-10100] p 16 N83-15743
FORTRAN implementation of Friedman's test for several related samples
[E83-10123] p 18 N83-15793

AGROCLIMATOLOGY
An application of cluster analysis for determining homogeneous subregions: The agroclimatological point of view --- Rio Grande do Sul, Brazil
[E83-10067] p 14 N83-14576

AGROMETEOROLOGY
Crop weather models of corn and soybeans for Agrophysical Units (APU's) in Iowa using monthly meteorological predictors
[E83-10054] p 13 N83-14563
The Group Agromet Monitoring Project (GAMP) --- using METEOSAT for rangeland management in Mali
p 23 N83-14615

AIR LAND INTERACTIONS
An evaluation of four thermal models used in thermal inertia analysis --- for thermal mapping from remotely sensed data p 67 A83-10098

AIR POLLUTION
Evidence for a central Eurasian source area of arctic haze in Alaska p 18 A83-11626
A study of atmospheric diffusion from the Landsat imagery p 20 A83-14504
Development of mathematical techniques for the assimilation of remote sensing data into atmospheric models
[E83-10062] p 22 N83-14571

AIR QUALITY
Technology needs assessment of an atmospheric observation system for tropospheric research missions, part 1
[NASA-CR-3556] p 21 N83-10645
Technology needs assessment of an atmospheric observation system for multidisciplinary air quality/meteorology missions, part 2
[NASA-CR-3557] p 21 N83-10646

AIR SAMPLING
Arctic haze and the Arctic gas and aerosol sampling program /AGASP/
[AIAA PAPER 83-0439] p 21 A83-16714
Aircraft and remote measurements of atmospheric transport of pollutants within the global integrated monitoring system p 22 N83-12620

AIR SEA ICE INTERACTIONS
The utilization of infrared /IR/ aerial and space observations of Arctic seas in navigation and during the solution of other national-economic problems
p 40 A83-10836

AIR WATER INTERACTIONS
On the circulation of the western Gulf of Mexico - A satellite view p 39 A83-10113
Satellite estimates of ocean-air heat fluxes during cold air outbreaks p 41 A83-13059
Effects of mesoscale atmospheric convection cells on the waters of the East China Sea p 41 A83-13270
On the use of laser profilometry for ocean wave studies p 42 A83-14502
Joint Air Sea Interaction (JASIN) experiment, Northwest coast of Scotland
[NASA-CR-169631] p 48 N83-14603
Western Boundary Eddies of the Gulf Stream
p 49 N83-14847

AIRBORNE EQUIPMENT
Use of reflectance spectra of native plant species for interpreting airborne multispectral scanner data in the East *Tintic Mountains, Utah* p 30 A83-10060
Ka-band passive/active airborne radar
p 68 A83-11239
On the use of laser profilometry for ocean wave studies p 42 A83-14502
Measurements of ocean surface spectrum from an aircraft using the two-frequency microwave resonance technique p 43 A83-17710
Passive microwave detection of river-plume fronts in the German Bight p 52 A83-17713
Experimental feasibility of the airborne measurement of absolute oil fluorescence spectral conversion efficiency
p 44 A83-18581
Effects of detection algorithm on accuracy degradation from logarithmic and difference processing for airborne laser bathymetry returns
[PB82-215138] p 44 N83-10707
Aircraft and remote measurements of atmospheric transport of pollutants within the global integrated monitoring system p 22 N83-12620

AIRBORNE INTEGRATED RECONNAISSANCE SYSTEM
Remote sensing software for airborne image analysis
p 58 A83-14273

AIRBORNE/SPACEBORNE COMPUTERS
Operational planning of the process of earth survey by satellites p 70 A83-14314

AIRCRAFT INSTRUMENTS
The use of thematic mapper simulator calibration data for assessment of data quality
[NASA-TM-82059] p 71 N83-13547

ALASKA
Evidence for a central Eurasian source area of arctic haze in Alaska p 18 A83-11626

ALBEDO
Investigations of the apparent temperature of snow cover in the submillimeter wavelength region
p 52 A83-15816

ALGAE
HCMM hydrological analysis in Utah
[E83-10026] p 53 N83-13520

ALGORITHMS
Effects of detection algorithm on accuracy degradation from logarithmic and difference processing for airborne laser bathymetry returns
[PB82-215138] p 44 N83-10707
Automated segment matching algorithm-theory, test, and evaluation
[E83-10096] p 16 N83-15740
Proceedings of the NASA Workshop on Surface Fitting
[E83-10117] p 64 N83-15759

ALTIMETERS
Mean Earth ellipsoid determined from SEASAT altimeter observations
[AD-A117910] p 45 N83-11570
The accuracy of Seasat-1 altimeter altitude measurments under various sea state conditions
[RAE-TR-82059] p 47 N83-14553

ALTITUDE
Collinear-track altimetry in the Gulf of Mexico from SEASAT: Measurements, models and surface truth
[AD-A118160] p 45 N83-11568

ANDES MOUNTAINS (SOUTH AMERICA)
Temporary lakes and salt plains in the high plateaus of the Andes /Bolivia/ - A continuing survey of periodic hydrologic phenomena using the geostationary satellite GOES-EST p 51 A83-14574

ANEMOMETERS
The measurement of the synoptic scale wind over the ocean p 47 N83-13773

ANNUAL VARIATIONS
Photointerpretation of LANDSAT images
p 61 N83-10462
Multitemporal and geobotanical approach in the remote detection of Greisenization areas in the Serra da Pedra Branca Granite, Goias State, Brazil
[E83-10071] p 35 N83-14580

ANTARCTIC REGIONS
The application of microwave remote sensing for snow and ice research p 38 A83-10088
Investigations of the Arctic, the Antarctic and the world ocean; Conference-Seminar, Moscow, USSR, February 9-13, 1981, Reports p 39 A83-10826
Japanese MAGSAT Team
[E83-10080] p 27 N83-14589
Investigation of Antarctic crust and upper mantle using MAGSAT and other geophysical data
[E83-10086] p 27 N83-14594

ANTICLINES
An example of a statistical analysis of the results of space imagery interpretation for the eastern part of the Fergana Valley p 33 A83-14315

ANTICYCLONES
On the circulation of the western Gulf of Mexico - A satellite view p 39 A83-10113

APPROXIMATION
Surfaces: Representation and approximation
p 30 N83-15763

AQUICULTURE
Application of remote sensing techniques in oceanographic studies of the British Columbia Salmon Fishery p 41 A83-14258

ARCHAEOLOGY
Subsurface valleys and geoarcheology of the eastern Sahara revealed by Shuttle radar p 32 A83-13349

ARCTIC OCEAN
Tidal phenomena in Arctic Ocean ice /according to space data/ p 40 A83-10832
Some features of the spatial structure of the Arctic Ocean ice cover in connection with turbulent friction and geostrophic capture of tide waves p 40 A83-10833
The utilization of infrared /IR/ aerial and space observations of Arctic seas in navigation and during the solution of other national-economic problems
p 40 A83-10836

ARCTIC REGIONS
The application of microwave remote sensing for snow and ice research p 38 A83-10088
Investigations of the Arctic, the Antarctic and the world ocean; Conference-Seminar, Moscow, USSR, February 9-13, 1981, Reports p 39 A83-10826
Using new methods in monitoring the thermal regime of the Arctic p 39 A83-10828
Evidence for a central Eurasian source area of arctic haze in Alaska p 18 A83-11626
Predicting permafrost conditions with infrared sensing techniques p 6 A83-14264
Arctic haze and the Arctic gas and aerosol sampling program /AGASP/
[AIAA PAPER 83-0439] p 21 A83-16714

AREA
Estimation of the sugar cane cultivated area from LANDSAT images using the two phase sampling method
[E83-10077] p 15 N83-14586

ARID LANDS
Special reflectance of some plant indicators of saline and nonsaline soils
[AD-A119727] p 16 N83-14655

Tectonics of west central Mexico and adjacent Arizona: A remote sensing and field study in arid and semi-arid areas
[DE82-002393] p 37 N83-14797

ARIZONA
Diurnal patterns of wheat spectral reflectances and their importance in the assessment of canopy parameters from remotely sensed observations --- Phoenix, Arizona
[E83-10050] p 13 N83-14559
Tectonics of west central Mexico and adjacent Arizona: A remote sensing and field study in arid and semi-arid areas
[DE82-002393] p 37 N83-14797

ARTIFICIAL INTELLIGENCE
Terrestrial applications: An intelligent Earth-sensing information system p 76 N83-15349

ARTIFICIAL SATELLITES
Comparison of multichannel and two-satellite methods for remote measurement of sea surface temperature
[AD-A118736] p 45 N83-12511

ASTRONOMICAL COORDINATES
Concerning a method for the determination of initial geodetic data p 24 A83-17679

ATLANTIC OCEAN
A comparison of surfaces temperatures from HCMM infrared data with field measurements
[E83-10046] p 47 N83-14555
Western Boundary Eddies of the Gulf Stream p 49 N83-14847

ATMOSPHERIC ATTENUATION
Adjusting the tasseled cap brightness and greenness factors for atmospheric path radiance and absorption on a pixel by pixel basis
[E83-10053] p 13 N83-14562

ATMOSPHERIC BOUNDARY LAYER
Joint Air Sea Interaction (JASIN) experiment, Northwest coast of Scotland
[NASA-CR-169631] p 48 N83-14603

ATMOSPHERIC CIRCULATION
Accuracy of operational snow and ice charts p 50 A83-10090
Effects of mesoscale atmospheric convection cells on the waters of the East China Sea p 41 A83-13270
Spatial and temporal variations of large-scale subsidence and convection regions derived from satellite data
[PB82-219817] p 71 N83-13750

ATMOSPHERIC COMPOSITION
Arctic haze and the Arctic gas and aerosol sampling program /AGASP/
[AIAA PAPER 83-0439] p 21 A83-16714
Development of mathematical techniques for the assimilation of remote sensing data into atmospheric models
[E83-10062] p 22 N83-14571

ATMOSPHERIC DIFFUSION
A study of atmospheric diffusion from the Landsat imagery p 20 A83-14504

ATMOSPHERIC EFFECTS
Atmospheric effects on radiation reflected from soil and vegetation as measured by orbital sensors using various scanning directions p 3 A83-12315
A tutorial assessment of atmospheric height uncertainties for high-precision satellite altimeter missions to monitor ocean currents p 42 A83-14851
Comparison of diverse methods for the correction of atmospheric effects on LANDSAT and SKYLAB images --- radiometric correction in Brazil
[E83-10079] p 72 N83-14588
The determination of soil moisture balances in tropical Africa by satellite infrared remote sensing: The atmospheric problem p 53 N83-14621

ATMOSPHERIC HEATING
Satellite estimates of ocean-air heat fluxes during cold air outbreaks p 41 A83-13059

ATMOSPHERIC MODELS
Accuracy of operational snow and ice charts p 50 A83-10090
Development of mathematical techniques for the assimilation of remote sensing data into atmospheric models
[E83-10062] p 22 N83-14571

ATMOSPHERIC MOISTURE
The possibility of measuring the moisture content of the upper layers of the atmosphere using radiometric techniques p 70 A83-14308
Validation and application of the SEASAT-SMMR geophysical algorithms
[NASA-CR-169390] p 71 N83-13767

ATMOSPHERIC OPTICS
Automated measurements of atmospheric visibility
[AIAA PAPER 83-0436] p 21 A83-16713

ATMOSPHERIC PRESSURE
Australian drifting buoy p 48 N83-14837

ATMOSPHERIC RADIATION
Methods of editing cloud and atmospheric layer affected pixels from satellite data
[E83-10103] p 64 N83-15746

ATMOSPHERIC SCATTERING
Application of the airborne microwave rain-scattered/radiometer system to the remote sensing of rains and wind vector measurements over the ocean p 70 A83-14293

ATMOSPHERIC TEMPERATURE
Using new methods in monitoring the thermal regime of the Arctic p 39 A83-10828
Airborne atmospheric temperature structure measurements of a Pacific coast marine inversion
[AIAA PAPER 83-0278] p 70 A83-19585
Remote sensing of temperature profiles in the atmosphere p 66 N83-15778

ATMOSPHERIC TIDES
The role of cross-equatorial tropical cyclone pairs in the southern oscillation p 40 A83-13057

ATMOSPHERIC WINDOWS
Concerning the determination of the temperature of the ocean surface from multichannel satellite measurements of radiation in infrared atmospheric windows p 42 A83-14316

AUSTRALIA
The MAGSAT project in Australia
[E83-10089] p 28 N83-14597

AUTOMATIC CONTROL
Automated measurements of atmospheric visibility
[AIAA PAPER 83-0436] p 21 A83-16713

AUTOMATION
Office automation in resource-management - The future is now --- agricultural land use map dissemination p 6 A83-14269
Automation of the search for and recognition of reference zones for precise coordinate control of space imagery p 59 A83-14311

B

BACKSCATTERING
Radar spectral observations of snow p 49 A83-10064
A backscatter model for a randomly perturbed periodic surface --- furrowed soils in agricultural fields p 1 A83-10107
A parametric study of tillage effects on radar backscatter p 2 A83-10108
Estimating wind speed from HF skywave radar sea backscatter p 40 A83-11352
Microwave remote sensing: Active and passive. Volume 2 - Radar remote sensing and surface scattering and emission theory --- Book p 69 A83-14040
An optimum statistical technique for ozone profile retrieval from backscattered UV radiances p 21 A83-14632
A simple relation between active and passive microwave remote sensing measurements of earth terrain p 24 A83-14857
A backscatter model for a randomly perturbed periodic surface --- radar imagery of earth soil with row structure p 7 A83-14859

BANDWIDTH
An evaluation of the NASA/GSFC Barnes field spectral reflecometer model 14-758, using signal/noise as a measure of utility
[NASA-TM-83969] p 71 N83-12396

BARLEY
Comparison of the CEAS and Williams-type barley yield models for North Dakota and Minnesota
[E83-10056] p 13 N83-14565
Crop weather models of barley and spring wheat yield for agrophysical units in North Dakota
[E83-10059] p 14 N83-14568
Evaluation of the Williams-type model for barley yields in North Dakota and Minnesota
[E83-10060] p 14 N83-14569

BAROCLINIC INSTABILITY
Drift buoy component, NORPAX anomaly dynamics study p 49 N83-14848

BARREN LAND
Extension of laboratory-measured soil spectra to field conditions
[E83-10021] p 11 N83-12504

BATHYMETERS
Radiance calculations for optimization of sensors designed for remote bathymetry, volume 1
[AD-A117743] p 44 N83-10739

BAY ICE
Ice distribution and winter surface circulation patterns, Kachemak Bay, Alaska p 50 A83-12038

BAYS (TOPOGRAPHIC FEATURES)
Passive microwave detection of river-plume fronts in the German Bight p 52 A83-17713

BEACON SATELLITES
Operation and maintenance of geodetic satellite observatory, McMurdo, Antarctica
[PB82-187923] p 25 N83-12107

BEDROCK
An investigation into the utilization of HCMM thermal data for the descrimination of volcanic and Eolian geological units --- Craters of the Moon volcanic field, Idaho; San Francisco volcanic field, Arizona; High Desert, California; and the Cascade Range, California and Oregon
[E83-10047] p 35 N83-14556
Neotectonics of the San Andreas Fault system: Basin and range province juncture
[E83-10090] p 36 N83-14598
Analysis of the characteristics appearing in LANDSAT multispectral images in the geological structural mapping of the midwestern portion of the Rio Grande do Sul shield --- Brazil
[E83-10126] p 37 N83-15795

BEETLES
The application of remote sensing in southern Alberta's mountain pine beetle management p 5 A83-14257

BERING SEA
Comparison of environmental conditions in the Bering Sea and Davis Strait and the effects on microwave signature returns; March and April, 1979
[NASA-CR-169473] p 46 N83-12828
The Bering Sea ice cover during March 1979: Comparison of surface and satellite data with the Nimbus-7 SMMR
[NASA-CR-169393] p 47 N83-13572

BIBLIOGRAPHIES
Geographic research in the US Geological Survey: Bibliography, 1966 - 1980
[USGS-CIRC-865] p 21 N83-11639
AgRISTARS documents tracking list report
[E83-10019] p 10 N83-12502

BIHARMONIC EQUATIONS
Surface fitting with biharmonic and harmonic models p 65 N83-15764

BIOMASS
Remote measurement of biomass p 6 A83-14306
Extension of laboratory-measured soil spectra to field conditions
[E83-10021] p 11 N83-12504
Estimating total standing herbaceous biomass production with LANDSAT MSS digital data
[E83-10045] p 12 N83-13536
Rangeland biomass estimation demonstration --- Texas Experimenta Ranch
[E83-10113] p 17 N83-15756

BIOPHYSICS
Rice scene radiation research plan p 9 N83-12496

BIRDS
Aerial thermal infrared census of Canada geese in South Dakota p 6 A83-14665

BRAZIL
Use of LANDSAT images to study cerrado vegetation --- Mato Grosso Sul, Brazil
[E83-10025] p 11 N83-13519
Geological-structural interpretation using products of remote sensing in the region of Carrancas, Minas Gerais, Brazil
[E83-10029] p 34 N83-13523
An introduction to project Freeze --- the location and intensity of freezing temperatures using infrared satellite imagery
[INPE-2435-NTE/186] p 22 N83-13703
Construction of a remotely sensed area sampling frame for Southern Brazil
[E83-10052] p 13 N83-14561
CNPq/INPE-LANDSAT system report of activities
[E83-10064] p 63 N83-14573
Automatic interpretation of MSS-LANDSAT data applied to coal refuse site studies in southern Santa Catarina State, Brazil
[E83-10066] p 35 N83-14575
Vegetation survey in Amazonia using LANDSAT data --- Brazil
[E83-10068] p 14 N83-14577
Spectral discrimination of lithologic facies in the granite of the Pedra Branca Goias using LANDSAT 1 digital imagery
[E83-10069] p 35 N83-14578
Multitemporal and geobotanical approach in the remote detection of Greisenization areas in the Serra da Pedra Branca Granite, Goias State, Brazil
[E83-10071] p 35 N83-14580
LANDSAT and radar mapping of intrusive rocks in SE-Brazil
[E83-10073] p 36 N83-14582
Interpretation of remotely sensed data and its applications in oceanography
[E83-10074] p 48 N83-14583

Evaluation of reforestation using remote sensing techniques
[E83-10076] p 15 N83-14585
The computer treatment of remotely sensed data: An introduction to techniques which have geologic applications --- image enhancement and thematic classification in Brazil
[E83-10078] p 36 N83-14587
Verification of LANDSAT imagery for morphametric and topological studies of drainage basins in a section of the western plateau of Sao Paulo State: Tiete-Aguapei watershed --- Brazil
[E83-10111] p 54 N83-15754
Analysis of the characteristics appearing in LANDSAT multispectral images in the geological structural mapping of the midwestern portion of the Rio Grande do Sul shield --- Brazil
[E83-10126] p 37 N83-15795

BRAZILIAN SPACE PROGRAM
INPE LANDSAT-D thematic mapper computer compatible tape format specification
[E83-10075] p 63 N83-14584

BRIGHTNESS
Remote measurement of biomass p 6 A83-14306
Adjusting the tasseled cap brightness and greenness factors for atmospheric path radiance and absorption on a pixel by pixel basis
[E83-10053] p 13 N83-14562
Comparisons among a new soil index and other two- and four-dimensional vegetation indices
[E83-10058] p 14 N83-14567
A review of crop canopy reflectance models
[E83-10110] p 17 N83-15753

BRIGHTNESS TEMPERATURE
Microwave emission signatures of snow in Finland p 50 A83-10065
Microwave radiance of early fall sea ice at 1.55 cm p 38 A83-10091
The effect of monomolecular surface films on the microwave brightness temperature of the sea surface p 43 A83-17714
Other remote sensing systems: Retrospect and outlook p 74 N83-10467
Measurement of soil moisture using remote sensing multisensor radiation techniques
[E83-10012] p 9 N83-12491

BUOYS
Australian drifting buoy p 48 N83-14837
Mesoscale ocean variability p 48 N83-14841
Lagrangian drift measurements of sea surface currents and iceberg tracking p 49 N83-14842
The RAMS collection of meterological and position data in the Norwegian Sea p 49 N83-14845
Drift buoy component, NORPAX anomaly dynamics study p 49 N83-14848

C

C BAND
Comparison of environmental conditions in the Bering Sea and Davis Strait and the effects on microwave signature returns; March and April, 1979
[NASA-CR-169473] p 46 N83-12828

CALIBRATING
The use of thematic mapper simulator calibration data for assessment of data quality
[NASA-TM-82059] p 71 N83-13547

CALIFORNIA
Gates to Gregg high voltage transmission line study --- California
[E83-10097] p 16 N83-15741
CIRSS vertical data integration, San Bernardino County study phases 1-A, 1-B
[E83-10124] p 67 N83-15794
Infrared satellite data from the first coastal ocean dynamics experiment, March - July 1981
[AD-A120068] p 49 N83-15799

CANADA
Canadian Symposium on Remote Sensing, 7th, Winnipeg, Canada, September 8-11, 1981, Proceedings p 73 A83-14226
The importance of remote sensing for Canada - Past achievements, future needs p 74 A83-14227
The reduction, verification and interpretation of MAGSAT magnetic data over Canada
[E83-10091] p 28 N83-14599
The reduction, verification and interpretation of MAGSAT magnetic data over Canada
[E83-10101] p 29 N83-15744

CANADIAN SPACE PROGRAMS
Conference on Using Next Generation Earth Observation Satellites: Summary handbook p 62 N83-12508

CANOPIES (VEGETATION)
Application of computer axial tomography /CAT/ to measuring crop canopy geometry --- corn and soybeans p 1 A83-10096
Reflectance of a vegetation canopy using the Adding method p 3 A83-12603
Effects of vegetation cover on the radar sensitivity to soil moisture p 6 A83-14856
Reflectance differences between untreated and Mepiquat Chloride-treated, field-grown cotton through a growing season p 7 A83-16909
Rice scene radiation research plan p 9 N83-12496
Development of thematic mapper vegetative indices for assessing biomass in corn, soybeans and wheat
[E83-10035] p 11 N83-13529
Diurnal patterns of wheat spectral reflectances and their importance in the assessment of canopy parameters from remotely sensed observations --- Phoenix, Arizona
[E83-10050] p 13 N83-14559
A review of crop canopy reflectance models
[E83-10110] p 17 N83-15753
Remote Sensing Program
[E83-10120] p 18 N83-15790

CARBON DIOXIDE LASERS
Dual-wavelength correlation measurements with an airborne pulsed carbon dioxide lidar system p 60 A83-16831

CARIBOUS
Digital colour enhancement of Landsat data for mapping vegetation of barrenground caribou winter range in northern Manitoba p 5 A83-14249

CELESTIAL REFERENCE SYSTEMS
Basic research for the geodynamics program
[NASA-CR-169470] p 26 N83-13537
Effects of adopting new precession, nutation and equinox corrections on the terrestrial reference frame p 26 N83-13538

CENTER OF GRAVITY
The accuracy of Seasat-1 altimeter altitude measurments under various sea state conditions
[RAE-TR-82059] p 47 N83-14553

CENTRAL AFRICAN REPUBLIC
Gravimetric maps of the Central African Republic
[E83-10084] p 27 N83-14592

CENTRAL PROCESSING UNITS
Earth Observations Division version of the Laboratory for Applications of Remote Sensing System (EOD-LARSYS) user guide for the IBM 370/148. Volume 1: System overview
[E83-10007] p 62 N83-12866

CEYLON
Multistage land use mapping and change monitoring in Sri Lanka p 15 N83-14625

CHANNELS (DATA TRANSMISSION)
An evaluation of the NASA/GSFC Barnes field spectral reflecometer model 14-758, using signal/noise as a measure of utility
[NASA-TM-83969] p 71 N83-12396

CHARGE COUPLED DEVICES
Technical issues in focal plane development; Proceedings of the Meeting, Washington, DC, April 21, 22, 1981 p 69 A83-13726

CHLOROPHYLLS
Analysis of high altitude remotely sensed data collected in the Nantucket Shoals experiment 4-15 May, 1981
[NASA-TM-84547] p 44 N83-10647

CITIES
An evaluation of Seasat SAR imagery for urban analysis p 60 A83-16904

CITRUS TREES
Use of near-infrared video recording system for the detection of freeze damaged citrus leaves
[E83-10049] p 12 N83-14558

CLASSIFICATIONS
Probabilistic cluster labeling of imagery data p 54 A83-11410
A means for utilizing ancillary information in multispectral classification --- of remotely sensed data p 60 A83-16905
Some fundamental concepts in remote sensing p 60 N83-10459
Near surface observations p 61 N83-10464
Appendix B: Principles of computer processing of LANDSAT data p 75 N83-10470
AgRISTARS. Semiannual program review presentation to level 1, interagency Coordination Committee
[E83-10006] p 8 N83-12486
Evaluation of small area crop estimation techniques using LANDSAT- and ground-derived data --- South Dakota
[E83-10008] p 8 N83-12487
Development of a corn and soybean labeling procedure for use with profile parameter classification
[E83-10014] p 9 N83-12493
Development of advanced acreage estimation methods
[E83-10015] p 9 N83-12494
System support documentation: IDIMS FUNCTION AMOEBA p 9 N83-12495
The Akaike information criterion and its application to mixture proportion estimation p 62 N83-12498
LANDSAT land cover analysis completed for CIRSS/San Bernardino County project
[E83-10024] p 22 N83-12507
Earth Observations Division version of the Laboratory for Applications of Remote Sensing System (EOD-LARSYS) user guide for the IBM 370/148. Volume 1: System overview
[E83-10007] p 62 N83-12866
Construction of a remotely sensed area sampling frame for Southern Brazil
[E83-10052] p 13 N83-14561
Vegetation survey in Amazonia using LANDSAT data --- Brazil
[E83-10068] p 14 N83-14577
The computer treatment of remotely sensed data: An introduction to techniques which have geologic applications --- image enhancement and thematic classification in Brazil
[E83-10078] p 36 N83-14587
Contextual classification of multispectral image data: An unbiased estimator for the context distribution
[E83-10087] p 63 N83-14595
Agroecological classification by remote sensing techniques p 23 N83-14622

CLIMATOLOGY
Commission for Marine Technology: Abridged report of the 8th Session --- resolutions and recommendations for ocean exploration and exploitation
[WMO-584] p 46 N83-12803
Comparison of environmental conditions in the Bering Sea and Davis Strait and the effects on microwave signature returns; March and April, 1979
[NASA-CR-169473] p 46 N83-12828

CLOUD SEEDING
FACE-2 data reductions (prior to disclosure of the treatment decisions). Part 5: Satellite-estimated rainfall from a geostationary platform in FACE-2
[PB82-216581] p 52 N83-10730

CLOUDS (METEOROLOGY)
Methods of editing cloud and atmospheric layer affected pixels from satellite data
[E83-10103] p 64 N83-15746

CLUSTER ANALYSIS
Development of advanced acreage estimation methods
[E83-10015] p 9 N83-12494
The Akaike information criterion and its application to mixture proportion estimation p 62 N83-12498
An application of cluster analysis for determining homogeneous subregions: The agroclimatological point of view --- Rio Grande do Sul, Brazil
[E83-10067] p 14 N83-14576
Agroecological classification by remote sensing techniques p 23 N83-14622

COAL
Automatic interpretation of MSS-LANDSAT data applied to coal refuse site studies in southern Santa Catarina State, Brazil
[E83-10066] p 35 N83-14575

COASTAL CURRENTS
Western Boundary Eddies of the Gulf Stream p 49 N83-14847

COASTAL WATER
Detection of coastal zone environmental conditions using synthetic aperture radar p 38 A83-10068
A comparison data set for the evaluation of remote sensing systems ability for ocean wave data collection p 38 A83-10071
Application of remote sensing techniques in oceanographic studies of the British Columbia Salmon Fishery p 41 A83-14258
Passive microwave detection of river-plume fronts in the German Bight p 52 A83-17713
Analysis of high altitude remotely sensed data collected in the Nantucket Shoals experiment 4-15 May, 1981
[NASA-TM-84547] p 44 N83-10647
Interpretation of remotely sensed data and its applications in oceanography
[E83-10074] p 48 N83-14583
Infrared satellite data from the first coastal ocean dynamics experiment, March - July 1981
[AD-A120068] p 49 N83-15799

COASTAL ZONE COLOR SCANNER
Phytoplankton pigment concentrations in the Middle Atlantic Bight - Comparison of ship determinations and CZCS estimates --- Coastal Zone Color Scanner p 43 A83-18580

COASTS
Super high altitude photography for coastal geomorphology --- from approximately 20 km altitude p 43 A83-17840
COLD FRONTS
Satellite estimates of ocean-air heat fluxes during cold air outbreaks p 41 A83-13059
COLD WEATHER
Use of thermal inertia determined by HCMM to predict nocturnal cold prone areas in Florida [E83-10028] p 62 N83-13522
Use of thermal inertia determined by HCMM to predict nocturnal cold prone areas in Florida [E83-10102] p 64 N83-15745
COLLINEARITY
Collinear-track altimetry in the Gulf of Mexico from SEASAT: Measurements, models and surface truth [AD-A118160] p 45 N83-11568
COLOR
Some spectral and spatial characteristics of LANDSAT data p 61 N83-10461
COLOR INFRARED PHOTOGRAPHY
Evaluation of photographic enhancements of Landsat imagery p 55 A83-12035
Environmental monitoring of the Athabasca Oil Sands Region p 19 A83-14238
Remote sensing applications for British Columbia wetlands using 35 mm aerial photography p 51 A83-14251
The application of remote sensing in southern Alberta's mountain pine beetle management p 5 A83-14257
Predicting permafrost conditions with infrared sensing techniques p 6 A83-14264
Remote measurement of biomass p 6 A83-14306
COLOR PHOTOGRAPHY
Remote sensing applications for British Columbia wetlands using 35 mm aerial photography p 51 A83-14251
Colour Landsat images and mosaics - Basic tools in areal and ecological differentiation in Canada p 57 A83-14265
COLORADO
Snowmelt runoff modeling in simulation and forecasting modes with the Martinec-Mango model [E83-10063] p 53 N83-14572
COMPUTER COMPATIBLE TAPES
Standardization of computer compatible tape formats for remote sensing data p 54 A83-10075
INPE LANDSAT-D thematic mapper computer compatible tape format specification [E83-10075] p 63 N83-14584
COMPUTER GRAPHICS
Results of stereoscopic image simulations for the SPOT HRV carried out at the Gun Lake site in British Columbia p 20 A83-14292
Geographic information systems p 61 N83-10465
A practical automated mapping system p 64 N83-14635
COMPUTER PROGRAMS
Remote sensing software for airborne image analysis p 58 A83-14273
The digital image processing system MOBI-DIVAH p 59 A83-14944
System support documentation: IDIMS FUNCTION AMOEBA p 9 N83-12495
Computer program documentation for the pasture/range condition assessment processor [E83-10100] p 16 N83-15743
FORTRAN implementation of Friedman's test for several related samples [E83-10123] p 18 N83-15793
COMPUTER TECHNIQUES
Application of computer axial tomography /CAT/ to measuring crop canopy geometry --- corn and soybeans p 1 A83-10096
An experimental Landsat Quicklook System for Alaska p 57 A83-14271
The LANDSAT tutorial workbook: Basics of satellite remote sensing [E83-10001] p 74 N83-10458
Computer processed LANDSAT data p 61 N83-10463
Appendix B: Principles of computer processing of LANDSAT data p 75 N83-10470
Analysis of geologic terrain models for determination of optimum SAR sensor configuration and optimum information extraction for exploration of global non-renewable resources. Pilot study: Arkansas Remote Sensing Laboratory, part 1, part 2, and part 3 [E83-10061] p 35 N83-14570
The computer treatment of remotely sensed data: An introduction to techniques which have geologic applications --- image enhancement and thematic classification in Brazil [E83-10078] p 36 N83-14587
The MAGSAT project in Australia [E83-10089] p 28 N83-14597
Methods of editing cloud and atmospheric layer affected pixels from satellite data [E83-10103] p 64 N83-15746
Proceedings of the NASA Workshop on Image Analysis [E83-10118] p 65 N83-15766
Automatic photointerpretation via texture and morphology analysis p 65 N83-15770
COMPUTERIZED SIMULATION
Geological terrain models p 31 A83-10080
Theoretical and experimental investigations on the accuracy of close-range photogrammetry [SER-C-266] p 25 N83-11564
CONFERENCES
Investigations of the Arctic, the Antarctic and the world ocean; Conference-Seminar, Moscow, USSR, February 9-13, 1981, Reports p 39 A83-10826
Spacelab, space platforms and the future; Proceedings of the Fourth Joint AAS/DGLR Symposium and Twentieth Goddard Memorial Symposium, Washington, DC, March 17-19, 1982 p 73 A83-11926
Electro-optical instrumentation for resources evaluation; Proceedings of the Meeting, Washington, DC, April 21, 22, 1981 p 68 A83-12669
Technical issues in focal plane development; Proceedings of the Meeting, Washington, DC, April 21, 22, 1981 p 69 A83-13726
Canadian Symposium on Remote Sensing, 7th, Winnipeg, Canada, September 8-11, 1981, Proceedings p 73 A83-14226
Global implications of space activities; Proceedings of the Conference, Aspen, CO, August 30-September 4, 1981 p 74 A83-17349
Conference on Using Next Generation Earth Observation Satellites: Summary handbook p 62 N83-12508
On the Development of Multimedia Monitoring of Environmental Pollution --- conferences [WMO-563] p 22 N83-12599
Report of the Monex review meeting [GARP-SPEC-REPT-38] p 45 N83-12707
Satellite remote sensing for developing countries --- conference [ESA-SP-175] p 75 N83-14608
Proceedings of the NASA Workshop on Image Analysis [E83-10118] p 65 N83-15766
Proceedings of the NASA Workshop on Density Estimation and Function Smoothing [E83-10119] p 66 N83-15774
CONGRESSIONAL REPORTS
A report to the President and the Congress [AR-11] p 75 N83-11532
CONICAL SCANNING
The conical scan radiometer --- satellite-borne radiometer p 72 N83-14804
CONIFERS
Assessment of spruce budworm defoliation using digital airborne MSS data p 5 A83-14248
The application of remote sensing in southern Alberta's mountain pine beetle management p 5 A83-14257
Detection of aspen-conifer forest mixes from LANDSAT digital data --- Utah-Idaho Bear River Range [E83-10106] p 17 N83-15749
CONTAMINANTS
Development of mathematical techniques for the assimilation of remote sensing data into atmospheric models [E83-10062] p 22 N83-14571
CONTEXT
Contextual classification of multispectral image data: An unbiased estimator for the context distribution [E83-10087] p 63 N83-14595
CONTINENTAL SHELVES
A report to the President and the Congress [AR-11] p 75 N83-11532
Western Boundary Eddies of the Gulf Stream p 49 N83-14847
CONVECTION CURRENTS
Effects of mesoscale atmospheric convection cells on the waters of the East China Sea p 41 A83-13270
CONVECTIVE FLOW
Spatial and temporal variations of large-scale subsidence and convection regions derived from satellite data [PB82-219817] p 71 N83-13750
CONVERGENCE
Topics in global convergence of density estimates p 66 N83-15775
COORDINATE TRANSFORMATIONS
Coordinate transformation during the geometric correction of the space scanner imagery of the earth p 70 A83-14313
COORDINATES
TOPEX orbit determination using GPS signals plus a sidetone ranging system [NASA-CR-169694] p 29 N83-14606
An upper bound on errors in the mean-of-date/instantaneous Earth-fixed vector transformation induced by interpolated nutation angles [AD-A119444] p 29 N83-14656
Surfaces: Representation and approximation p 30 N83-15763
CORN
Application of computer axial tomography /CAT/ to measuring crop canopy geometry --- corn and soybeans p 1 A83-10096
A three-part geometric model to predict the radar backscatter from wheat, corn, and sorghum [E83-10005] p 8 N83-12485
Development of a corn and soybean labeling procedure for use with profile parameter classification [E83-10014] p 9 N83-12493
Data documentation for the 1981 summer vegetation experiment --- Kansas River floodplain [E83-10016] p 10 N83-12499
Development, implementation and evaluation of satellite-aided agricultural monitoring systems [E83-10017] p 10 N83-12500
Analysis of the profile characteristics of corn and soybeans using field reflectance data [E83-10018] p 10 N83-12501
Remote sensing of agricultural crops and soils [E83-10023] p 11 N83-12506
Development of thematic mapper vegetative indices for assessing biomass in corn, soybeans and wheat [E83-10035] p 11 N83-13529
Crop weather models of corn and soybeans for Agrophysical Units (APU's) in Iowa using monthly meteorological predictors [E83-10054] p 13 N83-14563
CORRELATION
Analyses of oceanic subsurface features using space based radar imagery [AD-A118411] p 45 N83-11692
COSMONAUTS
Salyut-7 from June to August p 74 A83-17775
COST EFFECTIVENESS
Some closing thoughts: Practical payoffs from satellite systems p 74 N83-10468
COTTON
Reflectance measurement of artificially induced ultraviolet radiation stress on cotton leaves p 7 A83-16907
Reflectance differences between untreated and Mepiquat Chloride-treated, field-grown cotton through a growing season p 7 A83-16909
CRATERS
The geology of Europa p 24 A83-16239
CROP CALENDARS
Crop-phenology and LANDSAT-based irrigated lands inventory in the high plains --- Texas, New Mexico, Oklahma, Kansas, Colorado, Nebraska, Wyoming, and South Dakota [E83-10115] p 18 N83-15758
CROP GROWTH
Action plan for remote sensing applications for rice production --- Book [IFAORS-207] p 3 A83-14121
Second generation crop yield models review [E83-10003] p 7 N83-12483
Discrimination of growth and water stress in wheat by various vegetation indices through a clear a turbid atmosphere [E83-10009] p 8 N83-12488
CROP IDENTIFICATION
Satellite orbital dynamics and observation strategies in support of agricultural applications p 2 A83-10717
Satellite remote sensing for domestic crop reporting in the United States and Canada - A look to the future p 3 A83-14229
Vegetation change detection in an agricultural area - A simple approach for use with geo-data base p 4 A83-14236
Potentials of Landsat-D and SPOT-1 for crop identification in the maritimes p 4 A83-14240
Development of a corn and soybean labeling procedure for use with profile parameter classification [E83-10014] p 9 N83-12493
Rice scene radiation research plan p 9 N83-12496
Data documentation for the 1981 summer vegetation experiment --- Kansas River floodplain [E83-10016] p 10 N83-12499
Analysis of the profile characteristics of corn and soybeans using field reflectance data [E83-10018] p 10 N83-12501
Agricultural Research Service research highlights in remote sensing for calendar year 1981 [E83-10051] p 75 N83-14560

An automatic agricultural zone classification procedure for crop inventory satellite images
[E83-10065] p 14 N83-14574
Gates to Gregg high voltage transmission line study --- California
[E83-10097] p 16 N83-15741
A review of crop canopy reflectance models
[E83-10110] p 17 N83-15753
Crop-phenology and LANDSAT-based irrigated lands inventory in the high plains --- Texas, New Mexico, Oklahma, Kansas, Colorado, Nebraska, Wyoming, and South Dakota
[E83-10115] p 18 N83-15758
Cooperative processes in image segmentation
p 65 N83-15768

CROP INVENTORIES
AgRISTARS - Plans and first-year achievements --- Agriculture and Resources Inventory Surveys Through Aerospace Remote Sensing p 1 A83-10095
Visual analysis of 1:250,000 Landsat data for forage assessment during the 1980 drought in western Manitoba p 3 A83-14235
Aerial survey of crop losses due to grasshoppers /Orthoptera - Acrididae/ in Saskatchewan
p 5 A83-14255
The use of large-area spectral data in wheat yield estimation p 7 A83-16910
Second generation crop yield models review
[E83-10003] p 7 N83-12483
AgRISTARS. Semiannual program review presentation to level 1, interagency Coordination Committee
[E83-10006] p 8 N83-12486
Evaluation of small area crop estimation techniques using LANDSAT- and ground-derived data --- South Dakota
[E83-10008] p 8 N83-12487
Measurement of soil moisture using remote sensing multisensor radiation techniques
[E83-10012] p 9 N83-12491
Winter wheat stand density determination and yield estimates from handheld and airborne scanners --- Montana
[E83-10013] p 9 N83-12492
Development of a corn and soybean labeling procedure for use with profile parameter classification
[E83-10014] p 9 N83-12493
Development of advanced acreage estimation methods
[E83-10015] p 9 N83-12494
Development, implementation and evaluation of satellite-aided agricultural monitoring systems
[E83-10017] p 10 N83-12500
Missing observations in multiyear rotation sampling designs
[E83-10022] p 11 N83-12505
Evaluation of the Williams-type spring wheat model in North Dakota and Minnesota
[E83-10041] p 12 N83-13535
Estimating total standing herbaceous biomass production with LANDSAT MSS digital data
[E83-10045] p 12 N83-13536
Comparison of the CEAS and Williams-type barley yield models for North Dakota and Minnesota
[E83-10056] p 13 N83-14565
Crop weather models of barley and spring wheat yield for agrophysical units in North Dakota
[E83-10059] p 14 N83-14568
Evaluation of the Williams-type model for barley yields in North Dakota and Minnesota
[E83-10060] p 14 N83-14569
An automatic agricultural zone classification procedure for crop inventory satellite images
[E83-10065] p 14 N83-14574
An application of cluster analysis for determining homogeneous subregions: The agroclimatological point of view --- Rio Grande do Sul, Brazil
[E83-10067] p 14 N83-14576
Estimation of the sugar cane cultivated area from LANDSAT images using the two phase sampling method
[E83-10077] p 15 N83-14586
Crop proportion estimation problems in AgRISTARS
p 18 N83-15760
Remote Sensing Program
[E83-10120] p 18 N83-15790

CROP VIGOR
Application of computer axial tomography /CAT/ to measuring crop canopy geometry — corn and soybeans
p 1 A83-10096
Atmospheric effects on radiation reflected from soil and vegetation as measured by orbital sensors using various scanning directions p 3 A83-12315
Influence of environmental factors during seed development and after full-ripeness on pre-harvest sprouting in wheat
[E83-10002] p 7 N83-12482
Computer program documentation for the pasture/range condition assessment processor
[E83-10100] p 16 N83-15743

CRUSTAL FRACTURES
Basic research for the geodynamics program
[NASA-CR-169470] p 26 N83-13537

CUBA
Investigating the possibility of producing a land-use map for Cuba on the basis of space imagery
p 20 A83-14305

CYCLONES
The role of cross-equatorial tropical cyclone pairs in the southern oscillation p 40 A83-13057

D

DAMAGE
Use of near-infrared video recording system for the detection of freeze damaged citrus leaves
[E83-10049] p 12 N83-14558

DAMAGE ASSESSMENT
Landsat observations of Mount St. Helens
p 19 A83-12671
Mount St. Helens quick response damage assessment using high-altitude infrared photography
p 19 A83-12672

DATA ACQUISITION
Combining land use data acquired from Landsat with soil map data p 2 A83-10117
Analytical plotter for data input into geo-based information systems p 56 A83-12683
Reference quicklook images for monitor of Landsat image data acquisition p 58 A83-14286
Water survey of Canada's experience with data acquisition and telemetry systems p 51 A83-14287
Dual-wavelength correlation measurements with an airborne pulsed carbon dioxide lidar system
p 60 A83-16831
A means for utilizing ancillary information in multispectral classification --- of remotely sensed data
p 60 A83-16905
Remote sensing, a tool for managing the marine environment: Eight case studies
[PB82-220864] p 44 N83-10483
Operation and maintenance of geodetic satellite observatory, McMurdo, Antarctica
[PB82-187923] p 25 N83-12107
Manual on the global observing system. Volume 1 (annex to the WMO technical regulations): Global aspects, 1981 edition
[WMO-544-VOL-1-ANNEX] p 46 N83-12801
Neotectonics of the San Andreas Fault system: Basin and range province juncture
[E83-10090] p 36 N83-14598

DATA BASE MANAGEMENT SYSTEMS
A relational image data base system for remote sensing /LAND DBMS/ p 55 A83-11462

DATA BASES
Registration of a synthetic aperture radar /SAR/ reconnaissance image with a map reference data base
p 56 A83-12885
Definition and potential of geocoded satellite imagery products p 58 A83-14272
A means for utilizing ancillary information in multispectral classification --- of remotely sensed data
p 60 A83-16905
Geographic information systems p 61 N83-10465
Satellite observations of variations in Northern Hemisphere seasonal snow cover
[PB82-196668] p 52 N83-10734
Remote sensing applications to the development of an integrated data base for oil and gas exploration
p 37 N83-14628
The RAMS collection of meterological and position data in the Norwegian Sea p 49 N83-14845

DATA COLLECTION PLATFORMS
Performance assessment of future European remote sensing systems p 2 A83-10109
Water survey of Canada's experience with data acquisition and telemetry systems p 51 A83-14287
Nimbus 6 Random Access Measurement System applications experiments
[NASA-SP-457] p 48 N83-14835

DATA CORRELATION
Dual-wavelength correlation measurements with an airborne pulsed carbon dioxide lidar system
p 60 A83-16831
A comparison of HCMM surface temperatures with in situ temperature data — Nantucket shoals and the Gulf of Mexico regions
[E83-10040] p 46 N83-13534
An analysis of a relaxation scheme to improve terrain elevation data
[AD-A119257] p 27 N83-13550
Investigation of MAGSAT and TRIAD magnetometer data to provide corrective information on high-lattitude external fields
[E83-10093] p 28 N83-14600
Combined use of daily thermal cycle of METEOSAT imagery and multispectral LANDSAT data: Application to the Bandiagara plateau, Mali p 36 N83-14620
Space truth in oceanography p 48 N83-14636
Rangeland biomass estimation demonstration --- Texas Experimenta Ranch
[E83-10113] p 17 *N83-15756*

DATA INTEGRATION
CIRSS vertical data integration, San Bernardino County study phases 1-A, 1-B
[E83-10124] p 67 N83-15794
CIRSS vertical data integration, San Bernardino study
[E83-10127] p 67 N83-15796

DATA MANAGEMENT
Geographic information systems p 61 N83-10465
Development of a data management front end for use with a LANDSAT based information system --- assessing gypsy moth defoliation damage in Pennsylvania
[E83-10104] p 17 N83-15747

DATA PROCESSING
Use of reflectance spectra of native plant species for interpreting airborne multispectral scanner data in the East Tintic Mountains, Utah p 30 A83-10060
Standardization of computer compatible tape formats for remote sensing data p 54 A83-10075
Visual analysis of 1:250,000 Landsat data for forage assessment during the 1980 drought in western Manitoba p 3 A83-14235
Appendix A: The LANDSAT system
p 75 N83-10469
Appendix B: Principles of computer processing of LANDSAT data p 75 N83-10470
Evaluation of geodetic products produced by the NSWC reduction of SEASAT radar altimeter data
[AD-A117837] p 25 N83-11571
Earth Observations Division version of the Laboratory for Applications of Remote Sensing System (EOD-LARSYS) user guide for the IBM 370/148. Volume 1: System overview
[E83-10007] p 62 N83-12866
Use of thermal inertia determined by HCMM to predict nocturnal cold prone areas in Florida
[E83-10028] p 62 N83-13522
Gravity and magnetic anomaly data analysis
[E83-10031] p 26 N83-13525
MAGSAT and aeromagnetic data of the continental US
[E83-10033] p 26 N83-13527
Further SEASAT SAR coastal ocean wave analysis
[NASA-CR-169682] p 47 N83-13776
MAGSAT anomaly field inversion and interpretation for the US
[E83-10057] p 27 N83-14566
Development of mathematical techniques for the assimilation of remote sensing data into atmospheric models
[E83-10062] p 22 N83-14571
CNPq/INPE-LANDSAT system report of activities
[E83-10064] p 63 N83-14573
Japanese MAGSAT Team
[E83-10080] p 27 N83-14589
Equivalent source modeling of the main field using MAGSAT data
[E83-10094] p 28 N83-14601
Multitemporal analysis of Landsat data for investigations of agricultural land use: Problems and potentials
p 15 N83-14624
Use of thermal inertia determined by HCMM to predict nocturnal cold prone areas in Florida
[E83-10102] p 64 N83-15745
Proceedings of the NASA Workshop on Surface Fitting
[E83-10117] p 64 N83-15759
Fitting surfaces to scattered data p 65 N83-15761
C-1 surface interpolation for scattered data on a sphere p 65 N83-15762
Surfaces: Representation and approximation
p 30 N83-15763
Surface fitting with biharmonic and harmonic models
p 65 N83-15764
BSPLASH: A three-stage surface interpolant to scattered data p 65 N83-15765
FORTRAN implementation of Friedman's test for several related samples
[E83-10123] p 18 N83-15793

DATA PROCESSING TERMINALS
Operation plan for the data 100/LARS terminal system
[E83-10011] p 62 N83-12490

DATA RECORDING
CNPq/INPE-LANDSAT system report of activities
[E83-10064] p 63 N83-14573

DATA REDUCTION
Scene classification of Landsat multispectral scanner data by means of the Adaptive Learning Network methodology p 55 A83-11458
A means for utilizing ancillary information in multispectral classification — of remotely sensed data p 60 A83-16905
Computer processed LANDSAT data p 61 N83-10463
SEASAT-A SASS wind processing [NASA-CR-169433] p 44 N83-10473
Analysis of MAGSAT data of the Indian region [E83-10027] p 25 N83-13521
MAGSAT for geomagnetic studies over Indian region [E83-10032] p 26 N83-13526
Monitoring global vegetation [E83-10044] p 12 N83-14554
Investigation of Antarctic crust and upper mantle using MAGSAT and other geophysical data [E83-10086] p 27 N83-14594
The MAGSAT project in Australia [E83-10089] p 28 N83-14597
The reduction, verification and interpretation of MAGSAT magnetic data over Canada [E83-10091] p 28 N83-14599
Multitemporal analysis of Landsat data for investigations of agricultural land use: Problems and potentials p 15 N83-14624
The reduction, verification and interpretation of MAGSAT magnetic data over Canada [E83-10101] p 29 N83-15744
Detection of aspen-conifer forest mixes from LANDSAT digital data — Utah-Idaho Bear River Range [E83-10106] p 17 N83-15749
The application of remote sensing to resource management and environmental quality programs in Kansas [E83-10114] p 23 N83-15757
LANDSAT 4 investigations of thematic mapper and multispectral scanner applications [E83-10121] p 66 N83-15791

DATA SAMPLING
To mix or match - On choosing matched samples in comparative aerial surveys p 59 A83-14664
Missing observations in multiyear rotation sampling designs [E83-10022] p 11 N83-12505
Construction of a remotely sensed area sampling frame for Southern Brazil [E83-10052] p 13 N83-14561

DATA SIMULATION
Analysis of geologic terrain models for determination of optimum SAR sensor configuration and optimum information extraction for exploration of global non-renewable resources. Pilot study: Arkansas Remote Sensing Laboratory, part 1, part 2, and part 3 [E83-10061] p 35 N83-14570
Spectral characterization of the LANDSAT-D multispectral scanner subsystems [E83-10107] p 17 N83-15750

DATA SMOOTHING
Proceedings of the NASA Workshop on Density Estimation and Function Smoothing [E83-10119] p 66 N83-15774
Topics in global convergence of density estimates p 66 N83-15775

DATA SYSTEMS
Analytical plotter for data input into geo-based information systems p 56 A83-12683
Appendix A: The LANDSAT system p 75 N83-10469
System support documentation: IDIMS FUNCTION AMOEBA p 9 N83-12495
Some aspects of the presentation of remote sensing data p 63 N83-14617

DATA TRANSMISSION
Hydrological data transmission [WMO-559] p 53 N83-12514
Nimbus 6 Random Access Measurement System applications experiments [NASA-SP-457] p 48 N83-14835
Mesoscale ocean variability p 48 N83-14841

DEATH VALLEY (CA)
Geologic interpretation of HCMM and aircraft thermal data [E83-10036] p 62 N83-13530

DECIDUOUS TREES
Detection of aspen-conifer forest mixes from LANDSAT digital data — Utah-Idaho Bear River Range [E83-10106] p 17 N83-15749

DEER
Integration of Landsat imagery into a program for aerial surveying of deer populations in Alberta p 5 A83-14252
A multispectral approach to remote detection of deer p 6 A83-14666

DEFENSE INDUSTRY
Defense Mapping Agency /DMA/ overview of mapping, charting, and geodesy /MC&G/ applications of digital image pattern recognition p 24 A83-12877

DEFOLIATION
Assessment of spruce budworm defoliation using digital airborne MSS data p 5 A83-14248
Development of a data management front end for use with a LANDSAT based information system — assessing gypsy moth defoliation damage in Pennsylvania [E83-10104] p 17 N83-15747

DELINEATION
Landsat for delineation and mapping of saline soils in dryland areas in southern Alberta p 5 A83-14261

DENMARK
Multitemporal analysis of Landsat data for investigations of agricultural land use: Problems and potentials p 15 N83-14624

DEPTH MEASUREMENT
Evaluating depth to shallow groundwater using heat capacity mapping mission /HCMM/ data p 51 A83-14668
Effects of detection algorithm on accuracy degradation from logarithmic and difference processing for airborne laser bathymetry returns [PB82-215138] p 44 N83-10707
Radiance calculations for optimization of sensors designed for remote bathymetry, volume 1 [AD-A117743] p 44 N83-10739

DESERTLINE
Approaches to desertification monitoring in the Sudan p 23 N83-14623

DETECTORS
Radiance calculations for optimization of sensors designed for remote bathymetry, volume 1 [AD-A117743] p 44 N83-10739

DEVELOPING NATIONS
Photointerpretation, remote sensing, and photogrammetric elements applied to road-planning studies p 19 A83-11866
Satellite remote sensing for developing countries — conference [ESA-SP-175] p 75 N83-14608
The European Community, development and satellite technology p 75 N83-14609
Remote sensing in developing countries. FAO'S international experience p 76 N83-14614
Remote sensing of renewable natural resources in developing countries for national planning purposes p 76 N83-14616
Satellite remote sensing in mineral exploration in developing countries p 36 N83-14627
Satellite remote sensing for developing countries: Prospects and constraints p 76 N83-14631
Satellite remote sensing: ESA's experience with developing countries p 76 N83-14632
The role of EARSeL and EARSeL member laboratories — in developing nations p 76 N83-14633

DIELECTRICS
Remote sensing of dielectric media with periodic rough surfaces — microwave scattering from farmfields p 1 A83-10106

DIGITAL DATA
Analyzing and mapping regional land use trends by combining Landsat and topographic data p 2 A83-10119
Pattern recognition and digital image processing as applied to remote sensing in India p 54 A83-11450
Defense Mapping Agency /DMA/ overview of mapping, charting, and geodesy /MC&G/ applications of digital image pattern recognition p 24 A83-12877
Quality assessment of remote-sensing data - The SAR case p 56 A83-13845
Assessment of spruce budworm defoliation using digital airborne MSS data p 5 A83-14248
Surficial geology mapping from Landsat-Kaminak Lake, N.W.T. p 32 A83-14268
Geographic information systems p 61 N83-10465
Appendix A: The LANDSAT system p 75 N83-10469
Satellite observations of variations in Northern Hemisphere seasonal snow cover [PB82-196668] p 52 N83-10734
Spectral discrimination of lithologic facies in the granite of the Pedra Branca Goias using LANDSAT 1 digital imagery [E83-10069] p 35 N83-14578
The computer treatment of remotely sensed data: An introduction to techniques which have geologic applications — image enhancement and thematic classification in Brazil [E83-10078] p 36 N83-14587
Neotectonics of the San Andreas Fault system: Basin and range province juncture [E83-10090] p 36 N83-14598

DIGITAL RADAR SYSTEMS
The CCRS SAR processing system p 69 A83-14289

DIGITAL TECHNIQUES
Digital colour enhancement of Landsat data for mapping vegetation of barrenground caribou winter range in northern Manitoba p 5 A83-14249
Applications of Robert's gradient operator for the digital enhancement of icebergs from SAR imagery p 41 A83-14278
The digital image processing system MOBI-DIVAH p 59 A83-14944
Digital methods for lineament analysis p 37 N83-14634
Digital analysis of Landsat satellite imagery in Turkana, Northern Kenya p 64 N83-14637
Automated segment matching algorithm-theory, test, and evaluation [E83-10096] p 16 N83-15740

DISCRIMINANT ANALYSIS (STATISTICS)
Statistical Techniques Applied to Aerial Radiometric Surveys (STARRS): Discriminant-analysis methods applied to aerial radiometric data and their application to uranium favorability in South Texas. Nation uranium resource evaluation [DE82-020961] p 34 N83-12512

DISPLAY DEVICES
Some aspects of the presentation of remote sensing data p 63 N83-14617

DISTORTION
LANDSAT 3 return beam vidicon response artifacts: A report on RBV photographic product characteristics and quality coding system [E83-10122] p 67 N83-15792

DIURNAL VARIATIONS
Diurnal patterns of wheat spectral reflectances and their importance in the assessment of canopy parameters from remotely sensed observations — Phoenix, Arizona [E83-10050] p 13 N83-14559

DIVING (UNDERWATER)
A report to the President and the Congress [AR-11] p 75 N83-11532

DOCUMENTS
AgRISTARS documents tracking list report [E83-10019] p 10 N83-12502

DOPPLER EFFECT
Estimating wind speed from HF skywave radar sea backscatter p 40 A83-11352
Geometric adjustment of simultaneous Doppler-derived range differences p 26 N83-13540

DRAINAGE PATTERNS
Terrain analysis procedural guide for drainage and water resources (ETL series on guides for Army terrain analysts) [AD-A118318] p 52 N83-11569
Verification of LANDSAT imagery for morphametric and topological studies of drainage basins in a section of the western plateau of Sao Paulo State: Tiete-Aguapei watershed — Brazil [E83-10111] p 54 N83-15754

DROUGHT
Visual analysis of 1:250,000 Landsat data for forage assessment during the 1980 drought in western Manitoba p 3 A83-14235

E

EARTH ALBEDO
Determination of the radiation budget at the Earth's surface from satellite data p 29 N83-14808

EARTH CORE
Data use investigation for the magnetic field satellite (MAGSAT) mission: Geomagnetic field forecasting and fluid dynamics of the core [E83-10098] p 29 N83-15742

EARTH CRUST
MAGSAT project [E83-10030] p 25 N83-13524
The mineralogy of global magnetic anomalies [E83-10034] p 34 N83-13528
Crustal and upper mantle structure data analysis [E83-10038] p 26 N83-13532
Japanese MAGSAT Team [E83-10080] p 27 N83-14589
Use of MAGSAT anomaly data for crustal structure and mineral resources in the US midcontinent [E83-10082] p 36 N83-14590
Investigation of Antarctic crust and upper mantle using MAGSAT and other geophysical data [E83-10086] p 27 N83-14594
Investigating tectonic and bathymetric features of the Indian Ocean using MAGSAT magnetic anomaly data [E83-10095] p 28 N83-14602

EARTH MANTLE
Investigation of Antarctic crust and upper mantle using MAGSAT *and other geophysical data*
[E83-10086] p 27 N83-14594
EARTH MOVEMENTS
Utilization of range-difference observations in geodynamics p 26 N83-13539
EARTH OBSERVATIONS (FROM SPACE)
Earth observation - Evolution of requirements and systems p 72 A83-10429
The GDTA - Remote sensing at the service of users p 68 A83-11867
Shuttle imaging radar experiment p 32 A83-13348
Canadian Symposium on Remote Sensing, 7th, Winnipeg, Canada, September 8-11, 1981, Proceedings p 73 A83-14226
Measurements of the characteristic reflectance spectra of surficial deposits p 32 A83-14266
Operational planning of the process of earth survey by satellites p 70 A83-14314
Radar images of the earth from space p 59 A83-14598
Flight path design issues for the TOPEX mission --- Ocean Topography Experiment
[AIAA PAPER 83-0197] p 42 A83-16581
Global implications of space activities; Proceedings of *the Conference, Aspen, CO, August 30-September 4,* 1981 p 74 A83-17349
Some closing thoughts: Practical payoffs from satellite systems p 74 N83-10468
Appendix C. LANDSAT: A worldwide perspective p 75 N83-10471
Collinear-track altimetry in the Gulf of Mexico from SEASAT: *Measurements, models and surface truth*
[AD-A118160] p 45 N83-11568
Geographic research in the US Geological Survey: Bibliography, 1966 - 1980
[USGS-CIRC-865] p 21 N83-11639
Conference on Using Next Generation Earth Observation Satellites: Summary handbook p 62 N83-12508
The European Space Agency's Earth observation satellite programs in the 1980's p 75 N83-14610
EARTH ORBITS
Preliminary study of GPS orbit determination accuracy achievable from worldwide tracking data
[NASA-CR-169693] p 28 N83-14605
EARTH RESOURCES
Advanced operational earth resources satellite systems
[AAS 82-128] p 73 A83-11932
Electro-optical instrumentation for resources evaluation; Proceedings of the Meeting, Washington, DC, April 21, 22, 1981 p 68 A83-12669
Image enhancement through film recorder response contouring p 56 A83-12685
The importance of remote sensing for Canada - Past achievements, future needs p 74 A83-14227
A position-based resource mapping study of the Kananaskis Valley using Landsat p 19 A83-14232
Ecological land classification in the Yukon p 20 A83-14250
The accuracy of a component analysis in space studies of natural environments --- for thematic mapping of earth resources and photointerpretation p 59 A83-14304
Geographic research in the US Geological Survey: Bibliography, 1966 - 1980
[USGS-CIRC-865] p 21 N83-11639
The use of thematic mapper simulator calibration data for assessment of data quality
[NASA-TM-82059] p 71 N83-13547
Remote sensing of renewable natural resources in developing countries for national planning purposes p 76 N83-14616
Terrestrial applications: An intelligent Earth-sensing information system p 76 N83-15349
EARTH RESOURCES PROGRAM
Technical issues in focal plane development for terrestrial resource observations p 69 A83-13735
Radar signatures of terrain - Useful monitors of renewable resources p 21 A83-17248
EARTH RESOURCES SHUTTLE IMAGING RADAR
Earth resources observation with the Shuttle imaging radar p 68 A83-12676
EARTH RESOURCES SURVEY PROGRAM
AgRISTARS - Plans and first-year achievements --- Agriculture and Resources Inventory Surveys Through Aerospace Remote Sensing p 1 A83-10095
EARTH SATELLITES
Flight path design issues for the TOPEX mission --- Ocean Topography Experiment
[AIAA PAPER 83-0197] p 42 A83-16581
Geographic research in the US Geological Survey: Bibliography, 1966 - 1980
[USGS-CIRC-865] p 21 N83-11639
EARTH SURFACE
Construction and interpretation of a thermal inertia image *using airborne data* p 57 A83-14260
Measurements of the characteristic reflectance spectra of surficial deposits p 32 A83-14266
Coordinate transformation during the geometric correction of the space scanner imagery of the earth p 70 A83-14313
A simple relation between active and passive microwave remote sensing measurements of earth terrain p 24 A83-14857
A backscatter model for a randomly perturbed periodic surface --- radar imagery of earth soil with row structure p 7 A83-14859
The use of thematic mapper simulator calibration data for assessment of data quality
[NASA-TM-82059] p 71 N83-13547
Determination of the radiation budget at the Earth's surface from satellite data p 29 N83-14808
ECHO SOUNDING
Effects of detection algorithm on accuracy degradation from logarithmic and difference processing for airborne laser bathymetry returns
[PB82-215138] p 44 N83-10707
ECOLOGY
Ecological land classification in the Yukon p 20 A83-14250
Colour Landsat images and mosaics - Basic tools in areal and ecological differentiation in Canada p 57 A83-14265
Monitoring global vegetation
[E83-10044] p 12 N83-14554
ECONOMIC DEVELOPMENT
Future land remote sensing data and services - A commercial perspective
[AAS 82-129] p 73 A83-11933
ECOSYSTEMS
Remote sensing techniques for conservation and management of natural vegetation ecosystems
[E83-10070] p 15 N83-14579
EDITING
Methods of editing cloud and atmospheric layer affected pixels from satellite data
[E83-10103] p 64 N83-15746
EDUCATION
The LANDSAT tutorial workbook: Basics of satellite remote sensing
[E83-10001] p 74 N83-10458
ELECTRO-OPTICS
Electro-optical instrumentation for resources evaluation; Proceedings of the Meeting, Washington, DC, April 21, 22, 1981 p 68 A83-12669
ELECTROMAGNETIC SPECTRA
Some fundamental concepts in remote sensing p 60 N83-10459
ELEVATION
An analysis of a relaxation scheme to improve terrain elevation data
[AD-A119257] p 27 N83-13550
ELLIPSOIDS
Mean Earth ellipsoid determined from SEASAT altimeter observations
[AD-A117910] p 45 N83-11570
EMISSIVITY
Microwave radiance of early fall sea ice at 1.55 cm p 38 A83-10091
A simple relation between active and passive microwave remote sensing measurements of earth terrain p 24 A83-14857
ENERGY BUDGETS
An evaluation of four thermal models used in thermal inertia analysis --- for thermal mapping from remotely sensed data p 67 A83-10098
ENERGY CONVERSION EFFICIENCY
Spectroradiometer measurements in support of photovoltaic device testing p 70 A83-15458
ENERGY POLICY
Determination of the radiation budget at the Earth's surface from satellite data p 29 N83-14808
ENVIRONMENT EFFECTS
Ice distribution and winter surface circulation patterns, Kachemak Bay, Alaska p 50 A83-12038
ENVIRONMENT POLLUTION
On the Development of Multimedia Monitoring of Environmental Pollution --- conferences
[WMO-563] p 22 N83-12599
Monitoring of meteorological elements in a composite program for environmental pollution studies p 22 N83-12648
Automatic interpretation of MSS-LANDSAT data applied to coal refuse site studies in southern Santa Catarina State, Brazil
[E83-10066] p 35 N83-14575
ENVIRONMENT PROTECTION
Microwave remote sensing measurements of oil pollution on the ocean p 39 A83-10104
A case study in the practical use of LANDSAT data p 52 N83-10466
ENVIRONMENT SIMULATION
Results of stereoscopic image simulations for the SPOT HRV carried out at the Gun Lake site in British Columbia p 20 A83-14292
ENVIRONMENTAL MONITORING
Detection of coastal zone environmental conditions using synthetic aperture radar p 38 A83-10068
Using new methods in monitoring the thermal regime of the Arctic p 39 A83-10828
Advanced operational earth resources satellite systems
[AAS 82-128] p 73 A83-11932
Environmental monitoring of the Athabasca Oil Sands using Landsat data p 31 A83-11988
Renewable resources monitoring needs in Manitoba p 19 A83-14228
Toward an operational, satellite-based, wetland monitoring program for the Fraser River Estuary, British Columbia p 51 A83-14234
Environmental monitoring of the Athabasca Oil Sands Region p 19 A83-14238
Remote sensing and waste management p 20 A83-14263
An experimental Landsat Quicklook System for Alaska p 57 A83-14271
Temporary lakes and salt plains in the high plateaus of the Andes /Bolivia/ - A continuing survey of periodic hydrologic phenomena using the geostationary satellite GOES-EST p 51 A83-14574
An optimum statistical technique for ozone profile retrieval from backscattered UV radiances p 21 A83-14632
Automated measurements of atmospheric visibility
[AIAA PAPER 83-0436] p 21 A83-16713
Ocean pollution research, development and monitoring
[PB82-219049] p 45 N83-10740
On the Development of Multimedia Monitoring of Environmental Pollution --- conferences
[WMO-563] p 22 N83-12599
Monitoring of meteorological elements in a composite program for environmental pollution studies p 22 N83-12648
Monitoring global vegetation
[E83-10044] p 12 N83-14554
Remote sensing techniques for conservation and management of natural vegetation ecosystems
[E83-10070] p 15 N83-14579
Approaches to desertification monitoring in the Sudan p 23 N83-14623
Multistage land use mapping and change monitoring in Sri Lanka p 15 N83-14625
The application of remote sensing to resource management and environmental quality programs in Kansas
[E83-10114] p 23 N83-15757
ENVIRONMENTAL RESEARCH SATELLITES
Performance assessment of future European remote sensing systems p 2 A83-10109
EQUATORIAL ATMOSPHERE
The role of cross-equatorial tropical cyclone pairs in the southern oscillation p 40 A83-13057
EQUATORIAL ELECTROJET
MAGSAT for geomagnetic studies over Indian region
[E83-10032] p 26 N83-13526
EQUINOXES
Basic research for the geodynamics program
[NASA-CR-169470] p 26 N83-13537
Effects of adopting new precession, nutation and equinox corrections on the terrestrial reference frame p 26 N83-13538
EQUIPMENT SPECIFICATIONS
MSS D Multispectral Scanner System
[E83-10128] p 72 N83-15797
EROSION
Bank erosion and flood plain studies of the Annapolis River - An application of remote sensing data p 51 A83-14262
ERROR ANALYSIS
A tutorial assessment of atmospheric height uncertainties for high-precision satellite altimeter missions to monitor ocean currents p 42 A83-14851
GRAVSAT *error analysis by means of global spectral* analyses of the marine geoid from SEASAT altimeter data
[E83-10105] p 29 N83-15748
ERRORS
Evaluation of geodetic products produced by the NSWC reduction of SEASAT radar altimeter data
[AD-A117837] p 25 N83-11571
ERS-1 (ESA SATELLITE)
The microwave payload for the ESA Remote Sensing Satellite /ERS-1/ p 69 A83-14290

The European Space Agency's Earth observation satellite programs in the 1980's p 75 N83-14610
ESTIMATES
Evaluation of geodetic products produced by the NSWC reduction of SEASAT radar altimeter data
[AD-A117837] p 25 N83-11571
ESTIMATING
Crop proportion estimation problems in AgRISTARS p 18 N83-15760
Topics in global convergence of density estimates p 66 N83-15775
Characterization of a maximum-likelihood nonparametric density estimator of kernel type p 66 N83-15777
ESTUARIES
Remote sensing of water quality for estuarine environments p 50 A83-10073
Toward an operational, satellite-based, wetland monitoring program for the Fraser River Estuary, British Columbia p 51 A83-14234
EUROPA
The geology of Europa p 24 A83-16239
EUROPE
The European Community, development and satellite technology p 75 N83-14609
EUROPEAN SPACE AGENCY
Earthnet prepares for Landsat-D p 74 A83-17426
Satellite remote sensing: ESA's experience with developing countries p 76 N83-14632
The role of EARSeL and EARSeL member laboratories --- in developing nations p 76 N83-14633
EUROPEAN SPACE PROGRAMS
Performance assessment of future European remote sensing systems p 2 A83-10109
The European Space Agency's Earth observation satellite programs in the 1980's p 75 N83-14610
SPOT in the 1980's p 76 N83-14611
EVAPORATION
HCMM hydrological analysis in Utah
[E83-10026] p 53 N83-13520
EVAPOROGRAPHY
Remote determination of surface evaporation using thermal IR measurements p 50 A83-10101
EVOLUTION (DEVELOPMENT)
Aerial geologic log from Livermore, California to the Nevada Test Site, Nye County, Nevada
[DE82-018392] p 25 N83-10693
EXPLORATION
Airborne gamma-ray spectrometer and magnetometer survey. Volume 1. Detail areas, Christmas Mountains, Solitario, Green Valley/0-2 Ranch, Texas
[DE82-021614] p 34 N83-12513

F

FARM CROPS
A backscatter model for a randomly perturbed periodic surface --- furrowed soils in agricultural fields p 1 A83-10107
Satellite orbital dynamics and observation strategies in support of agricultural applications p 2 A83-10717
Land use/land cover mapping from enhanced Landsat imagery of the eastern provinces of the People's Republic of China p 4 A83-14241
Agricultural Research Service research highlights in remote sensing for calendar year 1981
[E83-10051] p 75 N83-14560
Automated segment matching algorithm-theory, test, and evaluation
[E83-10096] p 16 N83-15740
FARMLANDS
Remote sensing of dielectric media with periodic rough surfaces --- microwave scattering from farmfields p 1 A83-10106
A parametric study of tillage effects on radar backscatter p 2 A83-10108
Landsat for delineation and mapping of saline soils in dryland areas in southern Alberta p 5 A83-14261
Estimation of the sugar cane cultivated area from LANDSAT images using the two phase sampling method
[E83-10077] p 15 N83-14586
Multistage land use mapping and change monitoring in Sri Lanka p 15 N83-14625
Gates to Gregg high voltage transmission line study --- California
[E83-10097] p 16 N83-15741
Crop-phenology and LANDSAT-based irrigated lands inventory in the high plains --- Texas, New Mexico, Oklahma, Kansas, Colorado, Nebraska, Wyoming, and South Dakota
[E83-10115] p 18 N83-15758
FEASIBILITY ANALYSIS
Terrestrial applications: An intelligent Earth-sensing information system p 76 N83-15349
FISHERIES
Application of remote sensing techniques in oceanographic studies of the British Columbia Salmon Fishery p 41 A83-14258
FITTING
Proceedings of the NASA Workshop on Surface Fitting
[E83-10117] p 64 N83-15759
Fitting surfaces to scattered data p 65 N83-15761
C-1 surface interpolation for scattered data on a sphere p 65 N83-15762
Surface fitting with biharmonic and harmonic models p 65 N83-15764
BSPLASH: A three-stage surface interpolant to scattered data p 65 N83-15765
FLIGHT PATHS
Flight path design issues for the TOPEX mission --- Ocean Topography Experiment
[AIAA PAPER 83-0197] p 42 A83-16581
FLIR DETECTORS
FLIR target screening p 65 N83-15771
FLOOD CONTROL
Application of Landsat imagery to flood control and management of agricultural land - A case study of northern India p 3 A83-14233
FLOOD PLAINS
Bank erosion and flood plain studies of the Annapolis River - An application of remote sensing data p 51 A83-14262
The application of remote sensing to resource management and environmental quality programs in Kansas
[E83-10114] p 23 N83-15757
FLOOD PREDICTIONS
A report to the President and the Congress
[AR-11] p 75 N83-11532
FLORIDA
Use of thermal inertia determined by HCMM to predict nocturnal cold prone areas in Florida
[E83-10028] p 62 N83-13522
Use of thermal inertia determined by HCMM to predict nocturnal cold prone areas in Florida
[E83-10102] p 64 N83-15745
FLUID DYNAMICS
Data use investigation for the magnetic field satellite (MAGSAT) mission: Geomagnetic field forecasting and fluid dynamics of the core
[E83-10098] p 29 N83-15742
FLUORESCENCE
Experimental feasibility of the airborne measurement of absolute oil fluorescence spectral conversion efficiency p 44 A83-18581
FOLIAGE
Application of computer axial tomography /CAT/ to measuring crop canopy geometry --- corn and soybeans p 1 A83-10096
Effects of ground cover and leaf area on the spectral reflectance of vegetation-soil target
[AD-A119714] p 16 N83-14653
FORECASTING
Long-range water supply forecasting
[WMO-587] p 53 N83-12516
Snowmelt runoff modeling in simulation and forecasting modes with the Martinec-Mango model
[E83-10063] p 53 N83-14572
Use of remote sensing techniques for rice production forecasting in west Africa (Mali and Guinea: Niger-Bani Project) p 15 N83-14626
The RAMS collection of meterological and position data in the Norwegian Sea p 49 N83-14845
FOREST FIRE DETECTION
Determination of forest fire spread rates from infrared photographs p 6 A83-14307
FOREST MANAGEMENT
The application of remote sensing in southern Alberta's mountain pine beetle management p 5 A83-14257
Development of a data management front end for use with a LANDSAT based information system --- assessing gypsy moth defoliation damage in Pennsylvania
[E83-10104] p 17 N83-15747
Detection of aspen-conifer forest mixes from LANDSAT digital data --- Utah-Idaho Bear River Range
[E83-10106] p 17 N83-15749
FORESTS
Seasat L-band radar response to forest vegetation in eastern Virginia p 1 A83-10061
The use of R.B.V., colour additive viewer and M.S.S. products in the British Columbia Forest Inventory Depletion Monitoring Program --- Return Beam Vidicon and Multispectral Scanning p 4 A83-14246
Landsat-based forest mapping in Ontario north of latitude 52 deg north p 5 A83-14253
Multitemporal analysis of Landsat data for forest cutover mapping - A trial of two procedures p 5 A83-14254
Predicting forest land attributes from aerial photo interpretation variables p 5 A83-14259
Multistage land use mapping and change monitoring in Sri Lanka p 15 N83-14625
FORMAT
Standardization of computer compatible tape formats for remote sensing data p 54 A83-10075
INPE LANDSAT-D thematic mapper computer compatible tape format specification
[E83-10075] p 63 N83-14584
FREEZING
An introduction to project Freeze --- the location and intensity of freezing temperatures using infrared satellite imagery
[INPE-2435-NTE/186] p 22 N83-13703
Use of near-infrared video recording system for the detection of freeze damaged citrus leaves
[E83-10049] p 12 N83-14558
FROST
An introduction to project Freeze --- the location and intensity of freezing temperatures using infrared satellite imagery
[INPE-2435-NTE/186] p 22 N83-13703
FUNCTIONAL ANALYSIS
Remote sensing of temperature profiles in the atmosphere p 66 N83-15778
FUNCTIONALS
Proceedings of the NASA Workshop on Density Estimation and Function Smoothing
[E83-10119] p 66 N83-15774

G

GAMMA RAYS
Airborne measurement of surficial soil moisture using natural terrestrial gamma radiation p 50 A83-10120
GARP ATLANTIC TROPICAL EXPERIMENT
Global Weather Experiment. The GARP Atlantic Tropical Experiment (GATE) Monograph
[GARP-PUB-SER-25] p 45 N83-12724
Main achievements of GARP Atlantic Tropical Experiment (GATE) and its impact on FGGE --- first GARP Global Experiment (FGGE) p 46 N83-12735
GEOBOTANY
Spectral discrimination of lithologic facies in the granite of the Pedra Branca Goias using LANDSAT 1 digital imagery
[E83-10069] p 35 N83-14578
Multitemporal and geobotanical approach in the remote detection of Greisenization areas in the Serra da Pedra Branca Granite, Goias State, Brazil
[E83-10071] p 35 N83-14580
GEOCHEMISTRY
Remote determination of humus content in soils p 7 A83-15889
Airborne gamma-ray spectrometer and magnetometer survey. Volume 1. Detail areas, Christmas Mountains, Solitario, Green Valley/0-2 Ranch, Texas
[DE82-021614] p 34 N83-12513
GEODESY
Defense Mapping Agency /DMA/ overview of mapping, charting, and geodesy /MC&G/ applications of digital image pattern recognition p 24 A83-12877
Report on the special program 78 satellite geodesy of the technical university of Munich
[ASTRON-GEODAET-ARB-41] p 25 N83-11563
Applications of space science and technology --- Indian space program p 75 N83-12115
An upper bound on errors in the mean-of-date/instantaneous Earth-fixed vector transformation induced by interpolated nutation angles
[AD-A119444] p 29 N83-14656
GEODETIC COORDINATES
Concerning a method for the determination of initial geodetic data p 24 A83-17679
Report on the special program 78 satellite geodesy of the technical university of Munich
[ASTRON-GEODAET-ARB-41] p 25 N83-11563
GEODETIC SATELLITES
Geometric adjustment of simultaneous Doppler-derived range differences p 26 N83-13540
GEODETIC SURVEYS
Evaluation of geodetic products produced by the NSWC reduction of SEASAT radar altimeter data
[AD-A117837] p 25 N83-11571
GEODYNAMICS
Basic research for the geodynamics program
[NASA-CR-169470] p 26 N83-13537
Effects of adopting new precession, nutation and equinox corrections on the terrestrial reference frame p 26 N83-13538
Utilization of range-difference observations in geodynamics p 26 N83-13539
Geometric adjustment of simultaneous Doppler-derived range differences p 26 N83-13540

GEOGRAPHIC INFORMATION SYSTEMS
Analytical plotter for data input into geo-based information systems p 56 A83-12683
A position-based resource mapping study of the Kananaskis Valley using Landsat p 19 A83-14232
Office automation in resource-management - The future is now --- agricultural land use map dissemination p 6 A83-14269
An experimental Landsat Quicklook System for Alaska p 57 A83-14271
LANDSAT land cover analysis completed for CIRSS/San Bernardino County project
[E83-10024] p 22 N83-12507
Identifying environmental features for land management decisions
[E83-10109] p 23 N83-15752
CIRSS vertical data integration, San Bernardino County study phases 1-A, 1-B
[E83-10124] p 67 N83-15794
CIRSS vertical data integration, San Bernardino study
[E83-10127] p 67 N83-15796
GEOGRAPHY
Geographic information systems p 61 N83-10465
Geographic research in the US Geological Survey: Bibliography, 1966 - 1980
[USGS-CIRC-865] p 21 N83-11639
GEOIDS
Mean Earth ellipsoid determined from SEASAT altimeter observations
[AD-A117910] p 45 N83-11570
Evaluation of geodetic products produced by the NSWC reduction of SEASAT radar altimeter data
[AD-A117837] p 25 N83-11571
GRAVSAT error analysis by means of global spectral analyses of the marine geoid from SEASAT altimeter data
[E83-10105] p 29 N83-15748
GEOLOGICAL SURVEYS
Critical and strategic minerals in Alaska: Cobalt, the platinum-group metals and chromite
[PB82-193085] p 33 N83-10485
Aerial geologic log from Livermore, California to the Nevada Test Site, Nye County, Nevada
[DE82-018392] p 25 N83-10693
Statistical Techniques Applied to Aerial Radiometric Surveys (STARRS): Discriminant-analysis methods applied to aerial radiometric data and their application to uranium favorability in South Texas. Nation uranium resource evaluation
[DE82-020961] p 34 N83-12512
Low- to moderate-temperature geothermal resource assessment for Nevada: Area specific studies, Pumpernickel Valley, Carlin and Moana
[DE82-018598] p 34 N83-12584
LANDSAT and radar mapping of intrusive rocks in SE-Brazil
[E83-10073] p 36 N83-14582
Combined use of daily thermal cycle of METEOSAT imagery and multispectral LANDSAT data: Application to the Bandiagara plateau, Mali p 36 N83-14620
GEOLOGY
Remote sensing in geology: Current trends and future prospects with satellite data
[INPE-2514-PRE/193] p 33 N83-12509
Determination of the contribution of side-looking airborne radar to structural geologic mapping
[PB82-185042] p 34 N83-12713
GEOMAGNETISM
Analysis of MAGSAT data of the Indian region
[E83-10027] p 25 N83-13521
MAGSAT project
[E83-10030] p 25 N83-13524
Gravity and magnetic anomaly data analysis
[E83-10031] p 26 N83-13525
MAGSAT for geomagnetic studies over Indian region
[E83-10032] p 26 N83-13526
MAGSAT and aeromagnetic data of the continental US
[E83-10033] p 26 N83-13527
MAGSAT anomaly field inversion and interpretation for the US
[E83-10057] p 27 N83-14566
Japanese MAGSAT Team
[E83-10080] p 27 N83-14589
An investigation of MAGSAT and complementary data emphasizing Precambrian shields and adjacent areas of West Africa and South America
[E83-10085] p 36 N83-14593
Investigation of Antarctic crust and upper mantle using MAGSAT and other geophysical data
[E83-10086] p 27 N83-14594
The MAGSAT project in Australia
[E83-10089] p 28 N83-14597
The reduction, verification and interpretation of MAGSAT magnetic data over Canada
[E83-10091] p 28 N83-14599
Investigation of MAGSAT and TRIAD magnetometer data to provide corrective information on high-lattitude external fields
[E83-10093] p 28 N83-14600
Equivalent source modeling of the main field using MAGSAT data
[E83-10094] p 28 N83-14601
Data use investigation for the magnetic field satellite (MAGSAT) mission: Geomagnetic field forecasting and fluid dynamics of the core
[E83-10098] p 29 N83-15742
The reduction, verification and interpretation of MAGSAT magnetic data over Canada
[E83-10101] p 29 N83-15744
Geomagnetic modeling by optimal recursive filtering
[E83-10112] p 29 N83-15755
GEOMETRIC ACCURACY
LANDSAT-4 image data quality analysis
[E83-10039] p 63 N83-13533
GEOMETRIC RECTIFICATION (IMAGERY)
Some effects on the GCP success rate --- Ground Control Points for satellite image rectification p 58 A83-14285
Coordinate transformation during the geometric correction of the space scanner imagery of the earth p 70 A83-14313
The digital image processing system MOBI-DIVAH p 59 A83-14944
Rectification of Seasat radar on Landsat MSS with the aid of digital image correlation p 59 A83-14946
Familiarization with LANDSAT imagery p 60 N83-10460
GEOMORPHOLOGY
Drumlin fields and glaciated mountains - A contrast in geomorphic perception from Seasat radar images p 23 A83-10078
Imaging radar observations of volcanic features in Medicine Lake Highland, California p 30 A83-10079
Application of Landsat imagery to flood control and management of agricultural land - A case study of northern India p 3 A83-14233
The geology of Europa p 24 A83-16239
Super high altitude photography for coastal geomorphology --- from approximately 20 km altitude p 43 A83-17840
Geomorphological mapping using Landsat imagery - A case study in Argentina p 33 A83-17841
Some comparative aspects of SLAR and airphoto images for geomorphologic and geologic interpretation p 33 A83-17842
Verification of LANDSAT imagery for morphametric and topological studies of drainage basins in a section of the western plateau of Sao Paulo State: Tiete-Aguapei watershed --- Brazil
[E83-10111] p 54 N83-15754
GEOPHYSICAL FLUIDS
Data use investigation for the magnetic field satellite (MAGSAT) mission: Geomagnetic field forecasting and fluid dynamics of the core
[E83-10098] p 29 N83-15742
GEOPHYSICAL SATELLITES
Preliminary study of GPS orbit determination accuracy achievable from worldwide tracking data
[NASA-CR-169693] p 28 N83-14605
TOPEX orbit determination using GPS signals plus a sidetone ranging system
[NASA-CR-169694] p 29 N83-14606
GEOS SATELLITES (ESA)
The use of satellite information in weather forecasting at the Pacific Weather Centre p 20 A83-14277
GEOSTROPHIC WIND
Some features of the spatial structure of the Arctic Ocean ice cover in connection with turbulent friction and geostrophic capture of tide waves p 40 A83-10833
GEOTHERMAL RESOURCES
Radar and infrared remote sensing of geothermal features at Pilgrim Springs, Alaska p 31 A83-12036
Low- to moderate-temperature geothermal resource assessment for Nevada: Area specific studies, Pumpernickel Valley, Carlin and Moana
[DE82-018598] p 34 N83-12584
GERMINATION
Influence of environmental factors during seed development and after full-ripeness on pre-harvest sprouting in wheat
[E83-10002] p 7 N83-12482
GLACIAL DRIFT
Drumlin fields and glaciated mountains - A contrast in geomorphic perception from Seasat radar images p 23 A83-10078
GLACIOLOGY
Drumlin fields and glaciated mountains - A contrast in geomorphic perception from Seasat radar images p 23 A83-10078
GLOBAL AIR POLLUTION
Aircraft and remote measurements of atmospheric transport of pollutants within the global integrated monitoring system p 22 N83-12620
GLOBAL ATMOSPHERIC RESEARCH PROGRAM
Report of the Monex review meeting
[GARP-SPEC-REPT-38] p 45 N83-12707
Manual on the global observing system. Volume 1 (annex to the WMO technical regulations): Global aspects, 1981 edition
[WMO-544-VOL-1-ANNEX] p 46 N83-12801
The Global Weather Experiment. First GARP Global Experiment (FGGE) operations report series: Volume 5, summary of data collected 5 July - December 1979
[GARP-FOR-5] p 46 N83-12808
GOVERNMENT/INDUSTRY RELATIONS
Future land remote sensing data and services - A commercial perspective
[AAS 82-129] p 73 A83-11933
GRAINS (FOOD)
AgRISTARS. Semiannual program review presentation to level 1, interagency Coordination Committee
[E83-10006] p 8 N83-12486
GRANITE
Spectral discrimination of lithologic facies in the granite *of the Pedra Branca Goias using LANDSAT 1 digital* imagery
[E83-10069] p 35 N83-14578
Multitemporal and geobotanical approach in the remote detection of Greisenization areas in the Serra da Pedra Branca Granite, Goias State, Brazil
[E83-10071] p 35 N83-14580
Remote sensing of the granites of Southeast Asia p 37 N83-14629
GRASSES
Estimating total standing herbaceous biomass production with LANDSAT MSS digital data
[E83-10045] p 12 N83-13536
GRASSHOPPERS
Aerial survey of crop losses due to grasshoppers /Orthoptera - Acrididae/ in Saskatchewan p 5 A83-14255
GRASSLANDS
Landsat for delineation and mapping of saline soils in dryland areas in southern Alberta p 5 A83-14261
Computer program documentation for the pasture/range condition assessment processor
[E83-10100] p 16 N83-15743
GRAVIMETRY
Gravimetric maps of the Central African Republic
[E83-10084] p 27 N83-14592
GRAVITATIONAL FIELDS
Concerning a method for the determination of initial geodetic data p 24 A83-17679
GRAVITY ANOMALIES
Evaluation of geodetic products produced by the NSWC reduction of SEASAT radar altimeter data
[AD-A117837] p 25 N83-11571
Gravimetric maps of the Central African Republic
[E83-10084] p 27 N83-14592
GREEN WAVE EFFECT
Rangeland biomass estimation demonstration --- Texas Experimenta Ranch
[E83-10113] p 17 N83-15756
GROUND STATIONS
Earthnet prepares for Landsat-D p 74 A83-17426
GROUND TRUTH
Near surface observations p 61 N83-10464
Extension of laboratory-measured soil spectra to field conditions
[E83-10021] p 11 N83-12504
A comparison of surfaces temperatures from HCMM infrared data with field measurements
[E83-10046] p 47 N83-14555
GROUND WATER
Evaluating depth to shallow groundwater using heat capacity mapping mission /HCMM/ data p 51 A83-14668
GROUND WIND
Observations of oceanic surface-wind fields from the Nimbus-7 microwave radiometer p 42 A83-14861
GUINEA
Use of remote sensing techniques for rice production forecasting in west Africa (Mali and Guinea: Niger-Bani Project) p 15 N83-14626
GULF OF MEXICO
On the circulation of the western Gulf of Mexico - A satellite view p 39 A83-10113
A comparison of HCMM surface temperatures with in situ temperature data --- Nantucket shoals and the Gulf of Mexico regions
[E83-10040] p 46 N83-13534
A comparison of surfaces temperatures from HCMM infrared data with field measurements
[E83-10046] p 47 N83-14555

GULF STREAM
Western Boundary Eddies of the Gulf Stream p 49 N83-14847

H

HABITATS
Waterfowl habitat inventory of Alberta, Saskatchewan and Manitoba by remote sensing p 4 A83-14244
Digital colour enhancement of Landsat data for mapping vegetation of barrenground caribou winter range in northern Manitoba p 5 A83-14249
Integration of Landsat imagery into a program for aerial surveying of deer populations in Alberta p 5 A83-14252

HARMONIC ANALYSIS
Surface fitting with biharmonic and harmonic models p 65 N83-15764

HAZE
Arctic haze and the Arctic gas and aerosol sampling program /AGASP/ [AIAA PAPER 83-0439] p 21 A83-16714

HAZE DETECTION
Evidence for a central Eurasian source area of arctic haze in Alaska p 18 A83-11626

HEAT CAPACITY MAPPING MISSION
Some examples of the utility of HCMM data in geologic remote sensing --- Heat Capacity Mapping Mission p 31 A83-10099
Snow hydrology studies using data from the Heat Capacity Mapping Mission p 50 A83-10102
Construction and interpretation of a thermal inertia image using airborne data p 57 A83-14260
Evaluating depth to shallow groundwater using heat capacity mapping mission /HCMM/ data p 51 A83-14668

HEIGHT
Mean Earth ellipsoid determined from SEASAT altimeter observations [AD-A117910] p 45 N83-11570
The accuracy of Seasat-1 altimeter altitude measurments under various sea state conditions [RAE-TR-82059] p 47 N83-14553

HETEROJUNCTION DEVICES
Low threshold InGaAsP/InP lasers with microcleaved mirrors suitable for monolithic integration p 24 A83-10981

HIGH ALTITUDE
Super high altitude photography for coastal geomorphology --- from approximately 20 km altitude p 43 A83-17840

HIGHLANDS
Temporary lakes and salt plains in the high plateaus of the Andes /Bolivia/ - A continuing survey of periodic hydrologic phenomena using the geostationary satellite GOES-EST p 51 A83-14574

HIMALAYAS
Analysis of MAGSAT data of the Indian region [E83-10027] p 25 N83-13521

HUMIDITY MEASUREMENT
The possibility of measuring the moisture content of the upper layers of the atmosphere using radiometric techniques p 70 A83-14308

HYDRODYNAMICS
Analyses of oceanic subsurface features using space based radar imagery [AD-A118411] p 45 N83-11692

HYDROELECTRIC POWER STATIONS
Ice distribution and winter surface circulation patterns, Kachemak Bay, Alaska p 50 A83-12038

HYDROGEOLOGY
Application of satellite data to hydrogeological investigation in Damagaram-Mounio, Niger p 53 N83-14630

HYDROGRAPHY
Weather constraints on airborne laser hydrography operations [PB82-189754] p 52 N83-10745
Snowmelt runoff modeling in simulation and forecasting modes with the Martinec-Mango model [E83-10063] p 53 N83-14572

HYDROLOGY
Snow hydrology studies using data from the Heat Capacity Mapping Mission p 50 A83-10102
Temporary lakes and salt plains in the high plateaus of the Andes /Bolivia/ - A continuing survey of periodic hydrologic phenomena using the geostationary satellite GOES-EST p 51 A83-14574
A report to the President and the Congress [AR-11] p 75 N83-11532
Terrain analysis procedural guide for drainage and water resources (ETL series on guides for Army terrain analysts) [AD-A118318] p 52 N83-11569
Hydrological data transmission [WMO-559] p 53 N83-12514

HYDROLOGY MODELS
Long-range water supply forecasting [WMO-587] p 53 N83-12516
HCMM hydrological analysis in Utah [E83-10026] p 53 N83-13520
Snowmelt runoff modeling in simulation and forecasting modes with the Martinec-Mango model [E83-10063] p 53 N83-14572

HYDROMETEOROLOGY
Long-range water supply forecasting [WMO-587] p 53 N83-12516

I

ICE FLOES
Some features of the spatial structure of the Arctic Ocean ice cover in connection with turbulent friction and geostrophic capture of tide waves p 40 A83-10833
The RAMS collection of meterological and position data in the Norwegian Sea p 49 N83-14845

ICE FORMATION
Ice distribution and winter surface circulation patterns, Kachemak Bay, Alaska p 50 A83-12038

ICE MAPPING
The application of microwave remote sensing for snow and ice research p 38 A83-10088
Accuracy of operational snow and ice charts p 50 A83-10090
Microwave radiance of early fall sea ice at 1.55 cm p 38 A83-10091
Satellite laser altimeter for measurement of ice sheet topography p 38 A83-10092
Ice-sheet dynamics by satellite laser altimetry p 38 A83-10093
Tidal phenomena in Arctic Ocean ice /according to space data/ p 40 A83-10832
The utilization of infrared /IR/ aerial and space observations of Arctic seas in navigation and during the solution of other national-economic problems p 40 A83-10836
An algorithm to interface Nimbus-7 SMMR data with the AES ice modelling grid for the Beaufort Sea p 41 A83-14284
The permanently sparse areas of ice cover in the open regions of the Okhtsk Sea p 42 A83-15058
The RAMS collection of meterological and position data in the Norwegian Sea p 49 N83-14845

ICEBERGS
Ice-sheet dynamics by satellite laser altimetry p 38 A83-10093
Applications of Robert's gradient operator for the digital enhancement of icebergs from SAR imagery p 41 A83-14278
Lagrangian drift measurements of sea surface currents and iceberg tracking p 49 N83-14842

IMAGE CONTRAST
Drumlin fields and glaciated mountains - A contrast in geomorphic perception from Seasat radar images p 23 A83-10078
LANDSAT 3 return beam vidicon response artifacts: A report on RBV photographic product characteristics and quality coding system [E83-10122] p 67 N83-15792

IMAGE CORRELATORS
Rectification of Seasat radar on Landsat MSS with the aid of digital image correlation p 59 A83-14946

IMAGE ENHANCEMENT
Evaluation of photographic enhancements of Landsat imagery p 55 A83-12035
Contribution of Landsat imagery to the study of volcanic structures p 31 A83-12641
Image enhancement through film recorder response contouring p 56 A83-12685
Application of Landsat imagery to natural resources management in Sierra Leone, West Africa p 57 A83-14247
Digital colour enhancement of Landsat data for mapping vegetation of barrenground caribou winter range in northern Manitoba p 5 A83-14249
Applications of Robert's gradient operator for the digital enhancement of icebergs from SAR imagery p 41 A83-14278
OSTA-1/Ocean Color Experiment [AIAA PAPER 83-0415] p 42 A83-16701
Computer processed LANDSAT data p 61 N83-10463
Appendix B: Principles of computer processing of LANDSAT data p 75 N83-10470
The computer treatment of remotely sensed data: An introduction to techniques which have geologic applications --- image enhancement and thematic classification in Brazil [E83-10078] p 36 N83-14587
Analysis of the characteristics appearing in LANDSAT multispectral images in the geological structural mapping of the midwestern portion of the Rio Grande do Sul shield --- Brazil [E83-10126] p 37 N83-15795

IMAGE FILTERS
SAR squint analysis of directional extended targets --- using Doppler filtering of SAR signal film p 54 A83-10084

IMAGE PROCESSING
Rock type discrimination techniques using Landsat and Seasat image data p 30 A83-10057
Probabilistic cluster labeling of imagery data p 54 A83-11410
Pattern recognition and digital image processing as applied to remote sensing in India p 54 A83-11450
Automatic multitemporal segmentation for diachronic analysis of remotely sensed images p 55 A83-11461
Evaluation of photographic enhancements of Landsat imagery p 55 A83-12035
A comparison of unsupervised classification procedures on Landsat MSS data for an area of complex surface conditions in Basilicata, Southern Italy p 55 A83-12037
Technology and future ground processing systems p 56 A83-12678
Defense Mapping Agency /DMA/ overview of mapping, charting, and geodesy /MC&G/ applications of digital image pattern recognition p 24 A83-12877
Reconnaissance applications of image understanding p 56 A83-12882
Quality assessment of remote-sensing data - The SAR case p 56 A83-13845
Integration of Landsat imagery into a program for aerial surveying of deer populations in Alberta p 5 A83-14252
Construction and interpretation of a thermal inertia image using airborne data p 57 A83-14260
Remote sensing software for airborne image analysis p 58 A83-14273
A field portable reflectance spectrometer p 69 A83-14275
A refined destriping procedure for Landsat MSS data products p 58 A83-14281
Some effects on the GCP success rate --- Ground Control Points for satellite image rectification p 58 A83-14285
Reference quicklook images for monitor of Landsat image data acquisition p 58 A83-14286
The CCRS SAR processing system p 69 A83-14289
A system for the complex processing of aerial and space data for agriculture p 6 A83-14301
Automation of the search for and recognition of reference zones for precise coordinate control of space imagery p 59 A83-14311
Resolution versus speckle relative to geologic interpretability of spaceborne radar images - A survey of user preference p 33 A83-14852
Estimation of context for statistical classification of multispectral image data p 59 A83-14853
Investigations of interpretability of images by different sensors and platforms for small scale mapping p 70 A83-14943
The digital image processing system MOBI-DIVAH p 59 A83-14944
Phytoplankton pigment concentrations in the Middle Atlantic Bight - Comparison of ship determinations and CZCS estimates --- Coastal Zone Color Scanner p 43 A83-18580
The LANDSAT tutorial workbook: Basics of satellite remote sensing [E83-10001] p 74 N83-10458
Familiarization with LANDSAT imagery p 60 N83-10460
Some spectral and spatial characteristics of LANDSAT data p 61 N83-10461
Computer processed LANDSAT data p 61 N83-10463
Image processing techniques p 61 N83-11391
Image processing of remotely sensed phenomena p 61 N83-11400
System support documentation: IDIMS FUNCTION AMOEBA p 9 N83-12495
LANDSAT land cover analysis completed for CIRSS/San Bernardino County project [E83-10024] p 22 N83-12507
Remote sensing in geology: Current trends and future prospects with satellite data [INPE-2514-PRE/193] p 33 N83-12509
Determination of the contribution of side-looking airborne radar to structural geologic mapping [PB82-185042] p 34 N83-12713
Pass point determination and geometrical precision of the relative rectification of scanner data [SER-C-268] p 62 N83-13518

Geologic interpretation of HCMM and aircraft thermal data
[E83-10036] p 62 N83-13530
An analysis of a relaxation scheme to improve terrain elevation data
[AD-A119257] p 27 N83-13550
Further SEASAT SAR coastal ocean wave analysis
[NASA-CR-169682] p 47 N83-13776
Analysis of geologic terrain models for determination of optimum SAR sensor configuration and optimum information extraction for exploration of global non-renewable resources. Pilot study: Arkansas Remote Sensing Laboratory, part 1, part 2, and part 3
[E83-10061] p 35 N83-14570
An automatic agricultural zone classification procedure for crop inventory satellite images
[E83-10065] p 14 N83-14574
Method of interpretation of remotely sensed data and applications to land use
[E83-10072] p 23 N83-14581
Interpretation of remotely sensed data and its applications in oceanography
[E83-10074] p 48 N83-14583
Comparison of diverse methods for the correction of atmospheric effects on LANDSAT and SKYLAB images --- *radiometric correction in Brazil*
[E83-10079] p 72 N83-14588
Some aspects of the presentation of remote sensing data p 63 N83-14617
Digital methods for lineament analysis p 37 N83-14634
A practical automated mapping system p 64 N83-14635
Digital analysis of Landsat satellite imagery in Turkana, Northern Kenya p 64 N83-14637
Automated segment matching algorithm-theory, test, and evaluation
[E83-10096] p 16 N83-15740
Gates to Gregg high voltage transmission line study --- California
[E83-10097] p 16 N83-15741
Methods of editing cloud and atmospheric layer affected pixels from satellite data
[E83-10103] p 64 N83-15746
Proceedings of the NASA Workshop on Image Analysis
[E83-10118] p 65 N83-15766
Image segmentation survey p 65 N83-15767
Cooperative processes in image segmentation p 65 N83-15768
Shape and texture p 65 N83-15769
Automatic photointerpretation via texture and morphology analysis p 65 N83-15770
FLIR target screening p 65 N83-15771
Determining 3-D motion and structure from image sequences p 66 N83-15773
LANDSAT 4 investigations of thematic mapper and multispectral scanner applications
[E83-10121] p 66 N83-15791
Infrared satellite data from the first coastal ocean dynamics experiment, March - July 1981
[AD-A120068] p 49 N83-15799

IMAGE RECONSTRUCTION
Image processing techniques p 61 N83-11391

IMAGE RESOLUTION
Results of stereoscopic image simulations for the SPOT HRV carried out at the Gun Lake site in British Columbia p 20 A83-14292
Resolution versus speckle relative to geologic interpretability of spaceborne radar images - A survey of user preference p 33 A83-14852
Image processing techniques p 61 *N83-11391*
Evaluation of ERIM optically processed SEASAT SAR data
[E83-10037] p 63 N83-13531
LANDSAT-4 image data quality analysis
[E83-10039] p 63 N83-13533
An investigation into the utilization of HCMM thermal data for the descrimination of volcanic and Eolian geological units --- Craters of the Moon volcanic field, Idaho; San Francisco volcanic field, Arizona; High Desert, California; and the Cascade Range, California and Oregon
[E83-10047] p 35 N83-14556
The applicability of satellite remote sensing to small and medium scale mapping p 64 N83-14618
LANDSAT 3 return beam vidicon response artifacts: A report on RBV photographic product characteristics and quality coding system
[E83-10122] p 67 N83-15792

IMAGE TRANSDUCERS
Technical issues in focal plane development; Proceedings of the Meeting, Washington, DC, April 21, 22, 1981 p 69 A83-13726
Technical issues in focal plane development for terrestrial resource observations p 69 A83-13735

IMAGING TECHNIQUES
Geological terrain models p 31 A83-10080
Potentials for change detection using Seasat synthetic aperture radar data p 54 A83-10121
An automated mapping satellite system /Mapsat/ p 67 A83-10715
Spectroscopic imaging of the thermosphere from the Space Shuttle p 68 A83-12605
Image analysis unit (UAI-R) for meteorological applications
[INPE-2428-NTE/185] p 63 N83-13707
Land remote sensing activities in the US p 72 N83-14612

INDEXES (DOCUMENTATION)
AgRISTARS documents tracking list report
[E83-10019] p 10 N83-12502

INDIA
Analysis of MAGSAT data of the Indian region
[E83-10027] p 25 N83-13521
MAGSAT project
[E83-10030] p 25 N83-13524
MAGSAT for geomagnetic studies over Indian region
[E83-10032] p 26 N83-13526

INDIAN OCEAN
Investigating tectonic and bathymetric features of the *Indian Ocean using MAGSAT magnetic anomaly data*
[E83-10095] p 28 N83-14602
Australian drifting buoy p 48 N83-14837

INDIAN SPACE PROGRAM
Applications of space science and technology --- Indian space program p 75 N83-12115

INDIAN SPACECRAFT
Applications of space science and technology --- Indian space program p 75 N83-12115

INDIUM PHOSPHIDES
Low threshold InGaAsP/InP lasers with microcleaved mirrors suitable for monolithic integration p 24 A83-10981

INFESTATION
Landsat monitoring of Desert Locust breeding grounds in Africa, the Near East and Southwest Asia p 1 A83-10097
Action plan for remote sensing applications for rice production --- Book
[IFAORS-207] p 3 A83-14121
Assessment of spruce budworm defoliation using digital airborne MSS data p 5 A83-14248
Aerial survey of crop losses due to grasshoppers /Orthoptera - Acrididae/ in Saskatchewan p 5 A83-14255
The application of remote sensing in southern Alberta's mountain pine beetle management p 5 A83-14257
Development of a data management front end for use with a LANDSAT based information system --- assessing gypsy moth defoliation damage in Pennsylvania
[E83-10104] p 17 N83-15747

INFORMATION DISSEMINATION
Office automation in resource-management - The future is now --- agricultural land use map dissemination p 6 A83-14269
Data Announcement Bulletin: Space Shuttle OSTA 1 payload data
[NASA-TM-84884] p 72 N83-15344

INFORMATION SYSTEMS
Standardization of computer compatible tape formats for remote sensing data p 54 A83-10075
Geographic information systems p 61 N83-10465
Some closing thoughts: Practical payoffs from satellite systems p 74 N83-10468
World Integrated Oceanic Services System: General plan and operational program for 1982-1985
[WMO-582] p 46 N83-12802
Development of a data management front end for use with a LANDSAT based information system --- assessing gypsy moth defoliation damage in Pennsylvania
[E83-10104] p 17 N83-15747

INFORMATION THEORY
The Akaike information criterion and its application to mixture proportion estimation p 62 N83-12498

INFRARED DETECTORS
Investigations of the apparent temperature of snow cover in the submillimeter wavelength region p 52 A83-15816

INFRARED IMAGERY
On the circulation of the western Gulf of Mexico - A satellite view p 39 A83-10113
Analyzing and mapping regional land use trends by combining Landsat and topographic data p 2 A83-10119
Radar and infrared remote sensing of geothermal features at Pilgrim Springs, Alaska p 31 A83-12036
Technical issues in focal plane development; Proceedings of the Meeting, Washington, DC, April 21, 22, 1981 p 69 A83-13726
Environmental monitoring of the Athabasca Oil Sands Region p 19 A83-14238
Predicting permafrost conditions with infrared sensing techniques p 6 A83-14264
Other remote sensing systems: Retrospect and outlook p 74 N83-10467
An introduction to project Freeze --- the location and intensity of freezing temperatures using infrared satellite imagery
[INPE-2435-NTE/186] p 22 N83-13703
FLIR target screening p 65 N83-15771

INFRARED PHOTOGRAPHY
The utilization of infrared /IR/ aerial and space observations of Arctic seas in navigation and during the solution of other national-economic problems p 40 A83-10836
Mount St. Helens quick response damage assessment using high-altitude infrared photography p 19 A83-12672
Aerial survey of crop losses due to grasshoppers /Orthoptera - Acrididae/ in Saskatchewan p 5 A83-14255
Determination of forest fire spread rates from infrared photographs p 6 A83-14307
Aerial thermal infrared census of Canada geese in South Dakota p 6 A83-14665

INFRARED RADIATION
Comparison of multichannel and two-satellite methods for remote measurement of sea surface temperature
[AD-A118736] p 45 N83-12511

INFRARED RADIOMETERS
Mineral identification from orbit - Initial results from the Shuttle multispectral infrared radiometer p 32 A83-13350
Concerning the determination of the temperature of the ocean surface from multichannel satellite measurements of radiation in infrared atmospheric windows p 42 A83-14316
Data Announcement Bulletin: Space Shuttle OSTA 1 payload data
[NASA-TM-84884] p 72 N83-15344

INFRARED SPECTRA
The role of geological surfaces in determining visible-near infra red spectral signatures p 30 A83-10058
Use of near-infrared video recording system for the detection of freeze damaged citrus leaves
[E83-10049] p 12 N83-14558
Comparisons among a new soil index and other two- and four-dimensional vegetation indices
[E83-10058] p 14 N83-14567

INSTRUMENT ERRORS
Investigation of the geometrical stability of a photogrammetric recording system --- systems stability
[SER-C-267] p 71 N83-11565

INTEGRATED OPTICS
Low threshold InGaAsP/InP lasers with microcleaved mirrors suitable for monolithic integration p 24 A83-10981

INTERNATIONAL COOPERATION
Advanced operational earth resources satellite systems
[AAS 82-128] p 73 A83-11932
Main achievements of GARP Atlantic Tropical Experiment (GATE) and its impact on FGGE --- first GARP Global Experiment (FGGE) p 46 N83-12735
The European Community, development and satellite technology p 75 N83-14609
The role of EARSeL and EARSeL member laboratories --- in developing nations p 76 N83-14633

INTERPOLATION
Proceedings of the NASA Workshop on Surface Fitting
[E83-10117] p 64 N83-15759
C-1 surface interpolation for scattered data on a sphere p 65 N83-15762
Surfaces: Representation and approximation p 30 N83-15763
BSPLASH: A three-stage surface interpolant to scattered data p 65 N83-15765

INVENTORIES
Ecological land classification in the Yukon p 20 A83-14250

IONOSPHERIC CURRENTS
Investigation of MAGSAT and TRIAD magnetometer data to provide corrective information on high-lattitude external fields
[E83-10093] p 28 N83-14600

IONOSPHERIC PROPAGATION
Sky-wave radar sea-state sensing - Effects of ionospheric movement and propagation geometry p 43 A83-17709

IOWA
Crop weather models of corn and soybeans for Agrophysical Units (APU's) in Iowa using monthly meteorological predictors
[E83-10054] p 13 N83-14563

IRRIGATION
Crop-phenology and LANDSAT-based irrigated lands inventory in the high plains --- Texas, New Mexico, Oklahma, Kansas, Colorado, Nebraska, Wyoming, and South Dakota
[E83-10115] p 18 N83-15758

J

JAPAN
Japanese MAGSAT Team
[E83-10080] p 27 N83-14589

K

KALMAN FILTERS
Geomagnetic modeling by optimal recursive filtering
[E83-10112] p 29 N83-15755
KANSAS
Data documentation for the 1981 summer vegetation experiment --- Kansas River floodplain
[E83-10016] p 10 N83-12499
Assessment of radar resolution requirements for soil moisture estimation from simulated satellite imagery --- Kansas
[E83-10020] p 10 N83-12503
The application of remote sensing to resource management and environmental quality programs in Kansas
[E83-10114] p 23 N83-15757
KENYA
Multitemporal analysis of Landsat data for investigations of agricultural land use: Problems and potentials p 15 N83-14624
Digital analysis of Landsat satellite imagery in Turkana, Northern Kenya p 64 N83-14637
KERNEL FUNCTIONS
Characterization of a maximum-likelihood nonparametric density estimator of kernel type p 66 N83-15777
KINETIC FRICTION
Some features of the spatial structure of the Arctic Ocean ice cover in connection with turbulent friction and geostrophic capture of tide waves p 40 A83-10833
KOLMOGOROFF THEORY
The measurement of the synoptic scale wind over the ocean p 47 N83-13773

L

LAGRANGE COORDINATES
An upper bound on errors in the mean-of-date/instantaneous Earth-fixed vector transformation induced by interpolated nutation angles
[AD-A119444] p 29 N83-14656
Lagrangian drift measurements of sea surface currents and iceberg tracking p 49 N83-14842
LAKES
Surficial geology mapping from Landsat-Kaminak Lake, N.W.T. p 32 A83-14268
Temporary lakes and salt plains in the high plateaus of the Andes /Bolivia/ - A continuing survey of periodic hydrologic phenomena using the geostationary satellite GOES-EST p 51 A83-14574
HCMM hydrological analysis in Utah
[E83-10026] p 53 N83-13520
LAND ICE
Predicting permafrost conditions with infrared sensing techniques p 6 A83-14264
LAND MANAGEMENT
Application of Landsat imagery to flood control and management of agricultural land - A case study of northern India p 3 A83-14233
Identifying environmental features for land management decisions
[E83-10109] p 23 N83-15752
LAND USE
Ongoing microwave remote sensing-activities for land applications in Germany p 18 A83-10083
Analyzing and mapping regional land use trends by combining Landsat and topographic data p 2 A83-10119
Future land remote sensing data and services - A commercial perspective
[AAS 82-129] p 73 A83-11933
Operational land cover type mapping in Ontario by Landsat based digital analysis and map production p 19 A83-14230
A procedure to overlay thematic map and dominion land survey system data to geometrically-corrected Landsat images and its application to agricultural land use studies in western Canada p 3 A83-14231
Land use/land cover mapping from enhanced Landsat imagery of the eastern provinces of the People's Republic of China p 4 A83-14241
Vegetation and human impact mapping for the management of the sunshine area, Canadian Rocky Mountains p 20 A83-14242
Bank erosion and flood plain studies of the Annapolis River - An application of remote sensing data p 51 A83-14262
Office automation in resource-management - The future is now --- agricultural land use map dissemination p 6 A83-14269
Investigating the possibility of producing a land-use map for Cuba on the basis of space imagery p 20 A83-14305
LANDSAT land cover analysis completed for CIRSS/San Bernardino County project
[E83-10024] p 22 N83-12507
Construction of a remotely sensed area sampling frame for Southern Brazil
[E83-10052] p 13 N83-14561
Method of interpretation of remotely sensed data and applications to land use
[E83-10072] p 23 N83-14581
Agroecological classification by remote sensing techniques p 23 N83-14622
Automated segment matching algorithm-theory, test, and evaluation
[E83-10096] p 16 N83-15740
Identifying environmental features for land management decisions
[E83-10109] p 23 N83-15752
LANDFORMS
Predicting forest land attributes from aerial photo interpretation variables p 5 A83-14259
LANDSAT D PRIME
MSS D Multispectral Scanner System
[E83-10128] p 72 N83-15797
LANDSAT SATELLITES
Rock type discrimination techniques using Landsat and Seasat image data p 30 A83-10057
Wetland mapping with imaging radar p 50 A83-10072
Landsat monitoring of Desert Locust breeding grounds in Africa, the Near East and Southwest Asia p 1 A83-10097
A comparison of unsupervised classification procedures on Landsat MSS data for an area of complex surface conditions in Basilicata, Southern Italy p 55 A83-12037
Atmospheric effects on radiation reflected from soil and vegetation as measured by orbital sensors using various scanning directions p 3 A83-12315
Background reflectance effects in Landsat data p 55 A83-12602
Contribution of Landsat imagery to the study of volcanic structures p 31 A83-12641
Landsat observations of Mount St. Helens p 19 A83-12671
Operational land cover type mapping in Ontario by Landsat based digital analysis and map production p 19 A83-14230
A procedure to overlay thematic map and dominion land survey system data to geometrically-corrected Landsat images and its application to agricultural land use studies in western Canada p 3 A83-14231
Toward an operational, satellite-based, wetland monitoring program for the Fraser River Estuary, British Columbia p 51 A83-14234
Monitoring revision requirements for Canadian maps p 24 A83-14237
Land use/land cover mapping from enhanced Landsat imagery of the eastern provinces of the People's Republic of China p 4 A83-14241
Application of Landsat imagery to natural resources management in Sierra Leone, West Africa p 57 A83-14247
Digital colour enhancement of Landsat data for mapping vegetation of barrenground caribou winter range in northern Manitoba p 5 A83-14249
Integration of Landsat imagery into a program for aerial surveying of deer populations in Alberta p 5 A83-14252
Landsat-based forest mapping in Ontario north of latitude 52 deg north p 5 A83-14253
Multitemporal analysis of Landsat data for forest cutover mapping - A trial of two procedures p 5 A83-14254
Landsat for resource evaluation and management in the Alberta foothills p 32 A83-14256
Landsat for delineation and mapping of saline soils in dryland areas in southern Alberta p 5 A83-14261
Colour Landsat images and mosaics - Basic tools in areal and ecological differentiation in Canada p 57 A83-14265
A national Landsat collection and a proposal for a library of Landsat images p 57 A83-14270
An experimental Landsat Quicklook System for Alaska p 57 A83-14271
Definition and potential of geocoded satellite imagery products p 58 A83-14272
A refined destriping procedure for Landsat MSS data products p 58 A83-14281
Reference quicklook images for monitor of Landsat image data acquisition p 58 A83-14286
A study of atmospheric diffusion from the Landsat imagery p 20 A83-14504
Evaluating the effectiveness of Landsat data as a tool for locating buried pre-glacial valleys in eastern South Dakota p 33 A83-14667
Preparation of a sediment map of the North Frisian shoal areas on the basis of Landsat imagery p 59 A83-14945
The use of large-area spectral data in wheat yield estimation p 7 A83-16910
Geomorphological mapping using Landsat imagery - A case study in Argentina p 33 A83-17841
The LANDSAT tutorial workbook: Basics of satellite remote sensing
[E83-10001] p 74 N83-10458
Appendix A: The LANDSAT system p 75 N83-10469
Remote sensing of land resources: Application of LANDSAT satellite imagery p 11 N83-13517
Automatic interpretation of MSS-LANDSAT data applied to coal refuse site studies in southern Santa Catarina State, Brazil
[E83-10066] p 35 N83-14575
Combined use of daily thermal cycle of METEOSAT imagery and multispectral LANDSAT data: Application to the Bandiagara plateau, Mali p 36 N83-14620
Multitemporal analysis of Landsat data for investigations of agricultural land use: Problems and potentials p 15 N83-14624
A practical automated mapping system p 64 N83-14635
Digital analysis of Landsat satellite imagery in Turkana, Northern Kenya p 64 N83-14637
LANDSAT 4
The early 1981 view of Landsat-D progress p 73 A83-12673
Potentials of Landsat-D and SPOT-1 for crop identification in the maritimes p 4 A83-14240
Comparison study of future SPOT and Landsat-D satellite products from a simulation flight --- for determining spatial and spectral resolution p 57 A83-14243
Earthnet prepares for Landsat-D p 74 A83-17426
LANDSAT-4 image data quality analysis
[E83-10039] p 63 N83-13533
CNPq/INPE-LANDSAT system report of activities
[E83-10064] p 63 N83-14573
INPE LANDSAT-D thematic mapper computer compatible tape format specification
[E83-10075] p 63 N83-14584
Land remote sensing activities in the US p 72 N83-14612
LANDSAT-D: The new era of earth resources survey
[E83-10125] p 76 N83-15739
Spectral characterization of the LANDSAT-D multispectral scanner subsystems
[E83-10107] p 17 N83-15750
LANDSAT 4 investigations of thematic mapper and multispectral scanner applications
[E83-10121] p 66 N83-15791
MSS D Multispectral Scanner System
[E83-10128] p 72 N83-15797
LASER ALTIMETERS
Satellite laser altimeter for measurement of ice sheet topography p 38 A83-10092
Remote sensing of sea state using laser altimeters p 40 A83-12316
LASER APPLICATIONS
On the use of laser profilometry for ocean wave studies p 42 A83-14502
Weather constraints on airborne laser hydrography operations
[PB82-189754] p 52 N83-10745
LASER CAVITIES
Low threshold InGaAsP/InP lasers with microcleaved mirrors suitable for monolithic integration p 24 A83-10981
LASER INTERFEROMETRY
Basic research for the geodynamics program
[NASA-CR-169470] p 26 N83-13537
LASER RANGE FINDERS
Ice-sheet dynamics by satellite laser altimetry p 38 A83-10093
Utilization of range-difference observations in geodynamics p 26 N83-13539
Geometric adjustment of simultaneous Doppler-derived range differences p 26 N83-13540

LASERS
Effects of detection algorithm on accuracy degradation from logarithmic and difference processing for airborne laser bathymetry returns
[PB82-215138] p 44 N83-10707
LEAVES
Optical parameters of leaves of seven weed species
[E83-10010] p 9 N83-12489
Use of near-infrared video recording system for the detection of freeze damaged citrus leaves
[E83-10049] p 12 N83-14558
LIBERIA
The mineralogy of global magnetic anomalies
[E83-10034] p 34 N83-13528
LIBRARIES
A national Landsat collection and a proposal for a library of Landsat images p 57 A83-14270
LINEAR ARRAYS
An automated mapping satellite system /Mapsat/ p 67 A83-10715
LINEAR PROGRAMMING
Operational planning of the process of earth survey by satellites p 70 A83-14314
LITHOLOGY
Geological-structural interpretation using products of remote sensing in the region of Carrancas, Minas Gerais, Brazil
[E83-10029] p 34 N83-13523
MAGSAT project
[E83-10030] p 25 N83-13524
Spectral discrimination of lithologic facies in the granite of the Pedra Branca Goias using LANDSAT 1 digital imagery
[E83-10069] p 35 N83-14578
Multitemporal and geobotanical approach in the remote detection of Greisenization areas in the Serra da Pedra Branca Granite, Goias State, Brazil
[E83-10071] p 35 N83-14580
Combined use of daily thermal cycle of METEOSAT imagery and multispectral LANDSAT data: Application to the Bandiagara plateau, Mali p 36 N83-14620
LITHOSPHERE
The intermediate wavelength magnetic anomaly field of the north Pacific and possible source distributions
[E83-10088] p 27 N83-14596
The MAGSAT project in Australia
[E83-10089] p 28 N83-14597
LOCUSTS
Landsat monitoring of Desert Locust breeding grounds in Africa, the Near East and Southwest Asia p 1 A83-10097
LORAN C
Use of aerial photography with Loran C positioning to map offshore surface currents p 41 A83-14093
LOWER ATMOSPHERE
Technology needs assessment of an atmospheric observation system for multidisciplinary air quality/meteorology missions, part 2
[NASA-CR-3557] p 21 N83-10646

M

MAGNETIC ANOMALIES
Analysis of MAGSAT data of the Indian region
[E83-10027] p 25 N83-13521
MAGSAT project
[E83-10030] p 25 N83-13524
Gravity and magnetic anomaly data analysis
[E83-10031] p 26 N83-13525
MAGSAT for geomagnetic studies over Indian region
[E83-10032] p 26 N83-13526
MAGSAT and aeromagnetic data of the continental US
[E83-10033] p 26 N83-13527
The mineralogy of global magnetic anomalies
[E83-10034] p 34 N83-13528
MAGSAT anomaly field inversion and interpretation for the US
[E83-10057] p 27 N83-14566
Japanese MAGSAT Team
[E83-10080] p 27 N83-14589
Use of MAGSAT anomaly data for crustal structure and mineral resources in the US midcontinent
[E83-10082] p 36 N83-14590
Investigations of medium wavelength magnetic anomalies in the eastern Pacific using MAGSAT data
[E83-10083] p 27 N83-14591
An investigation of MAGSAT and complementary data *emphasizing Precambrian shields and adjacent areas of* West Africa and South America
[E83-10085] p 36 N83-14593
Investigation of Antarctic crust and upper mantle using MAGSAT and other geophysical data
[E83-10086] p 27 N83-14594
The intermediate wavelength magnetic anomaly field of the north Pacific and possible source distributions
[E83-10088] p 27 N83-14596
The reduction, verification and interpretation of MAGSAT magnetic data over Canada
[E83-10091] p 28 N83-14599
Investigating tectonic and bathymetric features of the Indian Ocean using MAGSAT magnetic anomaly data
[E83-10095] p 28 N83-14602
MAGNETIC DISTURBANCES
Investigation of MAGSAT and TRIAD magnetometer data to provide corrective information on high-lattitude external fields
[E83-10093] p 28 N83-14600
MAGNETIC EFFECTS
The MAGSAT project in Australia
[E83-10089] p 28 N83-14597
MAGNETIC FIELD INVERSIONS
MAGSAT anomaly field inversion and interpretation for the US
[E83-10057] p 27 N83-14566
MAGNETIC FIELDS
Equivalent source modeling of the main field using MAGSAT data
[E83-10094] p 28 N83-14601
Geomagnetic modeling by optimal recursive filtering
[E83-10112] p 29 N83-15755
MAGNETIC SURVEYS
Airborne gamma-ray spectrometer and magnetometer survey. Volume 1. Detail areas, Christmas Mountains, Sclitario, Green Valley/0-2 Ranch, Texas
[DE82-021614] p 34 N83-12513
Gravity and magnetic anomaly data analysis
[E83-10031] p 26 N83-13525
MAGSAT and aeromagnetic data of the continental US
[E83-10033] p 26 N83-13527
Japanese MAGSAT Team
[E83-10080] p 27 N83-14589
Use of MAGSAT anomaly data for crustal structure and mineral resources in the US midcontinent
[E83-10082] p 36 N83-14590
Investigations of medium wavelength magnetic anomalies in the eastern Pacific using MAGSAT data
[E83-10083] p 27 N83-14591
The intermediate wavelength magnetic anomaly field of the north Pacific and possible source distributions
[E83-10088] p 27 N83-14596
Investigation of MAGSAT and TRIAD magnetometer data to provide corrective information on high-lattitude external fields
[E83-10093] p 28 N83-14600
Equivalent source modeling of the main field using MAGSAT data
[E83-10094] p 28 N83-14601
Data use investigation for the magnetic field satellite (MAGSAT) mission: Geomagnetic field forecasting and fluid dynamics of the core
[E83-10098] p 29 N83-15742
The reduction, verification and interpretation of MAGSAT magnetic data over Canada
[E83-10101] p 29 N83-15744
MAINTENANCE
Operation and maintenance of geodetic satellite observatory, McMurdo, Antarctica
[PB82-187923] p 25 N83-12107
MALI
The Group Agromet Monitoring Project (GAMP) --- using METEOSAT for rangeland management in Mali p 23 N83-14615
Combined use of daily thermal cycle of METEOSAT imagery and multispectral LANDSAT data: Application to the Bandiagara plateau, Mali p 36 N83-14620
Use of remote sensing techniques for rice production forecasting in west Africa (Mali and Guinea:, Niger-Bani Project) p 15 N83-14626
MAN ENVIRONMENT INTERACTIONS
Monitoring global vegetation
[E83-10044] p 12 N83-14554
MAN MACHINE SYSTEMS
Operation plan for the data 100/LARS terminal system
[E83-10011] p 62 N83-12490
MANNED SPACE FLIGHT
Salyut-7 from June to August p 74 A83-17775
MAPPING
Analyzing and mapping regional land use trends by combining Landsat and topographic data p 2 A83-10119
An automated mapping satellite system /Mapsat/ p 67 A83-10715
Multitemporal analysis of Landsat data for forest cutover mapping - A trial of two procedures p 5 A83-14254
Cartographic aspects of dual-frequency dual-polarization SAR imagery p 58 A83-14280
Determination of the contribution of side-looking airborne radar to structural geologic mapping
[PB82-185042] p 34 N83-12713
Gravity and magnetic anomaly data analysis
[E83-10031] p 26 N83-13525
MAGSAT and aeromagnetic data of the continental US
[E83-10033] p 26 N83-13527
An analysis of a relaxation scheme to improve terrain elevation data
[AD-A119257] p 27 N83-13550
An investigation of MAGSAT and complementary data emphasizing Precambrian shields and adjacent areas of West Africa and South America
[E83-10085] p 36 N83-14593
The applicability of satellite remote sensing to small and medium scale mapping p 64 N83-14618
Tectonics of west central Mexico and adjacent Arizona: A remote sensing and field study in arid and semi-arid areas
[DE82-002393] p 37 N83-14797
The reduction, verification and interpretation of MAGSAT magnetic data over Canada
[E83-10101] p 29 N83-15744
Verification of LANDSAT imagery for morphametric and topological studies of drainage basins in a section of the western plateau of Sao Paulo State: Tiete-Aguapei watershed --- Brazil
[E83-10111] p 54 N83-15754
MAPS
Investigations of medium wavelength magnetic anomalies in the eastern Pacific using MAGSAT data
[E83-10083] p 27 N83-14591
Gravimetric maps of the Central African Republic
[E83-10084] p 27 N83-14592
MAPSAT
An automated mapping satellite system /Mapsat/ p 67 A83-10715
Geometry of a mapping satellite p 67 A83-10716
MARINE ENVIRONMENTS
Remote sensing, a tool for managing the marine environment: Eight case studies
[PB82-220864] p 44 N83-10483
Ocean pollution research, development and monitoring
[PB82-219049] p 45 N83-10740
A report to the President and the Congress
[AR-11] p 75 N83-11532
MARINE METEOROLOGY
Investigations of the Arctic, the Antarctic and the world ocean; Conference-Seminar, Moscow, USSR, February 9-13, 1981, Reports p 39 A83-10826
Application of the airborne microwave rain-scattered/radiometer system to the remote sensing of rains and wind vector measurements over the ocean p 70 A83-14293
Observations of oceanic surface-wind fields from the Nimbus-7 microwave radiometer p 42 A83-14861
Airborne atmospheric temperature structure measurements of a Pacific coast marine inversion
[AIAA PAPER 83-0278] p 70 A83-19585
SEASAT-A SASS wind processing
[NASA-CR-169433] p 44 N83-10473
Global Weather Experiment. The GARP Atlantic Tropical Experiment (GATE) Monograph
[GARP-PUB-SER-25] p 45 N83-12724
Commission for Marine Technology: Abridged report of the 8th Session --- resolutions and recommendations for ocean exploration and exploitation
[WMO-584] p 46 N83-12803
The measurement of the synoptic scale wind over the ocean p 47 N83-13773
Mesoscale ocean variability p 48 N83-14841
MATCHING
Relaxation matching applied to aerial images p 56 A83-12889
MATHEMATICAL MODELS
Radiative transfer model for heterogeneous 3-D scenes p 3 A83-12604
Second generation crop yield models review
[E83-10003] p 7 N83-12483
The possible modifications of the Hisse model for pure LANDSAT agricultural data p 10 N83-12497
Evaluation of the Williams-type spring wheat model in North Dakota and Minnesota
[E83-10041] p 12 N83-13535
Crop weather models of corn and soybeans for Agrophysical Units (APU's) in Iowa using monthly meteorological predictors
[E83-10054] p 13 N83-14563
Comparison of the CEAS and Williams-type barley yield models for North Dakota and Minnesota
[E83-10056] p 13 N83-14565
MAGSAT anomaly field inversion and interpretation for the US
[E83-10057] p 27 N83-14566

Crop weather models of barley and spring wheat yield for agrophysical units in North Dakota
[E83-10059] p 14 N83-14568
Evaluation of the Williams-type model for barley yields in North Dakota and Minnesota
[E83-10060] p 14 N83-14569
Analysis of geologic terrain models for determination of optimum SAR sensor configuration and optimum information extraction for exploration of global non-renewable resources. Pilot study: Arkansas Remote Sensing Laboratory, part 1, part 2, and part 3
[E83-10061] p 35 N83-14570
Data use investigation for the magnetic field satellite (MAGSAT) mission: Geomagnetic field forecasting and fluid dynamics of the core
[E83-10098] p 29 N83-15742
A review of crop canopy reflectance models
[E83-10110] p 17 N83-15753
Geomagnetic modeling by optimal recursive filtering
[E83-10112] p 29 N83-15755

MAXIMUM ENTROPY METHOD
The Akaike information criterion and its application to mixture proportion estimation p 62 N83-12498

MAXIMUM LIKELIHOOD ESTIMATES
Characterization of a maximum-likelihood nonparametric density estimator of kernel type p 66 N83-15777

MEASURING INSTRUMENTS
Instruments and methods for monitoring background soil pollution --- in the U.S.S.R. p 22 N83-12650

MESOSCALE PHENOMENA
Effects of mesoscale atmospheric convection cells on the waters of the East China Sea p 41 A83-13270
The measurement of the synoptic scale wind over the ocean p 47 N83-13773
Mesoscale ocean variability p 48 N83-14841

METEOROLOGICAL CHARTS
Accuracy of operational snow and ice charts p 50 A83-10090

METEOROLOGICAL PARAMETERS
Monitoring of meteorological elements in a composite program for environmental pollution studies p 22 N83-12648
Global Weather Experiment. The GARP Atlantic Tropical Experiment (GATE) Monograph
[GARP-PUB-SER-25] p 45 N83-12724
Main achievements of GARP Atlantic Tropical Experiment (GATE) and its impact on FGGE --- first GARP Global Experiment (FGGE) p 46 N83-12735
Manual on the global observing system. Volume 1 (annex to the WMO technical regulations): Global aspects, 1981 edition
[WMO-544-VOL-1-ANNEX] p 46 N83-12801
The RAMS collection of meterological and position data in the Norwegian Sea p 49 N83-14845

METEOROLOGICAL SATELLITES
Satellite estimates of ocean-air heat fluxes during cold air outbreaks p 41 A83-13059
The use of satellite information in weather forecasting at the Pacific Weather Centre p 20 A83-14277
Applications of space science and technology --- Indian space program p 75 N83-12115
Key scientific questions and the role of satellites p 64 N83-14830

METEOROLOGICAL SERVICES
Hydrological data transmission
[WMO-559] p 53 N83-12514
World Integrated Oceanic Services System: General plan and operational program for 1982-1985
[WMO-582] p 46 N83-12802

METEOROLOGY
Key scientific questions and the role of satellites p 64 N83-14830

METEOSAT SATELLITE
The European Space Agency's Earth observation satellite programs in the 1980's p 75 N83-14610
The Group Agromet Monitoring Project (GAMP) --- using METEOSAT for rangeland management in Mali p 23 N83-14615
Multitemporal soil and vegetation observations by METEOSAT over Central Africa p 15 N83-14619
Combined use of daily thermal cycle of METEOSAT imagery and multispectral LANDSAT data: Application to the Bandiagara plateau, Mali p 36 N83-14620

MICROWAVE EMISSION
Microwave emission signatures of snow in Finland p 50 A83-10065
Microwave radiance of early fall sea ice at 1.55 cm p 38 A83-10091

MICROWAVE FREQUENCIES
Evaluation of the potential of one to three SEASAT-SMMR channels in retrieving sea surface temperature
[NASA-CR-169660] p 48 N83-14604

MICROWAVE IMAGERY
The application of microwave remote sensing for snow and ice research p 38 A83-10088

MICROWAVE RADIOMETERS
Ka-band passive/active airborne radar p 68 A83-11239
An algorithm to interface Nimbus-7 SMMR data with the AES ice modelling grid for the Beaufort Sea p 41 A83-14284
Application of the airborne microwave rain-scattered/radiometer system to the remote sensing of rains and wind vector measurements over the ocean p 70 A83-14293
The possibility of measuring the moisture content of the upper layers of the atmosphere using radiometric techniques p 70 A83-14308
Snow-cover parameters retrieved from Nimbus-7 scanning multichannel microwave radiometer /SMMR/ data p 51 A83-14854
Passive microwave detection of river-plume fronts in the German Bight p 52 A83-17713
The effect of monomolecular surface films on the microwave brightness temperature of the sea surface p 43 A83-17714
Comparison of environmental conditions in the Bering Sea and Davis Strait and the effects on microwave signature returns; March and April, 1979
[NASA-CR-169473] p 46 N83-12828
Validation and application of the SEASAT-SMMR geophysical algorithms
[NASA-CR-169390] p 71 N83-13767
Evaluation of the potential of one to three SEASAT-SMMR channels in retrieving sea surface temperature
[NASA-CR-169660] p 48 N83-14604

MICROWAVE RESONANCE
Measurements of ocean surface spectrum from an aircraft using the two-frequency microwave resonance technique p 43 A83-17710

MICROWAVE SCATTERING
Remote sensing of dielectric media with periodic rough surfaces --- microwave scattering from farmfields p 1 A83-10106
Radar images of the earth from space p 59 A83-14598

MICROWAVE SENSORS
Ongoing microwave remote sensing-activities for land applications in Germany p 18 A83-10083
Microwave remote sensing: Active and passive. Volume 2 - Radar remote sensing and surface scattering and emission theory --- Book p 69 A83-14040
The microwave payload for the ESA Remote Sensing Satellite /ERS-1/ p 69 A83-14290
A simple relation between active and passive microwave remote sensing measurements of earth terrain p 24 A83-14857
Measurement of soil moisture using remote sensing multisensor radiation techniques
[E83-10012] p 9 N83-12491
Investigation of remote sensing techniques of measuring soil moisture
[E83-10048] p 12 N83-14557
Microwave remote sensing of soil moisture, volume 1 --- Guymon, Oklahoma and Dalhart, Texas
[E83-10108] p 17 N83-15751

MICROWAVE SOUNDING
Feasibility of mapping ocean surface currents using delta k-microwave radars mounted on geostationary satellite platforms p 39 A83-10094

MICROWAVE SPECTROMETERS
A field portable reflectance spectrometer p 69 A83-14275

MILITARY TECHNOLOGY
Ka-band passive/active airborne radar p 68 A83-11239

MINERAL DEPOSITS
Measurements of the characteristic reflectance spectra of surficial deposits p 32 A83-14266
Critical and strategic minerals in Alaska: Cobalt, the platinum-group metals and chromite
[PB82-193085] p 33 N83-10485

MINERAL EXPLORATION
The role of geological surfaces in determining visible-near infra red spectral signatures p 30 A83-10058
Use of reflectance spectra of native plant species for interpreting airborne multispectral scanner data in the East Tintic Mountains, Utah p 30 A83-10060
A method for the quantitative evaluation of the results of space imagery interpretation in prospecting applications p 33 A83-14302
Statistical Techniques Applied to Aerial Radiometric Surveys (STARRS): Discriminant-analysis methods applied to aerial radiometric data and their application to uranium favorability in South Texas. Nation uranium resource evaluation
[DE82-020961] p 34 N83-12512
Use of MAGSAT anomaly data for crustal structure and mineral resources in the US midcontinent
[E83-10082] p 36 N83-14590
Satellite remote sensing in mineral exploration in developing countries p 36 N83-14627

MINERALOGY
Derivation of compositional information from multispectral images --- for use in geologic remote sensing p 30 A83-10059
Cosmogeological structures of the Hissar Alai and their role in the distribution of endogenous mineralization p 31 A83-11959
Mineral identification from orbit - Initial results from the Shuttle multispectral infrared radiometer p 32 A83-13350
The mineralogy of global magnetic anomalies
[E83-10034] p 34 N83-13528

MINING
Automatic interpretation of MSS-LANDSAT data applied to coal refuse site studies in southern Santa Catarina State, Brazil
[E83-10066] p 35 N83-14575

MINNESOTA
Evaluation of the Williams-type spring wheat model in North Dakota and Minnesota
[E83-10041] p 12 N83-13535
Comparison of the CEAS and Williams-type barley yield models for North Dakota and Minnesota
[E83-10056] p 13 N83-14565
Evaluation of the Williams-type model for barley yields in North Dakota and Minnesota
[E83-10060] p 14 N83-14569

MISSION PLANNING
Operational planning of the process of earth survey by satellites p 70 A83-14314
LANDSAT-D: The new era of earth resources survey
[E83-10125] p 76 N83-15739

MISSISSIPPI RIVER (US)
A comparison of surfaces temperatures from HCMM infrared data with field measurements
[E83-10046] p 47 N83-14555

MOISTURE CONTENT
Remote determination of surface evaporation using thermal IR measurements p 50 A83-10101
Discrimination of growth and water stress in wheat by various vegetation indices through a clear a turbid atmosphere
[E83-10009] p 8 N83-12488

MOJAVE DESERT (CA)
Geologic interpretation of HCMM and aircraft thermal data
[E83-10036] p 62 N83-13530

MONITORS
Radar signatures of terrain - Useful monitors of renewable resources p 21 A83-17248

MONOMOLECULAR FILMS
The effect of monomolecular surface films on the microwave brightness temperature of the sea surface p 43 A83-17714

MONSOONS
Report of the Monex review meeting
[GARP-SPEC-REPT-38] p 45 N83-12707

MONTANA
Winter wheat stand density determination and yield estimates from handheld and airborne scanners --- Montana
[E83-10013] p 9 N83-12492

MORPHOLOGY
Automatic photointerpretation via texture and morphology analysis p 65 N83-15770

MOTION
Determining 3-D motion and structure from image sequences p 66 N83-15773

MULTISPECTRAL BAND SCANNERS
Use of reflectance spectra of native plant species for interpreting airborne multispectral scanner data in the East Tintic Mountains, Utah p 30 A83-10060
Scene classification of Landsat multispectral scanner data by means of the Adaptive Learning Network methodology p 55 A83-11458
A comparison of unsupervised classification procedures on Landsat MSS data for an area of complex surface conditions in Basilicata, Southern Italy p 55 A83-12037
Atmospheric effects on radiation reflected from soil and vegetation as measured by orbital sensors using various scanning directions p 3 A83-12315
Background reflectance effects in Landsat data p 55 A83-12602
Vegetation change detection in an agricultural area - A simple approach for use with geo-data base p 4 A83-14236
The use of R.B.V., colour additive viewer and M.S.S. products in the British Columbia Forest Inventory Depletion Monitoring Program --- Return Beam Vidicon and Multispectral Scanning p 4 A83-14246

Assessment of spruce budworm defoliation using digital airborne MSS data p 5 A83-14248
Definition and potential of geocoded satellite imagery products p 58 A83-14272
A refined destriping procedure for Landsat MSS data products p 58 A83-14281
Some effects on the GCP success rate --- Ground Control Points for satellite image rectification p 58 A83-14285
Spectral characterization of the LANDSAT-D multispectral scanner subsystems
[E83-10107] p 17 N83-15750
MSS D Multispectral Scanner System
[E83-10128] p 72 N83-15797

MULTISPECTRAL PHOTOGRAPHY
Derivation of compositional information from multispectral images --- for use in geologic remote sensing p 30 A83-10059
Automatic multitemporal segmentation for diachronic analysis of remotely sensed images p 55 A83-11461
The accuracy of a component analysis in space studies of natural environments --- for thematic mapping of earth resources and photointerpretation p 59 A83-14304
A multispectral approach to remote detection of deer p 6 A83-14666
Estimation of context for statistical classification of multispectral image data p 59 A83-14853
Some spectral and spatial characteristics of LANDSAT data p 61 N83-10461
Contextual classification of multispectral image data: An unbiased estimator for the context distribution
[E83-10087] p 63 N83-14595

MULTISPECTRAL RESOURCE SAMPLER
A means for utilizing ancillary information in multispectral classification --- of remotely sensed data p 60 A83-16905
Polarized visible light as an aid to vegetation classification p 7 A83-16908

MULTIVARIATE STATISTICAL ANALYSIS
The Akaike information criterion and its application to mixture proportion estimation p 62 N83-12498

N

NASA PROGRAMS
Land remote sensing activities in the US p 72 N83-14612

NATURAL GAS EXPLORATION
Landsat for resource evaluation and management in the Alberta foothills p 32 A83-14256
Remote sensing applications to the development of an integrated data base for oil and gas exploration p 37 N83-14628
Remote Sensing Program
[E83-10120] p 18 N83-15790

NAVIGATION SATELLITES
Operation and maintenance of geodetic satellite observatory, McMurdo, Antarctica
[PB82-187923] p 25 N83-12107

NEARSHORE WATER
Use of aerial photography with Loran C positioning to map offshore surface currents p 41 A83-14093

NEW JERSEY
A case study in the practical use of LANDSAT data p 52 N83-10466

NEW MEXICO
Tectonics of west central Mexico and adjacent Arizona: A remote sensing and field study in arid and semi-arid areas
[DE82-002393] p 37 N83-14797

NEW YORK
Remote Sensing Program
[E83-10120] p 18 N83-15790

NIGER
Application of satellite data to hydrogeological investigation in Damagaram-Mounio, Niger p 53 N83-14630

NIMBUS 6 SATELLITE
Nimbus 6 Random Access Measurement System applications experiments
[NASA-SP-457] p 48 N83-14835

NIMBUS 7 SATELLITE
An algorithm to interface Nimbus-7 SMMR data with the AES ice modelling grid for the Beaufort Sea p 41 A83-14284
Snow-cover parameters retrieved from Nimbus-7 scanning multichannel microwave radiometer /SMMR/ data p 51 A83-14854
Observations of oceanic surface-wind fields from the Nimbus-7 microwave radiometer p 42 A83-14861
The Bering Sea ice cover during March 1979: Comparison of surface and satellite data with the Nimbus-7 SMMR
[NASA-CR-169393] p 47 N83-13572

NOCTURNAL VARIATIONS
Use of thermal inertia determined by HCMM to predict nocturnal cold prone areas in Florida
[E83-10028] p 62 N83-13522
Use of thermal inertia determined by HCMM to predict nocturnal cold prone areas in Florida
[E83-10102] p 64 N83-15745

NOISE MEASUREMENT
An evaluation of the NASA/GSFC Barnes field spectral reflecometer model 14-758, using signal/noise as a measure of utility
[NASA-TM-83969] p 71 N83-12396

NONPARAMETRIC STATISTICS
Proceedings of the NASA Workshop on Density Estimation and Function Smoothing
[E83-10119] p 66 N83-15774
Cross-validation for densities and regressions p 66 N83-15776
Characterization of a maximum-likelihood nonparametric density estimator of kernel type p 66 N83-15777

NORTH DAKOTA
Evaluation of the Williams-type spring wheat model in North Dakota and Minnesota
[E83-10041] p 12 N83-13535
Comparison of the CEAS and Williams-type barley yield models for North Dakota and Minnesota
[E83-10056] p 13 N83-14565
Crop weather models of barley and spring wheat yield for agrophysical units in North Dakota
[E83-10059] p 14 N83-14568
Evaluation of the Williams-type model for barley yields in North Dakota and Minnesota
[E83-10060] p 14 N83-14569

NUMERICAL ANALYSIS
Fitting surfaces to scattered data p 65 N83-15761

NUTATION
Basic research for the geodynamics program
[NASA-CR-169470] p 26 N83-13537
Effects of adopting new precession, nutation and equinox corrections on the terrestrial reference frame p 26 N83-13538

O

OCEAN BOTTOM
Analyses of oceanic subsurface features using space based radar imagery
[AD-A118411] p 45 N83-11692

OCEAN COLOR SCANNER
OSTA-1/Ocean Color Experiment
[AIAA PAPER 83-0415] p 42 A83-16701
Analysis of high altitude remotely sensed data collected in the Nantucket Shoals experiment 4-15 May, 1981
[NASA-TM-84547] p 44 N83-10647
Data Announcement Bulletin: Space Shuttle OSTA 1 payload data
[NASA-TM-84884] p 72 N83-15344

OCEAN CURRENTS
Use of aerial photography with Loran C positioning to map offshore surface currents p 41 A83-14093
A tutorial assessment of atmospheric height uncertainties for high-precision satellite altimeter missions to monitor ocean currents p 42 A83-14851
Collinear-track altimetry in the Gulf of Mexico from SEASAT: Measurements, models and surface truth
[AD-A118160] p 45 N83-11568
Interpretation of remotely sensed data and its applications in oceanography
[E83-10074] p 48 N83-14583
Lagrangian drift measurements of sea surface currents and iceberg tracking p 49 N83-14842
The RAMS collection of meterological and position data in the Norwegian Sea p 49 N83-14845
Drift buoy component, NORPAX anomaly dynamics study p 49 N83-14848

OCEAN DATA ACQUISITIONS SYSTEMS
A comparison data set for the evaluation of remote sensing systems ability for ocean wave data collection p 38 A83-10071
Feasibility of mapping ocean surface currents using delta k-microwave radars mounted on geostationary satellite platforms p 39 A83-10094
OSTA-1/Ocean Color Experiment
[AIAA PAPER 83-0415] p 42 A83-16701
Spectral signal to clutter and thermal noise properties of ocean wave imaging synthetic aperture radars p 43 A83-17712
Global Weather Experiment. The GARP Atlantic Tropical Experiment (GATE) Monograph
[GARP-PUB-SER-25] p 45 N83-12724
Main achievements of GARP Atlantic Tropical Experiment (GATE) and its impact on FGGE --- first GARP Global Experiment (FGGE) p 46 N83-12735
World Integrated Oceanic Services System: General plan and operational program for 1982-1985
[WMO-582] p 46 N83-12802
Commission for Marine Technology: Abridged report of the 8th Session --- resolutions and recommendations for ocean exploration and exploitation
[WMO-584] p 46 N83-12803
Australian drifting buoy p 48 N83-14837
Mesoscale ocean variability p 48 N83-14841
Lagrangian drift measurements of sea surface currents and iceberg tracking p 49 N83-14842

OCEAN DYNAMICS
On the use of laser profilometry for ocean wave studies p 42 A83-14502
Flight path design issues for the TOPEX mission --- Ocean Topography Experiment
[AIAA PAPER 83-0197] p 42 A83-16581

OCEAN SURFACE
A comparison data set for the evaluation of remote sensing systems ability for ocean wave data collection p 38 A83-10071
Feasibility of mapping ocean surface currents using delta k-microwave radars mounted on geostationary satellite platforms p 39 A83-10094
Microwave remote sensing measurements of oil pollution on the ocean p 39 A83-10104
Estimating wind speed from HF skywave radar sea backscatter p 40 A83-11352
Remote sensing of sea state using laser altimeters p 40 A83-12316
The role of cross-equatorial tropical cyclone pairs in the southern oscillation p 40 A83-13057
Effects of mesoscale atmospheric convection cells on the waters of the East China Sea p 41 A83-13270
Concerning the determination of the temperature of the ocean surface from multichannel satellite measurements of radiation in infrared atmospheric windows p 42 A83-14316
Observations of oceanic surface-wind fields from the Nimbus-7 microwave radiometer p 42 A83-14861
Measurements of ocean surface spectrum from an aircraft using the two-frequency microwave resonance technique p 43 A83-17710
The effect of monomolecular surface films on the microwave brightness temperature of the sea surface p 43 A83-17714
Experimental feasibility of the airborne measurement of absolute oil fluorescence spectral conversion efficiency p 44 A83-18581
Collinear-track altimetry in the Gulf of Mexico from SEASAT: Measurements, models and surface truth
[AD-A118160] p 45 N83-11568
Mean Earth ellipsoid determined from SEASAT altimeter observations
[AD-A117910] p 45 N83-11570
Analyses of oceanic subsurface features using space based radar imagery
[AD-A118411] p 45 N83-11692
Comparison of multichannel and two-satellite methods for remote measurement of sea surface temperature
[AD-A118736] p 45 N83-12511
The Global Weather Experiment. First GARP Global Experiment (FGGE) operations report series: Volume 5, summary of data collected 5 July - December 1979
[GARP-FOR-5] p 46 N83-12808
A comparison of HCMM surface temperatures with in situ temperature data --- Nantucket shoals and the Gulf of Mexico regions
[E83-10040] p 46 N83-13534
Aircraft and satellite measurement of ocean wave directional spectra using scanning-beam microwave radars
[NASA-TM-84008] p 47 N83-13544
The intermediate wavelength magnetic anomaly field of the north Pacific and possible source distributions
[E83-10088] p 27 N83-14596
Joint Air Sea Interaction (JASIN) experiment, Northwest coast of Scotland
[NASA-CR-169631] p 48 N83-14603
Evaluation of the potential of one to three SEASAT-SMMR channels in retrieving sea surface temperature
[NASA-CR-169660] p 48 N83-14604
GRAVSAT error analysis by means of global spectral analyses of the marine geoid from SEASAT altimeter data
[E83-10105] p 29 N83-15748

OCEAN TEMPERATURE
Applicability of satellite-derived sea-surface temperatures in the Fiji region p 40 A83-12032
The role of cross-equatorial tropical cyclone pairs in the southern oscillation p 40 A83-13057
Satellite estimates of ocean-air heat fluxes during cold air outbreaks p 41 A83-13059

Concerning the determination of the temperature of the ocean surface from multichannel satellite measurements of radiation in infrared atmospheric windows p 42 A83-14316
Comparison of multichannel and two-satellite methods for remote measurement of sea surface temperature [AD-A118736] p 45 N83-12511
The Global Weather Experiment. First GARP Global Experiment (FGGE) operations report series: Volume 5, summary of data collected 5 July - December 1979 [GARP-FOR-5] p 46 N83-12808
Space truth in oceanography p 48 N83-14636
Australian drifting buoy p 48 N83-14837
Infrared satellite data from the first coastal ocean dynamics experiment, March - July 1981 [AD-A120068] p 49 N83-15799

OCEANOGRAPHIC PARAMETERS
The 100 days of Seasat-A p 39 A83-10115

OCEANOGRAPHY
Investigations of the Arctic, the Antarctic and the world ocean; Conference-Seminar, Moscow, USSR, February 9-13, 1981, Reports p 39 A83-10826
SEASAT-A SASS wind processing [NASA-CR-169433] p 44 N83-10473
Evaluation of geodetic products produced by the NSWC reduction of SEASAT radar altimeter data [AD-A117837] p 25 N83-11571
Naval Research Reviews, volume 34, no. 1 [AD-A117981] p 45 N83-12037
Interpretation of remotely sensed data and its applications in oceanography [E83-10074] p 48 N83-14583
Space truth in oceanography p 48 N83-14636
The RAMS collection of meterological and position data in the Norwegian Sea p 49 N83-14845

OCEANS
Ocean pollution research, development and monitoring [PB82-219049] p 45 N83-10740

OIL EXPLORATION
Environmental monitoring of the Athabasca Oil Sands Region p 19 A83-14238
Landsat for resource evaluation and management in the Alberta foothills p 32 A83-14256
Remote sensing applications to the development of an integrated data base for oil and gas exploration p 37 N83-14628

OIL POLLUTION
Remote sensing of water quality for estuarine environments p 50 A83-10073
Microwave remote sensing measurements of oil pollution on the ocean p 39 A83-10104
On detection of oil pollution in ice environment p 41 A83-14239

OIL SLICKS
The effect of monomolecular surface films on the microwave brightness temperature of the sea surface p 43 A83-17714
Experimental feasibility of the airborne measurement of absolute oil fluorescence spectral conversion efficiency p 44 A83-18581

OKLAHOMA
Microwave remote sensing of soil moisture, volume 1 --- Guymon, Oklahoma and Dalhart, Texas [E83-10108] p 17 N83-15751

OPTICAL DENSITY
Remote measurement of biomass p 6 A83-14306

OPTICAL MEASURING INSTRUMENTS
Electro-optical instrumentation for resources evaluation; Proceedings of the Meeting, Washington, DC, April 21, 22, 1981 p 68 A83-12669

OPTICAL PROPERTIES
Performance comparison for Barnes model 12-1000, Exotech model 100, and Ideas Inc. Biometer Mark 2 [E83-10004] p 8 N83-12484

OPTICAL RADAR
Dual-wavelength correlation measurements with an airborne pulsed carbon dioxide lidar system p 60 A83-16831
Experimental feasibility of the airborne measurement of absolute oil fluorescence spectral conversion efficiency p 44 A83-18581

OPTIMIZATION
Geomagnetic modeling by optimal recursive filtering [E83-10112] p 29 N83-15755

ORBIT CALCULATION
Flight path design issues for the TOPEX mission --- Ocean Topography Experiment [AIAA PAPER 83-0197] p 42 A83-16581

ORBITAL MECHANICS
Preliminary study of GPS orbit determination accuracy achievable from worldwide tracking data [NASA-CR-169693] p 28 N83-14605
TOPEX orbit determination using GPS signals plus a sidetone ranging system [NASA-CR-169694] p 29 N83-14606

ORGANIC MATERIALS
Determination of humus in soil on the basis of spectral measurements p 6 A83-14310

OROGRAPHY
Cosmogeological structures of the Hissar Alai and their role in the distribution of endogenous mineralization p 31 A83-11959

ORTHOPHOTOGRAPHY
A Digital Photogrammetric System (DPS) for producing Digital Elevation Models (DEM) and orthoplates by means of linear array scanner imagery [MBB-UA-618/81] p 71 N83-13567

OSTA-1 PAYLOAD
Use of the Space Shuttle for remote sensing research - Recent results and future prospects p 68 A83-13347
Data Announcement Bulletin: Space Shuttle OSTA 1 payload data [NASA-TM-84884] p 72 N83-15344

OZONE
An optimum statistical technique for ozone profile retrieval from backscattered UV radiances p 21 A83-14632

P

P-3 AIRCRAFT
Passive microwave detection of river-plume fronts in the German Bight p 52 A83-17713

PACIFIC OCEAN
Applicability of satellite-derived sea-surface temperatures in the Fiji region p 40 A83-12032
The role of cross-equatorial tropical cyclone pairs in the southern oscillation p 40 A83-13057
The use of satellite information in weather forecasting at the Pacific Weather Centre p 20 A83-14277
Airborne atmospheric temperature structure measurements of a Pacific coast marine inversion [AIAA PAPER 83-0278] p 70 A83-19585
Investigations of medium wavelength magnetic anomalies in the eastern Pacific using MAGSAT data [E83-10083] p 27 N83-14591
The intermediate wavelength magnetic anomaly field of the north Pacific and possible source distributions [E83-10088] p 27 N83-14596
Australian drifting buoy p 48 N83-14837
Drift buoy component, NORPAX anomaly dynamics study p 49 N83-14848

PARAMETER IDENTIFICATION
Investigation of the geometrical stability of a photogrammetric recording system --- systems stability [SER-C-267] p 71 N83-11565

PATTERN RECOGNITION
Probabilistic cluster labeling of imagery data p 54 A83-11410
Pattern recognition and digital image processing as applied to remote sensing in India p 54 A83-11450
Scene classification of Landsat multispectral scanner data by means of the Adaptive Learning Network methodology p 55 A83-11458
Defense Mapping Agency /DMA/ overview of mapping, charting, and geodesy /MC&G/ applications of digital image pattern recognition p 24 A83-12877
Reconnaissance applications of image understanding p 56 A83-12882
Automation of the search for and recognition of reference zones for precise coordinate control of space imagery p 59 A83-14311
Estimation of context for statistical classification of multispectral image data p 59 A83-14853
Some spectral and spatial characteristics of LANDSAT data p 61 N83-10461
Photointerpretation of LANDSAT images p 61 N83-10462
Computer processed LANDSAT data p 61 N83-10463
Appendix B: Principles of computer processing of LANDSAT data p 75 N83-10470
Remote sensing of agricultural crops and soils [E83-10023] p 11 N83-12506
Use of LANDSAT images to study cerrado vegetation --- Mato Grosso Sul, Brazil [E83-10025] p 11 N83-13519
Contextual classification of multispectral image data: An unbiased estimator for the context distribution [E83-10087] p 63 N83-14595
Automatic photointerpretation via texture and morphology analysis p 65 N83-15770
FLIR target screening p 65 N83-15771
Structural analysis techniqes for remote sensing p 66 N83-15772

PATTERN REGISTRATION
Registration of a synthetic aperture radar /SAR/ reconnaissance image with a map reference data base p 56 A83-12885
Near surface observations p 61 N83-10464

PENNSYLVANIA
Development of a data management front end for use with a LANDSAT based information system --- assessing gypsy moth defoliation damage in Pennsylvania [E83-10104] p 17 N83-15747

PERFORMANCE
Comparison study of future SPOT and Landsat-D satellite products from a simulation flight --- for determining spatial and spectral resolution p 57 A83-14243

PERFORMANCE PREDICTION
Satellite remote sensing for domestic crop reporting in the United States and Canada - A look to the future p 3 A83-14229

PERFORMANCE TESTS
MSS D Multispectral Scanner System [E83-10128] p 72 N83-15797

PERIODIC VARIATIONS
Vegetation change detection in an agricultural area - A simple approach for use with geo-data base p 4 A83-14236

PERIODICALS
Naval Research Reviews, volume 34, no. 1 [AD-A117981] p 45 N83-12037

PERMAFROST
Predicting permafrost conditions with infrared sensing techniques p 6 A83-14264

PESTICIDES
Reflectance differences between untreated and Mepiquat Chloride-treated, field-grown cotton through a growing season p 7 A83-16909

PHENOLOGY
Analysis of the profile characteristics of corn and soybeans using field reflectance data [E83-10018] p 10 N83-12501
Crop-phenology and LANDSAT-based irrigated lands inventory in the high plains --- Texas, New Mexico, Oklahma, Kansas, Colorado, Nebraska, Wyoming, and South Dakota [E83-10115] p 18 N83-15758

PHOTOGEOLOGY
Rock type discrimination techniques using Landsat and Seasat image data p 30 A83-10057
Derivation of compositional information from multispectral images --- for use in geologic remote sensing p 30 A83-10059
Geological terrain models p 31 A83-10080
Some examples of the utility of HCMM data in geologic remote sensing --- Heat Capacity Mapping Mission p 31 A83-10099
Cosmogeological structures of the Hissar Alai and their role in the distribution of endogenous mineralization p 31 A83-11959
Contribution of Landsat imagery to the study of volcanic structures p 31 A83-12641
Subsurface valleys and geoarcheology of the eastern Sahara revealed by Shuttle radar p 32 A83-13349
Mineral identification from orbit - Initial results from the Shuttle multispectral infrared radiometer p 32 A83-13350
Measurements of the characteristic reflectance spectra of surficial deposits p 32 A83-14266
Surficial geology mapping from Landsat-Kaminak Lake, N.W.T. p 32 A83-14268
A method for the quantitative evaluation of the results of space imagery interpretation in prospecting applications p 33 A83-14302
Lineaments and ring structures on the territory of Poland p 24 A83-14303
An example of a statistical analysis of the results of space imagery interpretation for the eastern part of the Fergana Valley p 33 A83-14315
Evaluating the effectiveness of Landsat data as a tool for locating buried pre-glacial valleys in eastern South Dakota p 33 A83-14667
Some comparative aspects of SLAR and airphoto images for geomorphologic and geologic interpretation p 33 A83-17842
Geological-structural interpretation using products of remote sensing in the region of Carrancas, Minas Gerais, Brazil [E83-10029] p 34 N83-13523
An investigation into the utilization of HCMM thermal data for the descrimination of volcanic and Eolian geological units --- Craters of the Moon volcanic field, Idaho; San Francisco volcanic field, Arizona; High Desert, California; and the Cascade Range, California and Oregon [E83-10047] p 35 N83-14556
Spectral discrimination of lithologic facies in the granite of the Pedra Branca Goias using LANDSAT 1 digital imagery [E83-10069] p 35 N83-14578

Multitemporal and geobotanical approach in the remote detection of Greisenization areas in the Serra da Pedra Branca Granite, Goias State, Brazil
[E83-10071] p 35 N83-14580
LANDSAT and radar mapping of intrusive rocks in SE-Brazil
[E83-10073] p 36 N83-14582
The computer treatment of remotely sensed data: An introduction to techniques which have geologic applications --- image enhancement and thematic classification in Brazil
[E83-10078] p 36 N83-14587
Neotectonics of the San Andreas Fault system: Basin and range province juncture
[E83-10090] p 36 N83-14598
Analysis of the characteristics appearing in LANDSAT multispectral images in the geological structural mapping of the midwestern portion of the Rio Grande do Sul shield --- Brazil
[E83-10126] p 37 N83-15795

PHOTOGRAMMETRY
Photointerpretation, remote sensing, and photogrammetric elements applied to road-planning studies p 19 A83-11866
Image enhancement through film recorder response contouring p 56 A83-12685
Some effects on the GCP success rate --- Ground Control Points for satellite image rectification p 58 A83-14285
To mix or match - On choosing matched samples in comparative aerial surveys p 59 A83-14664
Results of phototriangulation on the basis of space photographs p 60 A83-17299
Theoretical and experimental investigations on the accuracy of close-range photogrammetry
[SER-C-266] p 25 N83-11564
Investigation of the geometrical stability of a photogrammetric recording system --- systems stability
[SER-C-267] p 71 N83-11565
Pass point determination and geometrical precision of the relative rectification of scanner data
[SER-C-268] p 62 N83-13518
An analysis of a relaxation scheme to improve terrain elevation data
[AD-A119257] p 27 N83-13550
A Digital Photogrammetric System (DPS) for producing Digital Elevation Models (DEM) and orthoplates by means of linear array scanner imagery
[MBB-UA-618/81] p 71 N83-13567
The applicability of satellite remote sensing to small and medium scale mapping p 64 N83-14618

PHOTOGRAPHIC PROCESSING
Evaluation of photographic enhancements of Landsat imagery p 55 A83-12035

PHOTOGRAPHIC RECORDING
Investigation of the geometrical stability of a photogrammetric recording system --- systems stability
[SER-C-267] p 71 N83-11565

PHOTOINTERPRETATION
Automatic multitemporal segmentation for diachronic analysis of remotely sensed images p 55 A83-11461
Photointerpretation, remote sensing, and photogrammetric elements applied to road-planning studies p 19 A83-11866
Reconnaissance applications of image understanding p 56 A83-12882
The relationships between reflectance in the Landsat wavebands and the composition of an Australian semi-arid shrub rangeland p 19 A83-14095
Operational land cover type mapping in Ontario by Landsat based digital analysis and map production p 19 A83-14230
Visual analysis of 1:250,000 Landsat data for forage assessment during the 1980 drought in western Manitoba p 3 A83-14235
Waterfowl habitat inventory of Alberta, Saskatchewan and Manitoba by remote sensing p 4 A83-14244
Optical characteristics of Alberta rangeland as related to remote sensing p 4 A83-14245
Predicting forest land attributes from aerial photo interpretation variables p 5 A83-14259
Construction and interpretation of a thermal inertia image using airborne data p 57 A83-14260
Colour Landsat images and mosaics - Basic tools in areal and ecological differentiation in Canada p 57 A83-14265
A field portable reflectance spectrometer p 69 A83-14275
A system for the complex processing of aerial and space data for agriculture p 6 A83-14301
A method for the quantitative evaluation of the results of space imagery interpretation in prospecting applications p 33 A83-14302
The accuracy of a component analysis in space studies of natural environments --- for thematic mapping of earth resources and photointerpretation p 59 A83-14304
Determination of forest fire spread rates from infrared photographs p 6 A83-14307
An example of a statistical analysis of the results of space imagery interpretation for the eastern part of the Fergana Valley p 33 A83-14315
A multispectral approach to remote detection of deer p 6 A83-14666
Resolution versus speckle relative to geologic interpretability of spaceborne radar images - A survey of user preference p 33 A83-14852
Investigations of interpretability of images by different sensors and platforms for small scale mapping p 70 A83-14943
Familiarization with LANDSAT imagery p 60 N83-10460
Photointerpretation of LANDSAT images p 61 N83-10462
Appendix C. LANDSAT: A worldwide perspective p 75 N83-10471
Geological-structural interpretation using products of remote sensing in the region of Carrancas, Minas Gerais, Brazil
[E83-10029] p 34 N83-13523
Method of interpretation of remotely sensed data and applications to land use
[E83-10072] p 23 N83-14581
Interpretation of remotely sensed data and its applications in oceanography
[E83-10074] p 48 N83-14583
Evaluation of reforestation using remote sensing techniques
[E83-10076] p 15 N83-14585
Some aspects of the presentation of remote sensing data p 63 N83-14617
Proceedings of the NASA Workshop on Image Analysis
[E83-10118] p 65 N83-15766
Automatic photointerpretation via texture and morphology analysis p 65 N83-15770
Structural analysis techniqes for remote sensing p 66 N83-15772

PHOTOMAPPING
Geometry of a mapping satellite p 67 A83-10716
A relational image data base system for remote sensing /LAND DBMS/ p 55 A83-11462
Photointerpretation, remote sensing, and photogrammetric elements applied to road-planning studies p 19 A83-11866
Environmental monitoring of the Athabasca Oil Sands using Landsat data p 31 A83-11988
Landsat observations of Mount St. Helens p 19 A83-12671
Mount St. Helens quick response damage assessment using high-altitude infrared photography p 19 A83-12672
The early 1981 view of Landsat-D progress p 73 A83-12673
Analytical plotter for data input into geo-based information systems p 56 A83-12683
Defense Mapping Agency /DMA/ overview of mapping, charting, and geodesy /MC&G/ applications of digital image pattern recognition p 24 A83-12877
Use of aerial photography with Loran C positioning to map offshore surface currents p 41 A83-14093
Satellite remote sensing for domestic crop reporting in the United States and Canada - A look to the future p 3 A83-14229
Operational land cover type mapping in Ontario by Landsat based digital analysis and map production p 19 A83-14230
A position-based resource mapping study of the Kananaskis Valley using Landsat p 19 A83-14232
Monitoring revision requirements for Canadian maps p 24 A83-14237
Land use/land cover mapping from enhanced Landsat imagery of the eastern provinces of the People's Republic of China p 4 A83-14241
Vegetation and human impact mapping for the management of the sunshine area, Canadian Rocky Mountains p 20 A83-14242
Landsat-based forest mapping in Ontario north of latitude 52 deg north p 5 A83-14253
Landsat for resource evaluation and management in the Alberta foothills p 32 A83-14256
Predicting forest land attributes from aerial photo interpretation variables p 5 A83-14259
Surficial geology mapping from Landsat-Kaminak Lake, N.W.T. p 32 A83-14268
Office automation in resource-management - The future is now --- agricultural land use map dissemination p 6 A83-14269
A national Landsat collection and a proposal for a library of Landsat images p 57 A83-14270
Definition and potential of geocoded satellite imagery products p 58 A83-14272
Lineaments and ring structures on the territory of Poland p 24 A83-14303
Investigating the possibility of producing a land-use map for Cuba on the basis of space imagery p 20 A83-14305
Aerial thermal infrared census of Canada geese in South Dakota p 6 A83-14665
Investigations of interpretability of images by different sensors and platforms for small scale mapping p 70 A83-14943
Preparation of a sediment map of the North Frisian shoal areas on the basis of Landsat imagery p 59 A83-14945
Results of phototriangulation on the basis of space photographs p 60 A83-17299
Geomorphological mapping using Landsat imagery - A case study in Argentina p 33 A83-17841
The use of thematic mapper simulator calibration data for assessment of data quality
[NASA-TM-82059] p 71 N83-13547
A practical automated mapping system p 64 N83-14635

PHOTOMAPS
Familiarization with LANDSAT imagery p 60 N83-10460
Photointerpretation of LANDSAT images p 61 N83-10462

PHOTORECONNAISSANCE
Reconnaissance applications of image understanding p 56 A83-12882
Landsat for resource evaluation and management in the Alberta foothills p 32 A83-14256

PHOTOVOLTAIC CONVERSION
Spectroradiometer measurements in support of photovoltaic device testing p 70 A83-15458

PHYSIOLOGY
Second generation crop yield models review
[E83-10003] p 7 N83-12483

PIGMENTS
Phytoplankton pigment concentrations in the Middle Atlantic Bight - Comparison of ship determinations and CZCS estimates --- Coastal Zone Color Scanner p 43 A83-18580

PLAINS
Crop-phenology and LANDSAT-based irrigated lands inventory in the high plains --- Texas, New Mexico, Oklahma, Kansas, Colorado, Nebraska, Wyoming, and South Dakota
[E83-10115] p 18 N83-15758

PLANETARY SURFACES
Imaging radar observations of volcanic features in Medicine Lake Highland, California p 30 A83-10079

PLANKTON
Phytoplankton pigment concentrations in the Middle Atlantic Bight - Comparison of ship determinations and CZCS estimates --- Coastal Zone Color Scanner p 43 A83-18580

PLANT STRESS
Reflectance measurement of artificially induced ultraviolet radiation stress on cotton leaves p 7 A83-16907
Discrimination of growth and water stress in wheat by various vegetation indices through a clear a turbid atmosphere
[E83-10009] p 8 N83-12488
Agricultural Research Service research highlights in remote sensing for calendar year 1981
[E83-10051] p 75 N83-14560

PLANTS (BOTANY)
Use of reflectance spectra of native plant species for interpreting airborne multispectral scanner data in the East Tintic Mountains, Utah p 30 A83-10060
Second generation crop yield models review
[E83-10003] p 7 N83-12483
Comparison of LANDSAT-2 and field spectrometer reflectance signatures of south Texas rangeland plant communities
[E83-10055] p 13 N83-14564

PLOTTERS
Analytical plotter for data input into geo-based information systems p 56 A83-12683

PLOTTING
Earth Observations Division version of the Laboratory for Applications of Remote Sensing System (EOD-LARSYS) user guide for the IBM 370/148. Volume 1: System overview
[E83-10007] p 62 N83-12866

PLUMES
A study of atmospheric diffusion from the Landsat imagery p 20 A83-14504

POLAND
Lineaments and ring structures on the territory of Poland p 24 A83-14303

POLAR METEOROLOGY
Investigations of the Arctic, the Antarctic and the world ocean; Conference-Seminar, Moscow, USSR, February 9-13, 1981, Reports p 39 A83-10826
Using new methods in monitoring the thermal regime of the Arctic p 39 A83-10828
Arctic haze and the Arctic gas and aerosol sampling program /AGASP/
[AIAA PAPER 83-0439] p 21 A83-16714
POLAR REGIONS
Satellite laser altimeter for measurement of ice sheet topography p 38 A83-10092
POLAR WANDERING (GEOLOGY)
Effects of adopting new precession, nutation and equinox corrections on the terrestrial reference frame p 26 N83-13538
Utilization of range-difference observations in geodynamics p 26 N83-13539
POLARIZED LIGHT
Polarized visible light as an aid to vegetation classification p 7 A83-16908
POLLUTION MONITORING
Remote sensing of water quality for estuarine environments p 50 A83-10073
Microwave remote sensing measurements of oil pollution on the ocean p 39 A83-10104
Evidence for a central Eurasian source area of arctic haze in Alaska p 18 A83-11626
On detection of oil pollution in ice environment p 41 A83-14239
On the Development of Multimedia Monitoring of Environmental Pollution — conferences
[WMO-563] p 22 N83-12599
Instruments and methods for monitoring background soil pollution — in the U.S.S.R. p 22 N83-12650
Automatic interpretation of MSS-LANDSAT data applied to coal refuse site studies in southern Santa Catarina State, Brazil
[E83-10066] p 35 N83-14575
POLLUTION TRANSPORT
Aircraft and remote measurements of atmospheric transport of pollutants within the global integrated monitoring system p 22 N83-12620
PORTABLE EQUIPMENT
A field portable reflectance spectrometer p 69 A83-14275
PRECESSION
Effects of adopting new precession, nutation and equinox corrections on the terrestrial reference frame p 26 N83-13538
PREPROCESSING
Appendix A: The LANDSAT system p 75 N83-10469
Appendix B: Principles of computer processing of LANDSAT data p 75 N83-10470
PROBABILITY DENSITY FUNCTIONS
Proceedings of the NASA Workshop on Density Estimation and Function Smoothing
[E83-10119] p 66 N83-15774
Topics in global convergence of density estimates p 66 N83-15775
Cross-validation for densities and regressions p 66 N83-15776
PROFILOMETERS
On the use of laser profilometry for ocean wave studies p 42 A83-14502
PROGRAM VERIFICATION (COMPUTERS)
Validation and application of the SEASAT-SMMR geophysical algorithms
[NASA-CR-169390] p 71 N83-13767
PROJECT MANAGEMENT
Main achievements of GARP Atlantic Tropical Experiment (GATE) and its impact on FGGE — first GARP Global Experiment (FGGE) p 46 N83-12735
PROJECT PLANNING
World Integrated Oceanic Services System: General plan and operational program for 1982-1985
[WMO-582] p 46 N83-12802
SPOT in the 1980's p 76 N83-14611
PROPAGATION VELOCITY
Determination of forest fire spread rates from infrared photographs p 6 A83-14307
PROVING
Cross-validation for densities and regressions p 66 N83-15776
PULSED LASERS
Dual-wavelength correlation measurements with an airborne pulsed carbon dioxide lidar system p 60 A83-16831
PUSHBROOM SENSOR MODES
Technical issues in focal plane development for terrestrial resource observations p 69 A83-13735
A Digital Photogrammetric System (DPS) for producing Digital Elevation Models (DEM) and orthoplates by means of linear array scanner imagery
[MBB-UA-618/81] p 71 N83-13567

Q

QUALITY CONTROL
Quality assessment of remote-sensing data - The SAR case p 56 A83-13845

R

RADAR
Mean Earth ellipsoid determined from SEASAT altimeter observations
[AD-A117910] p 45 N83-11570
Aircraft and satellite measurement of ocean wave directional spectra using scanning-beam microwave radars
[NASA-TM-84008] p 47 N83-13544
RADAR ECHOES
Estimating wind speed from HF skywave radar sea backscatter p 40 A83-11352
RADAR EQUIPMENT
Ka-band passive/active airborne radar p 68 A83-11239
RADAR GEOLOGY
Geological-structural interpretation using products of remote sensing in the region of Carrancas, Minas Gerais, Brazil
[E83-10029] p 34 N83-13523
Analysis of geologic terrain models for determination of optimum SAR sensor configuration and optimum information extraction for exploration of global non-renewable resources. Pilot study: Arkansas Remote Sensing Laboratory, part 1, part 2, and part 3
[E83-10061] p 35 N83-14570
RADAR IMAGERY
Seasat L-band radar response to forest vegetation in eastern Virginia p 1 A83-10061
Wetland mapping with imaging radar p 50 A83-10072
Drumlin fields and glaciated mountains - A contrast in geomorphic perception from Seasat radar images p 23 A83-10078
Imaging radar observations of volcanic features in Medicine Lake Highland, California p 30 A83-10079
Geological terrain models p 31 A83-10080
A parametric study of tillage effects on radar backscatter p 2 A83-10108
Potentials for change detection using Seasat synthetic aperture radar data p 54 A83-10121
Radar and infrared remote sensing of geothermal features at Pilgrim Springs, Alaska p 31 A83-12036
Earth resources observation with the Shuttle imaging radar p 68 A83-12676
Shuttle imaging radar experiment p 32 A83-13348
Subsurface valleys and geoarcheology of the eastern Sahara revealed by Shuttle radar p 32 A83-13349
Quality assessment of remote-sensing data - The SAR case p 56 A83-13845
Microwave remote sensing: Active and passive. Volume 2 - Radar remote sensing and surface scattering and emission theory — Book p 69 A83-14040
Remote sensing software for airborne image analysis p 58 A83-14273
Applications of Robert's gradient operator for the digital enhancement of icebergs from SAR imagery p 41 A83-14278
Cartographic aspects of dual-frequency dual-polarization SAR imagery p 58 A83-14280
Radar images of the earth from space p 59 A83-14598
Resolution versus speckle relative to geologic interpretability of spaceborne radar images - A survey of user preference p 33 A83-14852
A backscatter model for a randomly perturbed periodic surface — radar imagery of earth soil with row structure p 7 A83-14859
The digital image processing system MOBI-DIVAH p 59 A83-14944
Rectification of Seasat radar on Landsat MSS with the aid of digital image correlation p 59 A83-14946
An evaluation of Seasat SAR imagery for urban analysis p 60 A83-16904
Spectral signal to clutter and thermal noise properties of ocean wave imaging synthetic aperture radars p 43 A83-17712
Other remote sensing systems: Retrospect and outlook p 74 N83-10467
Naval Research Reviews, volume 34, no. 1
[AD-A117981] p 45 N83-12037
Assessment of radar resolution requirements for soil moisture estimation from simulated satellite imagery — Kansas
[E83-10020] p 10 N83-12503
Evaluation of ERIM optically processed SEASAT SAR data
[E83-10037] p 63 N83-13531
Method of interpretation of remotely sensed data and applications to land use
[E83-10072] p 23 N83-14581
LANDSAT and radar mapping of intrusive rocks in SE-Brazil
[E83-10073] p 36 N83-14582
The applicability of satellite remote sensing to small and medium scale mapping p 64 N83-14618
Data Announcement Bulletin: Space Shuttle OSTA 1 payload data
[NASA-TM-84884] p 72 N83-15344
RADAR MAPS
Wetland mapping with imaging radar p 50 A83-10072
Feasibility of mapping ocean surface currents using delta k-microwave radars mounted on geostationary satellite platforms p 39 A83-10094
Registration of a synthetic aperture radar /SAR/ reconnaissance image with a map reference data base p 56 A83-12885
RADAR MEASUREMENT
Radar spectral observations of snow p 49 A83-10064
Effects of vegetation cover on the radar sensitivity to soil moisture p 6 A83-14856
Dual-wavelength correlation measurements with an airborne pulsed carbon dioxide lidar system p 60 A83-16831
Sky-wave radar sea-state sensing - Effects of ionospheric movement and propagation geometry p 43 A83-17709
Measurements of ocean surface spectrum from an aircraft using the two-frequency microwave resonance technique p 43 A83-17710
RADAR RESOLUTION
Assessment of radar resolution requirements for soil moisture estimation from simulated satellite imagery — Kansas
[E83-10020] p 10 N83-12503
RADAR SCATTERING
Radar spectral observations of snow p 49 A83-10064
A backscatter model for a randomly perturbed periodic surface — furrowed soils in agricultural fields p 1 A83-10107
A parametric study of tillage effects on radar backscatter p 2 A83-10108
Estimating wind speed from HF skywave radar sea backscatter p 40 A83-11352
Effects of vegetation cover on the radar sensitivity to soil moisture p 6 A83-14856
A three-part geometric model to predict the radar backscatter from wheat, corn, and sorghum
[E83-10005] p 8 N83-12485
Data documentation for the 1981 summer vegetation experiment — Kansas River floodplain
[E83-10016] p 10 N83-12499
RADAR SIGNATURES
Radar signatures of terrain - Useful monitors of renewable resources p 21 A83-17248
RADAR TARGETS
SAR squint analysis of directional extended targets — using Doppler filtering of SAR signal film p 54 A83-10084
RADIAL DISTRIBUTION
TOPEX orbit determination using GPS signals plus a sidetone ranging system
[NASA-CR-169694] p 29 N83-14606
RADIANCE
An optimum statistical technique for ozone profile retrieval from backscattered UV radiances p 21 A83-14632
Winter wheat stand density determination and yield estimates from handheld and airborne scanners — Montana
[E83-10013] p 9 N83-12492
RADIATION DAMAGE
Reflectance measurement of artificially induced ultraviolet radiation stress on cotton leaves p 7 A83-16907
RADIATION MEASUREMENT
Spectroradiometer measurements in support of photovoltaic device testing p 70 A83-15458
RADIATIVE TRANSFER
Radiative transfer model for heterogeneous 3-D scenes p 3 A83-12604
Other remote sensing systems: Retrospect and outlook p 74 N83-10467
Radiance calculations for optimization of sensors designed for remote bathymetry, volume 1
[AD-A117743] p 44 N83-10739
Adjusting the tasseled cap brightness and greenness factors for atmospheric path radiance and absorption on a pixel by pixel basis
[E83-10053] p 13 N83-14562

Comparison of diverse methods for the correction of atmospheric effects on LANDSAT and SKYLAB images --- radiometric correction in Brazil
[E83-10079] p 72 N83-14588
A review of crop canopy reflectance models
[E83-10110] p 17 N83-15753
Remote sensing of temperature profiles in the atmosphere p 66 N83-15778

RADII
Mean Earth ellipsoid determined from SEASAT altimeter observations
[AD-A117910] p 45 N83-11570

RADIO ALTIMETERS
Ice-sheet dynamics by satellite laser altimetry p 38 A83-10093
The microwave payload for the ESA Remote Sensing Satellite /ERS-1/ p 69 A83-14290
A tutorial assessment of atmospheric height uncertainties for high-precision satellite altimeter missions to monitor ocean currents p 42 A83-14851
Evaluation of geodetic products produced by the NSWC reduction of SEASAT radar altimeter data
[AD-A117837] p 25 N83-11571
GRAVSAT error analysis by means of global spectral analyses of the marine geoid from SEASAT altimeter data
[E83-10105] p 29 N83-15748

RADIOACTIVE WASTES
A report to the President and the Congress
[AR-11] p 75 N83-11532

RADIOMETERS
An evaluation of the NASA/GSFC Barnes field spectral reflecometer model 14-758, using signal/noise as a measure of utility
[NASA-TM-83969] p 71 N83-12396
Performance comparison for Barnes model 12-1000, Exotech model 100, and Ideas Inc. Biometer Mark 2
[E83-10004] p 8 N83-12484
Statistical Techniques Applied to Aerial Radiometric Surveys (STARRS): Discriminant-analysis methods applied to aerial radiometric data and their application to uranium favorability in South Texas. Nation uranium resource evaluation
[DE82-020961] p 34 N83-12512
Airborne gamma-ray spectrometer and magnetometer survey. Volume 1. Detail areas, Christmas Mountains, Solitario, Green Valley/0-2 Ranch, Texas
[DE82-021614] p 34 N83-12513
The conical scan radiometer --- satellite-borne radiometer p 72 N83-14804
The Earth Radiation Budget Satellite System (ERBSS) of the United States p 72 N83-14805

RADIOMETRIC CORRECTION
A refined destriping procedure for Landsat MSS data products p 58 A83-14281
Adjusting the tasseled cap brightness and greenness factors for atmospheric path radiance and absorption on a pixel by pixel basis
[E83-10053] p 13 N83-14562
Comparison of LANDSAT-2 and field spectrometer reflectance signatures of south Texas rangeland plant communities
[E83-10055] p 13 N83-14564
Comparison of diverse methods for the correction of atmospheric effects on LANDSAT and SKYLAB images --- radiometric correction in Brazil
[E83-10079] p 72 N83-14588

RADIOMETRIC RESOLUTION
Evaluation of ERIM optically processed SEASAT SAR data
[E83-10037] p 63 N83-13531
LANDSAT-4 image data quality analysis
[E83-10039] p 63 N83-13533

RAIN
Application of the airborne microwave rain-scattered/radiometer system to the remote sensing of rains and wind vector measurements over the ocean p 70 A83-14293
FACE-2 data reductions (prior to disclosure of the treatment decisions). Part 5: Satellite-estimated rainfall from a geostationary platform in FACE-2
[PB82-216581] p 52 N83-10730

RAINMAKING
FACE-2 data reductions (prior to disclosure of the treatment decisions). Part 5: Satellite-estimated rainfall from a geostationary platform in FACE-2
[PB82-216581] p 52 N83-10730

RANDOM ACCESS
Nimbus 6 Random Access Measurement System applications experiments
[NASA-SP-457] p 48 N83-14835

RANGEFINDING
Basic research for the geodynamics program
[NASA-CR-169470] p 26 N83-13537
Effects of adopting new precession, nutation and equinox corrections on the terrestrial reference frame p 26 N83-13538
Utilization of range-difference observations in geodynamics p 26 N83-13539
Geometric adjustment of simultaneous Doppler-derived range differences p 26 N83-13540

RANGELANDS
The relationships between reflectance in the Landsat wavebands and the composition of an Australian semi-arid shrub rangeland p 19 A83-14095
Optical characteristics of Alberta rangeland as related to remote sensing p 4 A83-14245
Use of LANDSAT images to study cerrado vegetation --- Mato Grosso Sul, Brazil
[E83-10025] p 11 N83-13519
Estimating total standing herbaceous biomass production with LANDSAT MSS digital data
[E83-10045] p 12 N83-13536
Comparison of LANDSAT-2 and field spectrometer reflectance signatures of south Texas rangeland plant communities
[E83-10055] p 13 N83-14564
The Group Agromet Monitoring Project (GAMP) --- using METEOSAT for rangeland management in Mali p 23 N83-14615
Computer program documentation for the pasture/range condition assessment processor
[E83-10100] p 16 N83-15743
Rangeland biomass estimation demonstration --- Texas Experimenta Ranch
[E83-10113] p 17 N83-15756
The application of remote sensing to resource management and environmental quality programs in Kansas
[E83-10114] p 23 N83-15757

RANK TESTS
FORTRAN implementation of Friedman's test for several related samples
[E83-10123] p 18 N83-15793

RECONNAISSANCE SPACECRAFT
Naval Research Reviews, volume 34, no. 1
[AD-A117981] p 45 N83-12037

REFLECTANCE
Application of computer axial tomography /CAT/ to measuring crop canopy geometry --- corn and soybeans p 1 A83-10096
Optical parameters of leaves of seven weed species
[E83-10010] p 9 N83-12489
Use of near-infrared video recording system for the detection of freeze damaged citrus leaves
[E83-10049] p 12 N83-14558
Special reflectance of some plant indicators of saline and nonsaline soils
[AD-A119727] p 16 N83-14655
A review of crop canopy reflectance models
[E83-10110] p 17 N83-15753

REFLECTED WAVES
Some fundamental concepts in remote sensing p 60 N83-10459

REFLECTOMETERS
An evaluation of the NASA/GSFC Barnes field spectral reflecometer model 14-758, using signal/noise as a measure of utility
[NASA-TM-83969] p 71 N83-12396

REFORESTATION
Use of LANDSAT images to study cerrado vegetation --- Mato Grosso Sul, Brazil
[E83-10025] p 11 N83-13519
Evaluation of reforestation using remote sensing techniques
[E83-10076] p 15 N83-14585

REGIONAL PLANNING
Photointerpretation, remote sensing, and photogrammetric elements applied to road-planning studies p 19 A83-11866
A case study in the practical use of LANDSAT data p 52 N83-10466
Vegetation survey in Amazonia using LANDSAT data --- Brazil
[E83-10068] p 14 N83-14577
Remote sensing of renewable natural resources in developing countries for national planning purposes p 76 N83-14616
CIRSS vertical data integration, San Bernardino study
[E83-10127] p 67 N83-15796

REGRESSION ANALYSIS
Evaluation of the potential of one to three SEASAT-SMMR channels in retrieving sea surface temperature
[NASA-CR-169660] p 48 N83-14604
Cross-validation for densities and regressions p 66 N83-15776

RELAXATION METHOD (MATHEMATICS)
Relaxation matching applied to aerial images p 56 A83-12889

REMOTE CONSOLES
Operation plan for the data 100/LARS terminal system
[E83-10011] p 62 N83-12490
Image analysis unit (UAI-R) for meteorological applications
[INPE-2428-NTE/185] p 63 N83-13707

REMOTE SENSING
The role of geological surfaces in determining visible-near infra red spectral signatures p 30 A83-10058
Derivation of compositional information from multispectral images --- for use in geologic remote sensing p 30 A83-10059
Seasat L-band radar response to forest vegetation in eastern Virginia p 1 A83-10061
Radar spectral observations of snow p 49 A83-10064
Microwave emission signatures of snow in Finland p 50 A83-10065
Detection of coastal zone environmental conditions using synthetic aperture radar p 38 A83-10068
A comparison data set for the evaluation of remote sensing systems ability for ocean wave data collection p 38 A83-10071
Remote sensing of water quality for estuarine environments p 50 A83-10073
Standardization of computer compatible tape formats for remote sensing data p 54 A83-10075
Imaging radar observations of volcanic features in Medicine Lake Highland, California p 30 A83-10079
Geological terrain models p 31 A83-10080
Ongoing microwave remote sensing-activities for land applications in Germany p 18 A83-10083
The application of microwave remote sensing for snow and ice research p 38 A83-10088
AgRISTARS - Plans and first-year achievements --- Agriculture and Resources Inventory Surveys Through Aerospace Remote Sensing p 1 A83-10095
Landsat monitoring of Desert Locust breeding grounds in Africa, the Near East and Southwest Asia p 1 A83-10097
An evaluation of four thermal models used in thermal inertia analysis --- for thermal mapping from remotely sensed data p 67 A83-10098
Some examples of the utility of HCMM data in geologic remote sensing --- Heat Capacity Mapping Mission p 31 A83-10099
Remote determination of surface evaporation using thermal IR measurements p 50 A83-10101
Microwave remote sensing measurements of oil pollution on the ocean p 39 A83-10104
Remote sensing of dielectric media with periodic rough surfaces --- microwave scattering from farmfields p 1 A83-10106
Performance assessment of future European remote sensing systems p 2 A83-10109
The 100 days of Seasat-A p 39 A83-10115
Soil spectral characterization p 2 A83-10118
Analyzing and mapping regional land use trends by combining Landsat and topographic data p 2 A83-10119
Potentials for change detection using Seasat synthetic aperture radar data p 54 A83-10121
Earth observation - Evolution of requirements and systems p 72 A83-10429
An automated mapping satellite system /Mapsat/ p 67 A83-10715
Selection of the optimum spectral bands for the SPOT satellite p 68 A83-10718
Pattern recognition and digital image processing as applied to remote sensing in India p 54 A83-11450
Automatic multitemporal segmentation for diachronic analysis of remotely sensed images p 55 A83-11461
A relational image data base system for remote sensing /LAND DBMS/ p 55 A83-11462
The GDTA - Remote sensing at the service of users p 68 A83-11867
Advanced operational earth resources satellite systems
[AAS 82-128] p 73 A83-11932
Future land remote sensing data and services - A commercial perspective
[AAS 82-129] p 73 A83-11933
Radar and infrared remote sensing of geothermal features at Pilgrim Springs, Alaska p 31 A83-12036
A comparison of unsupervised classification procedures on Landsat MSS data for an area of complex surface conditions in Basilicata, Southern Italy p 55 A83-12037
Remote sensing of sea state using laser altimeters p 40 A83-12316
Background reflectance effects in Landsat data p 55 A83-12602
Reflectance of a vegetation canopy using the Adding method p 3 A83-12603

Radiative transfer model for heterogeneous 3-D scenes p 3 A83-12604
Earth resources observation with the Shuttle imaging radar p 68 A83-12676
Use of the Space Shuttle for remote sensing research - Recent results and future prospects p 68 A83-13347
Mineral identification from orbit - Initial results from the Shuttle multispectral infrared radiometer p 32 A83-13350
Microwave remote sensing: Active and passive. Volume 2 - Radar remote sensing and surface scattering and emission theory — Book p 69 A83-14040
Action plan for remote sensing applications for rice production — Book
[IFAORS-207] p 3 A83-14121
Canadian Symposium on Remote Sensing, 7th, Winnipeg, Canada, September 8-11, 1981, Proceedings p 73 A83-14226
The importance of remote sensing for Canada - Past achievements, future needs p 74 A83-14227
Renewable resources monitoring needs in Manitoba p 19 A83-14228
Toward an operational, satellite-based, wetland monitoring program for the Fraser River Estuary, British Columbia p 51 A83-14234
Visual analysis of 1:250,000 Landsat data for forage assessment during the 1980 drought in western Manitoba p 3 A83-14235
Vegetation change detection in an agricultural area - A simple approach for use with geo-data base p 4 A83-14236
On detection of oil pollution in ice environment p 41 A83-14239
Vegetation and human impact mapping for the management of the sunshine area, Canadian Rocky Mountains p 20 A83-14242
Waterfowl habitat inventory of Alberta, Saskatchewan and Manitoba by remote sensing p 4 A83-14244
Optical characteristics of Alberta rangeland as related to remote sensing p 4 A83-14245
The use of R.B.V., colour additive viewer and M.S.S. products in the British Columbia Forest Inventory Depletion Monitoring Program — Return Beam Vidicon and Multispectral Scanning p 4 A83-14246
Assessment of spruce budworm defoliation using digital airborne MSS data p 5 A83-14248
Ecological land classification in the Yukon p 20 A83-14250
Remote sensing applications for British Columbia wetlands using 35 mm aerial photography p 51 A83-14251
The application of remote sensing in southern Alberta's mountain pine beetle management p 5 A83-14257
Application of remote sensing techniques in oceanographic studies of the British Columbia Salmon Fishery p 41 A83-14258
Bank erosion and flood plain studies of the Annapolis River - An application of remote sensing data p 51 A83-14262
Remote sensing and waste management p 20 A83-14263
Predicting permafrost conditions with infrared sensing techniques p 6 A83-14264
Remote sensing software for airborne image analysis p 58 A83-14273
Water survey of Canada's experience with data acquisition and telemetry systems p 51 A83-14287
The CCRS SAR processing system p 69 A83-14289
The microwave payload for the ESA Remote Sensing Satellite /ERS-1/ p 69 A83-14290
Results of stereoscopic image simulations for the SPOT HRV carried out at the Gun Lake site in British Columbia p 20 A83-14292
Application of the airborne microwave rain-scattered/radiometer system to the remote sensing of rains and wind vector measurements over the ocean p 70 A83-14293
Remote measurement of biomass p 6 A83-14306
Determination of forest fire spread rates from infrared photographs p 6 A83-14307
Determination of humus in soil on the basis of spectral measurements p 6 A83-14310
A multispectral approach to remote detection of deer p 6 A83-14666
Evaluating depth to shallow groundwater using heat capacity mapping mission /HCMM/ data p 51 A83-14668
A simple relation between active and passive microwave remote sensing measurements of earth terrain p 24 A83-14857
Rectification of Seasat radar on Landsat MSS with the aid of digital image correlation p 59 A83-14946
Investigations of the apparent temperature of snow cover in the submillimeter wavelength region p 52 A83-15816
Remote determination of humus content in soils p 7 A83-15889
A means for utilizing ancillary information in multispectral classification — of remotely sensed data p 60 A83-16905
Reflectance differences between untreated and Mepiquat Chloride-treated, field-grown cotton through a growing season p 7 A83-16909
Earthnet prepares for Landsat-D p 74 A83-17426
Measurements of ocean surface spectrum from an aircraft using the two-frequency microwave resonance technique p 43 A83-17710
The LANDSAT tutorial workbook: Basics of satellite remote sensing
[E83-10001] p 74 N83-10458
Some fundamental concepts in remote sensing p 60 N83-10459
Appendix C. LANDSAT: A worldwide perspective p 75 N83-10471
Remote sensing, a tool for managing the marine environment: Eight case studies
[PB82-220864] p 44 N83-10483
FACE-2 data reductions (prior to disclosure of the treatment decisions). Part 5: Satellite-estimated rainfall from a geostationary platform in FACE-2
[PB82-216581] p 52 N83-10730
Image processing of remotely sensed phenomena p 61 N83-11400
Geographic research in the US Geological Survey: Bibliography, 1966 - 1980
[USGS-CIRC-865] p 21 N83-11639
Applications of space science and technology — Indian space program p 75 N83-12115
Conference on Using Next Generation Earth Observation Satellites: Summary handbook p 62 N83-12508
Remote sensing in geology: Current trends and future prospects with satellite data
[INPE-2514-PRE/193] p 33 N83-12509
Remote sensing of land resources: Application of LANDSAT satellite imagery p 11 N83-13517
Aircraft and satellite measurement of ocean wave directional spectra using scanning-beam microwave radars
[NASA-TM-84008] p 47 N83-13544
The measurement of the synoptic scale wind over the ocean p 47 N83-13773
Satellite remote sensing for developing countries — conference
[ESA-SP-175] p 75 N83-14608
SPOT in the 1980's p 76 N83-14611
Land remote sensing activities in the US p 72 N83-14612
Remote sensing in developing countries. FAO'S international experience p 76 N83-14614
The Group Agromet Monitoring Project (GAMP) — using METEOSAT for rangeland management in Mali p 23 N83-14615
Remote sensing of renewable natural resources in developing countries for national planning purposes p 76 N83-14616
Some aspects of the presentation of remote sensing data p 63 N83-14617
The applicability of satellite remote sensing to small and medium scale mapping p 64 N83-14618
Agroecological classification by remote sensing techniques p 23 N83-14622
Satellite remote sensing in mineral exploration in developing countries p 36 N83-14627
Remote sensing applications to the development of an integrated data base for oil and gas exploration p 37 N83-14628
Remote sensing of the granites of Southeast Asia p 37 N83-14629
Application of satellite data to hydrogeological investigation in Damagaram-Mounio, Niger p 53 N83-14630
Satellite remote sensing for developing countries: Prospects and constraints p 76 N83-14631
Satellite remote sensing: ESA's experience with developing countries p 76 N83-14632
The role of EARSeL and EARSeL member laboratories — in developing nations p 76 N83-14633
Special reflectance of some plant indicators of saline and nonsaline soils
[AD-A119727] p 16 N83-14655
Tectonics of west central Mexico and adjacent Arizona: A remote sensing and field study in arid and semi-arid areas
[DE82-002393] p 37 N83-14797
Terrestrial applications: An intelligent Earth-sensing information system p 76 N83-15349

REMOTE SENSORS
Spectroscopic imaging of the thermosphere from the Space Shuttle p 68 A83-12605
Electro-optical instrumentation for resources evaluation; Proceedings of the Meeting, Washington, DC, April 21, 22, 1981 p 68 A83-12669
Technical issues in focal plane development; Proceedings of the Meeting, Washington, DC, April 21, 22, 1981 p 69 A83-13726
Technical issues in focal plane development for terrestrial resource observations p 69 A83-13735
Measurements of the characteristic reflectance spectra of surficial deposits p 32 A83-14266
Definition and potential of geocoded satellite imagery products p 58 A83-14272
A field portable reflectance spectrometer p 69 A83-14275
Investigations of interpretability of images by different sensors and platforms for small scale mapping p 70 A83-14943
Other remote sensing systems: Retrospect and outlook p 74 N83-10467
Radiance calculations for optimization of sensors designed for remote bathymetry, volume 1
[AD-A117743] p 44 N83-10739
Naval Research Reviews, volume 34, no. 1
[AD-A117981] p 45 N83-12037
Remote sensing techniques for conservation and management of natural vegetation ecosystems
[E83-10070] p 15 N83-14579

RESEARCH AND DEVELOPMENT
Spacelab, space platforms and the future; Proceedings of the Fourth Joint AAS/DGLR Symposium and Twentieth Goddard Memorial Symposium, Washington, DC, March 17-19, 1982 p 73 A83-11926
Future land remote sensing data and services - A commercial perspective
[AAS 82-129] p 73 A83-11933

RESONANCE LINES
The possibility of measuring the moisture content of the upper layers of the atmosphere using radiometric techniques p 70 A83-14308

RESOURCES
Remote sensing of land resources: Application of LANDSAT satellite imagery p 11 N83-13517

RESOURCES MANAGEMENT
Electro-optical instrumentation for resources evaluation; Proceedings of the Meeting, Washington, DC, April 21, 22, 1981 p 68 A83-12669
Canadian Symposium on Remote Sensing, 7th, Winnipeg, Canada, September 8-11, 1981, Proceedings p 73 A83-14226
The importance of remote sensing for Canada - Past achievements, future needs p 74 A83-14227
Renewable resources monitoring needs in Manitoba p 19 A83-14228
Vegetation and human impact mapping for the management of the sunshine area, Canadian Rocky Mountains p 20 A83-14242
Application of Landsat imagery to natural resources management in Sierra Leone, West Africa p 57 A83-14247
Landsat for resource evaluation and management in the Alberta foothills p 32 A83-14256
A case study in the practical use of LANDSAT data p 52 N83-10466
Some closing thoughts: Practical payoffs from satellite systems p 74 N83-10468
Remote sensing techniques for conservation and management of natural vegetation ecosystems
[E83-10070] p 15 N83-14579
Remote sensing in developing countries. FAO'S international experience p 76 N83-14614
Remote sensing of renewable natural resources in developing countries for national planning purposes p 76 N83-14616
LANDSAT-D: The new era of earth resources survey
[E83-10125] p 76 N83-15739
The application of remote sensing to resource management and environmental quality programs in Kansas
[E83-10114] p 23 N83-15757
CIRSS vertical data integration, San Bernardino study
[E83-10127] p 67 N83-15796

RETURN BEAM VIDICONS
The use of R.B.V., colour additive viewer and M.S.S. products in the British Columbia Forest Inventory Depletion Monitoring Program — Return Beam Vidicon and Multispectral Scanning p 4 A83-14246
LANDSAT 3 return beam vidicon response artifacts: A report on RBV photographic product characteristics and quality coding system
[E83-10122] p 67 N83-15792

RICE
Action plan for remote sensing applications for rice production --- Book
[IFAORS-207] p 3 A83-14121
Rice scene radiation research plan p 9 N83-12496
Multistage land use mapping and change monitoring in Sri Lanka p 15 N83-14625
Use of remote sensing techniques for rice production forecasting in west Africa (Mali and Guinea: Niger-Bani Project) p 15 N83-14626
RING CURRENTS
MAGSAT for geomagnetic studies over Indian region
[E83-10032] p 26 N83-13526
RIVER BASINS
Snowmelt runoff modeling in simulation and forecasting modes with the Martinec-Mango model
[E83-10063] p 53 N83-14572
RIVERS
Bank erosion and flood plain studies of the Annapolis River - An application of remote sensing data p 51 A83-14262
A report to the President and the Congress
[AR-11] p 75 N83-11532
ROADS
Photointerpretation, remote sensing, and photogrammetric elements applied to road-planning studies p 19 A83-11866
ROCK INTRUSIONS
LANDSAT and radar mapping of intrusive rocks in SE-Brazil
[E83-10073] p 36 N83-14582
ROCKS
The mineralogy of global magnetic anomalies
[E83-10034] p 34 N83-13528
RURAL AREAS
The Group Agromet Monitoring Project (GAMP) --- using METEOSAT for rangeland management in Mali p 23 N83-14615
RURAL LAND USE
Combining land use data acquired from Landsat with soil map data p 2 A83-10117
Use of LANDSAT images to study cerrado vegetation --- Mato Grosso Sul, Brazil
[E83-10025] p 11 N83-13519
Vegetation survey in Amazonia using LANDSAT data --- Brazil
[E83-10068] p 14 N83-14577
Multitemporal analysis of Landsat data for investigations of agricultural land use: Problems and potentials p 15 N83-14624
Multistage land use mapping and change monitoring in Sri Lanka p 15 N83-14625
Gates to Gregg high voltage transmission line study --- California
[E83-10097] p 16 N83-15741

S

SAHARA DESERT (AFRICA)
Subsurface valleys and geoarcheology of the eastern Sahara revealed by Shuttle radar p 32 A83-13349
SALINITY
Landsat for delineation and mapping of saline soils in dryland areas in southern Alberta p 5 A83-14261
Passive microwave detection of river-plume fronts in the German Bight p 52 A83-17713
Remote Sensing Program
[E83-10120] p 18 N83-15790
SALYUT SPACE STATION
Salyut-7 from June to August p 74 A83-17775
SAMPLING
Estimation of the sugar cane cultivated area from LANDSAT images using the two phase sampling method
[E83-10077] p 15 N83-14586
SAN ANDREAS FAULT
Neotectonics of the San Andreas Fault system: Basin and range province juncture
[E83-10090] p 36 N83-14598
SATELLITE CONFIGURATIONS
LANDSAT-D: The new era of earth resources survey
[E83-10125] p 76 N83-15739
SATELLITE NETWORKS
Terrestrial applications: An intelligent Earth-sensing information system p 76 N83-15349
SATELLITE OBSERVATION
Satellite laser altimeter for measurement of ice sheet topography p 38 A83-10092
Performance assessment of future European remote sensing systems p 2 A83-10109
On the circulation of the western Gulf of Mexico - A satellite view p 39 A83-10113
Combining land use data acquired from Landsat with soil map data p 2 A83-10117
Advanced operational earth resources satellite systems
[AAS 82-128] p 73 A83-11932
Future land remote sensing data and services - A commercial perspective
[AAS 82-129] p 73 A83-11933
Applicability of satellite-derived sea-surface temperatures in the Fiji region p 40 A83-12032
Toward an operational, satellite-based, wetland monitoring program for the Fraser River Estuary, British Columbia p 51 A83-14234
The use of satellite information in weather forecasting at the Pacific Weather Centre p 20 A83-14277
A tutorial assessment of atmospheric height uncertainties for high-precision satellite altimeter missions to monitor ocean currents p 42 A83-14851
Snow-cover parameters retrieved from Nimbus-7 scanning multichannel microwave radiometer /SMMR/ data p 51 A83-14854
An evaluation of Seasat SAR imagery for urban analysis p 60 A83-16904
Some closing thoughts: Practical payoffs from satellite systems p 74 N83-10468
Technology needs assessment of an atmospheric observation system for tropospheric research missions, part 1
[NASA-CR-3556] p 21 N83-10645
Technology needs assessment of an atmospheric observation system for multidisciplinary air quality/meteorology missions, part 2
[NASA-CR-3557] p 21 N83-10646
FACE-2 data reductions (prior to disclosure of the treatment decisions). Part 5: Satellite-estimated rainfall from a geostationary platform in FACE-2
[PB82-216581] p 52 N83-10730
Satellite observations of variations in Northern Hemisphere seasonal snow cover
[PB82-196668] p 52 N83-10734
Report on the special program 78 satellite geodesy of the technical university of Munich
[ASTRON-GEODAET-ARB-41] p 25 N83-11563
Conference on Using Next Generation Earth Observation Satellites: Summary handbook
p 62 N83-12508
An introduction to project Freeze --- the location and intensity of freezing temperatures using infrared satellite imagery
[INPE-2435-NTE/186] p 22 N83-13703
Image analysis unit (UAI-R) for meteorological applications
[INPE-2428-NTE/185] p 63 N83-13707
Further SEASAT SAR coastal ocean wave analysis
[NASA-CR-169682] p 47 N83-13776
Comparison of diverse methods for the correction of atmospheric effects on LANDSAT and SKYLAB images --- radiometric correction in Brazil
[E83-10079] p 72 N83-14588
TOPEX orbit determination using GPS signals plus a sidetone ranging system
[NASA-CR-169694] p 29 N83-14606
Satellite remote sensing for developing countries --- conference
[ESA-SP-175] p 75 N83-14608
The European Community, development and satellite technology p 75 N83-14609
The determination of soil moisture balances in tropical Africa by satellite infrared remote sensing: The atmospheric problem p 53 N83-14621
Determination of the radiation budget at the Earth's surface from satellite data p 29 N83-14808
Key scientific questions and the role of satellites p 64 N83-14830
SATELLITE ORBITS
Satellite orbital dynamics and observation strategies in support of agricultural applications p 2 A83-10717
SATELLITE SOUNDING
Prospects for the future --- satellite sounding data p 48 N83-14832
SATELLITE SURFACES
The geology of Europa p 24 A83-16239
SATELLITE TRACKING
Operation and maintenance of geodetic satellite observatory, McMurdo, Antarctica
[PB82-187923] p 25 N83-12107
SATELLITE-BORNE INSTRUMENTS
Microwave radiance of early fall sea ice at 1.55 cm p 38 A83-10091
Satellite laser altimeter for measurement of ice sheet topography p 38 A83-10092
Ice-sheet dynamics by satellite laser altimetry p 38 A83-10093
Technical issues in focal plane development for terrestrial resource observations p 69 A83-13735
An algorithm to interface Nimbus-7 SMMR data with the AES ice modelling grid for the Beaufort Sea p 41 A83-14284
Water survey of Canada's experience with data acquisition and telemetry systems p 51 A83-14287
The microwave payload for the ESA Remote Sensing Satellite /ERS-1/ p 69 A83-14290
The possibility of measuring the moisture content of the upper layers of the atmosphere using radiometric techniques p 70 A83-14308
Concerning the determination of the temperature of the ocean surface from multichannel satellite measurements of radiation in infrared atmospheric windows p 42 A83-14316
Observations of oceanic surface-wind fields from the Nimbus-7 microwave radiometer p 42 A83-14861
The conical scan radiometer --- satellite-borne radiometer p 72 N83-14804
The Earth Radiation Budget Satellite System (ERBSS) of the United States p 72 N83-14805
LANDSAT-D: The new era of earth resources survey
[E83-10125] p 76 N83-15739
SATELLITE-BORNE PHOTOGRAPHY
Geometry of a mapping satellite p 67 A83-10716
Satellite orbital dynamics and observation strategies in support of agricultural applications p 2 A83-10717
Tidal phenomena in Arctic Ocean ice /according to space data/ p 40 A83-10832
The utilization of infrared /IR/ aerial and space observations of Arctic seas in navigation and during the solution of other national-economic problems p 40 A83-10836
Evidence for a central Eurasian source area of arctic haze in Alaska p 18 A83-11626
The GDTA - Remote sensing at the service of users p 68 A83-11867
Cosmogeological structures of the Hissar Alai and their role in the distribution of endogenous mineralization p 31 A83-11959
Environmental monitoring of the Athabasca Oil Sands using Landsat data p 31 A83-11988
Evaluation of photographic enhancements of Landsat imagery p 55 A83-12035
Contribution of Landsat imagery to the study of volcanic structures p 31 A83-12641
Landsat observations of Mount St. Helens p 19 A83-12671
The early 1981 view of Landsat-D progress p 73 A83-12673
Technology and future ground processing systems p 56 A83-12678
Image enhancement through film recorder response contouring p 56 A83-12685
The relationships between reflectance in the Landsat wavebands and the composition of an Australian semi-arid shrub rangeland p 19 A83-14095
Satellite remote sensing for domestic crop reporting in the United States and Canada - A look to the future p 3 A83-14229
A procedure to overlay thematic map and dominion land survey system data to geometrically-corrected Landsat images and its application to agricultural land use studies in western Canada p 3 A83-14231
A position-based resource mapping study of the Kananaskis Valley using Landsat p 19 A83-14232
Application of Landsat imagery to flood control and management of agricultural land - A case study of northern India p 3 A83-14233
Monitoring revision requirements for Canadian maps p 24 A83-14237
Land use/land cover mapping from enhanced Landsat imagery of the eastern provinces of the People's Republic of China p 4 A83-14241
Waterfowl habitat inventory of Alberta, Saskatchewan and Manitoba by remote sensing p 4 A83-14244
Application of Landsat imagery to natural resources management in Sierra Leone, West Africa p 57 A83-14247
Ecological land classification in the Yukon p 20 A83-14250
Landsat for resource evaluation and management in the Alberta foothills p 32 A83-14256
Colour Landsat images and mosaics - Basic tools in areal and ecological differentiation in Canada p 57 A83-14265
Surficial geology mapping from Landsat-Kaminak Lake, N.W.T. p 32 A83-14268
A national Landsat collection and a proposal for a library of Landsat images p 57 A83-14270
An experimental Landsat Quicklook System for Alaska p 57 A83-14271
Definition and potential of geocoded satellite imagery products p 58 A83-14272
A refined destriping procedure for Landsat MSS data products p 58 A83-14281
Some effects on the GCP success rate --- Ground Control Points for satellite image rectification p 58 A83-14285

A system for the complex processing of aerial and space data for agriculture p 6 A83-14301
A method for the quantitative evaluation of the results of space imagery interpretation in prospecting applications p 33 A83-14302
Lineaments and ring structures on the territory of Poland p 24 A83-14303
The accuracy of a component analysis in space studies of natural environments --- for thematic mapping of earth resources and photointerpretation p 59 A83-14304
Investigating the possibility of producing a land-use map for Cuba on the basis of space imagery p 20 A83-14305
Remote measurement of biomass p 6 A83-14306
Automation of the search for and recognition of reference zones for precise coordinate control of space imagery p 59 A83-14311
Coordinate transformation during the geometric correction of the space scanner imagery of the earth p 70 A83-14313
Operational planning of the process of earth survey by satellites p 70 A83-14314
An example of a statistical analysis of the results of space imagery interpretation for the eastern part of the Fergana Valley p 33 A83-14315
Temporary lakes and salt plains in the high plateaus of the Andes /Bolivia/ - A continuing survey of periodic hydrologic phenomena using the geostationary satellite GOES-EST p 51 A83-14574
Evaluating the effectiveness of Landsat data as a tool for locating buried pre-glacial valleys in eastern South Dakota p 33 A83-14667
Resolution versus speckle relative to geologic interpretability of spaceborne radar images - A survey of user preference p 33 A83-14852
Estimation of context for statistical classification of multispectral image data p 59 A83-14853
The digital image processing system MOBI-DIVAH p 59 A83-14944
Preparation of a sediment map of the North Frisian shoal areas on the basis of Landsat imagery p 59 A83-14945
Rectification of Seasat radar on Landsat MSS with the aid of digital image correlation p 59 A83-14946
The permanently sparse areas of ice cover in the open regions of the Okhtsk Sea p 42 A83-15058
The use of large-area spectral data in wheat yield estimation p 7 A83-16910
Results of phototriangulation on the basis of space photographs p 60 A83-17299
Earthnet prepares for Landsat-D p 74 A83-17426
Geomorphological mapping using Landsat imagery - A case study in Argentina p 33 A83-17841

SATELLITE-BORNE RADAR
Seasat L-band radar response to forest vegetation in eastern Virginia p 1 A83-10061
Radar images of the earth from space p 59 A83-14598

SCANNING
Pass point determination and geometrical precision of the relative rectification of scanner data
[SER-C-268] p 62 N83-13518
The use of thematic mapper simulator calibration data for assessment of data quality
[NASA-TM-82059] p 71 N83-13547

SCATTERING COEFFICIENTS
A backscatter model for a randomly perturbed periodic surface --- radar imagery of earth soil with row structure p 7 A83-14859
Optical parameters of leaves of seven weed species
[E83-10010] p 9 N83-12489

SCATTEROMETERS
Comparison of environmental conditions in the Bering Sea and Davis Strait and the effects on microwave signature returns; March and April, 1979
[NASA-CR-169473] p 46 N83-12828

SCENE ANALYSIS
SAR squint analysis of directional extended targets --- using Doppler filtering of SAR signal film p 54 A83-10084
Scene classification of Landsat multispectral scanner data by means of the Adaptive Learning Network methodology p 55 A83-11458
Relaxation matching applied to aerial images p 56 A83-12889
Familiarization with LANDSAT imagery p 60 N83-10460
Computer processed LANDSAT data p 61 N83-10463
Appendix C. LANDSAT: A worldwide perspective p 75 N83-10471
Proceedings of the NASA Workshop on Image Analysis
[E83-10118] p 65 N83-15766
Cooperative processes in image segmentation p 65 N83-15768
Structural analysis techniqes for remote sensing p 66 N83-15772

SEA ICE
Microwave radiance of early fall sea ice at 1.55 cm p 38 A83-10091
Tidal phenomena in Arctic Ocean ice /according to space data/ p 40 A83-10832
The utilization of infrared /IR/ aerial and space observations of Arctic seas in navigation and during the solution of other national-economic problems p 40 A83-10836
On detection of oil pollution in ice environment p 41 A83-14239
An algorithm to interface Nimbus-7 SMMR data with the AES ice modelling grid for the Beaufort Sea p 41 A83-14284
The permanently sparse areas of ice cover in the open regions of the Okhtsk Sea p 42 A83-15058
Comparison of environmental conditions in the Bering Sea and Davis Strait and the effects on microwave signature returns; March and April, 1979
[NASA-CR-169473] p 46 N83-12828
The Bering Sea ice cover during March 1979: Comparison of surface and satellite data with the Nimbus-7 SMMR
[NASA-CR-169393] p 47 N83-13572

SEA LEVEL
The accuracy of Seasat-1 altimeter altitude measurments under various sea state conditions
[RAE-TR-82059] p 47 N83-14553

SEA OF OKHOTSK
The permanently sparse areas of ice cover in the open regions of the Okhtsk Sea p 42 A83-15058

SEA ROUGHNESS
GRAVSAT error analysis by means of global spectral analyses of the marine geoid from SEASAT altimeter data
[E83-10105] p 29 N83-15748

SEA STATES
Remote sensing of sea state using laser altimeters p 40 A83-12316
Sky-wave radar sea-state sensing - Effects of ionospheric movement and propagation geometry p 43 A83-17709
Further SEASAT SAR coastal ocean wave analysis
[NASA-CR-169682] p 47 N83-13776
The accuracy of Seasat-1 altimeter altitude measurments under various sea state conditions
[RAE-TR-82059] p 47 N83-14553

SEA TRUTH
Phytoplankton pigment concentrations in the Middle Atlantic Bight - Comparison of ship determinations and CZCS estimates --- Coastal Zone Color Scanner p 43 A83-18580
Space truth in oceanography p 48 N83-14636

SEAMOUNTS
The intermediate wavelength magnetic anomaly field of the north Pacific and possible source distributions
[E83-10088] p 27 N83-14596

SEASAT SATELLITES
Rock type discrimination techniques using Landsat and Seasat image data p 30 A83-10057
Wetland mapping with imaging radar p 50 A83-10072
Drumlin fields and glaciated mountains - A contrast in geomorphic perception from Seasat radar images p 23 A83-10078
Potentials for change detection using Seasat synthetic aperture radar data p 54 A83-10121
Radar signatures of terrain - Useful monitors of renewable resources p 21 A83-17248
Mean Earth ellipsoid determined from SEASAT altimeter observations
[AD-A117910] p 45 N83-11570
Evaluation of geodetic products produced by the NSWC reduction of SEASAT radar altimeter data
[AD-A117837] p 25 N83-11571
Evaluation of the potential of one to three SEASAT-SMMR channels in retrieving sea surface temperature
[NASA-CR-169660] p 48 N83-14604

SEASAT 1
The 100 days of Seasat-A p 39 A83-10115
SEASAT-A SASS wind processing
[NASA-CR-169433] p 44 N83-10473

SEDIMENTARY ROCKS
Rock type discrimination techniques using Landsat and Seasat image data p 30 A83-10057

SEDIMENTS
Preparation of a sediment map of the North Frisian shoal areas on the basis of Landsat imagery p 59 A83-14945

SEEDS
Influence of environmental factors during seed development and after full-ripeness on pre-harvest sprouting in wheat
[E83-10002] p 7 N83-12482

SEGMENTS
Proceedings of the NASA Workshop on Image Analysis
[E83-10118] p 65 N83-15766
Image segmentation survey p 65 N83-15767
Cooperative processes in image segmentation p 65 N83-15768
Shape and texture p 65 N83-15769

SEISMOGRAMS
Crustal and upper mantle structure data analysis
[E83-10038] p 26 N83-13532

SEMICONDUCTOR LASERS
Low threshold InGaAsP/InP lasers with microcleaved mirrors suitable for monolithic integration p 24 A83-10981

SHALE OIL
Environmental monitoring of the Athabasca Oil Sands using Landsat data p 31 A83-11988

SHAPES
Shape and texture p 65 N83-15769
Determining 3-D motion and structure from image sequences p 66 N83-15773

SHOALS
Preparation of a sediment map of the North Frisian shoal areas on the basis of Landsat imagery p 59 A83-14945

SHORELINES
Identifying environmental features for land management decisions
[E83-10109] p 23 N83-15752

SIDE-LOOKING RADAR
Registration of a synthetic aperture radar /SAR/ reconnaissance image with a map reference data base p 56 A83-12885
Radar images of the earth from space p 59 A83-14598
Some comparative aspects of SLAR and airphoto images for geomorphologic and geologic interpretation p 33 A83-17842
Determination of the contribution of side-looking airborne radar to structural geologic mapping
[PB82-185042] p 34 N83-12713

SIGNAL PROCESSING
SAR squint analysis of directional extended targets --- using Doppler filtering of SAR signal film p 54 A83-10084
Effects of detection algorithm on accuracy degradation from logarithmic and difference processing for airborne laser bathymetry returns
[PB82-215138] p 44 N83-10707
Nimbus 6 Random Access Measurement System applications experiments
[NASA-SP-457] p 48 N83-14835

SIGNAL TO NOISE RATIOS
Spectral signal to clutter and thermal noise properties of ocean wave imaging synthetic aperture radars p 43 A83-17712

SIGNATURE ANALYSIS
The role of geological surfaces in determining visible-near infra red spectral signatures p 30 A83-10058
Ongoing microwave remote sensing-activities for land applications in Germany p 18 A83-10083
AgRISTARS. Semiannual program review presentation to level 1, interagency Coordination Committee
[E83-10006] p 8 N83-12486
Comparison of LANDSAT-2 and field spectrometer reflectance signatures of south Texas rangeland plant communities
[E83-10055] p 13 N83-14564

SIMULATION
Assessment of radar resolution requirements for soil moisture estimation from simulated satellite imagery --- Kansas
[E83-10020] p 10 N83-12503

SIRIO SATELLITE
The European Space Agency's Earth observation satellite programs in the 1980's p 75 N83-14610

SITE SELECTION
Near surface observations p 61 N83-10464
Remote Sensing Program
[E83-10120] p 18 N83-15790

SKY WAVES
Sky-wave radar sea-state sensing - Effects of ionospheric movement and propagation geometry p 43 A83-17709

SMOKE TRAILS
A study of atmospheric diffusion from the Landsat imagery p 20 A83-14504

SNOW
Satellite observations of variations in Northern Hemisphere seasonal snow cover
[PB82-196668] p 52 N83-10734
Snowmelt runoff modeling in simulation and forecasting modes with the Martinec-Mango model
[E83-10063] p 53 N83-14572
SNOW COVER
Radar spectral observations of snow
p 49 A83-10064
Microwave emission signatures of snow in Finland
p 50 A83-10065
The application of microwave remote sensing for snow and ice research p 38 A83-10088
Accuracy of operational snow and ice charts
p 50 A83-10090
Snow hydrology studies using data from the Heat Capacity Mapping Mission p 50 A83-10102
Airborne measurement of surficial soil moisture using natural terrestrial gamma radiation p 50 A83-10120
Snow-cover parameters retrieved from Nimbus-7 scanning multichannel microwave radiometer /SMMR/ data p 51 A83-14854
Investigations of the apparent temperature of snow cover in the submillimeter wavelength region
p 52 A83-15816
SOIL MAPPING
Combining land use data acquired from Landsat with soil map data p 2 A83-10117
Operational land cover type mapping in Ontario by Landsat based digital analysis and map production
p 19 A83-14230
Landsat for delineation and mapping of saline soils in dryland areas in southern Alberta p 5 A83-14261
Determination of humus in soil on the basis of spectral measurements p 6 A83-14310
A backscatter model for a randomly perturbed periodic surface --- radar imagery of earth soil with row structure
p 7 A83-14859
Preparation of a sediment map of the North Frisian shoal areas on the basis of Landsat imagery
p 59 A83-14945
Remote determination of humus content in soils
p 7 *A83-15889*
Comparisons among a new soil index and other two- and four-dimensional vegetation indices
[E83-10058] p 14 N83-14567
Multitemporal soil and vegetation observations by METEOSAT over Central Africa p 15 N83-14619
SOIL MOISTURE
Airborne measurement of surficial soil moisture using natural terrestrial gamma radiation p 50 A83-10120
Atmospheric effects on radiation reflected from soil and vegetation as measured by orbital sensors using various scanning directions p 3 A83-12315
Effects of vegetation cover on the radar sensitivity to soil moisture p 6 A83-14856
A three-part geometric model to predict the radar backscatter from wheat, corn, and sorghum
[E83-10005] p 8 N83-12485
Measurement of soil moisture using remote sensing multisensor radiation techniques
[E83-10012] p 9 N83-12491
Assessment of radar resolution requirements for soil moisture estimation from simulated satellite imagery --- Kansas
[E83-10020] p 10 N83-12503
Extension of laboratory-measured soil spectra to field conditions
[E83-10021] p 11 N83-12504
Remote sensing of agricultural crops and soils
[E83-10023] p 11 N83-12506
Investigation of remote sensing techniques of measuring soil moisture
[E83-10048] p 12 N83-14557
Agricultural Research Service research highlights in remote sensing for calendar year 1981
[E83-10051] p 75 N83-14560
The determination of soil moisture balances in tropical Africa by satellite infrared remote sensing: The atmospheric problem p 53 N83-14621
Microwave remote sensing of soil moisture, volume 1 --- Guymon, Oklahoma and Dalhart, Texas
[E83-10108] p 17 N83-15751
FORTRAN implementation of Friedman's test for several related samples
[E83-10123] p 18 N83-15793
SOILS
A backscatter model for a randomly perturbed periodic surface --- furrowed soils in agricultural fields
p 1 A83-10107
Soil spectral characterization p 2 A83-10118
Instruments and methods for monitoring background soil pollution --- in the U.S.S.R. p 22 N83-12650
Special reflectance of some plant indicators of saline and nonsaline soils
[AD-A119727] p 16 N83-14655
Spectral characterization of the LANDSAT-D multispectral scanner subsystems
[E83-10107] p 17 N83-15750
SOLAR INSTRUMENTS
Spectroradiometer measurements in support of photovoltaic device testing p 70 A83-15458
SOLAR RADIATION
The Earth Radiation Budget Satellite System (ERBSS) of the United States p 72 N83-14805
Determination of the radiation budget at the Earth's surface from satellite data p 29 N83-14808
SOLID STATE DEVICES
Technical issues in focal plane development for terrestrial resource observations p 69 A83-13735
SORGHUM
A three-part geometric model to predict the radar backscatter from wheat, corn, and sorghum
[E83-10005] p 8 N83-12485
Comparisons among a new soil index and other two- and four-dimensional vegetation indices
[E83-10058] p 14 N83-14567
SOUTH AMERICA
The mineralogy of global magnetic anomalies
[E83-10034] p 34 N83-13528
Crustal and upper mantle structure data analysis
[E83-10038] p 26 N83-13532
An investigation of MAGSAT and complementary data emphasizing Precambrian shields and adjacent areas of West Africa and South America
[E83-10085] p 36 N83-14593
SOUTH DAKOTA
Evaluation of small area crop estimation techniques using LANDSAT- and ground-derived data --- South Dakota
[E83-10008] p 8 N83-12487
SOUTHEAST ASIA
Remote sensing of the granites of Southeast Asia
p 37 N83-14629
SOUTHERN CALIFORNIA
LANDSAT land cover analysis completed for CIRSS/San Bernardino County project
[E83-10024] p 22 N83-12507
CIRSS vertical data integration, San Bernardino County study phases 1-A, 1-B
[E83-10124] p 67 N83-15794
CIRSS vertical data integration, San Bernardino study
[E83-10127] p 67 N83-15796
SOYBEANS
Application of computer axial tomography /CAT/ to measuring crop canopy geometry --- corn and soybeans
p 1 A83-10096
AgRISTARS. Semiannual program review presentation to level 1, interagency Coordination Committee
[E83-10006] p 8 N83-12486
Development of a corn and soybean labeling procedure for use with profile parameter classification
[E83-10014] p 9 N83-12493
Data documentation for the 1981 summer vegetation experiment --- Kansas River floodplain
[E83-10016] p 10 N83-12499
Development, implementation and evaluation of satellite-aided agricultural monitoring systems
[E83-10017] p 10 N83-12500
Analysis of the profile characteristics of corn and soybeans using field reflectance data
[E83-10018] p 10 N83-12501
Remote sensing of agricultural crops and soils
[E83-10023] p 11 N83-12506
Development of thematic mapper vegetative indices for assessing biomass in corn, soybeans and wheat
[E83-10035] p 11 N83-13529
Crop weather models of corn and soybeans for Agrophysical Units (APU's) in Iowa using monthly meteorological predictors
[E83-10054] p 13 N83-14563
Spectral characterization of the LANDSAT-D multispectral scanner subsystems
[E83-10107] p 17 N83-15750
SPACE BASED RADAR
Shuttle imaging radar experiment p 32 A83-13348
SPACE PLATFORMS
Spacelab, space platforms and the future; Proceedings of the Fourth Joint AAS/DGLR Symposium and Twentieth Goddard Memorial Symposium, Washington, DC, March 17-19, 1982 p 73 A83-11926
SPACE PROGRAMS
Global implications of space activities; Proceedings of the Conference, Aspen, CO, August 30-September 4, 1981 p 74 A83-17349
SPACE SHUTTLE ORBITERS
Use of the Space Shuttle for remote sensing research - Recent results and future prospects
p 68 A83-13347
SPACE SHUTTLE PAYLOADS
Spectroscopic imaging of the thermosphere from the Space Shuttle p 68 A83-12605
Earth resources observation with the Shuttle imaging radar p 68 A83-12676
OSTA-1 - Shuttle's first scientific and applications payload p 73 A83-13715
OSTA-1/Ocean Color Experiment
[AIAA PAPER 83-0415] p 42 A83-16701
Land remote sensing activities in the US
p 72 N83-14612
SPACE TRANSPORTATION SYSTEM
Use of the Space Shuttle for remote sensing research - Recent results and future prospects
p 68 A83-13347
Shuttle imaging radar experiment p 32 A83-13348
SPACE TRANSPORTATION SYSTEM FLIGHTS
Subsurface valleys and geoarcheology of the eastern Sahara revealed by Shuttle radar p 32 A83-13349
Mineral identification from orbit - Initial results from the Shuttle multispectral infrared radiometer
p 32 A83-13350
SPACE TRANSPORTATION SYSTEM 2 FLIGHT
OSTA-1 - Shuttle's first scientific and applications payload p 73 A83-13715
SPACEBORNE EXPERIMENTS
Ongoing microwave remote sensing-activities for land applications in Germany p 18 A83-10083
OSTA-1/Ocean Color Experiment
[AIAA PAPER 83-0415] p 42 A83-16701
Salyut-7 from June to August p 74 A83-17775
SPACEBORNE PHOTOGRAPHY
Results of phototriangulation on the basis of space photographs p 60 A83-17299
SPACELAB
Spacelab, space platforms and the future; Proceedings of the Fourth Joint AAS/DGLR Symposium and Twentieth Goddard Memorial Symposium, Washington, DC, March 17-19, 1982 p 73 A83-11926
SPACELAB PAYLOADS
OSTA-1 - Shuttle's first scientific and applications payload p 73 A83-13715
The European Space Agency's Earth observation satellite programs in the 1980's p 75 *N83-14610*
SPATIAL DISTRIBUTION
Probabilistic cluster labeling of imagery data
p 54 A83-11410
Some spectral and spatial characteristics of LANDSAT data p 61 N83-10461
Development of advanced acreage estimation methods
[E83-10015] p 9 N83-12494
System support documentation: IDIMS FUNCTION AMOEBA p 9 N83-12495
The possible modifications of the Hisse model for pure LANDSAT agricultural data p 10 N83-12497
Spatial and temporal variations of large-scale subsidence and convection regions derived from satellite data
[PB82-219817] p 71 N83-13750
Contextual classification of multispectral image data: An unbiased estimator for the context distribution
[E83-10087] p 63 N83-14595
Methods of editing cloud and atmospheric layer affected pixels from satellite data
[E83-10103] p 64 N83-15746
Rangeland biomass estimation demonstration --- Texas Experimenta Ranch
[E83-10113] p 17 N83-15756
SPATIAL RESOLUTION
Comparison study of future SPOT and Landsat-D satellite products from a simulation flight --- for determining spatial and spectral resolution p 57 A83-14243
SPECTRAL BANDS
Selection of the optimum spectral bands for the SPOT satellite p 68 A83-10718
Spectral characterization of the LANDSAT-D multispectral scanner subsystems
[E83-10107] p 17 N83-15750
SPECTRAL REFLECTANCE
Derivation of compositional information from multispectral images --- for use in geologic remote sensing p 30 A83-10059
Use of reflectance spectra of native plant species for interpreting airborne multispectral scanner data in the East Tintic Mountains, Utah p 30 A83-10060
Soil spectral characterization p 2 A83-10118
Atmospheric effects on radiation reflected from soil and vegetation as measured by orbital sensors using various scanning directions p 3 A83-12315
Background reflectance effects in Landsat data
p 55 A83-12602
Reflectance of a vegetation canopy using the Adding method p 3 A83-12603
Radiative transfer model for heterogeneous 3-D scenes p 3 A83-12604

The relationships between reflectance in the Landsat wavebands and the composition of an Australian semi-arid shrub rangeland p 19 A83-14095
Measurements of the characteristic reflectance spectra of surficial deposits p 32 A83-14266
A field portable reflectance spectrometer p 69 A83-14275
Determination of humus in soil on the basis of spectral measurements p 6 A83-14310
Reflectance measurement of artificially induced ultraviolet radiation stress on cotton leaves p 7 A83-16907
Polarized visible light as an aid to vegetation classification p 7 A83-16908
Reflectance differences between untreated and Mepiquat Chloride-treated, field-grown cotton through a growing season p 7 A83-16909
Measurements of ocean surface spectrum from an aircraft using the two-frequency microwave resonance technique p 43 A83-17710
Discrimination of growth and water stress in wheat by various vegetation indices through a clear a turbid atmosphere
[E83-10009] p 8 N83-12488
Extension of laboratory-measured soil spectra to field conditions
[E83-10021] p 11 N83-12504
Remote sensing of agricultural crops and soils
[E83-10023] p 11 N83-12506
Development of thematic mapper vegetative indices for assessing biomass in corn, soybeans and wheat
[E83-10035] p 11 N83-13529
Diurnal patterns of wheat spectral reflectances and their importance in the assessment of canopy parameters from remotely sensed observations --- Phoenix, Arizona
[E83-10050] p 13 N83-14559
Agricultural Research Service research highlights in remote sensing for calendar year 1981
[E83-10051] p 75 N83-14560
Adjusting the tasseled cap brightness and greenness factors for atmospheric path radiance and absorption on a pixel by pixel basis
[E83-10053] p 13 N83-14562
Comparison of LANDSAT-2 and field spectrometer reflectance signatures of south Texas rangeland plant communities
[E83-10055] p 13 N83-14564
Effects of ground cover and leaf area on the spectral reflectance of vegetation-soil target
[AD-A119714] p 16 N83-14653
Rangeland biomass estimation demonstration --- Texas Experimenta Ranch
[E83-10113] p 17 N83-15756

SPECTRAL RESOLUTION
Comparison study of future SPOT and Landsat-D satellite products from a simulation flight --- for determining spatial and spectral resolution p 57 A83-14243

SPECTRAL SENSITIVITY
Microwave remote sensing of soil moisture, volume 1 --- Guymon, Oklahoma and Dalhart, Texas
[E83-10108] p 17 N83-15751

SPECTRAL SIGNATURES
Rock type discrimination techniques using Landsat and Seasat image data p 30 A83-10057
The role of geological surfaces in determining visible-near infra red spectral signatures p 30 A83-10058
Derivation of compositional information from multispectral images --- for use in geologic remote sensing p 30 A83-10059
Microwave emission signatures of snow in Finland p 50 A83-10065
Imaging radar observations of volcanic features in Medicine Lake Highland, California p 30 A83-10079
Soil spectral characterization p 2 A83-10118
Selection of the optimum spectral bands for the SPOT satellite p 68 A83-10718
Probabilistic cluster labeling of imagery data p 54 A83-11410
Effects of vegetation cover on the radar sensitivity to soil moisture p 6 A83-14856
Some fundamental concepts in remote sensing p 60 N83-10459
Some spectral and spatial characteristics of LANDSAT data p 61 N83-10461
Near surface observations p 61 N83-10464
Evaluation of small area crop estimation techniques using LANDSAT- and ground-derived data --- South Dakota
[E83-10008] p 8 N83-12487
Development of advanced acreage estimation methods
[E83-10015] p 9 N83-12494
Rice scene radiation research plan p 9 N83-12496
The possible modifications of the Hisse model for pure LANDSAT agricultural data p 10 N83-12497
Development, implementation and evaluation of satellite-aided agricultural monitoring systems
[E83-10017] p 10 N83-12500
Analysis of the profile characteristics of corn and soybeans using field reflectance data
[E83-10018] p 10 N83-12501

SPECTROMETERS
Spectroscopic imaging of the thermosphere from the Space Shuttle p 68 A83-12605

SPECTRORADIOMETERS
Spectroradiometer measurements in support of photovoltaic device testing p 70 A83-15458

SPECTRUM ANALYSIS
The use of large-area spectral data in wheat yield estimation p 7 A83-16910
Special reflectance of some plant indicators of saline and nonsaline soils
[AD-A119727] p 16 N83-14655
Computer program documentation for the pasture/range condition assessment processor
[E83-10100] p 16 N83-15743
GRAVSAT error analysis by means of global spectral analyses of the marine geoid from SEASAT altimeter data
[E83-10105] p 29 N83-15748

SPHERICAL COORDINATES
The reduction, verification and interpretation of MAGSAT magnetic data over Canada
[E83-10101] p 29 N83-15744
C-1 surface interpolation for scattered data on a sphere p 65 N83-15762

SPOT (FRENCH SATELLITE)
Earth observation - Evolution of requirements and systems p 72 A83-10429
Selection of the optimum spectral bands for the SPOT satellite p 68 A83-10718
Potentials of Landsat-D and SPOT-1 for crop identification in the maritimes p 4 A83-14240
Comparison study of future SPOT and Landsat-D satellite products from a simulation flight --- for determining spatial and spectral resolution p 57 A83-14243
Results of stereoscopic image simulations for the SPOT HRV carried out at the Gun Lake site in British Columbia p 20 A83-14292
SPOT in the 1980's p 76 N83-14611

SPRINGS (WATER)
Radar and infrared remote sensing of geothermal features at Pilgrim Springs, Alaska p 31 A83-12036

STATISTICAL ANALYSIS
A comparison of unsupervised classification procedures on Landsat MSS data for an area of complex surface conditions in Basilicata, Southern Italy p 55 A83-12037
An example of a statistical analysis of the results of space imagery interpretation for the eastern part of the Fergana Valley p 33 A83-14315
An optimum statistical technique for ozone profile retrieval from backscattered UV radiances p 21 A83-14632
Estimation of context for statistical classification of multispectral image data p 59 A83-14853
Proceedings of the NASA Workshop on Surface Fitting
[E83-10117] p 64 N83-15759
Crop proportion estimation problems in AgRISTARS p 18 N83-15760

STATISTICAL CORRELATION
Proceedings of the NASA Workshop on Density Estimation and Function Smoothing
[E83-10119] p 66 N83-15774

STATISTICAL DISTRIBUTIONS
Using new methods in monitoring the thermal regime of the Arctic p 39 A83-10828

STEREOPHOTOGRAPHY
An automated mapping satellite system /Mapsat/ p 67 A83-10715
Geometry of a mapping satellite p 67 A83-10716

STEREOSCOPY
Results of stereoscopic image simulations for the SPOT HRV carried out at the Gun Lake site in British Columbia p 20 A83-14292

STOCHASTIC PROCESSES
Geomagnetic modeling by optimal recursive filtering
[E83-10112] p 29 N83-15755

STORMS
Drift buoy component, NORPAX anomaly dynamics study p 49 N83-14848

STRATIFICATION
Construction of a remotely sensed area sampling frame for Southern Brazil
[E83-10052] p 13 N83-14561
An application of cluster analysis for determining homogeneous subregions: The agroclimatological point of view --- Rio Grande do Sul, Brazil
[E83-10067] p 14 N83-14576

STRUCTURAL PROPERTIES (GEOLOGY)
Cosmogeological structures of the Hissar Alai and their role in the distribution of endogenous mineralization p 31 A83-11959
Contribution of Landsat imagery to the study of volcanic structures p 31 A83-12641
Lineaments and ring structures on the territory of Poland p 24 A83-14303
Geological-structural interpretation using products of remote sensing in the region of Carrancas, Minas Gerais, Brazil
[E83-10029] p 34 N83-13523
Crustal and upper mantle structure data analysis
[E83-10038] p 26 N83-13532
Use of MAGSAT anomaly data for crustal structure and mineral resources in the US midcontinent
[E83-10082] p 36 N83-14590
Digital methods for lineament analysis p 37 N83-14634
Analysis of the characteristics appearing in LANDSAT multispectral images in the geological structural mapping of the midwestern portion of the Rio Grande do Sul shield --- Brazil
[E83-10126] p 37 N83-15795

SUBARCTIC REGIONS
Digital colour enhancement of Landsat data for mapping vegetation of barrenground caribou winter range in northern Manitoba p 5 A83-14249

SUBMILLIMETER WAVES
Investigations of the apparent temperature of snow cover in the submillimeter wavelength region p 52 A83-15816

SUBSIDENCE
Spatial and temporal variations of large-scale subsidence and convection regions derived from satellite data
[PB82-219817] p 71 N83-13750

SUDAN
Approaches to desertification monitoring in the Sudan p 23 N83-14623

SUGAR CANE
Estimation of the sugar cane cultivated area from LANDSAT images using the two phase sampling method
[E83-10077] p 15 N83-14586

SUNFLOWERS
Optical parameters of leaves of seven weed species
[E83-10010] p 9 N83-12489

SURFACE ROUGHNESS
Measurement of soil moisture using remote sensing multisensor radiation techniques
[E83-10012] p 9 N83-12491

SURFACE ROUGHNESS EFFECTS
Remote sensing of dielectric media with periodic rough surfaces --- microwave scattering from farmfields p 1 A83-10106
A parametric study of tillage effects on radar backscatter p 2 A83-10108
A backscatter model for a randomly perturbed periodic surface --- radar imagery of earth soil with row structure p 7 A83-14859

SURFACE TEMPERATURE
An evaluation of four thermal models used in thermal inertia analysis --- for thermal mapping from remotely sensed data p 67 A83-10098
Remote determination of surface evaporation using thermal IR measurements p 50 A83-10101
Applicability of satellite-derived sea-surface temperatures in the Fiji region p 40 A83-12032
HCMM hydrological analysis in Utah
[E83-10026] p 53 N83-13520
Use of thermal inertia determined by HCMM to predict nocturnal cold prone areas in Florida
[E83-10028] p 62 N83-13522
A comparison of HCMM surface temperatures with in situ temperature data --- Nantucket shoals and the Gulf of Mexico regions
[E83-10040] p 46 N83-13534
A comparison of surfaces temperatures from HCMM infrared data with field measurements
[E83-10046] p 47 N83-14555
Investigation of remote sensing techniques of measuring soil moisture
[E83-10048] p 12 N83-14557
Use of thermal inertia determined by HCMM to predict nocturnal cold prone areas in Florida
[E83-10102] p 64 N83-15745
Infrared satellite data from the first coastal ocean dynamics experiment, March - July 1981
[AD-A120068] p 49 N83-15799

SURFACE WATER
Ice distribution and winter surface circulation patterns, Kachemak Bay, Alaska p 50 A83-12038

SURVEYS
Airborne gamma-ray spectrometer and magnetometer survey. Volume 1. Detail areas, Christmas Mountains, Solitario, Green Valley/0-2 Ranch, Texas
[DE82-021614] p 34 N83-12513
Remote sensing of land resources: Application of LANDSAT satellite imagery p 11 N83-13517
SYNCHRONOUS PLATFORMS
Feasibility of mapping ocean surface currents using delta k-microwave radars mounted on geostationary satellite platforms p 39 A83-10094
SYNCHRONOUS SATELLITES
Satellite orbital dynamics and observation strategies in support of agricultural applications p 2 A83-10717
An upper bound on errors in the mean-of-date/instantaneous Earth-fixed vector transformation induced by interpolated nutation angles
[AD-A119444] p 29 N83-14656
SYNOPTIC MEASUREMENT
Advanced operational earth resources satellite systems
[AAS 82-128] p 73 A83-11932
SYNOPTIC METEOROLOGY
The use of satellite information in weather forecasting at the Pacific Weather Centre p 20 A83-14277
The measurement of the synoptic scale wind over the ocean p 47 N83-13773
SYNTHETIC APERTURE RADAR
Detection of coastal zone environmental conditions using synthetic aperture radar p 38 A83-10068
Drumlin fields and glaciated mountains - A contrast in geomorphic perception from Seasat radar images p 23 A83-10078
Ongoing microwave remote sensing-activities for land applications in Germany p 18 A83-10083
SAR squint analysis of directional extended targets --- using Doppler filtering of SAR signal film p 54 A83-10084
Potentials for change detection using Seasat synthetic aperture radar data p 54 A83-10121
Registration of a synthetic aperture radar /SAR/ reconnaissance image with a map reference data base p 56 A83-12885
Quality assessment of remote-sensing data - The SAR case p 56 A83-13845
Applications of Robert's gradient operator for the digital enhancement of icebergs from SAR imagery p 41 A83-14278
Cartographic aspects of dual-frequency dual-polarization SAR imagery p 58 A83-14280
The CCRS SAR processing system p 69 A83-14289
Radar images of the earth from space p 59 A83-14598
Resolution versus speckle relative to geologic interpretability of spaceborne radar images - A survey of user preference p 33 A83-14852
Rectification of Seasat radar on Landsat MSS with the aid of digital image correlation p 59 A83-14946
An evaluation of Seasat SAR imagery for urban analysis p 60 A83-16904
Radar signatures of terrain - Useful monitors of renewable resources p 21 A83-17248
Spectral signal to clutter and thermal noise properties of ocean wave imaging synthetic aperture radars p 43 A83-17712
Determination of the contribution of side-looking airborne radar to structural geologic mapping
[PB82-185042] p 34 N83-12713
Evaluation of ERIM optically processed SEASAT SAR data
[E83-10037] p 63 N83-13531
Further SEASAT SAR coastal ocean wave analysis
[NASA-CR-169682] p 47 N83-13776
Analysis of geologic terrain models for determination of optimum SAR sensor configuration and optimum information extraction for exploration of global non-renewable resources. Pilot study: Arkansas Remote Sensing Laboratory, part 1, part 2, and part 3
[E83-10061] p 35 N83-14570
SYSTEMS ANALYSIS
Performance comparison for Barnes model 12-1000, Exotech model 100, and Ideas Inc. Biometer Mark 2
[E83-10004] p 8 N83-12484
SYSTEMS MANAGEMENT
Operation plan for the data 100/LARS terminal system
[E83-10011] p 62 N83-12490
SYSTEMS SIMULATION
Comparison study of future SPOT and Landsat-D satellite products from a simulation flight --- for determining spatial and spectral resolution p 57 A83-14243
SYSTEMS STABILITY
Investigation of the geometrical stability of a photogrammetric recording system --- systems stability
[SER-C-267] p 71 N83-11565

T

TAR SANDS
Environmental monitoring of the Athabasca Oil Sands using Landsat data p 31 A83-11988
TARGET RECOGNITION
FLIR target screening p 65 N83-15771
TECHNOLOGICAL FORECASTING
Spacelab, space platforms and the future; Proceedings of the Fourth Joint AAS/DGLR Symposium and Twentieth Goddard Memorial Symposium, Washington, DC, March 17-19, 1982 p 73 A83-11926
Technology and future ground processing systems p 56 A83-12678
Satellite remote sensing for developing countries: Prospects and constraints p 76 N83-14631
TECHNOLOGY ASSESSMENT
Remote sensing, a tool for managing the marine environment: Eight case studies
[PB82-220864] p 44 N83-10483
Technology needs assessment of an atmospheric observation system for tropospheric research missions, part 1
[NASA-CR-3556] p 21 N83-10645
Technology needs assessment of an atmospheric observation system for multidisciplinary air quality/meteorology missions, part 2
[NASA-CR-3557] p 21 N83-10646
TECHNOLOGY TRANSFER
The LANDSAT tutorial workbook: Basics of satellite remote sensing
[E83-10001] p 74 N83-10458
Satellite remote sensing for developing countries --- conference
[ESA-SP-175] p 75 N83-14608
The European Community, development and satellite technology p 75 N83-14609
Remote sensing in developing countries. FAO'S international experience p 76 N83-14614
The application of remote sensing to resource management and environmental quality programs in Kansas
[E83-10114] p 23 N83-15757
TECHNOLOGY UTILIZATION
A case study in the practical use of LANDSAT data p 52 N83-10466
Appendix C. LANDSAT: A worldwide perspective p 75 N83-10471
TECTONICS
Lineaments and ring structures on the territory of Poland p 24 A83-14303
Determination of the contribution of side-looking airborne radar to structural geologic mapping
[PB82-185042] p 34 N83-12713
Crustal and upper mantle structure data analysis
[E83-10038] p 26 N83-13532
The intermediate wavelength magnetic anomaly field of the north Pacific and possible source distributions
[E83-10088] p 27 N83-14596
Neotectonics of the San Andreas Fault system: Basin and range province juncture
[E83-10090] p 36 N83-14598
Investigating tectonic and bathymetric features of the Indian Ocean using MAGSAT magnetic anomaly data
[E83-10095] p 28 N83-14602
Tectonics of west central Mexico and adjacent Arizona: A remote sensing and field study in arid and semi-arid areas
[DE82-002393] p 37 N83-14797
TELECOMMUNICATION
Applications of space science and technology --- Indian space program p 75 N83-12115
TELEMETRY
Water survey of Canada's experience with data acquisition and telemetry systems p 51 A83-14287
TELEPHOTOMETRY
Automated measurements of atmospheric visibility
[AIAA PAPER 83-0436] p 21 A83-16713
TELEVISION CAMERAS
Coordinate transformation during the geometric correction of the space scanner imagery of the earth p 70 A83-14313
TELEVISION SYSTEMS
Image analysis unit (UAI-R) for meteorological applications
[INPE-2428-NTE/185] p 63 N83-13707
TEMPERATURE EFFECTS
Influence of environmental factors during seed development and after full-ripeness on pre-harvest sprouting in wheat
[E83-10002] p 7 N83-12482
TEMPERATURE INVERSIONS
Airborne atmospheric temperature structure measurements of a Pacific coast marine inversion
[AIAA PAPER 83-0278] p 70 A83-19585
TEMPERATURE MEASUREMENT
Applicability of satellite-derived sea-surface temperatures in the Fiji region p 40 A83-12032
Investigations of the apparent temperature of snow cover in the submillimeter wavelength region p 52 A83-15816
Comparison of multichannel and two-satellite methods for remote measurement of sea surface temperature
[AD-A118736] p 45 N83-12511
TEMPERATURE PROFILES
Remote sensing of temperature profiles in the atmosphere p 66 N83-15778
TEMPORAL DISTRIBUTION
Spatial and temporal variations of large-scale subsidence and convection regions derived from satellite data
[PB82-219817] p 71 N83-13750
TEMPORAL RESOLUTION
Familiarization with LANDSAT imagery p 60 N83-10460
Photointerpretation of LANDSAT images p 61 N83-10462
TERRADYNAMICS
Utilization of range-difference observations in geodynamics p 26 N83-13539
TERRAIN ANALYSIS
Geological terrain models p 31 A83-10080
Scene classification of Landsat multispectral scanner data by means of the Adaptive Learning Network methodology p 55 A83-11458
A comparison of unsupervised classification procedures on Landsat MSS data for an area of complex surface conditions in Basilicata, Southern Italy p 55 A83-12037
Operational land cover type mapping in Ontario by Landsat based digital analysis and map production p 19 A83-14230
Predicting forest land attributes from aerial photo interpretation variables p 5 A83-14259
The geology of Europa p 24 A83-16239
Radar signatures of terrain - Useful monitors of renewable resources p 21 A83-17248
Image processing of remotely sensed phenomena p 61 N83-11400
Terrain analysis procedural guide for drainage and water resources (ETL series on guides for Army terrain analysts)
[AD-A118318] p 52 N83-11569
TERRESTRIAL PLANETS
Basic research for the geodynamics program
[NASA-CR-169470] p 26 N83-13537
TERRESTRIAL RADIATION
Airborne measurement of surficial soil moisture using natural terrestrial gamma radiation p 50 A83-10120
TEXAS
Comparison of LANDSAT-2 and field spectrometer reflectance signatures of south Texas rangeland plant communities
[E83-10055] p 13 N83-14564
Microwave remote sensing of soil moisture, volume 1 --- Guymon, Oklahoma and Dalhart, Texas
[E83-10108] p 17 N83-15751
TEXTURES
Proceedings of the NASA Workshop on Image Analysis
[E83-10118] p 65 N83-15766
Shape and texture p 65 N83-15769
Automatic photointerpretation via texture and morphology analysis p 65 N83-15770
THEMATIC MAPPING
The early 1981 view of Landsat-D progress p 73 A83-12673
Technology and future ground processing systems p 56 A83-12678
A procedure to overlay thematic map and dominion land survey system data to geometrically-corrected Landsat images and its application to agricultural land use studies in western Canada p 3 A83-14231
Optical characteristics of Alberta rangeland as related to remote sensing p 4 A83-14245
Digital colour enhancement of Landsat data for mapping vegetation of barrenground caribou winter range in northern Manitoba p 5 A83-14249
Integration of Landsat imagery into a program for aerial surveying of deer populations in Alberta p 5 A83-14252
The accuracy of a component analysis in space studies of natural environments --- for thematic mapping of earth resources and photointerpretation p 59 A83-14304
Investigating the possibility of producing a land-use map for Cuba on the basis of space imagery p 20 A83-14305
Remote determination of humus content in soils p 7 A83-15889
Earthnet prepares for Landsat-D p 74 A83-17426

Photointerpretation of LANDSAT images
p 61 N83-10462
Appendix A: The LANDSAT system
p 75 N83-10469
Conference on Using Next Generation Earth Observation Satellites: Summary handbook
p 62 N83-12508
Use of LANDSAT images to study cerrado vegetation — Mato Grosso Sul, Brazil
[E83-10025] p 11 N83-13519
Development of thematic mapper vegetative indices for assessing biomass in corn, soybeans and wheat
[E83-10035] p 11 N83-13529
LANDSAT-4 image data quality analysis
[E83-10039] p 63 N83-13533
The use of thematic mapper simulator calibration data for assessment of data quality
[NASA-TM-82059] p 71 N83-13547
Vegetation survey in Amazonia using LANDSAT data — Brazil
[E83-10068] p 14 N83-14577
Spectral discrimination of lithologic facies in the granite of the Pedra Branca Goias using LANDSAT 1 digital imagery
[E83-10069] p 35 N83-14578
Remote sensing techniques for conservation and management of natural vegetation ecosystems
[E83-10070] p 15 N83-14579
Multitemporal and geobotanical approach in the remote detection of Greisenization areas in the Serra da Pedra Branca Granite, Goias State, Brazil
[E83-10071] p 35 N83-14580
LANDSAT and radar mapping of intrusive rocks in SE-Brazil
[E83-10073] p 36 N83-14582
INPE LANDSAT-D thematic mapper computer compatible tape format specification
[E83-10075] p 63 N83-14584
Multitemporal soil and vegetation observations by METEOSAT over Central Africa p 15 N83-14619
Combined use of daily thermal cycle of METEOSAT imagery and multispectral LANDSAT data: Application to the Bandiagara plateau, Mali p 36 N83-14620
Agroecological classification by remote sensing techniques p 23 N83-14622
Multistage land use mapping and change monitoring in Sri Lanka p 15 N83-14625
Gates to Gregg high voltage transmission line study — California
[E83-10097] p 16 N83-15741
Detection of aspen-conifer forest mixes from LANDSAT digital data — Utah-Idaho Bear River Range
[E83-10106] p 17 N83-15749
Identifying environmental features for land management decisions
[E83-10109] p 23 N83-15752
LANDSAT 4 investigations of thematic mapper and multispectral scanner applications
[E83-10121] p 66 N83-15791
Analysis of the characteristics appearing in LANDSAT multispectral images in the geological structural mapping of the midwestern portion of the Rio Grande do Sul shield — Brazil
[E83-10126] p 37 N83-15795

THERMAL MAPPING
An evaluation of four thermal models used in thermal inertia analysis — for thermal mapping from remotely sensed data p 67 A83-10098
Some examples of the utility of HCMM data in geologic remote sensing — Heat Capacity Mapping Mission
p 31 A83-10099
Remote determination of surface evaporation using thermal IR measurements p 50 A83-10101
Snow hydrology studies using data from the Heat Capacity Mapping Mission p 50 A83-10102
Environmental monitoring of the Athabasca Oil Sands Region p 19 A83-14238
Aerial thermal infrared census of Canada geese in South Dakota p 6 A83-14665
Evaluating depth to shallow groundwater using heat capacity mapping mission /HCMM/ data
p 51 A83-14668
Other remote sensing systems: Retrospect and outlook p 74 N83-10467
HCMM hydrological analysis in Utah
[E83-10026] p 53 N83-13520
Use of thermal inertia determined by HCMM to predict nocturnal cold prone areas in Florida
[E83-10028] p 62 N83-13522
Geologic interpretation of HCMM and aircraft thermal data
[E83-10036] p 62 N83-13530
A comparison of HCMM surface temperatures with in situ temperature data — Nantucket shoals and the Gulf of Mexico regions
[E83-10040] p 46 N83-13534
A comparison of surfaces temperatures from HCMM infrared data with field measurements
[E83-10046] p 47 N83-14555
An investigation into the utilization of HCMM thermal data for the descrimination of volcanic and Eolian geological units — Craters of the Moon volcanic field, Idaho; San Francisco volcanic field, Arizona; High Desert, California; and the Cascade Range, California and Oregon
[E83-10047] p 35 N83-14556
Investigation of remote sensing techniques of measuring soil moisture
[E83-10048] p 12 N83-14557
Agricultural Research Service research highlights in remote sensing for calendar year 1981
[E83-10051] p 75 N83-14560
The determination of soil moisture balances in tropical Africa by satellite infrared remote sensing: The atmospheric problem p 53 N83-14621
Use of thermal inertia determined by HCMM to predict nocturnal cold prone areas in Florida
[E83-10102] p 64 N83-15745
Infrared satellite data from the first coastal ocean dynamics experiment, March - July 1981
[AD-A120068] p 49 N83-15799

THERMAL NOISE
Spectral signal to clutter and thermal noise properties of ocean wave imaging synthetic aperture radars
p 43 A83-17712

THERMAL STABILITY
Performance comparison for Barnes model 12-1000, Exotech model 100, and Ideas Inc. Biometer Mark 2
[E83-10004] p 8 N83-12484

THERMOSPHERE
Spectroscopic imaging of the thermosphere from the Space Shuttle p 68 A83-12605

THRESHOLD CURRENTS
Low threshold InGaAsP/InP lasers with microcleaved mirrors suitable for monolithic integration
p 24 A83-10981

TIDAL WAVES
Tidal phenomena in Arctic Ocean ice /according to space data/ p 40 A83-10832
Some features of the spatial structure of the Arctic Ocean ice cover in connection with turbulent friction and geostrophic capture of tide waves p 40 A83-10833

TIMBER IDENTIFICATION
Seasat L-band radar response to forest vegetation in eastern Virginia p 1 A83-10061
Detection of aspen-conifer forest mixes from LANDSAT digital data — Utah-Idaho Bear River Range
[E83-10106] p 17 N83-15749

TIMBER INVENTORY
The use of R.B.V., colour additive viewer and M.S.S. products in the British Columbia Forest Inventory Depletion Monitoring Program — Return Beam Vidicon and Multispectral Scanning p 4 A83-14246
Assessment of spruce budworm defoliation using digital airborne MSS data p 5 A83-14248
Landsat-based forest mapping in Ontario north of latitude 52 deg north p 5 A83-14253
Remote sensing techniques for conservation and management of natural vegetation ecosystems
[E83-10070] p 15 N83-14579
Evaluation of reforestation using remote sensing techniques
[E83-10076] p 15 N83-14585

TIROS N SATELLITE
The Bering Sea ice cover during March 1979: Comparison of surface and satellite data with the Nimbus-7 SMMR
[NASA-CR-169393] p 47 N83-13572
Prospects for the future — satellite sounding data
p 48 N83-14832

TOMOGRAPHY
Application of computer axial tomography /CAT/ to measuring crop canopy geometry — corn and soybeans
p 1 A83-10096

TOPEX
TOPEX orbit determination using GPS signals plus a sidetone ranging system
[NASA-CR-169694] p 29 N83-14606

TOPOGRAPHY
Satellite laser altimeter for measurement of ice sheet topography p 38 A83-10092
Monitoring revision requirements for Canadian maps
p 24 A83-14237
Investigations of interpretability of images by different sensors and platforms for small scale mapping
p 70 A83-14943
Flight path design issues for the TOPEX mission — Ocean Topography Experiment
[AIAA PAPER 83-0197] p 42 A83-16581
Analyses of oceanic subsurface features using space based radar imagery
[AD-A118411] p 45 N83-11692
TOPEX orbit determination using GPS signals plus a sidetone ranging system
[NASA-CR-169694] p 29 N83-14606
Verification of LANDSAT imagery for morphametric and topological studies of drainage basins in a section of the western plateau of Sao Paulo State: Tiete-Aguapei watershed — Brazil
[E83-10111] p 54 N83-15754

TOPOLOGY
Proceedings of the NASA Workshop on Surface Fitting
[E83-10117] p 64 N83-15759
Surfaces: Representation and approximation
p 30 N83-15763
Surface fitting with biharmonic and harmonic models
p 65 N83-15764
BSPLASH: A three-stage surface interpolant to scattered data p 65 N83-15765

TRACKING (POSITION)
Nimbus 6 Random Access Measurement System applications experiments
[NASA-SP-457] p 48 N83-14835
Lagrangian drift measurements of sea surface currents and iceberg tracking p 49 N83-14842
Drift buoy component, NORPAX anomaly dynamics study p 49 N83-14848
Determining 3-D motion and structure from image sequences p 66 N83-15773

TRACKING NETWORKS
Preliminary study of GPS orbit determination accuracy achievable from worldwide tracking data
[NASA-CR-169693] p 28 N83-14605

TRADEOFFS
Some closing thoughts: Practical payoffs from satellite systems p 74 N83-10468

TRAJECTORY ANALYSIS
Preliminary study of GPS orbit determination accuracy achievable from worldwide tracking data
[NASA-CR-169693] p 28 N83-14605
TOPEX orbit determination using GPS signals plus a sidetone ranging system
[NASA-CR-169694] p 29 N83-14606

TRANSFORMATIONS (MATHEMATICS)
An upper bound on errors in the mean-of-date/instantaneous Earth-fixed vector transformation induced by interpolated nutation angles
[AD-A119444] p 29 N83-14656

TRANSMISSION LINES
Gates to Gregg high voltage transmission line study — California
[E83-10097] p 16 N83-15741

TRANSMISSIVITY
Concerning the determination of the temperature of the ocean surface from multichannel satellite measurements of radiation in infrared atmospheric windows
p 42 A83-14316

TREES (PLANTS)
Evaluation of reforestation using remote sensing techniques
[E83-10076] p 15 N83-14585

TRIANGULATION
Results of phototriangulation on the basis of space photographs p 60 A83-17299

TROPICAL METEOROLOGY
Global Weather Experiment. The GARP Atlantic Tropical Experiment (GATE) Monograph
[GARP-PUB-SER-25] p 45 N83-12724

TROPICAL REGIONS
An introduction to project Freeze — the location and intensity of freezing temperatures using infrared satellite imagery
[INPE-2435-NTE/186] p 22 N83-13703
The determination of soil moisture balances in tropical Africa by satellite infrared remote sensing: The atmospheric problem p 53 N83-14621

TROPOSPHERE
Technology needs assessment of an atmospheric observation system for tropospheric research missions, part 1
[NASA-CR-3556] p 21 N83-10645

TURBULENT FLOW
Some features of the spatial structure of the Arctic Ocean ice cover in connection with turbulent friction and geostrophic capture of tide waves p 40 A83-10833

U

U.S.S.R.
Instruments and methods for monitoring background soil pollution — in the U.S.S.R. p 22 N83-12650

U.S.S.R. SPACE PROGRAM
Salyut-7 from June to August p 74 A83-17775

ULTRAVIOLET RADIATION
An optimum statistical technique for ozone profile retrieval from backscattered UV radiances p 21 A83-14632
Reflectance measurement of artificially induced ultraviolet radiation stress on cotton leaves p 7 A83-16907
UNITED NATIONS
Remote sensing in developing countries. FAO'S international experience p 76 N83-14614
UNITED STATES OF AMERICA
MAGSAT and aeromagnetic data of the continental US
[E83-10033] p 26 N83-13527
MAGSAT anomaly field inversion and interpretation for the US
[E83-10057] p 27 N83-14566
Use of MAGSAT anomaly data for crustal structure and mineral resources in the US midcontinent
[E83-10082] p 36 N83-14590
UPPER ATMOSPHERE
The possibility of measuring the moisture content of the upper layers of the atmosphere using radiometric techniques p 70 A83-14308
Technology needs assessment of an atmospheric observation system for multidisciplinary air quality/meteorology missions, part 2
[NASA-CR-3557] p 21 N83-10646
The Global Weather Experiment. First GARP Global Experiment (FGGE) operations report series: Volume 5, summary of data collected 5 July - December 1979
[GARP-FOR-5] p 46 N83-12808
URANIUM
Statistical Techniques Applied to Aerial Radiometric Surveys (STARRS): Discriminant-analysis methods applied to aerial radiometric data and their application to uranium favorability in South Texas. Nation uranium resource evaluation
[DE82-020961] p 34 N83-12512
USER MANUALS (COMPUTER PROGRAMS)
Earth Observations Division version of the Laboratory for Applications of Remote Sensing System (EOD-LARSYS) user guide for the IBM 370/148. Volume 1: System overview
[E83-10007] p 62 N83-12866
USER REQUIREMENTS
CIRSS vertical data integration, San Bernardino County study phases 1-A, 1-B
[E83-10124] p 67 N83-15794
UTAH
HCMM hydrological analysis in Utah
[E83-10026] p 53 N83-13520
Identifying environmental features for land management decisions
[E83-10109] p 23 N83-15752

V

VALLEYS
Subsurface valleys and geoarcheology of the eastern Sahara revealed by Shuttle radar p 32 A83-13349
Evaluating the effectiveness of Landsat data as a tool for locating buried pre-glacial valleys in eastern South Dakota p 33 A83-14667
VECTOR ANALYSIS
An upper bound on errors in the mean-of-date/instantaneous Earth-fixed vector transformation induced by interpolated nutation angles
[AD-A119444] p 29 N83-14656
VEGETATION
The relationships between reflectance in the Landsat wavebands and the composition of an Australian semi-arid shrub rangeland p 19 A83-14095
Vegetation and human impact mapping for the management of the sunshine area, Canadian Rocky Mountains p 20 A83-14242
Polarized visible light as an aid to vegetation classification p 7 A83-16908
An evaluation of the NASA/GSFC Barnes field spectral reflecometer model 14-758, using signal/noise as a measure of utility
[NASA-TM-83969] p 71 N83-12396
LANDSAT land cover analysis completed for CIRSS/San Bernardino County project
[E83-10024] p 22 N83-12507
Use of LANDSAT images to study cerrado vegetation --- Mato Grosso Sul, Brazil
[E83-10025] p 11 N83-13519
Estimating total standing herbaceous biomass production with LANDSAT MSS digital data
[E83-10045] p 12 N83-13536
Monitoring global vegetation
[E83-10044] p 12 N83-14554
An investigation into the utilization of HCMM thermal data for the descrimination of volcanic and Eolian geological units --- Craters of the Moon volcanic field, Idaho; San Francisco volcanic field, Arizona; High Desert, California; and the Cascade Range, California and Oregon
[E83-10047] p 35 N83-14556
Comparisons among a new soil index and other two- and four-dimensional vegetation indices
[E83-10058] p 14 N83-14567
Vegetation survey in Amazonia using LANDSAT data --- Brazil
[E83-10068] p 14 N83-14577
Remote sensing techniques for conservation and management of natural vegetation ecosystems
[E83-10070] p 15 N83-14579
Multitemporal and geobotanical approach in the remote detection of Greisenization areas in the Serra da Pedra Branca Granite, Goias State, Brazil
[E83-10071] p 35 N83-14580
Contextual classification of multispectral image data: An unbiased estimator for the context distribution
[E83-10087] p 63 N83-14595
Multitemporal soil and vegetation observations by METEOSAT over Central Africa p 15 N83-14619
Agroecological classification by remote sensing techniques p 23 N83-14622
Effects of ground cover and leaf area on the spectral reflectance of vegetation-soil target
[AD-A119714] p 16 N83-14653
Microwave remote sensing of soil moisture, volume 1 --- Guymon, Oklahoma and Dalhart, Texas
[E83-10108] p 17 N83-15751
Rangeland biomass estimation demonstration --- Texas Experimenta Ranch
[E83-10113] p 17 N83-15756
VEGETATION GROWTH
Radiative transfer model for heterogeneous 3-D scenes p 3 A83-12604
Visual analysis of 1:250,000 Landsat data for forage assessment during the 1980 drought in western Manitoba p 3 A83-14235
Vegetation change detection in an agricultural area - A simple approach for use with geo-data base p 4 A83-14236
VERY LONG BASE INTERFEROMETRY
Basic research for the geodynamics program
[NASA-CR-169470] p 26 N83-13537
VIDEO DATA
Automation of the search for and recognition of reference zones for precise coordinate control of space imagery p 59 A83-14311
LANDSAT 3 return beam vidicon response artifacts: A report on RBV photographic product characteristics and quality coding system
[E83-10122] p 67 N83-15792
VIDEO EQUIPMENT
Use of near-infrared video recording system for the detection of freeze damaged citrus leaves
[E83-10049] p 12 N83-14558
VINEYARDS
Remote Sensing Program
[E83-10120] p 18 N83-15790
VISIBILITY
Automated measurements of atmospheric visibility
[AIAA PAPER 83-0436] p 21 A83-16713
VISIBLE SPECTRUM
Comparisons among a new soil index and other two- and four-dimensional vegetation indices
[E83-10058] p 14 N83-14567
VOLCANOES
Imaging radar observations of volcanic features in Medicine Lake Highland, California p 30 A83-10079
Landsat observations of Mount St. Helens p 19 A83-12671
Mount St. Helens quick response damage assessment using high-altitude infrared photography p 19 A83-12672
An investigation into the utilization of HCMM thermal data for the descrimination of volcanic and Eolian geological units --- Craters of the Moon volcanic field, Idaho; San Francisco volcanic field, Arizona; High Desert, California; and the Cascade Range, California and Oregon
[E83-10047] p 35 N83-14556
VOLCANOLOGY
Contribution of Landsat imagery to the study of volcanic structures p 31 A83-12641
VORTICES
Western Boundary Eddies of the Gulf Stream p 49 N83-14847

W

WASTE DISPOSAL
Remote sensing and waste management p 20 A83-14263
A report to the President and the Congress
[AR-11] p 75 N83-11532
WATER CIRCULATION
On the circulation of the western Gulf of Mexico - A satellite view p 39 A83-10113
Ice distribution and winter surface circulation patterns, Kachemak Bay, Alaska p 50 A83-12038
WATER COLOR
Phytoplankton pigment concentrations in the Middle Atlantic Bight - Comparison of ship determinations and CZCS estimates --- Coastal Zone Color Scanner p 43 A83-18580
WATER DEPTH
Investigating tectonic and bathymetric features of the Indian Ocean using MAGSAT magnetic anomaly data
[E83-10095] p 28 N83-14602
WATER POLLUTION
Experimental feasibility of the airborne measurement of absolute oil fluorescence spectral conversion efficiency p 44 A83-18581
Ocean pollution research, development and monitoring
[PB82-219049] p 45 N83-10740
Interpretation of remotely sensed data and its applications in oceanography
[E83-10074] p 48 N83-14583
WATER QUALITY
Remote sensing of water quality for estuarine environments p 50 A83-10073
A case study in the practical use of LANDSAT data p 52 N83-10466
HCMM hydrological analysis in Utah
[E83-10026] p 53 N83-13520
Vegetation survey in Amazonia using LANDSAT data --- Brazil
[E83-10068] p 14 N83-14577
WATER RESOURCES
Action plan for remote sensing applications for rice production --- Book
[IFAORS-207] p 3 A83-14121
Water survey of Canada's experience with data acquisition and telemetry systems p 51 A83-14287
Terrain analysis procedural guide for drainage and water resources (ETL series on guides for Army terrain analysts)
[AD-A118318] p 52 N83-11569
Application of satellite data to hydrogeological investigation in Damagaram-Mounio, Niger p 53 N83-14630
WATER RUNOFF
Long-range water supply forecasting
[WMO-587] p 53 N83-12516
Snowmelt runoff modeling in simulation and forecasting modes with the Martinec-Mango model
[E83-10063] p 53 N83-14572
WATER TEMPERATURE
A comparison of surfaces temperatures from HCMM infrared data with field measurements
[E83-10046] p 47 N83-14555
WATER TREATMENT
A report to the President and the Congress
[AR-11] p 75 N83-11532
WATER VAPOR
Validation and application of the SEASAT-SMMR geophysical algorithms
[NASA-CR-169390] p 71 N83-13767
WATER WAVES
A comparison data set for the evaluation of remote sensing systems ability for ocean wave data collection p 38 A83-10071
On the use of laser profilometry for ocean wave studies p 42 A83-14502
Spectral signal to clutter and thermal noise properties of ocean wave imaging synthetic aperture radars p 43 A83-17712
Aircraft and satellite measurement of ocean wave directional spectra using scanning-beam microwave radars
[NASA-TM-84008] p 47 N83-13544
Further SEASAT SAR coastal ocean wave analysis
[NASA-CR-169682] p 47 N83-13776
WATERFOWL
Waterfowl habitat inventory of Alberta, Saskatchewan and Manitoba by remote sensing p 4 A83-14244
WATERSHEDS
Terrain analysis procedural guide for drainage and water resources (ETL series on guides for Army terrain analysts)
[AD-A118318] p 52 N83-11569

Snowmelt runoff modeling in simulation and forecasting modes with the Martinec-Mango model
[E83-10063] p 53 N83-14572
Verification of LANDSAT imagery for morphametric and topological studies of drainage basins in a section of the western plateau of Sao Paulo State: Tiete-Aguapei watershed — Brazil
[E83-10111] p 54 N83-15754

WAVE PROPAGATION
Some fundamental concepts in remote sensing
p 60 N83-10459

WAVELENGTHS
An evaluation of the NASA/GSFC Barnes field spectral reflecometer model 14-758, using signal/noise as a measure of utility
[NASA-TM-83969] p 71 N83-12396

WEATHER
Weather constraints on airborne laser hydrography operations
[PB82-189754] p 52 N83-10745
The Global Weather Experiment. First GARP Global Experiment (FGGE) operations report series: Volume 5, summary of data collected 5 July - December 1979
[GARP-FOR-5] p 46 N83-12808
Crop weather models of corn and soybeans for Agrophysical Units (APU's) in Iowa using monthly meteorological predictors
[E83-10054] p 13 N83-14563

WEATHER FORECASTING
The use of satellite information in weather forecasting at the Pacific Weather Centre p 20 A83-14277
A report to the President and the Congress
[AR-11] p 75 N83-11532

WEATHER STATIONS
Manual on the global observing system. Volume 1 (annex to the WMO technical regulations): Global aspects, 1981 edition
[WMO-544-VOL-1-ANNEX] p 46 N83-12801

WETLANDS
Wetland mapping with imaging radar
p 50 A83-10072
Toward an operational, satellite-based, wetland monitoring program for the Fraser River Estuary, British Columbia p 51 A83-14234
Remote sensing applications for British Columbia wetlands using 35 mm aerial photography
p 51 A83-14251
Identifying environmental features for land management decisions
[E83-10109] p 23 N83-15752

WETTING
Influence of environmental factors during seed development and after full-ripeness on pre-harvest sprouting in wheat
[E83-10002] p 7 N83-12482

WHEAT
The use of large-area spectral data in wheat yield estimation p 7 A83-16910
Influence of environmental factors during seed development and after full-ripeness on pre-harvest sprouting in wheat
[E83-10002] p 7 N83-12482
A three-part geometric model to predict the radar backscatter from wheat, corn, and sorghum
[E83-10005] p 8 N83-12485
Discrimination of growth and water stress in wheat by various vegetation indices through a clear a turbid atmosphere
[E83-10009] p 8 N83-12488
Winter wheat stand density determination and yield estimates from handheld and airborne scanners — Montana
[E83-10013] p 9 N83-12492
Data documentation for the 1981 summer vegetation experiment — Kansas River floodplain
[E83-10016] p 10 N83-12499
Development of thematic mapper vegetative indices for assessing biomass in corn, soybeans and wheat
[E83-10035] p 11 N83-13529
Evaluation of the Williams-type spring wheat model in North Dakota and Minnesota
[E83-10041] p 12 N83-13535
Diurnal patterns of wheat spectral reflectances and their importance in the assessment of canopy parameters from remotely sensed observations — Phoenix, Arizona
[E83-10050] p 13 N83-14559
Crop weather models of barley and spring wheat yield for agrophysical units in North Dakota
[E83-10059] p 14 N83-14568

WILDLIFE
Aerial thermal infrared census of Canada geese in South Dakota p 6 A83-14665
A multispectral approach to remote detection of deer
p 6 A83-14666

WIND (METEOROLOGY)
The Global Weather Experiment. First GARP Global Experiment (FGGE) operations report series: Volume 5, summary of data collected 5 July - December 1979
[GARP-FOR-5] p 46 N83-12808

WIND DIRECTION
SEASAT-A SASS wind processing
[NASA-CR-169433] p 44 N83-10473

WIND MEASUREMENT
Application of the airborne microwave rain-scattered/radiometer system to the remote sensing of rains and wind vector measurements over the ocean
p 70 A83-14293
The measurement of the synoptic scale wind over the ocean p 47 N83-13773

WIND VELOCITY
SEASAT-A SASS wind processing
[NASA-CR-169433] p 44 N83-10473

WIND VELOCITY MEASUREMENT
Estimating wind speed from HF skywave radar sea backscatter p 40 A83-11352
Observations of oceanic surface-wind fields from the Nimbus-7 microwave radiometer p 42 A83-14861

WORLD DATA CENTERS
World Integrated Oceanic Services System: General plan and operational program for 1982-1985
[WMO-582] p 46 N83-12802

WORLD METEOROLOGICAL ORGANIZATION
Commission for Marine Technology: Abridged report of the 8th Session — resolutions and recommendations for ocean exploration and exploitation
[WMO-584] p 46 N83-12803

Z

ZAMBIA
Multitemporal analysis of Landsat data for investigations of agricultural land use: Problems and potentials
p 15 N83-14624

Typical Personal Author Index Listing

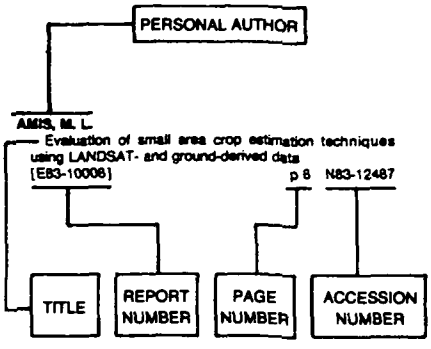

Listings in this index are arranged alphabetically by personal author. The title of the document provides the user with a brief description of the subject matter. The report number helps to indicate the type of document listed (e.g., NASA report, translation, NASA contractor report). The page and accession numbers are located beneath and to the right of the title. Under any one author's name the accession numbers are arranged in sequence with the AIAA accession numbers appearing first.

A

AASE, J. K.
Winter wheat stand density determination and yield estimates from handheld and airborne scanners
[E83-10013] p 9 N83-12492

ABRAMS, M.
Rock type discrimination techniques using Landsat and Seasat image data p 30 A83-10057

ABRAMS, M. J.
Some examples of the utility of HCMM data in geologic remote sensing p 31 A83-10099

ADAMS, J. B.
Derivation of compositional information from multispectral images p 30 A83-10059

AGARWAL, G. C.
Analysis of MAGSAT data of the Indian region
[E83-10027] p 25 N83-13521

AGGARWAL, R.
FLIR target screening p 65 N83-15771

AHERN, F. J.
Optical characteristics of Alberta rangeland as related to remote sensing p 4 A83-14245

ALBOUY, J.
Gravimetric maps of the Central African Republic
[E83-10084] p 27 N83-14592

ALEXANDER, T. M.
Future land remote sensing data and services - A commercial perspective
[AAS 82-129] p 73 A83-11933

ALLEN, C.
Data documentation for the 1981 summer vegetation experiment
[E83-10016] p 10 N83-12499

ALLEN, L. H., JR.
Use of thermal inertia determined by HCMM to predict nocturnal cold prone areas in Florida
[E83-10028] p 62 N83-13522
Use of thermal inertia determined by HCMM to predict nocturnal cold prone areas in Florida
[E83-10102] p 64 N83-15745

ALLEY, R. E.
Some examples of the utility of HCMM data in geologic remote sensing p 31 A83-10099

ALMEIDA, F. C.
An introduction to project Freeze
[INPE-2435-NTE/186] p 22 N83-13703

ALMEIDO, R., JR.
Spectral discrimination of lithologic facies in the granite of the Pedra Branca Goias using LANDSAT 1 digital imagery
[E83-10069] p 35 N83-14578

ALPERS, W.
Spectral signal to clutter and thermal noise properties of ocean wave imaging synthetic aperture radars p 43 A83-17712
The effect of monomolecular surface films on the microwave brightness temperature of the sea surface p 43 A83-17714

ALVARADO, D. R.
Technology needs assessment of an atmospheric observation system for tropospheric research missions, part 1
[NASA-CR-3556] p 21 N83-10645

ALVARADO, U. R.
Technology needs assessment of an atmospheric observation system for multidisciplinary air quality/meteorology missions, part 2
[NASA-CR-3557] p 21 N83-10646

ALYEA, F.
Technology needs assessment of an atmospheric observation system for multidisciplinary air quality/meteorology missions, part 2
[NASA-CR-3557] p 21 N83-10646

AMIS, M. L.
Evaluation of small area crop estimation techniques using LANDSAT- and ground-derived data
[E83-10008] p 8 N83-12487

ANDERSON, D. R.
A multispectral approach to remote detection of deer p 6 A83-14666

ANDO, K. J.
Land remote sensing activities in the US p 72 N83-14612

ANDREEV, G. G.
A system for the complex processing of aerial and space data for agriculture p 6 A83-14301

ANUTA, P. E.
LANDSAT-4 image data quality analysis
[E83-10039] p 63 N83-13533

ARAI, K.
Some effects on the GCP success rate p 58 A83-14285

ARNASON, R.
Visual analysis of 1:250,000 Landsat data for forage assessment during the 1980 drought in western Manitoba p 3 A83-14235

ARONOFF, S.
Environmental monitoring of the Athabasca Oil Sands using Landsat data p 31 A83-11988
Environmental monitoring of the Athabasca Oil Sands Region p 19 A83-14238

ARUR, M. G.
Analysis of MAGSAT data of the Indian region
[E83-10027] p 25 N83-13521

ASLAM, A.
Radar spectral observations of snow p 49 A83-10064
Effects of vegetation cover on the radar sensitivity to soil moisture p 6 A83-14856

ATLAS, D.
Satellite estimates of ocean-air heat fluxes during cold air outbreaks p 41 A83-13059
Prospects for the future p 48 N83-14832

AUCOIN, P. J.
Earth Observations Division version of the Laboratory for Applications of Remote Sensing System (EOD-LARSYS) user guide for the IBM 370/148. Volume 1: System overview
[E83-10007] p 62 N83-12866

AUDET, H.
Conference on Using Next Generation Earth Observation Satellites: Summary handbook p 62 N83-12508

AVANESOV, G. A.
Automation of the search for and recognition of reference zones for precise coordinate control of space imagery p 59 A83-14311

B

BABKINA, E.
Instruments and methods for monitoring background soil pollution p 22 N83-12650

BAINUM, P. M.
Spacelab, space platforms and the future; Proceedings of the Fourth Joint AAS/DGLR Symposium and Twentieth *Goddard Memorial Symposium, Washington, DC, March* 17-19, 1982 p 73 A83-11926

BAKER, M. C. W.
Contribution of Landsat imagery to the study of volcanic structures p 31 A83-12641

BAKER, P. L.
Aircraft and satellite measurement of ocean wave directional spectra using scanning-beam microwave radars
[NASA-TM-84008] p 47 N83-13544

BAKLANOV, A. D.
An example of a statistical analysis of the results of space imagery interpretation for the eastern part of the Fergana Valley p 33 A83-14315

BALASHOV, A. A.
Results of phototriangulation on the basis of space photographs p 60 A83-17299

BALDRIDGE, W. S.
Tectonics of west central Mexico and adjacent Arizona: A remote sensing and field study in arid and semi-arid areas
[DE82-002393] p 37 N83-14797

BALLESTER, A.
Space truth in oceanography p 48 N83-14636

BANNER, A. V.
Multitemporal analysis of Landsat data for forest cutover mapping - A trial of two procedures p 5 A83-14254

BARATOV, R. B.
Cosmogeological structures of the Hissar Alai and their role in the distribution of endogenous mineralization p 31 A83-11959

BARBOSA, M. N.
CNPq/INPE-LANDSAT system report of activities
[E83-10064] p 63 N83-14573

BARBOSA, M. P.
Geological-structural interpretation using products of remote sensing in the region of Carrancas, Minas Gerais, Brazil
[E83-10029] p 34 N83-13523
LANDSAT and radar mapping of intrusive rocks in SE-Brazil
[E83-10073] p 36 N83-14582

BARDINET, C.
Combined use of daily thermal cycle of METEOSAT imagery and multispectral LANDSAT data: Application to the Bandiagara plateau, Mali p 36 N83-14620

BARKER, J. C.
Critical and strategic minerals in Alaska: Cobalt, the platinum-group metals and chromite
[PB82-193085] p 33 N83-10485

BARKER, J. L.
Spectral characterization of the LANDSAT-D *multispectral scanner subsystems*
[E83-10107] p 17 N83-15750

BARNARD, T.
Waterfowl habitat inventory of Alberta, Saskatchewan and Manitoba by remote sensing p 4 A83-14244

BARNES, J. C.
Snow hydrology studies using data from the Heat Capacity Mapping Mission p 50 A83-10102

BARNETT, T. L.
The use of large-area spectral data in wheat yield estimation p 7 A83-16910
Evaluation of the Williams-type model for barley yields in North Dakota and Minnesota
[E83-10060] p 14 N83-14569

BARNHILL, R. E.
Surfaces: Representation and approximation p 30 N83-15763
BARNUM, J. R.
Estimating wind speed from HF skywave radar sea backscatter p 40 A83-11352
BARR, B. G.
The application of remote sensing to resource management and environmental quality programs in Kansas
[E83-10114] p 23 N83-15757
BARRETT, E. C.
The role of EARSeL and EARSeL member laboratories p 76 N83-14633
BARTOV, Y.
Tectonics of west central Mexico and adjacent Arizona: A remote sensing and field study in arid and semi-arid areas
[DE82-002393] p 37 N83-14797
BASEDOW, R. W.
Spectroscopic imaging of the thermosphere from the Space Shuttle p 68 A83-12605
BAUER, M. E.
Remote sensing of agricultural crops and soils
[E83-10023] p 11 N83-12506
BAUMGARDNER, M. F.
Soil spectral characterization p 2 A83-10118
Extension of laboratory-measured soil spectra to field conditions
[E83-10021] p 11 N83-12504
BAZHINSKII, IU.
Lineaments and ring structures on the territory of Poland p 24 A83-14303
BEGNI, G.
Selection of the optimum spectral bands for the SPOT satellite p 68 A83-10718
BEHIE, G.
Remote sensing, a tool for managing the marine environment: Eight case studies
[PB82-220864] p 44 N83-10483
BELCHANSKII, G. I.
A system for the complex processing of aerial and space data for agriculture p 6 A83-14301
BELL, E. J.
Low- to moderate-temperature geothermal resource assessment for Nevada: Area specific studies, Pumpernickel Valley, Carlin and Moana
[DE82-018598] p 34 N83-12584
BELL, R.
An evaluation of the NASA/GSFC Barnes field spectral reflecometer model 14-758, using signal/noise as a measure of utility
[NASA-TM-83969] p 71 N83-12396
BELOV, G.
Instruments and methods for monitoring background soil pollution p 22 N83-12650
BEMENT, T. R.
Statistical Techniques Applied to Aerial Radiometric Surveys (STARRS): Discriminant-analysis methods applied to aerial radiometric data and their application to uranium favorability in South Texas. Nation uranium resource evaluation
[DE82-020961] p 34 N83-12512
BENDER, P. L.
Preliminary study of GPS orbit determination accuracy achievable from worldwide tracking data
[NASA-CR-169693] p 28 N83-14605
TOPEX orbit determination using GPS signals plus a sidetone ranging system
[NASA-CR-169694] p 29 N83-14606
BENTLEY, C. R.
Investigation of Antarctic crust and upper mantle using MAGSAT and other geophysical data
[E83-10086] p 27 N83-14594
BENTON, E. R.
Data use investigation for the magnetic field satellite (MAGSAT) mission: Geomagnetic field forecasting and fluid dynamics of the core
[E83-10098] p 29 N83-15742
BERG, A.
Use of remote sensing techniques for rice production forecasting in west Africa (Mali and Guinea: Niger-Bani Project) p 15 N83-14626
BERGIS, V.
Gates to Gregg high voltage transmission line study
[E83-10097] p 16 N83-15741
BERNIER, M.
Construction and interpretation of a thermal inertia image using airborne data p 57 A83-14260
BEST, R. G.
Aerial thermal infrared census of Canada geese in South Dakota p 6 A83-14665
BEST, W. G.
Canadian Symposium on Remote Sensing, 7th, Winnipeg, Canada, September 8-11, 1981, Proceedings p 73 A83-14226
Renewable resources monitoring needs in Manitoba p 19 A83-14228
BHARTIA, P. K.
An optimum statistical technique for ozone profile retrieval from backscattered UV radiances p 21 A83-14632
BICKNELL, T. J.
SAR squint analysis of directional extended targets p 54 A83-10084
BIEHL, L. L.
Extension of laboratory-measured soil spectra to field conditions
[E83-10021] p 11 N83-12504
BIERLY, E. W.
Key scientific questions and the role of satellites p 64 N83-14830
BINDSCHADLER, R. A.
Ice-sheet dynamics by satellite laser altimetry p 38 A83-10093
BLAD, B. L.
Development of thematic mapper vegetative indices for assessing biomass in corn, soybeans and wheat
[E83-10035] p 11 N83-13529
BLAIR, S. C.
Analyzing and mapping regional land use trends by combining Landsat and topographic data p 2 A83-10119
BLANCHARD, A. J.
A simple relation between active and passive microwave remote sensing measurements of earth terrain p 24 A83-14857
Investigation of remote sensing techniques of measuring soil moisture
[E83-10048] p 12 N83-14557
BLOM, R.
Rock type discrimination techniques using Landsat and Seasat image data p 30 A83-10057
Imaging radar observations of volcanic features in Medicine Lake Highland, California p 30 A83-10079
Subsurface valleys and geoarcheology of the eastern Sahara revealed by Shuttle radar p 32 A83-13349
BLUME, H.-J. C.
Microwave remote sensing measurements of oil pollution on the ocean p 39 A83-10104
Passive microwave detection of river-plume fronts in the German Bight p 52 A83-17713
The effect of monomolecular surface films on the microwave brightness temperature of the sea surface p 43 A83-17714
BLY, B. G.
Landsat observations of Mount St. Helens p 19 A83-12671
BOBOVNIKOVA, T.
Instruments and methods for monitoring background soil pollution p 22 N83-12650
BODECHTEL, J.
Performance assessment of future European remote sensing systems p 2 A83-10109
BOETTINGER, W. U.
Theoretical and experimental investigations on the accuracy of close-range photogrammetry
[SER-C-266] p 25 N83-11564
BOGGIO, G.
The European Community, development and satellite technology p 75 N83-14609
BOGORODSKII, V. V.
Tidal phenomena in Arctic Ocean ice /according to space data/ p 40 A83-10832
BOHN, C. G.
Landsat observations of Mount St. Helens p 19 A83-12671
BONDERUD, J.
Gates to Gregg high voltage transmission line study
[E83-10097] p 16 N83-15741
BONN, F.
Comparison study of future SPOT and Landsat-D satellite products from a simulation flight p 57 A83-14243
Construction and interpretation of a thermal inertia image using airborne data p 57 A83-14260
BORN, G. H.
Collinear-track altimetry in the Gulf of Mexico from SEASAT: Measurements, models and surface truth
[AD-A118160] p 45 N83-11568
BORSTAD, G. A.
Application of remote sensing techniques in oceanographic studies of the British Columbia Salmon Fishery p 41 A83-14258
BORTNER, M. H.
Technology needs assessment of an atmospheric observation system for tropospheric research missions, part 1
[NASA-CR-3556] p 21 N83-10645
Technology needs assessment of an atmospheric observation system for multidisciplinary air quality/meteorology missions, part 2
[NASA-CR-3557] p 21 N83-10646
BOTKIN, D. B.
Monitoring global vegetation
[E83-10044] p 12 N83-14554
BOURQUE, H. H.
Remote sensing and waste management p 20 A83-14263
BOWEN, A. J., JR.
Operation plan for the data 100/LARS terminal system
[E83-10011] p 62 N83-12490
BOWEN, R. L.
Use of near-infrared video recording system for the detection of freeze damaged citrus leaves
[E83-10049] p 12 N83-14558
BOWLEY, C. J.
Snow hydrology studies using data from the Heat Capacity Mapping Mission p 50 A83-10102
BOYD, J. E.
Image enhancement through film recorder response contouring p 56 A83-12685
BOYD, M.
Integration of Landsat imagery into a program for aerial surveying of deer populations in Alberta p 5 A83-14252
BOYD, W. E.
Rangeland biomass estimation demonstration
[E83-10113] p 17 N83-15756
BRACHET, G.
Earth observation - Evolution of requirements and systems p 72 A83-10429
BRADLEY, P. A.
Sky-wave radar sea-state sensing - Effects of ionospheric movement and propagation geometry p 43 A83-17709
BRAILE, L. W.
Gravity and magnetic anomaly data analysis
[E83-10031] p 26 N83-13525
BRAMLEY, E. N.
Sky-wave radar sea-state sensing - Effects of ionospheric movement and propagation geometry p 43 A83-17709
BRANDNER, T. M.
Combining land use data acquired from Landsat with soil map data p 2 A83-10117
BRANN, H. N.
Australian drifting buoy p 48 N83-14837
BREED, C.
Shuttle imaging radar experiment p 32 A83-13348
BREED, C. S.
Subsurface valleys and geoarcheology of the eastern Sahara revealed by Shuttle radar p 32 A83-13349
BREHM, W. F.
Technology needs assessment of an atmospheric observation system for multidisciplinary air quality/meteorology missions, part 2
[NASA-CR-3557] p 21 N83-10646
BRINK, J. V.
The application of remote sensing in southern Alberta's mountain pine beetle management p 5 A83-14257
BRINKMAN, K. L.
MSS D Multispectral Scanner System
[E83-10128] p 72 N83-15797
BRISCO, B.
Data documentation for the 1981 summer vegetation experiment
[E83-10016] p 10 N83-12499
BROCHU, R.
Construction and interpretation of a thermal inertia image using airborne data p 57 A83-14260
BROENKOW, W. W.
Phytoplankton pigment concentrations in the Middle Atlantic Bight - Comparison of ship determinations and CZCS estimates p 43 A83-18580
BROWN, J. W.
Phytoplankton pigment concentrations in the Middle Atlantic Bight - Comparison of ship determinations and CZCS estimates p 43 A83-18580
BROWN, O. B.
Phytoplankton pigment concentrations in the Middle Atlantic Bight - Comparison of ship determinations and CZCS estimates p 43 A83-18580
BROWN, R. J.
Satellite remote sensing for domestic crop reporting in the United States and Canada - A look to the future p 3 A83-14229
Optical characteristics of Alberta rangeland as related to remote sensing p 4 A83-14245
BROWN, R. M.
Application of remote sensing techniques in oceanographic studies of the British Columbia Salmon Fishery p 41 A83-14258

BROWN, W. E.
Shuttle imaging radar experiment p 32 A83-13348
BRUCE, W. D.
Application of Landsat imagery to natural resources management in Sierra Leone, West Africa p 57 A83-14247
BRUZZI, S.
Quality assessment of remote-sensing data - The SAR case p 56 A83-13845
BRYAN, M. L.
Potentials for change detection using Seasat synthetic aperture radar data p 54 A83-10121
BRYANT, J.
System support documentation: IDIMS FUNCTION AMOEBA p 9 N83-12495
BUCKINGHAM, W. F.
The role of geological surfaces in determining visible-near infra red spectral signatures p 30 A83-10058
BUFTON, J. L.
Satellite laser altimeter for measurement of ice sheet topography p 38 A83-10092
Dual-wavelength correlation measurements with an airborne pulsed carbon dioxide lidar system p 60 A83-16831
BURT, W. V.
Effects of mesoscale atmospheric convection cells on the waters of the East China Sea p 41 A83-13270
BUSINGER, J. A.
Joint Air Sea Interaction (JASIN) experiment, Northwest coast of Scotland
[NASA-CR-169631] p 48 N83-14603

C

CAMARA, G.
Comparison of diverse methods for the correction of atmospheric effects on LANDSAT and SKYLAB images
[E83-10079] p 72 N83-14588
CAMARGO, J. C. G.
Verification of LANDSAT imagery for morphametric and topological studies of drainage basins in a section of the western plateau of Sao Paulo State: Tiete-Aguapei watershed
[E83-10111] p 54 N83-15754
CAMPBELL, W. J.
The application of microwave remote sensing for snow and ice research p 38 A83-10088
Geographic information systems p 61 N83-10465
CANDE, S. C.
The intermediate wavelength magnetic anomaly field of the north Pacific and possible source distributions
[E83-10088] p 27 N83-14596
CANOBA, C. A.
Geomorphological mapping using Landsat imagery - A case study in Argentina p 33 A83-17841
CAPPELLETTI, C. A.
An application of cluster analysis for determining homogeneous subregions: The agroclimatological point of view
[E83-10067] p 14 N83-14576
Estimation of the sugar cane cultivated area from LANDSAT images using the two phase sampling method
[E83-10077] p 15 N83-14586
CAPPELLINI, V.
Agroecological classification by remote sensing techniques p 23 N83-14622
CARLSON, T. N.
Remote determination of surface evaporation using thermal IR measurements p 50 A83-10101
Use of thermal inertia determined by HCMM to predict nocturnal cold prone areas in Florida
[E83-10102] p 64 N83-15745
CARMICHAEL, R. S.
Use of MAGSAT anomaly data for crustal structure and mineral resources in the US midcontinent
[E83-10082] p 36 N83-14590
CARROLL, T. R.
Airborne measurement of surficial soil moisture using natural terrestrial gamma radiation p 50 A83-10120
CARSEY, F. D.
Microwave radiance of early fall sea ice at 1.55 cm p 38 A83-10091
CAUDILL, C. E.
AgRISTARS - Plans and first-year achievements p 1 A83-10095
CAVALIERI, D. J.
The Bering Sea ice cover during March 1979: Comparison of surface and satellite data with the Nimbus-7 SMMR
[NASA-CR-169393] p 47 N83-13572
CAZABAT, C.
Photointerpretation, remote sensing, and photogrammetric elements applied to road-planning studies p 19 A83-11866
CHAMARD, R. R. S.
Analytical plotter for data input into geo-based information systems p 56 A83-12683
CHAN, W. C.
Technical issues in focal plane development; Proceedings of the Meeting, Washington, DC, April 21, 22, 1981 p 69 A83-13726
CHANG, A. T. C.
Observations of oceanic surface-wind fields from the Nimbus-7 microwave radiometer p 42 A83-14861
CHAVRO, A. I.
Concerning the determination of the temperature of the ocean surface from multichannel satellite measurements of radiation in infrared atmospheric windows p 42 A83-14316
CHEBOTAREVA, V. A.
The utilization of infrared /IR/ aerial and space observations of Arctic seas in navigation and during the solution of other national-economic problems p 40 A83-10836
CHEN, D. T.
On the use of laser profilometry for ocean wave studies p 42 A83-14502
CHEN, E.
Use of thermal inertia determined by HCMM to predict nocturnal cold prone areas in Florida
[E83-10028] p 62 N83-13522
Use of thermal inertia determined by HCMM to predict nocturnal cold prone areas in Florida
[E83-10102] p 64 N83-15745
CHEN, T. R.
Low threshold InGaAsP/InP lasers with microcleaved mirrors suitable for monolithic integration p 24 A83-10981
CHITTINENI, C. B.
Probabilistic cluster labeling of imagery data p 54 A83-11410
CHIZHIK, V. N.
Cosmogeological structures of the Hissar Alai and their role in the distribution of endogenous mineralization p 31 A83-11959
CHOU, S.-H.
Satellite estimates of ocean-air heat fluxes during cold air outbreaks p 41 A83-13059
CHRISTENSON, J.
CIRSS vertical data integration, San Bernardino County study phases 1-A, 1-B
[E83-10124] p 67 N83-15794
CIRSS vertical data integration, San Bernardino study
[E83-10127] p 67 N83-15796
CHUANG, S. L.
Remote sensing of dielectric media with periodic rough surfaces p 1 A83-10106
CHUSN, G., JR.
Low- to moderate-temperature geothermal resource assessment for Nevada: Area specific studies, Pumpernickel Valley, Carlin and Moana
[DE82-018598] p 34 N83-12584
CICONE, R.
Development, implementation and evaluation of satellite-aided agricultural monitoring systems
[E83-10017] p 10 N83-12500
CIHA, A. J.
Influence of environmental factors during seed development and after full-ripeness on pre-harvest sprouting in wheat
[E83-10002] p 7 N83-12482
CIHLAR, J.
Renewable resources monitoring needs in Manitoba p 19 A83-14228
CIMINO, J. B.
Shuttle imaging radar experiment p 32 A83-13348
CLAASEN, D. B. V. R.
Landsat for resource evaluation and management in the Alberta foothills p 32 A83-14256
CLARK, B. P.
LANDSAT 3 return beam vidicon response artifacts: A report on RBV photographic product characteristics and quality coding system
[E83-10122] p 67 N83-15792
CLARK, B. V.
Rangeland biomass estimation demonstration
[E83-10113] p 17 N83-15756
CLARK, D. K.
Phytoplankton pigment concentrations in the Middle Atlantic Bight - Comparison of ship determinations and CZCS estimates p 43 A83-18580
CLEMENTE-COLON, P.
On the circulation of the western Gulf of Mexico - A satellite view p 39 A83-10113
CLICHE, G.
Comparison study of future SPOT and Landsat-D satellite products from a simulation flight p 57 A83-14243
COBERLY, W. A.
The Akaike information criterion and its application to mixture proportion estimation p 62 N83-12498
COBURN, V. L.
Analyzing and mapping regional land use trends by combining Landsat and topographic data p 2 A83-10119
COLES, R. L.
The reduction, verification and interpretation of MAGSAT magnetic data over Canada
[E83-10091] p 28 N83-14599
The reduction, verification and interpretation of MAGSAT magnetic data over Canada
[E83-10101] p 29 N83-15744
COLVOCORESSES, A. P.
An automated mapping satellite system /Mapsat/ p 67 A83-10715
COLWELL, R. N.
Remote sensing of water quality for estuarine environments p 50 A83-10073
CONESE, C.
Agroecological classification by remote sensing techniques p 23 N83-14622
CONRAD, C.
Rock type discrimination techniques using Landsat and Seasat image data p 30 A83-10057
CONROW, E. H.
An evaluation of four thermal models used in thermal inertia analysis p 67 A83-10098
COOK, A.
Integration of Landsat imagery into a program for aerial surveying of deer populations in Alberta p 5 A83-14252
COOK, D. O.
Use of aerial photography with Loran C positioning to map offshore surface currents p 41 A83-14093
COOK, F. J.
Scene classification of Landsat multispectral scanner data by means of the Adaptive Learning Network methodology p 55 A83-11458
COOPER, G.
Use of near-infrared video recording system for the detection of freeze damaged citrus leaves
[E83-10049] p 12 N83-14558
COOPER, K.
Reflectance of a vegetation canopy using the Adding method p 3 A83-12603
CORNILLON, P.
Remote sensing, a tool for managing the marine environment: Eight case studies
[PB82-220864] p 44 N83-10483
COTE, C. E.
Nimbus 6 Random Access Measurement System applications experiments
[NASA-SP-457] p 48 N83-14835
COX, K.
An experimental Landsat Quicklook System for Alaska p 57 A83-14271
COX, S.
A case study in the practical use of LANDSAT data p 52 N83-10466
CRIST, E. P.
Development, implementation and evaluation of satellite-aided agricultural monitoring systems
[E83-10017] p 10 N83-12500
Analysis of the profile characteristics of corn and soybeans using field reflectance data
[E83-10018] p 10 N83-12501
CROMBIE, M. A.
An analysis of a relaxation scheme to improve terrain elevation data
[AD-A119257] p 27 N83-13550
CROSWELL, W. F.
Microwave remote sensing measurements of oil pollution on the ocean p 39 A83-10104
CROWELL, J. C.
Neotectonics of the San Andreas Fault system: Basin and range province juncture
[E83-10090] p 36 N83-14598
CROWLEY, J.
Seasat L-band radar response to forest vegetation in eastern Virginia p 1 A83-10061
CUMMING, C.
A field portable reflectance spectrometer p 69 A83-14275
CURRAN, P. J.
Polarized visible light as an aid to vegetation classification p 7 A83-16908
CUTTING, E.
Flight path design issues for the TOPEX mission
[AIAA PAPER 83-0197] p 42 A83-16581

D

DAILY, M.
Imaging radar observations of volcanic features in Medicine Lake Highland, California p 30 A83-10079
DAILY, M. I.
SAR squint analysis of directional extended targets p 54 A83-10084
DANA, R. W.
Background reflectance effects in Landsat data p 55 A83-12602
DANEL-DANELSKAIA, B.
Lineaments and ring structures on the territory of Poland p 24 A83-14303
DAVIDSON, S. A.
FORTRAN implementation of Friedman's test for several related samples
[E83-10123] p 18 N83-15793
DAVIES, J. H.
A field portable reflectance spectrometer p 69 A83-14275
DAVIS, D. N.
The CCRS SAR processing system p 69 A83-14289
DAVIS, G. R.
Use of aerial photography with Loran C positioning to map offshore surface currents p 41 A83-14093
DAVIS, L. S.
Cooperative processes in image segmentation p 65 N83-15768
DAWE, B.
On detection of oil pollution in ice environment p 41 A83-14239
DEAN, K. G.
Evaluation of photographic enhancements of Landsat imagery p 55 A83-12035
Radar and infrared remote sensing of geothermal features at Pilgrim Springs, Alaska p 31 A83-12036
DEAQUINO, L. C. S.
Vegetation survey in Amazonia using LANDSAT data
[E83-10068] p 14 N83-14577
DEEKSHATULU, B. L.
Pattern recognition and digital image processing as applied to remote sensing in India p 54 A83-11450
DEEPAK, A.
Action plan for remote sensing applications for rice production
[IFAORS-207] p 3 A83-14121
DELANEY, E. A.
Lagrangian drift measurements of sea surface currents and iceberg tracking p 49 N83-14842
DELVALLE, G.
Use of thermal inertia determined by HCMM to predict nocturnal cold prone areas in Florida
[E83-10102] p 64 N83-15745
DEMARCKE, J. S.
Wetland mapping with imaging radar p 50 A83-10072
DEMAS, L. J.
OSTA-1 - Shuttle's first scientific and applications payload p 73 A83-13715
DEMORAESNOVO, E. M. L.
Method of interpretation of remotely sensed data and applications to land use
[E83-10072] p 23 N83-14581
DENEGRE, J.
Photointerpretation, remote sensing, and photogrammetric elements applied to road-planning studies p 19 A83-11666
DENNERT-MOELLER, E.
The digital image processing system MOBI-DIVAH p 59 A83-14944
Preparation of a sediment map of the North Frisian shoal areas on the basis of Landsat imagery p 59 A83-14945
DEOLIVEIRA, M. O. B.
An automatic agricultural zone classification procedure for crop inventory satellite images
[E83-10065] p 14 N83-14574
DERENYI, E.
Potentials of Landsat-D and SPOT-1 for crop identification in the maritimes p 4 A83-14240
Cartographic aspects of dual-frequency dual-polarization SAR imagery p 58 A83-14280
DERENYI, E. E.
Vegetation change detection in an agricultural area - A simple approach for use with geo-data base p 4 A83-14236
DERYDER, L. J.
Technology needs assessment of an atmospheric observation system for tropospheric research missions, part 1
[NASA-CR-3556] p 21 N83-10645
DESOUZA, R. C. M.
INPE LANDSAT-D thematic mapper computer compatible tape format specification
[E83-10075] p 63 N83-14584
Comparison of diverse methods for the correction of atmospheric effects on LANDSAT and SKYLAB images
[E83-10079] p 72 N83-14588
DEVROYE, L.
Topics in global convergence of density estimates p 66 N83-15775
DEWEY, K. F.
Satellite observations of variations in Northern Hemisphere seasonal snow cover
[PB82-196668] p 52 N83-10734
DHOORE, J.
Multitemporal soil and vegetation observations by METEOSAT over Central Africa p 15 N83-14619
DIAS, L. A. V.
Comparison of diverse methods for the correction of atmospheric effects on LANDSAT and SKYLAB images
[E83-10079] p 72 N83-14588
DICK, R.
A field portable reflectance spectrometer p 69 A83-14275
DICKINSON, K.
Remote sensing software for airborne image analysis p 58 A83-14273
DIETERLE, G.
The microwave payload for the ESA Remote Sensing Satellite /ERS-1/ p 69 A83-14290
DIXON, R. J.
Digital colour enhancement of Landsat data for mapping vegetation of barrenground caribou winter range in northern Manitoba p 5 A83-14249
DIXON, T.
Shuttle imaging radar experiment p 32 A83-13348
DOBSON, M. C.
Effects of vegetation cover on the radar sensitivity to soil moisture p 6 A83-14856
Assessment of radar resolution requirements for soil moisture estimation from simulated satellite imagery
[E83-10020] p 10 N83-12503
DODD, J. K.
An evaluation of four thermal models used in thermal inertia analysis p 67 A83-10098
DORRER, G. A.
Determination of forest fire spread rates from infrared photographs p 6 A83-14307
DOSANJOS, C. E.
Geological-structural interpretation using products of remote sensing in the region of Carrancas, Minas Gerais, Brazil
[E83-10029] p 34 N83-13523
LANDSAT and radar mapping of intrusive rocks in SE-Brazil
[E83-10073] p 36 N83-14582
DOSSANTOS, A. P.
Method of interpretation of remotely sensed data and applications to land use
[E83-10072] p 23 N83-14581
DOSSANTOS, A. R.
Geological-structural interpretation using products of remote sensing in the region of Carrancas, Minas Gerais, Brazil
[E83-10029] p 34 N83-13523
LANDSAT and radar mapping of intrusive rocks in SE-Brazil
[E83-10073] p 36 N83-14582
DOSSANTOS, J. R.
Vegetation survey in Amazonia using LANDSAT data
[E83-10068] p 14 N83-14577
Remote sensing techniques for conservation and management of natural vegetation ecosystems
[E83-10070] p 15 N83-14579
Evaluation of reforestation using remote sensing techniques
[E83-10076] p 15 N83-14585
DOYLE, F. J.
Electro-optical instrumentation for resources evaluation; Proceedings of the Meeting, Washington, DC, April 21, 22, 1981 p 68 A83-12669
DUGDALE, G.
The determination of soil moisture balances in tropical Africa by satellite infrared remote sensing: The atmospheric problem p 53 N83-14621
DUGGIN, M.
Measurements of the characteristic reflectance spectra of surficial deposits p 32 A83-14266
DYHR-NIELSEN, M.
Long-range water supply forecasting
[WMO-587] p 53 N83-12516

E

EASTERWOOD, P.
Gates to Gregg high voltage transmission line study
[E83-10097] p 16 N83-15741
EASTES, J. W.
Special reflectance of some plant indicators of saline and nonsaline soils
[AD-A119727] p 16 N83-14655
EATON, F. D.
Radar and infrared remote sensing of geothermal features at Pilgrim Springs, Alaska p 31 A83-12036
EBNER, H.
A Digital Photogrammetric System (DPS) for producing Digital Elevation Models (DEM) and orthoplates by means of linear array scanner imagery
[MBB-UA-618/81] p 71 N83-13567
EGER, G. W., III
A three-part geometric model to predict the radar backscatter from wheat, corn, and sorghum
[E83-10005] p 8 N83-12485
EHLERS, M.
The digital image processing system MOBI-DIVAH p 59 A83-14944
Rectification of Seasat radar on Landsat MSS with the aid of digital image correlation p 59 A83-14946
ELACHI, C.
Imaging radar observations of volcanic features in Medicine Lake Highland, California p 30 A83-10079
Earth resources observation with the Shuttle imaging radar p 68 A83-12676
Shuttle imaging radar experiment p 32 A83-13348
Subsurface valleys and geoarcheology of the eastern Sahara revealed by Shuttle radar p 32 A83-13349
Radar images of the earth from space p 59 A83-14598
ELLENBECK, K. H.
Investigation of the geometrical stability of a photogrammetric recording system
[SER-C-267] p 71 N83-11565
ELLIS, T. J.
Operational land cover type mapping in Ontario by Landsat based digital analysis and map production p 19 A83-14230
ENGLAND, A.
Seasat L-band radar response to forest vegetation in eastern Virginia p 1 A83-10061
Shuttle imaging radar experiment p 32 A83-13348
ESCOBAR, D. E.
Reflectance measurement of artificially induced ultraviolet radiation stress on cotton leaves p 7 A83-16907
Use of near-infrared video recording system for the detection of freeze damaged citrus leaves
[E83-10049] p 12 N83-14558
Comparison of LANDSAT-2 and field spectrometer reflectance signatures of south Texas rangeland plant communities
[E83-10055] p 13 N83-14564
ESERKEPOVA, I. B.
Using new methods in monitoring the thermal regime of the Arctic p 39 A83-10828
ESTES, J. E.
Monitoring global vegetation
[E83-10044] p 12 N83-14554
Neotectonics of the San Andreas Fault system: Basin and range province juncture
[E83-10090] p 36 N83-14598
ESTES, R. H.
Equivalent source modeling of the main field using MAGSAT data
[E83-10094] p 28 N83-14601
Geomagnetic modeling by optimal recursive filtering
[E83-10112] p 29 N83-15755
EVANS, D. L.
Derivation of compositional information from multispectral images p 30 A83-10059
Shuttle imaging radar experiment p 32 A83-13348
EVANS, R. H.
Phytoplankton pigment concentrations in the Middle Atlantic Bight - Comparison of ship determinations and CZCS estimates p 43 A83-18580
EVANS, W. E.
Automated measurements of atmospheric visibility
[AIAA PAPER 83-0436] p 21 A83-16713
EVERITT, J. H.
Estimating total standing herbaceous biomass production with LANDSAT MSS digital data
[E83-10045] p 12 N83-13536
Comparison of LANDSAT-2 and field spectrometer reflectance signatures of south Texas rangeland plant communities
[E83-10055] p 13 N83-14564

F

FARR, T. G.
Imaging radar observations of volcanic features in Medicine Lake Highland, California p 30 A83-10079
FECSO, R.
Construction of a remotely sensed area sampling frame for Southern Brazil
[E83-10052] p 13 N83-14561
FEDCHENKO, P. P.
Determination of humus in soil on the basis of spectral measurements p 6 A83-14310
Remote determination of humus content in soils p 7 A83-15889
FEDOSEEV, L. I.
Investigations of the apparent temperature of snow cover in the submillimeter wavelength region p 52 A83-15816
FEDOSEJEVS, G.
Optical characteristics of Alberta rangeland as related to remote sensing p 4 A83-14245
FEMIANO, M. D.
Satellite laser altimeter for measurement of ice sheet topography p 38 A83-10092
FENNER, R. G.
A parametric study of tillage effects on radar backscatter p 2 A83-10108
FERNANDES, L.
Investigating the possibility of producing a land-use map for Cuba on the basis of space imagery p 20 A83-14305
FILHO, P. H.
Use of LANDSAT images to study cerrado vegetation
[E83-10025] p 11 N83-13519
Evaluation of reforestation using remote sensing techniques
[E83-10076] p 15 N83-14585
FILHO, R. A.
Multitemporal and geobotanical approach in the remote detection of Greisenization areas in the Serra da Pedra Branca Granite, Goias State, Brazil
[E83-10071] p 35 N83-14580
FLANDERS, A. F.
Hydrological data transmission
[WMO-559] p 53 N83-12514
FLATOW, F. S.
Satellite laser altimeter for measurement of ice sheet topography p 38 A83-10092
FLEMING, E.
Monitoring revision requirements for Canadian maps p 24 A83-14237
A national Landsat collection and a proposal for a library of Landsat images p 57 A83-14270
FLYNN, T.
Low- to moderate-temperature geothermal resource assessment for Nevada: Area specific studies, Pumpernickel Valley, Carlin and Moana
[DE82-018598] p 34 N83-12584
FLYNN, T. L.
Use of aerial photography with Loran C positioning to map offshore surface currents p 41 A83-14093
FOLDER, P.
Technology needs assessment of an atmospheric observation system for multidisciplinary air quality/meteorology missions, part 2
[NASA-CR-3557] p 21 N83-10646
FOLEY, T. A.
BSPLASH: A three-stage surface interpolant to scattered data p 65 N83-15765
FOLLESTAD, B.
Digital methods for lineament analysis p 37 N83-14634
FOOTE, H. P.
Analyzing and mapping regional land use trends by combining Landsat and topographic data p 2 A83-10119
FORBES, R. B.
Radar and infrared remote sensing of geothermal features at Pilgrim Springs, Alaska p 31 A83-12036
FORD, J. P.
Drumlin fields and glaciated mountains - A contrast in geomorphic perception from Seasat radar images p 23 A83-10078
Shuttle imaging radar experiment p 32 A83-13348
Resolution versus speckle relative to geologic interpretability of spaceborne radar images - A survey of user preference p 33 A83-14852
FORESTI, C.
Method of interpretation of remotely sensed data and applications to land use
[E83-10072] p 23 N83-14581
FORMAN, M. L.
The use of thematic mapper simulator calibration data for assessment of data quality
[NASA-TM-82059] p 71 N83-13547
FOWLER, R.
Aerial thermal infrared census of Canada geese in South Dakota p 6 A83-14665
FRANKLIN, R. A.
Use of aerial photography with Loran C positioning to map offshore surface currents p 41 A83-14093
FRAUTNICK, J. C.
Flight path design issues for the TOPEX mission
[AIAA PAPER 83-0197] p 42 A83-16581
FREDEN, S. C.
Appendix A: The LANDSAT system p 75 N83-10469
FREDHJEM, K. O.
Digital analysis of Landsat satellite imagery in Turkana, Northern Kenya p 64 N83-14637
FREI, W.
Automatic multitemporal segmentation for diachronic analysis of remotely sensed images p 55 A83-11461
FRICK, D. M.
Snowmelt runoff modeling in simulation and forecasting modes with the Martinec-Mango model
[E83-10063] p 53 N83-14572
FRIDMAN, S. D.
Aircraft and remote measurements of atmospheric transport of pollutants within the global integrated monitoring system p 22 N83-12620
FRIPPEL, G. G.
Technology needs assessment of an atmospheric observation system for tropospheric research missions, part 1
[NASA-CR-3556] p 21 N83-10645
Technology needs assessment of an atmospheric observation system for multidisciplinary air quality/meteorology missions, part 2
[NASA-CR-3557] p 21 N83-10646
FROST, F. S.
Analysis of geologic terrain models for determination of optimum SAR sensor configuration and optimum information extraction for exploration of global non-renewable resources. Pilot study: Arkansas Remote Sensing Laboratory, part 1, part 2, and part 3
[E83-10061] p 35 N83-14570
FUGONO, N.
Application of the airborne microwave rain-scattered/radiometer system to the remote sensing of rains and wind vector measurements over the ocean p 70 A83-14293
FUJITA, M.
Application of the airborne microwave rain-scattered/radiometer system to the remote sensing of rains and wind vector measurements over the ocean p 70 A83-14293
FUKUSHIMA, N.
Japanese MAGSAT Team
[E83-10080] p 27 N83-14589
FUNG, A. K.
Radar spectral observations of snow p 49 A83-10064
A backscatter model for a randomly perturbed periodic surface p 1 A83-10107
Microwave remote sensing: Active and passive. Volume 2 - Radar remote sensing and surface scattering and emission theory p 69 A83-14040
A backscatter model for a randomly perturbed periodic surface p 7 A83-14859

G

GAIKOVICH, K. P.
The possibility of measuring the moisture content of the upper layers of the atmosphere using radiometric techniques p 70 A83-14308
GARCIA, M.
Space truth in oceanography p 48 N83-14636
GARDNER, B. R.
Development of thematic mapper vegetative indices for assessing biomass in corn, soybeans and wheat
[E83-10035] p 11 N83-13529
GARDNER, C. S.
Remote sensing of sea state using laser altimeters p 40 A83-12316
GARDNER, W.
Construction of a remotely sensed area sampling frame for Southern Brazil
[E83-10052] p 13 N83-14561
GARRETT, J.
Mesoscale ocean variability p 48 N83-14841
GARRETT, W. D.
The effect of monomolecular surface films on the microwave brightness temperature of the sea surface p 43 A83-17714
GATTO, L. W.
Ice distribution and winter surface circulation patterns, Kachemak Bay, Alaska p 50 A83-12038
GAUSMAN, H. W.
Reflectance measurement of artificially induced ultraviolet radiation stress on cotton leaves p 7 A83-16907
Reflectance differences between untreated and Mepiquat Chloride-treated, field-grown cotton through a growing season p 7 A83-16909
Optical parameters of leaves of seven weed species
[E83-10010] p 9 N83-12489
Use of near-infrared video recording system for the detection of freeze damaged citrus leaves
[E83-10049] p 12 N83-14558
Comparison of LANDSAT-2 and field spectrometer reflectance signatures of south Texas rangeland plant communities
[E83-10055] p 13 N83-14564
GAZIEV, Y.
Instruments and methods for monitoring background soil pollution p 22 N83-12650
GBUR, E. E.
Missing observations in multiyear rotation sampling designs
[E83-10022] p 11 N83-12505
GEISER, U.
Multistage land use mapping and change monitoring in Sri Lanka p 15 N83-14625
GEMAN, S.
Cross-validation for densities and regressions p 66 N83-15776
Characterization of a maximum-likelihood nonparametric density estimator of kernel type p 66 N83-15777
GENTLE, M. R.
The relationships between reflectance in the Landsat wavebands and the composition of an Australian semi-arid shrub rangeland p 19 A83-14095
GERACI, A. L.
Remote sensing of water quality for estuarine environments p 50 A83-10073
GERHARDT, L. A.
Image processing techniques p 61 N83-11391
GERLACH, F. L.
Predicting forest land attributes from aerial photo interpretation variables p 5 A83-14259
GEYSER, J. E.
Observations of oceanic surface-wind fields from the Nimbus-7 microwave radiometer p 42 A83-14861
GIBBS, B. P.
Geomagnetic modeling by optimal recursive filtering
[E83-10112] p 29 N83-15755
GIERLOFF-EMDEN, H. G.
Super high altitude photography for coastal geomorphology p 43 A83-17840
GILBERT, E.
Nimbus 6 Random Access Measurement System applications experiments
[NASA-SP-457] p 48 N83-14835
GLOERSEN, P.
The Bering Sea ice cover during March 1979: Comparison of surface and satellite data with the Nimbus-7 SMMR
[NASA-CR-169393] p 47 N83-13572
GODBY, E. A.
The importance of remote sensing for Canada - Past achievements, future needs p 74 A83-14227
GODIVIER, R.
Gravimetric maps of the Central African Republic
[E83-10084] p 27 N83-14592
GOEL, N. S.
A review of crop canopy reflectance models
[E83-10110] p 17 N83-15753
GOETZ, A. F. H.
Mineral identification from orbit - Initial results from the Shuttle multispectral infrared radiometer p 32 A83-13350
GOLCHIN, J.
Remote sensing of land resources: Application of LANDSAT satellite imagery p 11 N83-13517
GOLDHIRSH, J.
A tutorial assessment of atmospheric height uncertainties for high-precision satellite altimeter missions to monitor ocean currents p 42 A83-14851
GOLDSTEIN, W. A.
Influence of environmental factors during seed development and after full-ripeness on pre-harvest sprouting in wheat
[E83-10002] p 7 N83-12482
GOMBEER, R.
Multitemporal soil and vegetation observations by METEOSAT over Central Africa p 15 N83-14619
GOODENOUGH, D. G.
Remote sensing software for airborne image analysis p 58 A83-14273

GOODFELLOW, L. C.
A procedure to overlay thematic map and dominion land survey system data to geometrically-corrected Landsat images and its application to agricultural land use studies in western Canada p 3 A83-14231
GORDON, H. R.
Phytoplankton pigment concentrations in the Middle Atlantic Bight - Comparison of ship determinations and CZCS estimates p 43 A83-18580
GOUGEON, F. A.
Assessment of spruce budworm defoliation using digital airborne MSS data p 5 A83-14248
GOWER, J. F. F.
Application of remote sensing techniques in oceanographic studies of the British Columbia Salmon Fishery p 41 A83-14258
GRAETZ, R. D.
The relationships between reflectance in the Landsat wavebands and the composition of an Australian semi-arid shrub rangeland p 19 A83-14095
GRANICHNYI, M.
Lineaments and ring structures on the territory of Poland p 24 A83-14303
GRAZIANI, M. E.
Geographic research in the US Geological Survey: Bibliography, 1966 - 1980
[USGS-CIRC-865] p 21 N83-11639
GREGOIRE, J. M.
Use of remote sensing techniques for rice production forecasting in west Africa (Mali and Guinea: Niger-Bani Project) p 15 N83-14626
GRENDA, R. N.
Technology needs assessment of an atmospheric observation system for tropospheric research missions, part 1
[NASA-CR-3556] p 21 N83-10645
Technology needs assessment of an atmospheric observation system for multidisciplinary air quality/meteorology missions, part 2
[NASA-CR-3557] p 21 N83-10646
GREY, J.
Global implications of space activities; Proceedings of the Conference, Aspen, CO, August 30-September 4, 1981 p 74 A83-17349
GRIFFITH, C. G.
FACE-2 data reductions (prior to disclosure of the treatment decisions). Part 5: Satellite-estimated rainfall from a geostationary platform in FACE-2
[PB82-216581] p 52 N83-10730
GROLEMUND, D. A.
Dual-wavelength correlation measurements with an airborne pulsed carbon dioxide lidar system p 60 A83-16831
GROLIER, M. J.
Subsurface valleys and geoarcheology of the eastern Sahara revealed by Shuttle radar p 32 A83-13349
GUDMANSEN, P.
The application of microwave remote sensing for snow and ice research p 38 A83-10088
GUENTHER, G. C.
Effects of detection algorithm on accuracy degradation from logarithmic and difference processing for airborne laser bathymetry returns
[PB82-215138] p 44 N83-10707
GUEPET, G.
The GDTA - Remote sensing at the service of users p 68 A83-11867
GUERTIN, F. E.
Standardization of computer compatible tape formats for remote sensing data p 54 A83-10075
Definition and potential of geocoded satellite imagery products p 58 A83-14272
GUIGNARD, J.-P.
Quality assessment of remote-sensing data - The SAR case p 56 A83-13845
GUILLOT, B.
Temporary lakes and salt plains in the high plateaus of the Andes /Bolivia/ - A continuing survey of periodic hydrologic phenomena using the geostationary satellite GOES-EST p 51 A83-14574
GUINDON, B.
Remote sensing software for airborne image analysis p 58 A83-14273
GUSEMAN, L. F., JR.
Development of advanced acreage estimation methods
[E83-10015] p 9 N83-12494
Proceedings of the NASA Workshop on Surface Fitting
[E83-10117] p 64 N83-15759
Proceedings of the NASA Workshop on Image Analysis
[E83-10118] p 65 N83-15766
Proceedings of the NASA Workshop on Density Estimation and Function Smoothing
[E83-10119] p 66 N83-15774

H

HAEFNER, H.
Remote sensing of renewable natural resources in developing countries for national planning purposes p 76 N83-14616
Multistage land use mapping and change monitoring in Sri Lanka p 15 N83-14625
HAGEMANN, M. G.
Influence of environmental factors during seed development and after full-ripeness on pre-harvest sprouting in wheat
[E83-10002] p 7 N83-12482
HAGGERTY, S. E.
The mineralogy of global magnetic anomalies
[E83-10034] p 34 N83-13528
HAINES, G. V.
The reduction, verification and interpretation of MAGSAT magnetic data over Canada
[E83-10091] p 28 N83-14599
The reduction, verification and interpretation of MAGSAT magnetic data over Canada
[E83-10101] p 29 N83-15744
HALE, B.
Construction of a remotely sensed area sampling frame for Southern Brazil
[E83-10052] p 13 N83-14561
HALL, F. G.
AgRISTARS - Plans and first-year achievements p 1 A83-10095
HALL, R. J.
Remote sensing applications to the development of an integrated data base for oil and gas exploration p 37 N83-14628
HALL, W.
Integration of Landsat imagery into a program for aerial surveying of deer populations in Alberta p 5 A83-14252
HALSEY, H.
Technology needs assessment of an atmospheric observation system for tropospheric research missions, part 1
[NASA-CR-3556] p 21 N83-10645
HANDCOCK, D. E.
Australian drifting buoy p 48 N83-14837
HARALICK, R. M.
Image segmentation survey p 65 N83-15767
HARDY, R. L.
Surface fitting with biharmonic and harmonic models p 65 N83-15764
HARRINGTON, L.
To mix or match - On choosing matched samples in comparative aerial surveys p 59 A83-14664
HARRISON, C. G. A.
Investigations of medium wavelength magnetic anomalies in the eastern Pacific using MAGSAT data
[E83-10083] p 27 N83-14591
HART, W. D.
On the use of laser profilometry for ocean wave studies p 42 A83-14502
HARTL, P.
Ongoing microwave remote sensing-activities for land applications in Germany p 18 A83-10083
HASSELMANN, K.
Spectral signal to clutter and thermal noise properties of ocean wave imaging synthetic aperture radars p 43 A83-17712
HASSON, A.
Low threshold InGaAsP/InP lasers with microcleaved mirrors suitable for monolithic integration p 24 A83-10981
HASTINGS, D. A.
An investigation of MAGSAT and complementary data emphasizing Precambrian shields and adjacent areas of West Africa and South America
[E83-10085] p 36 N83-14593
HATHOUT, S.
Land use/land cover mapping from enhanced Landsat imagery of the eastern provinces of the People's Republic of China p 4 A83-14241
HAUSE, D.
Aerial thermal infrared census of Canada geese in South Dakota p 6 A83-14665
HAWKINS, J.
Comparison of multichannel and two-satellite methods for remote measurement of sea surface temperature
[AD-A118736] p 45 N83-12511
HAWKINS, J. L.
AgRISTARS documents tracking list report
[E83-10019] p 10 N83-12502
HAYDN, R.
Some aspects of the presentation of remote sensing data p 63 N83-14617
HAYNES, C. V.
Subsurface valleys and geoarcheology of the eastern Sahara revealed by Shuttle radar p 32 A83-13349
HAYNES, J. E.
Remote sensing and waste management p 20 A83-14263
HEAD, J. W., III
An investigation into the utilization of HCMM thermal data for the descrimination of volcanic and Eolian geological units
[E83-10047] p 35 N83-14556
HEGYI, F.
The use of R.B.V., colour additive viewer and M.S.S. products in the British Columbia Forest Inventory Depletion Monitoring Program p 4 A83-14246
HEILMAN, J.
Rice scene radiation research plan p 9 N83-12496
HEILMAN, J. L.
Evaluating depth to shallow groundwater using heat capacity mapping mission /HCMM/ data p 51 A83-14668
HEIM, R., JR.
Satellite observations of variations in Northern Hemisphere seasonal snow cover
[PB82-196668] p 52 N83-10734
HELLDEN, U.
Approaches to desertification monitoring in the Sudan p 23 N83-14623
HENDERSON, F. M.
An evaluation of Seasat SAR imagery for urban analysis p 60 A83-16904
HENDERSON, K. E.
Development of thematic mapper vegetative indices for assessing biomass in corn, soybeans and wheat
[E83-10035] p 11 N83-13529
HENLEY, P.
Effects of ground cover and leaf area on the spectral reflectance of vegetation-soil target
[AD-A119714] p 16 N83-14653
HENNINGS, D.
The conical scan radiometer p 72 N83-14804
HESSION, J. P.
Office automation in resource-management - The future is now p 6 A83-14269
HEYDORN, R. P.
Monitoring global vegetation
[E83-10044] p 12 N83-14554
Crop proportion estimation problems in AgRISTARS p 18 N83-15760
HICKS, T. I.
Evaluation of geodetic products produced by the NSWC reduction of SEASAT radar altimeter data
[AD-A117837] p 25 N83-11571
HIELKEMA, J. U.
Landsat monitoring of Desert Locust breeding grounds in Africa, the Near East and Southwest Asia p 1 A83-10097
HINKLE, R. E.
Mount St. Helens quick response damage assessment using high-altitude infrared photography p 19 A83-12672
HINZE, W. J.
Gravity and magnetic anomaly data analysis
[E83-10031] p 26 N83-13525
HODGES, T.
Second generation crop yield models review
[E83-10003] p 7 N83-12483
HODSON, W.
CIRSS vertical data integration, San Bernardino study
[E83-10127] p 67 N83-15796
HOFMANN, O.
A Digital Photogrammetric System (DPS) for producing Digital Elevation Models (DEM) and orthoplates by means of linear array scanner imagery
[MBB-UA-618/81] p 71 N83-13567
HOGE, F. E.
Experimental feasibility of the airborne measurement of absolute oil fluorescence spectral conversion efficiency p 44 A83-18581
HOGG, R. C.
AgRISTARS - Plans and first-year achievements p 1 A83-10095
HOLTZMAN, J. C.
Analysis of geologic terrain models for determination of optimum SAR sensor configuration and optimum information extraction for exploration of global non-renewable resources. Pilot study: Arkansas Remote Sensing Laboratory, part 1, part 2, and part 3
[E83-10061] p 35 N83-14570
HOLYER, R.
Comparison of multichannel and two-satellite methods for remote measurement of sea surface temperature
[AD-A118736] p 45 N83-12511
HONEA, D. L.
Operation and maintenance of geodetic satellite observatory, McMurdo, Antarctica
[PB82-187923] p 25 N83-12107

HOOD, V. A.
Satellite remote sensing: ESA's experience with developing countries p 76 N83-14632
HORN, L.
Digital colour enhancement of Landsat data for mapping vegetation of barrenground caribou winter range in northern Manitoba p 5 A83-14249
HORVATH, P.
Scene classification of Landsat multispectral scanner data by means of the Adaptive Learning Network methodology p 55 A83-11458
HOUSTON, A. G.
Monitoring global vegetation
[E83-10044] p 12 N83-14554
HOWARD, J. A.
Remote sensing in developing countries. FAO'S international experience p 76 N83-14614
HUANG, T. S.
Determining 3-D motion and structure from image sequences p 66 N83-15773
HUEHNERFUSS, H.
The effect of monomolecular surface films on the microwave brightness temperature of the sea surface p 43 A83-17714
HUEMMRICH, K. F.
Microwave radiance of early fall sea ice at 1.55 cm p 38 A83-10091

I

IDSO, S. B.
Diurnal patterns of wheat spectral reflectances and their importance in the assessment of canopy parameters from remotely sensed observations
[E83-10050] p 13 N83-14559
IGARASHI, T.
Reference quicklook images for monitor of Landsat image data acquisition p 58 A83-14286
INOMATA, H.
Application of the airborne microwave rain-scattered/radiometer system to the remote sensing of rains and wind vector measurements over the ocean p 70 A83-14293
INOSTROZA, H. M.
Interpretation of remotely sensed data and its applications in oceanography
[E83-10074] p 48 N83-14583
IONOV, V. A.
Aircraft and remote measurements of atmospheric transport of pollutants within the global integrated monitoring system p 22 N83-12620
ISSAWI, B.
Subsurface valleys and geoarcheology of the eastern Sahara revealed by Shuttle radar p 32 A83-13349
ITABE, T.
Dual-wavelength correlation measurements with an airborne pulsed carbon dioxide lidar system p 60 A83-16831
ITTEN, K. I.
Multistage land use mapping and change monitoring in Sri Lanka p 15 N83-14625

J

JACKSON, F. C.
Aircraft and satellite measurement of ocean wave directional spectra using scanning-beam microwave radars
[NASA-TM-84008] p 47 N83-13544
JACKSON, P. L.
Further SEASAT SAR coastal ocean wave analysis
[NASA-CR-169682] p 47 N83-13776
JACKSON, R. D.
Atmospheric effects on radiation reflected from soil and vegetation as measured by orbital sensors using various scanning directions p 3 A83-12315
Discrimination of growth and water stress in wheat by various vegetation indices through a clear a turbid atmosphere
[E83-10009] p 8 N83-12488
Diurnal patterns of wheat spectral reflectances and their importance in the assessment of canopy parameters from remotely sensed observations
[E83-10050] p 13 N83-14559
Adjusting the tasseled cap brightness and greenness factors for atmospheric path radiance and absorption on a pixel by pixel basis
[E83-10053] p 13 N83-14562
JACOBSEN, J.
Waterfowl habitat inventory of Alberta, Saskatchewan and Manitoba by remote sensing p 4 A83-14244
JANO, A.
Landsat-based forest mapping in Ontario north of latitude 52 deg north p 5 A83-14253
JARRARD, R. D.
The intermediate wavelength magnetic anomaly field of the north Pacific and possible source distributions
[E83-10088] p 27 N83-14596
JAYNES, R. A.
Detection of aspen-conifer forest mixes from LANDSAT digital data
[E83-10106] p 17 N83-15749
JEANSOULIN, R.
Automatic multitemporal segmentation for diachronic analysis of remotely sensed images p 55 A83-11461
JENSEN, C. K.
The RAMS collection of meterological and position data in the Norwegian Sea p 49 N83-14845
JOHNSON, J. W.
Microwave remote sensing measurements of oil pollution on the ocean p 39 A83-10104
Measurements of ocean surface spectrum from an aircraft using the two-frequency microwave resonance technique p 43 A83-17710
JOHNSON, M. E.
Statistical Techniques Applied to Aerial Radiometric Surveys (STARRS): Discriminant-analysis methods applied to aerial radiometric data and their application to uranium favorability in South Texas. Nation uranium resource evaluation
[DE82-020961] p 34 N83-12512
JOHNSON, M. P.
Methods of editing cloud and atmospheric layer affected pixels from satellite data
[E83-10103] p 64 N83-15746
JOHNSON, R. L.
MSS D Multispectral Scanner System
[E83-10128] p 72 N83-15797
JOHNSON, V.
Construction of a remotely sensed area sampling frame for Southern Brazil
[E83-10052] p 13 N83-14561
JOLLY, J. P.
Application of Landsat imagery to natural resources management in Sierra Leone, West Africa p 57 A83-14247
JONES, C. L.
Microwave remote sensing of soil moisture, volume 1
[E83-10108] p 17 N83-15751
JONES, E. B.
Snowmelt runoff modeling in simulation and forecasting modes with the Martinec-Mango model
[E83-10063] p 53 N83-14572
JONES, P. H.
Use of thermal inertia determined by HCMM to predict nocturnal cold prone areas in Florida
[E83-10028] p 62 N83-13522
Use of thermal inertia determined by HCMM to predict nocturnal cold prone areas in Florida
[E83-10102] p 64 N83-15745
JONES, W. L.
Measurements of ocean surface spectrum from an aircraft using the two-frequency microwave resonance technique p 43 A83-17710
JUSTICE, C.
A comparison of unsupervised classification procedures on Landsat MSS data for an area of complex surface conditions in Basilicata, Southern Italy p 55 A83-12037

K

KAGAN, R. L.
Using new methods in monitoring the thermal regime of the Arctic p 39 A83-10828
KAHLE, A. B.
Some examples of the utility of HCMM data in geologic remote sensing p 31 A83-10099
KALCIC, M. T.
Automated segment matching algorithm-theory, test, and evaluation
[E83-10096] p 16 N83-15740
KALININA, N. A.
Determination of forest fire spread rates from infrared photographs p 6 A83-14307
KANEMASU, E. T.
A three-part geometric model to predict the radar backscatter from wheat, corn, and sorghum
[E83-10005] p 8 N83-12485
KASISCHKE, E. S.
Detection of coastal zone environmental conditions using synthetic aperture radar p 38 A83-10068
Further SEASAT SAR coastal ocean wave analysis
[NASA-CR-169682] p 47 N83-13776
KATSAROS, K. B.
Validation and application of the SEASAT-SMMR geophysical algorithms
[NASA-CR-169390] p 71 N83-13767
KAUPP, V. H.
Wetland mapping with imaging radar p 50 A83-10072
Geological terrain models p 31 A83-10080
Analysis of geologic terrain models for determination of optimum SAR sensor configuration and optimum information extraction for exploration of global non-renewable resources. Pilot study: Arkansas Remote Sensing Laboratory, part 1, part 2, and part 3
[E83-10061] p 35 N83-14570
KEAFER, L. S.
Technology needs assessment of an atmospheric observation system for tropospheric research missions, part 1
[NASA-CR-3556] p 21 N83-10645
KEEN, R. A.
The role of cross-equatorial tropical cyclone pairs in the southern oscillation p 40 A83-13057
KELLER, G. R.
Crustal and upper mantle structure data analysis
[E83-10038] p 26 N83-13532
KELLER, S. W.
Land remote sensing activities in the US p 72 N83-14612
KELLY, K. A.
Infrared satellite data from the first coastal ocean dynamics experiment, March - July 1981
[AD-A120068] p 49 N83-15799
KHIZHNICHENKO, V. I.
Coordinate transformation during the geometric correction of the space scanner imagery of the earth p 70 A83-14313
KHORRAM, S.
Remote sensing of water quality for estuarine environments p 50 A83-10073
KHREBTOV, B. A.
Determination of forest fire spread rates from infrared photographs p 6 A83-14307
KILGORE, R. W.
Application of computer axial tomography /CAT/ to measuring crop canopy geometry p 1 A83-10096
KIM, H. H.
OSTA-1/Ocean Color Experiment
[AIAA PAPER 83-0415] p 42 A83-16701
KIMES, D. S.
Radiative transfer model for heterogeneous 3-D scenes p 3 A83-12604
KINGSTON, M. J.
Mineral identification from orbit - Initial results from the Shuttle multispectral infrared radiometer p 32 A83-13350
KIPP, E. R.
Crop-phenology and LANDSAT-based irrigated lands inventory in the high plains
[E83-10115] p 18 N83-15758
KIRBY, M. E.
Applications of Robert's gradient operator for the digital enhancement of icebergs from SAR imagery p 41 A83-14278
KIRCHNER, J. A.
Radiative transfer model for heterogeneous 3-D scenes p 3 A83-12604
KIREMIDJIAN, G. K.
Registration of a synthetic aperture radar /SAR/ reconnaissance image with a map reference data base p 56 A83-12885
KIRWAN, A. D., JR.
Drift buoy component, NORPAX anomaly dynamics study p 49 N83-14848
KITAGAWA, G.
The Akaike information criterion and its application to mixture proportion estimation p 62 N83-12498
KITAI, SH. D.
The possibility of measuring the moisture content of the upper layers of the atmosphere using radiometric techniques p 70 A83-14308
KLENK, K. F.
An optimum statistical technique for ozone profile retrieval from backscattered UV radiances p 21 A83-14632
KLOOSTER, A., JR.
Evaluation of ERIM optically processed SEASAT SAR data
[E83-10037] p 63 N83-13531
KNIFFEN, S.
Evaluation of the potential of one to three SEASAT-SMMR channels in retrieving sea surface temperature
[NASA-CR-169660] p 48 N83-14604
KOCH, C. D.
Statistical Techniques Applied to Aerial Radiometric Surveys (STARRS): Discriminant-analysis methods applied to aerial radiometric data and their application to uranium favorability in South Texas. Nation uranium resource evaluation
[DE82-020961] p 34 N83-12512

KOELLE, D. E.
Spacelab, space platforms and the future; Proceedings of the Fourth Joint AAS/DGLR Symposium and Twentieth Goddard Memorial Symposium, Washington, DC, March 17-19, 1982 p 73 A83-11926
KOENIG, B. A.
Low- to moderate-temperature geothermal resource assessment for Nevada: Area specific studies, Pumpernickel Valley, Carlin and Moana
[DE82-018598] p 34 N83-12584
KOLM, K. E.
Evaluating the effectiveness of Landsat data as a tool for locating buried pre-glacial valleys in eastern South Dakota p 33 A83-14667
KOLOUCH, D.
The digital image processing system MOBI-DIVAH p 59 A83-14944
KONDRATEV, K. IA.
Remote determination of humus content in soils p 7 A83-15889
KONECNY, G.
Investigations of interpretability of images by different sensors and platforms for small scale mapping p 70 A83-14943
KONG, J. A.
Remote sensing of dielectric media with periodic rough surfaces p 1 A83-10106
A simple relation between active and passive microwave remote sensing measurements of earth terrain p 24 A83-14857
KOOPMANS, B. N.
Some comparative aspects of SLAR and airphoto images for geomorphologic and geologic interpretation p 33 A83-17842
KOREN, U.
Low threshold InGaAsP/InP lasers with microcleaved mirrors suitable for monolithic integration p 24 A83-10981
KORNILOV, N. A.
Investigations of the Arctic, the Antarctic and the world ocean; Conference-Seminar, Moscow, USSR, February 9-13, 1981, Reports p 39 A83-10826
KOUYATE, F.
A backscatter model for a randomly perturbed periodic surface p 1 A83-10107
A backscatter model for a randomly perturbed periodic surface p 7 A83-14859
KOVSHOV, V. A.
The permanently sparse areas of ice cover in the open regions of the Okhtsk Sea p 42 A83-15058
KRAIMAN, H.
Technology needs assessment of an atmospheric observation system for multidisciplinary air quality/meteorology missions, part 2
[NASA-CR-3557] p 21 N83-10646
KRIEGER, H.
Crop-phenology and LANDSAT-based irrigated lands inventory in the high plains
[E83-10115] p 18 N83-15758
KRIKORIAN, E.
Technical issues in focal plane development; Proceedings of the Meeting, Washington, DC, April 21, 22, 1981 p 69 A83-13726
KRITIKOS, H.
Technology needs assessment of an atmospheric observation system for tropospheric research missions, part 1
[NASA-CR-3556] p 21 N83-10645
KROHN, M. D.
Seasat L-band radar response to forest vegetation in *eastern Virginia* p 1 A83-10061
KRON, A.
Tectonics of west central Mexico and adjacent Arizona: A remote sensing and field study in arid and semi-arid areas
[DE82-002393] p 37 N83-14797
KROWITZ, L.
Technology needs assessment of an atmospheric observation system for multidisciplinary air quality/meteorology missions, part 2
[NASA-CR-3557] p 21 N83-10646
KUKLA, G.
Accuracy of operational snow and ice charts p 50 A83-10090
KUNZI, K. F.
Snow-cover parameters retrieved from Nimbus-7 scanning multichannel microwave radiometer /SMMR/ data p 51 A83-14854
KUX, H. J. H.
Automatic interpretation of MSS-LANDSAT data applied to coal refuse site studies in southern Santa Catarina State, Brazil
[E83-10066] p 35 N83-14575
KUZNETSOV, I. V.
Investigations of the apparent temperature of snow cover in the submillimeter wavelength region p 52 A83-15816

L

LABOVITZ, M. L.
An evaluation of the NASA/GSFC Barnes field spectral reflecometer model 14-758, using signal/noise as a measure of utility
[NASA-TM-83969] p 71 N83-12396
LABRECQUE, J. L.
The intermediate wavelength magnetic anomaly field of *the north Pacific and possible source distributions*
[E83-10088] p 27 N83-14596
LAN, F. KH.
Concerning a method for the determination of initial geodetic data p 24 A83-17679
LANDGREBE, D. A.
A means for utilizing ancillary information in multispectral classification p 60 A83-16905
LANGFORD, G.
Integration of Landsat imagery into a program for aerial surveying of deer populations in Alberta p 5 A83-14252
LANGLAND, R. A.
SEASAT-A SASS wind processing
[NASA-CR-169433] p 44 N83-10473
LARDEN, D. R.
Preliminary study of GPS orbit determination accuracy achievable from worldwide tracking data
[NASA-CR-169693] p 28 N83-14605
TOPEX orbit determination using GPS signals plus a sidetone ranging system
[NASA-CR-169694] p 29 N83-14606
LARGE, P.
Application of Landsat imagery to natural resources management in Sierra Leone, West Africa p 57 A83-14247
LASCANO, R.
Investigation of remote sensing techniques of measuring soil moisture
[E83-10048] p 12 N83-14557
LAUER, D. T.
LANDSAT 4 investigations of thematic mapper and multispectral scanner applications
[E83-10121] p 66 N83-15791
LAULETTA, A. M.
MSS D Multispectral Scanner System
[E83-10128] p 72 N83-15797
LAWRENCE, G.
Remote sensing and waste management p 20 A83-14263
LAWSON, C. L.
C-1 surface interpolation for scattered data on a sphere p 65 N83-15762
LAZAREWICZ, A. R.
Investigating tectonic and bathymetric features of the Indian Ocean using MAGSAT magnetic anomaly data
[E83-10095] p 28 N83-14602
LEBERL, F. W.
The applicability of satellite remote sensing to small and medium scale mapping p 64 N83-14618
LECKIE, D. G.
Assessment of spruce budworm defoliation using digital airborne MSS data p 5 A83-14248
LEDUC, S.
Evaluation of the Williams-type spring wheat model in North Dakota and Minnesota
[E83-10041] p 12 N83-13535
Crop weather models of corn and soybeans for Agrophysical Units (APU's) in Iowa using monthly meteorological predictors
[E83-10054] p 13 N83-14563
Comparison of the CEAS and Williams-type barley yield models for North Dakota and Minnesota
[E83-10056] p 13 N83-14565
Crop weather models of barley and spring wheat yield for agrophysical units in North Dakota
[E83-10059] p 14 N83-14568
LEE, D. C. L.
Estimation of the sugar cane cultivated area from LANDSAT images using the two phase sampling method
[E83-10077] p 15 N83-14586
LEGAL, L. R.
The use of satellite information in weather forecasting at the Pacific Weather Centre p 20 A83-14277
LEGECKIS, R.
On the circulation of the western Gulf of Mexico - A satellite view p 39 A83-10113
LENNERTZ, D.
The European Space Agency's Earth observation satellite programs in the 1980's p 75 N83-14610
LENNINGTON, R. K.
Probabilistic cluster labeling of imagery data p 54 A83-11410
LEONHART, L. S.
Analyzing and mapping regional land use trends by combining Landsat and topographic data p 2 A83-10119
LESCURE, W. J., III
Naval Research Reviews, volume 34, no. 1
[AD-A117981] p 45 N83-12037
LEVY, G.
Satellite remote sensing for developing countries
[ESA-SP-175] p 75 N83-14608
LEVY, L.
Global implications of space activities; Proceedings of the Conference, Aspen, CO, August 30-September 4, 1981 p 74 A83-17349
LIANG, T.
Remote Sensing Program
[E83-10120] p 18 N83-15790
LICHY, D. E.
A comparison data set for the evaluation of remote sensing systems ability for ocean wave data collection p 38 A83-10071
LIDIAK, E. G.
Crustal and upper mantle structure data analysis
[E83-10038] p 26 N83-13532
LIKENS, W.
LANDSAT land cover analysis completed for CIRSS/San Bernardino County project
[E83-10024] p 22 N83-12507
LITVINENKO, K. I.
Cosmogeological structures of the Hissar Alai and their role in the distribution of endogenous mineralization p 31 A83-11959
LODWICK, G. D.
A position-based resource mapping study of the Kananaskis Valley using Landsat p 19 A83-14232
LOHMANN, P.
The digital image processing system MOBI-DIVAH p 59 A83-14944
LOMBARDO, M. A.
Method of interpretation of remotely sensed data and applications to land use
[E83-10072] p 23 N83-14581
LONGDON, N.
Satellite remote sensing for developing countries
[ESA-SP-175] p 75 N83-14608
LUCCHITTA, B. K.
The geology of Europa p 24 A83-16239
LUGINA, K. M.
Using new methods in monitoring the thermal regime of the Arctic p 39 A83-10828
LYNHAM, T.
Multitemporal analysis of Landsat data for forest cutover mapping - A trial of two procedures p 5 A83-14254
LYZENGA, D. R.
Evaluation of ERIM optically processed SEASAT SAR data
[E83-10037] p 63 N83-13531

M

MACDONALD, H. C.
Wetland mapping with imaging radar p 50 A83-10072
Geological terrain models p 31 A83-10080
Analysis of geologic terrain models for determination of optimum SAR sensor configuration and optimum information extraction for exploration of global non-renewable resources. Pilot study: Arkansas Remote Sensing Laboratory, part 1, part 2, and part 3
[E83-10061] p 35 N83-14570
MACDONALD, R. B.
Monitoring global vegetation
[E83-10044] p 12 N83-14554
MACFARLANE, R. J.
Waterfowl habitat inventory of Alberta, Saskatchewan and Manitoba by remote sensing p 4 A83-14244
MACK, A. R.
A procedure to overlay thematic map and dominion land survey system data to geometrically-corrected Landsat images and its application to agricultural land use studies in western Canada p 3 A83-14231
MAES, J.
Multitemporal soil and vegetation observations by METEOSAT over Central Africa p 15 N83-14619
MAGNESS, E. R.
Development of a corn and soybean labeling procedure for use with profile parameter classification
[E83-10014] p 9 N83-12493
MAHONEY, W. C.
Defense Mapping Agency /DMA/ overview of mapping, charting, and geodesy /MC&G/ applications of digital image pattern recognition p 24 A83-12877

MAKHONKO, E.
Instruments and methods for monitoring background soil pollution p 22 N83-12650
MALAKHOV, S.
Instruments and methods for monitoring background soil pollution p 22 N83-12650
MALLICK, D. I. J.
Remote sensing of the granites of Southeast Asia p 37 N83-14629
MALYSHEV, V. V.
Operational planning of the process of earth survey by satellites p 70 A83-14314
MARACCHI, G. P.
Agroecological classification by remote sensing techniques p 23 N83-14622
MARELLI, L.
Earthnet prepares for Landsat-D p 74 A83-17426
MARESCA, J. W., JR.
Estimating wind speed from HF skywave radar sea backscatter p 40 A83-11352
MARGALIT, S.
Low threshold InGaAsP/InP lasers with microcleaved mirrors suitable for monolithic integration p 24 A83-10981
MARKHAM, B. L.
Spectral characterization of the LANDSAT-D multispectral scanner subsystems
[E83-10107] p 17 N83-15750
MARKS, J.
Evaluation of ERIM optically processed SEASAT SAR data
[E83-10037] p 63 N83-13531
MARTIN, F. C., JR.
Predicting forest land attributes from aerial photo interpretation variables p 5 A83-14259
MARTIN, M. V.
Evaluation of small area crop estimation techniques using LANDSAT- and ground-derived data
[E83-10008] p 8 N83-12487
MARTIN, S.
Comparison of environmental conditions in the Bering Sea and Davis Strait and the effects on microwave signature returns; March and April, 1979
[NASA-CR-169473] p 46 N83-12828
The Bering Sea ice cover during March 1979: Comparison of surface and satellite data with the Nimbus-7 SMMR
[NASA-CR-169393] p 47 N83-13572
MARTINKO, E. A.
The application of remote sensing to resource management and environmental quality programs in Kansas
[E83-10114] p 23 N83-15757
Crop-phenology and LANDSAT-based irrigated lands inventory in the high plains
[E83-10115] p 18 N83-15758
MARTSOLF, J. D.
Use of thermal inertia determined by HCMM to predict nocturnal cold prone areas in Florida
[E83-10028] p 62 N83-13522
Use of thermal inertia determined by HCMM to predict nocturnal cold prone areas in Florida
[E83-10102] p 64 N83-15745
MASCARENHAS, N. D. D.
Comparison of diverse methods for the correction of atmospheric effects on LANDSAT and SKYLAB images
[E83-10079] p 72 N83-14588
MASUKO, H.
Application of the airborne microwave rain-scattered/radiometer system to the remote sensing of rains and wind vector measurements over the ocean p 70 A83-14293
MASURSKY, H.
Shuttle imaging radar experiment p 32 A83-13348
MATEER, C. L.
An optimum statistical technique for ozone profile retrieval from backscattered UV radiances p 21 A83-14632
MAUGHAN, P. M.
Advanced operational earth resources satellite systems
[AAS 82-128] p 73 A83-11932
Future land remote sensing data and services - A commercial perspective
[AAS 82-129] p 73 A83-11933
MAUL, G. A.
Collinear-track altimetry in the Gulf of Mexico from SEASAT: Measurements, models and surface truth
[AD-A118160] p 45 N83-11568
MAW, K.
LANDSAT land cover analysis completed for CIRSS/San Bernardino County project
[E83-10024] p 22 N83-12507
Gates to Gregg high voltage transmission line study
[E83-10097] p 16 N83-15741
MAXIM, L. D.
To mix or match - On choosing matched samples in comparative aerial surveys p 59 A83-14664
MAYBEE, J. D.
Spectroradiometer measurements in support of photovoltaic device testing p 70 A83-15458
MAYHEW, M. A.
MAGSAT anomaly field inversion and interpretation for the US
[E83-10057] p 27 N83-14566
Equivalent source modeling of the main field using MAGSAT data
[E83-10094] p 28 N83-14601
MCCANDLESS, S. W.
Advanced operational earth resources satellite systems
[AAS 82-128] p 73 A83-11932
Analyses of oceanic subsurface features using space based radar imagery
[AD-A118411] p 45 N83-11692
MCCANDLESS, S. W., JR.
The 100 days of Seasat-A p 39 A83-10115
MCCAULEY, J. F.
Subsurface valleys and geoarcheology of the eastern Sahara revealed by Shuttle radar p 32 A83-13349
MCCLAIN, C. R.
On the use of laser profilometry for ocean wave studies p 42 A83-14502
MCCLURE, D. E.
Characterization of a maximum-likelihood nonparametric density estimator of kernel type p 66 N83-15777
MCFARLAND, M. J.
Microwave remote sensing of soil moisture, volume 1
[E83-10108] p 17 N83-15751
MCGUIRE, W. G.
Evaluation of small area crop estimation techniques using LANDSAT- and ground-derived data
[E83-10008] p 8 N83-12487
MCINTOSH, R. E.
Feasibility of mapping ocean surface currents using delta k-microwave radars mounted on geostationary satellite platforms p 39 A83-10094
MCINTYRE, K. S.
Computer program documentation for the pasture/range condition assessment processor
[E83-10100] p 16 N83-15743
MCKAY, M. F.
Earth Observations Division version of the Laboratory for Applications of Remote Sensing System (EOD-LARSYS) user guide for the IBM 370/148. Volume 1: System overview
[E83-10007] p 62 N83-12866
MCKENZIE, R. L.
Applicability of satellite-derived sea-surface temperatures in the Fiji region p 40 A83-12032
MCLAURIN, I.
Water survey of Canada's experience with data acquisition and telemetry systems p 51 A83-14287
MCMURDIE, L. A.
Validation and application of the SEASAT-SMMR geophysical algorithms
[NASA-CR-169390] p 71 N83-13767
MCNUTT, S. L.
Comparison of environmental conditions in the Bering Sea and Davis Strait and the effects on microwave signature returns; March and April, 1979
[NASA-CR-169473] p 46 N83-12828
The Bering Sea ice cover during March 1979: Comparison of surface and satellite data with the Nimbus-7 SMMR
[NASA-CR-169393] p 47 N83-13572
MEADOWS, G. A.
Detection of coastal zone environmental conditions using synthetic aperture radar p 38 A83-10068
Further SEASAT SAR coastal ocean wave analysis
[NASA-CR-169682] p 47 N83-13776
MEITIN, J. G., JR.
FACE-2 data reductions (prior to disclosure of the treatment decisions). Part 5: Satellite-estimated rainfall from a geostationary platform in FACE-2
[PB82-216581] p 52 N83-10730
MENDONCA, F. J.
Estimation of the sugar cane cultivated area from LANDSAT images using the two phase sampling method
[E83-10077] p 15 N83-14586
MENGES, R. M.
Optical parameters of leaves of seven weed species
[E83-10010] p 9 N83-12489
MEROLA, J. A.
Detection of aspen-conifer forest mixes from LANDSAT digital data
[E83-10106] p 17 N83-15749
MESSMORE, J. A.
Terrain analysis procedural guide for drainage and water resources (ETL series on guides for Army terrain analysts)
[AD-A118318] p 52 N83-11569
METZLER, M.
Development, implementation and evaluation of satellite-aided agricultural monitoring systems
[E83-10017] p 10 N83-12500
MEUNIER, J.-F.
Remote sensing software for airborne image analysis p 58 A83-14273
MICHEL, R.
CIRSS vertical data integration, San Bernardino County study phases 1-A, 1-B
[E83-10124] p 67 N83-15794
CIRSS vertical data integration, San Bernardino study
[E83-10127] p 67 N83-15796
MIGLIETTA, F.
Agroecological classification by remote sensing techniques p 23 N83-14622
MILFORD, J. R.
The determination of soil moisture balances in tropical Africa by satellite infrared remote sensing: The atmospheric problem p 53 N83-14621
MILLARD, J. P.
Winter wheat stand density determination and yield estimates from handheld and airborne scanners
[E83-10013] p 9 N83-12492
MILLER, A. W.
HCMM hydrological analysis in Utah
[E83-10026] p 53 N83-13520
MILLER, J. R.
Observations of oceanic surface-wind fields from the Nimbus-7 microwave radiometer p 42 A83-14861
MILLER, T. G.
Computer program documentation for the pasture/range condition assessment processor
[E83-10100] p 16 N83-15743
MILTON, N. M.
Use of reflectance spectra of native plant species for interpreting airborne multispectral scanner data in the East Tintic Mountains, Utah p 30 A83-10060
Seasat L-band radar response to forest vegetation in eastern Virginia p 1 A83-10061
MINTER, T. C.
Probabilistic cluster labeling of imagery data p 54 A83-11410
MISRA, K. S.
Application of Landsat imagery to flood control and management of agricultural land - A case study of northern India p 3 A83-14233
MOESER, W.
Determination of the radiation budget at the Earth's surface from satellite data p 29 N83-14808
MOEZZI, S.
Assessment of radar resolution requirements for soil moisture estimation from simulated satellite imagery
[E83-10020] p 10 N83-12503
MOISEEV, D. V.
Operational planning of the process of earth survey by satellites p 70 A83-14314
MONGET, J. M.
Combined use of daily thermal cycle of METEOSAT imagery and multispectral LANDSAT data: Application to the Bandiagara plateau, Mali p 36 N83-14620
MOORE, D. G.
Evaluating depth to shallow groundwater using heat capacity mapping mission /HCMM/ data p 51 A83-14668
MOORE, R. K.
Microwave remote sensing: Active and passive. Volume 2 - Radar remote sensing and surface scattering and emission theory p 69 A83-14040
MORALEV, V. M.
A method for the quantitative evaluation of the results of space imagery interpretation in prospecting applications p 33 A83-14302
MOREIRA, J. C.
LANDSAT and radar mapping of intrusive rocks in SE-Brazil
[E83-10073] p 36 N83-14582
MORRISON, N. R.
Colour Landsat images and mosaics - Basic tools in areal and ecological differentiation in Canada p 57 A83-14265
MOWATT, T. C.
Critical and strategic minerals in Alaska: Cobalt, the platinum-group metals and chromite
[PB82-193085] p 33 N83-10485
MRAZEK, C. P.
Analyses of oceanic subsurface features using space based radar imagery
[AD-A118411] p 45 N83-11692

MROCZYNSKI, R. P.
Waterfowl habitat inventory of Alberta, Saskatchewan and Manitoba by remote sensing p 4 A83-14244
MUELLER, I. I.
Basic research for the geodynamics program
[NASA-CR-169470] p 26 N83-13537
Effects of adopting new precession, nutation and equinox corrections on the terrestrial reference frame p 26 N83-13538
Geometric adjustment of simultaneous Doppler-derived range differences p 26 N83-13540
MULLIGAN, J. J.
Critical and strategic minerals in Alaska: Cobalt, the platinum-group metals and chromite
[PB82-193085] p 33 N83-10485
MULLIGAN, T. R.
Application of remote sensing techniques in oceanographic studies of the British Columbia Salmon Fishery p 41 A83-14258
MURPHY, J.
A refined destriping procedure for Landsat MSS data products p 58 A83-14281
MURRAY, H.
Influence of environmental factors during seed development and after full-ripeness on pre-harvest sprouting in wheat
[E83-10002] p 7 N83-12482

N

NAGATA, M.
A relational image data base system for remote sensing /LAND DBMS/ p 55 A83-11462
NARAYANAN, V.
Analysis of geologic terrain models for determination of optimum SAR sensor configuration and optimum information extraction for exploration of global non-renewable resources. Pilot study: Arkansas Remote Sensing Laboratory, part 1, part 2, and part 3
[E83-10061] p 35 N83-14570
NAVE, P.
A Digital Photogrammetric System (DPS) for producing Digital Elevation Models (DEM) and orthoplates by means of linear array scanner imagery
[MBB-UA-618/81] p 71 N83-13567
NAZAROV, I. M.
Aircraft and remote measurements of atmospheric transport of pollutants within the global integrated monitoring system p 22 N83-12620
NAZAROV, L.
Instruments and methods for monitoring background soil pollution p 22 N83-12650
NAZIROV, M. G.
Tidal phenomena in Arctic Ocean ice /according to space data/ p 40 A83-10832
Some features of the spatial structure of the Arctic Ocean ice cover in connection with turbulent friction and geostrophic capture of tide waves p 40 A83-10833
NEMETH, J.
The use of R.B.V., colour additive viewer and M.S.S. products in the British Columbia Forest Inventory Depletion Monitoring Program p 4 A83-14246
NERAASEN, T.
Waterfowl habitat inventory of Alberta, Saskatchewan and Manitoba by remote sensing p 4 A83-14244
NESHYBA, S. J.
Effects of mesoscale atmospheric convection cells on the waters of the East China Sea p 41 A83-13270
NESTE, S. L.
Technology needs assessment of an atmospheric observation system for tropospheric research missions, part 1
[NASA-CR-3556] p 21 N83-10645
NETO, G. C.
An automatic agricultural zone classification procedure for crop inventory satellite images
[E83-10065] p 14 N83-14574
NEWITT, L. R.
The reduction, verification and interpretation of MAGSAT magnetic data over Canada
[E83-10091] p 28 N83-14599
The reduction, verification and interpretation of MAGSAT magnetic data over Canada
[E83-10101] p 29 N83-15744
NEWLAND, W.
Gates to Gregg high voltage transmission line study
[E83-10097] p 16 N83-15741
NEWMAN, C. K.
Statistical Techniques Applied to Aerial Radiometric Surveys (STARRS): Discriminant-analysis methods applied to aerial radiometric data and their application to uranium favorability in South Texas. Nation uranium resource evaluation
[DE82-020961] p 34 N83-12512
NEWTON, R. W.
A simple relation between active and passive microwave remote sensing measurements of earth terrain p 24 A83-14857
Investigation of remote sensing techniques of measuring soil moisture
[E83-10048] p 12 N83-14557
Rangeland biomass estimation demonstration
[E83-10113] p 17 N83-15756
NIEBER, J. L.
Investigation of remote sensing techniques of measuring soil moisture
[E83-10048] p 12 N83-14557
NIERO, M.
Method of interpretation of remotely sensed data and applications to land use
[E83-10072] p 23 N83-14581
NIKITIN, S. A.
Salyut-7 from June to August p 74 A83-17775
NISBET, R. M.
Applicability of satellite-derived sea-surface temperatures in the Fiji region p 40 A83-12032
NIXON, P. R.
Methods of editing cloud and atmospheric layer affected pixels from satellite data
[E83-10103] p 64 N83-15746
NORDO, J.
The RAMS collection of meterological and position data in the Norwegian Sea p 49 N83-14845
NUESCH, D.
Development, implementation and evaluation of satellite-aided agricultural monitoring systems
[E83-10017] p 10 N83-12500

O

OHARA, T.
Analysis of the characteristics appearing in LANDSAT multispectral images in the geological structural mapping of the midwestern portion of the Rio Grande do Sul shield
[E83-10126] p 37 N83-15795
OHLHORST, C. W.
Analysis of high altitude remotely sensed data collected in the Nantucket Shoals experiment 4-15 May, 1981
[NASA-TM-84547] p 44 N83-10647
OJIMA, T.
Application of the airborne microwave rain-scattered/radiometer system to the remote sensing of rains and wind vector measurements over the ocean p 70 A83-14293
OKAMOTO, K.
Application of the airborne microwave rain-scattered/radiometer system to the remote sensing of rains and wind vector measurements over the ocean p 70 A83-14293
OLFERT, O.
Aerial survey of crop losses due to grasshoppers /Orthoptera - Acrididae/ in Saskatchewan p 5 A83-14255
OLSSON, L.
Approaches to desertification monitoring in the Sudan p 23 N83-14623
OSULLIVAN, F.
Remote sensing of temperature profiles in the atmosphere p 66 N83-15778
OSWALD, E. T.
Ecological land classification in the Yukon p 20 A83-14250
OTTEN, L. J., III
Airborne atmospheric temperature structure measurements of a Pacific coast marine inversion
[AIAA PAPER 83-0278] p 70 A83-19585

P

PAINE, S. H.
A position-based resource mapping study of the Kananaskis Valley using Landsat p 19 A83-14232
PALA, S.
Operational land cover type mapping in Ontario by Landsat based digital analysis and map production p 19 A83-14230
Landsat-based forest mapping in Ontario north of latitude 52 deg north p 5 A83-14253
A practical automated mapping system p 64 N83-14635
PALFREY, K. M.
Lagrangian drift measurements of sea surface currents and iceberg tracking p 49 N83-14842
PAMPALONI, P.
Agroecological classification by remote sensing techniques p 23 N83-14622
PANDEY, P. C.
Evaluation of the potential of one to three SEASAT-SMMR channels in retrieving sea surface temperature
[NASA-CR-169660] p 48 N83-14604
PARADA, N. D. J.
Use of LANDSAT images to study cerrado vegetation
[E83-10025] p 11 N83-13519
Geological-structural interpretation using products of remote sensing in the region of Carrancas, Minas Gerais, Brazil
[E83-10029] p 34 N83-13523
CNPq/INPE-LANDSAT system report of activities
[E83-10064] p 63 N83-14573
An automatic agricultural zone classification procedure for crop inventory satellite images
[E83-10065] p 14 N83-14574
Automatic interpretation of MSS-LANDSAT data applied to coal refuse site studies in southern Santa Catarina State, Brazil
[E83-10066] p 35 N83-14575
An application of cluster analysis for determining homogeneous subregions: The agroclimatological point of view
[E83-10067] p 14 N83-14576
Vegetation survey in Amazonia using LANDSAT data
[E83-10068] p 14 N83-14577
Spectral discrimination of lithologic facies in the granite of the Pedra Branca Goias using LANDSAT 1 digital imagery
[E83-10069] p 35 N83-14578
Remote sensing techniques for conservation and management of natural vegetation ecosystems
[E83-10070] p 15 N83-14579
Multitemporal and geobotanical approach in the remote detection of Greisenization areas in the Serra da Pedra Branca Granite, Goias State, Brazil
[E83-10071] p 35 N83-14580
Method of interpretation of remotely sensed data and applications to land use
[E83-10072] p 23 N83-14581
LANDSAT and radar mapping of intrusive rocks in SE-Brazil
[E83-10073] p 36 N83-14582
Interpretation of remotely sensed data and its applications in oceanography
[E83-10074] p 48 N83-14583
INPE LANDSAT-D thematic mapper computer compatible tape format specification
[E83-10075] p 63 N83-14584
Evaluation of reforestation using remote sensing techniques
[E83-10076] p 15 N83-14585
Estimation of the sugar cane cultivated area from LANDSAT images using the two phase sampling method
[E83-10077] p 15 N83-14586
The computer treatment of remotely sensed data: An introduction to techniques which have geologic applications
[E83-10078] p 36 N83-14587
Comparison of diverse methods for the correction of atmospheric effects on LANDSAT and SKYLAB images
[E83-10079] p 72 N83-14588
Verification of LANDSAT imagery for morphametric and topological studies of drainage basins in a section of the western plateau of Sao Paulo State: Tiete-Aguapei watershed
[E83-10111] p 54 N83-15754
Analysis of the characteristics appearing in LANDSAT multispectral images in the geological structural mapping of the midwestern portion of the Rio Grande do Sul shield
[E83-10126] p 37 N83-15795
PARADELLA, W. R.
Remote sensing in geology: Current trends and future prospects with satellite data
[INPE-2514-PRE/193] p 33 N83-12509
The computer treatment of remotely sensed data: An introduction to techniques which have geologic applications
[E83-10078] p 36 N83-14587
PARAMONOV, A. I.
The utilization of infrared /IR/ aerial and space observations of Arctic seas in navigation and during the solution of other national-economic problems p 40 A83-10836
PARASHAR, S.
On detection of oil pollution in ice environment p 41 A83-14239
PARKS, A. D.
An upper bound on errors in the mean-of-date/instantaneous Earth-fixed vector transformation induced by interpolated nutation angles
[AD-A119444] p 29 N83-14656

PASCUCCI, R. F.
Determination of the contribution of side-looking airborne radar to structural geologic mapping
[PB82-185042] p 34 N83-12713
PATIL, S.
Snow-cover parameters retrieved from Nimbus-7 scanning multichannel microwave radiometer /SMMR/ data p 51 A83-14854
PATOUREAUX, Y.
Combined use of daily thermal cycle of METEOSAT imagery and multispectral LANDSAT data: Application to the Bandiagara plateau, Mali p 36 N83-14620
PATTERSON, D. A.
Statistical Techniques Applied to Aerial Radiometric Surveys (STARRS): Discriminant-analysis methods applied to aerial radiometric data and their application to uranium favorability in South Texas. Nation uranium resource evaluation
[DE82-020961] p 34 N83-12512
PAVLASEK, S.
Construction of a remotely sensed area sampling frame for Southern Brazil
[E83-10052] p 13 N83-14561
PEARCE, C. M.
Optical characteristics of Alberta rangeland as related to remote sensing p 4 A83-14245
PEARSON, J. E.
Determination of the contribution of side-looking airborne radar to structural geologic mapping
[PB82-185042] p 34 N83-12713
PELS, G. F.
A parametric study of tillage effects on radar backscatter p 2 A83-10108
PEREIRA, A. E. C.
Comparison of diverse methods for the correction of atmospheric effects on LANDSAT and SKYLAB images
[E83-10079] p 72 N83-14588
PERFILEV, IU. S.
A method for the quantitative evaluation of the results of space imagery interpretation in prospecting applications p 33 A83-14302
PETERS, C.
The possible modifications of the Hisse model for pure LANDSAT agricultural data p 10 N83-12497
PETROSSIANTS, M. A.
Main achievements of GARP Atlantic Tropical Experiment (GATE) and its impact on FGGE
p 46 N83-12735
PETROV, N. A.
Monitoring of meteorological elements in a composite program for environmental pollution studies
p 22 N83-12648
PHILIPSON, W. R.
Remote Sensing Program
[E83-10120] p 18 N83-15790
PHILPOT, W. D.
Remote Sensing Program
[E83-10120] p 18 N83-15790
PIERSON, W. J.
The measurement of the synoptic scale wind over the ocean p 47 N83-13773
PIHOS, G. G.
SEASAT-A SASS wind processing
[NASA-CR-169433] p 44 N83-10473
PIKE, T.
Quality assessment of remote-sensing data - The SAR case p 56 A83-13845
PINTER, P. J.
Discrimination of growth and water stress in wheat by various vegetation indices through a clear a turbid atmosphere
[E83-10009] p 8 N83-12488
Adjusting the tasseled cap brightness and greenness factors for atmospheric path radiance and absorption on a pixel by pixel basis
[E83-10053] p 13 N83-14562
PINTER, P. J., JR.
Diurnal patterns of wheat spectral reflectances and their importance in the assessment of canopy parameters from remotely sensed observations
[E83-10050] p 13 N83-14559
PIRKLE, F. L.
Statistical Techniques Applied to Aerial Radiometric Surveys (STARRS): Discriminant-analysis methods applied to aerial radiometric data and their application to uranium favorability in South Texas. Nation uranium resource evaluation
[DE82-020961] p 34 N83-12512
PITTS, D.
Reflectance of a vegetation canopy using the Adding method p 3 A83-12603
POLCYN, F.
Radiance calculations for optimization of sensors designed for remote bathymetry, volume 1
[AD-A117743] p 44 N83-10739
POLOVA, N. K.
Investigations of the apparent temperature of snow cover in the submillimeter wavelength region
p 52 A83-15816
PORACSKY, J.
Crop-phenology and LANDSAT-based irrigated lands inventory in the high plains
[E83-10115] p 18 N83-15758
PORADISH, F. J.
Ka-band passive/active airborne radar
p 68 A83-11239
POTEMRA, T. A.
Investigation of MAGSAT and TRIAD magnetometer data to provide corrective information on high-lattitude external fields
[E83-10093] p 28 N83-14600
PRICE, J. C.
Satellite orbital dynamics and observation strategies in support of agricultural applications p 2 A83-10717
PRICE, K. E.
Relaxation matching applied to aerial images
p 56 A83-12889
PRICE, M.
Vegetation and human impact mapping for the management of the sunshine area, Canadian Rocky Mountains p 20 A83-14242
PRILL, J. C.
Mount St. Helens quick response damage assessment using high-altitude infrared photography
p 19 A83-12672
PRINCZ, G. J.
The CCRS SAR processing system
p 69 A83-14289
PROSCH, T.
The conical scan radiometer p 72 N83-14804
PROUT, N. A.
Landsat for delineation and mapping of saline soils in dryland areas in southern Alberta p 5 A83-14261
PRUITT, J. R.
Mount St. Helens quick response damage assessment using high-altitude infrared photography
p 19 A83-12672
PUNCHAK, A. A.
A comparison data set for the evaluation of remote sensing systems ability for ocean wave data collection
p 38 A83-10071

Q

QUENET, R. V.
The use of R.B.V., colour additive viewer and M.S.S. products in the British Columbia Forest Inventory Depletion Monitoring Program p 4 A83-14246

R

RASCHKE, E.
The Earth Radiation Budget Satellite System (ERBSS) of the United States p 72 N83-14805
RASMUSSEN, K.
Multitemporal analysis of Landsat data for investigations of agricultural land use: Problems and potentials
p 15 N83-14624
RASTOGI, R. G.
MAGSAT for geomagnetic studies over Indian region
[E83-10032] p 26 N83-13526
REDNER, R. A.
The Akaike information criterion and its application to mixture proportion estimation p 62 N83-12498
REGINATO, R. J.
Diurnal patterns of wheat spectral reflectances and their importance in the assessment of canopy parameters from remotely sensed observations
[E83-10050] p 13 N83-14559
REID, S. C.
A parametric study of tillage effects on radar backscatter p 2 A83-10108
REITLINGER, A. S.
A method for the quantitative evaluation of the results of space imagery interpretation in prospecting applications p 33 A83-14302
REMPEL, G.
Renewable resources monitoring needs in Manitoba
p 19 A83-14228
RENCZ, A. N.
Surficial geology mapping from Landsat-Kaminak Lake, N.W.T. p 32 A83-14268
RESHETOV, E. A.
Results of phototriangulation on the basis of space photographs p 60 A83-17299
RICHARDS, J. A.
A means for utilizing ancillary information in multispectral classification p 60 A83-16905
RICHARDSON, A. J.
Reflectance differences between untreated and Mepiquat Chloride-treated, field-grown cotton through a growing season p 7 A83-16909
Optical parameters of leaves of seven weed species
[E83-10010] p 9 N83-12489
Estimating total standing herbaceous biomass production with LANDSAT MSS digital data
[E83-10045] p 12 N83-13536
Comparison of LANDSAT-2 and field spectrometer reflectance signatures of south Texas rangeland plant communities
[E83-10055] p 13 N83-14564
Comparisons among a new soil index and other two- and four-dimensional vegetation indices
[E83-10058] p 14 N83-14567
Methods of editing cloud and atmospheric layer affected pixels from satellite data
[E83-10103] p 64 N83-15746
RINDSTAD, B.
Digital methods for lineament analysis
p 37 N83-14634
RINGROSE, S. M.
Application of Landsat imagery to natural resources management in Sierra Leone, West Africa
p 57 A83-14247
RITCHIE, J. C.
Agricultural Research Service research highlights in *remote sensing for calendar year 1981*
[E83-10051] p 75 N83-14560
ROBERTS, J. L.
Reconnaissance applications of image understanding
p 56 A83-12882
ROBINSON, B.
Performance comparison for Barnes model 12-1000, Exotech model 100, and Ideas Inc. Biometer Mark 2
[E83-10004] p 8 N83-12484
ROBINSON, B. F.
Extension of laboratory-measured soil spectra to field conditions
[E83-10021] p 11 N83-12504
ROBINSON, D.
Accuracy of operational snow and ice charts
p 50 A83-10090
ROBINSON, J. E.
Satellite laser altimeter for measurement of ice sheet topography p 38 A83-10092
RODRIGUEZ, R. R.
Optical parameters of leaves of seven weed species
[E83-10010] p 9 N83-12489
ROND, B.
The GDTA - Remote sensing at the service of users
p 68 A83-11867
ROSE, W. C.
Airborne atmospheric temperature structure measurements of a Pacific coast marine inversion
[AIAA PAPER 83-0278] p 70 A83-19585
ROSEMA, A.
The Group Agromet Monitoring Project (GAMP)
p 23 N83-14615
ROSENFELD, A.
Shape and texture p 65 N83-15769
ROSENTHAL, W. D.
Microwave remote sensing of soil moisture, volume 1
[E83-10108] p 17 N83-15751
ROSS, G. A.
Environmental monitoring of the Athabasca Oil Sands using Landsat data p 31 A83-11988
Environmental monitoring of the Athabasca Oil Sands Region p 19 A83-14238
Landsat for resource evaluation and management in the Alberta foothills p 32 A83-14256
ROSS, W. A.
Environmental monitoring of the Athabasca Oil Sands using Landsat data p 31 A83-11988
Environmental monitoring of the Athabasca Oil Sands Region p 19 A83-14238
ROTT, H.
Snow-cover parameters retrieved from Nimbus-7 scanning multichannel microwave radiometer /SMMR/ data p 51 A83-14854
ROWAN, L. C.
Mineral identification from orbit - Initial results from the Shuttle multispectral infrared radiometer
p 32 A83-13350
ROWLAND, J. R.
A tutorial assessment of atmospheric height uncertainties for high-precision satellite altimeter missions to monitor ocean currents p 42 A83-14851
RUBEC, C. D. A.
Colour Landsat images and mosaics - Basic tools in areal and ecological differentiation in Canada
p 57 A83-14265
RUGGLES, K. W.
Technology and future ground processing systems
p 56 A83-12678

RYERSON, R. A.
Satellite remote sensing for domestic crop reporting in the United States and Canada - A look to the future p 3 A83-14229
Visual analysis of 1:250,000 Landsat data for forage assessment during the 1980 drought in western Manitoba p 3 A83-14235
Vegetation change detection in an agricultural area - A simple approach for use with geo-data base p 4 A83-14236

S

SAILOR, R. V.
Investigating tectonic and bathymetric features of the Indian Ocean using MAGSAT magnetic anomaly data [E83-10095] p 28 N83-14602
SALOMONSON, V. V.
The early 1981 view of Landsat-D progress p 73 A83-12673
SANDHAM, W. A.
Sky-wave radar sea-state sensing - Effects of ionospheric movement and propagation geometry p 43 A83-17709
SATO, H.
Reference quicklook images for monitor of Landsat image data acquisition p 58 A83-14286
SATTERWHITE, M. B.
Effects of ground cover and leaf area on the spectral reflectance of vegetation-soil target [AD-A119714] p 16 N83-14653
Special reflectance of some plant indicators of saline and nonsaline soils [AD-A119727] p 16 N83-14655
SAUNDERS, R. S.
Shuttle imaging radar experiment p 32 A83-13348
SAVELEV, B. I.
Results of phototriangulation on the basis of space photographs p 60 A83-17299
SAZONOV, N. V.
A system for the complex processing of aerial and space data for agriculture p 6 A83-14301
SCHABER, G. G.
Subsurface valleys and geoarcheology of the eastern Sahara revealed by Shuttle radar p 32 A83-13349
SCHIELDGE, J. P.
Some examples of the utility of HCMM data in geologic remote sensing p 31 A83-10099
SCHMIDT, R.
Waterfowl habitat inventory of Alberta, Saskatchewan and Manitoba by remote sensing p 4 A83-14244
SCHNEIDER, M.
Report on the special program 78 satellite geodesy of the technical university of Munich [ASTRON-GEODAET-ARB-41] p 25 N83-11563
SCHNEIDER, W. H.
An optimum statistical technique for ozone profile retrieval from backscattered UV radiances p 21 A83-14632
SCHNELL, R. C.
Arctic haze and the Arctic gas and aerosol sampling program /AGASP/ [AIAA PAPER 83-0439] p 21 A83-16714
SCHOCH, R.
Remote sensing of renewable natural resources in developing countries for national planning purposes p 76 N83-14616
SCHREIER, H.
Predicting permafrost conditions with infrared sensing techniques p 6 A83-14264
SCHUHR, W.
Investigations of interpretability of images by different sensors and platforms for small scale mapping p 70 A83-14943
SCHUMAKER, L. L.
Fitting surfaces to scattered data p 65 N83-15761
SCOTT, R.
Weather constraints on airborne laser hydrography operations [PB82-189754] p 52 N83-10745
SEELEY-HEUSE, L.
An algorithm to interface Nimbus-7 SMMR data with the AES ice modelling grid for the Beaufort Sea p 41 A83-14284
SEGAL, D.
Seasat L-band radar response to forest vegetation in eastern Virginia p 1 A83-10061
SEINFELD, J. H.
Development of mathematical techniques for the assimilation of remote sensing data into atmospheric models [E83-10062] p 22 N83-14571
SELBY, C.
Predicting permafrost conditions with infrared sensing techniques p 6 A83-14264
SERAPINAS, B. B.
The accuracy of a component analysis in space studies of natural environments p 59 A83-14304
SETTLE, M.
Use of the Space Shuttle for remote sensing research - Recent results and future prospects p 68 A83-13347
SHAFER, B.
Snowmelt runoff modeling in simulation and forecasting modes with the Martinec-Mango model [E83-10063] p 53 N83-14572
SHANMUGAM, K. S.
Analysis of geologic terrain models for determination of optimum SAR sensor configuration and optimum information extraction for exploration of global non-renewable resources. Pilot study: Arkansas Remote Sensing Laboratory, part 1, part 2, and part 3 [E83-10061] p 35 N83-14570
SHAPIRO, L. G.
Structural analysis techniqes for remote sensing p 66 N83-15772
SHAW, E.
Definition and potential of geocoded satellite imagery products p 58 A83-14272
SHAW, G. E.
Evidence for a central Eurasian source area of arctic haze in Alaska p 18 A83-11626
SHEARMAN, E. D. R.
Sky-wave radar sea-state sensing - Effects of ionospheric movement and propagation geometry p 43 A83-17709
SHEN, S. S.
Evaluation of small area crop estimation techniques using LANDSAT- and ground-derived data [E83-10008] p 8 N83-12487
SHEREMET, O. G.
A method for the quantitative evaluation of the results of space imagery interpretation in prospecting applications p 33 A83-14302
SHIELDS, J. A.
A procedure to overlay thematic map and dominion land survey system data to geometrically-corrected Landsat images and its application to agricultural land use studies in western Canada p 3 A83-14231
SHILINA, A.
Instruments and methods for monitoring background soil pollution p 22 N83-12650
SHILTS, W. W.
Surficial geology mapping from Landsat-Kaminak Lake, N.W.T. p 32 A83-14268
SHIMABUKURO, Y. E.
Vegetation survey in Amazonia using LANDSAT data [E83-10068] p 14 N83-14577
Evaluation of reforestation using remote sensing techniques [E83-10076] p 15 N83-14585
Estimation of the sugar cane cultivated area from LANDSAT images using the two phase sampling method [E83-10077] p 15 N83-14586
SHINE, J. A.
An analysis of a relaxation scheme to improve terrain elevation data [AD-A119257] p 27 N83-13550
SHORT, N. M.
The LANDSAT tutorial workbook: Basics of satellite remote sensing [E83-10001] p 74 N83-10458
SHUCHMAN, R.
Evaluation of ERIM optically processed SEASAT SAR data [E83-10037] p 63 N83-13531
SHUCHMAN, R. A.
Detection of coastal zone environmental conditions using synthetic aperture radar p 38 A83-10068
Further SEASAT SAR coastal ocean wave analysis [NASA-CR-169682] p 47 N83-13776
SHVETSOV, A. A.
Investigations of the apparent temperature of snow cover in the submillimeter wavelength region p 52 A83-15816
SIDDOWAY, F. H.
Winter wheat stand density determination and yield estimates from handheld and airborne scanners [E83-10013] p 9 N83-12492
SIEBER, A.
Ongoing microwave remote sensing-activities for land applications in Germany p 18 A83-10083
SIEBER, A. J.
A backscatter model for a randomly perturbed periodic surface p 7 A83-14859
SIELKEN, R. L., JR.
Missing observations in multiyear rotation sampling designs [E83-10022] p 11 N83-12505
SIGMAN, R. S.
Satellite remote sensing for domestic crop reporting in the United States and Canada - A look to the future p 3 A83-14229
SIMARD, R.
Results of stereoscopic image simulations for the SPOT HRV carried out at the Gun Lake site in British Columbia p 20 A83-14292
SINGHROY, V.
Bank erosion and flood plain studies of the Annapolis River - An application of remote sensing data p 51 A83-14262
Measurements of the characteristic reflectance spectra of surficial deposits p 32 A83-14266
SINIURIN, IU. N.
The permanently sparse areas of ice cover in the open regions of the Okhtsk Sea p 42 A83-15058
SINNOTT, D.
LANDSAT land cover analysis completed for CIRSS/San Bernardino County project [E83-10024] p 22 N83-12507
Gates to Gregg high voltage transmission line study [E83-10097] p 16 N83-15741
SLATER, P. M.
Discrimination of growth and water stress in wheat by various vegetation indices through a clear a turbid atmosphere [E83-10009] p 8 N83-12488
SLATER, P. N.
Atmospheric effects on radiation reflected from soil and vegetation as measured by orbital sensors using various scanning directions p 3 A83-12315
Adjusting the tasseled cap brightness and greenness factors for atmospheric path radiance and absorption on a pixel by pixel basis [E83-10053] p 13 N83-14562
SMIL, V.
Land use/land cover mapping from enhanced Landsat imagery of the eastern provinces of the People's Republic of China p 4 A83-14241
SMIRNOVA, I. P.
Using new methods in monitoring the thermal regime of the Arctic p 39 A83-10828
SMITH, A. F.
Determination of the contribution of side-looking airborne radar to structural geologic mapping [PB82-185042] p 34 N83-12713
SMITH, J. A.
Reflectance of a vegetation canopy using the Adding method p 3 A83-12603
SMITH, S. A.
Analysis of geologic terrain models for determination of optimum SAR sensor configuration and optimum information extraction for exploration of global non-renewable resources. Pilot study: Arkansas Remote Sensing Laboratory, part 1, part 2, and part 3 [E83-10061] p 35 N83-14570
SMITH, S. L., III
Evaluation of geodetic products produced by the NSWC reduction of SEASAT radar altimeter data [AD-A117837] p 25 N83-11571
SNELLEN, J.
On detection of oil pollution in ice environment p 41 A83-14239
SNYDER, J. P.
Geometry of a mapping satellite p 67 A83-10716
SODERBLOM, L. A.
The geology of Europa p 24 A83-16239
SOMMER, M.
Multistage land use mapping and change monitoring in Sri Lanka p 15 N83-14625
SOMMER, S. E.
The role of geological surfaces in determining visible-near infra red spectral signatures p 30 A83-10058
SOMMERFELDT, T. G.
Landsat for delineation and mapping of saline soils in dryland areas in southern Alberta p 5 A83-14261
SPENCER, J. P.
Evaluation of photographic enhancements of Landsat imagery p 55 A83-12035
SPERANSKAIA, N. A.
Using new methods in monitoring the thermal regime of the Arctic p 39 A83-10828
STABLEIN, N. K.
Statistical Techniques Applied to Aerial Radiometric Surveys (STARRS): Discriminant-analysis methods *applied to aerial radiometric data and their application to* uranium favorability in South Texas. Nation uranium resource evaluation [DE82-020961] p 34 N83-12512
STAENZ, K.
Optical characteristics of Alberta rangeland as related to remote sensing p 4 A83-14245

STAPLETON, G.
On detection of oil pollution in ice environment p 41 A83-14239
STEFFENSON, R.
A procedure to overlay thematic map and dominion land survey system data to geometrically-corrected Landsat images and its application to agricultural land use studies in western Canada p 3 A83-14231
STEPHENS, E. A.
Satellite remote sensing in mineral exploration in developing countries p 36 N83-14627
STEPHENS, P. L.
SEASAT-A SASS wind processing
[NASA-CR-169433] p 44 N83-10473
STERN, M.
Approaches to desertification monitoring in the Sudan p 23 N83-14623
STILES, J. A.
Analysis of geologic terrain models for determination of optimum SAR sensor configuration and optimum information extraction for exploration of global non-renewable resources. Pilot study: Arkansas Remote Sensing Laboratory, part 1, part 2, and part 3
[E83-10061] p 35 N83-14570
STILES, W. H.
Radar spectral observations of snow p 49 A83-10064
STILL, J. C.
Critical and strategic minerals in Alaska: Cobalt, the platinum-group metals and chromite
[PB82-193085] p 33 N83-10485
STONER, E. R.
Soil spectral characterization p 2 A83-10118
Extension of laboratory-measured soil spectra to field conditions
[E83-10021] p 11 N83-12504
STRAHLR, A. H.
Monitoring global vegetation
[E83-10044] p 12 N83-14554
SUBBOTIN, V. V.
Using new methods in monitoring the thermal regime of the Arctic p 39 A83-10828
SUGIURA, M.
Investigation of MAGSAT and TRIAD magnetometer data to provide corrective information on high-lattitude external fields
[E83-10093] p 28 N83-14600
SUKHININ, A. I.
Determination of forest fire spread rates from infrared photographs p 6 A83-14307
SULLIVAN, K. D.
Radar and infrared remote sensing of geothermal features at Pilgrim Springs, Alaska p 31 A83-12036
SWAIN, P. H.
Estimation of context for statistical classification of multispectral image data p 59 A83-14853
A means for utilizing ancillary information in multispectral classification p 60 A83-16905
Contextual classification of multispectral image data: An unbiased estimator for the context distribution
[E83-10087] p 63 N83-14595
SWIFT, R. N.
Experimental feasibility of the airborne measurement of absolute oil fluorescence spectral conversion efficiency p 44 A83-18581
SZABO, L.
Cartographic aspects of dual-frequency dual-polarization SAR imagery p 58 A83-14280

T

TAIZET, M.
SPOT in the 1980's p 76 N83-14611
TAMEZ, S.
Optical parameters of leaves of seven weed species
[E83-10010] p 9 N83-12489
TANAKA, K.
Interpretation of remotely sensed data and its applications in oceanography
[E83-10074] p 48 N83-14583
TANIS, F. J.
Radiance calculations for optimization of sensors designed for remote bathymetry, volume 1
[AD-A117743] p 44 N83-10739
TARANIK, J. V.
Use of the Space Shuttle for remote sensing research - Recent results and future prospects p 68 A83-13347
OSTA-1 - Shuttle's first scientific and applications payload p 73 A83-13715
TAYLOR, R.
Nimbus 6 Random Access Measurement System applications experiments
[NASA-SP-457] p 48 N83-14835
TEILLET, P. M.
Remote sensing software for airborne image analysis p 58 A83-14273
THEIS, S. W.
Microwave remote sensing of soil moisture, volume 1
[E83-10108] p 17 N83-15751
THEODORIDIS, S.
Sky-wave radar sea-state sensing - Effects of ionospheric movement and propagation geometry p 43 A83-17709
THIE, J.
The importance of remote sensing for Canada - Past achievements, future needs p 74 A83-14227
THOMAS, R. H.
Ice-sheet dynamics by satellite laser altimetry p 38 A83-10093
THOMAS, V. L.
Standardization of computer compatible tape formats for remote sensing data p 54 A83-10075
THOMPSON, D. R.
The use of large-area spectral data in wheat yield estimation p 7 A83-16910
Development of thematic mapper vegetative indices for assessing biomass in corn, soybeans and wheat
[E83-10035] p 11 N83-13529
THOMPSON, J. D.
Collinear-track altimetry in the Gulf of Mexico from SEASAT: Measurements, models and surface truth
[AD-A118160] p 45 N83-11568
THOMPSON, L. L.
Technical issues in focal plane development for terrestrial resource observations p 69 A83-13735
THOMPSON, M. D.
Landsat for delineation and mapping of saline soils in dryland areas in southern Alberta p 5 A83-14261
THOMSON, K. P. B.
Toward an operational, satellite-based, wetland monitoring program for the Fraser River Estuary, British Columbia p 51 A83-14234
Optical characteristics of Alberta rangeland as related to remote sensing p 4 A83-14245
Conference on Using Next Generation Earth Observation Satellites: Summary handbook p 62 N83-12508
THORNBURY, G.
Gates to Gregg high voltage transmission line study
[E83-10097] p 16 N83-15741
TILTON, J. C.
Estimation of context for statistical classification of multispectral image data p 59 A83-14853
Contextual classification of multispectral image data: An unbiased estimator for the context distribution
[E83-10087] p 63 N83-14595
TIURI, M.
Microwave emission signatures of snow in Finland p 50 A83-10065
TOLSTIKOV, E. I.
Investigations of the Arctic, the Antarctic and the world ocean; Conference-Seminar, Moscow, USSR, February 9-13, 1981, Reports p 39 A83-10826
TOMLINS, G. F.
Toward an operational, satellite-based, wetland monitoring program for the Fraser River Estuary, British Columbia p 51 A83-14234
TORR, D. G.
Spectroscopic imaging of the thermosphere from the Space Shuttle p 68 A83-12605
TORR, M. R.
Spectroscopic imaging of the thermosphere from the Space Shuttle p 68 A83-12605
TORSANI, J. A.
A study of atmospheric diffusion from the Landsat imagery p 20 A83-14504
TORSHIN, V. I.
A system for the complex processing of aerial and space data for agriculture p 6 A83-14301
TOU, J. T.
Automatic photointerpretation via texture and morphology analysis p 65 N83-15770
TOUTANT, C.
Comparison study of future SPOT and Landsat-D satellite products from a simulation flight p 57 A83-14243
TOWNSHEND, J.
A comparison of unsupervised classification procedures on Landsat MSS data for an area of complex surface conditions in Basilicata, Southern Italy p 55 A83-12037
TREXLER, D. T.
Low- to moderate-temperature geothermal resource assessment for Nevada: Area specific studies, Pumpernickel Valley, Carlin and Moana
[DE82-018598] p 34 N83-12584
TRIVEDI, M. M.
A multispectral approach to remote detection of deer p 6 A83-14666
TROFIMOVA, V. G.
Some features of the spatial structure of the Arctic Ocean ice cover in connection with turbulent friction and geostrophic capture of tide waves p 40 A83-10833
TRUAX, D.
Application of remote sensing techniques in oceanographic studies of the British Columbia Salmon Fishery p 41 A83-14258
TRUMP, C. L.
Effects of mesoscale atmospheric convection cells on the waters of the East China Sea p 41 A83-13270
TSAI, B. M.
Remote sensing of sea state using laser altimeters p 40 A83-12316
TSANG, L.
A simple relation between active and passive microwave remote sensing measurements of earth terrain p 24 A83-14857
Investigation of remote sensing techniques of measuring soil moisture
[E83-10048] p 12 N83-14557
TSENG, Y.
Further SEASAT SAR coastal ocean wave analysis
[NASA-CR-169682] p 47 N83-13776
TSUCHIYA, K.
Some effects on the GCP success rate p 58 A83-14285
TUCKER, A. J.
Operation and maintenance of geodetic satellite observatory, McMurdo, Antarctica
[PB82-187923] p 25 N83-12107
TURNER, B. J.
Development of a data management front end for use with a LANDSAT based information system
[E83-10104] p 17 N83-15747
TURNER, D. L.
Radar and infrared remote sensing of geothermal features at Pilgrim Springs, Alaska p 31 A83-12036

U

ULABY, F. T.
Radar spectral observations of snow p 49 A83-10064
A backscatter model for a randomly perturbed periodic surface p 1 A83-10107
Microwave remote sensing: Active and passive. Volume 2 - Radar remote sensing and surface scattering and emission theory p 69 A83-14040
Effects of vegetation cover on the radar sensitivity to soil moisture p 6 A83-14856
A backscatter model for a randomly perturbed periodic surface p 7 A83-14859
Radar signatures of terrain - Useful monitors of renewable resources p 21 A83-17248
A three-part geometric model to predict the radar backscatter from wheat, corn, and sorghum
[E83-10005] p 8 N83-12485
Data documentation for the 1981 summer vegetation experiment
[E83-10016] p 10 N83-12499
Assessment of radar resolution requirements for soil moisture estimation from simulated satellite imagery
[E83-10020] p 10 N83-12503
ULBRICHT, K. A.
Image processing of remotely sensed phenomena p 61 N83-11400

V

VALENDIK, E. N.
Determination of forest fire spread rates from infrared photographs p 6 A83-14307
VALERIANO, D. D. M.
Automatic interpretation of MSS-LANDSAT data applied to coal refuse site studies in southern Santa Catarina State, Brazil
[E83-10066] p 35 N83-14575
VAN DER PIEPEN, H.
OSTA-1/Ocean Color Experiment
[AIAA PAPER 83-0415] p 42 A83-16701
VAN RYSWYK, A. L.
Remote sensing applications for British Columbia wetlands using 35 mm aerial photography p 51 A83-14251
VANBAVEL, C. H. M.
Investigation of remote sensing techniques of measuring soil moisture
[E83-10048] p 12 N83-14557
VANBEEK, G. J.
The reduction, verification and interpretation of MAGSAT magnetic data over Canada
[E83-10091] p 28 N83-14599

The reduction, verification and interpretation of MAGSAT magnetic data over Canada
[E83-10101] p 29 N83-15744
VANDERBILT, V. C.
Application of computer axial tomography /CAT/ to measuring crop canopy geometry p 1 A83-10096
VARDEMAN, S. B.
Estimation of context for statistical classification of multispectral image data p 59 A83-14853
Contextual classification of multispectral image data: An unbiased estimator for the context distribution
[E83-10087] p 63 N83-14595
VAVAEV, V. A.
Automation of the search for and recognition of reference zones for precise coordinate control of space imagery p 59 A83-14311
VELASCO, F. R. D.
An automatic agricultural zone classification procedure for crop inventory satellite images
[E83-10065] p 14 N83-14574
VENEZIANI, P.
Geological-structural interpretation using products of remote sensing in the region of Carrancas, Minas Gerais, Brazil
[E83-10029] p 34 N83-13523
LANDSAT and radar mapping of intrusive rocks in SE-Brazil
[E83-10073] p 36 N83-14582
VERDESIO, J. J.
Remote sensing techniques for conservation and management of natural vegetation ecosystems
[E83-10070] p 15 N83-14579
Interpretation of remotely sensed data and its applications in oceanography
[E83-10074] p 48 N83-14583
VERNEKAR, A. D.
Spatial and temporal variations of large-scale subsidence and convection regions derived from satellite data
[PB82-219817] p 71 N83-13750
VIEZEE, W.
Automated measurements of atmospheric visibility
[AIAA PAPER 83-0436] p 21 A83-16713
VILCHINSKII, M.
Lineaments and ring structures on the territory of Poland p 24 A83-14303
VINOGRADOV, B. V.
Remote measurement of biomass p 6 A83-14306
VIRCHENKO, E.
Instruments and methods for monitoring background soil pollution p 22 N83-12650
VISWANADHAM, Y.
A study of atmospheric diffusion from the Landsat imagery p 20 A83-14504
VITORELLO, I.
Remote sensing in geology: Current trends and future prospects with satellite data
[INPE-2514-PRE/193] p 33 N83-12509
The computer treatment of remotely sensed data: An introduction to techniques which have geologic applications
[E83-10078] p 36 N83-14587
VONFRESE, R. R. B.
Gravity and magnetic anomaly data analysis
[E83-10031] p 26 N83-13525
VOUTE, C.
Satellite remote sensing for developing countries: Prospects and constraints p 76 N83-14631
VUKOVICH, F. M.
A comparison of HCMM surface temperatures with in situ temperature data
[E83-10040] p 46 N83-13534
A comparison of surfaces temperatures from HCMM infrared data with field measurements
[E83-10046] p 47 N83-14555
VUKOVICH, F. V.
Western Boundary Eddies of the Gulf Stream p 49 N83-14847

W

WAGONER, J. L.
Aerial geologic log from Livermore, California to the Nevada Test Site, Nye County, Nevada
[DE82-018392] p 25 N83-10693
WAITE, W. P.
Wetland mapping with imaging radar p 50 A83-10072
Geological terrain models p 31 A83-10080
Measurement of soil moisture using remote sensing multisensor radiation techniques
[E83-10012] p 9 N83-12491
Analysis of geologic terrain models for determination of optimum SAR sensor configuration and optimum information extraction for exploration of global non-renewable resources. Pilot study: Arkansas Remote Sensing Laboratory, part 1, part 2, and part 3
[E83-10061] p 35 N83-14570
WALKER, J. K.
The reduction, verification and interpretation of MAGSAT magnetic data over Canada
[E83-10091] p 28 N83-14599
The reduction, verification and interpretation of MAGSAT magnetic data over Canada
[E83-10101] p 29 N83-15744
WALTER, H.
Optical parameters of leaves of seven weed species
[E83-10010] p 9 N83-12489
WALTON, W. T.
Aircraft and satellite measurement of ocean wave directional spectra using scanning-beam microwave radars
[NASA-TM-84008] p 47 N83-13544
WARD, N. R.
The determination of soil moisture balances in tropical Africa by satellite infrared remote sensing: The atmospheric problem p 53 N83-14621
WATERMAN, S. E.
An algorithm to interface Nimbus-7 SMMR data with the AES ice modelling grid for the Beaufort Sea p 41 A83-14284
WATSON, E. K.
Remote sensing applications for British Columbia wetlands using 35 mm aerial photography p 51 A83-14251
WEHDE, M.
Aerial thermal infrared census of Canada geese in South Dakota p 6 A83-14665
WEISMILLER, R. A.
Extension of laboratory-measured soil spectra to field conditions
[E83-10021] p 11 N83-12504
WEISSMAN, D. E.
Measurements of ocean surface spectrum from an aircraft using the two-frequency microwave resonance technique p 43 A83-17710
WESELAKE, S.-A.
Canadian Symposium on Remote Sensing, 7th, Winnipeg, Canada, September 8-11, 1981, Proceedings p 73 A83-14226
WEST, G. B.
Mean Earth ellipsoid determined from SEASAT altimeter observations
[AD-A117910] p 45 N83-11570
WESTIN, F. C.
Combining land use data acquired from Landsat with soil map data p 2 A83-10117
WHITE, C.
The European Community, development and satellite technology p 75 N83-14609
WHITE, D. B.
Operational land cover type mapping in Ontario by Landsat based digital analysis and map production p 19 A83-14230
WHITE, G. C.
The accuracy of Seasat-1 altimeter altitude measurments under various sea state conditions
[RAE-TR-82059] p 47 N83-14553
WIEGAND, C. L.
Estimating total standing herbaceous biomass production with LANDSAT MSS digital data
[E83-10045] p 12 N83-13536
Comparisons among a new soil index and other two- and four-dimensional vegetation indices
[E83-10058] p 14 N83-14567
Methods of editing cloud and atmospheric layer affected pixels from satellite data
[E83-10103] p 64 N83-15746
WIESEL, W. J.
Pass point determination and geometrical precision of the relative rectification of scanner data
[SER-C-268] p 62 N83-13518
WIGHTMAN, J. F.
Bank erosion and flood plain studies of the Annapolis River - An application of remote sensing data p 51 A83-14262
WIKEN, E. B.
Colour Landsat images and mosaics - Basic tools in areal and ecological differentiation in Canada p 57 A83-14265
WILHEIT, T. T., JR.
Observations of oceanic surface-wind fields from the Nimbus-7 microwave radiometer p 42 A83-14861
WILKINSON, G. G.
The determination of soil moisture balances in tropical Africa by satellite infrared remote sensing: The atmospheric problem p 53 N83-14621
WINQUEST, E.
The application of remote sensing in southern Alberta's mountain pine beetle management p 5 A83-14257
WON, I. J.
MAGSAT and aeromagnetic data of the continental US
[E83-10033] p 26 N83-13527
WOOD, B. J.
Technology and future ground processing systems p 56 A83-12678
WOOD, G. M.
Remote sensing and waste management p 20 A83-14263
WOODLEY, W. L.
FACE-2 data reductions (prior to disclosure of the treatment decisions). *Part 5: Satellite-estimated rainfall* from a geostationary platform in FACE-2
[PB82-216581] p 52 N83-10730
WORSFOLD, R.
On detection of oil pollution in ice environment p 41 A83-14239
WU, J.
Investigations of interpretability of images by different sensors and platforms for small scale mapping p 70 A83-14943
WUKELIC, G. W.
Analyzing and mapping regional land use trends by combining Landsat and topographic data p 2 A83-10119
WYATT, C. L.
A multispectral approach to remote detection of deer p 6 A83-14666

Y

YARIV, A.
Low threshold InGaAsP/InP lasers with microcleaved mirrors suitable for monolithic integration p 24 A83-10981
YATES, R.
An algorithm to interface Nimbus-7 SMMR data with the AES ice modelling grid for the Beaufort Sea p 41 A83-14284
YAZDANI, R.
Vegetation change detection in an agricultural area - A simple approach for use with geo-data base p 4 A83-14236
Potentials of Landsat-D and SPOT-1 for crop identification in the maritimes p 4 A83-14240
YOSHIKADO, S.
Application of the airborne microwave rain-scattered/radiometer system to the remote sensing of rains and wind vector measurements over the ocean p 70 A83-14293
YU, K. L.
Low threshold InGaAsP/InP lasers with microcleaved mirrors suitable for monolithic integration p 24 A83-10981

Z

ZAFIRYADIS, J. P.
Application of satellite data to hydrogeological investigation in Damagaram-Mounio, Niger p 53 N83-14630
ZANETTIC, L. J.
Investigation of MAGSAT and TRIAD magnetometer data to provide corrective information on high-lattitude external fields
[E83-10093] p 28 N83-14600
ZERLAUT, G. A.
Spectroradiometer measurements in support of photovoltaic device testing p 70 A83-15458
ZHANG, C.
Geometric adjustment of simultaneous Doppler-derived range differences p 26 N83-13540
ZHU, S. Y.
Effects of adopting new precession, nutation and equinox corrections on the terrestrial reference frame p 26 N83-13538
ZIGICH, D. K.
Evaluating the effectiveness of Landsat data as a tool for locating buried pre-glacial valleys in eastern South Dakota p 33 A83-14667
ZWALLY, H. J.
Ice-sheet dynamics by satellite laser altimetry p 38 A83-10093

Typical Corporate Source Index Listing

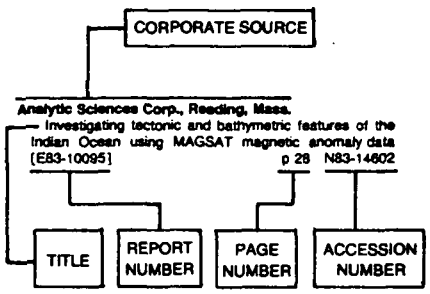

The title of the document is used to provide a brief description of the subject matter. The page number and the accession number are included in each entry to assist the user in locating the abstract in the abstract section. If applicable, a report number is also included as an aid in identifying the document.

A

Agricultural Research Service, Phoenix, Ariz.
Discrimination of growth and water stress in wheat by various vegetation indices through a clear a turbid atmosphere
[E83-10009] p 8 N83-12488
Adjusting the tasseled cap brightness and greenness factors for atmospheric path radiance and absorption on a pixel by pixel basis
[E83-10053] p 13 N83-14562

Agricultural Research Service, Pullman, Wash.
Influence of environmental factors during seed development and after full-ripeness on pre-harvest sprouting in wheat
[E83-10002] p 7 N83-12482

Agricultural Research Service, Weslaco, Tex.
Estimating total standing herbaceous biomass production with LANDSAT MSS digital data
[E83-10045] p 12 N83-13536
Use of near-infrared video recording system for the detection of freeze damaged citrus leaves
[E83-10049] p 12 N83-14558
Comparison of LANDSAT-2 and field spectrometer reflectance signatures of south Texas rangeland plant communities
[E83-10055] p 13 N83-14564
Comparisons among a new soil index and other two- and four-dimensional vegetation indices
[E83-10058] p 14 N83-14567
Methods of editing cloud and atmospheric layer affected pixels from satellite data
[E83-10103] p 64 N83-15746

Agricultural Research Services, Beltsville, Md.
Agricultural Research Service research highlights in remote sensing for calendar year 1981
[E83-10051] p 75 N83-14560

Alaska Univ., Fairbanks.
Evaluation of photographic enhancements of Landsat imagery p 55 A83-12035
Radar and infrared remote sensing of geothermal features at Pilgrim Springs, Alaska p 31 A83-12036

Analytic Sciences Corp., Reading, Mass.
Investigating tectonic and bathymetric features of the Indian Ocean using MAGSAT magnetic anomaly data
[E83-10095] p 28 N83-14602

Applied Physics Lab., Johns Hopkins Univ., Laurel, Md.
A tutorial assessment of atmospheric height uncertainties for high-precision satellite altimeter missions to monitor ocean currents p 42 A83-14851
Investigation of MAGSAT and TRIAD magnetometer data to provide corrective information on high-lattitude external fields
[E83-10093] p 28 N83-14600

Arizona Univ., Tucson.
Atmospheric effects on radiation reflected from soil and vegetation as measured by orbital sensors using various scanning directions p 3 A83-12315
Subsurface valleys and geoarcheology of the eastern Sahara revealed by Shuttle radar p 32 A83-13349

Arkansas Univ., Fayetteville.
Wetland mapping with imaging radar p 50 A83-10072
Geological terrain models p 31 A83-10080
Measurement of soil moisture using remote sensing multisensor radiation techniques
[E83-10012] p 9 N83-12491
Analysis of geologic terrain models for determination of optimum SAR sensor configuration and optimum information extraction for exploration of global non-renewable resources. Pilot study: Arkansas Remote Sensing Laboratory, part 1, part 2, and part 3
[E83-10061] p 35 N83-14570

Army Engineer Topographic Labs., Fort Belvoir, Va.
Terrain analysis procedural guide for drainage and water resources (ETL series on guides for Army terrain analysts)
[AD-A118318] p 52 N83-11569
An analysis of a relaxation scheme to improve terrain elevation data
[AD-A119257] p 27 N83-13550
Effects of ground cover and leaf area on the spectral reflectance of vegetation-soil target
[AD-A119714] p 16 N83-14653
Special reflectance of some plant indicators of saline and nonsaline soils
[AD-A119727] p 16 N83-14655

Aster Consulting Associates, Binghamton, N.Y.
A review of crop canopy reflectance models
[E83-10110] p 17 N83-15753

Autometric Corp., Inc., Falls Church, Va.
Determination of the contribution of side-looking airborne radar to structural geologic mapping
[PB82-185042] p 34 N83-12713

B

Bayerische Akademie der Wissenschaften, Munich (West Germany).
Report on the special program 78 satellite geodesy of the technical university of Munich
[ASTRON-GEODAET-ARB-41] p 25 N83-11563
Theoretical and experimental investigations on the accuracy of close-range photogrammetry
[SER-C-266] p 25 N83-11564
Investigation of the geometrical stability of a photogrammetric recording system
[SER-C-267] p 71 N83-11565
Pass point determination and geometrical precision of the relative rectification of scanner data
[SER-C-268] p 62 N83-13518

Bendix Field Engineering Corp., Columbia, Md.
Dual-wavelength correlation measurements with an airborne pulsed carbon dioxide lidar system p 60 A83-16831

Bendix Field Engineering Corp., Grand Junction, Colo.
Statistical Techniques Applied to Aerial Radiometric Surveys (STARRS): Discriminant-analysis methods applied to aerial radiometric data and their application to uranium favorability in South Texas. Nation uranium resource evaluation
[DE82-020961] p 34 N83-12512

Brigham Young Univ., Provo, Utah.
HCMM hydrological analysis in Utah
[E83-10026] p 53 N83-13520

Bristol Univ. (England).
The role of EARSeL and EARSeL member laboratories p 76 N83-14633

Brown Univ., Providence, R. I.
An investigation into the utilization of HCMM thermal data for the descrimination of volcanic and Eolian geological units
[E83-10047] p 35 N83-14556
Cross-validation for densities and regressions p 66 N83-15776
Characterization of a maximum-likelihood nonparametric density estimator of kernel type p 66 N83-15777

Bureau of Land Management, Anchorage, Alaska.
Evaluation of photographic enhancements of Landsat imagery p 55 A83-12035

Bureau of Meteorology, Melbourne (Australia).
Australian drifting buoy p 48 N83-14837

Bureau of Mines, Anchorage, Alaska.
Critical and strategic minerals in Alaska: Cobalt, the platinum-group metals and chromite
[PB82-193085] p 33 N83-10485

Business and Technological Systems, Inc., Seabrook, Md.
MAGSAT anomaly field inversion and interpretation for the US
[E83-10057] p 27 N83-14566
Equivalent source modeling of the main field using MAGSAT data
[E83-10094] p 28 N83-14601
Geomagnetic modeling by optimal recursive filtering
[E83-10112] p 29 N83-15755

C

California Inst. of Tech., Pasadena.
Development of mathematical techniques for the assimilation of remote sensing data into atmospheric models
[E83-10062] p 22 N83-14571

California Polytechnic State Univ., San Luis Obispo.
BSPLASH: A three-stage surface interpolant to scattered data p 65 N83-15765

California Univ., Livermore. Lawrence Livermore Lab.
Aerial geologic log from Livermore, California to the Nevada Test Site, Nye County, Nevada
[DE82-018392] p 25 N83-10693

California Univ., Santa Barbara.
Monitoring global vegetation
[E83-10044] p 12 N83-14554
Neotectonics of the San Andreas Fault system: Basin and range province juncture
[E83-10090] p 36 N83-14598

Canada Centre for Remote Sensing, Ottawa (Ontario).
Standardization of computer compatible tape formats for remote sensing data p 54 A83-10075

Canada Centre for Remote Sensing, Toronto (Ontario).
A practical automated mapping system p 64 N83-14635

Center for Remote Sensing, Colombo (Sri Lanka).
Multistage land use mapping and change monitoring in Sri Lanka p 15 N83-14625

Centre National de la Recherche Scientifique, Paris (France).
SPOT in the 1980's p 76 N83-14611

City Univ. Inst. of Marine and Atmospheric Sciences, New York.
The measurement of the synoptic scale wind over the ocean p 47 N83-13773

Coast Guard, Washington, D.C.
Lagrangian drift measurements of sea surface currents and iceberg tracking p 49 N83-14842

SOURCE

Cologne Univ. (West Germany).
The conical scan radiometer p 72 N83-14804
The Earth Radiation Budget Satellite System (ERBSS) of the United States p 72 N83-14805
Determination of the radiation budget at the Earth's surface from satellite data p 29 N83-14808
Colorado State Univ., Fort Collins.
Reflectance of a vegetation canopy using the Adding method p 3 A83-12603
Colorado Univ., Boulder.
Data use investigation for the magnetic field satellite (MAGSAT) mission: Geomagnetic field forecasting and fluid dynamics of the core
[E83-10098] p 29 N83-15742
Commission of the European Communities, Brussels (Belgium).
The European Community, development and satellite technology p 75 N83-14609
Computer Sciences Corp., Silver Spring, Md.
Microwave radiance of early fall sea ice at 1.55 cm p 38 A83-10091
Landsat observations of Mount St. Helens p 19 A83-12671
Estimation of context for statistical classification of multispectral image data p 59 A83-14853
Computer Sciences-Technicolor Associates, Greenbelt, Md.
LANDSAT 3 return beam vidicon response artifacts: A report on RBV photographic product characteristics and quality coding system
[E83-10122] p 67 N83-15792
Consiglio Nazionale delle Ricerche, Florence (Italy).
Agroecological classification by remote sensing techniques p 23 N83-14622
Copenhagen Univ. (Denmark).
Multitemporal analysis of Landsat data for investigations of agricultural land use: Problems and potentials p 15 N83-14624
Cornell Univ., Ithaca, N. Y.
Remote Sensing Program
[E83-10120] p 18 N83-15790

D

Department of Agriculture, Columbia, Mo.
Second generation crop yield models review
[E83-10003] p 7 N83-12483
Department of Agriculture, Houston, Tex.
Optical parameters of leaves of seven weed species
[E83-10010] p 9 N83-12489
Department of Agriculture, Phoenix, Ariz.
Atmospheric effects on radiation reflected from soil and vegetation as measured by orbital sensors using various scanning directions p 3 A83-12315
Diurnal patterns of wheat spectral reflectances and their importance in the assessment of canopy parameters from remotely sensed observations
[E83-10050] p 13 N83-14559
Department of Agriculture, Sydney, Mont.
Winter wheat stand density determination and yield estimates from handheld and airborne scanners
[E83-10013] p 9 N83-12492
Department of Agriculture, Washington, D.C.
AgRISTARS - Plans and first-year achievements p 1 A83-10095
Construction of a remotely sensed area sampling frame for Southern Brazil
[E83-10052] p 13 N83-14561
Deutsche Forschungs- und Versuchsanstalt fuer Luft- und Raumfahrt, Oberpfaffenhofen (West Germany).
OSTA-1/Ocean Color Experiment
[AIAA PAPER 83-0415] p 42 A83-16701
Image processing of remotely sensed phenomena p 61 N83-11400

E

Ecole Nationale Superieure des Mines, Sophia-Antipolis (France).
Combined use of daily thermal cycle of METEOSAT imagery and multispectral LANDSAT data: Application to the Bandiagara plateau, Mali p 36 N83-14620
Eidgenoessische Technische Hochschule, Zurich (Switzerland).
Remote sensing of renewable natural resources in developing countries for national planning purposes p 76 N83-14616
Electromagnetic Systems Labs., Inc., Sunnyvale, Calif.
Remote sensing applications to the development of an integrated data base for oil and gas exploration p 37 N83-14628
Energy, Mines and Resources Canada, Ottawa (Ontario).
The reduction, verification and interpretation of MAGSAT magnetic data over Canada
[E83-10091] p 28 N83-14599
The reduction, verification and interpretation of MAGSAT magnetic data over Canada
[E83-10101] p 29 N83-15744
Environment Canada, Victoria (British Columbia).
Mesoscale ocean variability p 48 N83-14841
Environmental Analysis and Remote Sensing, Delft (Netherlands).
The Group Agromet Monitoring Project (GAMP) p 23 N83-14615
Environmental Research and Technology, Inc., Concord, Mass.
Snow hydrology studies using data from the Heat Capacity Mapping Mission p 50 A83-10102
Environmental Research Inst. of Michigan, Ann Arbor.
Radiance calculations for optimization of sensors designed for remote bathymetry, volume 1
[AD-A117743] p 44 N83-10739
Development, implementation and evaluation of satellite-aided agricultural monitoring systems
[E83-10017] p 10 N83-12500
Analysis of the profile characteristics of corn and soybeans using field reflectance data
[E83-10018] p 10 N83-12501
Evaluation of ERIM optically processed SEASAT SAR data
[E83-10037] p 63 N83-13531
Further SEASAT SAR coastal ocean wave analysis
[NASA-CR-169682] p 47 N83-13776
Environmental Systems Research Inst., Redlands, Calif.
CIRSS vertical data integration, San Bernardino County study phases 1-A, 1-B
[E83-10124] p 67 N83-15794
CIRSS vertical data integration, San Bernardino study
[E83-10127] p 67 N83-15796
European Space Agency, Paris (France).
Satellite remote sensing for developing countries
[ESA-SP-175] p 75 N83-14608
Satellite remote sensing: ESA's experience with developing countries p 76 N83-14632
European Space Agency, Toulouse (France).
The European Space Agency's Earth observation satellite programs in the 1980's p 75 N83-14610
EG and G Washington Analytical Services Center, Inc., Pocomoke City, Md.
Experimental feasibility of the airborne measurement of absolute oil fluorescence spectral conversion efficiency p 44 A83-18581
EROS Data Center, Sioux Falls, S. Dak.
LANDSAT 4 investigations of thematic mapper and multispectral scanner applications
[E83-10121] p 66 N83-15791
LANDSAT 3 return beam vidicon response artifacts: A report on RBV photographic product characteristics and quality coding system
[E83-10122] p 67 N83-15792

F

Florence Univ. (Italy).
Agroecological classification by remote sensing techniques p 23 N83-14622
Florida Univ., Gainesville.
Use of thermal inertia determined by HCMM to predict nocturnal cold prone areas in Florida
[E83-10028] p 62 N83-13522
Use of thermal inertia determined by HCMM to predict nocturnal cold prone areas in Florida
[E83-10102] p 64 N83-15745
Automatic photointerpretation via texture and morphology analysis p 65 N83-15770
Food and Agriculture Organization of the United Nations, Rome (Italy).
Remote sensing in developing countries. FAO'S international experience p 76 N83-14614

G

General Electric Co., Fairfield, Conn.
LANDSAT-D: The new era of earth resources survey
[E83-10125] p 76 N83-15739
General Electric Co., Philadelphia, Pa.
Measurements of ocean surface spectrum from an aircraft using the two-frequency microwave resonance technique p 43 A83-17710
Technology needs assessment of an atmospheric observation system for tropospheric research missions, part 1
[NASA-CR-3556] p 21 N83-10645
Technology needs assessment of an atmospheric observation system for multidisciplinary air quality/meteorology missions, part 2
[NASA-CR-3557] p 21 N83-10646
Geological Survey of Norway, Trondheim.
Digital methods for lineament analysis p 37 N83-14634
Geological Survey, Flagstaff, Ariz.
Shuttle imaging radar experiment p 32 A83-13348
Subsurface valleys and geoarcheology of the eastern Sahara revealed by Shuttle radar p 32 A83-13349
The geology of Europa p 24 A83-16239
Geological Survey, Reston, Va.
Seasat L-band radar response to forest vegetation in eastern Virginia p 1 A83-10061
Mineral identification from orbit - Initial results from the Shuttle multispectral infrared radiometer p 32 A83-13350
Geological Survey, Washington, D. C.
Geographic research in the US Geological Survey: Bibliography, 1966 - 1980
[USGS-CIRC-865] p 21 N83-11639
Graz Univ. (Austria).
The applicability of satellite remote sensing to small and medium scale mapping p 64 N83-14618

H

Hamburg Univ. (West Germany).
The effect of monomolecular surface films on the microwave brightness temperature of the sea surface p 43 A83-17714
High Life Helicopters, Inc., Puyallup, Wash.
Airborne gamma-ray spectrometer and magnetometer survey. Volume 1. Detail areas, Christmas Mountains, Solitario, Green Valley/0-2 Ranch, Texas
[DE82-021614] p 34 N83-12513
Hofstra Univ., Hempstead, N. Y.
Measurements of ocean surface spectrum from an aircraft using the two-frequency microwave resonance technique p 43 A83-17710
Honeywell Systems and Research Center, Minneapolis, Minn.
FLIR target screening p 65 N83-15771
Houston Univ., Tex.
The possible modifications of the Hisse model for pure LANDSAT agricultural data p 10 N83-12497
Hughes Aircraft Co., Los Angeles, Calif.
MSS D Multispectral Scanner System
[E83-10128] p 72 N83-15797
Hydrometeorological Centre of the USSR (Moscow).
Aircraft and remote measurements of atmospheric transport of pollutants within the global integrated monitoring system p 22 N83-12620
Monitoring of meteorological elements in a composite program for environmental pollution studies p 22 N83-12648
Instruments and methods for monitoring background soil pollution p 22 N83-12650
Main achievements of GARP Atlantic Tropical Experiment (GATE) and its impact on FGGE p 46 N83-12735

I

Illinois Univ., Urbana.
Remote sensing of sea state using laser altimeters p 40 A83-12316
Determining 3-D motion and structure from image sequences p 66 N83-15773
Indian Inst. of Geomagnetism, Bombay.
MAGSAT project
[E83-10030] p 25 N83-13524
MAGSAT for geomagnetic studies over Indian region
[E83-10032] p 26 N83-13526
Indian Space Research Organization, Bangalore.
Applications of space science and technology p 75 N83-12115
Institute of Geological Sciences, Nottingham (England).
Satellite remote sensing in mineral exploration in developing countries p 36 N83-14627
Remote sensing of the granites of Southeast Asia p 37 N83-14629
Instituto de Investigaciones Pesqueras, Barcelona (Spain).
Space truth in oceanography p 48 N83-14636
Instituto de Pesquisas Espaciais, Sao Jose dos Campos (Brazil).
Remote sensing in geology: Current trends and future prospects with satellite data
[INPE-2514-PRE/193] p 33 N83-12509
Use of LANDSAT images to study cerrado vegetation
[E83-10025] p 11 N83-13519

Geological-structural interpretation using products of remote sensing in the region of Carrancas, Minas Gerais, Brazil
[E83-10029] p 34 N83-13523
An introduction to project Freeze
[INPE-2435-NTE/186] p 22 N83-13703
Image analysis unit (UAI-R) for meteorological applications
[INPE-2428-NTE/185] p 63 N83-13707
CNPq/INPE-LANDSAT system report of activities
[E83-10064] p 63 N83-14573
An automatic agricultural zone classification procedure for crop inventory satellite images
[E83-10065] p 14 N83-14574
Automatic interpretation of MSS-LANDSAT data applied to coal refuse site studies in southern Santa Catarina State, Brazil
[E83-10066] p 35 N83-14575
An application of cluster analysis for determining homogeneous subregions: The agroclimatological point of view
[E83-10067] p 14 N83-14576
Vegetation survey in Amazonia using LANDSAT data
[E83-10068] p 14 N83-14577
Spectral discrimination of lithologic facies in the granite of the Pedra Branca Goias using LANDSAT 1 digital imagery
[E83-10069] p 35 N83-14578
Remote sensing techniques for conservation and management of natural vegetation ecosystems
[E83-10070] p 15 N83-14579
Multitemporal and geobotanical approach in the remote detection of Greisenization areas in the Serra da Pedra Branca Granite, Goias State, Brazil
[E83-10071] p 35 N83-14580
Method of interpretation of remotely sensed data and applications to land use
[E83-10072] p 23 N83-14581
LANDSAT and radar mapping of intrusive rocks in SE-Brazil
[E83-10073] p 36 N83-14582
Interpretation of remotely sensed data and its applications in oceanography
[E83-10074] p 48 N83-14583
INPE LANDSAT-D thematic mapper computer compatible tape format specification
[E83-10075] p 63 N83-14584
Evaluation of reforestation using remote sensing techniques
[E83-10076] p 15 N83-14585
Estimation of the sugar cane cultivated area from LANDSAT images using the two phase sampling method
[E83-10077] p 15 N83-14586
The computer treatment of remotely sensed data: An introduction to techniques which have geologic applications
[E83-10078] p 36 N83-14587
Comparison of diverse methods for the correction of atmospheric effects on LANDSAT and SKYLAB images
[E83-10079] p 72 N83-14588
Verification of LANDSAT imagery for morphametric and topological studies of drainage basins in a section of the western plateau of Sao Paulo State: Tiete-Aguapei watershed
[E83-10111] p 54 N83-15754
Analysis of the characteristics appearing in LANDSAT multispectral images in the geological structural mapping of the midwestern portion of the Rio Grande do Sul shield
[E83-10126] p 37 N83-15795

International Inst. for Aerial Survey and Earth Sciences, Delft (Netherlands).
Satellite remote sensing for developing countries: Prospects and constraints p 76 N83-14631

International Council of Scientific Unions, Rome (Italy).
Report of the Monex review meeting
[GARP-SPEC-REPT-38] p 45 N83-12707
Global Weather Experiment. The GARP Atlantic Tropical Experiment (GATE) Monograph
[GARP-PUB-SER-25] p 45 N83-12724
The Global Weather Experiment. First GARP Global Experiment (FGGE) operations report series: Volume 5, summary of data collected 5 July - December 1979
[GARP-FOR-5] p 46 N83-12808

Iowa State Univ. of Science and Technology, Ames.
Estimation of context for statistical classification of multispectral image data p 59 A83-14853
Remote sensing of land resources: Application of LANDSAT satellite imagery p 11 N83-13517
Surface fitting with biharmonic and harmonic models p 65 N83-15764

Iowa Univ., Iowa City.
Use of MAGSAT anomaly data for crustal structure and mineral resources in the US midcontinent
[E83-10082] p 36 N83-14590

J

Jet Propulsion Lab., California Inst. of Tech., Pasadena.
Rock type discrimination techniques using Landsat and Seasat image data p 30 A83-10057
Drumlin fields and glaciated mountains - A contrast in geomorphic perception from Seasat radar images p 23 A83-10078
Imaging radar observations of volcanic features in Medicine Lake Highland, California p 30 A83-10079
SAR squint analysis of directional extended targets p 54 A83-10084
Some examples of the utility of HCMM data in geologic remote sensing p 31 A83-10099
Potentials for change detection using Seasat synthetic aperture radar data p 54 A83-10121
Earth resources observation with the Shuttle imaging radar p 68 A83-12676
Shuttle imaging radar experiment p 32 A83-13348
Subsurface valleys and geoarcheology of the eastern Sahara revealed by Shuttle radar p 32 A83-13349
Mineral identification from orbit - Initial results from the Shuttle multispectral infrared radiometer p 32 A83-13350
Radar images of the earth from space p 59 A83-14598
Resolution versus speckle relative to geologic interpretability of spaceborne radar images - A survey of user preference p 33 A83-14852
Flight path design issues for the TOPEX mission
[AIAA PAPER 83-0197] p 42 A83-16581
SEASAT-A SASS wind processing
[NASA-CR-169433] p 44 N83-10473
Geologic interpretation of HCMM and aircraft thermal data
[E83-10036] p 62 N83-13530
Evaluation of the potential of one to three SEASAT-SMMR channels in retrieving sea surface temperature
[NASA-CR-169660] p 48 N83-14604
C-1 surface interpolation for scattered data on a sphere p 65 N83-15762

Joint Inst. for Lab. Astrophysics, Boulder, Colo.
Preliminary study of GPS orbit determination accuracy achievable from worldwide tracking data
[NASA-CR-169693] p 28 N83-14605
TOPEX orbit determination using GPS signals plus a sidetone ranging system
[NASA-CR-169694] p 29 N83-14606

Joint Research Centre of the European Communities, Ispra (Italy).
Use of remote sensing techniques for rice production forecasting in west Africa (Mali and Guinea: Niger-Bani Project) p 15 N83-14626

K

Kansas Univ. Center for Research, Inc., Lawrence.
Radar spectral observations of snow p 49 A83-10064
A backscatter model for a randomly perturbed periodic surface p 1 A83-10107
A three-part geometric model to predict the radar backscatter from wheat, corn, and sorghum
[E83-10005] p 8 N83-12485
Data documentation for the 1981 summer vegetation experiment
[E83-10016] p 10 N83-12499
Assessment of radar resolution requirements for soil moisture estimation from simulated satellite imagery
[E83-10020] p 10 N83-12503
Analysis of geologic terrain models for determination of optimum SAR sensor configuration and optimum information extraction for exploration of global non-renewable resources. Pilot study: Arkansas Remote Sensing Laboratory, part 1, part 2, and part 3
[E83-10061] p 35 N83-14570
Crop-phenology and LANDSAT-based irrigated lands inventory in the high plains
[E83-10115] p 18 N83-15758

Kansas Univ., Lawrence.
Microwave remote sensing: Active and passive. Volume 2 - Radar remote sensing and surface scattering and emission theory p 69 A83-14040
The application of remote sensing to resource management and environmental quality programs in Kansas
[E83-10114] p 23 N83-15757

Katholieke Universiteit te Leuven (Belgium).
Multitemporal soil and vegetation observations by METEOSAT over Central Africa p 15 N83-14619

Krueger (I.) A/S, Copenhagen (Denmark).
Application of satellite data to hydrogeological investigation in Damagaram-Mounio, Niger p 53 N83-14630

L

Lamont-Doherty Geological Observatory, Palisades, N. Y.
The intermediate wavelength magnetic anomaly field of the north Pacific and possible source distributions
[E83-10088] p 27 N83-14596

Lockheed Engineering and Management Services Co., Inc., Houston, Tex.
A parametric study of tillage effects on radar backscatter p 2 A83-10108
Probabilistic cluster labeling of imagery data p 54 A83-11410
Evaluation of small area crop estimation techniques using LANDSAT- and ground-derived data
[E83-10008] p 8 N83-12487
Operation plan for the data 100/LARS terminal system
[E83-10011] p 62 N83-12490
Development of a corn and soybean labeling procedure for use with profile parameter classification
[E83-10014] p 9 N83-12493
AgRISTARS documents tracking list report
[E83-10019] p 10 N83-12502
Earth Observations Division version of the Laboratory for Applications of Remote Sensing System (EOD-LARSYS) user guide for the IBM 370/148. Volume 1: System overview
[E83-10007] p 62 N83-12866
Computer program documentation for the pasture/range condition assessment processor
[E83-10100] p 16 N83-15743
FORTRAN implementation of Friedman's test for several related samples
[E83-10123] p 18 N83-15793

Los Alamos Scientific Lab., N. Mex.
Statistical Techniques Applied to Aerial Radiometric Surveys (STARRS): Discriminant-analysis methods applied to aerial radiometric data and their application to uranium favorability in South Texas. Nation uranium resource evaluation
[DE82-020961] p 34 N83-12512
Tectonics of west central Mexico and adjacent Arizona: A remote sensing and field study in arid and semi-arid areas
[DE82-002393] p 37 N83-14797

Lund Univ. (Sweden).
Approaches to desertification monitoring in the Sudan p 23 N83-14623

M

MacQuarie Univ., North Ryde (Australia).
The MAGSAT project in Australia
[E83-10089] p 28 N83-14597

Maryland Univ., College Park.
The role of geological surfaces in determining visible-near infra red spectral signatures p 30 A83-10058
Spatial and temporal variations of large-scale subsidence and convection regions derived from satellite data
[PB82-219817] p 71 N83-13750
Cooperative processes in image segmentation p 65 N83-15768
Shape and texture p 65 N83-15769

Massachusetts Univ., Amherst.
The mineralogy of global magnetic anomalies
[E83-10034] p 34 N83-13528

Max-Planck-Institut fuer Meteorologie, Hamburg (West Germany).
The effect of monomolecular surface films on the microwave brightness temperature of the sea surface p 43 A83-17714

McGill Univ., Montreal (Quebec).
Topics in global convergence of density estimates p 66 N83-15775

Messerschmitt-Boelkow-Blohm G.m.b.H., Ottobrunn (West Germany).
A Digital Photogrammetric System (DPS) for producing Digital Elevation Models (DEM) and orthoplates by means of linear array scanner imagery
[MBB-UA-618/81] p 71 N83-13567

Miami Univ., Coral Gables, Fla.
Phytoplankton pigment concentrations in the Middle Atlantic Bight - Comparison of ship determinations and CZCS estimates p 43 A83-18580

Miami Univ., Fla.
Phytoplankton pigment concentrations in the Middle Atlantic Bight - Comparison of ship determinations and CZCS estimates p 43 A83-18580
Investigations of medium wavelength magnetic anomalies in the eastern Pacific using MAGSAT data
[E83-10083] p 27 N83-14591
Ministere de l'Energie et des Ressources (Quebec).
Conference on Using Next Generation Earth Observation Satellites: Summary handbook
p 62 N83-12508
Missouri Univ., Columbia.
Second generation crop yield models review
[E83-10003] p 7 N83-12483
Moss Landing Marine Labs., Calif.
Phytoplankton pigment concentrations in the Middle Atlantic Bight - Comparison of ship determinations and CZCS estimates p 43 A83-18580

N

National Aeronautics and Space Administration, Washington, D. C.
AgRISTARS - Plans and first-year achievements
p 1 A83-10095
Use of the Space Shuttle for remote sensing research - Recent results and future prospects
p 68 A83-13347
OSTA-1 - Shuttle's first scientific and applications payload p 73 A83-13715
Land remote sensing activities in the US
p 72 N83-14612
National Oceanic and Atmospheric Administration, Washington, D. C.
Phytoplankton pigment concentrations in the Middle Atlantic Bight - Comparison of ship determinations and CZCS estimates p 43 A83-18580
National Oceanic and Atmospheric Administration, Boulder, Colo.
FACE-2 data reductions (prior to disclosure of the treatment decisions). Part 5: Satellite-estimated rainfall from a geostationary platform in FACE-2
[PB82-216581] p 52 N83-10730
Ocean pollution research, development and monitoring
[PB82-219049] p 45 N83-10740
National Oceanic and Atmospheric Administration, Columbia, Mo.
Evaluation of the Williams-type spring wheat model in North Dakota and Minnesota
[E83-10041] p 12 N83-13535
Crop weather models of corn and soybeans for Agrophysical Units (APU's) in Iowa using monthly meteorological predictors
[E83-10054] p 13 N83-14563
Comparison of the CEAS and Williams-type barley yield models for North Dakota and Minnesota
[E83-10056] p 13 N83-14565
Crop weather models of barley and spring wheat yield for agrophysical units in North Dakota
[E83-10059] p 14 N83-14568
National Oceanic and Atmospheric Administration, Rockville, Md.
Effects of detection algorithm on accuracy degradation from logarithmic and difference processing for airborne laser bathymetry returns
[PB82-215138] p 44 N83-10707
Weather constraints on airborne laser hydrography operations
[PB82-189754] p 52 N83-10745
National Science Foundation, Washington, D.C.
Key scientific questions and the role of satellites
p 64 N83-14830
National Advisory Committee on Oceans and Atmosphere, Washington, D.C.
A report to the President and the Congress
[AR-11] p 75 N83-11532
Naval Ocean Research and Development Activity, Bay St. Louis, Miss.
Collinear-track altimetry in the Gulf of Mexico from SEASAT: Measurements, models and surface truth
[AD-A118160] p 45 N83-11568
Comparison of multichannel and two-satellite methods for remote measurement of sea surface temperature
[AD-A118736] p 45 N83-12511
Naval Research Lab., Washington, D. C.
On the use of laser profilometry for ocean wave studies p 42 A83-14502
The effect of monomolecular surface films on the microwave brightness temperature of the sea surface
p 43 A83-17714
Naval Surface Weapons Center, Dahlgren, Va.
Mean Earth ellipsoid determined from SEASAT altimeter observations
[AD-A117910] p 45 N83-11570
Evaluation of geodetic products produced by the NSWC reduction of SEASAT radar altimeter data
[AD-A117837] p 25 N83-11571
An upper bound on errors in the mean-of-date/instantaneous Earth-fixed vector transformation induced by interpolated nutation angles
[AD-A119444] p 29 N83-14656
Nebraska Univ., Lincoln.
Satellite observations of variations in Northern Hemisphere seasonal snow cover
[PB82-196668] p 52 N83-10734
Nevada Univ., Reno.
Low- to moderate-temperature geothermal resource assessment for Nevada: Area specific studies, Pumpernickel Valley, Carlin and Moana
[DE82-018598] p 34 N83-12584
New South Wales Univ., Kensington (Australia).
A means for utilizing ancillary information in multispectral classification p 60 A83-16905
New York State Univ., Albany.
An evaluation of Seasat SAR imagery for urban analysis p 60 A83-16904
North Carolina State Univ., Raleigh.
MAGSAT and aeromagnetic data of the continental US
[E83-10033] p 26 N83-13527
Norwegian Meteorological Inst., Blindern.
The RAMS collection of meterological and position data in the Norwegian Sea p 49 N83-14845
National Aeronautics and Space Administration. Ames Research Center, Moffett Field, Calif.
LANDSAT land cover analysis completed for CIRSS/San Bernardino County project
[E83-10024] p 22 N83-12507
Terrestrial applications: An intelligent Earth-sensing information system p 76 N83-15349
Gates to Gregg high voltage transmission line study
[E83-10097] p 16 N83-15741
National Aeronautics and Space Administration. Earth Resources Labs., Bay St. Louis, Miss.
Soil spectral characterization p 2 A83-10118
Automated segment matching algorithm-theory, test, and evaluation
[E83-10096] p 16 N83-15740
National Aeronautics and Space Administration. Goddard Space Flight Center, Greenbelt, Md.
Standardization of computer compatible tape formats for remote sensing data p 54 A83-10075
Microwave radiance of early fall sea ice at 1.55 cm
p 38 A83-10091
Satellite laser altimeter for measurement of ice sheet topography p 38 A83-10092
Ice-sheet dynamics by satellite laser altimetry
p 38 A83-10093
Radiative transfer model for heterogeneous 3-D scenes p 3 A83-12604
Landsat observations of Mount St. Helens
p 19 A83-12671
The early 1981 view of Landsat-D progress
p 73 A83-12673
Satellite estimates of ocean-air heat fluxes during cold air outbreaks p 41 A83-13059
Technical issues in focal plane development for terrestrial resource observations p 69 A83-13735
On the use of laser profilometry for ocean wave studies p 42 A83-14502
Observations of oceanic surface-wind fields from the Nimbus-7 microwave radiometer p 42 A83-14861
OSTA-1/Ocean Color Experiment
[AIAA PAPER 83-0415] p 42 A83-16701
Dual-wavelength correlation measurements with an airborne pulsed carbon dioxide lidar system
p 60 A83-16831
The LANDSAT tutorial workbook: Basics of satellite remote sensing
[E83-10001] p 74 N83-10458
Some fundamental concepts in remote sensing
p 60 N83-10459
Familiarization with LANDSAT imagery
p 60 N83-10460
Some spectral and spatial characteristics of LANDSAT data p 61 N83-10461
Photointerpretation of LANDSAT images
p 61 N83-10462
Computer processed LANDSAT data
p 61 N83-10463
Near surface observations p 61 N83-10464
Geographic information systems p 61 N83-10465
A case study in the practical use of LANDSAT data
p 52 N83-10466
Other remote sensing systems: Retrospect and outlook p 74 N83-10467
Some closing thoughts: Practical payoffs from satellite systems p 74 N83-10468
Appendix A: The LANDSAT system
p 75 N83-10469
Appendix B: Principles of computer processing of LANDSAT data p 75 N83-10470
Appendix C. LANDSAT: A worldwide perspective
p 75 N83-10471
An evaluation of the NASA/GSFC Barnes field spectral reflecometer model 14-758, using signal/noise as a measure of utility
[NASA-TM-83969] p 71 N83-12396
Aircraft and satellite measurement of ocean wave directional spectra using scanning-beam microwave radars
[NASA-TM-84008] p 47 N83-13544
The use of thematic mapper simulator calibration data for assessment of data quality
[NASA-TM-82059] p 71 N83-13547
The Bering Sea ice cover during March 1979: Comparison of surface and satellite data with the Nimbus-7 SMMR
[NASA-CR-169393] p 47 N83-13572
Prospects for the future p 48 N83-14832
Nimbus 6 Random Access Measurement System applications experiments
[NASA-SP-457] p 48 N83-14835
Data Announcement Bulletin: Space Shuttle OSTA 1 payload data
[NASA-TM-84884] p 72 N83-15344
Spectral characterization of the LANDSAT-D multispectral scanner subsystems
[E83-10107] p 17 N83-15750
National Aeronautics and Space Administration. Langley Research Center, Hampton, Va.
Microwave remote sensing measurements of oil pollution on the ocean p 39 A83-10104
Measurements of ocean surface spectrum from an aircraft using the two-frequency microwave resonance technique p 43 A83-17710
Passive microwave detection of river-plume fronts in the German Bight p 52 A83-17713
The effect of monomolecular surface films on the microwave brightness temperature of the sea surface
p 43 A83-17714
Analysis of high altitude remotely sensed data collected in the Nantucket Shoals experiment 4-15 May, 1981
[NASA-TM-84547] p 44 N83-10647
National Aeronautics and Space Administration. Lyndon B. Johnson Space Center, Houston, Tex.
Seasat L-band radar response to forest vegetation in eastern Virginia p 1 A83-10061
AgRISTARS - Plans and first-year achievements
p 1 A83-10095
A parametric study of tillage effects on radar backscatter p 2 A83-10108
Radar and infrared remote sensing of geothermal features at Pilgrim Springs, Alaska p 31 A83-12036
Reflectance of a vegetation canopy using the Adding method p 3 A83-12603
Shuttle imaging radar experiment p 32 A83-13348
The use of large-area spectral data in wheat yield estimation p 7 A83-16910
AgRISTARS. Semiannual program review presentation to level 1, interagency Coordination Committee
[E83-10006] p 8 N83-12486
Development of thematic mapper vegetative indices for assessing biomass in corn, soybeans and wheat
[E83-10035] p 11 N83-13529
Monitoring global vegetation
[E83-10044] p 12 N83-14554
Evaluation of the Williams-type model for barley yields in North Dakota and Minnesota
[E83-10060] p 14 N83-14569
Crop proportion estimation problems in AgRISTARS
p 18 N83-15760
National Aeronautics and Space Administration. Wallops Flight Center, Wallops Island, Va.
Experimental feasibility of the airborne measurement of absolute oil fluorescence spectral conversion efficiency
p 44 A83-18581

O

Ocean Data Systems, Inc., Monterey, Calif.
Technology and future ground processing systems
p 56 A83-12678
SEASAT-A SASS wind processing
[NASA-CR-169433] p 44 N83-10473
Office de la Recherche Scientifique et Technique Outre-Mer, Paris (France).
Gravimetric maps of the Central African Republic
[E83-10084] p 27 N83-14592
Office of Naval Research, Arlington, Va.
Naval Research Reviews, volume 34, no. 1
[AD-A117981] p 45 N83-12037
Ohio State Univ., Columbus.
Basic research for the geodynamics program
[NASA-CR-169470] p 26 N83-13537

Effects of adopting new precession, nutation and equinox corrections on the terrestrial reference frame
p 26 N83-13538
Utilization of range-difference observations in geodynamics p 26 N83-13539
Geometric adjustment of simultaneous Doppler-derived range differences p 26 N83-13540

Oslo Univ. (Norway).
Digital analysis of Landsat satellite imagery in Turkana, Northern Kenya p 64 N83-14637

OAO Corp., Beltsville, Md.
Ice-sheet dynamics by satellite laser altimetry
p 38 A83-10093

P

Pacific Gas and Electric Co., San Francisco, Calif.
Gates to Gregg high voltage transmission line study
[E83-10097] p 16 N83-15741

Pennsylvania State Univ., University Park.
Development of a data management front end for use with a LANDSAT based information system
[E83-10104] p 17 N83-15747

Phoenix Corp., McLean, Va.
GRAVSAT error analysis by means of global spectral analyses of the marine geoid from SEASAT altimeter data
[E83-10105] p 29 N83-15748

Purdue Univ., Lafayette, Ind.
Application of computer axial tomography /CAT/ to measuring crop canopy geometry p 1 A83-10096
Soil spectral characterization p 2 A83-10118
Estimation of context for statistical classification of multispectral image data p 59 A83-14853
A means for utilizing ancillary information in multispectral classification p 60 A83-16905
Performance comparison for Barnes model 12-1000, Exotech model 100, and Ideas Inc. Biometer Mark 2
[E83-10004] p 8 N83-12484
Extension of laboratory-measured soil spectra to field conditions
[E83-10021] p 11 N83-12504
Remote sensing of agricultural crops and soils
[E83-10023] p 11 N83-12506
Gravity and magnetic anomaly data analysis
[E83-10031] p 26 N83-13525
LANDSAT-4 image data quality analysis
[E83-10039] p 63 N83-13533
Contextual classification of multispectral image data: An unbiased estimator for the context distribution
[E83-10087] p 63 N83-14595

Q

QEB, Inc., Lakewood, Colo.
Airborne gamma-ray spectrometer and magnetometer survey. Volume 1. Detail areas, Christmas Mountains, Solitario, Green Valley/0-2 Ranch, Texas
[DE82-021614] p 34 N83-12513

R

Reading Univ. (England).
The determination of soil moisture balances in tropical Africa by satellite infrared remote sensing: The atmospheric problem p 53 N83-14621

Rensselaer Polytechnic Inst., Troy, N. Y.
Image processing techniques p 61 N83-11391

Research Triangle Inst., Research Triangle Park, N.C.
A comparison of HCMM surface temperatures with in situ temperature data
[E83-10040] p 46 N83-13534
A comparison of surfaces temperatures from HCMM infrared data with field measurements
[E83-10046] p 47 N83-14555
Western Boundary Eddies of the Gulf Stream
p 49 N83-14847

Resource Consultants, Inc., Fort Collins, Colo.
Snowmelt runoff modeling in simulation and forecasting modes with the Martinec-Mango model
[E83-10063] p 53 N83-14572

Rhode Island Univ., Narragansett.
Remote sensing, a tool for managing the marine environment: Eight case studies
[PB82-220864] p 44 N83-10483

Royal Aircraft Establishment, Farnborough (England).
The accuracy of Seasat-1 altimeter altitude measurments under various sea state conditions
[RAE-TR-82059] p 47 N83-14553

Rutgers Univ., New Brunswick, N. J.
Observations of oceanic surface-wind fields from the Nimbus-7 microwave radiometer p 42 A83-14861

S

Science Systems and Applications, Inc., Lanham, Md.
On the use of laser profilometry for ocean wave studies p 42 A83-14502

Scripps Institution of Oceanography, La Jolla, Calif.
Infrared satellite data from the first coastal ocean dynamics experiment, March - July 1981
[AD-A120068] p 49 N83-15799

Soil Conservation Service, Denver, Colo.
Snowmelt runoff modeling in simulation and forecasting modes with the Martinec-Mango model
[E83-10063] p 53 N83-14572

South Dakota State Univ., Brookings.
Combining land use data acquired from Landsat with soil map data p 2 A83-10117
Aerial thermal infrared census of Canada geese in South Dakota p 6 A83-14665
Evaluating depth to shallow groundwater using heat capacity mapping mission /HCMM/ data
p 51 A83-14668

Survey of India, Dehra Dun.
Analysis of MAGSAT data of the Indian region
[E83-10027] p 25 N83-13521

T

Technicolor Government Services, Inc., Moffett Field, Calif.
Gates to Gregg high voltage transmission line study
[E83-10097] p 16 N83-15741

Technicolor Graphic Services, Inc., Sioux Falls, S. Dak.
An investigation of MAGSAT and complementary data emphasizing Precambrian shields and adjacent areas of West Africa and South America
[E83-10085] p 36 N83-14593

Texas A&M Univ., College Station.
Evaluating depth to shallow groundwater using heat capacity mapping mission /HCMM/ data
p 51 A83-14668
Development of advanced acreage estimation methods
[E83-10015] p 9 N83-12494
System support documentation: IDIMS FUNCTION AMOEBA p 9 N83-12495
Rice scene radiation research plan p 9 N83-12496
Missing observations in multiyear rotation sampling designs
[E83-10022] p 11 N83-12505
Investigation of remote sensing techniques of measuring soil moisture
[E83-10048] p 12 N83-14557
Drift buoy component, NORPAX anomaly dynamics study p 49 N83-14848
Microwave remote sensing of soil moisture, volume 1
[E83-10108] p 17 N83-15751
Rangeland biomass estimation demonstration
[E83-10113] p 17 N83-15756
Proceedings of the NASA Workshop on Surface Fitting
[E83-10117] p 64 N83-15759
Fitting surfaces to scattered data p 65 N83-15761
Proceedings of the NASA Workshop on Image Analysis
[E83-10118] p 65 N83-15766
Proceedings of the NASA Workshop on Density Estimation and Function Smoothing
[E83-10119] p 66 N83-15774

Texas Univ., Austin.
Operation and maintenance of geodetic satellite observatory, McMurdo, Antarctica
[PB82-187923] p 25 N83-12107

Texas Univ., El Paso.
Crustal and upper mantle structure data analysis
[E83-10038] p 26 N83-13532

Tokyo Univ. (Japan).
Japanese MAGSAT Team
[E83-10080] p 27 N83-14589

Tulsa Univ., Okla.
The Akaike information criterion and its application to mixture proportion estimation p 62 N83-12498

U

Underwater Systems, Inc., Rockville, Md.
Analyses of oceanic subsurface features using space based radar imagery
[AD-A118411] p 45 N83-11692

United Nations Educational, Scientific and Cultural Organization, Paris (France).
World Integrated Oceanic Services System: General plan and operational program for 1982-1985
[WMO-582] p 46 N83-12802

Utah State Univ., Logan.
Spectroscopic imaging of the thermosphere from the Space Shuttle p 68 A83-12605

Utah Univ., Salt Lake City.
Detection of aspen-conifer forest mixes from LANDSAT digital data
[E83-10106] p 17 N83-15749
Identifying environmental features for land management decisions
[E83-10109] p 23 N83-15752
Surfaces: Representation and approximation
p 30 N83-15763

V

Virginia Polytechnic Inst. and State Univ., Blacksburg.
Image segmentation survey p 65 N83-15767
Structural analysis techniqes for remote sensing
p 66 N83-15772

W

Washington Univ., Seattle.
Comparison of environmental conditions in the Bering Sea and Davis Strait and the effects on microwave signature returns; March and April, 1979
[NASA-CR-169473] p 46 N83-12828
The Bering Sea ice cover during March 1979: Comparison of surface and satellite data with the Nimbus-7 SMMR
[NASA-CR-169393] p 47 N83-13572
Validation and application of the SEASAT-SMMR geophysical algorithms
[NASA-CR-169390] p 71 N83-13767
Joint Air Sea Interaction (JASIN) experiment, Northwest coast of Scotland
[NASA-CR-169631] p 48 N83-14603

Wisconsin Univ., Madison.
Investigation of Antarctic crust and upper mantle using MAGSAT and other geophysical data
[E83-10086] p 27 N83-14594
Remote sensing of temperature profiles in the atmosphere p 66 N83-15778

World Meteorological Organization, Geneva (Switzerland).
Hydrological data transmission
[WMO-559] p 53 N83-12514
Long-range water supply forecasting
[WMO-587] p 53 N83-12516
On the Development of Multimedia Monitoring of Environmental Pollution
[WMO-563] p 22 N83-12599
Report of the Monex review meeting
[GARP-SPEC-REPT-38] p 45 N83-12707
Global Weather Experiment. The GARP Atlantic Tropical Experiment (GATE) Monograph
[GARP-PUB-SER-25] p 45 N83-12724
Manual on the global observing system. Volume 1 (annex to the WMO technical regulations): Global aspects, 1981 edition
[WMO-544-VOL-1-ANNEX] p 46 N83-12801
World Integrated Oceanic Services System: General plan and operational program for 1982-1985
[WMO-582] p 46 N83-12802
Commission for Marine Technology: Abridged report of the 8th Session
[WMO-584] p 46 N83-12803
The Global Weather Experiment. First GARP Global Experiment (FGGE) operations report series: Volume 5, summary of data collected 5 July - December 1979
[GARP-FOR-5] p 46 N83-12808

Z

Zentralstelle fuer Geo-Photogrammetrie und Fernerkundung, Munich (West Germany).
Some aspects of the presentation of remote sensing data p 63 N83-14617

Typical Contract Number Index Listing

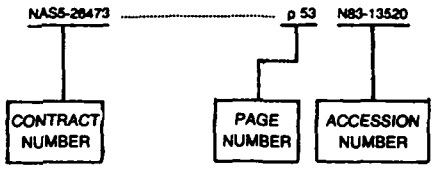

Listings in this index are arranged alphanumerically by contract number. Under each contract number, the accession numbers denoting documents that have been produced as a result of research done under that contract are arranged in ascending order with the AIAA accession numbers appearing first. The accession number denotes the number by which the citation is identified in the abstract section. Preceding the accession number is the page number on which the citation may be found.

AF-AFOSR-3514-78 ..... p 66 N83-15776
p 66 N83-15777
BLM-AA550-CT6-53 ..... p 41 A83-14093
DA PROJ. 4A7-62707-A-855 ..... p 52 N83-11569
p 27 N83-13550
DAAG-80-K-0006 ..... p 66 N83-15777
DAAG29-79-C-0199 ..... p 3 A83-12603
DAAG29-80-K-0006 ..... p 66 N83-15776
DAAG29-80-K-0042 ..... p 66 N83-15778
DACW39-79-M-3958 ..... p 55 A83-11458
DE-AC08-81NV-10220 ..... p 34 N83-12584
DE-AC13-76GJ-01664 ..... p 34 N83-12512
p 34 N83-12513
DE-43SS-KM601-0-2050 ..... p 41 A83-14284
DI-12-14-5001-38 ..... p 13 N83-14562
DI-14-08-0001-20129 ..... p 36 N83-14593
DSS-O6SU-323-8050 ..... p 6 A83-14264
DSS-0S2-80-00026 ..... p 5 A83-14261
FINEP-B/54-81-042-00-00 ..... p 20 A83-14504
F19628-80-C-0052 ..... p 1 A83-10106
JPL-954940 ..... p 50 A83-10072
JPL-955370 ..... p 44 N83-10473
JPL-955528 ..... p 48 N83-14603
JPL-956105 ..... p 63 N83-13531
MO-A01-78-00-4335 ..... p 47 N83-13572
MO-A01-78-00-4339 ..... p 47 N83-13776
NAGW-266 ..... p 47 N83-13773
NAGW-376 ..... p 68 A83-13347
NAGW-95 ..... p 17 N83-15749
NAG1-71 ..... p 22 N83-14571
NAG2-57 ..... p 18 N83-15758
NAG5-161 ..... p 46 N83-12828
p 47 N83-13572
NAG5-177 ..... p 36 N83-14598
NAG5-196 ..... p 3 A83-12315
NAG5-20 ..... p 50 A83-10072
NAG5-30 ..... p 1 A83-10107
NAG5-31 ..... p 12 N83-14557
NAG9-3 ..... p 31 A83-10080
p 35 N83-14570
NAG9-8 ..... p 31 A83-12036
NAS 5-26425 ..... p 36 N83-14590
NAS 5-26442 ..... p 47 N83-14555
NASA ORDER S-53876-AG ..... p 13 N83-14564
p 14 N83-14567
NASA ORDER S-63971-B ..... p 53 N83-14572
NASA ORDER S-70251-AG ..... p 14 N83-14567
NASA ORDER W-08395 ..... p 24 A83-16239
NASA ORDER W-13709 ..... p 24 A83-16239
NASA TASK 146-40-15-25 ..... p 42 A83-14502
NAS1-15669 ..... p 47 N83-13773
NAS1-16312 ..... p 21 N83-10645
p 21 N83-10646
NAS1-5345 ..... p 2 A83-10117
NAS2-10741 ..... p 67 N83-15794
p 67 N83-15796
NAS2-11101 ..... p 16 N83-15741
NAS5-15977 ..... p 27 N83-14594
NAS5-22963 ..... p 43 A83-18580
NAS5-24206 ..... p 51 A83-14668
NAS5-24316 ..... p 50 *A83-10102*
NAS5-25050 ..... p 72 N83-15797
NAS5-25888 ..... p 26 N83-13537
p 26 N83-13539
NAS5-25891 ..... p 27 N83-14596
NAS5-25957 ..... p 29 N83-15742
NAS5-26025 ..... p 56 A83-12678
NAS5-26032 ..... p 60 A83-16904
NAS5-26047 ..... p 28 N83-14601
NAS5-26062 ..... p 53 N83-14572
NAS5-26123 ..... p 42 A83-14861
NAS5-26157 ..... p 26 N83-13527
NAS5-26250 ..... p 29 N83-15755
NAS5-26326 ..... p 26 N83-13532
NAS5-26414 ..... p 34 N83-13528
NAS5-26424 ..... p 28 N83-14602
NAS5-26453 ..... p 62 N83-13522
p 64 N83-15745
NAS5-26468 ..... p 17 N83-15747
NAS5-26473 ..... p 53 N83-13520
NAS5-26579 ..... p 29 N83-15748
NAS5-26728 ..... p 35 N83-14556
NAS5-26859 ..... p 63 N83-13533
NAS5-26863 ..... p 46 N83-13534
NAS7-100 ..... p 30 A83-10057
p 23 A83-10078
p 54 A83-10084
p 31 A83-10099
p 54 A83-10121
p 68 A83-12676
p 63 N83-13531
NAS8-33992 ..... p 68 A83-12605
NAS9-14251 ..... p 9 N83-12491
NAS9-14689 ..... p 9 N83-12494
p 10 N83-12497
p 62 N83-12498
p 11 N83-12505
NAS9-15421 ..... p 8 N83-12485
p 10 N83-12499
NAS9-15466 ..... p 1 A83-10096
p 59 A83-14853
p 60 A83-16905
p 8 N83-12484
p 11 N83-12504
p 11 N83-12506
p 63 N83-14595
NAS9-15800 ..... p 54 A83-11410
p 8 N83-12487
p 62 N83-12490
p 9 N83-12493
p 10 N83-12502
p 62 N83-12866
p 16 N83-15743
p 18 N83-15793
NAS9-16369 ..... p 17 N83-15756
NAS9-16419 ..... p 10 N83-12503
NAS9-16447 ..... p 64 N83-15759
p 65 N83-15766
p 66 N83-15774
NAS9-16505 ..... p 17 N83-15753
NAS9-16538 ..... p 10 N83-12500
p 10 N83-12501
NAVAIR TASK WF59553000 ..... p 42 A83-14502
NAVY PROJECT RR-032-08-41 ..... p 42 A83-14502
NA78-SAC-04102 ..... p 71 N83-13767
NA80AA-D-00035 ..... p 71 N83-13750
NA81RAC000-13 ..... p 47 N83-13572
NERC-GR/3/4076 ..... p 7 A83-16908
NGL-02-001-092 ..... p 55 A83-12035
NGL-17-004-024 ..... p 23 N83-15757
NGL-33-010-171 ..... p 18 N83-15790
NGL-42-003-007 ..... p 6 A83-14665
NGT-06-002-800 ..... p 3 A83-12603
NOAA-MO-A01-78-00-4339 ..... p 38 A83-10068
NOAA-NA-79SA00741 ..... p 43 A83-18580
NOAA-03-7-022-35111 ..... p 40 A83-11352
NOAA-04-8M01-129 ..... p 43 A83-18580
NR PROJECT 083-102 ..... p 41 A83-13270
NSERC-A-6043 ..... p 57 A83-14260
NSF ATM-77-28522 ..... p 50 A83-10090
NSF ATM-80-01470 ..... p 50 A83-10090
NSF ATM-80-24881 ..... p 71 N83-13750
NSF BA-28004 ..... p 41 A83-13270
NSF DPP-68-00508 ..... p 25 N83-12107
NSF DPP-79-19816 ..... p 18 A83-11626
NSF ECS-80-14579 ..... p 24 A83-14857
NSF ENG-78-23145 ..... p 1 A83-10106
NSF MCS 81-01854 ..... p 30 N83-15763
NSF MCS-78-04366 ..... p 59 A83-14853
p 63 N83-14595
NSF OCE-80-16991 ..... p 43 A83-18580
NSG-5049 ..... p 40 A83-12316
NSG-5134 ..... p 17 N83-15751
NSG-5265 ..... p 26 N83-13537
NSG-5335 ..... p 49 A83-10064
NSG-7226 ..... p 23 N83-15752
N00014-C-0435 ..... p 18 A83-11626
N00014-75-C-0300 ..... p 49 N83-15799
N00014-76-C-0067 ..... p 41 A83-13270
N00014-76-C-1048 ..... p 38 A83-10068
N00014-80-C-0042 ..... p 43 A83-18580
N00014-80-C-0440 ..... p 49 N83-15799
N00014-81-C-2350 ..... p 44 N83-10739
N00014-82-C-0114 ..... p 45 N83-11692
N0024-81-C-5301 ..... p 42 A83-14851
OSURF PROJ. 711055 ..... p 26 N83-13537
OSURF PROJ. 712407 ..... p 26 N83-13537
PROJ. AGRISTARS ..... p 7 N83-12482
p 7 N83-12483
p 8 N83-12484
p 8 N83-12485
p 8 N83-12486
p 8 N83-12488
p 9 N83-12489
p 62 N83-12490
p 9 N83-12491
p 9 N83-12492
p 9 N83-12493
p 9 N83-12494
p 10 N83-12499
p 10 N83-12500
p 10 N83-12501
p 10 N83-12502
p 10 N83-12503
p 11 N83-12504
p 11 N83-12505
p 11 N83-12506
p 62 N83-12866
p 11 N83-13529
p 12 N83-13535
p 12 N83-13536
p 12 N83-14554
p 12 N83-14557
p 12 N83-14558
p 13 N83-14559
p 75 N83-14560
p 13 N83-14561
p 13 N83-14562
p 13 N83-14563
p 13 N83-14564
p 13 N83-14565
p 14 N83-14567
p 14 N83-14568
p 14 N83-14569
p 16 N83-15740
p 16 N83-15743
p 18 N83-15793
PROJECT VOYAGER ..... p 24 A83-16239
SG-NA79AA-D-00096 ..... p 44 N83-10483
USDA-12-14-5001-38 ..... p 3 A83-12315
USDA-53-3148-200 ..... p 2 A83-10117
USDA-53-3187-0-29 ..... p 19 A83-12672
USGS-14-08-001-16439 ..... p 56 A83-12685
W-7405-ENG-36 ..... p 34 N83-12512
p 37 N83-14797
W-7405-ENG-48 ..... p 25 N83-10693
004-72-470 ..... p 16 N83-15743

146-40-15-07	p 44	N83-10647
658-70-04	p 16	N83-15741
658-80-05	p 67	N83-15794
	p 67	N83-15796
677-16-15	p 22	N83-12507

Typical Report/Accession Number Index Listing

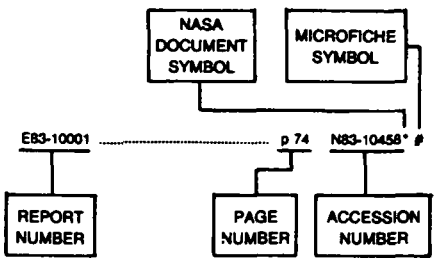

Listings in this index are arranged alphanumerically by report number. The page number indicates the page on which the citation is located. The accession number denotes the number by which the citation is identified. An asterisk (*) indicates that the item is a NASA report. A pound sign (#) indicates that the item is available on microfiche.

A-8920 ..... p 22 N83-12507* #
A-9182 ..... p 16 N83-15741* #

AAS 82-128 ..... p 73 A83-11932 #
AAS 82-129 ..... p 73 A83-11933 #

AD-A117743 ..... p 44 N83-10739 #
AD-A117837 ..... p 25 N83-11571 #
AD-A117910 ..... p 45 N83-11570 #
AD-A117981 ..... p 45 N83-12037 #
AD-A118160 ..... p 45 N83-11568 #
AD-A118318 ..... p 52 N83-11569 #
AD-A118411 ..... p 45 N83-11692 #
AD-A118736 ..... p 45 N83-12511 #
AD-A119257 ..... p 27 N83-13550 #
AD-A119444 ..... p 29 N83-14656 #
AD-A119714 ..... p 16 N83-14653 #
AD-A119727 ..... p 16 N83-14655 #
AD-A120068 ..... p 49 N83-15799 #

AGES-820526 ..... p 13 N83-14561* #

AIAA PAPER 83-0197 ..... p 42 A83-16581* #
AIAA PAPER 83-0278 ..... p 70 A83-19585 #
AIAA PAPER 83-0415 ..... p 42 A83-16701* #
AIAA PAPER 83-0436 ..... p 21 A83-16713 #
AIAA PAPER 83-0439 ..... p 21 A83-16714 #

AP-L2-04116 ..... p 10 N83-12502* #

AR-11 ..... p 75 N83-11532 #

ARL-TR-81-49 ..... p 25 N83-12107 #

ARSL-TR-81-2 ..... p 35 N83-14570* #

ASTRON-GEODAET-ARB-41 ..... p 25 N83-11563 #

BM-IC-8869 ..... p 33 N83-10485 #

BR82059 ..... p 47 N83-14553 #

BTS-FR-81-147 ..... p 29 N83-15755* #

BTS33-82-60/BR ..... p 28 N83-14601* #
BTS33-82-79/RB ..... p 27 N83-14566* #

CONF-811133-1 ..... p 37 N83-14797 #

CONTRIB-616 ..... p 71 N83-13767* #

CRSC-82-4 ..... p 17 N83-15749* #

DC-L2-04264 ..... p 8 N83-12487* #

DC-Y2-04325 ..... p 16 N83-15740* #

DE82-002393 ..... p 37 N83-14797 #
DE82-018392 ..... p 25 N83-10693 #
DE82-018598 ..... p 34 N83-12584 #
DE82-020961 ..... p 34 N83-12512 #
DE82-021614 ..... p 34 N83-12513 #

DOE/NV-10220/1 ..... p 34 N83-12584 #

ERIM-138600-6-F ..... p 47 N83-13776* #
ERIM-155800-1-F1 ..... p 44 N83-10739 #
ERIM-157800-1-F ..... p 63 N83-13531* #
ERIM-160300-18-P ..... p 10 N83-12500* #
ERIM-160300-19-T ..... p 10 N83-12501* #

ESA-SP-175 ..... p 75 N83-14608 #

ETL-R038 ..... p 16 N83-14655 #
ETL-R039 ..... p 16 N83-14653 #

ETL-0285 ..... p 52 N83-11569 #
ETL-0298 ..... p 27 N83-13550 #

EW-L2-04340 ..... p 16 N83-15743* #

EW-R2-04345 ..... p 75 N83-14560* #

EW-U2-04298 ..... p 8 N83-12488* #
EW-U2-04319 ..... p 7 N83-12482* #
EW-U2-04320 ..... p 12 N83-13536* #
EW-U2-04327 ..... p 9 N83-12492* #
EW-U2-04328 ..... p 9 N83-12489* #
EW-U2-04334 ..... p 13 N83-14562* #
EW-U2-04335 ..... p 13 N83-14564* #
EW-U2-04349 ..... p 13 N83-14559* #
EW-U2-04350 ..... p 14 N83-14567* #
EW-U2-04351 ..... p 12 N83-14558* #

E83-10001 ..... p 74 N83-10458* #
E83-10002 ..... p 7 N83-12482* #
E83-10003 ..... p 7 N83-12483* #
E83-10004 ..... p 8 N83-12484* #
E83-10005 ..... p 8 N83-12485* #
E83-10006 ..... p 8 N83-12486* #
E83-10007 ..... p 62 N83-12866* #
E83-10008 ..... p 8 N83-12487* #
E83-10009 ..... p 8 N83-12488* #
E83-10010 ..... p 9 N83-12489* #
E83-10011 ..... p 62 N83-12490* #
E83-10012 ..... p 9 N83-12491* #
E83-10013 ..... p 9 N83-12492* #
E83-10014 ..... p 9 N83-12493* #
E83-10015 ..... p 9 N83-12494* #
E83-10016 ..... p 10 N83-12499* #
E83-10017 ..... p 10 N83-12500* #
E83-10018 ..... p 10 N83-12501* #
E83-10019 ..... p 10 N83-12502* #
E83-10020 ..... p 10 N83-12503* #
E83-10021 ..... p 11 N83-12504* #
E83-10022 ..... p 11 N83-12505* #
E83-10023 ..... p 11 N83-12506* #
E83-10024 ..... p 22 N83-12507* #
E83-10025 ..... p 11 N83-13519* #
E83-10026 ..... p 53 N83-13520* #
E83-10027 ..... p 25 N83-13521* #
E83-10028 ..... p 62 N83-13522* #
E83-10029 ..... p 34 N83-13523* #
E83-10030 ..... p 25 N83-13524* #
E83-10031 ..... p 26 N83-13525* #
E83-10032 ..... p 26 N83-13526* #
E83-10033 ..... p 26 N83-13527* #
E83-10034 ..... p 34 N83-13528* #
E83-10035 ..... p 11 N83-13529* #
E83-10036 ..... p 62 N83-13530* #
E83-10037 ..... p 63 N83-13531* #
E83-10038 ..... p 26 N83-13532* #
E83-10039 ..... p 63 N83-13533* #
E83-10040 ..... p 46 N83-13534* #
E83-10041 ..... p 12 N83-13535* #
E83-10044 ..... p 12 N83-14554* #
E83-10045 ..... p 12 N83-13536* #
E83-10046 ..... p 47 N83-14555* #

E83-10047 ..... p 35 N83-14556* #
E83-10048 ..... p 12 N83-14557* #
E83-10049 ..... p 12 N83-14558* #
E83-10050 ..... p 13 N83-14559* #
E83-10051 ..... p 75 N83-14560* #
E83-10052 ..... p 13 N83-14561* #
E83-10053 ..... p 13 N83-14562* #
E83-10054 ..... p 13 N83-14563* #
E83-10055 ..... p 13 N83-14564* #
E83-10056 ..... p 13 N83-14565* #
E83-10057 ..... p 27 N83-14566* #
E83-10058 ..... p 14 N83-14567* #
E83-10059 ..... p 14 N83-14568* #
E83-10060 ..... p 14 N83-14569* #
E83-10061 ..... p 35 N83-14570* #
E83-10062 ..... p 22 N83-14571* #
E83-10063 ..... p 53 N83-14572* #
E83-10064 ..... p 63 N83-14573* #
E83-10065 ..... p 14 N83-14574* #
E83-10066 ..... p 35 N83-14575* #
E83-10067 ..... p 14 N83-14576* #
E83-10068 ..... p 14 N83-14577* #
E83-10069 ..... p 35 N83-14578* #
E83-10070 ..... p 15 N83-14579* #
E83-10071 ..... p 35 N83-14580* #
E83-10072 ..... p 23 N83-14581* #
E83-10073 ..... p 36 N83-14582* #
E83-10074 ..... p 48 N83-14583* #
E83-10075 ..... p 63 N83-14584* #
E83-10076 ..... p 15 N83-14585* #
E83-10077 ..... p 15 N83-14586* #
E83-10078 ..... p 36 N83-14587* #
E83-10079 ..... p 72 N83-14588* #
E83-10080 ..... p 27 N83-14589* #
E83-10082 ..... p 36 N83-14590* #
E83-10083 ..... p 27 N83-14591* #
E83-10084 ..... p 27 N83-14592* #
E83-10085 ..... p 36 N83-14593* #
E83-10086 ..... p 27 N83-14594* #
E83-10087 ..... p 63 N83-14595* #
E83-10088 ..... p 27 N83-14596* #
E83-10089 ..... p 28 N83-14597* #
E83-10090 ..... p 36 N83-14598* #
E83-10091 ..... p 28 N83-14599* #
E83-10093 ..... p 28 N83-14600* #
E83-10094 ..... p 28 N83-14601* #
E83-10095 ..... p 28 N83-14602* #
E83-10096 ..... p 16 N83-15740* #
E83-10097 ..... p 16 N83-15741* #
E83-10098 ..... p 29 N83-15742* #
E83-10100 ..... p 16 N83-15743* #
E83-10101 ..... p 29 N83-15744* #
E83-10102 ..... p 64 N83-15745* #
E83-10103 ..... p 64 N83-15746* #
E83-10104 ..... p 17 N83-15747* #
E83-10105 ..... p 29 N83-15748* #
E83-10106 ..... p 17 N83-15749* #
E83-10107 ..... p 17 N83-15750* #
E83-10108 ..... p 17 N83-15751* #
E83-10109 ..... p 23 N83-15752* #
E83-10110 ..... p 17 N83-15753* #
E83-10111 ..... p 54 N83-15754* #
E83-10112 ..... p 29 N83-15755* #
E83-10113 ..... p 17 N83-15756* #
E83-10114 ..... p 23 N83-15757* #
E83-10115 ..... p 18 N83-15758* #
E83-10117 ..... p 64 N83-15759* #
E83-10118 ..... p 65 N83-15766* #
E83-10119 ..... p 66 N83-15774* #
E83-10120 ..... p 18 N83-15790* #
E83-10121 ..... p 66 N83-15791* #
E83-10122 ..... p 67 N83-15792* #
E83-10123 ..... p 18 N83-15793* #
E83-10124 ..... p 67 N83-15794* #
E83-10125 ..... p 76 N83-15739* #
E83-10126 ..... p 37 N83-15795* #
E83-10127 ..... p 67 N83-15796* #
E83-10128 ..... p 72 N83-15797* #

GARP-FOR-5 ..... p 46 N83-12808

GARP-PUB-SER-25 ..... p 45 N83-12724

GARP-SPEC-REPT-38 ..... p 45 N83-12707

GJBX-156-82 ..... p 34 N83-12512 #
GJBX-195-82-VOL-1 ..... p 34 N83-12513 #

HAC-E1966 ..... p 72 N83-15797* #

IFAORS-207 ..... p 3 A83-14121

INPE-2261-MD/016 ..... p 23 N83-14581* #
INPE-2264-PRE/045 ..... p 15 N83-14579* #
INPE-2368-MD/019 ..... p 48 N83-14583* #
INPE-2409-PRE/118 ..... p 14 N83-14577* #
INPE-2410-PRE/119 ..... p 35 N83-14575* #
INPE-2413-PRE/121 ..... p 15 N83-14585* #
INPE-2417-PRE/125 ..... p 36 N83-14582* #
INPE-2418-PRE/126 ..... p 35 N83-14578* #
INPE-2419-PRE/127 ..... p 36 N83-14587* #
INPE-2428-NTE/185 ..... p 63 N83-13707 #
INPE-2435-NTE/186 ..... p 22 N83-13703 #
INPE-2444-TDL/093 ..... p 54 N83-15754* #
INPE-2446-PRE/145 ..... p 35 N83-14580* #
INPE-2471-PRE/160 ..... p 72 N83-14588* #
INPE-2482-PRE/166 ..... p 14 N83-14574* #
INPE-2489-PRE/172 ..... p 15 N83-14586* #
INPE-2490-PRE/173 ..... p 14 N83-14576* #
INPE-2514-PRE/193 ..... p 33 N83-12509 #
INPE-2524-TDL/100 ..... p 37 N83-15795* #
INPE-2526-PRE/195 ..... p 11 N83-13519* #
INPE-2528-RPE/416 ..... p 34 N83-13523* #
INPE-2553-PRE/207 ..... p 63 N83-14584* #
INPE-2554-PRE-208 ..... p 63 N83-14573* #

IR-2 ..... p 18 N83-15758* #

ISBN-3-7696-9318-3 ..... p 25 N83-11564 #
ISBN-3-7696-9319-1 ..... p 71 N83-11565 #
ISBN-3-7696-93205 ..... p 62 N83-13518 #
ISBN-3-7696-9784-7 ..... p 25 N83-11563 #
ISBN-92-63-10559-6 ..... p 53 N83-12514
ISBN-92-63-10563-4 ..... p 22 N83-12599
ISBN-92-63-10584-7 ..... p 46 N83-12803
ISBN-92-63-10587-1 ..... p 53 N83-12516
ISBN-92-63-12544-9 ..... p 46 N83-12801
ISBN-92-63-20582-5 ..... p 46 N83-12802

ISSN-0065-5325 ..... p 25 N83-11564 #
ISSN-0065-5325 ..... p 71 N83-11565 #
ISSN-0065-5325 ..... p 62 N83-13518 #
ISSN-0340-7691 ..... p 25 N83-11563 #
ISSN-0379-6566 ..... p 75 N83-14608 #

IT-E2-04310 ..... p 10 N83-12501* #
IT-E2-04311 ..... p 10 N83-12500* #

IT-T2-04323 ..... p 11 N83-12505* #

IT-U2-04332 ..... p 13 N83-14561* #

ITJ2-04267 ..... p 8 N83-12486* #

JPL-PUB-82-89 ..... p 48 N83-14604* #

JPL-9950-738 ..... p 44 N83-10473* #

JSC-13821-VOL-1-REV-A ..... p 62 N83-12866* #
JSC-16747 ..... p 62 N83-12490* #
JSC-17816 ..... p 18 N83-15793* #
JSC-17829 ..... p 8 N83-12487* #
JSC-17830 ..... p 8 N83-12486* #
JSC-18233 ..... p 12 N83-13535* #
JSC-18234 ..... p 14 N83-14569* #
JSC-18237 ..... p 13 N83-14565* #
JSC-18241 ..... p 8 N83-12488* #
JSC-18242 ..... p 12 N83-14554* #
JSC-18245 ..... p 7 N83-12483* #
JSC-18254 ..... p 7 N83-12482* #
JSC-18255 ..... p 12 N83-13536* #
JSC-18256 ..... p 14 N83-14568* #
JSC-18257 ..... p 9 N83-12493* #
JSC-18258 ..... p 9 N83-12492* #
JSC-18259 ..... p 9 N83-12489* #
JSC-18260 ..... p 13 N83-14562* #
JSC-18261 ..... p 13 N83-14564* #
JSC-18264 ..... p 11 N83-13529* #
JSC-18265 ..... p 16 N83-15743* #
JSC-18268 ..... p 75 N83-14560* #
JSC-18272 ..... p 13 N83-14563* #
JSC-18561 ..... p 13 N83-14559* #
JSC-18562 ..... p 14 N83-14567* #
JSC-18563 ..... p 12 N83-14558* #

LA-UR-81-2920 ..... p 37 N83-14797 #

LARS-CR-110982 ..... p 63 N83-13533* #

LARS-TR-070381 ..... p 63 N83-14595* #

LARS-052680 ..... p 11 N83-12504* #
LARS-113081 ..... p 11 N83-12506* #

LC-81-600117 ..... p 74 N83-10458* #
LC-82-14553 ..... p 48 N83-14835* #

LEMSCO-12653-VOL-1-REV-A ..... p 62 N83-12866* #
LEMSCO-15128 ..... p 62 N83-12490* #
LEMSCO-17502 ..... p 18 N83-15793* #
LEMSCO-17597 ..... p 8 N83-12487* #
LEMSCO-17765 ..... p 9 N83-12493* #
LEMSCO-18627 ..... p 16 N83-15743* #

MBB-UA-618/81 ..... p 71 N83-13567 #

NAS 1.15:82059 ..... p 71 N83-13547* #
NAS 1.15:83955 ..... p 17 N83-15750* #
NAS 1.15:83969 ..... p 71 N83-12396* #
NAS 1.15:84008 ..... p 47 N83-13544* #
NAS 1.15:84244 ..... p 22 N83-12507* #
NAS 1.15:84314 ..... p 16 N83-15741* #
NAS 1.15:84547 ..... p 44 N83-10647* #
NAS 1.15:84878 ..... p 8 N83-12486* #
NAS 1.15:84884 ..... p 72 N83-15344* #
NAS 1.15:85166 ..... p 12 N83-14554* #
NAS 1.15:85169 ..... p 14 N83-14569* #
NAS 1.15:85170 ..... p 11 N83-13529* #
NAS 1.15:85192 ..... p 16 N83-15740* #
NAS 1.26:165122 ..... p 72 N83-14588* #
NAS 1.26:166355 ..... p 67 N83-15794* #
NAS 1.26:166373 ..... p 67 N83-15796* #
NAS 1.26:166819 ..... p 29 N83-15748* #
NAS 1.26:166822 ..... p 17 N83-15751* #
NAS 1.26:167633 ..... p 63 N83-14595* #
NAS 1.26:167634 ..... p 17 N83-15756* #
NAS 1.26:167646 ..... p 8 N83-12484* #
NAS 1.26:167648 ..... p 9 N83-12491* #
NAS 1.26:167701 ..... p 9 N83-12494* #
NAS 1.26:167716 ..... p 17 N83-15753* #
NAS 1.26:167718 ..... p 10 N83-12499* #
NAS 1.26:167720 ..... p 9 N83-12493* #
NAS 1.26:167721 ..... p 11 N83-12506* #
NAS 1.26:167728 ..... p 10 N83-12502* #
NAS 1.26:167729 ..... p 10 N83-12501* #
NAS 1.26:167746 ..... p 16 N83-15743* #
NAS 1.26:167748 ..... p 10 N83-12503* #
NAS 1.26:167752 ..... p 8 N83-12487* #
NAS 1.26:167754 ..... p 62 N83-12490* #
NAS 1.26:167755 ..... p 62 N83-12866* #
NAS 1.26:167778 ..... p 65 N83-15766* #
NAS 1.26:167779 ..... p 64 N83-15759* #
NAS 1.26:167780 ..... p 66 N83-15774* #
NAS 1.26:169390 ..... p 71 N83-13767* #
NAS 1.26:169393 ..... p 47 N83-13572* #
NAS 1.26:169433 ..... p 44 N83-10473* #
NAS 1.26:169470 ..... p 26 N83-13537* #
NAS 1.26:169473 ..... p 46 N83-12828* #
NAS 1.26:169490 ..... p 9 N83-12489* #
NAS 1.26:169491 ..... p 8 N83-12488* #
NAS 1.26:169493 ..... p 7 N83-12482* #
NAS 1.26:169498 ..... p 11 N83-13519* #
NAS 1.26:169499 ..... p 53 N83-13520* #
NAS 1.26:169500 ..... p 25 N83-13521* #
NAS 1.26:169501 ..... p 62 N83-13522* #
NAS 1.26:169502 ..... p 34 N83-13523* #
NAS 1.26:169505 ..... p 26 N83-13526* #
NAS 1.26:169507 ..... p 34 N83-13528* #
NAS 1.26:169509 ..... p 63 N83-13531* #
NAS 1.26:169511 ..... p 63 N83-13533* #
NAS 1.26:169512 ..... p 46 N83-13534* #
NAS 1.26:169530 ..... p 47 N83-14555* #
NAS 1.26:169549 ..... p 12 N83-13535* #
NAS 1.26:169563 ..... p 35 N83-14556* #
NAS 1.26:169564 ..... p 12 N83-14557* #
NAS 1.26:169565 ..... p 12 N83-14558* #
NAS 1.26:169566 ..... p 13 N83-14559* #
NAS 1.26:169567 ..... p 75 N83-14560* #
NAS 1.26:169568 ..... p 13 N83-14561* #
NAS 1.26:169569 ..... p 13 N83-14562* #
NAS 1.26:169570 ..... p 13 N83-14564* #
NAS 1.26:169571 ..... p 13 N83-14565* #
NAS 1.26:169572 ..... p 14 N83-14568* #
NAS 1.26:169574 ..... p 22 N83-14571* #
NAS 1.26:169575 ..... p 63 N83-14573* #
NAS 1.26:169576 ..... p 14 N83-14574* #
NAS 1.26:169577 ..... p 35 N83-14575* #
NAS 1.26:169578 ..... p 14 N83-14576* #
NAS 1.26:169579 ..... p 14 N83-14577* #
NAS 1.26:169580 ..... p 35 N83-14578* #
NAS 1.26:169581 ..... p 15 N83-14579* #
NAS 1.26:169582 ..... p 35 N83-14580* #
NAS 1.26:169583 ..... p 23 N83-14581* #
NAS 1.26:169584 ..... p 36 N83-14582* #
NAS 1.26:169585 ..... p 48 N83-14583* #
NAS 1.26:169586 ..... p 63 N83-14584* #
NAS 1.26:169587 ..... p 15 N83-14585* #
NAS 1.26:169588 ..... p 15 N83-14586* #
NAS 1.26:169589 ..... p 36 N83-14587* #
NAS 1.26:169590 ..... p 27 N83-14589* #
NAS 1.26:169591 ..... p 27 N83-14566* #
NAS 1.26:169592 ..... p 14 N83-14567* #
NAS 1.26:169594 ..... p 36 N83-14590* #
NAS 1.26:169595 ..... p 27 N83-14591* #
NAS 1.26:169596 ..... p 27 N83-14592* #
NAS 1.26:169597 ..... p 27 N83-14594* #
NAS 1.26:169598 ..... p 27 N83-14596* #
NAS 1.26:169599 ..... p 28 N83-14597* #
NAS 1.26:169600 ..... p 36 N83-14598* #
NAS 1.26:169601 ..... p 28 N83-14599* #
NAS 1.26:169603 ..... p 28 N83-14600* #
NAS 1.26:169604 ..... p 28 N83-14601* #
NAS 1.26:169605 ..... p 28 N83-14602* #
NAS 1.26:169606 ..... p 12 N83-13536* #
NAS 1.26:169607 ..... p 36 N83-14593* #
NAS 1.26:169612 ..... p 13 N83-14563* #
NAS 1.26:169631 ..... p 48 N83-14603* #
NAS 1.26:169660 ..... p 48 N83-14604* #
NAS 1.26:169675 ..... p 29 N83-15742* #
NAS 1.26:169677 ..... p 29 N83-15744* #
NAS 1.26:169678 ..... p 64 N83-15745* #
NAS 1.26:169679 ..... p 64 N83-15746* #
NAS 1.26:169680 ..... p 17 N83-15749* #
NAS 1.26:169681 ..... p 23 N83-15752* #
NAS 1.26:169682 ..... p 47 N83-13776* #
NAS 1.26:169693 ..... p 28 N83-14605* #
NAS 1.26:169694 ..... p 29 N83-14606* #
NAS 1.26:169695 ..... p 54 N83-15754* #
NAS 1.26:169696 ..... p 29 N83-15755* #
NAS 1.26:169697 ..... p 23 N83-15757* #
NAS 1.26:169698 ..... p 18 N83-15758* #
NAS 1.26:169723 ..... p 18 N83-15790* #
NAS 1.26:169724 ..... p 66 N83-15791* #
NAS 1.26:169725 ..... p 67 N83-15792* #
NAS 1.26:169726 ..... p 18 N83-15793* #
NAS 1.26:169727 ..... p 76 N83-15739* #
NAS 1.26:169728 ..... p 37 N83-15795* #
NAS 1.26:170452 ..... p 53 N83-14572* #
NAS 1.26:170457 ..... p 72 N83-15797* #
NAS 1.26:170461 ..... p 17 N83-15747* #
NAS 1.26:3556 ..... p 21 N83-10645* #
NAS 1.26:3557 ..... p 21 N83-10646* #
NAS 1.61:1078 ..... p 74 N83-10458* #

NASA-CR-165122 ..... p 72 N83-14588* #
NASA-CR-166355 ..... p 67 N83-15794* #
NASA-CR-166373 ..... p 67 N83-15796* #
NASA-CR-166819 ..... p 29 N83-15748* #
NASA-CR-166822 ..... p 17 N83-15751* #
NASA-CR-167633 ..... p 63 N83-14595* #
NASA-CR-167634 ..... p 17 N83-15756* #
NASA-CR-167646 ..... p 8 N83-12484* #
NASA-CR-167648 ..... p 9 N83-12491* #
NASA-CR-167700 ..... p 11 N83-12505* #
NASA-CR-167701 ..... p 9 N83-12494* #
NASA-CR-167702 ..... p 10 N83-12500* #
NASA-CR-167713 ..... p 8 N83-12485* #
NASA-CR-167716 ..... p 17 N83-15753* #
NASA-CR-167718 ..... p 10 N83-12499* #
NASA-CR-167720 ..... p 9 N83-12493* #
NASA-CR-167721 ..... p 11 N83-12506* #
NASA-CR-167722 ..... p 11 N83-12504* #
NASA-CR-167728 ..... p 10 N83-12502* #
NASA-CR-167729 ..... p 10 N83-12501* #
NASA-CR-167746 ..... p 16 N83-15743* #
NASA-CR-167748 ..... p 10 N83-12503* #
NASA-CR-167752 ..... p 8 N83-12487* #
NASA-CR-167754 ..... p 62 N83-12490* #
NASA-CR-167755 ..... p 62 N83-12866* #
NASA-CR-167778 ..... p 65 N83-15766* #
NASA-CR-167779 ..... p 64 N83-15759* #
NASA-CR-167780 ..... p 66 N83-15774* #
NASA-CR-169390 ..... p 71 N83-13767* #
NASA-CR-169393 ..... p 47 N83-13572* #
NASA-CR-169433 ..... p 44 N83-10473* #
NASA-CR-169470 ..... p 26 N83-13537* #
NASA-CR-169473 ..... p 46 N83-12828* #
NASA-CR-169489 ..... p 9 N83-12492* #
NASA-CR-169490 ..... p 9 N83-12489* #
NASA-CR-169491 ..... p 8 N83-12488* #
NASA-CR-169492 ..... p 7 N83-12483* #
NASA-CR-169493 ..... p 7 N83-12482* #
NASA-CR-169498 ..... p 11 N83-13519* #
NASA-CR-169500 ..... p 25 N83-13521* #
NASA-CR-169501 ..... p 62 N83-13522* #
NASA-CR-169502 ..... p 34 N83-13523* #
NASA-CR-169503 ..... p 25 N83-13524* #
NASA-CR-169504 ..... p 26 N83-13525* #
NASA-CR-169505 ..... p 26 N83-13526* #
NASA-CR-169506 ..... p 26 N83-13527* #
NASA-CR-169507 ..... p 34 N83-13528* #

NASA-CR-169508 ..... p 62 N83-13530* #
NASA-CR-169509 ..... p 63 N83-13531* #
NASA-CR-169510 ..... p 26 N83-13532* #
NASA-CR-169511 ..... p 63 N83-13533* #
NASA-CR-169512 ..... p 46 N83-13534* #
NASA-CR-169530 ..... p 47 N83-14555* #
NASA-CR-169549 ..... p 12 N83-13535* #
NASA-CR-169563 ..... p 35 N83-14556* #
NASA-CR-169564 ..... p 12 N83-14557* #
NASA-CR-169565 ..... p 12 N83-14558* #
NASA-CR-169566 ..... p 13 N83-14559* #
NASA-CR-169567 ..... p 75 N83-14560* #
NASA-CR-169568 ..... p 13 N83-14561* #
NASA-CR-169569 ..... p 13 N83-14562* #
NASA-CR-169570 ..... p 13 N83-14564* #
NASA-CR-169571 ..... p 13 N83-14565* #
NASA-CR-169572 ..... p 14 N83-14568* #
NASA-CR-169573 ..... p 35 N83-14570* #
NASA-CR-169574 ..... p 22 N83-14571* #
NASA-CR-169575 ..... p 63 N83-14573* #
NASA-CR-169576 ..... p 14 N83-14574* #
NASA-CR-169577 ..... p 35 N83-14575* #
NASA-CR-169578 ..... p 14 N83-14576* #
NASA-CR-169579 ..... p 14 N83-14577* #
NASA-CR-169580 ..... p 35 N83-14578* #
NASA-CR-169581 ..... p 15 N83-14579* #
NASA-CR-169582 ..... p 35 N83-14580* #
NASA-CR-169583 ..... p 23 N83-14581* #
NASA-CR-169584 ..... p 36 N83-14582* #
NASA-CR-169585 ..... p 48 N83-14583* #
NASA-CR-169586 ..... p 63 N83-14584* #
NASA-CR-169587 ..... p 15 N83-14585* #
NASA-CR-169588 ..... p 15 N83-14586* #
NASA-CR-169589 ..... p 36 N83-14587* #
NASA-CR-169590 ..... p 27 N83-14589* #
NASA-CR-169591 ..... p 27 N83-14566* #
NASA-CR-169592 ..... p 14 N83-14567* #
NASA-CR-169594 ..... p 36 N83-14590* #
NASA-CR-169595 ..... p 27 N83-14591* #
NASA-CR-169596 ..... p 27 N83-14592* #
NASA-CR-169597 ..... p 27 N83-14594* #
NASA-CR-169598 ..... p 27 N83-14596* #
NASA-CR-169599 ..... p 28 N83-14597* #
NASA-CR-169600 ..... p 36 N83-14598* #
NASA-CR-169601 ..... p 28 N83-14599* #
NASA-CR-169603 ..... p 28 N83-14600* #
NASA-CR-169604 ..... p 28 N83-14601* #
NASA-CR-169605 ..... p 28 N83-14602* #
NASA-CR-169606 ..... p 12 N83-13536* #
NASA-CR-169607 ..... p 36 N83-14593* #
NASA-CR-169612 ..... p 13 N83-14563* #
NASA-CR-169631 ..... p 48 N83-14603* #
NASA-CR-169660 ..... p 48 N83-14604* #
NASA-CR-169675 ..... p 29 N83-15742* #
NASA-CR-169677 ..... p 29 N83-15744* #
NASA-CR-169678 ..... p 64 N83-15745* #
NASA-CR-169679 ..... p 64 N83-15746* #
NASA-CR-169680 ..... p 17 N83-15749* #
NASA-CR-169681 ..... p 23 N83-15752* #
NASA-CR-169682 ..... p 47 N83-13776* #
NASA-CR-169693 ..... p 28 N83-14605* #
NASA-CR-169694 ..... p 29 N83-14606* #
NASA-CR-169695 ..... p 54 N83-15754* #
NASA-CR-169696 ..... p 29 N83-15755* #
NASA-CR-169697 ..... p 23 N83-15757* #
NASA-CR-169698 ..... p 18 N83-15758* #
NASA-CR-169723 ..... p 18 N83-15790* #
NASA-CR-169724 ..... p 66 N83-15791* #
NASA-CR-169725 ..... p 67 N83-15792* #
NASA-CR-169726 ..... p 18 N83-15793* #
NASA-CR-169727 ..... p 76 N83-15739* #
NASA-CR-169728 ..... p 37 N83-15795* #
NASA-CR-170452 ..... p 53 N83-14572* #
NASA-CR-170457 ..... p 72 N83-15797* #
NASA-CR-170461 ..... p 17 N83-15747* #
NASA-CR-170492 ..... p 53 N83-13520* #
NASA-CR-3556 ..... p 21 N83-10645* #
NASA-CR-3557 ..... p 21 N83-10646* #

NASA-RP-1078 ..... p 74 N83-10458* #

NASA-SP-457 ..... p 48 N83-14835* #

NASA-TM-82059 ..... p 71 N83-13547* #
NASA-TM-83955 ..... p 17 N83-15750* #
NASA-TM-83969 ..... p 71 N83-12396* #
NASA-TM-84008 ..... p 47 N83-13544* #
NASA-TM-84244 ..... p 22 N83-12507* #
NASA-TM-84314 ..... p 16 N83-15741* #
NASA-TM-84547 ..... p 44 N83-10647* #
NASA-TM-84878 ..... p 8 N83-12486* #
NASA-TM-84884 ..... p 72 N83-15344* #
NASA-TM-85166 ..... p 12 N83-14554* #
NASA-TM-85169 ..... p 14 N83-14569* #
NASA-TM-85170 ..... p 11 N83-13529* #
NASA-TM-85192 ..... p 16 N83-15740* #

NOAA-TM-ERL-OWRM-11 ..... p 52 N83-10730 #

NOAA-TM-OTES-3 ..... p 52 N83-10745 #

NOAA-TR-NESS-87 ..... p 52 N83-10734 #

NOAA-TR-OTES-6 ..... p 44 N83-10707 #

NOAA-81072405 ..... p 44 N83-10483 #
NOAA-82021005 ..... p 52 N83-10745 #
NOAA-82041501 ..... p 44 N83-10707 #
NOAA-82042703 ..... p 45 N83-10740 #
NOAA-82042903 ..... p 52 N83-10730 #
NOAA-82051011 ..... p 47 N83-13572* #
NOAA-82051012 ..... p 71 N83-13767* #
NOAA-82052402 ..... p 47 N83-13776* #

NORDA-TN-162 ..... p 45 N83-12511 #
NORDA-TN-57 ..... p 45 N83-11568 #

NSSDC/WDC-A-R/S-82-25 ..... p 72 N83-15344* #

NSTL/ERL-209 ..... p 16 N83-15740* #

NSWC/TR-252 ..... p 45 N83-11570 #
NSWC/TR-81-260 ..... p 25 N83-11571 #
NSWC/TR-82-75 ..... p 29 N83-14656 #

OHR-14 ..... p 53 N83-12514
OHR-20 ..... p 53 N83-12516

PB82-185042 ..... p 34 N83-12713 #
PB82-187923 ..... p 25 N83-12107 #
PB82-189754 ..... p 52 N83-10745 #
PB82-193085 ..... p 33 N83-10485 #
PB82-196668 ..... p 52 N83-10734 #
PB82-215138 ..... p 44 N83-10707 #
PB82-216581 ..... p 52 N83-10730 #
PB82-219049 ..... p 45 N83-10740 #
PB82-219817 ..... p 71 N83-13750 #
PB82-220864 ..... p 44 N83-10483 #
PB82-230350 ..... p 47 N83-13776* #
PB82-230400 ..... p 47 N83-13572* #
PB82-237934 ..... p 71 N83-13767* #

PR-1325-6 ..... p 28 N83-14602* #
PR-1 ..... p 63 N83-13533* #
PR-3 ..... p 26 N83-13526* #
PR-6 ..... p 27 N83-14589* #
PR-6 ..... p 28 N83-14599* #
PR-7 ..... p 29 N83-15744* #

QR-7 ..... p 36 N83-14590* #

QSTPR-10 ..... p 27 N83-14594* #

RAE-SPACE-616 ..... p 47 N83-14553 #

RAE-TR-82059 ..... p 47 N83-14553 #

REPT-4 ..... p 25 N83-13521* #
REPT-8 ..... p 52 N83-11569 #

RSC-3458-129-VOL-1 ..... p 17 N83-15751* #
RSC-4242-1 ..... p 12 N83-14557* #
RSC-4496-132 ..... p 17 N83-15756* #

RSL-TR-360-18 ..... p 8 N83-12485* #
RSL-TR-551-2 ..... p 10 N83-12503* #

SASR-6 ..... p 26 N83-13537* #
SASR-9 ..... p 26 N83-13537* #

SER-C-266 ..... p 25 N83-11564 #
SER-C-267 ..... p 71 N83-11565 #
SER-C-268 ..... p 62 N83-13518 #

SER-15 ..... p 22 N83-12599

SIO-REF-82-15 ..... p 49 N83-15799 #

SM-A2-04322 ..... p 9 N83-12491* #

SM-K2-04356 ..... p 10 N83-12503* #

SM-L2-04234 ..... p 18 N83-15793* #

SM-T2-04363 ..... p 12 N83-14557* #

SR-J2-04300 ..... p 12 N83-14554* #
SR-J2-04337 ..... p 11 N83-13529* #

SR-K2-04313 ..... p 8 N83-12485* #
SR-K2-04336 ..... p 10 N83-12499* #

SR-L2-00750 ..... p 9 N83-12493* #

SR-P1-04090 ..... p 8 N83-12484* #
SR-P2-04266 ..... p 11 N83-12506* #
SR-P2-04326 ..... p 11 N83-12504* #

SR-T2-04371 ..... p 9 N83-12494* #

UCRL-53217 ..... p 25 N83-10693 #

URI-MTR-77 ..... p 44 N83-10483 #

USGS-CIRC-865 ..... p 21 N83-11639 #

WMO-544-VOL-1-ANNEX ..... p 46 N83-12801
WMO-559 ..... p 53 N83-12514
WMO-563 ..... p 22 N83-12599
WMO-582 ..... p 46 N83-12802
WMO-584 ..... p 46 N83-12803
WMO-587 ..... p 53 N83-12516

YM-I2-04348 ..... p 13 N83-14563* #

YM-U2-04286 ..... p 12 N83-13535* #
YM-U2-04287 ..... p 14 N83-14569* #
YM-U2-04290 ..... p 13 N83-14565* #

YM-1-4-4(80-01.1) ..... p 12 N83-13535* #
YM-12-04306 ..... p 7 N83-12483* #
YM-12-04321 ..... p 14 N83-14568* #

YMD-1-4-1(81-12.2) ..... p 14 N83-14569* #
YMD-1-4-2(82-1.2) ..... p 13 N83-14565* #

Typical Accession Number Index Listing

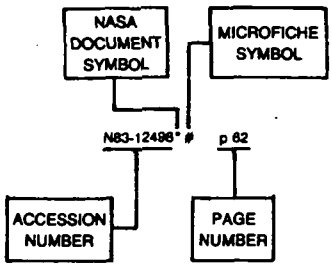

Listings in this index are arranged alphanumerically by accession number. The page number listed to the right indicates the page on which the citation is located. An asterisk (*) indicates that the item is a NASA report. A pound sign (#) indicates that the item is available on microfiche.

A83-10057* # p 30
A83-10058* # p 30
A83-10059 # p 30
A83-10060 # p 30
A83-10061* # p 1
A83-10064* # p 49
A83-10065 # p 50
A83-10068 # p 38
A83-10071 # p 38
A83-10072* # p 50
A83-10073 # p 50
A83-10075* # p 54
A83-10078* # p 23
A83-10079* # p 30
A83-10080* # p 31
A83-10083 # p 18
A83-10084* # p 54
A83-10088 # p 38
A83-10090 # p 50
A83-10091* # p 38
A83-10092* # p 38
A83-10093* # p 38
A83-10094 # p 39
A83-10095* # p 1
A83-10096* # p 1
A83-10097 # p 1
A83-10098 # p 67
A83-10099* # p 31
A83-10101 # p 50
A83-10102* # p 50
A83-10104* # p 39
A83-10106 # p 1
A83-10107* # p 1
A83-10108* # p 2
A83-10109 # p 2
A83-10113 # p 39
A83-10115 # p 39
A83-10117* # p 2
A83-10118* # p 2
A83-10119 # p 2
A83-10120 # p 50
A83-10121* # p 54
A83-10429 # p 72
A83-10715 # p 67
A83-10716 # p 67
A83-10717 # p 2
A83-10718 # p 68
A83-10826 p 39
A83-10828 # p 39
A83-10832 # p 40
A83-10833 # p 40
A83-10836 # p 40
A83-10981 # p 24
A83-11239 # p 68
A83-11352 # p 40
A83-11410* # p 54
A83-11450 # p 54
A83-11458 # p 55
A83-11461 # p 55
A83-11462 # p 55
A83-11626 # p 18
A83-11866 # p 19
A83-11867 # p 68
A83-11926 p 73
A83-11932 # p 73
A83-11933 # p 73
A83-11959 # p 31
A83-11988 # p 31
A83-12032 # p 40
A83-12035* # p 55
A83-12036* # p 31
A83-12037 # p 55
A83-12038 # p 50
A83-12315* # p 3
A83-12316* # p 40
A83-12602 # p 55
A83-12603* # p 3
A83-12604* # p 3
A83-12605* # p 68
A83-12641 # p 31
A83-12669 p 68
A83-12671* # p 19
A83-12672 # p 19
A83-12673* # p 73
A83-12676* # p 68
A83-12678* # p 56
A83-12683 # p 56
A83-12685 # p 56
A83-12877 # p 24
A83-12882 # p 56
A83-12885 # p 56
A83-12889 # p 56
A83-13057 # p 40
A83-13059* # p 41
A83-13270 # p 41
A83-13347* # p 68
A83-13348* # p 32
A83-13349* # p 32
A83-13350* # p 32
A83-13715* # p 73
A83-13726 p 69
A83-13735* # p 69
A83-13845 # p 56
A83-14040* # p 69
A83-14093 # p 41
A83-14095 # p 19
A83-14121 p 3
A83-14226 p 73
A83-14227 # p 74
A83-14228 # p 19
A83-14229 # p 3
A83-14230 # p 19
A83-14231 # p 3
A83-14232 # p 19
A83-14233 # p 3
A83-14234 # p 51
A83-14235 # p 3
A83-14236 # p 4
A83-14237 # p 24
A83-14238 # p 19
A83-14239 # p 41
A83-14240 # p 4
A83-14241 # p 4
A83-14242 # p 20
A83-14243 # p 57
A83-14244 # p 4
A83-14245 # p 4
A83-14246 # p 4
A83-14247 # p 57
A83-14248 # p 5
A83-14249 # p 5
A83-14250 # p 20
A83-14251 # p 51
A83-14252 # p 5
A83-14253 # p 5
A83-14254 # p 5
A83-14255 # p 5
A83-14256 # p 32
A83-14257 # p 5
A83-14258 # p 41
A83-14259 # p 5
A83-14260 # p 57
A83-14261 # p 5
A83-14262 # p 51
A83-14263 # p 20
A83-14264 # p 6
A83-14265 # p 57
A83-14266 # p 32
A83-14268 # p 32
A83-14269 # p 6
A83-14270 # p 57
A83-14271 # p 57
A83-14272 # p 58
A83-14273 # p 58
A83-14275 # p 69
A83-14277 # p 20
A83-14278 # p 41
A83-14280 # p 58
A83-14281 # p 58
A83-14284 # p 41
A83-14285 # p 58
A83-14286 # p 58
A83-14287 # p 51
A83-14289 # p 69
A83-14290 # p 69
A83-14292 # p 20
A83-14293 # p 70
A83-14301 # p 6
A83-14302 # p 33
A83-14303 # p 24
A83-14304 # p 59
A83-14305 # p 20
A83-14306 # p 6
A83-14307 # p 6
A83-14308 # p 70
A83-14310 # p 6
A83-14311 # p 59
A83-14313 # p 70
A83-14314 # p 70
A83-14315 # p 33
A83-14316 # p 42
A83-14502* # p 42
A83-14504 # p 20
A83-14574 # p 51
A83-14598* # p 59
A83-14632 # p 21
A83-14664 # p 59
A83-14665* # p 6
A83-14666 # p 6
A83-14667 # p 33
A83-14668* # p 51
A83-14851* # p 42
A83-14852* # p 33
A83-14853* # p 59
A83-14854 # p 51
A83-14856 # p 6
A83-14857 # p 24
A83-14859 # p 7
A83-14861* # p 42
A83-14943 # p 70
A83-14944 # p 59
A83-14945 # p 59
A83-14946 # p 59
A83-15058 # p 42
A83-15458 # p 70
A83-15816 # p 52
A83-15889 # p 7
A83-16239* # p 24
A83-16581* # p 42
A83-16701* # p 42
A83-16713 # p 21
A83-16714 # p 21
A83-16831* # p 60
A83-16904* # p 60
A83-16905* # p 60
A83-16907 # p 7
A83-16908 # p 7
A83-16909 # p 7
A83-16910* # p 7
A83-17248 # p 21
A83-17299 # p 60
A83-17349 p 74
A83-17426 # p 74
A83-17679 # p 24
A83-17709 # p 43
A83-17710* # p 43
A83-17712 # p 43
A83-17713* # p 52
A83-17714* # p 43
A83-17775 # p 74
A83-17840 # p 43
A83-17841 # p 33
A83-17842 # p 33
A83-18580* # p 43
A83-18581* # p 44
A83-19585 # p 70
N83-10458* # p 74
N83-10459* # p 60
N83-10460* # p 60
N83-10461* # p 61
N83-10462* # p 61
N83-10463* # p 61
N83-10464* # p 61
N83-10465* # p 61
N83-10466* # p 52
N83-10467* # p 74
N83-10468* # p 74
N83-10469* # p 75
N83-10470* # p 75
N83-10471* # p 75
N83-10473* # p 44
N83-10483 # p 44
N83-10485 # p 33
N83-10645* # p 21
N83-10646* # p 21
N83-10647* # p 44
N83-10693 # p 25
N83-10707 # p 44
N83-10730 # p 52
N83-10734 # p 52
N83-10739 # p 44
N83-10740 # p 45
N83-10745 # p 52
N83-11391 # p 61
N83-11400 # p 61
N83-11532 # p 75
N83-11563 # p 25
N83-11564 # p 25
N83-11565 # p 71
N83-11568 # p 45
N83-11569 # p 52
N83-11570 # p 45
N83-11571 # p 25
N83-11639 # p 21
N83-11692 # p 45
N83-12037 # p 45
N83-12107 # p 25
N83-12115 # p 75
N83-12396* # p 71
N83-12482* # p 7
N83-12483* # p 7
N83-12484* # p 8
N83-12485* # p 8
N83-12486* # p 8
N83-12487* # p 8
N83-12488* # p 8
N83-12489* # p 9
N83-12490* # p 62
N83-12491* # p 9
N83-12492* # p 9
N83-12493* # p 9
N83-12494* # p 9
N83-12495* # p 9
N83-12496* # p 9
N83-12497* # p 10
N83-12498* # p 62
N83-12499* # p 10
N83-12500* # p 10
N83-12501* # p 10
N83-12502* # p 10
N83-12503* # p 10
N83-12504* # p 11
N83-12505* # p 11
N83-12506* # p 11
N83-12507* # p 22
N83-12508 # p 62
N83-12509 # p 33
N83-12511 # p 45
N83-12512 # p 34
N83-12513 # p 34
N83-12514 p 53
N83-12516 p 53
N83-12584 # p 34
N83-12599 p 22
N83-12620 p 22
N83-12648 p 22
N83-12650 p 22
N83-12707 p 45
N83-12713 # p 34
N83-12724 p 45
N83-12735 p 46
N83-12801 p 46
N83-12802 p 46
N83-12803 p 46
N83-12808 p 46
N83-12828* # p 46
N83-12866* # p 62
N83-13517 # p 11
N83-13518 # p 62
N83-13519* # p 11
N83-13520* # p 53
N83-13521* # p 25
N83-13522* # p 62
N83-13523* # p 34
N83-13524* # p 25
N83-13525* # p 26
N83-13526* # p 26
N83-13527* # p 26
N83-13528* # p 34
N83-13529* # p 11
N83-13530* # p 62
N83-13531* # p 63
N83-13532* # p 26
N83-13533* # p 63
N83-13534* # p 46
N83-13535* # p 12
N83-13536* # p 12
N83-13537* # p 26
N83-13538* # p 26
N83-13539* # p 26
N83-13540* # p 26
N83-13544* # p 47
N83-13547* # p 71
N83-13550 # p 27
N83-13567 # p 71
N83-13572* # p 47
N83-13703 # p 22
N83-13707 # p 63

N83-13750 # p 71
N83-13767* # p 71
N83-13773* # p 47
N83-13776* # p 47
N83-14553 # p 47
N83-14554* # p 12
N83-14555* # p 47
N83-14556* # p 35
N83-14557* # p 12
N83-14558* # p 12
N83-14559* # p 13
N83-14560* # p 75
N83-14561* # p 13
N83-14562* # p 13
N83-14563* # p 13
N83-14564* # p 13
N83-14565* # p 13
N83-14566* # p 27
N83-14567* # p 14
N83-14568* # p 14
N83-14569* # p 14
N83-14570* # p 35
N83-14571* # p 22
N83-14572* # p 53
N83-14573* # p 63
N83-14574* # p 14
N83-14575* # p 35
N83-14576* # p 14
N83-14577* # p 14
N83-14578* # p 35
N83-14579* # p 15
N83-14580* # p 35
N83-14581* # p 23
N83-14582* # p 36
N83-14583* # p 48
N83-14584* # p 63
N83-14585* # p 15
N83-14586* # p 15
N83-14587* # p 36
N83-14588* # p 72
N83-14589* # p 27
N83-14590* # p 36
N83-14591* # p 27
N83-14592* # p 27
N83-14593* # p 36
N83-14594* # p 27
N83-14595* # p 63
N83-14596* # p 27
N83-14597* # p 28
N83-14598* # p 36
N83-14599* # p 28
N83-14600* # p 28
N83-14601* # p 28
N83-14602* # p 28
N83-14603* # p 48
N83-14604* # p 48
N83-14605* # p 28
N83-14606* # p 29
N83-14608 # p 75
N83-14609 # p 75
N83-14610 # p 75
N83-14611 # p 76
N83-14612* # p 72
N83-14614 # p 76
N83-14615 # p 23
N83-14616 # p 76
N83-14617 # p 63
N83-14618 # p 64
N83-14619 # p 15
N83-14620 # p 36
N83-14621 # p 53
N83-14622 # p 23
N83-14623 # p 23
N83-14624 # p 15
N83-14625 # p 15
N83-14626 # p 15
N83-14627 # p 36
N83-14628 # p 37
N83-14629 # p 37
N83-14630 # p 53
N83-14631 # p 76
N83-14632 # p 76
N83-14633 # p 76
N83-14634 # p 37
N83-14635 # p 64
N83-14636 # p 48
N83-14637 # p 64
N83-14653 # p 16
N83-14655 # p 16
N83-14656 # p 29
N83-14797 # p 37
N83-14804 # p 72
N83-14805 # p 72
N83-14808 # p 29
N83-14830* # p 64
N83-14832* # p 48
N83-14835* # p 48
N83-14837* # p 48
N83-14841* # p 48
N83-14842* # p 49
N83-14845* # p 49
N83-14847* # p 49
N83-14848* # p 49
N83-15344* # p 72
N83-15349* # p 76
N83-15739* # p 76
N83-15740* # p 16
N83-15741* # p 16
N83-15742* # p 29
N83-15743* # p 16
N83-15744* # p 29
N83-15745* # p 64
N83-15746* # p 64
N83-15747* # p 17
N83-15748* # p 29
N83-15749* # p 17
N83-15750* # p 17
N83-15751* # p 17
N83-15752* # p 23
N83-15753* # p 17
N83-15754* # p 54
N83-15755* # p 29
N83-15756* # p 17
N83-15757* # p 23
N83-15758* # p 18
N83-15759* # p 64
N83-15760* # p 18
N83-15761* # p 65
N83-15762* # p 65
N83-15763* # p 30
N83-15764* # p 65
N83-15765* # p 65
N83-15766* # p 65
N83-15767* # p 65
N83-15768* # p 65
N83-15769* # p 65
N83-15770* # p 65
N83-15771* # p 65
N83-15772* # p 66
N83-15773* # p 66
N83-15774* # p 66
N83-15775* # p 66
N83-15776* # p 66
N83-15777* # p 66
N83-15778* # p 66
N83-15790* # p 18
N83-15791* # p 66
N83-15792* # p 67
N83-15793* # p 18
N83-15794* # p 67
N83-15795* # p 37
N83-15796* # p 67
N83-15797* # p 72
N83-15799 # p 49

1. Report No.	2. Government Accession No.	3. Recipient's Catalog No.
NASA SP-7041(37)		

4. Title and Subtitle	5. Report Date
EARTH RESOURCES A Continuing Bibliography (Issue 37)	April 1983
	6. Performing Organization Code
7. Author(s)	8. Performing Organization Report No.
	10. Work Unit No.
9. Performing Organization Name and Address National Aeronautics and Space Administration Washington, D.C. 20546	11. Contract or Grant No.
	13. Type of Report and Period Covered
12. Sponsoring Agency Name and Address	14. Sponsoring Agency Code

15. Supplementary Notes

16. Abstract

This bibliography lists 512 reports, articles,and other documents introduced into the NASA scientific and technical information system between January 1 and March 31, 1983. Emphasis is placed on the use of remote sensing and geophysical instrumentation in spacecraft and aircraft to survey and inventory natural resources and urban areas. Subject matter is grouped according to agriculture and forestry, environmental changes and cultural resources, geodesy and cartography, geology and mineral resources, hydrology and water management, data processing and distribution systems, instrumentation and sensors, and economic analysis.

17. Key Words (Suggested by Author(s))	18. Distribution Statement
Bibliographies Earth Resources Remote Sensors	Unclassified - Unlimited

19. Security Classif. (of this report)	20. Security Classif. (of this page)	21. No. of Pages	22. Price*
Unclassified	Unclassified	146	$12.00 HC

*For sale by the National Technical Information Service, Springfield, Virginia 22161

NASA-Langley, 1983

PUBLIC COLLECTIONS OF NASA DOCUMENTS

DOMESTIC

NASA distributes its technical documents and bibliographic tools to eleven special libraries located in the organizations listed below. Each library is prepared to furnish the public such services as reference assistance, interlibrary loans, photocopy service, and assistance in obtaining copies of NASA documents for retention.

CALIFORNIA
University of California, Berkeley
COLORADO
University of Colorado, Boulder
DISTRICT OF COLUMBIA
Library of Congress
GEORGIA
Georgia Institute of Technology, Atlanta
ILLINOIS
The John Crerar Library, Chicago
MASSACHUSETTS
Massachusetts Institute of Technology, Cambridge
MISSOURI
Linda Hall Library, Kansas City
NEW YORK
Columbia University, New York
OKLAHOMA
University of Oklahoma, Bizzell Library
PENNSYLVANIA
Carnegie Library of Pittsburgh
WASHINGTON
University of Washington, Seattle

NASA publications (those indicated by an '*' following the accession number) are also received by the following public and free libraries:

CALIFORNIA
Los Angeles Public Library
San Diego Public Library
COLORADO
Denver Public Library
CONNECTICUT
Hartford Public Library
MARYLAND
Enoch Pratt Free Library, Baltimore
MASSACHUSETTS
Boston Public Library
MICHIGAN
Detroit Public Library
MINNESOTA
Minneapolis Public Library and Information Center
NEW JERSEY
Trenton Public Library
NEW YORK
Brooklyn Public Library
Buffalo and Erie County Public Library
Rochester Public Library
New York Public Library
OHIO
Akron Public Library
Cincinnati and Hamilton County Public Library
Cleveland Public Library
Dayton Public Library
Toledo and Lucas County Public Library
TEXAS
Dallas Public Library
Fort Worth Public Library
WASHINGTON
Seattle Public Library
WISCONSIN
Milwaukee Public Library

An extensive collection of NASA and NASA-sponsored documents and aerospace publications available to the public for reference purposes is maintained by the American Institute of Aeronautics and Astronautics, Technical Information Service, 555 West 57th Street, 12th Floor, New York, New York 10019.

EUROPEAN

An extensive collection of NASA and NASA-sponsored publications is maintained by the British Library Lending Division, Boston Spa, Wetherby, Yorkshire, England. By virtue of arrangements other than with NASA, the British Library Lending Division also has available many of the non-NASA publications cited in *STAR*. European requesters may purchase facsimile copy of microfiche of NASA and NASA-sponsored documents, those identified by both the symbols '#' and '*', from: ESA - Information Retrieval Service, European Space Agency, 8-10 rue Mario-Nikis, 75738 Paris CEDEX 15, France.

National Aeronautics and
Space Administration

Washington, D.C.
20546

Official Business
Penalty for Private Use, $300

THIRD-CLASS BULK RATE

Postage and Fees Paid
National Aeronautics and
Space Administration
NASA-451

NASA

POSTMASTER: If Undeliverable (Section 158
Postal Manual) Do Not Return